University of Strathclyde

Department of Electronic and Electrical Engineering

VOLTAGE STABILITY ANALYSIS AND CONTROL IN POWER SYSTEMS

BY

XIAORUI (RAY) ZHANG

A thesis presented in
fulfilment of the
requirements for
the degree of
Doctor of Philosophy
2007

ACKNOWLEDGEMENT

Firstly I like to express my sincere gratitude to Prof. K L Lo for not only his constructive supervision and guidance in this PhD project, but also his fatherly care, support in my personal life, which enabled me finally complete this thesis.

I am very grateful to the University of Strathclyde for their kind consideration and permission for me to submit this thesis after so many years.

I also wish to thank all my friends and family for their constant love, patience and encouragement during the time when I was working on the research and writing up this thesis.

CONTENTS

TABLES

FIGURES

ABSTRACT

Under the title of Voltage Stability Analysis and Control, three major subjects have been examined in this PhD project: the fundamental study of voltage stability, the on-line prediction method for voltage collapse, and secondary voltage control systems.

The fundamental study was aimed to lay a theoretical foundation for the rest of research in this project. The on-line prediction method and secondary voltage control systems are particularly targeting on the "early prediction and prevention" strategy to tackle the rapid and "uncontrollable" nature of the voltage collapse phenomenon.

The work on the fundamental study was presented in chapter 3 of this thesis. The basic characteristics of voltage collapse were examined, the theory concerning the voltage stability determining factors (VSDFs) was established. Based on this fundamental study, a knowledge based system for the on-line prediction of voltage collapse was proposed in chapter 4. The pattern recognition technique was used in this prediction system, and the design and development of such a system were intensively discussed in this chapter.

As a well recognised prevention measure to voltage collapse, secondary voltage control systems were systematically investigated in chapter 5, 6, and 7 of this thesis. Chapter 5 deals with the principle of secondary voltage control, and the design and analysis of such a system by classic and optimal control were presented in chapter 6 and 7 respectively.

As a further study, improving voltage stability through generation dispatch was also briefly discussed at the end of this thesis. An algorithm aimed at this purpose was proposed to determine the generation participation pattern upon system load increase.

All the studies in this project were simulated on the standard IEEE test power systems, some of the study results have been published in the different international conferences or academic forums [51] [53] [54] [55] [56].

CHAPTER 1 GENERAL INTRODUCTION

1.1 INTRODUCTION

1. Voltage Collapse

Over the past decades, the phenomenon of voltage collapse has been observed in many large power systems in the world. As the phenomenon may lead to a blackout of a whole power system, it has been regarded as one of the major threats to the security of a power system.

Voltage collapse normally occurred under heavily loaded conditions in a power system. It has been characterised by two typical periods: an initial slowly progressive voltage decline and a final rapid voltage drop. The final voltage drop was often trigged by a severe disturbance such as tripping of transmission lines. Conventional voltage control facilities usually become ineffective or even aggravate the situation. Either as a direct cause or some consequential effects such as angular swing due to the low voltage, this voltage collapse phenomenon may result in a cascade tripping of power system protections, eventually lead to the collapse of the whole power network.

2. Voltage Stability

Voltage collapse phenomenon is recognised as a voltage stability problem in power systems. Voltage stability can be broadly defined as the ability of a power system to maintain an acceptable voltage at all buses under normal and post fault conditions. Voltage stability is related to a variety of structural and operational issues in a power system. These include reactive power reserves, network running arrangement, loading conditions as well as load characteristics. Some voltage control devices such as automatic transformer tap changers, shunt reactive plant, Static Var. Compensators (SVCs) also have significant impacts on voltage stability of a power system.

There may be certain interactions between power system voltage stability and angular stability. An angular instability often leads to a voltage collapse as a secondary effect. However, as a dedicated research, this thesis is specifically concerned with the voltage stability problem that has its own genetic causes.

1.2 RESEARCH BACKGROUND

1. Study Scope

In the area of voltage stability study, the stability analysis and control are the two topics of general concern.

Voltage stability analysis mainly involves mechanism study and stability assessment. The mechanism study is aimed to explore why voltage collapse happens, and what the influencing factors are to the problem. Assessment of voltage stability is to assess or predict how close a power system is from a voltage collapse. The mechanism study is the foundation for the voltage stability study.

Voltage stability control is the ultimate purpose for voltage stability analysis. Due to the rapid and uncontrollable nature of voltage collapse, it is rather difficult to stop the phenomenon once it starts. This makes "early prediction and prevention" the best control strategy to deal with the problem.

As a recognised measure to prevent voltage collapse, secondary voltage control systems have recently drawn increasing attention in the area of power system study [6] [7] [8] [41] [42] [45]. The idea of secondary voltage control is to decentralise a power system into several regions based on electrical decoupling, and control system voltage profile through maintaining voltage at some pre-selected load buses (called pilot buses) by regulating reactive generation within each region. It has been proven [7] [8] [41] that secondary voltage control systems are not only able to maintain a desired voltage profile, but also improve voltage stability within a power network. This is due to two main reasons: firstly secondary voltage control systems move the constant voltage points from generators to the load centre; secondly secondary voltage control best utilise and co-ordinate reactive generation resources to control voltage within a power network.

2. Research History

Both dynamic and static approaches have been used for the study of voltage stability. The previous research covered the topics of the mechanism of voltage stability [1] [15] [20], prediction of voltage collapse [9] [19] [26] [22] [31], impacts of voltage control equipment on voltage stability [30] [38] [39], as well as secondary voltage control [7] [8] [41][42] [48], etc. In chapter 2 of this thesis, the previous research in the area of voltage stability will be reviewed.

As the dynamics of voltage stability are relatively slow, many aspects of the problem can be well examined by static approaches. Static approaches are good at examining the viability of a steady operation state specified by a wide range of system conditions in a power system. They are particularly useful for identifying the influencing factors to voltage stability. On the other hand, dynamic approaches have strong advantage in exploring whether and how a steady operation state (equilibrium points) is reached.

The previous literature review (Chapter2) shows, although many proposed methods are capable of accurately predicting voltage collapse, most of them are rather time-consuming because of algorithm-based numerical computations which often require human intervention during decision-making process, there is no one suitable for on-line applications. As to the prevention of voltage collapse, secondary voltage control was one of a very few recognised measures to improve voltage stability. Despite some successful industrial trials with European utilities, there is urgent need for a systematic study in design and analysis of secondary voltage control systems before such a system can be used in a real power system.

1.3 RESEARCH OBJECTIVES

Based on the above background, the following objectives are identified for this research project:

1. Voltage stability characteristics

Aimed to establish a theoretical foundation for the research in this project, some fundamental properties of voltage stability problem will be examined. This study will focus on the basic characteristics and the voltage stability determining factors.

2. Fast and accurate prediction of voltage collapse

Speed and accuracy are the two essential qualities for prediction of voltage collapse. They are especially important for an on-line application. In this project, an Artificial Intelligence (AI) method is going to be explored for on-line prediction of voltage collapse. It is aimed to take advantage of algorithm-based methods for the accuracy and the knowledge based system for speedy decision-making.

3. Secondary voltage control systems

Secondary voltage control systems will be systematically investigated as a major objective in this project. The study will particularly target on design and analyses of such a system by both classical and optimal control. To prepare a consistent and systematic environment for the design and analysis, the pilot bus based control principle will be theoretically formularised based on power system analysis, a complete set of system modelling and descriptions will be established for secondary voltage control.

4. Improvement of voltage stability by generation dispatch

Improving voltage stability through generation dispatch will also be briefly examined in this project. This will be based on the study of voltage stability characteristics. As this study was not originally planned for this project, some preliminary work will be presented as further study at the end of this thesis.

1.4 ORGANISATION OF THIS THESIS

All the research work in this project will be presented in eight chapters in this thesis.

As a general introduction, Chapter 1 gives an overview about this research project. The research objectives are identified in this chapter.

The previous literature in the area of voltage stability study will be reviewed in Chapter 2. The review will be divided into main sections: voltage stability analysis and secondary voltage control. The merits of the previous studies will be discussed at the end of each review.

Chapters 3 deals with the fundamental aspects of voltage stability problem. The basic characteristics of voltage stability will be examined, and the voltage stability determining factors (VSDFs) will be identified and defined in this chapter. These VSDFs are the load pattern, the load distribution pattern as well as the generation pattern and the generation participation pattern. Some special features with the VSDFs will be discussed, and the unique property of the VSDFs will be generalised into a hypothesis of which theoretical validation will be given. All the study will be backed up by numerical simulations on the IEEE 30 bus power system.

In Chapter 4, a knowledge based system will be proposed for on-line prediction of voltage collapse. This will be based on the fundamental study in Chapter 3 that a power system will have similar voltage stability when the VSDFs are in the same pattern classes. The proposed system consists of a knowledge based system and a pattern recognition module. The knowledge base contains pre-calculated voltage stability results (power margins) for the prototypes of all the pattern classes identified for the VSDFs in a power system. By using pattern recognition technique, the pattern classes of VSDFs for the current state of the power system can be recognised, and the results to the current prediction of voltage collapse can be found in the knowledge base. Simulations of the proposed system on the IEEE 30 bus system will also be presented in this chapter.

The study concerned with secondary voltage control will be presented in Chapter 5, Chapter 6 and Chapter 7. In Chapter 5, the principle of secondary voltage control will be mathematically formularised. The discussion will cover the contents of the pilot bus control principle, the centralised and decentralised control scheme, as well as the multi-level control structure. A complete set of system models and descriptions for secondary voltage control will be established in this chapter.

A secondary voltage control system by classical PI control design will be described in Chapter 6. All the design equations concerning PQR, RVR as well as their integration relationship will be presented. The closed loop stability and performance of this PI based voltage control system will be analysed by using the traditional frequency domain(s) method. The simulation results of this control design on the IEEE 39 bus system will be given in this chapter.

In Chapter 7, an optimal control design will be discussed for secondary voltage control. Both the RVR and PQR of the secondary voltage control will be formularised as the constrained optimal control (quadratic programming – QP) problems. Full details of the design procedure will be given in this chapter. A constructive time domain method will be proposed and used for the closed loop stability and integration analyses for this control system. The simulation results of this optimal control design on the IEEE 39 bus system will also be included with this chapter.

The whole research in this project will be summarised and concluded in Chapter 8. As further study, a method for improving voltage stability through generation dispatch will be briefly discussed in this chapter. Some preliminary simulation results on the ward-hale 6 bus system will be given to show the improvement of voltage stability by using the proposed method.

Apart from the References, there are three appendixes attached to this thesis. Appendix 1 gives the details of all the test power systems used for the simulations in this study. Appendix 2 lists the definitions and notations in the design and analysis of secondary voltage control. Appendix 3 includes all the detailed information about the simulations in Chapter 3 and 4 of this thesis.

1.5 ORIGINAL CONTRIBUTION OF THE THESIS

The original contribution of the research could be summarized in the following three major points,

- Through examining the mechanism of voltage collapse phenomenon, a theory concerning the voltage stability determining factors was established
- Aimed at on-line application, a knowledge based system was proposed for the prediction of voltage collapse using pattern recognition technique
- As a counter-measure to voltage collapse, the design and analysis of the secondary voltage control systems by both classical and optimal control were systemically investigated

Through the research work performed in this thesis, the following technical papers and a EU technical report were published,

[1] Zhang, X., M. A. Johnson, 'Stability Analysis of the Integrated Multi-level Voltage Regulation in Power System' IMPROVE Report 2.3.1 ESPRINT, April 1996.

[2] Lo, K L, Zhang, X "Dispatching Outputs of Generators for Enhancing the Power Margins from the Viewpoint of Voltage Stability", the proceeding of the IEE 2nd International Conference on Advances in Power System Control, Operation and Management, Dec 1993, Hong Kong, pp.60-65.

[3] Lo, K L, Zhang, X, "The Effect of Load Increase Distribution Pattern and Generator Participation Pattern on Voltage Collapse in Power Systems" UPEC 1993, Staffordshire, UK.

[4] Lo, K L, Zhang, X "The Use Of Pattern Recognition Technique for Identifying Electrically Weak Segments In Power Systems", the proceeding of the IEEE Power Tech Conference 1993, Athens, Greece, pp.916-920.

[5] Lo, K L, Zhang, X "A Real-Time Method to determine the Power Margins and Identify Electrically Weak Segments of a Power System with Respect to Voltage Collapse", the proceeding of the 27th UPEC 1992, Bath, UK, Vol.2 pp.704-707.

CHAPTER 2 REVIEW OF PREVIOUS LITERATURE

2.1 INTRODUCTION

The previous literature concerning voltage stability study will be reviewed in this chapter. This review is divided into two main parts: Voltage Stability and secondary Voltage Control. Based on the study methodology, the review on voltage stability will be further classified into static and dynamic methods. For secondary voltage control, as the previous literature exhibits a methodological structure of principle, design and analysis, the review will follow this structure. The previous publications about the impact of secondary voltage control systems on voltage stability will also be reviewed in the second part of the chapter. Merits of the previous studies will be discussed at the end of each review.

2.2 VOLTAGE STABILITY

There have been a large number of papers and reports published in the area of voltage stability study. Those previous literature can be broadly categorised under two main subjects: mechanism study and prediction of voltage collapse. The mechanism study mainly explores the cause for voltage collapse; while the prediction of voltage collapse targets on assessing how close a power system is from a voltage collapse. Those previous studies will be reviewed under headings of static methods and dynamic methods.

2.2.1 Static Methods

The static analysis is usually used to examine the viability of a steady operation state specified by the certain operating conditions in a power system. The load flow analysis tends to be a major tool for this kind of methods.

2.2.1.1 The Minimum Singular Value (MSV) method

Tiranuchit and Thomas in reference [1] have proven that the Jacobian matrix of the load flow equations will become singular when a power system experiences voltage collapse; the minimum singular value of the Jacobian matrix can be used as a Voltage Collapse Proximity Indictor (VCPI) to predict voltage collapse. The VCPI proposed in this study can be described as:

$$\mathrm{VCPI} = \sigma_{MIN}(\mathbf{J}) \qquad (2.2.1\text{–}1)$$

$$\sigma_{MIN}(\mathbf{J}) = \mathbf{Min}\{\sigma_1, \sigma_2, \ldots, \sigma_n\}$$

$$\mathbf{J} = \mathbf{U}\Sigma\mathbf{V}$$

$$\Sigma = \mathrm{diag}[\sigma_1, \sigma_2, \ldots, \sigma_n]$$

Where,

J is Jacobian matrix of the load flow equation,

σ_i is the singular value of **J**, i=1, 2, ... n, σ_{min} is the minimum singular value.

U and **V** are orthogonal matrices.

Improvement of voltage stability through the minimum singular value was also suggested by the same authors in reference [2]. This was based on the study about the influence of system power injections on the minimum singular value. This study can be summarised by the following equation:

$$\Delta\sigma_{\mathbf{min}} = \mathbf{C}^{\mathrm{T}}\Delta\mathbf{S} \qquad (2.2.1\text{–}2)$$

Where,

$\mathbf{C}^T \in \Re^r$ is the vector of system parameters, it is function of **J, U**, and **V**.

S is the vector of power injections to a power system.

Using this equation, an optimisation algorithm was formularised to maximise the minimum singular value through generation dispatch. The optimisation problem was subject to all the operation constraints and the balance between generation and demand.

From this equation (2.1.1-2), it can be seen that voltage stability will benefit from the shunting capacitors as negative reactive power injections to a power system.

A major difficulty with this method is the Singular Value Decomposition (SVD). The numerical computation burden for the SVD is proportional to the cubic power of the size of the Jacobian matrix. Thus, by conventional computer, the SVD computation is unacceptably slow. Addressing to this problem, Tiranuchit and Thomas also proposed the SVD computation schemes by parallel processors in reference [3]. The simulation results showed that the SVD computation speed was significantly improved by the proposed schemes.

The application of this MSV method in the National Grid Company's transmission system was presented by Ekwue et. al in reference [4]. It was shown that this method was good at accurately assessing voltage stability.

2.2.1.2 The Power Margins (PM) method

The power margins method for assessing voltage stability was discussed in reference [9 - 14]. This method is based on the fact that there are maximum limits for the power which can be transmitted to the load buses in a power system; voltage collapse may occur when the power system is loaded near or above these limits. The concept of power margins is defined as the differences between the initial load level and its maximum limits at one bus or in a whole power system. Two typical methods for determining the power margins are going to be reviewed below.

1. By the load flow simulation

The method to determine the power margins by load flow simulation was extensively discussed by Fishchl, et al. and Tamura in the reference [9-10]. The principle of this method is to progressively simulate load flow with increase of system load until the maximum loading limits are reached. This is probably one of the most direct ways to calculate the power margins, however the non-convergence due to the singular Jacobian matrix in the vicinity of voltage collapse is the major problem with this method.

To solve this problem, Lemaitre, et. al in reference [11] modified the simulation method by introducing the linearisation technique for the load flow calculation. To enhance the accuracy, the major non-linearity and dynamics in a power system, such as generators reaching reactive power limits, were taken into account. The application of this method involves the following procedure:

<u>Step1</u>: simulate linear increase in active and reactive load by

$$\begin{bmatrix} \Delta \mathbf{P}_L \\ \Delta \mathbf{Q}_L \end{bmatrix} = \alpha_K \begin{bmatrix} \mathbf{P}_L \\ \mathbf{Q}_L \end{bmatrix}$$, α_K is the load increase rate;

Step2: simulate the balance between active power generation and demand;

Step3: determining variations of network variables (V, θ, Q) by linear approximation:

$$[\theta]_{K+1} = [\theta]_K + \left[\frac{\Delta\theta}{\Delta\alpha}\right]_K \alpha_K$$

$$[\mathbf{V}]_{K+1} = [\mathbf{V}]_K + \left[\frac{\Delta \mathbf{V}}{\Delta\alpha}\right]_K \alpha_K$$

$$[Q]_{K+1} = [Q]_K + \left[\frac{\Delta Q}{\Delta\alpha}\right]_K \alpha_K$$

where,

$\left[\frac{\Delta Q}{\Delta\alpha}\right]_K, \left[\frac{\Delta\theta}{\Delta\alpha}\right]_K, \left[\frac{\Delta V}{\Delta\alpha}\right]_K$ are the sensitivity coefficients obtained from the Jacobian matrix. These sensitivity coefficients will be updated each time when a non-linearity occurs, e.g. each time a generator reaches its reactive generation limit. α_k can be determined by the following equation when a generator reaches it reactive generation limit:

$$\left[Q_K + \left[\frac{\Delta Q}{\Delta\alpha}\right]_K \alpha_K = Q_{MAX} \right]$$, Q_{max} is the reactive power limit of a generator.

Step4: terminate simulation, when margin in load is considered sufficient or a bus voltage becomes unstable ($\partial Q/\partial V$ or $\partial P/\partial V$ becomes negative).

The power margins then can be determined by:

$$\Delta P^i = \left[\sum_{K=1}^{N} \alpha_K\right] P^i_{L0}; \quad \Delta Q^i = \left[\sum_{K=1}^{N} \alpha_K\right] Q^i_{L0}$$

Where,

$P_{L0}{}^i$ and $Q_{L0}{}^I$ are the initial active and reactive power injections at bus i.

Although the convergence problem is avoided by this method, a dichotomic search is normally needed for determining the load increase steps in the vicinity of voltage collapse. This may influence the speed of this method. Another shortcoming of this method is that the load distribution and generation participation were not considered, which could significantly influence voltage stability in a power system.

2. By optimisation

Obadina and Berg in reference [12] formularised the determination of power margins into an optimisation problem. The objective of this optimisation is to maximise the total MVA load, subject to the power system operation constraints. The optimisation algorithm was given as:

$$\textbf{MAX.}\ S_{Total} = \sum_{i=1}^{M} (P_i^2 + Q_i^2)^{1/2}$$

Subject to

(a) Distribution constraints at load buses

(b) MVar and MW limits on generators

(c) Generators MW participation

(d) Power factor constraint for demand

(e) Limits on controlled voltages and OLTC transformer taps

Where, M is the number of load buses in a power system.

By solving this optimisation problem, the maximum MVA demand S_{Total}^{Limit} before voltage becomes unstable can be obtained. And power margins can be calculated by

$$S_M = S_{Total}^{\mathbf{lim}\,it} - S_{Total}^{initial}$$

Where, $S_{Total}^{initial}$ is the initial load.

A similar algorithm was also proposed for determining the reactive power margin by T. Van Cutsem in reference [14]. In order to consider the influence of active power flow but avoid explicitly treating active power/phase angle relationship, a special PQ transformation was introduced in this proposal. This transformation assumed that active power flow in all network branches is constant. It was believed that this assumption only influenced the solution marginally.

As the power margins determined by the optimisation methods are normally the maximum values under the specified operation constraints, they may be too optimistic for prediction of voltage collapse. In addition, solving optimisation problems is usually time-consuming, and often involves some tedious exercise for fine tuning constraints before a satisfactory solution is obtained.

2.2.1.3 The multiple load flow solutions method

As the load flow equations are quadratic in term of voltage magnitude and involve sines and cosins of voltage angle, it is possible to have multiple load flow solutions for an operation condition. The link between voltage instability and the multiple load flow solutions was investigated by Tamura in reference [15]. This study suggested that, individuals of a load flow solution pair could have completely different features: one being voltage stable, another being voltage unstable. Under heavily loaded conditions, the solution pair could become very close so that both of them appeared to be operable. In this situation, the system could easily jump from the stable solution to the unstable one following a disturbance. In this study, three criteria were proposed for assessing voltage stability of a closely located load flow solution pair. These three criteria are:

Criterion 1 The sign of the determinant of the Jacobian matrix

This criterion was based on the method proposed for estimating the power system angular stability by Venikov in reference [16]. It was given that,

$$\det \mathbf{J} = C \det \mathbf{A} = C\prod_{i=1}^{2m} \lambda_i \qquad (2.2.1\text{–}3)$$

Where,

$\mathbf{J}$ is the Jacobian matrix of load flow equation,

C is a constant related to the inertia constants and angular frequencies of all generators,

$\mathbf{A}$ is the Jacobian matrix for linearised state equation (the load flow and swing equations),

λ_i is the i-th eigenvalue of $\mathbf{A}$.

It is known that the system stability can be assessed by the sign of the real part of the eignevalues. From equation (2.2.1-3) the sign change of the real part of the eignevalues may be observed through the sign of det **J.** Thus assuming the initial state S_0 is a stable operation point, by comparing with the sign of det **J** at S_0, the voltage stability for other states S_1, S_2, ..., S_K can be assessed by

$$\mathbf{F}(S_K)\begin{cases} = \mathbf{F}(S_0) \rightarrow \text{stable} \\ \neq \mathbf{F}(S_0) \rightarrow \text{unstable} \end{cases} \qquad (2.2.1\text{–}4)$$

Where, $\mathbf{F}(S_K) = \mathbf{sign}\{\mathbf{det\,J}(S_K)\}$.

With this criterion, an unstable state may be overlooked when the real part of even number of eigenvalues change sign from negative into positive at the same time, as the sign of det J will not be affected.

Criterion 2 The voltage sensitivity

The second criterion was based on the voltage sensitivity analysis. It was found that the voltage sensitivity to power injections and other network parameters are opposite in sign for a load flow solution pair. Thus by comparing the sign of these sensitivities $(\frac{\partial V_i}{\partial Q_j}, \frac{\partial V_i}{\partial \eta_j})$ with those at stable situations, the stable and unstable solutions of a load flow solution pair can be distinguished.

Criterion 3 The stored energy

The third criterion was based on the principle of energy balance. It was suggested that a power system could be regarded as a LC network. For a frequency (f) variation, the stored energy E in the inductance L and capacitance C should possess the following property:

$$\left.\frac{\partial E}{\partial f}\right|_{S_i} > 0 \quad \text{if } S_i \text{ is a stable load flow solution;}$$

$$\left.\frac{\partial E}{\partial f}\right|_{S_i} < 0 \quad \text{if } S_i \text{ is an unstable load flow solution.}$$

By this property, the voltage stability of a load flow solution pair can be assessed. The formulas for calculating the total stored energy E were also proposed in the study.

The simulation results showed that all the three criteria could identify the stable or unstable solution for a load flow solution pair. However, the biggest problem with this method is to calculate the multiple load flow solution pairs, which requires heavy numerical computation and human intervention. Furthermore, it is rather difficult to perform the eigenvalue analysis or to formularise the stored energy for a large power system.

2.2.1.4 The Load Flow Feasibility Region method

Based on the concepts of the load flow Feasibility Region (FR) and Feasibility Margin (FM), a Voltage Collapse Proximity Indicator (VCPI) was proposed by F.D. Galiana in reference [19]. In references [17,18] Jarjis and Galiana defined the load flow FR as a set of bus injections (P, Q, or V^2 at each bus) for which load flow solutions exist; and the load flow FM is the proximity of a bus injection vector to the FR boundary. The value of this FM measures the angle between a given bus injection vector and the nearest injection vector on the FR boundary. Therefore, when FM > 0 indicates that the bus injection vector is inside the FR; while FM = 0 implies that the injection vector is on the FR boundary, which corresponding to the starting point of voltage collapse.

This VCPI was mathematically written as:

$$\mathrm{VCPI}(\alpha) = [\mathrm{FM}\{\mathbf{Z}(\alpha)\}]^{-K}$$

and

$$\mathrm{FM}\{\mathbf{Z}_0\} = \sin\{\mathbf{Z}_0, \mathbf{Z}_1\}$$

$$\cos\{\mathbf{Z}_0, \mathbf{Z}_1\} = \frac{\mathbf{Z}_0^{\,T}\mathbf{Z}_1}{\|\mathbf{Z}_0\|\|\mathbf{Z}_1\|}$$

$$\mathbf{Z}(\alpha) = \mathbf{Z}_0 + \alpha\Delta\mathbf{Z} \qquad 0 < \alpha < 1$$

with $\mathbf{Z}(1) = \mathbf{Z}_1$

Where,

$\mathbf{Z}_0$ is the given bus injection vector,

$\mathbf{Z}_1$ is the nearest injection vector on the boundary of FR,

$\Delta\mathbf{Z}$ is the specified change direction for a given injection vector.

The application of this VCPI for a simple two-bus system was demonstrated in this paper, the simulation results were encouraging.

As the VCPI does not directly use the load flow calculation, the convergence problem associated with the singular Jacobian matrix near voltage collapse seems to be avoided. However, this method relies on the boundary of load flow feasibility region, which is very difficult to determine for a multiple-bus power system. In addition, there is no guarantee that voltage collapse will not occur within the load flow feasibility region.

2.2.1.5 The PQ controllability method

The concept of PQ controllability was introduced to voltage stability study by Schlueter et. al. in reference [20, 21, 22]. It was suggested that loss of the PQ controllability could be a cause for voltage collapse.

The whole study was based on the following equation which could be derived either from the transient stability model or the load flow model:

$$\Delta\mathbf{V} = \mathbf{S}_{\mathrm{Q_L V}}^{-1}\Delta\mathbf{Q}_{\mathrm{L}} + \mathbf{S}_{\mathrm{VE}}\Delta\mathbf{E}$$

Where, E is voltage set points at generator (PV) buses. By using this equation, the PQ controllability was defined as:

'A system is called PQ controllable at any time t along the transient stability model trajectory or at the equilibrium if

(i) when $\Delta E(t)=0$, any non-zero non-negative disturbance $\Delta Q_L(t)$ causes the PQ state $\Delta V(t)$ to become non-negative; and for each j there is a non-zero non-negative disturbance $\Delta Q_L(t)$ causes $\Delta V_j(t)$ to become positive;

(ii) when $\Delta Q_L(t)=0$, any non-zero non-negative disturbance ΔE (t) causes the PQ state $\Delta V(t)$ to become non-negative; and for each j there is a non-zero non-negative control $\Delta E(t)$ causes $\Delta V_j(t)$ to become positive.'

A theorem for assessing the PQ controllability was given in this study as *'the system is PQ controllable if* $S_{Q_L V}$ *is invertible and* S_{VE} *is non-negative with no zero rows'*.

Associated with the PQ controllability, the concept of the voltage control area was proposed. It was defined as 'a set of load and generator buses where voltage responds very similarly (coherently) to the reactive load and generation changes outside this voltage control area'. An algorithm for identifying voltage control areas in a power system was also presented in this study.

Utilising these study results to predict voltage collapse was discussed in reference [21]. The reactive power reserve within a voltage control area boundary was identified as a measure for prediction of voltage collapse. As this reactive power reserve represents the limit of the reactive power that could be imported to the voltage control area before voltage collapse occurs, it reflects the weakness of the voltage control area. It was demonstrated the same algorithm for identifying voltage control areas could also be used to determine the reactive power reserve. Using the changes in sensitivity matrices S_{VE} and $S_{Q_L V}$, which would occur as voltage collapse developing, was also proposed as other measures for prediction of voltage collapse in this study.

As the determination of the reactive power reserve requires the heuristic knowledge and human intervention, it would only be used for the off-line prediction of voltage stability. The other measures are actually sensitivity analysis based methods, which will be specifically reviewed in a separate section below.

In this study, it was also proven that the necessary conditions for voltage stability derived from the dynamic model are identical to those from the static model. This was done by examining the singularity of Jacobian matrices for both the linearised transient stability model and the load flow model at the bifurcation point (voltage collapse). This result united the static and dynamic method for voltage stability study.

2.2.1.6 The sensitivity analysis method

The sensitivity analysis was one of the earliest static methods proposed for voltage stability study. By this method, Venikov in reference [23] developed a criterion for assessing voltage stability for a simple two bus power system. This criterion was given as

$$\frac{dV_s}{dV_i} > 0 \text{ if } V_i \text{ is stable.}$$

Where, V_s and V_i are voltages at sources end and load end respectively.

Borremans et.al in reference [25] proposed the following sensitivity based criteria for assessing voltage stability in a multi-bus power system:

(i) $\frac{V_i}{E_i} > 1/(2\cos(\frac{\xi-\alpha}{2}))$,

(ii) $\frac{\Delta Q_L}{\Delta Q_G} = \left.\frac{\partial Q_L}{\partial Q_G}\right|_{P_L=P_0} > 0$,

(iii) $\left.\frac{\partial V_i / V_i}{\partial Q_j / Q_j}\right|_{P_L=P_0} > 0$,

(iv) $P_L \le P_{L\,\max}$ and $Q_L \le Q_{L\,\max}$.

Where

V_i and E_i are the voltage and open circuit voltage at bus i,

$Z_{ii}\angle\xi$ and $Z_{iL}\angle\phi$ are the equivalent source and load impedance at bus i.

Based on a two bus system, Carpentier in reference [24] developed a set of constraints for voltage stability by sensitivity analysis. These constraints are:

(i) the constraint on reactive load: $Q_L < Q_{LC} = \frac{E^2}{4X}$,

(ii) the constraint on reactive supply : $Q_G < Q_{GC} = \frac{E^2}{2X}$.

Where, E is source voltage and X is the transmission line reactance.

It was shown that the voltage at the load end of the two bus system satisfies

$$V_L / E = \frac{1}{2}(1 + (1 - Q_L / Q_{LC})^{\frac{1}{2}}),$$

and the ratio V_L/E dropped rapidly from 1 to 1/2 as the Q_L approached the constraint Q_{LC} from 0. This was believed to be a scenario of voltage collapse.

By regarding a voltage control area as a bus and the rest of a system as another bus, these constraints were extended to a multi-bus power system. And a voltage stability indicator was proposed as

$$Z = \frac{Q_G}{Q_L} = \frac{1}{(1 - Q_L / Q_{LC})^{1/2}}.$$

It can be seen the value of Z will approach infinity when Q_L researches the constraint Q_{LC}. Thus, Q_G/Q_L becoming infinity was generalised as a criterion for assessing voltage stability. The Q_G, Q_L here are the total reactive generation and the reactive demand in a area or whole power system.

The sensitivity analysis methods provide a clear and direct insight to voltage stability of a power system. However, the sensitivity matrix can be difficult to calculate when a power system is close to voltage collapse. This is a major obstacle for the application of these sensitivity methods, particularly in a real time environment.

2.2.1.7 The optimal impedance solution method

A voltage stability study based on the theory of the optimal impedance solution was presented by Chebbo et.al in reference [26, 27]. The optimal impedance solution is known as that, in a two bus power system, the power transmitted to the load bus from the source reaches its maximum level when

$$Z_S / Z_L = 1$$

Where, Z_S, Z_L are the magnitudes of transmission line impedance and load impedance respectively.

It was believed the voltage at the load bus corresponding to this maximum transmission power was the critical voltage for voltage collapse. By the Thevenin's theorem, this solution was extended to a multi-bus system in reference [26], and a VCPI was proposed as

$$\mathrm{VCPI} = \frac{Z_{ii}}{Z_i} \leq 1 .$$

Where, $Z_{ii}\angle\beta_i$ is the Thevenin's equivalent impedance looking into to the port between bus-i and the ground, and $Z_i\angle\phi_i$ is load impedance at bus i.

$Z_{ii}\angle\beta_i$ was actually the i-th diagonal element of the system resistance matrix $[Z]$, it can be obtained from the system admittance matrix [Y] by $[Z]=[Y]^{-1}$. $Z_i\angle\phi_i$ can be directly calculated from the load flow solutions as

$$Z_i\angle\phi_i = \frac{V_i^2 \cos\phi_i}{P_i}\angle\phi_i , \ \angle\phi_i = \tan^{-1}\left(\frac{Q_i}{P_i}\right).$$

Using this VCPI, a linear programming algorithm was proposed in reference [27] to maximise voltage stability by reactive generation dispatch. The sparse dual revised simplex method was used in the algorithm to minimise the possibility of voltage collapse. Four different objective functions were given for the sake of comparison. These objective functions are

(i) Maximise $\sum\limits_{i \in J}(Z_{ii}/Z_i)$;

(ii) Maximise $\sum\limits_{i \in J}(Z_{ii}/Z_i)V_i$;

(iii) Maximise $\sum\limits_{i \in J} V_i$;

(iv) Maximise $\sum\limits_{i \in J} Z_i$.

Where, J is the set of load buses in a power system.

All these four objective functions were subject to the same set of system operational constraints. The state variables include the reactive generations of generators and the voltage magnitudes at load buses. The control variables were the transformer tap positions, the generator excitation settings, as well as the shunting reactive compensation plant. The simulation results showed that the objective function (ii) was the best among the four proposed functions in terms of system voltage profile, the VCPI values and decision-making time.

This VCPI was also suggested for determining the critical power (the maximum transmission power). But it was found that it was more accurate for single bus than for a whole system. The reason for it was that this VCPI uses the linearised system model, the load increase in the whole system may not be fully reflected.

In this study, it was assumed that voltage collapse would occur when the active transmission power reached its maximum level. However, voltage stability is also strongly influenced by the reactive power. It is likely that voltage collapse occurs before the maximum active transmission power is reached.

2.2.1.8 The impact of the Static Var Compensators (SVCs)

The impact of SVCs on voltage stability was examined by Hiskens and Mclean in reference [30]. The voltage-susceptance diagram was used to analyse the relationship between SVC operations and voltage characteristics in a power system. On this diagram, it was believed that "the positive slope" was a voltage stable region, and "a negative one" was an unstable region. To distinguish the effects of SVC from generator and transformer tap changer (due to the different response times), the voltage characteristics was examined in the scales of instantaneous, short term and long term individually.

The instantaneous characteristic represented the initial relationship between voltage and susceptance at a SVC without considering generator and transformer tap changer. The short term characteristic took into account the generator response but not tap-changers. The long term one included all these three components. With a voltage dependent load model, it was shown that the instantaneous characteristic alone could satisfy a 'positive slope requirement'. This indicated that SVC could have a voltage stable operation on the long term voltage-susceptance diagram which had negative slopes. The study also showed that the encountering limits of SVCs could lead to voltage collapse, especially when the operating points were in negative slope of the long term voltage-susceptance curve.

This study is a typical example of a static analysis for a dynamic subject. One of its outstanding contributions is to prove feasibility that SVCs can have a voltage stable operation on a negative slope of the long term voltage-susceptance characteristics. Practically, this means transmission capability may be improved by utilising the SVCs in a power system.

2.2.2 Dynamic Methods

In a power system, the voltage stability problem is often regarded as a "slow dynamic issue", and some dynamic analyses have been previously used to study this problem.

2.2.2.1 The eigenvalue analysis method

Based on the small disturbance principle, the eigenvalue analysis similar to the one for the power system machine stability was applied for the dynamic analysis of voltage stability in reference [31, 32, 33, 34]. The model used in these studies consisted of a set of differential equations for synchronous generators or motors, and a set of algebraic equations for machine excitations and power network as:

$$\dot{\mathbf{x}} = f(\mathbf{x}, \mathbf{y}) \qquad (2.2.2\text{–}1)$$

$$\mathbf{0} = g(\mathbf{x}, \mathbf{y}) \qquad (2.2.2\text{–}2)$$

Where, $\mathbf{x}$ represents the state variables of machines and excitation systems, y represents the stator currents of machines, power injections and voltages at all buses.

By linearisation and direct substitution, an equation in the format shown in 2.2.2-3 can be derived from the equation (2.2.2-1) and (2.2.2-2):

$$\frac{d\Delta\mathbf{x}}{dt} = (\mathbf{A} - \mathbf{B}\mathbf{D}^{-1}\mathbf{C})\Delta\mathbf{x} = \tilde{\mathbf{A}}\Delta\mathbf{x} \qquad (2.2.2\text{–}3)$$

Where, A, B, C and D are system metrics.

From this equation, it can be found that the static bifurcation occurred when det [D] = 0. By assuming that $\det[D] \neq 0$ and D^{-1} exists, the dynamic properties of voltage stability can be examined by monitoring the eigenvalues of $\tilde{\mathbf{A}}$.

Rajagopalan, et al., discussed the basic methodology of the eigenvalue analysis method for the study of voltage stability in reference [31]. Sekine et al in reference [32] extended this method by including the induction motor with system load. Lee and Lee in reference [33, 34] presented a comprehensive eigenvalue method for the voltage stability analysis. In reference [33], the dynamic mechanism of voltage collapse phenomenon was investigated from the physical point of view. By including the synchronous motor as a system load, it was observed that a voltage drop caused by interaction between machines and the system network could lead to voltage collapse. Study in reference [34] further developed the method by taking into account the synchronous machine excitations, transformer tap changers, shunting capacitors as well as the power system stabilisers. To enhance voltage dynamic stability, an optimisation algorithm for determining the control parameters was also proposed in this study.

It has been seen that the eigenvalue method is a powerful tool for examining the dynamic properties of voltage stability. It is also interesting to note that this method can also be used to study the static voltage stability around an equilibrium point.

2.2.2.2 The dynamic simulation method

The voltage stability study by dynamic simulation was discussed in references [5, 35, 36]. The basic procedure of this method is to numerically solve the dynamic model for voltage stability for a given period of time under certain system conditions. As voltage stability problem is normally a "slow dynamic event", the typical simulation period is the scale of several minuets.

Kundar in reference [5] described the details of a dynamic simulation method for voltage stability analysis. This study was based on an 11 bus power system, and the loss of a transmission line was used as the disturbance. The generator over-excitation limits, transformer tap changers and load characteristics were included in the simulation model. Deuse et al. in reference [36] presented a similar study using the dynamic simulation program "EUROSTAG". To demonstrate the capability of the dynamic simulations, three study cases were given. The first case showed the basics of voltage instability by using a model containing an infinite bus feeding to a reactive load through a purely reactive line. The second case used a two bus system to illustrate the system operation on the lower part of the PV curve, and the effect of load characteristics and SVC were also examined in this case. The third one showed the influence of automatic transformer tap changers on voltage stability.

Another voltage stability study by the dynamic simulation was carried out by Lachs et al in reference [37]. The simulation was performed following a disturbance of losing five lines simultaneously in a 92 bus system. This study covered the cases both with and without countermeasures for voltage collapse. It was found that an under-voltage load shedding scheme could be more efficient than expected for maintaining the voltage stability in a power system.

In comparison with the load flow simulation, the dynamic simulation methods provide more comprehensive and detailed understanding of the voltage stability problem. It is especially useful for a post fault analysis following a severe disturbance such as transmission line tripping, or sudden generation loss. Two drawbacks of those methods are the high stiffness of the differential equations due to long term dynamic simulation, and time-consuming numerical computation. The implicit integration methods were recommended in reference [5] to cope with the high stiffness problem. Reference [35] suggested that the computation efficiency could be improved by automatically adjusting the integration time step with solution progressing and fast transient decaying.

2.2.2.3 The impact of the Automatic Tap-changer Control (ATCC)

The impact of the ATCC on voltage stability was investigated in reference [38, 39]. The small disturbance method (the eigenvalue analysis) was used in those studies.

Liu in reference [37] examined the voltage collapse phenomenon caused by the operation of the ATCC. This study was based on a simple power system with an

ATCC on the transformer between the source (generator) bus and a load bus. The dynamics of this ATCC were modelled by

$$\frac{dn}{dt} = \frac{1}{T}(V_0 - V)$$

Where,

n is the transformer turn ratio related to a tap position,

V_0, V are the target voltage and the controlled voltage respectively.

T is time constant.

By solving the equation dn/dt = 0 with load flow equations, two equilibrium points (n_1, n_2 where $n_1 > n_2$) were obtained. By using the eigenvalue analysis, it was found that the equilibrium point n_2 is asymptotically stable, and n_1 is unstable. Thus, the stability region was established as

$$D = \{n: \quad n < n_1\}.$$

Liu and UV in reference [39] extended the study into a power system which has M transformers with ATCC. It was proved that there exist as many as 2^M classes of equilibriums, only one class could contain a stable equilibrium; in the class with the stable equilibrium, there exists a smallest equilibrium, which representing the worst case of the voltage stability. The Non-singular Jacobian matrix was used as a criterion to assess the stability of the smallest equilibrium. A method was also proposed for determining the stability region around the smallest equilibrium in the form of hyperboxes union.

The studies in reference [38, 39] mathematically modelled the dynamic impact of the ATCC on voltage stability. It theoretically revealed the mechanism of the voltage collapse phenomena caused by the operation of the ATCC.

2.2.2.4 The impact of the static load characteristic

Vournas and Krassass used a dynamic approach in reference [28] to investigate the impact of the static load characteristic on voltage stability. The excitation field dynamics of synchronous machines were taken into account in this study. The dependence of real and reactive load on voltage were modelled as

$$P = P_0\left(\frac{V}{V_0}\right)^{N1}, Q = Q_0\left(\frac{V}{V_0}\right)^{N2}.$$

Those equations were linearised and incorporated into the admittance matrix of power system model.

A single machine power system was firstly examined by using the Heffron-Phillips generator model described in reference [29]. In this model, the coefficient K_3 was derived to reflect the voltage stability of a power system. This study showed that K_3 was positive for the constant impedance loads, indicating that the system was voltage stable under all operation conditions; K_3 might become negative for the constant power loads, which suggesting that the system voltage controllability limit could be fairly close to the nominal voltage level. The voltage stability region as a function of the voltage dependent load was formularised in this study. It covered the cases both with and without the automatic voltage regulation.

This study was then extended to a multi-machine power system, and a set of approximate voltage stability criteria were developed. By using the extended linearisation coefficient matrices, voltage stability could be estimated through the eigenvalue analysis of a reduced dimension matrices. This significantly speeded up the voltage stability analysis for a large power system.

Apart from the extensive study of the impact of the static load characteristic on voltage stability, this study also provided a feasible means to predict voltage collapse by analysing the load characteristics in a power system.

2.2.3 Remarks

Both static and dynamic methods have been used for voltage stability study. The examination of voltage stability mechanism and prediction of voltage collapse were two focal points. The impact of the ATCC, SVCs, and the load static characteristics were also popular subjects in this study area. There was very little research published in terms of control or prevention of voltage collapse.

The static methods are normally used to examine viability of a steady operation state (voltage stability) specified by certain operation conditions in a power system. System parameters or variables are assumed to be time invariant in these methods. It has been seen that static methods are particularly good at examining a wide range of system conditions. The load flow analysis is a major tool for those methods.

One common problem with the static methods is the non-convergence of the load flow calculation in the vicinity of voltage collapse. Although some methods were proposed to overcome this problem, they were usually a "trade-off" with either the speed or accuracy of the decision-making.

The dynamic methods tend to be used to explore why or how a steady operation state (equilibrium point) is reached. As the dynamic methods provide comprehensive and detailed insight to the problem, they are particularly useful for the mechanism study or special case analysis of voltage stability problems. The model for the dynamic methods normally consists of a set of differential equations for system dynamics and a set of algebraic equations for power network.

The major drawback of the dynamic methods is the time-consuming numerical computation. In addition, those methods do not always conceptually distinguish between voltage stability and power system angular stability, which may cause some confusion under certain circumstances.

Many proposed methods are able to accurately predict voltage collapse. Most of them rely on algorithm based numerical computation, their decision-making speed tends to be unbearably slow, hence unsuitable for on-line applications.

2.3 SECONDARY VOLTAGE CONTROL

In this section, the previous literature on secondary voltage control will be reviewed under four headings: the impact of secondary voltage control on voltage stability, the control principle, control system designs as well as control system analyses.

2.3.1 The impact of secondary voltage control on voltage stability

Idea of secondary voltage control is to decentralise a power system into several regions based on electrical decoupling, and maintain a desired voltage profile through controlling the voltage profile for each region independently by a secondary voltage control system (Regional Voltage Regulator-RVR) using the regional reactive generation. In reference [7, 8, 41], the impact of secondary voltage control schemes on voltage stability was investigated. It was proven that a secondary voltage control scheme is not only able to maintain a desired voltage profile, but also improves voltage stability in a power system.

In reference [7, 41], the following points were concluded as to why secondary voltage control schemes improve voltage stability. Firstly a secondary voltage control scheme automatically maintains voltage profile of a power system at a desired level. Secondly a secondary voltage control scheme moves the voltage control points from generator terminal busbars to some strategically selected busbars called "pilot buses", so that the constant voltage points are closer to load centre. Most importantly secondary voltage control systems co-ordinately utilise reactive generation resources in a power system.

A detailed study about this impact was described by Popovic in reference [7]. This study examined the change of voltage stability margin by a secondary voltage control scheme in a power system. The voltage stability margin in form of "the critical regimes" was determined by finding the critical system load level. At this critical load level, it was observed that one complex-conjugate eigenvalue pair of the linearised system matrix becomes purely imaginary. Both the analysis and simulation results showed that with the secondary voltage control scheme, the voltage stability margin was increased in comparison with the situation where only primary voltage control (AVR) was used. It was also shown that the secondary voltage control scheme enhanced the loading capability for the power system.

In this study, the local voltage stability in the neighbourhood of "the critical point" was also examined using the Hopf bifurcation method. The study concluded that although a secondary voltage control scheme might not be able to stop an already started voltage collapse, it would extend its transition time, which will allow more time for control engineers in the control centre to take some actions.

An "emergency assist control mode" was proposed in this study for the secondary voltage control scheme. When voltage instability is predicted, this emergency control mode will be switched on, and the control scheme will use the most influential reactive generation to control the voltage at the jeopardised critical buses. The numerical simulations in this study demonstrated that this emergency mode was particularly beneficial for dumping already initiated voltage oscillations.

Aiming at improving the ability to prevent voltage collapse, a real-time voltage stability index was introduced into the secondary voltage control scheme by Arcidiacono, et al in reference [8]. This index was given as:

$$I_j(t) = q_j(t) + \rho \frac{\partial q_j(t)}{\partial (t)}$$

Where,

$q_j(t)$ is the percentage of reactive generation with respect to its limit in region j,

$I_j(t)$ satisfies $0 \leq I_j(t) \leq 1$.

This index was designed to avoid the saturation of secondary voltage regulator. When the index indicated that the reactive generation was close to or has reached its limit, the shunting capacitors or on-load transformer tap-changer would be used to support the voltage. In this way, the local generator units would be automatically discharged, consequently the control margins and voltage stability margins would be enhanced.

The previous studies clearly show that secondary voltage control scheme has beneficial impacts on voltage stability. It improves the voltage stability margin, and increases the transitional period of an already initiated voltage collapse in a power system.

2.3.2 The Control Principle

The principle of a secondary voltage control scheme is to decentralise a power system into several "voltage independent" regions based on electrical decoupling, and control the voltage profile in each region independently using the Secondary Voltage Controller, otherwise known as the Regional Voltage Regulator (RVR).

The RVR controls the voltage profile of a region by maintaining the voltage at pilot buses through regulating the reactive generation of the regional control power plants. In a power system, the pilot buses are such buses in a region that if their voltages are maintained at pre-defined values (references), the voltage at other buses in the region will stay within certain limits. The control power plants are the power plants, of which reactive outputs have stronger influences on the voltage at the pilot buses than other power plants in a region. The control power plants in one region are supposed to have limited influences on the voltage at the pilot buses in other regions.

Clearly the selection of the pilot buses and control power plants is the key task for the decentralisation of a power system. Some research work on this subject was presented in reference [7, 41, 42, 44, 45, 46]. Two typical methods using the sensitivity analysis and the optimisation modelling will be reviewed in this section.

2.3.2.1 The sensitivity method

A sensitivity method for selecting the pilot buses and control power plants was proposed by Arcidiacono et al in reference [42]. This method was based on the dependence analysis between bus voltages and reactive loads in a power system.

From the load flow equations and a simple voltage control law

$$\Delta Q_G = \Lambda(\Delta V_R - \Delta V) \qquad (2.3.2\text{–}1)$$

the following equations were derived:

$$\Delta V = S\Delta Q_G + S\Delta Q_L \qquad (2.3.2\text{–}2)$$

$$\Delta V = \tilde{S}\Lambda\Delta V_R + \tilde{S}\Delta Q_L \qquad (2.3.2\text{–}3)$$

Where,

$\Delta \mathbf{Q}_L$ were the variation vector of reactive load at all the buses,

ΔV and ΔV_R are the variation vector of the voltage at normal buses and reference voltage at pilot buses respectively,

$\Lambda = \text{diag}\{\alpha_i\}$, $\Lambda \in R^{nxn}$, $\alpha_i = 0$ for non-generator buses,

$\tilde{S}$ and S are the sensitivity matrixes.

1. Selection of Pilot Buses

The sensitivity matrix $\tilde{S}$ represents the dependence of the voltage variation from the reactive load variation at all the buses in a power network.

Using the matrix $\tilde{S}$, a procedure was developed for selecting the pilot buses within a whole network as:

Step 1: Selecting a pilot bus i by finding the smallest diagonal element

$$\tilde{S}_{ii} = \mathbf{min}\{\tilde{S}_{ii}, \tilde{S}_{(i+1)(i+1)}, \cdots, \tilde{S}_{(i+n)(i+n)}\},$$

Step 2: Remove the buses which have coupling coefficients with pilot bus i greater than a

pre-set value i.e. $(\tilde{S}_{ji} / \tilde{S}_{ii}) > E_p$,

Step 3: Repeat step (1) and (2) for the remaining buses in $\tilde{S}$, until the all the elements of matrix $\tilde{S}$ have been processed.

In the end of the above process, a group of remained buses in the matrix will be the pilot buses.

2. Selection of Control Power Plant

Based on the sensitivity matrix S and the selected pilot buses, a procedure for selecting the control power plants was developed as:

Step1: rearrange a new sub-matrix S_p from S, which columns corresponding to the power plants, and rows corresponding to the pilot buses;

Step2: for each pilot bus, identify the power plants that have higher sensitivity coefficients to the pilot bus than other pilot buses.

Step3: among the identified power plants, those reactive generation capacities are greater than a pre-set limit are selected as the control power plants for each pilot bus.

Both the load disturbance and the voltage interactions between different pilot buses were taken into account in the selection procedures for the pilot buses and control power plants. This will help to prevent the dynamic interaction between secondary voltage controls in different regions. As this method uses the sensitivity analysis, the heavy numerical computation is avoided.

2.3.2.2 The optimisation method

An optimisation method for selection of the pilot buses and control power plants was proposed by Popovic in reference [7]. Targeting on the minimisation of a quadratic index of expected value of voltage deviation throughout all load buses in a power system, the problem was formularised as:

$$\underset{(P)}{\mathrm{Min}}\,\mathbf{E}\ \{\Delta V_L^T Q_x\, \Delta V_L\}$$

Subject to

$$\Delta V_P = P\,\Delta V_L$$

$$\Delta V_L = P\,M\,\Delta Q_L + P\,B\,\Delta V_G$$

$$\Delta V_G = -\,K\,\Delta Q_P$$

Where,

E{.} is the expectation operator,

ΔV_P and ΔV_L are the voltage deviation vectors at pilot buses and load bus respectively,

ΔQ_L is the reactive load disturbance,

ΔQ_X is a diagonal weighting matrix,

K is the control law matrix for secondary voltage controller,

M and B are the sensitivity matrices from the Jacobian matrix of the load flow equations,

P is the pilot bus selection matrix, Pij=1 if bus j is the i-th pilot bus, 0 otherwise.

By solving this optimisation problem, a set of optimal pilot buses could be obtained for a power system.

The selection of the control power plants was also proposed in this study. It was also based on sensitivity analysis, and involving a two-stage process:

STAGE 1:

(i) Select pilot buses with all power plants in control mode,

(ii) Calculate and normalise the sensitivity matrix between ΔV_P and ΔQ_G,

(iii) A power plant is selected as a control one if its participation factor ($\Delta V_P/\Delta Q_G$) is greater than pre-defined threshold α,

(iv) Select pilot buses with new set of power plants.

STAGE 2:

(i) Consider the maximum VAR demand in the power system by simulation,

(ii) Modify the threshold α and select a new set of control power plants,

(iii) Select a new set of pilot buses based on the new set of control power plants.

This two-stage joint selection procedure ensures that the selected pilot buses will be supported from the most efficient power plants for their voltage control. In the meantime, the selected control power plants will also have sufficient reactive capacity to maintain a desired voltage at the selected pilot buses. Due to the adoption of the optimisation formulation, the pilot buses selected by this method will be the optimal with respect to the voltage deviations caused by the random load disturbance.

However, the pilot buses are supposed to be those that have strong influences on the voltage at load buses in the same region and limited influences on the voltage at the load buses in other regions. This was not transparent in this optimal selection method.

2.3.3 Control System Designs

A secondary voltage control system normally involves three level regulations. These are the Regional Voltage Regulation (RVR), Power Plant Reactive Power Regulation (PQR), and Generator Automatic Voltage Regulation (AVR). As AVRs are normally built in with the generator units, only RVRs and PQRs are the main issues in the design of a secondary voltage control system.

The RVR is the outer loop of this multi-level control structure. Its direct objective is to maintain the desired voltage levels at the regional pilot buses. Co-ordination of the regional reactive power generation is integrated into this objective. The PQRs provide the inner loop controls to achieve the demanded reactive generation for controlling the pilot bus voltages. A PQR targets on either the reactive generation or the HV busbar voltage, or a combination of these two at a control power plant. This inner control loop also ensures that the demanded reactive generation is evenly distributed among the generators within the control power plant. Some Secondary Voltage Control systems were designed to directly interface with the AVRs without the PQR.

Both classical control and optimal control designs have been proposed for secondary voltage control. Some of these proposals will be reviewed in this section.

2.3.3.1 The classical control design

Arcidiacono proposed a classical control design for the RVR in reference [8,42,43]. For a power network, the linearised relationship between the pilot bus voltages and the reactive generation of the generators was given by:

$$\Delta V_P = S_Q \Delta Q_G = S_Q \mathrm{Diag}\{Q_{\mathrm{lim}}\} \Delta q \qquad (2.3.3\text{–}1)$$

Where,

S_Q is a block diagonal matrix, each of the blocks is diagonal dominant and represents a region,

ΔQ_G and Δq represent the reactive generation variations at the control power plants and the generators respectively.

By using the following control law, a pure Integral control was applied to the RVR:

$$\Delta Q_G = (S_Q)^{-1} R_{(r)} (\Delta V_{\mathbf{Pr\,ef}} - \Delta V_P) \qquad (2.3.3\text{–}2)$$

$$\Delta q = (S_Q \mathrm{Diag}\{Q_{\mathbf{lim}}\})^{-1} R_{(r)} (\Delta V_{\mathbf{Pr\,ef}} - \Delta V_P) \qquad (2.3.3\text{–}3)$$

Where,

$R_{(r)}$ is a diagonal matrix,

$(\Delta V_{pref} - \Delta V_p)$ represents the voltage variations at the pilot buses.

In this design, the $\Delta q(\text{desired}) = \Delta q(\text{obtained})$ was assumed because the reactive power loops at PQR level are normally much faster than the pilot buses voltage loop, and they are also dynamically decoupled due to the PQR control law. $R_{(r)}$ is a strictly diagonal matrix and can be subdivided into r blocks corresponding to the r regions. It showed that the decoupled loops could be obtained by decentralised regional controllers, each of them corresponding to a block of matrix S_Q.

A PI control law was also suggested in the reference [8] for each regional voltage control loop. The PI law was the standard textbook decoupled form. But the details of control design were not presented.

In fact that the proportional parameter K_p and integral parameter K_I of the PI control are very important for time domain performance and transient shape specifications in the outer loop of RVR. In particular, K_p is needed to take into account the $\Delta V_{pj}(t)$ kicks in face of network perturbations. It would be useful to investigate the closed loop performance of this design such as reference tracking, disturbance rejection, integral windup, proportional kick as well as robustness to model mismatch.

Florez et al in reference [47] further developed the above RVR design by introducing the robust multi-variable PI controller. The general structure of the RVR was retained, and the controller had the following equations:

$$\dot{e}_r(t) = V_z(t) - V_r(t)$$

$$Q_G(t) = -K_p(t)V_z(t) + K_I(t)e_r(t)$$

Where,

$V_r(t)$ is the voltage reference given from the tertiary control,

$V_z(t)$ is the vector of the pilot bus voltage,

$Q_G(t)$ is the vector of regional reactive powers to be generated (one element/region),

$K_p(t)$ and $K_I(t)$ are the proportional and integral matrix coefficients.

The block diagram for this design was given as shown in Figure 2.3.3-1.

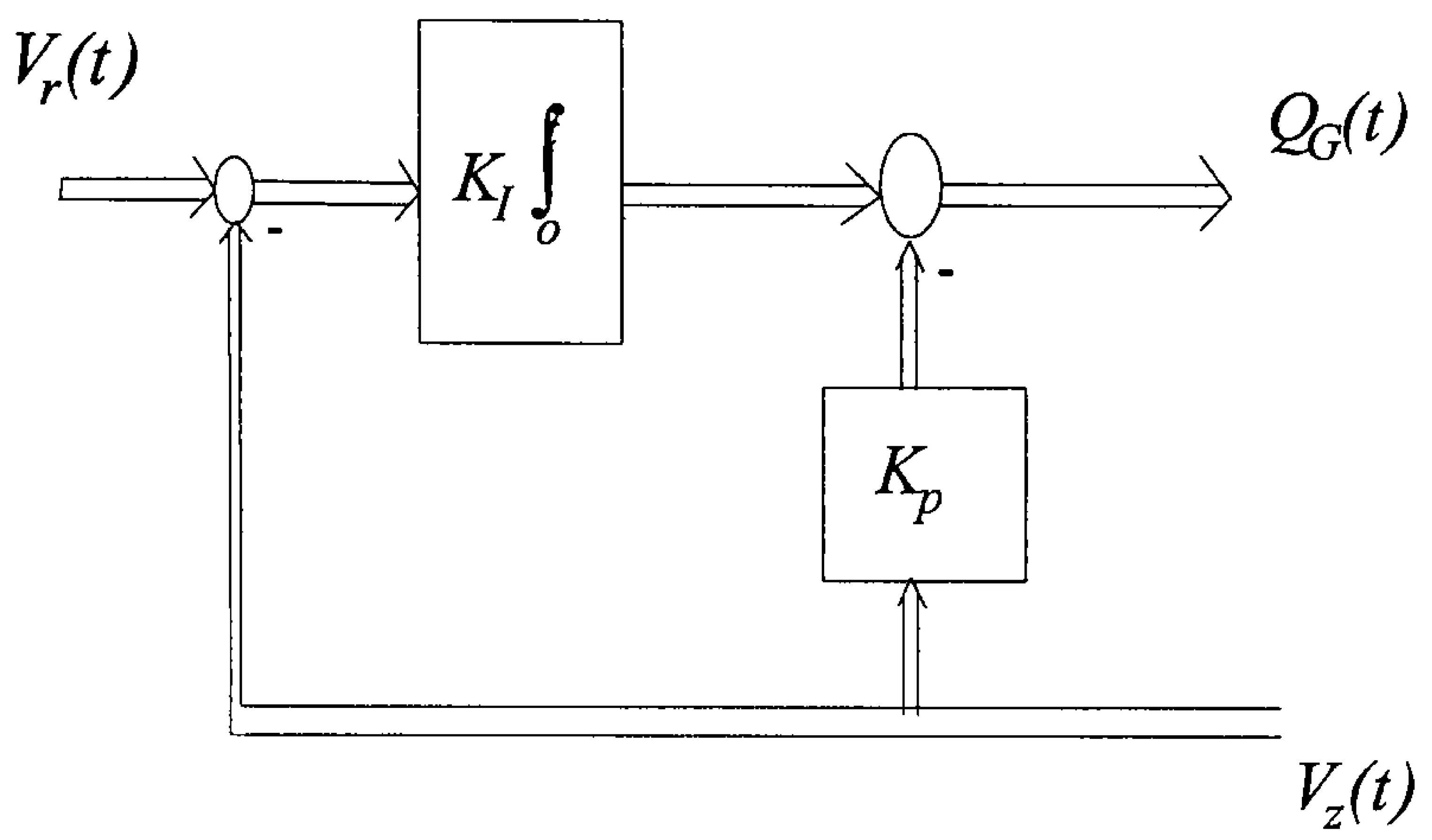

Figure 2.3.3-1 Robust Multi-variable PI Controller

The notable advantage of this design is that K_p does not operate on the error signal $\tilde{e}_r(t) = V_r(t) - V_z(t)$, this will protect $Q_G(t)$ against proportional kick coming from $V_r(t)$.

2.3.3.2 The optimal control design

Based on the Infinite Time Optimal Control, an optimal Regional Voltage Regulator was presented by Gomez et al in reference [48, 49]. Both centralised and decentralised versions of a state-space derivation were given in this study. The system equation was described as

$$y_{k+1} = y_k + [EB+D]\Delta u_k + EM\Delta q_k$$

Where,

y_k is the vector of output variables comprising pilot bus voltage magnitudes and reactive power output,

Δu_k is the vector of voltage variations at control power plants,

Δq_k is the vector of disturbance variables being reactive load changes at load buses,

E, B, D, M are the matrices derived from the power system sensitivity equations.

The cost function was formularised as

$$J = E\left\{ \sum_{k=0}^{\infty} \left[(y_k - y_c)^T Q_y (y_k - y_c) + (\Delta u_{k+1} - \Delta\bar{u})^T Q_u (\Delta u_{k+1} - \Delta\bar{u}) \right] \right\}$$

Where y_c is the commanded output and the solution procedure of Mita (1985) is followed.

The major difficulty with this formulation is that the cost function involves an expectation operator presumably reflecting a *stochastic* description for Δq_k; and the solution procedure of Mita has all the hallmarks of being a *deterministic* optimal control solution procedure. Thus, the solution procedures and the cost functions are incompatible in the same paper. The complete structure of the problem formulation and the correct solution procedure lead to some fairly complicated solutions depending on whether an observation equation is utilised.

Based on the Single Stage Optimisation Method, the use of the *"one-step at a time"* optimisation procedures for the RVR design problem was first described by Paul et al in reference [50]. Sancha et al in reference [44, 52] has also used the technique in a modified form where the main difference between the approaches being the reactive power generation management. Paul et al in reference [50] modelled the power system as:

$$\Delta V_p = C_v \Delta U$$

$$\Delta V_{ps} = C_{vs} \Delta U$$

$$\Delta Q = C_q \Delta U$$

Where,

ΔV_p is the vector of pilot bus voltages,

ΔV_{ps} is the vector of voltages at critical points,

ΔQ is the vector of change in reactive power produced by generators,

ΔU is the vector of change in voltage set-points of generator regulators (AVRs),

C_v, C_{vs}, C_q are Jacobian matrices correspond to a given control region.

The Cost Function was then proposed as:

$$J = \left\|\alpha(V_c - V_p(k)) - C_v\Delta U(k)\right\|^2 + q_o\Big(\left\|\alpha(Q_{ref} - Q(k)) - C_q\Delta U(k)\right\|^2$$
$$+ h\left\|\alpha(U_{ref} - U(k)) - \Delta U(k)\right\|^2\Big)$$

Subject to

$$V_{ps}^{\min} \le V_{ps}(k) + C_{vs}\Delta U(k) \le V_{ps}^{\max}$$

$$a_{ij}[Q_j(k) + C_q^j\Delta U_i(k)] + b_{ij}\Delta U_j(k) \le c_{ij} \text{ for all } i, j$$

$$|\Delta U(k)| \le \Delta U^{\max}$$

Where,

V_c, Q_{ref}, U_{ref} are set-point values,

α, q_o and h are cost weighting parameters,

C_v, C_{vs} and C_q are sensitivity matrices,

$V_{ps}^{\min}$, $V_{ps}^{\max}$ are voltage limits at the critical points.

The constraint $a_{ij}[Q_j(k) + C_q^j\Delta U_i(k)] + b_{ij}\Delta U_j(k) \le c_{ij}$ represents generator operating domains (j=1 ,.., n), and $\Delta U^{\max}$ represents a limit placed on the change in the control signal which may be applied in one time step. The procedure was to solve this constrained Quadratic Programming problem for $\Delta U(k)$ and then implement an update of the power plant voltage regulator reference as:

$$U(k+1) = U(k) + \Delta U(k)$$

The single stage optimisation approach proposed by Sancha et in reference [44, 52] further developed the above design by introducing the reactive power generation management. This method is also able to implement the different operation schemes such as RVR operating on AVR references, RVR operating on PQR references, and RVR operating on both the PQRs and the AVRs.

A typical formulation was given as follows:

$$\underset{\Delta v_{gref}, d(k)}{\mathbf{Min}} \ \mathbf{J} = \left\{ \left\| \alpha \Delta v_p(k) - S_{vv} \Delta v_{gref}(k) \right\|_2^2 + q_o \left\| \alpha \Delta q_g(k) - S_{qv} \Delta v_{gref}(k) \right\|_2^2 \right\}$$

Subject to

$$v_{g\,min} \le V_g(k) + \Delta v_{gref}(k) \le v_{g\,max}$$

$$q_{g\,min} \le q_g(k) + S_{qv}^{g} \Delta v_{gref}(k) \le q_{g\,max}$$

$$\Delta v_{gref}(k) \le \left\| \Delta v_{g\,max} \right\|$$

$$v_{c\,min} \le V_c(k) + S_{cv}^{c} \Delta v_{gref}(k) \le v_{c\,max}$$

$$\mathbf{max}\left(\frac{q_{min_i} - q_g^{ref_i}}{M_{iz}} \right) \le d_z \le \mathbf{min}\left(\frac{q_{max_i} - q_g^{ref_i}}{M_{iz}} \right) \quad \text{for all i in zone, z}$$

Where,

$v_p(k)$ and $v_{gref}(k)$ are the vectors of the pilot bus voltages and the control power plant references at time instant k (AVR set-point),

q_{gi} is the reactive generation of the control power plant i.

S_{vv} and S_{qv} are the sensitivity matrices.

A management scheme of reactive generation was proposed in this algorithm to co-ordinate the reactive output of the control power pants in a decentralised region. This scheme was introduced by the displacement variable d(k) as

$$q_{gref}(k) = q_g^{ref} + Md(k)$$

Where,

q_g^{ref} is the vector of the fixed reactive generation references for the control power plants, $q_{gref}(k)$ and $q_g(k)$ are the reactive power generation reference and actual value at time instant k,

M is the matrix specifies the slope of the working line for each generator.

The above equation is the linear relationship for the desired evolution of reactive power in each zone. To manage the evolution of reactive power, the derivation below would be minimised:

$$\Delta q_g(k) = q_{gref}(k) - q_g(k).$$

This expands as,

$$\Delta q_g(k) = q_g^{ref} + Md(k) - q_g(k)$$

This *single-stage* cost function would be over a finite horizon from time k up to max$\{N_{12}, N_{22}, N_{32}\}$ and involve the future behaviour of the system. It is then very important to consider the control principle being used. Implement the current control at time $t = k$, and re-performing the optimisation at time $t = k + 1$ leads to a receding horizon optimal control law. However in the algorithm by Sancha, this is not always clearly indicated. Furthermore it can be proved (Zhang et al in reference [51]) that, this control design will result in an incomplete controllability of the secondary voltage control system.

2.3.4 Control System Analyses

The purpose of control system analysis is to assess the functionality of a control system by a certain control design. Stability analysis is a major content for this analysis. As secondary control systems have a hierarchical structure, the integration analysis between different level of controls is also very important for the analysis.

The stability analysis of a control system normally includes the study of the closed loop stability and the closed loop performance. The closed loop stability covers the Steady State Stability and Robust Stability. For the study of the steady-state stability, a small change model around an operating point is used to test that all modes in the closed loop systems are asymptotically stable. For the robust stability analysis, model perturbations or representations of model uncertainty are used to test that the closed loop system remains asymptotically stable.

The closed loop performance is about the time domain behaviour of a closed loop control system. It includes Reference Tracking, Disturbance Rejection as well as Robust Performance.

The integration analysis of a secondary voltage control system is mainly concerned with the integration between PQR and RVR through a certain integration signal. As the integration problem will directly affect the success of a secondary voltage control, this analysis is essential for a control design.

Through the literature review in this section, it has been found that the previous publication does not contain any material concerning the control system analysis of secondary voltage control systems. This will be one of the major objectives to be achieved in this thesis.

2.3.5 Remarks

The previous literature concerning secondary voltage control in power systems has been reviewed in this section. The review covered the subjects of the impact of secondary voltage control schemes on voltage stability, the control principle, control system designs and control system analyses.

The previous studies have proven that a secondary voltage control scheme has a beneficial impact on voltage stability. It not only improves the voltage stability margin in a power system, but also prolongs the transient procedure for an already initiated voltage collapse.

The pilot bus control is the basic principle for a secondary voltage control scheme. A number of methods have been proposed for decentralisation of a power system and selection of the pilot buses/control power plants. The typical ones include the sensitivity method and the optimisation method. It has been noticed that the issues concerning the theoretical justification and formularisation of the control principle were missing in the previous literature.

As to the control system design, both classic control and optimal control designs have been used for secondary voltage control as some industrial trials by some European utilities. Despite some novel ideas and successful pioneer work, a systematic study is urgently needed in the area of system design and analysis before such a system can be applied to a real power system.

It has also been noted that the previous literature contains very little material about the stability analysis and integration analysis of secondary voltage control systems.

2.4 CONCLUSIONS

The previous literature in the area of voltage stability analysis and control has been reviewed in this chapter. The review was divided into two main sections: Voltage Stability analysis and secondary Voltage Control. The logic link between these two subjects is the fact that secondary voltage control has been recognised as a major countermeasure to voltage collapse.

For voltage stability analysis, it was found that the previous research mainly focused on the mechanism study and prediction of voltage collapse. The impact on voltage stability from some voltage control devices (e.g. the ATCCs and SVCs) and load static characteristics in a power system has also been an active research area.

Typical methods previously used for voltage stability analysis include static methods and dynamic methods. Generally-speaking a static method is good at examining the viability of a steady operation state specified by a wide range of system conditions in a power system; while the dynamic methods have a strong advantage in exploring whether and how a steady operation state (equilibrium points) is reached.

Many methods have been developed for accurately predicting voltage collapse. Most of them rely on algorithm based numerical computations which often require human intervention, hence the decision-making speed of those methods tends to be rather slow.

It has been noted that apart from secondary voltage control schemes, there was very little published work concerning the control or prevention of voltage collapse.

The previous study has proven that secondary voltage control is not only able to maintain a desired voltage profile, but also improve voltage stability and prolong the transient procedure of an already started voltage collapse in a power system.

Both classic control and optimal control design have been applied for secondary voltage control as industrial trials by some European utilities. However, there is an urgent need for a systematic study in the design and analysis of such control systems before they can be used to a real power system. The theoretical analyses for the closed loop stability and performance of such a multi-level control system is the particular area requiring significant further development.

CHAPTER 3 FUNDAMENTALS OF VOLTAGE STABILITY

3.1 INTRODUCTION

This chapter deals with the fundamental aspects of voltage stability problems. Two issues are particularly concerned in this chapter. These are the basic characteristics and the determining factors of voltage stability. The objective of this chapter is to establish a theoretical foundation for the rest of research in this thesis.

To examine the basic characteristics of voltage stability, the study will be starting from a two bus simple system, and extended to a multi-bus general power system. The V-P and V-Q curves will be used to explore the typical trajectory of voltage collapse incorporating the power system major non-linearity and dynamics.

The voltage stability determining factors of (VSDF) will be identified and defined in his chapter. These VSDFs include the Load Pattern (L), the Load Distribution Pattern (LD), The Generation Pattern (G) and The Generation Participation Pattern (GP). The case study on the IEEE 30 bus system will be presented to illustrate the impact of these VSDFs on voltage stability.

Some important properties of the VSDFs will also be discussed in this chapter. The property that the VSDFs uniquely determine the voltage stability of a power system will be generalised into a hypothesis, and the theoretical validation will be given for the hypothesis. Other properties revealed in this study include the pattern class feature of the VSDFs and the similarity of voltage stability when the VSDFs are in the same pattern classes. All those study will be backed up by the simulations on the IEEE 30 bus power system.

3.2 VOLTAGE STABILITY CHARACTERISTICS

In this section, some basic concepts and characteristics related to voltage stability in a power system will be discussed. The discussion will be starting from a two-bus power system, and then extended to a multi-bus power system. The V-P and V-Q curves will be used to present the relationship between voltage/power at load buses. By including the system major non-linearity and dynamics such as the generators reaching the reactive generation limits, a typical trajectory of voltage collapse will be plotted.

3.2.1 A Two Bus Power System

3.2.1.1 The V-P and V-Q curves

A simple power system consisting of one source bus and one load bus is shown by Figure 3.2.1-1. In the steady state, the relationship between the voltage and the power received at the load bus can be expressed as:

$$P_L = \frac{V_S V_L}{Z_T} \cos(\alpha + \theta) - \frac{V_L^2}{Z_T} \cos(\theta) \qquad (3.2.1\text{–}1)$$

$$Q_L = \frac{V_S V_L}{Z_T} \sin(\alpha + \theta) - \frac{V_L^2}{Z_T} \sin(\theta) \qquad (3.2.1\text{–}2)$$

where,

P_L and Q_L are the active and reactive power received at the load bus,

$V_S\angle 0$ and $V_L\angle\alpha$ are the voltages at the source bus and the load bus respectively,

$Z_T\angle\theta$ is the impedance of the transmission line between the source bus and the load bus.

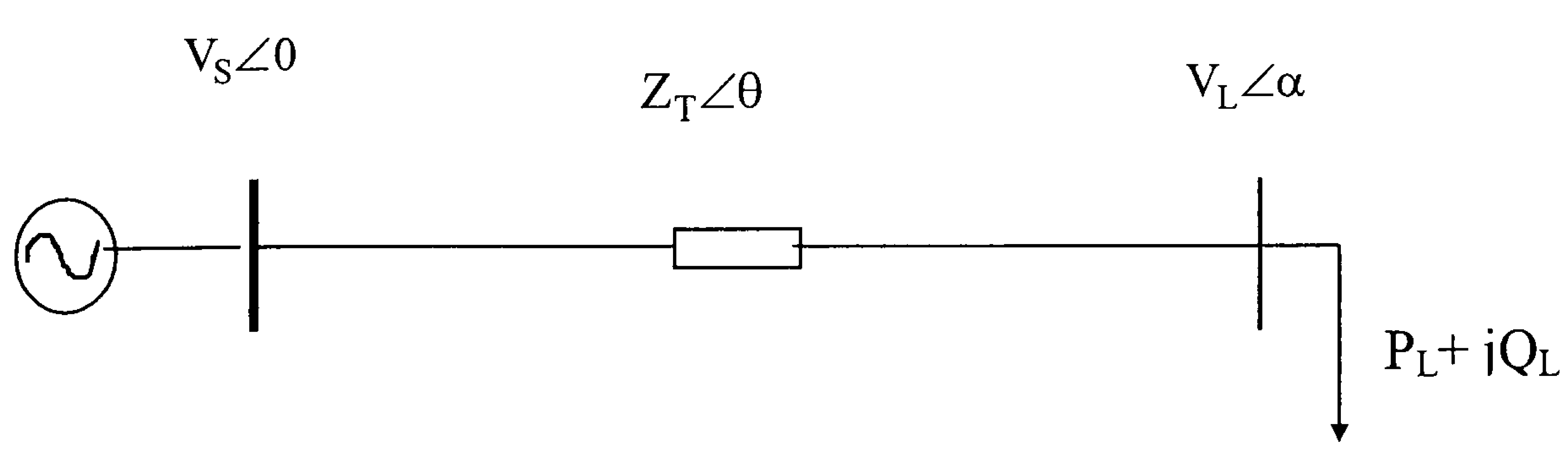

Figure 3.2.1-1 A two bus power system

Based on the equation (3.2.1-1), the V-P curve can be portrayed to show the voltage magnitude vs. the active power received at the load bus. Figure (3.2.1-2) displays a group of the V-P curves with different values of V_S. Similarly a group of the V-Q Curves can be obtained to present the voltage magnitude (simplified as voltage hereafter) vs. the reactive power received at the load bus based on equation (3.2.1-2). The V-Q curves will have similar shape to the V-P curves.

Generally the load characteristics can be assumed to have a non-linear relationship with the voltage a load bus, thus another curve (load curve) showing the relationship between the voltage and load can be plotted on to the PV curves.

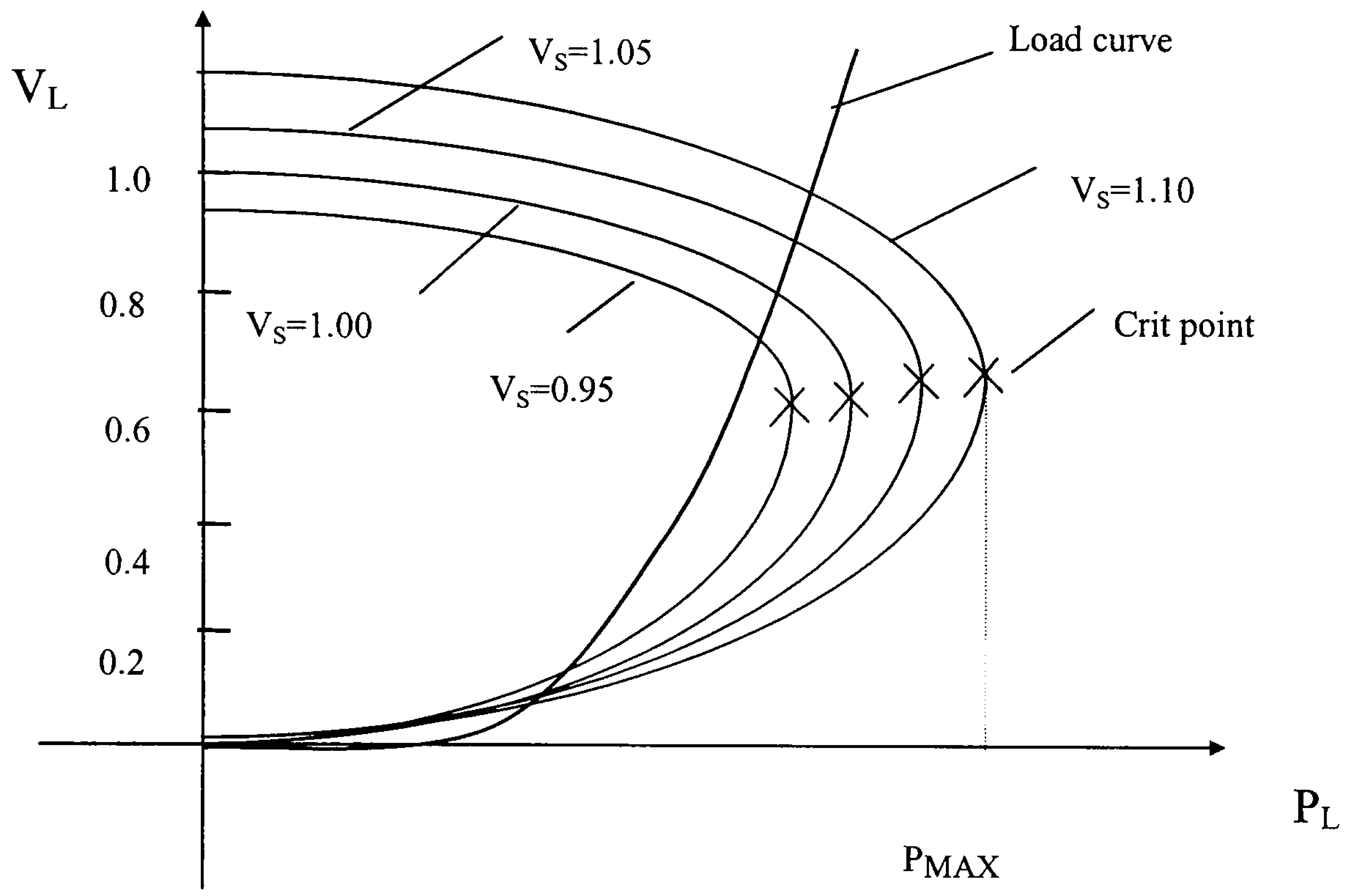

Figure 3.2.1-2 The V-P Curves at the load bus

3.2.1.2 Basic properties of voltage stability at the load bus

By using Figure 3.2.1-1, some basic properties of voltage stability can be examined.

1. **Voltage stability**

In Figure 3.2.1-2, there are two crossing points between the load curve and a VP curve. These two points represent the possible operation points for a given source voltage and a load. For the point on the upper portion of the PV curve, if there is a small disturbance to increase (decrease) the load, the operating point will move to the right (left) along the VP curve, and the voltage at the load bus will go down (up). By following the load curve it can be seen that the voltage drop (rise) will result in load decrease (increase) which will bring the system back to the original point. Therefore, the voltage is stable when the system operating on the upper portion of the VP curve. By using the same analysis, it is easy to know that the voltage will become unstable when the system operating on the lower portion of the VP curve.

It can also be seen that on the upper portion of the VP curves, the voltage at the load bus can be raised (lowered) by decreasing (increasing) the load or increasing (decreasing) the source voltage. Hence, the voltage is controllable when the system is operating on the upper portion of the VP curves.

It is not difficult to find out that the voltage becomes uncontrollable by changing the load or the source voltage when the system is operating on the lower portion of a VP curve.

2. The critical state of voltage stability

From Figure 3.2.1-2, it has been seen that the voltage stability on the upper portion of a VP or VQ curve has an opposite property to the one on the lower portion. The "knee point" dividing a VP or VQ curve into an upper and a lower portion is called 'bifurcation point' or 'critical point'. Under heavy loaded conditions, the two possible operating points on a given VP or VQ curve may both be very close to the critical point. With some disturbance, the system operating on the upper portion could easily move cross the critical point to the lower portion of the curve. Therefore, this critical point is where voltage collapse starts. The system state corresponding to this critical point is called 'critical state', and the load level at this critical state is "the maximum power" which can be transmitted from the source bus to the load bus. The voltage at the critical state is called 'the critical voltage'.

3. The necessary conditions for Voltage collapse

By performing the partial derivative with the equation (3.2.1-1) and (3.2.1-2),

$$\partial P/\partial V = 0,\ \partial Q/\partial V = 0$$

two different 'critical voltages' V^P_{Crit} V^Q_{Crit} can be obtained:

$$V^P_{Crit} = \frac{V_S \cos(\alpha + \theta)}{2\cos(\theta)} \qquad (3.2.1\text{–}3)$$

$$V^Q_{Crit} = \frac{V_S \sin(\alpha + \theta)}{2\sin(\theta)} \qquad (3.2.1\text{–}4).$$

The $V_{crit}{}^P$ and $V_{crit}{}^Q$ are corresponding to the active and reactive maximum transmission power respectively, and normally

$$V_{crit}{}^P \neq V_{crit}{}^Q \qquad (3.2.1\text{–}5)$$

The equation (3.2.1-1) (3.2.1-2) (3.2.1-3) revealed a very important nature about voltage stability: **it is not necessary for both the real and reactive load to reach their theoretical maximum transmission level before voltage collapse starts. The voltage at the load bus may become unstable when the load reaches either its active or reactive maximum transmission power.**

4. Voltage sensitivity

From the V-P curves, it can be observed that

$\partial V/\partial P < 0$ when the load voltage is stable, and

$\partial V/\partial P > 0$ when the load voltage is unstable.

Similarly, from the V-Q curves there are

$\partial V/\partial Q < 0$ when the load voltage is stable, and

$\partial V/\partial Q > 0$ when the load voltage is unstable.

By considering the necessary conditions for the voltage collapse discussed above, this sensitivity property can be re-stated as:

When the voltage is stable at the load bus, there are both $\partial V/\partial P < 0$ and $\partial V/\partial Q < 0$; when the system experiencing voltage collapse, at least one of $\partial V/\partial P < 0$ and $\partial V/\partial Q < 0$ will hold. $\partial V/\partial P = 0$ or $\partial V/\partial Q = 0$ whichever comes first will determine the critical point of voltage collapse.

5. The influence of source voltage and line impedance

Based on the above discussion, it becomes apparent that voltage stability is linked to the maximum transmission power and the critical voltage. From equations (3.2.1-1) and (3.2.1-2), it is easy to work out that this maximum transmission power and the critical voltage are the functions of the source voltage V_S and the transmission line impedance Z_T. Thus, another simple but important property is revealed: **voltage stability is related to the source voltage V_S and transmission line impedance Z_T.**

3.2.2 A Multi-bus Power System

3.2.2.1 Voltage stability trajectory

1. Equivalency of a multi-bus power system

By looking into the port between a load bus i and ground, a multi-bus power system can be equivalent to a simple system as shown in Figure 3.2.1-1. In the equivalent system, line impedance will be the i-th diagonal element $Z_{ii}\angle\beta_i$ of the system impedance matrix **Z**. The source voltage $V_S\angle 0$ will be the open circuit voltage at bus i. The source voltage is a function of all the voltage control devices including generators, transformers and reactive compensation plant etc. in the power system.

Based on this equivalency, the discussions and conclusions for a two bus simple system can be extended to the multi-bus general power system.

2. A typical voltage stability trajectory

From the equivalent system, a set of VP and VQ curves can be plotted in the steady state for a load bus in a power system. Each of the curves represents the relationship between voltage and power injection at the load bus under a given operation condition (equivalent source voltage and line impedance). In reality, the voltage at the load bus does not always stay on a fixed VP or VQ curve. With change of load and other system conditions, the voltage operating point is constantly moving from one curve to another. Its trajectory often involves many non-linearities caused by events such as generators reaching operational limits, automatic voltage control actions, transformer tap changes or reactive compensation plant switching. The system dynamics and non-linearity will be reflected through the source voltage and line impedance in the equivalent system.

A typical trajectory of voltage stability including system dynamics and major non-linearities is illustrated in Figure 3.2.2-1. This trajectory shows the system operation that induces a critical state X_A^i at load bus i from a given initial state X_0^i. In this figure, only VP curve is presented, the VQ curve will have a similar shape and features.

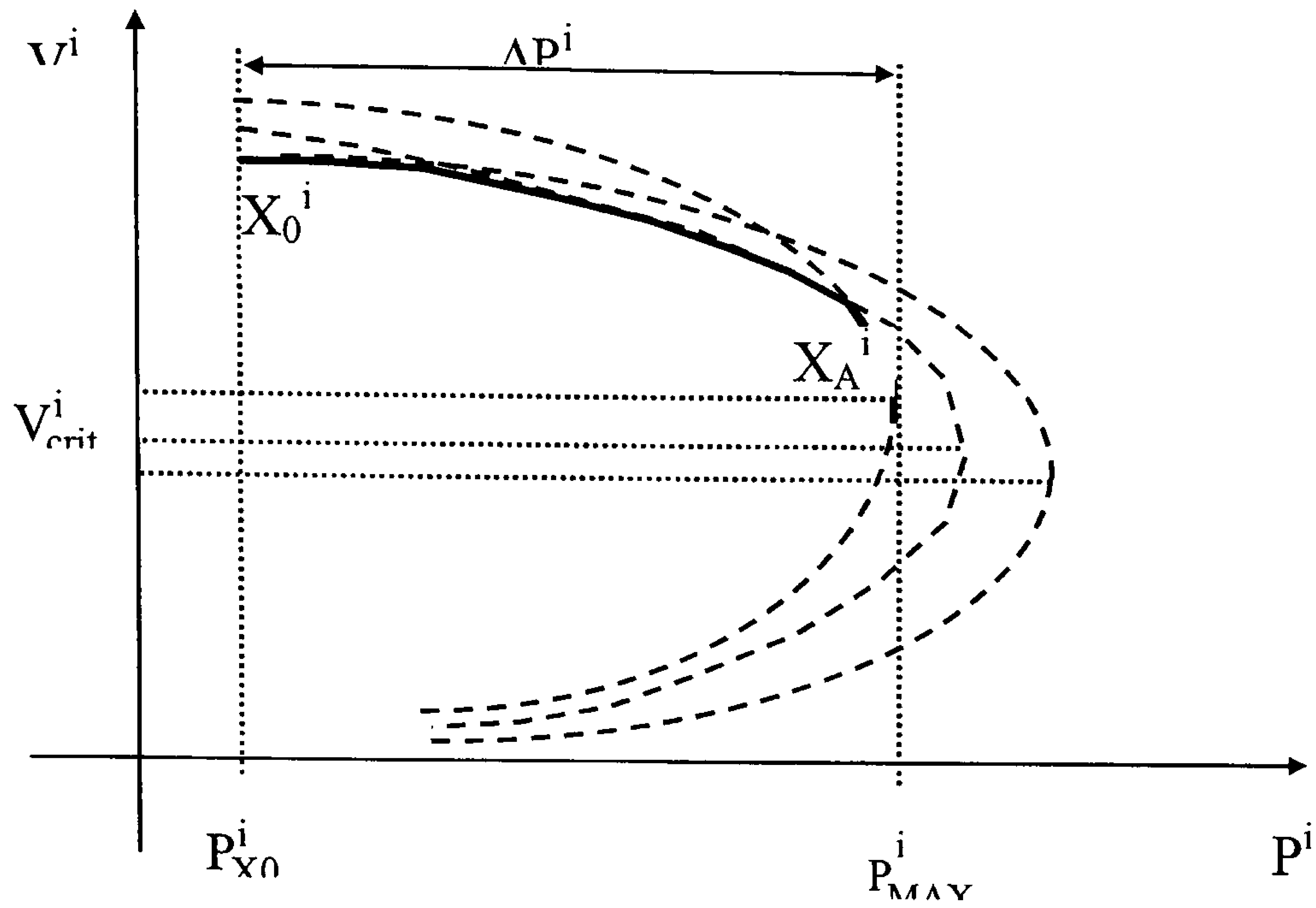

Figure 3.2.2-1 The typical voltage stability trajectory

3.2.2.2 Voltage stability characteristics

1. Basic characteristics

By using the equivalent system and the typical voltage stability trajectory, some basic characteristics of voltage stability in a multiple bus power system can be generalised.

(i) When voltage is stable at a bus, the sensitivity $\partial V/\partial P$ and $\partial V/\partial Q$ are both negative at this bus. This is a sufficient and necessary condition. The default power convention in this thesis is that load having a positive value, and generation having a negative value.

(ii) When voltage becomes unstable at a bus, at least one of the sensitivity coefficients $\partial V/\partial P$ and $\partial V/\partial Q$ will becomes positive. This is a necessary condition.

(iii) In steady state, there is a maximum power (active P_{MAX} and reactive Q_{MAX}) which can be transmitted to a load bus in a power system before its voltage becomes unstable. The voltage corresponding to this maximum transmission power (P_{MAX} or Q_{MAX}) is the critical voltage for the load bus. The system state corresponding to the critical voltage or the maximum transmission power is known as the critical state.

(iv) The maximum transmission power and the critical voltage are also related to the running arrangement and operation settings of a power network. Therefore the voltage stability of a power system is affected by those factors.

(v) Voltage collapse may start from one or several buses in a power system. The system voltage is regarded as unstable if any bus voltage becomes unstable in the power system.

(vi) The Jacobian matrix of the load flow equations becomes singular when voltage collapse starts in a power system.

(vii) When voltage at a load bus is stable, it can be controlled by voltage control facilities such as generator terminal voltages, transformer tap changers or reactive compensation plant. Load shredding is an efficient but last resort for voltage control.

(viii) When voltage becomes unstable at a load bus, the normal voltage control facilities become be ineffective or even aggravate the situation.

2. Definition of voltage stability

Having discussed the basic characteristics of voltage stability, the concept of voltage stability can be formally defined as:

Voltage stability is the capability of a power system to maintain the voltage at all the buses to an acceptable level subject to certain disturbances. When the system voltage becomes unstable (voltage collapse), the voltage at some or all the buses will experience a rapidly and uncontrollable drop.

From this definition, it is known that voltage stability contains contents of both stability and controllability .

3. Voltage stability margin

Voltage stability margin measures how close a power system is from voltage collapse. Many methods have been proposed to measure this stability margin in the form of a voltage collapse proximity indicator (VCPI), such as the minimum singular value method, the load flow feasibility margin method (See chapter 2). Among all the proposed methods, the one using power margins as a VCPI is the most direct and efficient method.

The power margins are defined as the difference between the initial load level and the maximum transmittable power to a load bus through a power network before voltage collapse starts. It can be either for a bus or for a whole power system. The power margin can be mathematically defined as:

(1) Power margins for a bus

$$\Delta P_M^i = P_{MAX}^i - P_0^i$$

$$\Delta Q_M^i = Q_{MAX}^i - Q_0^i$$

(2) Power margins for a system:

$$\Delta P_M = P_{MAX} - P_0 = \sum_i^N \Delta P^i$$

$$\Delta Q_M = Q_{MAX} - Q_0 = \sum_1^N \Delta Q^i$$

Where,

$$P_{MAX} = \sum_i^N \Delta P_{MAX}^i,$$

$$Q_{MAX} = \sum_1^N \Delta Q_{MAX}^i.$$

$$P_0 = \sum_i^N \Delta P_0^i,$$

$$Q_0 = \sum_{1}^{N} \Delta Q_0^i$$

ΔP_M^i and ΔQ_M^i are the active and reactive power margins for bus *i* in a *N* bus power system,

P_0^i and Q_0^i are the active and reactive power injections of bus *i* at an initial operation state,

P_{MAX}^i and Q_{MAX}^i are the maximum active and reactive load levels at bus *i*.

3.3 THE VOLTAGE STABILITY DETERMINING FACTORS (VSDFS)

The voltage stability determining factors (VSDFs) will be identified and defined in this section. This will be based on the analysis of load distribution and generation participation and their impact on voltage stability in a power system. The simulation results on the IEEE 30 bus power system will be presented to numerically demonstrate the impacts of these VSDFs. The unique property about the VSDFs will be discussed and generalised into a hypothesis, of which the theoretical validation will be given at the end of this section.

3.3.1 The Impact of the Load Distribution and Generation Participation

The load distribution describes how the demand and its changes are distributed among the load buses in a power system. The generation participation shows how each power plant contributes to the demand and its changes in the system.

The impact of load distribution and generation participation on voltage stability can be examined by analysing their influences on the power margins in a power system. The power margins are defined as the difference between the initial load level and the maximum transmittable power to a load bus. Based on the equivalent system model in last section, it is known that the maximum transmission power is related to the running arrangement (equivalent line impedance) and operation conditions (equivalent source voltage, etc) of a power network. From network dispatching point of view, the running arrangement of a power network has to be made to satisfy the load distribution requirements. And reactive generation participation is controlled by regulating the HV voltages of power plants, which have a direct impact on the "equivalent source voltage". Therefore, it can be concluded that both of load distribution and generation participation will have a significant impact on voltage stability.

In addition, the load distribution and generation participation directly affect the load flow distribution in a power system, and inappropriate load flow distribution is one of the major causes for voltage collapse.

The theoretical validation about the impact of load distribution and generation participation on voltage stability will be given in Section 3.4 of this chapter.

3.3.2 Definitions of the VSDFs

Based on the above analysis, four Voltage Stability Determining Factors (VSDFs) can be identified in a power system. These VSDFs are the load pattern, the load distribution pattern, the generation pattern and the generation participation pattern. The definitions of the VSDFs are as fellows.

1. The Load Pattern (L)

The Load pattern describes the load level at all the buses in a power system at a given time or for a given period. It can be written in a vector form as:

$$\mathbf{L} = [\, L_1^P\; L_2^P \ldots L_i^P \ldots L_N^P\;\; L_1^Q\; L_2^Q \ldots L_i^Q \ldots L_N^Q \,]$$

where,

L_i^P and L_i^Q are the real and reactive power injections at bus i,

N is the total number of buses in the power system.

2. The Load Distribution Pattern (LD)

The Load distribution pattern describes how a load increase is distributed among the all the buses in a power system at a given time or for a given period. It can be written as:

$$\mathbf{LD} = [\, LD_1^P\; LD_2^P \ldots LD_i^P \ldots LD_N^P\;\; LD_1^Q\; LD_2^Q \ldots LD_i^Q \ldots LD_N^Q \,]$$

and

$$\Delta P_i^L = LD_i^P \Delta P_{Ltotal}, \qquad i=1,2, \ldots, N$$

$$\Delta Q_i^L = LD_i^P \Delta Q_{Ltotal}, \qquad i=1,2, \ldots, M$$

$$\sum_{i=1}^{N} LD_i^P = 1,$$

$$\sum_{i=1}^{N} LD_i^Q = 1.$$

Where,

LD_i^P and LD_i^Q are the real and reactive load distribution coefficients at bus i,

ΔP_i^L and ΔQ_i^L are the real and reactive load increase at bus i,

ΔP_{Ltotal} and ΔQ_{Ltotal} are the total real and reactive load increase for the power system.

3. The Generation Pattern (G)

The Generation Pattern describes the generation outputs at all the power plants in a power system at a given time or for a given period. It can be written as

$$\mathbf{G} = [G_1^P\ G_2^P \ldots G_i^P \ldots G_N^P\ \ G_1^Q\ G_2^Q \ldots G_i^Q \ldots G_N^Q]$$

Where,

G_i^P and G_i^Q are the real and reactive outputs of power plant i,

4. The Generation Participation Pattern (GP)

Generation participation pattern describes how each power plant participates in a generation change demanded by a load changes in a power system at a given time or for a given period. It can be written as:

$$\mathbf{GP} = [GP_1^P\ GP_2^P \ldots GP_i^P \ldots GP_N^P\ \ GP_1^Q\ GP_2^Q \ldots GP_i^Q \ldots GP_N^Q]$$

and

$$\Delta P_i^G = GP_i^P(\Delta P_{Ltotal} + \Delta P_{Loss}), \qquad i=1,2,\ldots,N$$

$$\Delta Q_i^G = GP_i^Q(\Delta Q_{Ltotal} + \Delta Q_{Loss}), \qquad i=1,2,\ldots,M$$

$$\sum_{i=1}^{N} GP_i^P = 1,$$

$$\sum_{i=1}^{N} GP_i^Q = 1.$$

Where,

GP_i^P and GP_i^Q are the real and reactive participation coefficients at power plant i,

ΔP_i^G and ΔQ_i^G are the real and reactive generation increases at the power plant i,

ΔP_{loss} and ΔQ_{loss} are the real and reactive power transmission losses caused by the total load increase ΔP_{Ltotal} and ΔQ_{Ltotal} in the power system.

3.3.3 Case study

Some simulation results on IEEE 30 bus system are presented in this section to numerically demonstrate the impact of the identified VSDFs on voltage stability. Four groups of study cases were set up in this simulation to show the impact of each type of the VSDFs. The load flow simulation was used to determine power margins for each the study case. The details of the IEEE 30 bus power system are listed in Appendix 1, and all the simulation results and configuration information for each study case are given in Appendix 3 of this thesis.

1. The impact of the load pattern

To demonstrate the impact of the load pattern on voltage stability, two comparison cases were included in the simulation for the power margins. These two study cases as shown in the Table A3-1 (Case30F01) and Table A3-2 (Case30F02) of Appendix 3, have different load patterns but almost the same other VSDFs and system conditions,. The simulation results for this study group are summarised in the table below.

BUS	PM(F01)		PM(F02)		Max load(F01)		PM Diff (p.u.)		PM Diff (%)	
	ΔP	ΔQ	ΔPa	ΔQa	Pmax	Qmax	ε_P	ε_Q	μ_P	μ_Q
1	0.00	0.00	0.00	0.00	0.00	0.00	0.00	0.00	n/a	n/a
2	0.00	0.00	0.00	0.00	0.00	0.00	0.00	0.00	n/a	n/a
3	1.49	0.74	1.79	1.04	3.89	1.94	0.30	0.30	7.71%	15.46%
4	4.71	2.23	5.80	3.04	12.31	5.83	1.09	0.81	8.85%	13.89%
5	0.00	0.00	0.00	0.00	0.00	0.00	0.00	0.00	n/a	n/a
6	0.00	0.00	0.00	0.00	0.00	0.00	0.00	0.00	n/a	n/a
7	7.94	3.66	9.80	4.96	20.74	9.56	1.86	1.30	8.97%	13.60%
8	**7.13**	**2.67**	**30.13**	**17.28**	**18.63**	**6.97**	**23.00**	**14.61**	**123.46%**	**209.61%**
9	5.58	3.10	20.90	10.24	14.58	8.10	15.32	7.14	105.08%	88.15%
10	3.60	1.24	10.82	6.38	9.40	3.24	7.22	5.14	76.81%	158.64%
11	0.00	0.00	0.00	0.00	0.00	0.00	0.00	0.00	n/a	n/a
12	6.94	3.41	8.56	4.64	18.14	8.91	1.62	1.23	8.93%	13.80%
13	0.00	0.00	0.00	0.00	0.00	0.00	0.00	0.00	n/a	n/a
14	3.84	2.23	4.69	3.04	10.04	5.83	0.85	0.81	8.47%	13.89%
15	5.08	3.41	6.35	4.64	13.28	8.91	1.27	1.23	9.56%	13.80%
16	2.17	1.12	2.62	1.52	5.67	2.92	0.45	0.40	7.94%	13.70%
17	5.58	3.60	6.90	4.88	14.58	9.40	1.32	1.28	9.05%	13.62%
18	20.34	11.10	3.82	1.52	53.14	29.00	16.52	9.58	31.09%	33.03%
19	14.26	6.82	3.66	3.28	37.26	17.82	10.60	3.54	28.45%	19.87%
20	7.56	4.15	2.98	0.98	19.76	10.85	4.58	3.17	23.18%	29.22%
21	4.65	1.98	5.80	2.72	12.15	5.18	1.15	0.74	9.47%	14.29%
22	0.00	0.00	0.00	0.00	0.00	0.00	0.00	0.00	n/a	n/a
23	0.00	0.00	0.00	0.00	0.00	0.00	0.00	0.00	n/a	n/a
24	2.91	2.29	3.59	3.12	7.61	5.99	0.68	0.83	8.94%	13.86%
25	0.62	0.43	0.83	0.56	1.62	1.13	0.21	0.13	12.96%	11.50%
26	2.17	1.43	2.62	1.92	5.67	3.73	0.45	0.49	7.94%	13.14%
27	0.00	0.00	0.00	0.00	0.00	0.00	0.00	0.00	n/a	n/a
28	0.00	0.00	0.00	0.00	0.00	0.00	0.00	0.00	n/a	n/a
29	1.67	1.18	2.07	1.60	4.37	3.08	0.40	0.42	9.15%	13.64%
30	3.47	1.80	4.28	2.48	9.07	4.70	0.81	0.68	8.93%	14.47%
Total	**111.71**	**58.59**	**138.01**	**79.84**	**291.91**	**153.09**	**26.30**	**21.25**	**9.01%**	**13.88%**
Ave									**24.95%**	**35.48%**

NB:PM=Power Margins, $\varepsilon_P = |\Delta Pa - \Delta P|$, $\varepsilon_Q = |\Delta Qa - \Delta Q|$, $\mu_P = \varepsilon_P / Pmax$, $\mu_Q = \varepsilon_Q / Qmax$

Table 3.3.3-1 The impact of the load pattern on voltage stability

It can be seen that between the two study cases, the average differences of power margins are $\mu_P = 24.95\%$ and $\mu_Q = 35.48\%$, the maximum differences are $\mu_P = 123.46\%$ and $\mu_Q = 209.61\%$. This clearly shows that different load patterns may result in significant difference in voltage stability.

2. The impact of the load distribution pattern

Similarly three comparison cases were included in this study group to show the impact of the load distribution pattern on voltage stability. Those cases were configured to have different load distribution patterns, but almost identical other VSDFs and system operation conditions as shown in the Table A3-3 (Case30F01p), Table A3-4 (Case30F06) and Table A3-5 (Case30F07p) of Appendix 3. The simulation results for this study group are summarised below in Table 3.3.3-2 and Table 3.3.3-3.

BUS	PM(F01p)		PM(F06)		Max load(F01p)		PM Diff (p.u.)		PM Diff (%)	
	ΔP	ΔQ	ΔPa	ΔQa	Pmax	Qmax	ε_P	ε_Q	μ_P	μ_Q
1	0.00	0.00	0.00	0.00	0.00	0.00	0.00	0.00	n/a	n/a
2	0.00	0.00	0.00	0.00	0.00	0.00	0.00	0.00	n/a	n/a
3	3.65	1.82	15.00	9.00	3.89	1.94	11.35	7.18	291.77%	370.10%
4	11.55	5.47	15.00	9.00	12.31	5.83	3.45	3.53	28.03%	60.55%
5	0.00	0.00	0.00	0.00	0.00	0.00	0.00	0.00	n/a	n/a
6	0.00	0.00	0.00	0.00	0.00	0.00	0.00	0.00	n/a	n/a
7	19.46	8.97	15.00	9.00	20.74	9.56	4.46	0.03	21.50%	0.31%
8	17.48	6.54	15.00	9.00	18.63	6.97	2.48	2.46	13.31%	35.29%
9	13.68	7.60	15.00	9.00	14.58	8.10	1.32	1.40	9.05%	17.28%
10	8.82	3.04	15.00	9.00	9.40	3.24	6.18	5.96	65.74%	183.95%
11	0.00	0.00	0.00	0.00	0.00	0.00	0.00	0.00	n/a	n/a
12	17.02	8.36	15.00	9.00	18.14	8.91	2.02	0.64	11.14%	7.18%
13	0.00	0.00	0.00	0.00	0.00	0.00	0.00	0.00	n/a	n/a
14	9.42	5.47	15.00	9.00	10.04	5.83	5.58	3.53	55.58%	60.55%
15	12.46	8.36	15.00	9.00	13.28	8.91	2.54	0.64	19.13%	7.18%
16	5.32	2.74	15.00	9.00	5.67	2.92	9.68	6.26	170.72%	214.38%
17	13.68	8.82	15.00	9.00	14.58	9.40	1.32	0.18	9.05%	1.91%
18	49.86	27.21	15.00	9.00	53.14	29.00	34.86	18.21	65.60%	62.79%
19	34.96	16.72	15.00	9.00	37.26	17.82	19.96	7.72	53.57%	43.32%
20	18.54	10.18	15.00	9.00	19.76	10.85	3.54	1.18	17.91%	10.88%
21	11.40	4.86	15.00	9.00	12.15	5.18	3.60	4.14	29.63%	79.92%
22	0.00	0.00	0.00	0.00	0.00	0.00	0.00	0.00	n/a	n/a
23	0.00	0.00	0.00	0.00	0.00	0.00	0.00	0.00	n/a	n/a
24	7.14	5.62	15.00	9.00	7.61	5.99	7.86	3.38	103.29%	56.43%
25	**1.52**	**1.06**	**15.00**	**9.00**	**1.62**	**1.13**	**13.48**	**7.94**	**832.10 %**	**702.65 %**
26	5.32	3.50	15.00	9.00	5.67	3.73	9.68	5.50	170.72%	147.45%
27	0.00	0.00	0.00	0.00	0.00	0.00	0.00	0.00	n/a	n/a
28	0.00	0.00	0.00	0.00	0.00	0.00	0.00	0.00	n/a	n/a
29	4.10	2.89	15.00	9.00	4.37	3.08	10.90	6.11	249.43%	198.38%
30	8.51	4.41	15.00	9.00	9.07	4.70	6.49	4.59	71.55%	97.66%
Total	**273.89**	**143.64**	**300.00**	**180.00**	**291.91**	**153.09**	**26.11**	**36.36**	**8.94%**	**23.75%**
Ave									**109.42 %**	**113.43 %**

NB:PM=Power Margins, $\varepsilon_P = |\Delta Pa - \Delta P|$, $\varepsilon_Q = |\Delta Qa - \Delta Q|$, $\mu_P = \varepsilon_P / Pmax$, $\mu_Q = \varepsilon_Q / Qmax$

Table 3.3.3-2 The impact of the load distribution pattern on voltage stability

BUS	PM(F07p)		PM(F06)		Max load(F07p)		PM Diff (p.u.)		PM Diff (%)	
	ΔP	ΔQ	ΔPa	ΔQa	Pmax	Qmax	ε_P	ε_Q	μ_P	μ_Q
1	0.00	0.00	0.00	0.00	0.00	0.00	0.00	0.00	n/a	n/a
2	0.00	0.00	0.00	0.00	0.00	0.00	0.00	0.00	n/a	n/a
3	2.45	1.43	15.00	9.00	2.69	1.55	12.55	7.57	466.54%	488.39%
4	9.80	5.72	15.00	9.00	10.56	6.08	5.20	3.28	49.24%	53.95%
5	0.00	0.00	0.00	0.00	0.00	0.00	0.00	0.00	n/a	n/a
6	0.00	0.00	0.00	0.00	0.00	0.00	0.00	0.00	n/a	n/a
7	9.80	5.72	15.00	9.00	11.08	6.31	5.20	3.28	46.93%	51.98%
8	12.25	7.15	15.00	9.00	13.40	7.58	2.75	1.85	20.52%	24.41%
9	12.25	7.15	15.00	9.00	13.15	7.65	2.75	1.85	20.91%	24.18%
10	7.35	4.29	15.00	9.00	7.93	4.49	7.65	4.71	96.47%	104.90%
11	0.00	0.00	0.00	0.00	0.00	0.00	0.00	0.00	n/a	n/a
12	12.25	7.15	15.00	9.00	13.37	7.70	2.75	1.85	20.57%	24.03%
13	0.00	0.00	0.00	0.00	0.00	0.00	0.00	0.00	n/a	n/a
14	12.25	7.15	15.00	9.00	12.87	7.51	2.75	1.85	21.37%	24.63%
15	12.25	7.15	15.00	9.00	13.07	7.70	2.75	1.85	21.04%	24.03%
16	9.80	5.72	15.00	9.00	10.15	5.90	5.20	3.28	51.23%	55.59%
17	12.25	7.15	15.00	9.00	13.15	7.73	2.75	1.85	20.91%	23.93%
18	49.00	28.60	15.00	9.00	52.28	30.39	34.00	19.60	65.03%	64.49%
19	24.50	14.30	15.00	9.00	26.80	15.40	9.50	5.30	35.45%	34.42%
20	24.50	14.30	15.00	9.00	25.72	14.97	9.50	5.30	36.94%	35.40%
21	12.25	7.15	15.00	9.00	13.00	7.47	2.75	1.85	21.15%	24.77%
22	0.00	0.00	0.00	0.00	0.00	0.00	0.00	0.00	n/a	n/a
23	0.00	0.00	0.00	0.00	0.00	0.00	0.00	0.00	n/a	n/a
24	4.90	2.86	15.00	9.00	5.37	3.23	10.10	6.14	188.08%	190.09%
25	**2.45**	**1.43**	**15.00**	**9.00**	**2.55**	**1.50**	**12.55**	**7.57**	**492.1%**	**504.6%**
26	4.90	2.86	15.00	9.00	5.25	3.09	10.10	6.14	192.38%	198.71%
27	0.00	0.00	0.00	0.00	0.00	0.00	0.00	0.00	n/a	n/a
28	0.00	0.00	0.00	0.00	0.00	0.00	0.00	0.00	n/a	n/a
29	2.45	1.43	15.00	9.00	2.72	1.62	12.55	7.57	461.40%	467.28%
30	7.35	4.29	15.00	9.00	7.91	4.58	7.65	4.71	96.71%	102.84%
Total	**245.00**	**143.00**	**300.00**	**180.00**	**263.02**	**152.45**	**55.00**	**37.00**	**20.91%**	**24.27%**
Ave									**116.47 %**	**121.28 %**

NB:PM=Power Margins, $\varepsilon_P = |\Delta Pa - \Delta P|$, $\varepsilon_Q = |\Delta Qa - \Delta Q|$, $\mu_P = \varepsilon_P / Pmax$, $\mu_Q = \varepsilon_Q / Qmax$

Table 3.3.3-3 The impact of the load distribution pattern on voltage stability

Between Case30F01p and Case30F06, the average differences of power margins are μ_P = 109.42% and μ_Q =113.43%, the maximum differences are μ_P =832.10% and μ_Q=702.65%. Between the Case30F07p and Case30F06, the average differences of power margins are μ_P = 116.47% and μ_Q =121.28%, the maximum differences are μ_P =492.16% and μ_Q=504.67%. This shows that different load distribution patterns may result in significant difference in voltage stability.

3. The impact of the generation pattern

Two study cases are included in this simulation to show the impact of the generation pattern on voltage stability. Those cases were configured to have different generation patterns, but almost identical other VSDFs and system operation conditions, as shown in the Table A3-6 (Case30F08), Table A3-7 (Case30F09) of Appendix 3. The simulation results for this study group are summarised in the table below.

BUS	PM(F08)		PM(F09)		Max load(F08)		PM Diff (p.u.)		PM Diff (%)	
	ΔP	**ΔQ**	**ΔPa**	**ΔQa**	**Pmax**	**Qmax**	**ε_P**	**ε_Q**	**μ_P**	**μ_Q**
1	0.00	0.00	0.00	0.00	0.00	0.00	0.00	0.00	n/a	n/a
2	0.00	0.00	0.00	0.00	0.00	0.00	0.00	0.00	n/a	n/a
3	1.43	0.86	1.65	1.00	1.67	0.98	0.22	0.14	13.17%	14.29%
4	5.72	3.44	6.60	4.00	6.48	3.80	0.88	0.56	13.58%	14.74%
5	0.00	0.00	0.00	0.00	0.00	0.00	0.00	0.00	n/a	n/a
6	0.00	0.00	0.00	0.00	0.00	0.00	0.00	0.00	n/a	n/a
7	5.72	3.44	6.60	4.00	7.00	4.03	0.88	0.56	12.57%	13.90%
8	7.15	4.30	8.25	5.00	8.30	4.73	1.10	0.70	13.25%	14.80%
9	7.15	4.30	8.25	5.00	8.05	4.80	1.10	0.70	13.66%	14.58%
10	4.29	2.58	4.95	3.00	4.87	2.78	0.66	0.42	13.55%	15.11%
11	0.00	0.00	0.00	0.00	0.00	0.00	0.00	0.00	n/a	n/a
12	7.15	4.30	8.25	5.00	8.27	4.85	1.10	0.70	13.30%	14.43%
13	0.00	0.00	0.00	0.00	0.00	0.00	0.00	0.00	n/a	n/a
14	7.15	4.30	8.25	5.00	7.77	4.66	1.10	0.70	14.16%	15.02%
15	8.58	4.30	9.90	5.00	9.40	4.85	1.32	0.70	14.04%	14.43%
16	**5.72**	**3.44**	**6.60**	**4.00**	**6.07**	**3.62**	**0.88**	**0.56**	**14.50%**	**15.47%**
17	7.15	4.30	8.25	5.00	8.05	4.88	1.10	0.70	13.66%	14.34%
18	21.45	17.20	24.75	20.00	24.73	18.99	3.30	2.80	13.34%	14.74%
19	17.16	8.60	19.80	10.00	19.46	9.70	2.64	1.40	13.57%	14.43%
20	17.16	8.60	19.80	10.00	18.38	9.27	2.64	1.40	14.36%	15.10%
21	7.15	4.30	8.25	5.00	7.90	4.62	1.10	0.70	13.92%	15.15%
22	0.00	0.00	0.00	0.00	0.00	0.00	0.00	0.00	n/a	n/a
23	0.00	0.00	0.00	0.00	0.00	0.00	0.00	0.00	n/a	n/a
24	2.86	1.72	3.30	2.00	3.33	2.09	0.44	0.28	13.21%	13.40%
25	1.43	0.86	1.65	1.00	1.53	0.93	0.22	0.14	14.38%	15.05%
26	2.86	1.72	3.30	2.00	3.21	1.95	0.44	0.28	13.71%	14.36%
27	0.00	0.00	0.00	0.00	0.00	0.00	0.00	0.00	n/a	n/a
28	0.00	0.00	0.00	0.00	0.00	0.00	0.00	0.00	n/a	n/a
29	1.43	0.86	1.65	1.00	1.70	1.05	0.22	0.14	12.94%	13.33%
30	4.29	2.58	4.95	3.00	4.85	2.87	0.66	0.42	13.61%	14.63%
Total	**143.00**	**86.00**	**165.00**	**100.00**	**161.02**	**95.45**	**22.00**	**14.00**	**13.66%**	**14.67%**
Ave									**13.63%**	**14.57%**

NB:PM=Power Margins, $\varepsilon_P = \lvert \Delta Pa - \Delta P \rvert$, $\varepsilon_Q = \lvert \Delta Qa - \Delta Q \rvert$, $\mu_P = \varepsilon_P / Pmax$, $\mu_Q = \varepsilon_Q / Qmax$

Table 3.3.3-4 The impact of the generation pattern on voltage stability

Between Case30F08 and Case30F09, the average differences of power margins are μ_P = 13.63% and μ_Q =14.57%, the maximum differences μ_P =14.50% and μ_Q=715.47%. This proves that different generation patterns may result in different voltage stabilities.

4. The impact of the generation participation pattern

In the same way, two simulation cases are presented here to show the impact of the generation participation pattern on voltage stability. Those cases were configured to have different generation patterns, but almost the same other VSDFs and system operation conditions, as shown in the Table A3-3 (Case30F01p), Table A3-8 (Case30F04) of Appendix 3. The simulation results for this study group are summarised in the table below.

BUS	PM(F04)		PM(F01p)		Max load(F04)		PM Diff (p.u.)		PM Diff (%)	
	ΔP	ΔQ	ΔPa	ΔQa	Pmax	Qmax	ε_P	ε_Q	μ_P	μ_Q
1	0.00	0.00	0.00	0.00	0.00	0.00	0.00	0.00	n/a	n/a
2	0.00	0.00	0.00	0.00	0.00	0.00	0.00	0.00	n/a	n/a
3	**2.42**	**1.21**	**3.65**	**1.82**	**2.66**	**1.33**	**1.23**	**0.61**	**46.24%**	**45.86%**
4	7.68	3.64	11.55	5.47	8.44	4.00	3.87	1.83	45.85%	45.75%
5	0.00	0.00	0.00	0.00	0.00	0.00	0.00	0.00	n/a	n/a
6	0.00	0.00	0.00	0.00	0.00	0.00	0.00	0.00	n/a	n/a
7	12.93	5.96	19.46	8.97	14.21	6.55	6.53	3.01	45.95%	45.95%
8	11.62	4.34	17.48	6.54	12.77	4.77	5.86	2.20	45.89%	46.12%
9	9.09	5.05	13.68	7.60	9.99	5.55	4.59	2.55	45.95%	45.95%
10	5.86	2.02	8.82	3.04	6.44	2.22	2.96	1.02	45.96%	45.95%
11	0.00	0.00	0.00	0.00	0.00	0.00	0.00	0.00	n/a	n/a
12	11.31	5.56	17.02	8.36	12.43	6.11	5.71	2.80	45.94%	45.83%
13	0.00	0.00	0.00	0.00	0.00	0.00	0.00	0.00	n/a	n/a
14	6.26	3.64	9.42	5.47	6.88	4.00	3.16	1.83	45.93%	45.75%
15	8.28	5.56	12.46	8.36	9.10	6.11	4.18	2.80	45.93%	45.83%
16	3.54	1.82	5.32	2.74	3.89	2.00	1.78	0.92	45.76%	46.00%
17	9.09	5.86	13.68	8.82	9.99	6.44	4.59	2.96	45.95%	45.96%
18	33.13	18.08	49.86	27.21	36.41	19.87	16.73	9.13	45.95%	45.95%
19	23.23	11.11	34.96	16.72	25.53	12.21	11.73	5.61	45.95%	45.95%
20	12.32	6.77	18.54	10.18	13.54	7.44	6.22	3.41	45.94%	45.83%
21	7.58	3.23	11.40	4.86	8.33	3.55	3.82	1.63	45.86%	45.92%
22	0.00	0.00	0.00	0.00	0.00	0.00	0.00	0.00	n/a	n/a
23	0.00	0.00	0.00	0.00	0.00	0.00	0.00	0.00	n/a	n/a
24	4.75	3.74	7.14	5.62	5.22	4.11	2.39	1.88	45.79%	45.74%
25	1.01	0.71	1.52	1.06	1.11	0.78	0.51	0.35	45.95%	44.87%
26	3.54	2.32	5.32	3.50	3.89	2.55	1.78	1.18	45.76%	46.27%
27	0.00	0.00	0.00	0.00	0.00	0.00	0.00	0.00	n/a	n/a
28	0.00	0.00	0.00	0.00	0.00	0.00	0.00	0.00	n/a	n/a
29	2.73	1.92	4.10	2.89	3.00	2.11	1.37	0.97	45.67%	45.97%
30	5.66	2.93	8.51	4.41	6.22	3.22	2.85	1.48	45.82%	45.96%
Total	**182.03**	**95.47**	**273.89**	**143.64**	**200.05**	**104.92**	**91.86**	**48.17**	**45.92%**	**45.91%**
Ave									**45.90%**	**45.87%**

NB:PM=Power Margins, $\varepsilon_P = |\Delta Pa - \Delta P|$, $\varepsilon_Q = |\Delta Qa - \Delta Q|$, $\mu_P = \varepsilon_P/Pmax$, $\mu_Q = \varepsilon_Q/Qmax$

Table 3.3.3-5 The impact of the generation participation pattern on voltage stability

Between Case30F01p and Case30F04, the average differences of power margins are μ_P=45.90and μ_Q =45.87, the maximum differences are μ_P =46.24% and μ_Q=45.86%. This clearly demonstrates that different generation participation patterns may result in rather different voltage stabilities in a power system.

5. Remarks

The above simulation results clearly demonstrated that the VSDFs have significant impacts on voltage stability (power margins) in a power system. In fact, in a steady state, these determining factors uniquely determine the voltage stability of a power system. This property will be discussed and theoretically validated in next section.

3.4 THE UNIQUE PROPERTY OF THE VSDFS

A hypothesis to generalise the unique relationship between the VSDFs and voltage stability is going to be presented and theoretically validated in this section.

3.4.1 Hypothesis

In the steady state, the VSDFs have a unique relationship with voltage stability in a power system, this unique relationship can be generalised into a hypothesis as:

HYPOTHESIS: For a power system, voltage stability is directly related to the VSDFs, namely the load pattern, the load distribution pattern, the generation pattern and the generation participation pattern. In the steady state, these factors uniquely determine the voltage stability; once the VSDFs are fixed the voltage stability of the power system will remain unchanged.

3.4.2 Validation of the Hypothesis

By regarding the voltage magnitude of each bus as a dimension, the state of a power system can be presented in a multi-dimensional space. Each point in the space represents a set of load flow solution for the power system. Several points can be assumed in the multi-dimensional space to represent the critical states for voltage collapse. Figure 3.4.2-1 shows such a multi-dimensional space for a three bus power system.

For a power system with n buses, let bus 1 to M be load buses and bus M+1 to N be generator buses. In the steady state, a voltage state K of the power system can be described by the load flow equations:

$$P_i^k = \sum_{j=1}^{N} V_i^k V_j^k Y_{ij}^k \cos(\delta_i^k - \delta_j^k - \phi_{ij}^k) \qquad (3.4.2\text{–}1)$$

$$Q_i^k = \sum_{j=1}^{N} V_i^k V_j^k Y_{ij}^k \sin(\delta_i^k - \delta_j^k - \phi_{ij}^k) \qquad (3.4.2\text{–}2)$$

$$i=1, 2, 3, ..., N$$

Where,

P_i^k and Q_i^k are the net active and reactive power injection at bus i at the voltage state k,

$V_i^k \angle \delta_i^k$ is the voltage at bus i at the voltage state k,

$Y_{ij}^k \angle \phi_{ij}^k$ is the (i, j)th entry of the network bus admittance at the voltage state k.

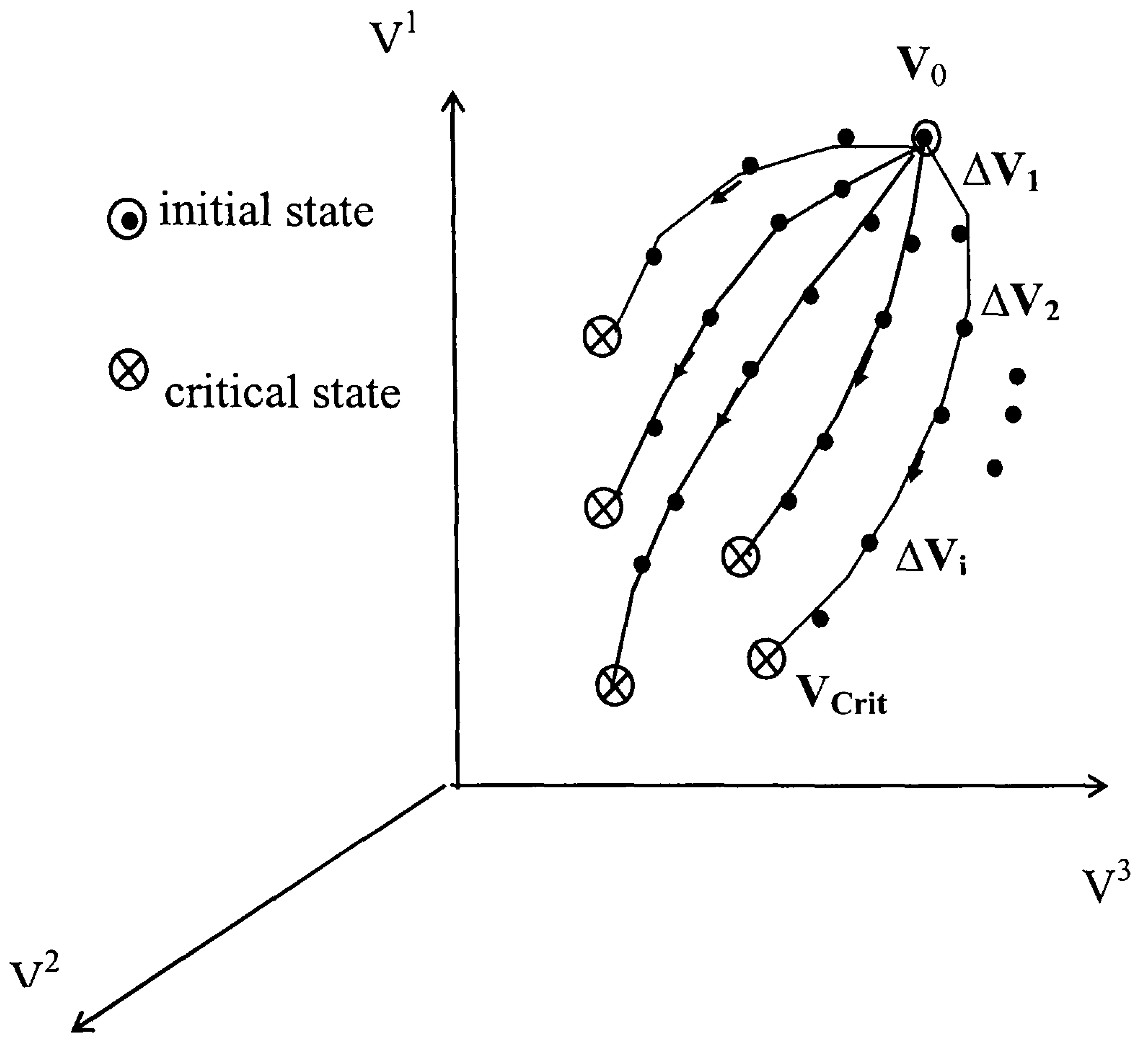

Figure 3.4.2-1 **The voltage state space of a three bus power system**

By recalling the definitions of the VSDFs, it is known that P_i^k and Q_i^k, i=1, 2, ..., N form the load and the generation patterns, which determines the voltage state k.

Linearising the load flow equations (3.4.2-1) and (3.4.2-2) at the state K produces:

$$\begin{bmatrix} \Delta P^k \\ \Delta Q^k \end{bmatrix} = \left[J^k\right] \begin{bmatrix} \Delta \theta^k \\ \Delta V^k \end{bmatrix} \qquad (3.4.2\text{–}3)$$

where,

$\Delta\mathbf{P}^k$ and $\Delta\mathbf{Q}^K$ are the variation vectors of the active and reactive power injections at all the buses of the power system at the voltage state k,

$\Delta\boldsymbol{\theta}^k$ and $\Delta\mathbf{V}^k$ are the variation vectors of voltage angle and magnitude at all the buses of the power system at the voltage state k,

$[\ \mathbf{J}^k\ ]$ is the Jocobian matrix at the voltage state k.

From equation (3.4.2-3), it can be seen that for a set of vector $\Delta\mathbf{P}^k$ and $\Delta\mathbf{Q}^k$, there will be a vector $\Delta\mathbf{V}^k$, and the vector $\Delta\mathbf{P}^k$, $\Delta\mathbf{Q}^k$ and $\Delta\mathbf{V}^k$ can be written as:

$$\Delta\mathbf{P}^k = \begin{bmatrix} \Delta\mathbf{P}^{Lk} \\ \Delta\mathbf{P}^{Gk} \end{bmatrix} \qquad (3.4.2\text{–}4)$$

$$\Delta\mathbf{Q}^k = \begin{bmatrix} \Delta\mathbf{Q}^{Lk} \\ \Delta\mathbf{Q}^{Gk} \end{bmatrix} \qquad (3.4.2\text{–}5)$$

and

$$\Delta\mathbf{V}^k = \left[\Delta V_1^k,\ \ \Delta V_2^k,\ \ ...,\ \ \Delta V_i^k,\ \ ...,\ \ \Delta V_N^k\right]^T \qquad (3.4.2\text{–}6)$$

Where,

$$\Delta\mathbf{P}^{Lk} = \left[\Delta P_1^{Lk},\ \ \Delta P_2^{Lk},\ \ ...,\ \ \Delta P_i^{Lk},\ \ ...,\ \ \Delta P_M^{Lk}\right]^T \qquad (3.4.2\text{–}7)$$

$$\Delta\mathbf{P}^{Gk} = \left[\Delta P_{M+1}^{Gk},\ \ \Delta P_{M+2}^{Gk},\ \ ...,\ \ \Delta P_{M+i}^{Gk},\ \ ...,\ \ \Delta P_N^{Gk}\right]^T \qquad (3.4.2\text{–}8)$$

$$\Delta\mathbf{Q}^{Lk} = \left[\Delta Q_1^{Lk},\ \ \Delta Q_2^{Lk},\ \ ...,\ \ \Delta Q_i^{Lk},\ \ ...,\ \ \Delta Q_M^{Lk}\right]^T \qquad (3.4.2\text{–}9)$$

$$\Delta\mathbf{Q}^{Gk} = \left[\Delta Q_{M+1}^{Gk},\ \ \Delta Q_{M+2}^{Gk},\ \ ...,\ \ \Delta Q_{M+i}^{Gk},\ \ ...,\ \ \Delta Q_N^{Gk}\right]^T \qquad (3.4.2\text{–}10)$$

The vector $\Delta\mathbf{V}^k$ represents the direction in which the system voltage will move from state k.

From the definitions of the load distribution and generation participation pattern, it is known that

$$\Delta P_i^{LK} = LD_i^P \Delta P_{Ltotal}^K \qquad (3.4.2\text{–}11)$$

$$\Delta Q_i^{LK} = LD_i^Q \Delta Q_{Ltotal}^K \qquad (3.4.2\text{–}12)$$

$$i=1, 2, ..., M$$

and

$$\Delta P_i^{GK} = GP_i^P(\Delta P_{Ltotal}^K + \Delta P_{Loss}) \qquad (3.4.2\text{–}13)$$

$$\Delta Q_i^{GK} = GP_i^Q(\Delta Q_{Ltotal}^K + \Delta Q_{Loss}) \qquad (3.4.2\text{–}14)$$

$$i=M+1,\ M+2,\ ...,\ N$$

Where,

$\mathbf{LD} = [LG_1^P, LG_2^P, ..., LG_i^P, ..., LG_1^Q, LG_2^Q, ..., LG_i^Q, ...]$ is the load distribution pattern at the voltage state k.

$\mathbf{GP} = [GP_1^P, GP_2^P, ..., GP_i^P, ..., GP_1^Q, GP_2^Q, ..., GP_i^Q, ...]$ is the generation participation pattern at the voltage state K.

From equations (3.4.2-3) to (3.4.2-14), it is clearly seen that the system voltage changing direction ΔV_K at the state k is determined by the load distribution pattern and generation participation pattern.

By knowing that the load pattern and generation pattern determine a voltage state, and the load distribution pattern and generation participation pattern set changing directions for a given voltage state, it can be concluded that voltage stability is determined by the VSDFs.

The above analysis can be further extended to validate the unique property of the VSDFs, as Based on equation (3.4.2-6), a series of $\Delta\mathbf{V}^0$, $\Delta\mathbf{V}^1$, $\Delta\mathbf{V}^2$..., $\Delta\mathbf{V}_{crit}$ can be produced with progressively increasing system load. This series of voltage changing vectors will form a trajectory from the initial operation state to a critical state of voltage collapse. It is easy to see that this voltage collapse trajectory is uniquely determined by the VSDFs. For the different VSDFs, the power system will move towards different critical states of voltage collapse.

3.5 Pattern Classes of the VSDFs

The pattern class feature of the VSDFs will be discussed in this section.

3.5.1 Pattern Classes for the Load and Load Distribution

By analysing load data, it is easy to find out that there exist some pattern classes which cover all the likely states of the load and load distribution in a power system. This pattern class feature can be explained from the following viewpoints:

Firstly, the load in a power system does not always change dramatically. It normally stays around a certain level for a period of time. The popularly used terminology 'peak load', 'trough load' and 'day average" are typical examples for this pattern class feature. In fact, these are the three major pattern classes for the load pattern in a power system.

Secondly, when the system load does change, it tends to follow certain fixed patterns. These changing patterns are related to the factors such as geographical locations, weather conditions, seasons, time of a day, industrial demand change as well as electricity regulation, pricing policy etc.

3.5.2 The Pattern Class for the Generation and Generation Participation

This pattern class feature can also be observed with the generation and generation participation patterns. Those pattern classes represent all likely states of the generation and generation participation of the power plants in a power system. The generator unit commitments, power plant maintenances, generation dispatch schedules, power network running arrangements are the common influencing factors to the pattern classes of generation and generation participation.

3.5.3 Pattern Class Determination

The pattern class is a natural feature for the VSDFs in a power system. However, to identify those pattern classes is a decision-making process. If a power system has a relatively stable load and regular load change pattern, only a few pattern classes are needed to represent all the likely states of the load and load distribution. A small number of power plants and limited generation capacity will require a few pattern classes to cover the possible states of generation and generation participation.

The pattern class determination also depend on how accurate it is required to represent the states of the VSDFs. Obviously higher accuracy is required, more pattern classes will be needed. For an extreme example, in order to archive one hundred percent accuracy, every possible state of the VSDFs has to be a pattern class, and the total number of the pattern classes will be infinite.

Furthermore, as the change of the load or load distribution will normally cause some changes in the generation or generation participation pattern, the pattern class determination also needs to take into account of the interactions between the VSDFs in a power system.

3.6 VOLTAGE STABILITY SIMILARITIES IN THE PATTERN CLASS

3.6.1 The Similarity of Voltage Stability

In this study, it has also been discovered that a power system has very similar voltage stability when the VSDFs stay in the same pattern class. This is another important and useful property of the VSDFs. The knowledge based system for prediction of voltage collapse presented in chapter 4 is based this similarity feature.

It must be emphasised here that a pattern class for a set of VSDFs contains four different sub-pattern classes associated with the load pattern, the load distribution pattern, and the generation pattern and the generation participation pattern. When the VSDFs is claimed to be in the same pattern class, all the individual determining factors have to remain in their won sub-pattern classes respectively.

This property can be easily explained by using the hypothesis given in section **Error! Reference source not found.**. From the hypothesis, it is known that in the steady state, the VSDFs uniquely determine voltage stability of a power system. When the VSDFs of a power system stay in the same pattern class, the load and load distribution as well as generation and generation participation will not change significantly. Therefore, the voltage stability of the power system will remain similar.

3.6.2 Case Study

Some numerical simulations have been performed on the IEEE 30 bus system to show the similarities of voltage stability when the VSDFs are in the same pattern class. Three typical pattern classes of the VSDFs were set up in this simulation to represent lightly, normally and heavily loaded system conditions. Each pattern class contains a group of four or five study cases, and power margins for each of the cases were determined by load flow simulations. The simulation results and details of the configurations for all the study cases are given in Appendix 3 of this thesis.

To ensure the study cases within each pattern class having similar but not the same VSDFs, 10% to 20% variations (+/-) were "randomly" made to at least one of the four VSDFs between any two cases, so that

$$20\% \geq \frac{|\beta_a^P i - \beta_b^P i|}{|\beta_a^P i|} \geq 10\%,$$

$$20\% \geq \frac{|\beta_a^Q i - \beta_b^Q i|}{|\beta_a^Q i|} \geq 10\%,$$

where,

$\beta_a = [\beta_a^P 1, \beta_a^P 2, ... \beta_a^P i \quad \beta_a^Q 1, \beta_a^Q 2, ... \beta_a^Q i ...]$

$\beta_b = [\beta_b^P 1, \beta_b^P 2, ... \beta_b^P i \quad \beta_b^Q 1, \beta_b^Q 2, ... \beta_b^Q i ...]$

$\boldsymbol{\beta}_a$ and $\boldsymbol{\beta}_b$ are the same type VSDF for study case a and b within a pattern class.

1. Pattern class I – lightly loaded conditions

(1) Simulation results

Five simulation cases are included in this pattern class to demonstrate the voltage stability similarity under lightly load conditions. The simulation details for this group of study cases are listed in Table A3-10 to Table A3 – 14 of Appendix 3. The simulation results between every two of the cases are compared and summarised in the following tables:

BUS	PM(F07a)		PM(F07b)		Max load(F07b)		PM Diff (p.u.)		PM Diff (%)	
	ΔP	ΔQ	ΔPa	ΔQa	Pmax	Qmax	ε_P	ε_Q	μ_P	μ_Q
1	0.00	0.00	0.00	0.00	0.00	0.00	0.00	0.00	n/a	n/a
2	0.00	0.00	0.00	0.00	0.00	0.00	0.00	0.00	n/a	n/a
3	2.48	1.48	2.50	1.50	2.79	1.64	0.02	0.02	0.79%	0.98%
4	9.92	5.92	10.00	6.00	10.91	6.43	0.08	0.08	0.71%	1.21%
5	0.00	0.00	0.00	0.00	0.00	0.00	0.00	0.00	n/a	n/a
6	0.00	0.00	0.00	0.00	0.00	0.00	0.00	0.00	n/a	n/a
7	9.92	5.92	10.00	6.00	11.54	6.71	0.08	0.08	0.73%	1.22%
8	12.40	7.40	12.50	7.50	13.88	8.02	0.10	0.10	0.72%	1.30%
9	12.40	7.40	12.50	7.50	13.58	8.10	0.10	0.10	0.74%	1.23%
10	7.44	4.44	7.50	4.50	8.20	4.74	0.06	0.06	0.78%	1.27%
11	0.00	0.00	0.00	0.00	0.00	0.00	0.00	0.00	n/a	n/a
12	12.40	7.40	12.50	7.50	13.84	8.16	0.10	0.10	0.69%	1.23%
13	0.00	0.00	0.00	0.00	0.00	0.00	0.00	0.00	n/a	n/a
14	12.40	7.40	12.50	7.50	13.24	7.93	0.10	0.10	0.73%	1.24%
15	14.88	8.88	15.00	9.00	15.98	9.66	0.12	0.12	0.73%	1.24%
16	**9.92**	**5.92**	**10.00**	**6.00**	**10.29**	**6.15**	**0.08**	**0.08**	**0.82%**	**1.32%**
17	12.40	7.40	12.50	7.50	13.23	7.98	0.10	0.10	0.73%	1.25%
18	37.20	22.20	37.50	22.50	40.17	23.98	0.30	0.30	0.74%	1.24%
19	29.76	17.76	30.00	18.00	31.88	18.91	0.24	0.24	0.77%	1.27%
20	29.76	17.76	30.00	18.00	30.99	18.55	0.24	0.24	0.76%	1.27%
21	12.40	7.40	12.50	7.50	13.11	7.76	0.10	0.10	0.75%	1.22%
22	0.00	0.00	0.00	0.00	0.00	0.00	0.00	0.00	n/a	n/a
23	0.00	0.00	0.00	0.00	0.00	0.00	0.00	0.00	n/a	n/a
24	4.96	2.96	5.00	3.00	5.38	3.31	0.04	0.04	0.68%	1.32%
25	2.48	1.48	2.50	1.50	2.58	1.56	0.02	0.02	0.72%	1.41%
26	4.96	2.96	5.00	3.00	5.42	3.28	0.04	0.04	0.74%	1.34%
27	0.00	0.00	0.00	0.00	0.00	0.00	0.00	0.00	n/a	n/a
28	0.00	0.00	0.00	0.00	0.00	0.00	0.00	0.00	n/a	n/a
29	2.48	1.48	2.50	1.50	2.82	1.73	0.02	0.02	0.57%	1.27%
30	7.44	4.44	7.50	4.50	8.17	4.85	0.06	0.06	0.71%	1.28%
Total	**248.00**	**148.00**	**249.98**	**150.00**	**268.00**	**159.45**	**1.98**	**2.00**	**0.74%**	**1.25%**
Ave									**0.73%**	**1.26%**

NB:PM=Power Margins, $\varepsilon_P = |\Delta Pa - \Delta P|$, $\varepsilon_Q = |\Delta Qa - \Delta Q|$, $\mu_P = \varepsilon_P/Pmax$, $\mu_Q = \varepsilon_Q/Qmax$

Table 3.6.2-1 Power margins for Case30F07a and Case30F07b within pattern class I

BUS	PM(F07c)		PM(F07b)		Max load(F07b)		PM Diff (p.u.)		PM Diff (%)	
	ΔP	ΔQ	ΔPa	ΔQa	Pmax	Qmax	ε_P	ε_Q	μ_P	μ_Q
1	0.00	0.00	0.00	0.00	0.00	0.00	0.00	0.00	n/a	n/a
2	0.00	0.00	0.00	0.00	0.00	0.00	0.00	0.00	n/a	n/a
3	2.51	1.50	2.50	1.50	2.79	1.64	0.01	0.00	0.36%	0.00%
4	10.04	6.00	10.00	6.00	10.91	6.43	0.04	0.00	0.37%	0.00%
5	0.00	0.00	0.00	0.00	0.00	0.00	0.00	0.00	n/a	n/a
6	0.00	0.00	0.00	0.00	0.00	0.00	0.00	0.00	n/a	n/a
7	10.04	6.00	10.00	6.00	11.54	6.71	0.04	0.00	0.35%	0.00%
8	12.55	7.50	12.50	7.50	13.88	8.02	0.05	0.00	0.36%	0.00%
9	12.55	7.50	12.50	7.50	13.58	8.10	0.05	0.00	0.37%	0.00%
10	7.53	4.50	7.50	4.50	8.20	4.74	0.03	0.00	0.37%	0.00%
11	0.00	0.00	0.00	0.00	0.00	0.00	0.00	0.00	n/a	n/a
12	12.55	7.50	12.50	7.50	13.84	8.16	0.05	0.00	0.36%	0.00%
13	0.00	0.00	0.00	0.00	0.00	0.00	0.00	0.00	n/a	n/a
14	12.55	7.50	12.50	7.50	13.24	7.93	0.05	0.00	0.38%	0.00%
15	15.06	9.00	15.00	9.00	15.98	9.66	0.06	0.00	0.38%	0.00%
16	10.04	6.00	10.00	6.00	10.29	6.15	0.04	0.00	0.39%	0.00%
17	12.55	7.50	12.50	7.50	13.23	7.98	0.05	0.00	0.38%	0.00%
18	37.65	22.50	37.50	22.50	40.17	23.98	0.15	0.00	0.37%	0.00%
19	30.12	18.00	30.00	18.00	31.88	18.91	0.12	0.00	0.38%	0.00%
20	**30.12**	**18.00**	**30.00**	**18.00**	**30.99**	**18.55**	**0.12**	**0.00**	**0.39%**	**0.00%**
21	12.55	7.50	12.50	7.50	13.11	7.76	0.05	0.00	0.38%	0.00%
22	0.00	0.00	0.00	0.00	0.00	0.00	0.00	0.00	n/a	n/a
23	0.00	0.00	0.00	0.00	0.00	0.00	0.00	0.00	n/a	n/a
24	5.02	3.00	5.00	3.00	5.38	3.31	0.02	0.00	0.37%	0.00%
25	2.51	1.50	2.50	1.50	2.58	1.56	0.01	0.00	0.39%	0.00%
26	5.02	3.00	5.00	3.00	5.42	3.28	0.02	0.00	0.37%	0.00%
27	0.00	0.00	0.00	0.00	0.00	0.00	0.00	0.00	n/a	n/a
28	0.00	0.00	0.00	0.00	0.00	0.00	0.00	0.00	n/a	n/a
29	2.51	1.50	2.50	1.50	2.82	1.73	0.01	0.00	0.35%	0.00%
30	7.53	4.50	7.50	4.50	8.17	4.85	0.03	0.00	0.37%	0.00%
Total	**250.98**	**150.00**	**249.98**	**150.00**	**268.00**	**159.45**	**1.00**	**0.00**	**0.37%**	**0.00%**
Ave									**0.37%**	**0.00%**

NB:PM=Power Margins, $\varepsilon_P=|\Delta Pa-\Delta P|$, $\varepsilon_Q=|\Delta Qa-\Delta Q|$, $\mu_P=\varepsilon_P/Pmax$, $\mu_Q=\varepsilon_Q/Qmax$

Table 3.6.2-2 Power margins for Case30F07c and Case30F07b within pattern class 1

BUS	PM(F07c)		PM(F07d)		Max load(F07d)		PM Diff (p.u.)		PM Diff (%)	
	ΔP	ΔQ	ΔPa	ΔQa	Pmax	Qmax	ε_P	ε_Q	μ_P	μ_Q
1	0.00	0.00	0.00	0.00	0.00	0.00	0.00	0.00	n/a	n/a
2	0.00	0.00	0.00	0.00	0.00	0.00	0.00	0.00	n/a	n/a
3	2.51	1.50	2.49	1.48	2.78	1.62	0.02	0.02	0.72%	1.23%
4	10.04	6.00	9.96	5.92	10.87	6.35	0.08	0.08	0.74%	1.26%
5	0.00	0.00	0.00	0.00	0.00	0.00	0.00	0.00	n/a	n/a
6	0.00	0.00	0.00	0.00	0.00	0.00	0.00	0.00	n/a	n/a
7	10.04	6.00	9.96	5.92	11.50	6.63	0.08	0.08	0.70%	1.21%
8	12.55	7.50	12.45	7.40	13.83	7.92	0.10	0.10	0.72%	1.26%
9	12.55	7.50	12.45	7.40	13.53	8.00	0.10	0.10	0.74%	1.25%
10	7.53	4.50	7.47	4.44	8.17	4.68	0.06	0.06	0.73%	1.28%
11	0.00	0.00	0.00	0.00	0.00	0.00	0.00	0.00	n/a	n/a
12	12.55	7.50	12.45	7.40	13.79	8.06	0.10	0.10	0.73%	1.24%
13	0.00	0.00	0.00	0.00	0.00	0.00	0.00	0.00	n/a	n/a
14	12.55	7.50	12.45	7.40	13.19	7.83	0.10	0.10	0.76%	1.28%
15	15.06	9.00	14.94	8.88	15.92	9.54	0.12	0.12	0.75%	1.26%
16	**10.04**	**6.00**	**9.96**	**5.92**	**10.25**	**6.07**	**0.08**	**0.08**	**0.78%**	**1.32%**
17	12.55	7.50	12.45	7.40	13.18	7.88	0.10	0.10	0.76%	1.27%
18	37.65	22.50	37.35	22.20	40.02	23.68	0.30	0.30	0.75%	1.27%
19	30.12	18.00	29.88	17.76	31.76	18.67	0.24	0.24	0.76%	1.29%
20	30.12	18.00	29.88	17.76	30.87	18.31	0.24	0.24	0.78%	1.31%
21	12.55	7.50	12.45	7.40	13.06	7.66	0.10	0.10	0.77%	1.31%
22	0.00	0.00	0.00	0.00	0.00	0.00	0.00	0.00	n/a	n/a
23	0.00	0.00	0.00	0.00	0.00	0.00	0.00	0.00	n/a	n/a
24	5.02	3.00	4.98	2.96	5.36	3.27	0.04	0.04	0.75%	1.22%
25	2.51	1.50	2.49	1.48	2.57	1.54	0.02	0.02	0.78%	1.30%
26	5.02	3.00	4.98	2.96	5.40	3.24	0.04	0.04	0.74%	1.23%
27	0.00	0.00	0.00	0.00	0.00	0.00	0.00	0.00	n/a	n/a
28	0.00	0.00	0.00	0.00	0.00	0.00	0.00	0.00	n/a	n/a
29	2.51	1.50	2.49	1.48	2.81	1.71	0.02	0.02	0.71%	1.17%
30	7.53	4.50	7.47	4.44	8.14	4.79	0.06	0.06	0.74%	1.25%
Total	**250.98**	**150.00**	**248.98**	**148.00**	**267.00**	**157.45**	**2.00**	**2.00**	**0.75%**	**1.27%**
Ave									**0.74%**	**1.26%**

NB:PM=Power Margins, $\varepsilon_P = |\Delta Pa - \Delta P|$, $\varepsilon_Q = |\Delta Qa - \Delta Q|$, $\mu_P = \varepsilon_P / Pmax$, $\mu_Q = \varepsilon_Q / Qmax$

Table 3.6.2-3 Power margins for Case30F07c and Case30F07d within pattern class I

BUS	PM(F07)		PM(F07a)		Max load(F07a)		PM Diff (p.u.)		PM Diff (%)	
	ΔP	ΔQ	ΔPa	ΔQa	Pmax	Qmax	ε_P	ε_Q	μ_P	μ_Q
1	0.00	0.00	0.00	0.00	0.00	0.00	0.00	0.00	n/a	n/a
2	0.00	0.00	0.00	0.00	0.00	0.00	0.00	0.00	n/a	n/a
3	2.77	1.66	2.48	1.48	2.72	1.60	0.29	0.18	10.66%	11.25%
4	9.07	5.44	9.92	5.92	10.68	6.28	0.85	0.48	7.96%	7.64%
5	0.00	0.00	0.00	0.00	0.00	0.00	0.00	0.00	n/a	n/a
6	0.00	0.00	0.00	0.00	0.00	0.00	0.00	0.00	n/a	n/a
7	11.09	6.64	9.92	5.92	11.20	6.51	1.17	0.72	10.45%	11.06%
8	11.34	6.80	12.40	7.40	13.55	7.83	1.06	0.60	7.82%	7.66%
9	13.86	8.31	12.40	7.40	13.30	7.90	1.46	0.91	10.98%	11.52%
10	6.80	4.08	7.44	4.44	8.02	4.64	0.64	0.36	7.98%	7.76%
11	0.00	0.00	0.00	0.00	0.00	0.00	0.00	0.00	n/a	n/a
12	13.86	8.31	12.40	7.40	13.52	7.95	1.46	0.91	10.80%	11.45%
13	0.00	0.00	0.00	0.00	0.00	0.00	0.00	0.00	n/a	n/a
14	11.34	6.80	12.40	7.40	13.02	7.76	1.06	0.60	8.14%	7.73%
15	16.63	9.97	14.88	8.88	15.70	9.43	1.75	1.09	11.15%	11.56%
16	9.07	5.44	9.92	5.92	10.27	6.10	0.85	0.48	8.28%	7.87%
17	13.86	8.31	12.40	7.40	13.30	7.98	1.46	0.91	10.98%	11.40%
18	34.02	20.39	37.20	22.20	40.48	23.99	3.18	1.81	7.86%	7.54%
19	33.26	19.93	29.76	17.76	32.06	18.86	3.50	2.17	10.92%	11.51%
20	27.22	16.31	29.76	17.76	30.98	18.43	2.54	1.45	8.20%	7.87%
21	**13.86**	**8.31**	**12.40**	**7.40**	**13.15**	**7.72**	**1.46**	**0.91**	**11.10 %**	**11.79 %**
22	0.00	0.00	0.00	0.00	0.00	0.00	0.00	0.00	n/a	n/a
23	0.00	0.00	0.00	0.00	0.00	0.00	0.00	0.00	n/a	n/a
24	5.54	3.32	4.96	2.96	5.43	3.33	0.58	0.36	10.68%	10.81%
25	2.27	1.36	2.48	1.48	2.58	1.55	0.21	0.12	8.14%	7.74%
26	5.54	3.32	4.96	2.96	5.31	3.19	0.58	0.36	10.92%	11.29%
27	0.00	0.00	0.00	0.00	0.00	0.00	0.00	0.00	n/a	n/a
28	0.00	0.00	0.00	0.00	0.00	0.00	0.00	0.00	n/a	n/a
29	2.27	1.36	2.48	1.48	2.75	1.67	0.21	0.12	7.64%	7.19%
30	8.32	4.98	7.44	4.44	8.00	4.73	0.88	0.54	11.00%	11.42%
Total	**251.99**	**151.04**	**248.00**	**148.00**	**266.02**	**157.45**	**3.99**	**3.04**	**1.50%**	**1.93%**
Ave									**9.20%**	**9.33%**

NB:PM=Power Margins, $\varepsilon_P = |\Delta Pa - \Delta P|$, $\varepsilon_Q = |\Delta Qa - \Delta Q|$, $\mu_P = \varepsilon_P/Pmax$, $\mu_Q = \varepsilon_Q/Qmax$

Table 3.6.2-4 Power margins for Case30F07 and Case30F07a within pattern class I

(2) Remarks

It can be seen from the above tables that both the average and maximum differences of power margins between any two cases within pattern class I are well below 2%, except for those between Case30F07 and Case30F07a (as shown in the Table 3.6.2-4, the average differences are 9.20% and 9.33 %, the maximum differences are 11.10% and 11.79%). The slightly higher figures observed in the Table 3.6.2-4 are due to the variations made for load distribution patterns between the two cases. In Chapter 4, a compensation method will be discussed for these voltage stability discrepancies.

2. Pattern class II – Normally loaded conditions

(1) Simulation results

Four simulation cases are included in this pattern class to demonstrate the voltage stability similarity under normally loaded conditions. The simulation details for those cases are listed in Table A3-15 to Table A3 – 18 of Appendix 3. The simulation results between every two of the cases are compared and summarised in the following tables:

BUS	PM(F015)		PM(F015a)		Max load(F015a)		PM Diff (p.u.)		PM Diff (%)	
	ΔP	ΔQ	ΔPa	ΔQa	Pmax	Qmax	ε_P	ε_Q	μ_P	μ_Q
1	0.00	0.00	0.00	0.00	0.00	0.00	0.00	0.00	n/a	n/a
2	0.00	0.00	0.00	0.00	0.00	0.00	0.00	0.00	n/a	n/a
3	1.56	0.92	1.64	0.98	2.96	1.64	0.08	0.06	2.70%	3.66%
4	3.12	1.84	3.28	1.96	7.46	3.94	0.16	0.12	2.14%	3.05%
5	0.00	0.00	0.00	0.00	0.00	0.00	0.00	0.00	n/a	n/a
6	0.00	0.00	0.00	0.00	0.00	0.00	0.00	0.00	n/a	n/a
7	2.34	1.38	2.46	1.47	9.50	4.72	0.12	0.09	1.26%	1.91%
8	3.90	2.30	4.10	2.45	10.43	4.82	0.20	0.15	1.92%	3.11%
9	3.90	2.30	4.10	2.45	9.05	5.20	0.20	0.15	2.21%	2.88%
10	2.34	1.38	2.46	1.47	5.65	2.57	0.12	0.09	2.12%	3.50%
11	0.00	0.00	0.00	0.00	0.00	0.00	0.00	0.00	n/a	n/a
12	3.12	1.84	3.28	1.96	8.32	4.44	0.16	0.12	1.92%	2.70%
13	0.00	0.00	0.00	0.00	0.00	0.00	0.00	0.00	n/a	n/a
14	4.68	2.76	4.92	2.94	7.71	4.56	0.24	0.18	3.11%	3.95%
15	3.90	2.30	4.10	2.45	7.79	4.93	0.20	0.15	2.57%	3.04%
16	**3.12**	**1.84**	**3.28**	**1.96**	**4.86**	**2.77**	**0.16**	**0.12**	**3.29%**	**4.33%**
17	3.90	2.30	4.10	2.45	8.15	5.06	0.20	0.15	2.45%	2.96%
18	15.60	9.20	16.40	9.81	31.16	17.86	0.80	0.61	2.57%	3.42%
19	7.80	4.60	8.20	4.90	18.55	9.85	0.40	0.30	2.16%	3.05%
20	7.80	4.60	8.20	4.90	13.69	7.92	0.40	0.30	2.92%	3.79%
21	3.90	2.30	4.10	2.45	8.23	4.21	0.20	0.15	2.43%	3.56%
22	0.00	0.00	0.00	0.00	0.00	0.00	0.00	0.00	n/a	n/a
23	0.00	0.00	0.00	0.00	0.00	0.00	0.00	0.00	n/a	n/a
24	1.56	0.92	1.64	0.98	4.23	3.02	0.08	0.06	1.89%	1.99%
25	0.78	0.46	0.82	0.49	1.37	0.88	0.04	0.03	2.92%	3.41%
26	2.34	1.38	2.45	1.47	4.38	2.73	0.11	0.09	2.51%	3.30%
27	0.00	0.00	0.00	0.00	0.00	0.00	0.00	0.00	n/a	n/a
28	0.00	0.00	0.00	0.00	0.00	0.00	0.00	0.00	n/a	n/a
29	0.78	0.46	0.82	0.49	2.31	1.53	0.04	0.03	1.73%	1.96%
30	1.56	0.92	1.64	0.98	4.72	2.58	0.08	0.06	1.69%	2.33%
Total	**78.00**	**46.00**	**81.99**	**49.01**	**170.52**	**95.23**	**3.99**	**3.01**	**2.34%**	**3.16%**
Ave									**2.33%**	**3.10%**

NB:PM=Power Margins, $\varepsilon_P = |\Delta Pa - \Delta P|$, $\varepsilon_Q = |\Delta Qa - \Delta Q|$, $\mu_P = \varepsilon_P / Pmax$, $\mu_Q = \varepsilon_Q / Qmax$

Table 3.6.2-5 Power margins for Case30F015 and Case30F015a in pattern class II

BUS	PM(F015b)		PM(F015a)		Max load(F015a)		PM Diff (p.u.)		PM Diff (%)	
	ΔP	ΔQ	ΔPa	ΔQa	Pmax	Qmax	ε_P	ε_Q	μ_P	μ_Q
1	0.00	0.00	0.00	0.00	0.00	0.00	0.00	0.00	n/a	n/a
2	0.00	0.00	0.00	0.00	0.00	0.00	0.00	0.00	n/a	n/a
3	1.76	1.06	1.64	0.98	2.96	1.64	0.12	0.08	4.05%	4.88%
4	3.52	2.11	3.28	1.96	7.46	3.94	0.24	0.15	3.22%	3.81%
5	0.00	0.00	0.00	0.00	0.00	0.00	0.00	0.00	n/a	n/a
6	0.00	0.00	0.00	0.00	0.00	0.00	0.00	0.00	n/a	n/a
7	2.64	1.58	2.46	1.47	9.50	4.72	0.18	0.11	1.89%	2.33%
8	4.40	2.64	4.10	2.45	10.43	4.82	0.30	0.19	2.88%	3.94%
9	4.40	2.64	4.10	2.45	9.05	5.20	0.30	0.19	3.31%	3.65%
10	2.64	1.58	2.46	1.47	5.65	2.57	0.18	0.11	3.19%	4.28%
11	0.00	0.00	0.00	0.00	0.00	0.00	0.00	0.00	n/a	n/a
12	3.52	2.11	3.28	1.96	8.32	4.44	0.24	0.15	2.88%	3.38%
13	0.00	0.00	0.00	0.00	0.00	0.00	0.00	0.00	n/a	n/a
14	5.28	3.17	4.92	2.94	7.71	4.56	0.36	0.23	4.67%	5.04%
15	4.40	2.64	4.10	2.45	7.79	4.93	0.30	0.19	3.85%	3.85%
16	3.52	2.11	3.28	1.96	4.86	2.77	0.24	0.15	4.94%	5.42%
17	3.60	2.16	4.10	2.45	8.15	5.06	0.50	0.29	6.13%	5.73%
18	14.40	8.64	16.40	9.81	31.16	17.86	2.00	1.17	6.42%	6.55%
19	7.20	4.32	8.20	4.90	18.55	9.85	1.00	0.58	5.39%	5.89%
20	**7.20**	**4.32**	**8.20**	**4.90**	**13.69**	**7.92**	**1.00**	**0.58**	**7.30%**	**7.32%**
21	3.60	2.16	4.10	2.45	8.23	4.21	0.50	0.29	6.08%	6.89%
22	0.00	0.00	0.00	0.00	0.00	0.00	0.00	0.00	n/a	n/a
23	0.00	0.00	0.00	0.00	0.00	0.00	0.00	0.00	n/a	n/a
24	1.76	1.06	1.64	0.98	4.23	3.02	0.12	0.08	2.84%	2.65%
25	0.88	0.53	0.82	0.49	1.37	0.88	0.06	0.04	4.38%	4.55%
26	2.64	1.58	2.45	1.47	4.38	2.73	0.19	0.11	4.34%	4.03%
27	0.00	0.00	0.00	0.00	0.00	0.00	0.00	0.00	n/a	n/a
28	0.00	0.00	0.00	0.00	0.00	0.00	0.00	0.00	n/a	n/a
29	0.88	0.53	0.82	0.49	2.31	1.53	0.06	0.04	2.60%	2.61%
30	1.76	1.06	1.64	0.98	4.72	2.58	0.12	0.08	2.54%	3.10%
Total	**80.00**	**48.00**	**81.99**	**49.01**	**170.52**	**95.23**	**1.99**	**1.01**	**1.17%**	**1.06%**
Ave									**4.00%**	**4.33%**

NB:PM=Power Margins, $\varepsilon_P = |\Delta Pa - \Delta P|$, $\varepsilon_Q = |\Delta Qa - \Delta Q|$, $\mu_P = \varepsilon_P/Pmax$, $\mu_Q = \varepsilon_Q/Qmax$

Table 3.6.2-6 Power margins for Case30F015a and Case30F015b in pattern class II

BUS	PM(F015b)		PM(F015c)		Max load(F015c)		PM Diff (p.u.)		PM Diff (%)	
	ΔP	ΔQ	ΔPa	ΔQa	Pmax	Qmax	ε_P	ε_Q	μ_P	μ_Q
1	0.00	0.00	0.00	0.00	0.00	0.00	0.00	0.00	n/a	n/a
2	0.00	0.00	0.00	0.00	0.00	0.00	0.00	0.00	n/a	n/a
3	**1.76**	**1.06**	**1.76**	**1.03**	**2.96**	**1.63**	**0.00**	**0.03**	**0.00%**	**1.84%**
4	3.52	2.11	3.52	2.07	7.32	3.87	0.00	0.04	0.00%	1.03%
5	0.00	0.00	0.00	0.00	0.00	0.00	0.00	0.00	n/a	n/a
6	0.00	0.00	0.00	0.00	0.00	0.00	0.00	0.00	n/a	n/a
7	2.64	1.58	2.64	1.55	9.04	4.50	0.00	0.03	0.00%	0.67%
8	4.40	2.64	4.40	2.59	10.15	4.74	0.00	0.05	0.00%	1.05%
9	4.40	2.64	4.40	2.59	8.90	5.09	0.00	0.05	0.00%	0.98%
10	2.64	1.58	2.64	1.55	5.54	2.55	0.00	0.03	0.00%	1.18%
11	0.00	0.00	0.00	0.00	0.00	0.00	0.00	0.00	n/a	n/a
12	3.52	2.11	3.52	2.07	9.12	4.82	0.00	0.04	0.00%	0.83%
13	0.00	0.00	0.00	0.00	0.00	0.00	0.00	0.00	n/a	n/a
14	5.28	3.17	5.28	3.10	8.38	4.90	0.00	0.07	0.00%	1.43%
15	4.40	2.64	4.40	2.59	8.50	5.34	0.00	0.05	0.00%	0.94%
16	3.52	2.11	3.52	2.07	5.27	2.97	0.00	0.04	0.00%	1.35%
17	3.60	2.16	3.60	2.12	8.10	5.02	0.00	0.04	0.00%	0.80%
18	14.40	8.64	14.40	8.46	30.80	17.41	0.00	0.18	0.00%	1.03%
19	7.20	4.32	7.20	4.23	18.70	9.73	0.00	0.09	0.00%	0.92%
20	7.20	4.32	7.20	4.23	13.30	7.58	0.00	0.09	0.00%	1.19%
21	3.60	2.16	3.60	2.12	7.35	3.72	0.00	0.04	0.00%	1.08%
22	0.00	0.00	0.00	0.00	0.00	0.00	0.00	0.00	n/a	n/a
23	0.00	0.00	0.00	0.00	0.00	0.00	0.00	0.00	n/a	n/a
24	1.76	1.06	1.76	1.03	4.11	2.88	0.00	0.03	0.00%	1.04%
25	0.88	0.53	0.88	0.52	1.38	0.87	0.00	0.01	0.00%	1.15%
26	2.64	1.58	2.64	1.55	4.39	2.70	0.00	0.03	0.00%	1.11%
27	0.00	0.00	0.00	0.00	0.00	0.00	0.00	0.00	n/a	n/a
28	0.00	0.00	0.00	0.00	0.00	0.00	0.00	0.00	n/a	n/a
29	0.88	0.53	0.88	0.52	2.23	1.47	0.00	0.01	0.00%	0.68%
30	1.76	1.06	1.76	1.03	4.56	2.48	0.00	0.03	0.00%	1.21%
Total	**80.00**	**48.00**	**80.00**	**47.02**	**170.10**	**94.27**	**0.00**	**0.98**	**0.00%**	**1.04%**
Ave									**0.00%**	**1.07%**

NB:PM=Power Margins, $\varepsilon_P = |\Delta Pa - \Delta P|$, $\varepsilon_Q = |\Delta Qa - \Delta Q|$, $\mu_P = \varepsilon_P/Pmax$, $\mu_Q = \varepsilon_Q/Qmax$

Table 3.6.2-7 Power margins for Case30F015b and Case30F015c in pattern class II

(2) Remarks

It can be seen that within pattern class II, the average differences of power margins between any two study cases are below 5%, the maximum differences are round 7%.

3. Pattern class III – Heavily loaded conditions

(1) Simulation results

Similarly four simulation cases are included in this pattern class to demonstrate the voltage stability similarity under heavily loaded conditions. The simulation details for this group of study cases are listed in Table A3-20 to Table A3 – 23 of Appendix 3. The simulation results between every two of the cases are compared and summarised in the following tables:

BUS	PM(F020)		PM(F020a)		Max load(F020a)		PM Diff (p.u.)		PM Diff (%)	
	ΔP	ΔQ	ΔPa	ΔQa	Pmax	Qmax	ε_P	ε_Q	μ_P	μ_Q
1	0.00	0.00	0.00	0.00	0.00	0.00	0.00	0.00	n/a	n/a
2	0.00	0.00	0.00	0.00	0.00	0.00	0.00	0.00	n/a	n/a
3	**2.95**	**1.75**	**3.80**	**2.30**	**7.10**	**4.28**	**0.85**	**0.55**	**11.97 %**	**12.85 %**
4	0.00	0.00	0.00	0.00	9.90	5.94	0.00	0.00	0.00%	0.00%
5	0.00	0.00	0.00	0.00	0.00	0.00	0.00	0.00	n/a	n/a
6	0.00	0.00	0.00	0.00	0.00	0.00	0.00	0.00	n/a	n/a
7	2.95	1.75	3.80	2.30	17.88	8.79	0.85	0.55	4.75%	6.26%
8	2.95	1.75	3.80	2.30	15.35	7.03	0.85	0.55	5.54%	7.82%
9	2.95	1.75	3.80	2.30	13.70	7.80	0.85	0.55	6.20%	7.05%
10	2.95	1.75	3.80	2.30	10.40	6.26	0.85	0.55	8.17%	8.79%
11	0.00	0.00	0.00	0.00	0.00	0.00	0.00	0.00	n/a	n/a
12	2.95	1.75	3.80	2.30	13.88	8.60	0.85	0.55	6.12%	6.40%
13	0.00	0.00	0.00	0.00	0.00	0.00	0.00	0.00	n/a	n/a
14	5.90	3.50	7.60	4.60	33.70	20.80	1.70	1.10	5.04%	5.29%
15	5.90	3.50	7.60	4.60	35.95	21.70	1.70	1.10	4.73%	5.07%
16	2.95	1.75	3.80	2.30	8.30	5.00	0.85	0.55	10.24%	11.00%
17	2.95	1.75	3.80	2.30	11.90	7.52	0.85	0.55	7.14%	7.31%
18	5.90	3.50	7.60	4.60	22.00	12.70	1.70	1.10	7.73%	8.66%
19	2.95	1.75	3.80	2.30	14.60	9.50	0.85	0.55	5.82%	5.79%
20	0.00	0.00	0.00	0.00	4.95	2.97	0.00	0.00	0.00%	0.00%
21	2.95	1.75	3.80	2.30	12.05	5.82	0.85	0.55	7.05%	9.45%
22	0.00	0.00	0.00	0.00	0.00	0.00	0.00	0.00	n/a	n/a
23	0.00	0.00	0.00	0.00	0.00	0.00	0.00	0.00	n/a	n/a
24	2.95	1.75	3.80	2.30	8.97	6.37	0.85	0.55	9.48%	8.63%
25	2.95	1.75	3.80	2.30	7.10	4.50	0.85	0.55	11.97%	12.22%
26	0.00	0.00	0.00	0.00	6.05	3.63	0.00	0.00	0.00%	0.00%
27	0.00	0.00	0.00	0.00	0.00	0.00	0.00	0.00	n/a	n/a
28	0.00	0.00	0.00	0.00	0.00	0.00	0.00	0.00	n/a	n/a
29	2.95	1.75	3.80	2.30	8.20	4.94	0.85	0.55	10.37%	11.13%
30	2.95	1.75	3.80	2.30	12.16	6.70	0.85	0.55	6.99%	8.21%
Total	**59.00**	**35.00**	**76.00**	**46.00**	**274.14**	**160.85**	**17.00**	**11.00**	**6.20%**	**6.84%**
Ave									**6.45%**	**7.08%**

NB:PM=Power Margins, $\varepsilon_P = |\Delta Pa - \Delta P|$, $\varepsilon_Q = |\Delta Qa - \Delta Q|$, $\mu_P = \varepsilon_P/Pmax$, $\mu_Q = \varepsilon_Q/Qmax$

Table 3.6.2-8 Power margins for Case30F020 and Case30F020a in pattern class III

BUS	PM(F020b)		PM(F020)		Max load(F020)		PM Diff (p.u.)		PM Diff (%)	
	ΔP	ΔQ	ΔPa	ΔQa	Pmax	Qmax	ε_P	ε_Q	μ_P	μ_Q
1	0.00	0.00	0.00	0.00	0.00	0.00	0.00	0.00	n/a	n/a
2	0.00	0.00	0.00	0.00	0.00	0.00	0.00	0.00	n/a	n/a
3	2.52	1.53	2.95	1.75	5.95	3.55	0.43	0.22	7.23%	6.20%
4	0.00	0.00	0.00	0.00	9.00	5.40	0.00	0.00	0.00%	0.00%
5	0.00	0.00	0.00	0.00	0.00	0.00	0.00	0.00	n/a	n/a
6	0.00	0.00	0.00	0.00	0.00	0.00	0.00	0.00	n/a	n/a
7	2.52	1.53	2.95	1.75	15.75	7.65	0.43	0.22	2.73%	2.88%
8	2.52	1.53	2.95	1.75	13.45	6.05	0.43	0.22	3.20%	3.64%
9	2.52	1.53	2.95	1.75	11.95	6.75	0.43	0.22	3.60%	3.26%
10	2.52	1.53	2.95	1.75	8.95	5.35	0.43	0.22	4.80%	4.11%
11	0.00	0.00	0.00	0.00	0.00	0.00	0.00	0.00	n/a	n/a
12	3.08	1.87	2.95	1.75	14.15	8.75	0.13	0.12	0.92%	1.37%
13	0.00	0.00	0.00	0.00	0.00	0.00	0.00	0.00	n/a	n/a
14	6.16	3.74	5.90	3.50	34.90	21.50	0.26	0.24	0.74%	1.12%
15	6.16	3.74	5.90	3.50	37.40	22.50	0.26	0.24	0.70%	1.07%
16	3.08	1.87	2.95	1.75	7.95	4.75	0.13	0.12	1.64%	2.53%
17	3.08	1.87	2.95	1.75	11.95	7.55	0.13	0.12	1.09%	1.59%
18	6.16	3.74	5.90	3.50	21.90	12.50	0.26	0.24	1.19%	1.92%
19	3.08	1.87	2.95	1.75	14.95	9.75	0.13	0.12	0.87%	1.23%
20	0.00	0.00	0.00	0.00	5.50	3.30	0.00	0.00	0.00%	0.00%
21	2.52	1.53	2.95	1.75	10.45	4.95	0.43	0.22	4.11%	4.44%
22	0.00	0.00	0.00	0.00	0.00	0.00	0.00	0.00	n/a	n/a
23	0.00	0.00	0.00	0.00	0.00	0.00	0.00	0.00	n/a	n/a
24	2.52	1.53	2.95	1.75	7.65	5.45	0.43	0.22	5.62%	4.04%
25	**2.52**	**1.53**	**2.95**	**1.75**	**5.95**	**3.75**	**0.43**	**0.22**	**7.23%**	**5.87%**
26	0.00	0.00	0.00	0.00	5.50	3.30	0.00	0.00	0.00%	0.00%
27	0.00	0.00	0.00	0.00	0.00	0.00	0.00	0.00	n/a	n/a
28	0.00	0.00	0.00	0.00	0.00	0.00	0.00	0.00	n/a	n/a
29	2.52	1.53	2.95	1.75	6.95	4.15	0.43	0.22	6.19%	5.30%
30	2.52	1.53	2.95	1.75	10.55	5.75	0.43	0.22	4.08%	3.83%
Total	**56.00**	**34.00**	**59.00**	**35.00**	**260.80**	**152.70**	**3.00**	**1.00**	**1.15%**	**0.65%**
Ave									**2.72%**	**2.62%**

NB:PM=Power Margins, $\varepsilon_P = |\Delta Pa - \Delta P|$, $\varepsilon_Q = |\Delta Qa - \Delta Q|$, $\mu_P = \varepsilon_P / Pmax$, $\mu_Q = \varepsilon_Q / Qmax$

Table 3.6.2-9 Power margins for Case30F020 and Case30F020b in pattern class III

BUS	PM(F020b)		PM(F020c)		Max load(F020c)		PM Diff (p.u.)		PM Diff (%)	
	ΔP	ΔQ	ΔPa	ΔQa	Pmax	Qmax	ε_P	ε_Q	μ_P	μ_Q
1	0.00	0.00	0.00	0.00	0.00	0.00	0.00	0.00	n/a	n/a
2	0.00	0.00	0.00	0.00	0.00	0.00	0.00	0.00	n/a	n/a
3	**2.52**	**1.53**	**2.38**	**1.40**	**5.38**	**3.20**	**0.14**	**0.13**	**2.60%**	**4.06%**
4	0.00	0.00	0.00	0.00	9.00	5.40	0.00	0.00	0.00%	0.00%
5	0.00	0.00	0.00	0.00	0.00	0.00	0.00	0.00	n/a	n/a
6	0.00	0.00	0.00	0.00	0.00	0.00	0.00	0.00	n/a	n/a
7	2.52	1.53	2.39	1.40	15.19	7.30	0.13	0.13	0.86%	1.78%
8	2.52	1.53	2.39	1.40	12.89	5.70	0.13	0.13	1.01%	2.28%
9	2.52	1.53	2.39	1.40	11.39	6.40	0.13	0.13	1.14%	2.03%
10	2.52	1.53	2.38	1.40	8.38	5.00	0.14	0.13	1.67%	2.60%
11	0.00	0.00	0.00	0.00	0.00	0.00	0.00	0.00	n/a	n/a
12	3.08	1.87	2.92	1.71	14.12	8.71	0.16	0.16	1.13%	1.84%
13	0.00	0.00	0.00	0.00	0.00	0.00	0.00	0.00	n/a	n/a
14	6.16	3.74	5.83	3.41	34.83	21.41	0.33	0.33	0.95%	1.54%
15	6.16	3.74	5.83	3.41	37.33	22.41	0.33	0.33	0.88%	1.47%
16	3.08	1.87	2.92	1.71	7.92	4.71	0.16	0.16	2.02%	3.40%
17	3.08	1.87	2.92	1.70	11.92	7.50	0.16	0.17	1.34%	2.27%
18	6.16	3.74	5.83	3.41	21.83	12.41	0.33	0.33	1.51%	2.66%
19	3.08	1.87	2.92	1.71	14.92	9.71	0.16	0.16	1.07%	1.65%
20	0.00	0.00	0.00	0.00	5.50	3.30	0.00	0.00	0.00%	0.00%
21	2.52	1.53	2.38	1.40	9.88	4.60	0.14	0.13	1.42%	2.83%
22	0.00	0.00	0.00	0.00	0.00	0.00	0.00	0.00	n/a	n/a
23	0.00	0.00	0.00	0.00	0.00	0.00	0.00	0.00	n/a	n/a
24	2.52	1.53	2.39	1.40	7.09	5.10	0.13	0.13	1.83%	2.55%
25	2.52	1.53	2.38	1.40	5.38	3.40	0.14	0.13	2.60%	3.82%
26	0.00	0.00	0.00	0.00	5.50	3.30	0.00	0.00	0.00%	0.00%
27	0.00	0.00	0.00	0.00	0.00	0.00	0.00	0.00	n/a	n/a
28	0.00	0.00	0.00	0.00	0.00	0.00	0.00	0.00	n/a	n/a
29	2.52	1.53	2.38	1.39	6.38	3.79	0.14	0.14	2.19%	3.69%
30	2.52	1.53	2.38	1.40	9.98	5.40	0.14	0.13	1.40%	2.41%
Total	**56.00**	**34.00**	**53.01**	**31.05**	**254.81**	**148.75**	**2.99**	**2.95**	**1.17%**	**1.98%**
Ave									**1.28%**	**2.14%**

NB:PM=Power Margins, $\varepsilon_P = |\Delta Pa - \Delta P|$, $\varepsilon_Q = |\Delta Qa - \Delta Q|$, $\mu_P = \varepsilon_P/Pmax$, $\mu_Q = \varepsilon_Q/Qmax$

Table 3.6.2-10 Power margins for Case30F020b and Case30F020c in pattern class III

(2) Remarks

Same again, within this simulation group (pattern class III), the average differences of power margins between the study cases are well below 10%. A few relatively high figures (up to 12.85%) have been observed between Case30F20 and Case30F20a. This is due to the severe system non-linerities under heavily loaded conditions.

4. Case study summaries

The simulation results from all the three groups (VSDF pattern classes) have consistently shown that the power system has very similar voltage stability when the VSDFs are in the same pattern class.

It is emphasised here that the 'similarity' of voltage stability is directly related to the pattern class determination for the VSDFs. The more pattern classes, the better the VSDFs can be represented, and consequently the more similar voltage stability will be for the same pattern class of VSDFs.

3.7 DISCUSSIONS AND CONCLUSIONS

In this chapter, some fundamental aspects of voltage stability problems have been examined. These include the basic characteristics and the determining factors of voltage stability. All the discussions were based on steady state analysis.

The basic characteristics study was initiated by examining voltage stability with a two bus simple system, and then extended into a multi-bus power system. The VP and VQ curves were used to explore the fundamental properties about voltage stability. A typical trajectory of voltage collapse with consideration of power system major dynamics and non-linearities was presented in this chapter.

Following the basic characteristics study, the voltage stability determining factors (VSDFs) were identified and defined. These determining factors are the load pattern, the load distribution patterns as well as the generation pattern and the generation participation pattern. The unique property of the VSDFs was investigated and generalised into a hypothesis. The theoretical validation for the hypothesis was also given in this chapter.

In this study, the pattern class feature was also observed with the voltage stability determining factors. It was found that a power system will have similar voltage stability when the VSDFs stay in the same pattern classes.

A large number of study cases were simulated on the IEEE 30 bus power system to study the impact of these determining factors. The results of the three testing groups under different system loading conditions were presented in this chapter to demonstrate the voltage stability similarity for the VSDFs in the same pattern classes.

The study presented in this chapter has laid a theoretical groundwork for the other parts of research in this project. The voltage stability determining factors theory is a significant development in revealing the mechanism of voltage stability in the steady state. Based on this theory, a knowledge based system for the prediction of voltage collapse using pattern recognition technique will be proposed in chapter 4, and a method for improving voltage stability through generation dispatch will be briefly discussed as a further study at end of this thesis.

CHAPTER 4 A KNOWLEDGE BASED SYSTEM FOR PREDICTION OF VOLTAGE COLLAPSE USING PATTERN RECOGNITION TECHNIQUE

4.1 INTRODUCTION

In this chapter, a knowledge-based system is proposed for prediction of voltage collapse by using pattern recognition technique. This system is based on the study results in chapter 3 that a power system will have similar voltage stability when the determining factors of voltage stability (VSDFs) belong to the same pattern class.

The principle of this prediction system is to compare a power network to a pre-studied system of which voltage stability is known. It consists of a basic knowledge based system and a pattern recognition module. The knowledge base of this system contains the pre-calculated power margin (PM) results for the prototypes of all the pattern classes for the VSDFs in a power system. By using pattern recognition technique, the pattern class of the VSDFs for a current state of the power system is identified, the solution to the current assessment of voltage stability can be found in the knowledge base.

This chapter starts with a brief review of basic theory about the knowledge based systems and pattern recognition techniques. Then the details for the design and implementation of the proposed system will be discussed. This prediction system has been simulated on the IEEE 30 bus power system, six study cases are presented in this chapter.

The simulation results show that the proposed system is capable of producing rather accurate results with speedy decision-making, hence has a good potential for the on-line application for prediction of voltage collapse.

2. Knowledge Base

The knowledge base comprises "all known knowledge" related to an application domain. It includes facts, laws/rules, descriptions of relations/phenomena, possible methods, heuristics and ideas for solving problems in the domain. Presentation of the knowledge is the key issue for a knowledge base. The "production rules" in the format of 'IF-THEN' have been widely used for the knowledge presentation.

3. Inference Engine

The main function of an inference engine is to infer solutions for a target problem based on certain inference strategies. It relies on the data in the data base and knowledge in the knowledge base. The inference strategies are the heart of the inference engine. Generally there are three kinds of inference strategies: the forward chaining, the backward chaining and the combination of these two.

(1) Forward chaining

The forward chaining strategy searches solutions from data to hypotheses, hence it is also called 'data directed' strategy. The forward chaining strategy as shown in Figure 4.2.1-2 includes following main steps:

Step 1: access the current data from the database; match the conditions of each rule in the knowledge base with the data.

Step 2: if the conditions of a rule are matched, add the conclusions of the rule as new facts into the data base.

Step 3: use the updated data to repeat step 1 to step 2 until no more new facts can be produced.

4.2 TECHNICAL BACKGROUND

In this section, some basic theory about the knowledge based system and pattern recognition techniques are going to be reviewed.

4.2.1 Knowledge Based Systems

Generally-speaking, a knowledge based system is a computer programme that has knowledge in a particular domain and is capable of solving the problems that require the knowledge. As such a system behaves like an expert in a specific area, it is also called Expert System.

A typical knowledge based system consists of four basic components: a data base, a knowledge base, an inference engine and a man-machine interface. The basic structure of a knowledge-based system is shown in Figure 4.2.1-1.

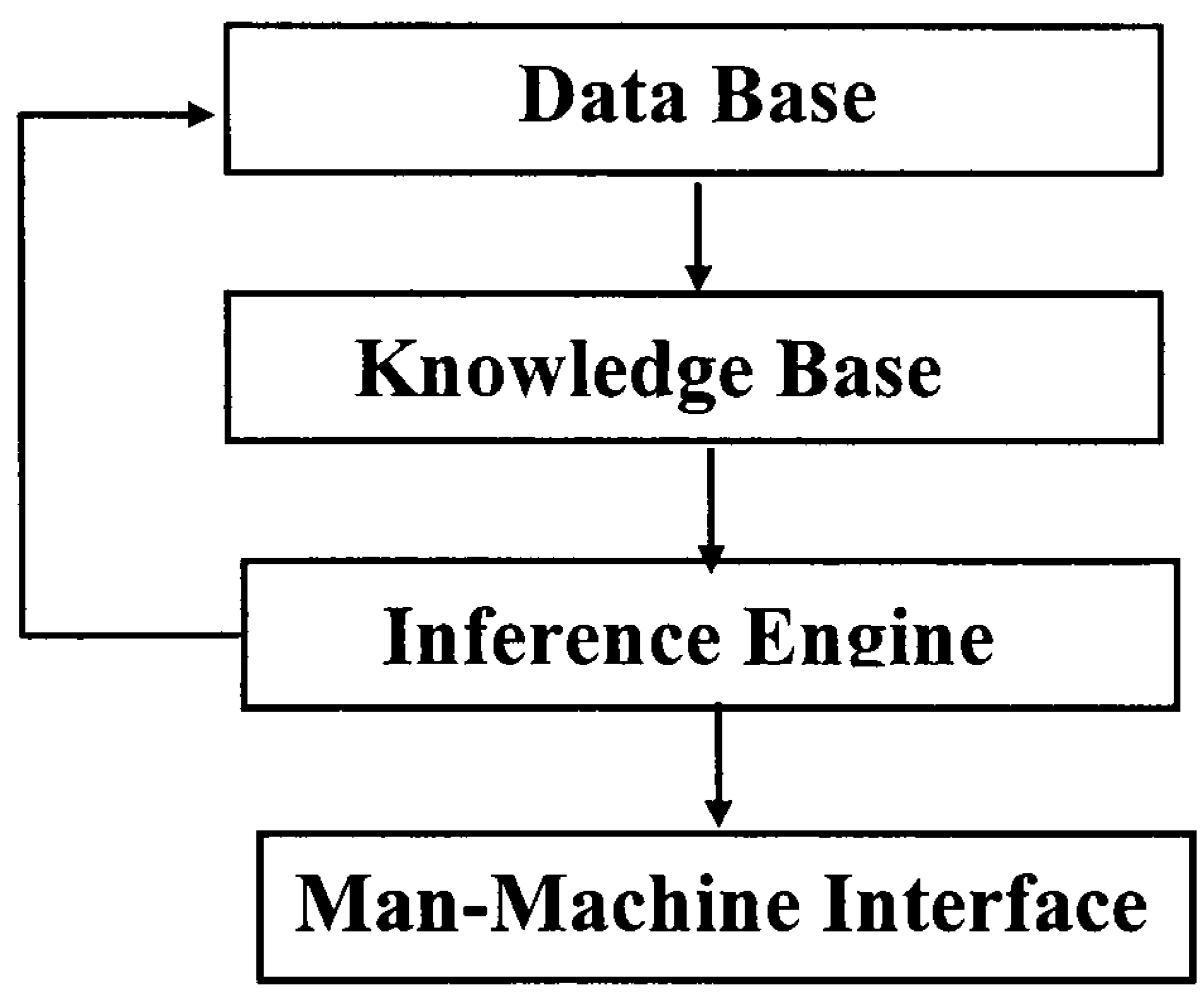

Figure 4.2.1-1 The basic structure of a knowledge based system

1. Data Base

The data base stores the data of a target system, on which decision-makings will be based. Sometimes the database is also used to keep the interim results of inferring actions. There are many methods for designing a data base. "Data tables" known as 'facts' is a most common and direct format for a data base.

2. Knowledge Base

The knowledge base comprises "all known knowledge" related to an application domain. It includes facts, laws/rules, descriptions of relations/phenomena, possible methods, heuristics and ideas for solving problems in the domain. Presentation of the knowledge is the key issue for a knowledge base. The "production rules" in the format of 'IF-THEN' have been widely used for the knowledge presentation.

3. Inference Engine

The main function of an inference engine is to infer solutions for a target problem based on certain inference strategies. It relies on the data in the data base and knowledge in the knowledge base. The inference strategies are the heart of the inference engine. Generally there are three kinds of inference strategies: the forward chaining, the backward chaining and the combination of these two.

(1) Forward chaining

The forward chaining strategy searches solutions from data to hypotheses, hence it is also called 'data directed' strategy. The forward chaining strategy as shown in Figure 4.2.1-2 includes following main steps:

Step 1: access the current data from the database; match the conditions of each rule in the knowledge base with the data.

Step 2: if the conditions of a rule are matched, add the conclusions of the rule as new facts into the data base.

Step 3: use the updated data to repeat step 1 to step 2 until no more new facts can be produced.

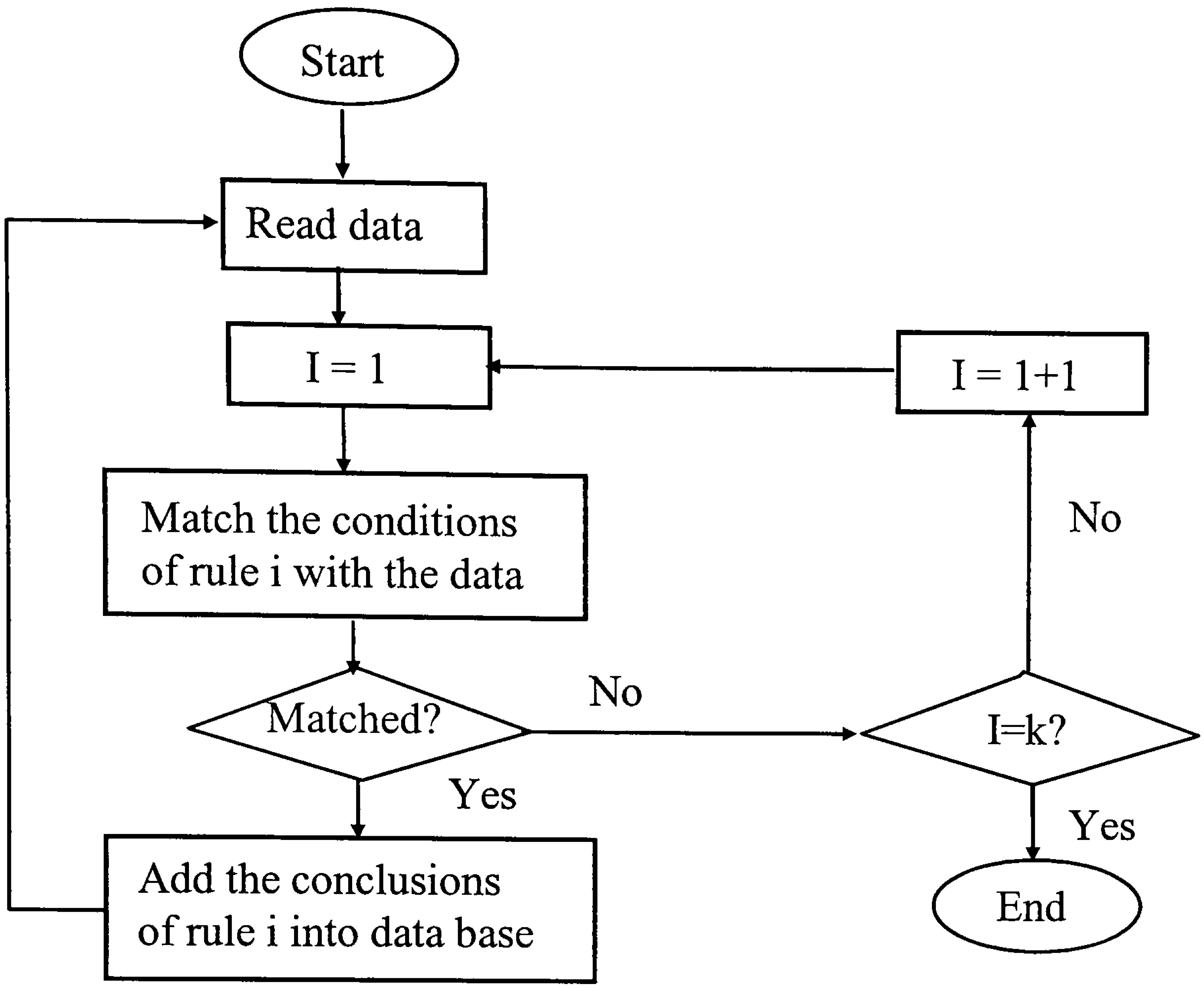

Figure 4.2.1-2 The flow chart of the forward chaining strategy

(2) Backward chaining

The backward chaining strategy searches for data to prove or disprove a hypothesis, it is also called 'goal directed' strategy. Its working procedure involves:

Step 1: propose a set of hypotheses (conclusions), check if the proposed hypotheses are in the data base. If they are, then inference is finished. Otherwise go to step 2.

Step 2: search the rules in the knowledge base. For the rules of which conclusions are matched to the hypotheses, treat their conditions as new hypotheses go to step 1 until no more new hypotheses are produced.

The flow chart for this backward chaining strategy is shown in Figure 4.2.1-3.

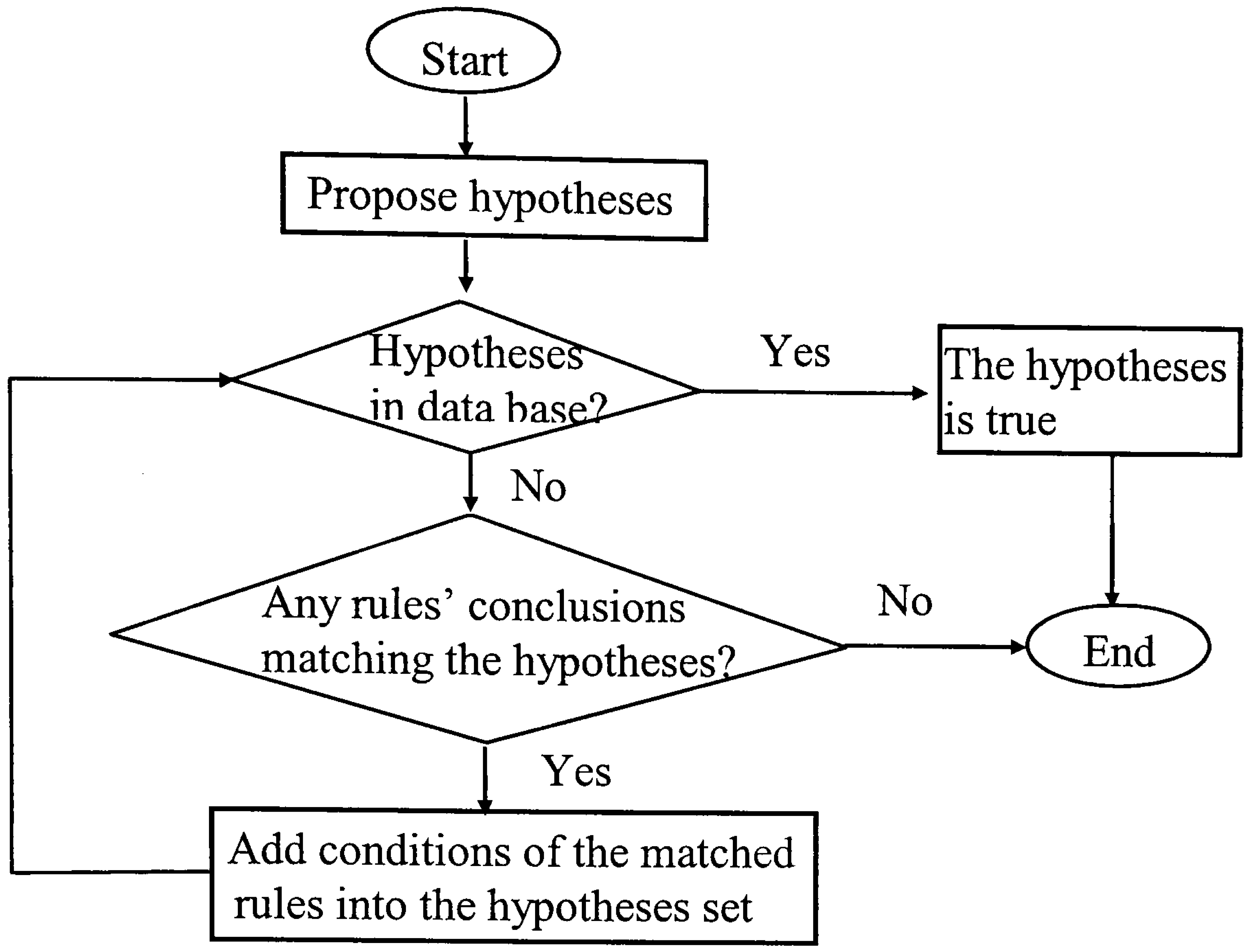

Figure 4.2.1-3 The flow chart of the backward chaining strategy

(3) Combined chaining

The pure forward chaining strategy may lead to unfocused questioning, whereas the sole backward chaining tends to be rather relentless in its goal-directed questioning. To copy with those problems, a new strategy is designed by combining the above two strategies, called the 'combined chaining'.

For a questioned problem, the combined chaining strategy uses the forward chaining to help to propose a set of hypotheses. Then, backward chaining will be used to verify the proposed hypotheses. This combined chaining strategy is usually used under following three conditions:

(i) There are insufficient facts in the data base, such that no rules can be fully matched by the data.

(ii) The data or inferred hypotheses have low credibility. There may be more than one solution searched out.

(iii) To confirm whether there are any or more solutions. This is specifically targeting on the relentlessness problem of the backward chaining.

The above inference strategies are three basic ones. There are many others strategies for solving special or complicated problems, such as the fuzzy logic strategy for tackling uncertain issues.

4. Man-Machine Interface

The man-machine interface provides communication media between users and the knowledge-based system. It can also provide the user with an insight into the problem-solving process executed by the inference engine. A common method to implement this function is to retrace the reasoning steps that lead to questions or conclusions.

It must be pointed out that in the area of Artificial Intelligence, there are different opinions concerning the structures of knowledge-based systems. For instance, the data base is sometimes merged with the knowledge base, the man-machine interface is often regarded as part of inference engine, etc. What have been reviewed in this section are some basic concepts to illustrate the principle of a knowledge-based system.

4.2.2 Pattern Recognition

The function of pattern recognition is to assign a new object on the basis of a set of measurements to one of the known groups (pattern classes). A typical pattern recognition task involves data acquisition, pattern analysis, and pattern classification.

1. Data acquisition

The main function of data acquisition is to gather analogue data from physical sources and converting them into a digitised-format. Those digitised data will be kept in a data base for further processing. This is normally the first phase of a pattern recognition task.

2. Pattern analysis

After data acquisition, the data will be analysed for some recognisable structures or features that can be formulated for further systematic investigation. The pattern analysis usually includes feature extraction and selection, and pattern class determination. This is the second phase for a pattern recognition task.

(1) Feature extraction and selection

So-called 'features' are normally variables which are used to describe the state of a target object (pattern). These variables can be extracted from the collected data. Selection of appropriate features is crucial to the success of a pattern recognition task. There may be a large number of features that could be used to describe the state of an object. If all these features were selected, it would cause massive computation burden to slow down the pattern recognition process. However, if too few features were selected, the accuracy of the pattern recognition would not be guaranteed.

(2) Pattern class determination

Pattern class determination is also called 'cluster' determination. It decides the number of classes into which the patterns can be classified. The pattern classes must be determined in such way that they are able to represent all the likely states of a target object. How many pattern classes are needed depends on the requirement of a pattern recognition task. Compromise between the speed and accuracy often has to be made in order to choose a right number of pattern classes.

(3) Pattern vectors and pattern space

Each of the selected features can be regarded as a variable in an n-dimensional space, where each feature is assigned to a dimension. This space is called feature space or pattern space. Thus, a state of the target object or a pattern presents a point in the pattern space. When a pattern is described by more than one feature, it is multi-dimensional, and can be expressed by a vector X:

$$\mathbf{X} = [\, X_1 \;\; X_2 \;\; \dots \;\; X_i \;\; \dots \;\; X_N \,]^T$$

where,

X_i is the i-th feature, $i = 1, 2, ..., N$,

N is the total number of features.

3. Pattern classification

Pattern classification is the final phase of a pattern recognition task. Its function is to best match the analysed information to a known class of patterns. This is achieved by using some computer algorithms called 'classifiers'.

As mentioned above, the patterns can be presented as points in a pattern space. All the patterns belonging to the same class will form a distinct cluster (class) in the pattern space. The classifier determines to which class a target pattern belongs.

(1) Decision functions

The classifiers are usually designed as a set of functions. Those functions are called 'decision functions'. Geometrically it is known that in a two dimensional system, one decision function separates two classes; and it needs several functions to separate three or more classes. The decision functions can be either linear or non-linear. In the n dimensional case, a set of the linear decision functions can be written as:

$$\mathbf{W} \bullet \mathbf{X} = \mathbf{0}$$

$$\mathbf{W}=\begin{bmatrix} w_{11} & w_{12} & \cdots & \cdots & w_{1N} \\ w_{21} & w_{22} & \cdots & \cdots & w_{2N} \\ \cdots & \cdots & \cdots & \cdots & \cdots \\ w_{M1} & w_{M2} & \cdots & \cdots & w_{MN} \end{bmatrix}$$

where

$\mathbf{X} \in \Re^{NX1}$	is the vector of pattern features (variables),
$\mathbf{W} \in \Re^{MXN}$	is the coefficients matrix,
N	is the number of features,
M	is the number of decision functions.

(2) Classifiers

Two most popular classifiers are the multi-category classifier and the minimum distance classifier. Those two classifiers are briefly introduced below.

(i) Multi-category classifier

There are many variants for the multi-category classifier. A basic one is to consider a given class as one class and rest of classes as the second class. Following this idea, it is easy to see that one decision function is needed to separate two classes. To separate N classes, N decision functions will be required.

(ii) Minimum distance classifier

The principal of the minimum distance classifier is to measure the Euclidean distance between a given pattern to the prototypes of each pattern class. The one whose prototype is nearest will be identified as the class for the given pattern. The prototype or cluster centre represents the typical values of a pattern class. It is usually located at an average distance from the all patterns (points) in the cluster it represents. For a cluster of N points, the value of a prototype point can be determined by

$$\mathbf{Z}=\frac{1}{N}\sum_{i=1}^{N}\mathbf{X}^{i}$$

where,

$\mathbf{X}^{i}$ is the i-th pattern (point) in the pattern class, i=1, 2, ..., N.

Thus the Euclidean distance from a given pattern point $\mathbf{X}$ to a prototype point $\mathbf{Z}^{i}$ can be calculated by:

$$D^i = [\omega_1(X_1 - Z_1^i)^2 + \omega_2(X_2 - Z_2^i)^2 + \ldots + \omega_K(X_K - Z_K^i)^2 + \ldots + \omega_N(X_N - Z_N^i)^2]^{1/2}$$

where,

$\mathbf{D}^i$ is the Euclidean distance from a given pattern $\mathbf{X}$ to the prototype of a pattern class $\mathbf{Z}^i$,

X_K is the value of feature K for the given pattern $\mathbf{X}$,

ω_K is the weighting factor for feature K,

Z_K^i is the value of feature K for the prototype $\mathbf{Z}^i$.

It is easy to see that to distinguish N pattern classes, the Euclidean distance has to be calculated N times.

(3) Training set

Decision functions have to be "trained" by trying them on a set of patterns for which the classifications are already known, and the modifying them until a satisfactory result is obtained. This set of known patterns is called the training set. The training set can be expressed by matrix as:

$$\mathbf{T} = \begin{bmatrix} X_1^1 & X_1^2 & \cdots & \cdots & X_1^M \\ X_2^1 & X_2^2 & \cdots & \cdots & X_2^M \\ \cdots & \cdots & \cdots & \cdots & \cdots \\ X_N^1 & X_N^2 & \cdots & \cdots & X_N^M \end{bmatrix}$$

where

$\mathbf{X}^i = \begin{bmatrix} X_1^i & X_2^i & \cdots & \cdots & X_N^i \end{bmatrix}^T$ is pattern i in the training set T, i = 1, 2, ..., M,

M is the number of patterns in the training set.

4.3 A KNOWLEDGE BASED SYSTEM FOR PREDICTION OF VOLTAGE COLLAPSE

In this section, the principle and basic structure of a knowledge based for prediction of voltage collapse system will be discussed.

4.3.1 System Principle

1. Basic principle

As discussed in Chapter 3 that the Voltage Stability Determining Factors (VSDFs) uniquely determine the voltage stability for a power system, and the power system will have similar voltage stability when the VSDFs stay in the same pattern class. Therefore, for a power system, if its pattern classes of VSDFs can be determined, and power margins for the prototypes of the pattern classes can be pre-calculated, the voltage stability at any moment can be predicted by simply identifying the pattern class of VSDFs for the current state of the power system. Based on this idea, a real time system is proposed for fast prediction of voltage collapse by using an Artificial Intelligence approach.

This prediction system consists of a knowledge-based system and a pattern recognition module. The knowledge base in the system contains pre-calculated voltage stability results (power margins) for the prototypes of all the pattern classes of VSDFs extracted for a power system. The data base of this knowledge-based system will be linked to a SCADA system and regularly fed with real time data of the power system. By using pattern recognition technique, the pattern class of the VSDFs for the current state (target state) of the power system can be recognised, and the power margins results for identified pattern class will be found in the knowledge base as the initial solution to the current assessment of voltage stability.

As mentioned in Chapter 3, a pattern class for the VSDFs contains 4 sub-pattern classes associated with 4 different types of VSDFs, hence the prototype for a pattern class of the VSDFs will contains 4 segments.

2. Solution Compensation

Although a power system has similar voltage stability when its VSDFs are in the same pattern class, the power margins will not be exactly the same. This means that the initial solution produced by the knowledge based system may not be sufficiently accurate, particularly when there are only a small number of the pattern classes determined for the VSDFs. This inaccuracy is largely due to discrepancies of the Load pattern and load distribution pattern between the target state and the prototype of a pattern class. It can be analysed as the follows:

From the discussions in Chapter 3, it is known that

$$\Delta P_i = P_i^{MAX} - P_i^0 = X_i^{LDP} * \Delta P_\Sigma^{MAX} \qquad (4.3.1\text{–}1)$$

$$\Delta Q_i = Q_i^{MAX} - Q_i^0 = X_i^{LDQ} * \Delta Q_\Sigma^{MAX} \qquad (4.3.1\text{–}2)$$

where,

ΔP_i, ΔQ_i and ΔP_Σ, ΔQ_Σ are the active and reactive power margins for a bus i and the whole system respectively,

P_i^0, Q_i^0 are the active and reactive power load at an initial operation state for a bus I,

P_i^{MAX}, Q_i^{MAX} and P_Σ^{MAX}, $Q_\Sigma^{MA\Xi}$ are the maximum active and reactive loads for a load bus i and the whole system.

X_i^{LDP}, X_i^{LDQ} are the active and reactive coefficients of the load distribution pattern at bus i.

By using the "α" to note the results produced by the knowledge based system, a similar set of equations are obtained as

$$\Delta P_i^\alpha = P_i^{\alpha MAX} - P_i^{\alpha 0} = LD_i^P * \Delta P_\Sigma^{\alpha MAX} \qquad (4.3.1\text{–}3)$$

$$\Delta Q_i^\alpha = Q_i^{\alpha MAX} - Q_i^{\alpha 0} = LD_i^Q * \Delta Q_\Sigma^{\alpha MAX} \qquad (4.3.1\text{–}4)$$

where,

LD_i^P and LD_i^Q are the active and reactive load distribution coefficients for the prototype of the pattern class at bus i.

From equations (4.3.1 – 1), (4.3.1 – 2), (4.3.1 – 3), (4.3.1 – 4), the error between the real power margins and the predicted ones can be calculated as

$$\begin{aligned}\delta_P^i &= \Delta P_i - \Delta P_i^\alpha \\ &= X_i^{LDP} * \Delta P_\Sigma^{MAX} - LD_i^P * \Delta P_\Sigma^{\alpha MAX}\end{aligned} \qquad (4.3.1\text{–}5)$$

$$\delta_Q^i = \Delta Q_i - \Delta Q_i^{\alpha}$$
$$= X_i^{LDP} * \Delta Q_\Sigma^{MAX} - LD_i^Q * \Delta Q_\Sigma^{\alpha MAX} \qquad (4.3.1\text{–}6)$$

It is also known that,

$$\Delta P_\Sigma^{MAX} = P_\Sigma^{MAX} - P_\Sigma^0 \qquad (4.3.1\text{–}7)$$

$$\Delta Q_\Sigma^{MAX} = Q_\Sigma^{MAX} - Q_\Sigma^0 \qquad (4.3.1\text{–}8)$$

Where,

$$P_\Sigma^{MAX} = \sum_{i=1}^{n} P_i^{MAX}$$

$$Q_\Sigma^{MAX} = \sum_{i=1}^{n} Q_i^{MAX}$$

$$P_\Sigma^0 = \sum_{i=1}^{n} P_i^0$$

$$Q_\Sigma^0 = \sum_{i=1}^{n} Q_i^0$$

$P_\Sigma{}^0$, $Q_\Sigma{}^0$ are the active and reactive power load at an initial operation state for the whole system,

n is the total number of buses in a power system.

Similarly there are,

$$\Delta P_\Sigma^{\alpha MAX} = P_\Sigma^{\alpha MAX} - P_\Sigma^{\alpha 0} \qquad (4.3.1\text{–}9)$$

$$\Delta Q_\Sigma^{\alpha MAX} = Q_\Sigma^{\alpha MAX} - Q_\Sigma^{\alpha 0} \qquad (4.3.1\text{–}10)$$

where,

$$P_\Sigma^{\alpha MAX} = \sum_{i=1}^{n} P_i^{\alpha MAX}$$

$$Q_\Sigma^{\alpha MAX} = \sum_{i=1}^{n} Q_i^{\alpha MAX}$$

$$P_\Sigma^{\alpha 0} = \sum_{i=1}^{n} P_i^{\alpha 0}$$

$$Q_\Sigma^{\alpha 0} = \sum_{i=1}^{n} Q_i^{\alpha 0}$$

When the VSDFs belong to the same pattern class, it can be assumed that the total maximum loading level for the power system remain roughly the same, hence

$$P_\Sigma^{MAX} \approx P_\Sigma^{\alpha MAX} \qquad (4.3.1\text{–}11)$$

$$Q_\Sigma^{MAX} \approx Q_\Sigma^{\alpha MAX} \qquad (4.3.1\text{–}12)$$

With substitution using equations (4.3.1 – 7), (4.3.1 – 8), (4.3.1 – 9), (4.3.1 – 10), (4.3.1– 11), (4.3.1 – 12), equations (4.3.1 – 5) and (4.3.1 – 6) become:

$$\delta_P^i = \Delta P_i - \Delta P_i^\alpha = X_i^{LDP}(P_\Sigma^{a0} - P_\Sigma^0) + \Delta P_\Sigma^{\alpha MAX} * (X_i^{LDP} - LD_i^P) \qquad (4.3.1\text{–}13)$$

$$\delta_Q^i = \Delta Q_i - \Delta Q_{\alpha i} = X_i^{LDQ}(Q_\Sigma^{a0} - Q_\Sigma^0) + \Delta Q_\Sigma^{\alpha MAX} * (X_i^{LDQ} - LD_i^Q) \qquad (4.3.1\text{–}14)$$

Re-ordering equations (4.3.1 – 13) and (4.3.1 – 14) produces:

$$\Delta P_i = \Delta P_i^\alpha + \delta_P^i = \Delta P_i^\alpha + X_i^{LDP}(P_\Sigma^{a0} - P_\Sigma^0) + \Delta P_\Sigma^{\alpha MAX} * (X_i^{LDP} - LD_i^P) \qquad (4.3.1\text{–}15)$$

$$\Delta Q_i = \Delta Q_i^\alpha + \delta_Q^i = \Delta Q_i^\alpha + X_i^{LDQ}(Q_\Sigma^{a0} - Q_\Sigma^0) + \Delta Q_\Sigma^{\alpha MAX} * (X_i^{LDQ} - LD_i^Q) \qquad (4.3.1\text{–}16)$$

Equations (4.3.1–15) and (4.3.1–16) provide a compensation method to improve the accuracy of the initial results produced by the knowledge based system. All the parameters involved in these equations are either already in the data base or become available as interim results from the solution searching of the knowledge based system.

The application of this compensation method will be demonstrated in the simulation section of this Chapter. Accuracy analyses on the simulation results are also included in the section.

4.3.2 System Structure

The high level structure of this knowledge based system will be outlined in this section. The details of each function modules will be further discussed in the section of system implementation.

The proposed system consists of a data base, a knowledge base, an inference engine, a pattern recogniser and a man-machine interface. A supporting kit is also included in this system. As the basic functions of these modules have been discussed in the section 4.2, only a few special points of this system are emphasised below.

1. The Database

The data base of the proposed system stores all the required "raw data" for a power system. Those raw data include the current and historic load and generation information, structural and operational parameters of the power network, weather forecast information, time etc. This data base will be linked or merged with the data base for the Supervisory Control and Data Acquisition (SCADA) system for a power system. It will be periodically updated.

2. Knowledge base

The knowledge base mainly contains two categories of "knowledge". The first category includes the pattern recognition related rules, formulas and heuristic information. The second one consists of the power margins for the prototypes of all pattern classes for the VSDFs.

3. Inference engine

As this knowledge based system relies on the data in the database to reach a solution, the forward chaining is chosen as the inferring strategy for the system.

4. The man-machine interface

The man-machine interface provides a two way communication between the proposed system and users. It takes instructions from users at start, and represents the predication results into a user-friendly format with some explanations once a solution is reached. It also provides an access for the designers or authorised users to change system settings or conduct some further development work.

5. The supporting kit

The supporting kit has three major functions. The first one is for on-line application, including calculation of the VSDFs for the current state of the power system, calculation of the Euclidean distance for the pattern recognition, and the accuracy compensation for the initial prediction solution. The second function is the power system analysis, which will be called to calculate power margins for a target state when the solution can not be reached by the prediction system. This function requires user intervention for the decision-making. The third function is the off-training package which used to accommodate newly identified pattern classes or other further development work. The structure of this prediction system is shown in Figure 4.3.2-1 below.

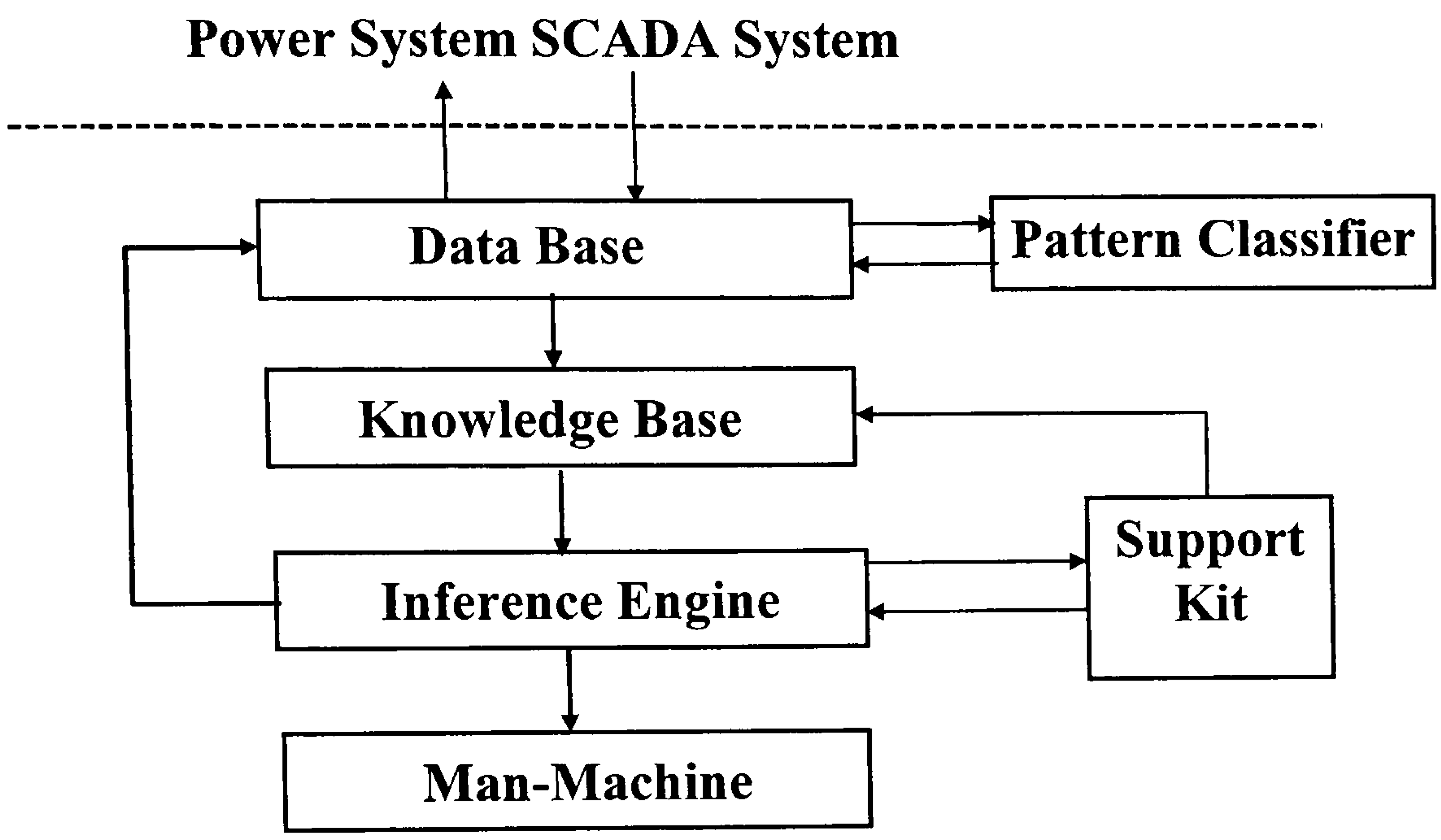

Figure 4.3.2-1 The structure of the prediction system

4.3.3 System operation

The operation of this knowledge based system involves a two stage process: the off-line training and the on-line decision-making.

1. The off-line training

This prediction system is designed with a generic infrastructure, which can be used for any power systems. To apply this system to a specific power system, there is a need to configure and train the system with the information about the power system. As this customisation process is off-line implemented, it is called 'off-line training'. The off-line training involves the following activities:

(1) Pattern Feature selection,

(2) Pattern class determination,

(3) Power margins calculation,

(4) System training and commissioning.

The details about this off-line training will be discussed at later stage of this chapter.

2. The on-line decision-making

The on-line decision-making fulfils the ultimate function of this prediction system. At this stage of operation, the data in the database will be periodically updated. When a decision-making is initiated manually or automatically, the system will try to search the solutions following the procedure below:

<u>Step 1</u>: Read the data from the database, calculate the VSDFs for the current state;

<u>Step2:</u> Recognise the pattern class of the VSDFs for the target state;

<u>Step 3</u>: Start the inference engine to search solutions

<u>Step 4:</u> If a solution is reached, perform accuracy compensation calculation, go to Step 7.

<u>Step 5:</u> Ask user if the power system analysis is required? If the answer is yes, the software in the supporting kit will be called to calculate power margins, go to Step 6. If not, feed 'No solution reached' to the man-machine interface.

Step 7: The man-machine interface presenting the final results in a required format (tables), end the decision-making.

The on-line decision-making process is shown in the flow chart Figure 4.3.3-1.

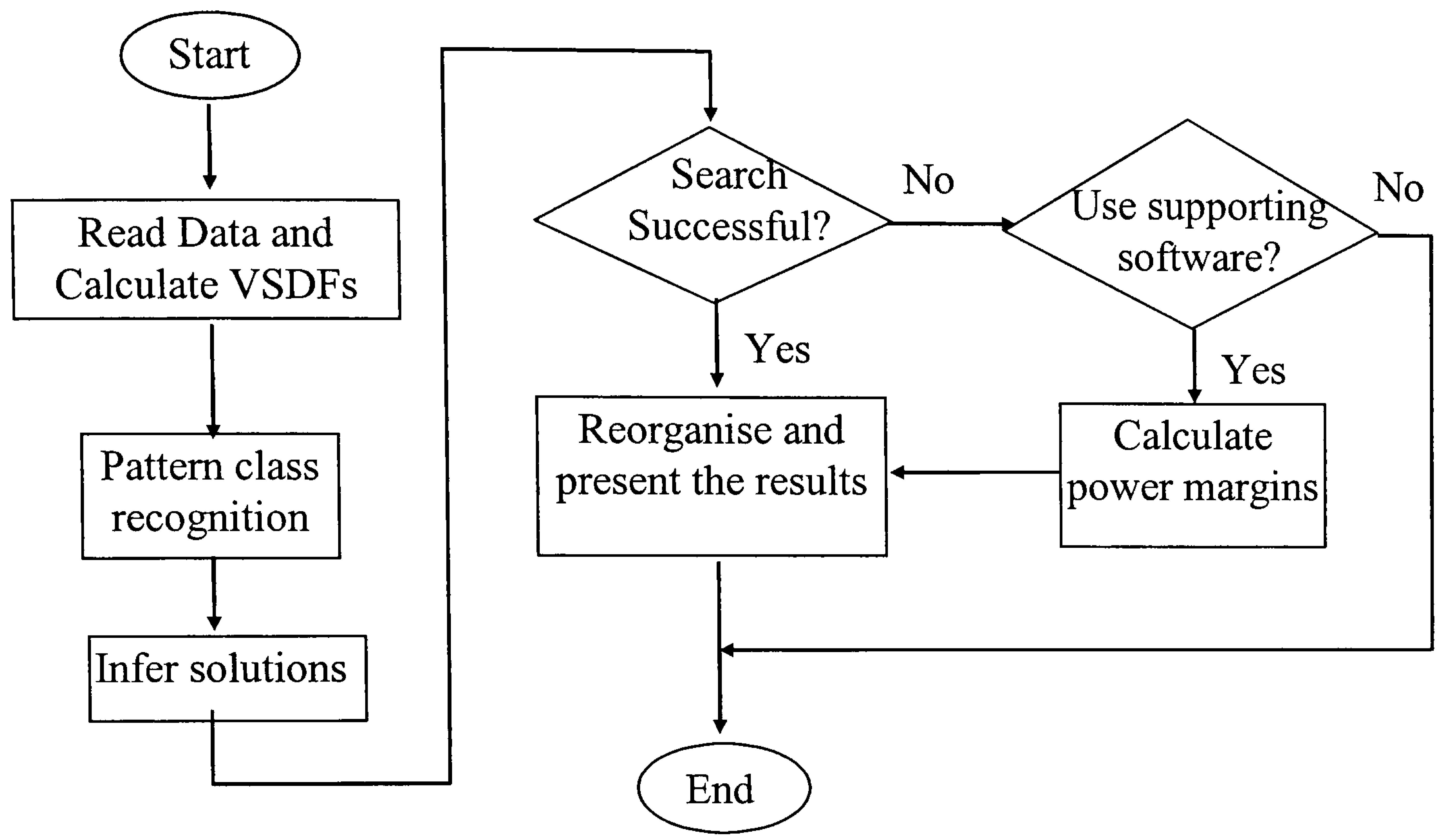

Figure 4.3.3-1 The flow chart of the on-line decision-making process

4.4 SYSTEM IMPLEMENTATION

This section deals with the details about implementing the knowledge based system for prediction of voltage collapse.

4.4.1 The Pattern Recognition Module

Implementation of the pattern recognition module involves the following three steps:

1. Pattern feature selection,
2. Training set creation,
3. Pattern classification (recognition).

1. Pattern Feature Selection

As discussed in Section 4.2, appropriately selecting a set of pattern features is critical to the success of a pattern recognition function. The features shall be selected in such way that, on one hand they are capable of sufficiently describing the state (pattern) of a target object to secure the accuracy of the results; on the other hand the features shall not be too many in order to achieve a good decision-making speed.

For this application, a pattern of VSDFs can be accurately described by their coefficients as defined in Chapter 3. However, it is impractical to select all those coefficients as pattern features, as a real power system can easily have over a thousand buses, and the total number of VSDF coefficients will be as many as eight times of the bus number.

It is known from the discussions in chapter 3, that the state of the VSDFs is strongly influenced by the environmental and operational conditions of a power system. The seasons of a year, hours of a day, weather conditions, power system operation arrangement are the typical influencing factors. Therefore, those influencing factors together with some key VSDF coefficients can be used as the pattern features for the VSDFs. Based on this consideration, the following pattern features are proposed for each type of the VSDFs:

(1) The pattern features for the load pattern

(i) Load levels at some heavy loaded buses,

(ii) Month of a year, from January to December,

(iii) Day of a week, i.e. Monday to Sunday

(iv) Time of a day, i.e. the real time: Hours: Minutes

(v) Weather condition, including fine, cloudy, raining or snowing,

(vi) Temperature, in °C,

(vii) Power system running arrangement (network topology) numbered by 1,2, 3...,

By using those selected features, the load pattern can be represented by

$$\mathbf{X}_\rho = \begin{bmatrix} X_{\rho 1} & X_{\rho 2} & \cdots & X_{\rho i} & \cdots & X_{\rho N_\rho} \end{bmatrix}^T$$

where,

$X_{\rho i}$ is the i-th feature for the load pattern, i=1, 2, ..., N_ρ,

N_ρ is the total number of selected features for the load pattern.

(2) The pattern features for the load distribution pattern

Most the pattern features selected for the load distribution pattern are the same as those for the load pattern except the first one, which is the load distribution coefficients at some selected buses. Those load distribution coefficients can be calculated by using current and historical load data as:

$$LD_i^P(t) = \frac{L_i^P(t) - L_i^P(t_1)}{\sum_{I=1}^{N_L}\left(L_i^P(t) - L_i^P(t_1)\right)}$$

$$LD_i^Q(K) = \frac{L_i^Q(t) - L_i^Q(t_1)}{\sum_{I=1}^{N_L}\left(L_i^Q(t) - L_i^Q(t_1)\right)}$$

where

$LD_i^P(t), LD_i^Q(t)$ are the active and reactive load distribution coefficients for a load bus i at time instant t,

$L_i^P(t), L_i^Q(t)$ and $L_i^P(t_1), L_i^Q(t_1)$ are the active and reactive load at a load bus i at time instant t and t_1 respectively,

N_L is the total number of load buses in a power system.

By these selected features, the load distribution pattern can be represented by:

$$X_a = \begin{bmatrix} X_{a1} & X_{a2} & \cdots & X_{ai} & \cdots & X_{aN_a} \end{bmatrix}^T$$

where,

$X_{\alpha i}$ is the i-th feature for the load distribution pattern, i=1, 2, ..., N_α,

N_α is the total number of selected features for the load distribution pattern.

(3) The pattern features for the generation and the generation participation pattern

The pattern features selected for the generation pattern and the generation participation pattern are almost identical except for the first one:

- (i) Generation outputs of major power plants for the generation pattern, or the Generation participation coefficients at major power plants for the generation participation pattern,
- (ii) Month of a year, from January to December,
- (iii) Day of a week, i.e. Monday to Sunday
- (iv) Time of a day, i.e. the real time: Hours:Minutes
- (v) Weather condition, including fine, cloudy, raining/snowing,
- (vi) Unit commitment arrangement: numbered by 1, 2, 3...,

The coefficients of the generation participation pattern can be calculated as

$$GP_i^P(t) = \frac{G_i^P(t) - G_i^P(t_1)}{\sum_{I=1}^{N_G}\left(G_i^P(t) - G_i^P(t_1)\right)}$$

$$GP_i^Q(t) = \frac{G_i^Q(t) - G_i^Q(t_1)}{\sum_{I=1}^{N_G}\left(G_i^Q(t) - G_i^Q(t_1)\right)}$$

where

$GP_i^P(t), GP_i^Q(t)$ are the active and reactive generation participation coefficients for a generation bus i at time instant t,

$G_i^P(t), G_i^Q(t)$ and $G_i^P(t_1), G_i^Q(t_1)$ are the active and reactive generation output at a generation bus i at time instant t and t_1 respectively,

N_G is the total number of generation buses in a power system.

By those pattern features, the generation pattern can be represented as:

$$\mathbf{X}_\Gamma = \left[X_{\Gamma 1} \quad X_{\Gamma 2} \quad \dots \quad X_{\Gamma i} \quad \dots \quad X_{\Gamma N_\Gamma}\right]^T$$

and the generation participation pattern can be represented:

$$\mathbf{X}_\beta = \left[X_{\beta 1} \quad X_{\beta 2} \quad \dots \quad X_{\beta i} \quad \dots \quad X_{\beta N_\beta}\right]^T$$

where,

$X_{\Gamma i}$ is the i-th feature for the generation pattern, i=1, 2, ..., N_Γ,

N_Γ is the total number of selected features for the generation pattern.

$X_{\beta i}$ is the i-th feature for the generation participation pattern, i=1, 2, ..., N_β,

N_β is the total number of selected features for the generation participation pattern.

It should be pointed out that in most power systems, the number of power plants is much less than the number of load buses. Thus, all the coefficients of generation and generation participation patterns may be directly selected as the pattern features for these two VSDFs, i.e.:

$$\mathbf{X}_G = \mathbf{G}$$

$$\mathbf{X}_\beta = \mathbf{GP}$$

Where

$$\mathbf{G} = [\mathbf{G}^\mathbf{P}, \mathbf{G}^\mathbf{Q}]$$

$$\mathbf{G}^\mathbf{P} = [\, G^P1, G^P2 \dots G^Pi \dots G^Pn]$$

$$\mathbf{G}^\mathbf{Q} = [G^Q1, G^Q 2 \dots G^Q i \dots G^Q n,]$$

$$\mathbf{GP} = [\mathbf{GP}^\mathbf{P}, \mathbf{GP}^\mathbf{Q}]$$

$$\mathbf{GP}^\mathbf{P} = [\, GP^P1, GP^P2 \dots GP^Pi \dots GP^Pn]$$

$$\mathbf{GP}^\mathbf{Q} = [GP^Q1, GP^Q 2 \dots GP^Q i \dots GP^Q n,]$$

2. Training Set Creation

The pattern recognition technique is used in this prediction system by comparing the states of the voltage stability determining factors (VSDFs) of a real power system (the target state) to a large training set. This training set contains the prototypes of all the pattern classes selected to represent all the likely states of the VSDFs of the power system.

As the VSDFs include four different factors, there is a need to create four training sub-sets for the pattern recognition in the proposed system. Using load pattern as an example, its training sub-set can be expressed in matrix as:

$$\mathbf{T}_\rho = \begin{bmatrix} \mathbf{X}_\rho^1 & \mathbf{X}_\rho^2 & \cdots & \mathbf{X}_\rho^i & \cdots & \mathbf{X}_\rho^{N_{C\rho}} \end{bmatrix}$$

$$= \begin{bmatrix} X_{\rho 1}^1 & X_{\rho 1}^2 & \cdots & X_{\rho 1}^i & \cdots & X_{\rho 1}^{N_{C\rho}} \\ X_{\rho 2}^1 & X_{\rho 2}^2 & \cdots & X_{\rho 2}^i & \cdots & X_{\rho 2}^{N_{C\rho}} \\ \cdots & \cdots & \cdots & \cdots & \cdots & \cdots \\ X_{\rho N_\rho}^1 & X_{\rho N_\rho}^2 & \cdots & X_{\rho N_\rho}^i & \cdots & X_{\rho N_\rho}^{N_{C\rho}} \end{bmatrix}$$

where,

$$\mathbf{X}_\rho^i = \begin{bmatrix} X_{\rho 1}^i & X_{\rho 2}^i & \cdots & X_{\rho j}^i & \cdots & X_{\rho N_\rho}^i \end{bmatrix}^T$$

is the prototype of the i-th pattern class for the load pattern, i= 1, 2, ... $N_{C\rho}$,

$N_{C\rho}$ is the number of pattern classes for the load pattern.

The training sub-sets for the load distribution pattern, generation pattern and generation participation pattern have a very similar format.

3. Pattern Recognition

The task of pattern recognition in this prediction system is to recognise the pattern class of the VSDFs to which a target state of a power system belongs. It is the final step of the whole pattern recognition process. Based on nature of the VDSFs, the minimum distance is chosen to be classifier for the pattern recognition in this application.

From the technical background, it is known that the minimum distance classifier uses the Euclidean distance as the decision function. The Euclidean distance between a target pattern and the prototype of a pattern class for is calculated by

$$D^i = [\omega_1(X_1 - Z_1^i)^2 + \omega_2(X_2 - Z_2^i)^2 + \ldots + \omega_K(X_K - Z_K^i)^2 + \ldots + \omega_N(X_N - Z_N^i)^2]^{1/2}$$

where,

D^i is the Euclidean distance from a target pattern $\mathbf{X}$ to the prototype of pattern class i,

$\mathbf{Z}^i$ is the prototype of pattern class i,

$$X=\begin{bmatrix} X_1 & X_2 & \dots & X_K & \dots & X_{N_f} \end{bmatrix},$$

$$Z^i=\begin{bmatrix} Z_1^i & Z_2^i & \dots & Z_K^i & \dots & Z_{N_f}^i \end{bmatrix},$$

X_K is the value of feature K for the target pattern, K=1, 2, ..., N_f,

Z_K^i is the value of feature K for the prototype of class i, K=1, 2, ..., N_f,

N_f is the number of selected features,

ω_K is the weighting factor for feature K.

Weighting factors introduced here is to reflect different influencing power that each pattern features may have on the pattern recognition.

The Euclidean distance in the proposed system includes four segments, each associated with a type of VSDF.

4.4.2 The Knowledge Based System

As shown in Figure 4.3.2-1, the knowledge-based system in this application includes a data base, a knowledge base, an inference set, a man-machine interface as well as a supporting kit.

1. The database

The database in the proposed system has two main functions. One is to store and regularly update "raw data" of a power system. The raw data contain all the structural and operational information about a power system, including the system parameter (e.g. line impedance), network running arrangement, the active and reactive power injections and voltage measurement etc. Most of the raw data are directly fed from the SCADA system of the power system. Other function of the database is acting as a buffer to keep the 'new facts' - the final or interim results produced by function modules of the proposed system such as the pattern recognition mechanism or the inference engine.

All the data in this database are organised in the format of tables. This type of database can be easily developed by using any of the computer languages such as database tools 'oracle', the 'sequence' or numerical languages 'FORTRAN' or 'C^{++}'

.

2. The inference engine

The forward chaining is selected as the inference strategy in this system for two main reasons. Firstly the conditions and conclusions are one to one matching for all the knowledge rules in this system, there will not be the case of "multiple solutions" for the same set of conditions. Secondly the use of the minimum distance classifier minimises the possibility for a target state to be classified into more than one pattern class. Therefore, the typical "unfocused questioning situation" for the forward chaining will not be a problem for this application.

3. The knowledge base

The knowledge base of the proposed system contains two types of knowledge: pattern recognition rules and pre-calculated power margin results for the prototypes of all pattern classes of the VSDFs for a power system. These "knowledge" are presented by the production rules in the format of 'IF-THEN' as:

RULES	CONTENTS	NOTES
Rule (i)	**IF** $D^{LDk} = \min\{D^{LD05}, D^{LD15}, D^{LD20}\}$ **Then** $X^{LD} \in \mathbf{LDk}$, K=05, 15, 20	If LD k has the min E distance, Then the target state has the load dist pattern LD k
…	… …	… …
Rule (j)	**IF** $X^{L} \in \mathbf{L01}, X^{G} \in \mathbf{G02}, X^{LD} \in \mathbf{LD05}, X^{GP} \in \mathbf{GP01}$ **Then** $X^{VSDF} \in \Phi 1$	If the target state has L01, G02, LD 05 and GP01, Then it belongs to Pattern Class 1
…	… …	… …
Rule (k)	**IF** $X^{VSDF} \in \Phi 3$ **Then** $\mathbf{PM_0}$ = Table 4.5.1 – 7	If target state belongs to Pattern Class 3 Then initial solution as listed in Table 4.5.1 - 7
…	… …	… …

Bus	L (p.u.)		LD (%)		G(p.u.)		GP (%)		PMo (p.u.)	
	LP	LQ	LDP	LDQ	GP	GQ	GPP	GPQ	**ΔP**	**ΔQ**
1	0.3	0.18	3	3.8	3.2	2.0	33.1	28.8	**10.0**	**8.00**
2	0.9	0.45	11	6	.....	.....	.....	.....	**6.80**	**3.80**
...	.....	.....	.....	.....	.....	.....	.....	.....	.....	.....
...	.....	.....	.....	.....	7.9	4.5	17	15	.....	.....
...	.....	.....	.....	.....	.....	.....	.....	.....	.....	.....
N	1.2	0.6	6	7.8	0	0	0	0	**7.50**	**3.02**
Total	18.1	11.2	100	100	20.5	9.6	100	100	**132**	**98**

Table 4.4.2-1 The example for the knowledge in the format of "production rules"

4. The Man-machine Interface

All the information processed within this knowledge based system is digitised or specially coded. This includes the interim or final results produced by the inference engine or pattern recognition module. The man-machine interface is responsible for interpreting those coded information into a user-friendly format. It can also provide some explanations regarding why or how the solutions were reached. When the explanations are required, the man-machine interface simply gathers together all the conditions of the rules used for the solution searching, and presents them out in a logic order as they were searched.

The principle and generic structure of this knowledge based system for prediction of voltage stability have discussed in the above sections. More detailed discussions for applying such a system to a power system will be presented in the simulation section below.

4.5 SYSTEM SIMULATION

The simulation of the proposed system on the IEEE 30 bus power system is presented in this section. It covers the contents of simulation configuration, case study and simulation evolution.

4.5.1 Simulation Configuration

1. Pattern features

By considering the totally number buses in the IEEE 30 bus power system, all the coefficients for the VSDFs are selected as the pattern features. Thus, there is no need to introduce any additional pattern features. The VSDFs for the pattern recognition purpose in this simulation have exactly the same format as defined in Chapter 3:

(1) Load pattern K:

$$\mathbf{L_k} = [\mathbf{L_k^P}, \mathbf{L_k^Q}]^T$$

$$\mathbf{L_k^P} = [\, L_k^P 1, L_k^P 2 \ldots L_k^P i \ldots L_k^P 30]$$

$$\mathbf{L_k^Q} = [L_k^Q 1, L_k^Q 2 \ldots L_k^Q i \ldots L_k^Q 30]$$

(2) Load distribution Pattern K:

$$\mathbf{LD_k} = [\mathbf{LD_k^P}, \mathbf{LD_k^Q}]^T$$

$$\mathbf{LD_k^P} = [\, LD_k^P 1, LD_k^P 2 \ldots LD_k^P i \ldots LD_k^P 30]$$

$$\mathbf{LD_k^Q} = [LD_k^Q 1, LD_k^Q 2 \ldots LD_k^Q i \ldots LD_k^Q 30]$$

(3) Generation Pattern K:

$$\mathbf{G_k} = [\mathbf{G_k^P}, \mathbf{G_k^Q}]^T$$

$$\mathbf{G_k^P} = [\, G_k^P 1, G_k^P 2 \ldots G_k^P i \ldots G_k^P 30]$$

$$\mathbf{G_k^Q} = [G_k^Q 1, G_k^Q 2 \ldots G_k^Q i \ldots G_k^Q 30]$$

(4) Generation Participation Pattern K

$$\mathbf{GP_k} = [\mathbf{GP_k^P}, \mathbf{GP_k^Q}]^T$$

$$\mathbf{GP_k^P} = [\, GP_k^P 1, GP_k^P 2 \ldots GP_k^P i \ldots GP_k^P 30]$$

$$\mathbf{GP_k^Q} = [GP_k^Q 1, GP_k^Q 2 \ldots GP_k^Q i \ldots GP_k^Q 30]$$

2. Pattern classes

Three pattern classes were set up for this simulation. Each of the pattern classes represents a typical system loading condition, namely lightly loaded conditions (load level less than 5% of the maximum generation capacity), normally loaded conditions (load level around 50% of the maximum generation capacity) and heavily loaded conditions (around 70% of the maximum generation capacity).

(1) Pattern class I

This pattern class is set up to represent the VSDFs under lightly loaded system conditions. The prototype of the pattern class 1 includes

(i) Load Pattern $\mathbf{L01} = [\mathbf{L01}^P, \mathbf{L01}^Q]^T$

(ii) Load Distribution Pattern $\mathbf{LD05} = [\mathbf{LD05}^P, \mathbf{LD05}^Q]^T$

(iii) Generation Pattern $\mathbf{G02} = [\mathbf{G02}^P, \mathbf{G02}^Q]^T$

(iv) Generation Participation Pattern $\mathbf{GP01} = [\mathbf{GP01}^P, \mathbf{GP01}^Q]^T$

Details of the prototype and its associated power margins for pattern class I are given in Table 4.5.1-1 (also see Table A3-10, Appendix 3):

Bus	L01 (p.u.)		G02 (p.u.)		LD05		GP01		PM (p.u.)	
	$L01^P$	$L01^Q$	$G02^P$	$G02^Q$	$LD05^P$	$LD05^Q$	$GP01^P$	$GP01^Q$	ΔP_L	ΔQ_L
1	0.00	0.00	4.47	-0.79	0.00%	0.00%	23.97%	10.99%	**0.00**	**0.00**
2	0.00	0.00	4.27	-1.40	0.00%	0.00%	23.92%	17.13%	**0.00**	**0.00**
3	0.24	0.12	0.00	0.00	1.00%	1.00%	0.00%	0.00%	**2.48**	**1.48**
4	0.76	0.36	0.00	0.00	4.00%	4.00%	0.00%	0.00%	**9.92**	**5.92**
5	0.00	0.00	0.00	0.00	0.00%	0.00%	0.00%	0.00%	**0.00**	**0.00**
6	0.00	0.00	0.00	0.00	0.00%	0.00%	0.00%	0.00%	**0.00**	**0.00**
7	1.28	0.59	0.00	0.00	4.00%	4.00%	0.00%	0.00%	**9.92**	**5.92**
8	1.15	0.43	0.00	0.00	5.00%	5.00%	0.00%	0.00%	**12.40**	**7.40**
9	0.90	0.50	0.00	0.00	5.00%	5.00%	0.00%	0.00%	**12.40**	**7.40**
10	0.58	0.20	0.00	0.00	3.00%	3.00%	0.00%	0.00%	**7.44**	**4.44**
11	0.00	0.00	0.00	0.00	0.00%	0.00%	0.00%	0.00%	**0.00**	**0.00**
12	1.12	0.55	0.00	0.00	5.00%	5.00%	0.00%	0.00%	**12.40**	**7.40**
13	0.00	0.00	2.14	-1.17	0.00%	0.00%	11.96%	14.95%	**0.00**	**0.00**
14	0.62	0.36	0.00	0.00	5.00%	5.00%	0.00%	0.00%	**12.40**	**7.40**
15	0.82	0.55	0.00	0.00	6.00%	6.00%	0.00%	0.00%	**14.88**	**8.88**
16	0.35	0.18	0.00	0.00	4.00%	4.00%	0.00%	0.00%	**9.92**	**5.92**
17	0.90	0.58	0.00	0.00	5.00%	5.00%	0.00%	0.00%	**12.40**	**7.40**
18	3.28	1.79	0.00	0.00	15.00%	15.00%	0.00%	0.00%	**37.20**	**22.20**
19	2.30	1.10	0.00	0.00	12.00%	12.00%	0.00%	0.00%	**29.76**	**17.76**
20	1.22	0.67	0.00	0.00	12.00%	12.00%	0.00%	0.00%	**29.76**	**17.76**
21	0.75	0.32	0.00	0.00	5.00%	5.00%	0.00%	0.00%	**12.40**	**7.40**
22	0.00	0.00	2.67	-1.63	0.00%	0.00%	14.90%	22.77%	**0.00**	**0.00**
23	0.00	0.00	1.60	-1.12	0.00%	0.00%	8.82%	14.95%	**0.00**	**0.00**
24	0.47	0.37	0.00	0.00	2.00%	2.00%	0.00%	0.00%	**4.96**	**2.96**
25	0.10	0.07	0.00	0.00	1.00%	1.00%	0.00%	0.00%	**2.48**	**1.48**
26	0.35	0.23	0.00	0.00	2.00%	2.00%	0.00%	0.00%	**4.96**	**2.96**
27	0.00	0.00	2.94	-1.52	0.00%	0.00%	16.42%	19.21%	**0.00**	**0.00**
28	0.00	0.00	0.00	0.00	0.00%	0.00%	0.00%	0.00%	**0.00**	**0.00**
29	0.27	0.19	0.00	0.00	1.00%	1.00%	0.00%	0.00%	**2.48**	**1.48**
30	0.56	0.29	0.00	0.00	3.00%	3.00%	0.00%	0.00%	**7.44**	**4.44**
Total	18.02	9.45	18.09	-7.63	100.00%	100.00%	100.00%	100.00%	**248.00**	**148.00**

Table 4.5.1-1 The prototype and its associated power margins for pattern class I

(2) Pattern class II

This pattern class is set up to represent the VSDFs under normally loaded system conditions. The prototype of pattern class 2 includes

(i) Load Pattern **L10** = $[L10^P, L10^Q]^T$

(ii) Load Distribution Pattern **LD15** = $[LD15^P, LD15^Q]^T$

(iii) Generation Pattern **G06** = **[G06^P, G06^Q]^T**

(iv) Generation Participation Pattern **GP03** =**[GP03^P, GP03^Q]^T**

The prototype of pattern class 2 and its associated power margins for pattern class II are detailed in Table 4.5.1-2 (also see Table A3-15, Appendix 3):

Bus	**L10** (p.u.)		**G06** (p.u.)		**LD15**		**GP03**		**PM** (p.u.)	
	L10^P	**L10^Q**	**G06^P**	**G06^Q**	**LD15^P**	**LD15^Q**	**GP03^P**	**GP03^Q**	**ΔP_L**	**ΔQ_L**
1	0.00	0.00	36.99	14.92	0.00%	0.00%	37.24%	33.92%	**0.00**	**0.00**
2	0.00	0.00	36.20	14.58	0.00%	0.00%	37.66%	35.58%	**0.00**	**0.00**
3	1.20	0.60	0.00	0.00	2.00%	2.00%	0.00%	0.00%	**1.56**	**0.92**
4	3.80	1.80	0.00	0.00	4.00%	4.00%	0.00%	0.00%	**3.12**	**1.84**
5	0.00	0.00	0.00	0.00	0.00%	0.00%	0.00%	0.00%	**0.00**	**0.00**
6	0.00	0.00	0.00	0.00	0.00%	0.00%	0.00%	0.00%	**0.00**	**0.00**
7	6.40	2.95	0.00	0.00	3.00%	3.00%	0.00%	0.00%	**2.34**	**1.38**
8	5.75	2.15	0.00	0.00	5.00%	5.00%	0.00%	0.00%	**3.90**	**2.30**
9	4.50	2.50	0.00	0.00	5.00%	5.00%	0.00%	0.00%	**3.90**	**2.30**
10	2.90	1.00	0.00	0.00	3.00%	3.00%	0.00%	0.00%	**2.34**	**1.38**
11	0.00	0.00	0.00	0.00	0.00%	0.00%	0.00%	0.00%	**0.00**	**0.00**
12	5.60	2.75	0.00	0.00	4.00%	4.00%	0.00%	0.00%	**3.12**	**1.84**
13	0.00	0.00	0.00	0.00	0.00%	0.00%	0.00%	0.00%	**0.00**	**0.00**
14	3.10	1.80	0.00	0.00	6.00%	6.00%	0.00%	0.00%	**4.68**	**2.76**
15	4.10	2.75	0.00	0.00	5.00%	5.00%	0.00%	0.00%	**3.90**	**2.30**
16	1.75	0.90	0.00	0.00	4.00%	4.00%	0.00%	0.00%	**3.12**	**1.84**
17	4.50	2.90	0.00	0.00	5.00%	5.00%	0.00%	0.00%	**3.90**	**2.30**
18	16.40	8.95	0.00	0.00	20.00%	20.00%	0.00%	0.00%	**15.60**	**9.20**
19	11.50	5.50	0.00	0.00	10.00%	10.00%	0.00%	0.00%	**7.80**	**4.60**
20	6.10	3.35	0.00	0.00	10.00%	10.00%	0.00%	0.00%	**7.80**	**4.60**
21	3.75	1.60	0.00	0.00	5.00%	5.00%	0.00%	0.00%	**3.90**	**2.30**
22	0.00	0.00	0.00	0.00	0.00%	0.00%	0.00%	0.00%	**0.00**	**0.00**
23	0.00	0.00	0.00	0.00	0.00%	0.00%	0.00%	0.00%	**0.00**	**0.00**
24	2.35	1.85	0.00	0.00	2.00%	2.00%	0.00%	0.00%	**1.56**	**0.92**
25	0.50	0.35	0.00	0.00	1.00%	1.00%	0.00%	0.00%	**0.78**	**0.46**
26	1.75	1.15	0.00	0.00	3.00%	3.00%	0.00%	0.00%	**2.34**	**1.38**
27	0.00	0.00	19.90	13.08	0.00%	0.00%	25.10%	30.50%	**0.00**	**0.00**
28	0.00	0.00	0.00	0.00	0.00%	0.00%	0.00%	0.00%	**0.00**	**0.00**
29	1.35	0.95	0.00	0.00	1.00%	1.00%	0.00%	0.00%	**0.78**	**0.46**
30	2.80	1.45	0.00	0.00	2.00%	2.00%	0.00%	0.00%	**1.56**	**0.92**
Total	90.10	47.25	93.09	42.58	100.00%	100.00%	100.00%	100.00%	**78.00**	**46.00**

Table 4.5.1-2 The prototype and its associated power margins for pattern class II

(3) Pattern class III

This pattern class is to represent the VSDFs under heavily loaded system condition. The prototype of pattern class 3 includes

(i) Load Pattern **L20** = **[L20^P, L20^Q]^T**

(ii) Load Distribution Pattern **LD20=[LD20^P, LD20^Q]^T**

(iii) Generation Pattern **G20** = **[G20^P, G20^Q]^T**

(iv) Generation Participation Pattern **GP20** =**[GP20^P, GP20^Q]^T**

The prototype and its associated power margins for pattern class III are detailed in the table below (also see Table A3-20, Appendix 3):

Bus	**L20 (p.u.)**		**G20 (p.u.)**		**LD20**		**GP20**		**PM (p.u.)**	
	L20^P	**L20^Q**	**G20^P**	**G20^Q**	**LD20^P**	**LD20^Q**	**GP20^P**	**GP20^Q**	**ΔP_L**	**ΔQ_L**
1	0.00	0.00	57.90	36.80	0.00%	0.00%	26.04%	27.51%	**0.00**	**0.00**
2	0.00	0.00	57.00	37.00	0.00%	0.00%	27.36%	26.81%	**0.00**	**0.00**
3	3.00	1.80	0.00	0.00	5.00%	5.00%	0.00%	0.00%	**2.95**	**1.75**
4	9.00	5.40	0.00	0.00	0.00%	0.00%	0.00%	0.00%	**0.00**	**0.00**
5	0.00	0.00	0.00	0.00	0.00%	0.00%	0.00%	0.00%	**0.00**	**0.00**
6	0.00	0.00	0.00	0.00	0.00%	0.00%	0.00%	0.00%	**0.00**	**0.00**
7	12.80	5.90	0.00	0.00	5.00%	5.00%	0.00%	0.00%	**2.95**	**1.75**
8	10.50	4.30	0.00	0.00	5.00%	5.00%	0.00%	0.00%	**2.95**	**1.75**
9	9.00	5.00	0.00	0.00	5.00%	5.00%	0.00%	0.00%	**2.95**	**1.75**
10	6.00	3.60	0.00	0.00	5.00%	5.00%	0.00%	0.00%	**2.95**	**1.75**
11	0.00	0.00	0.00	0.00	0.00%	0.00%	0.00%	0.00%	**0.00**	**0.00**
12	11.20	7.00	0.00	0.00	5.00%	5.00%	0.00%	0.00%	**2.95**	**1.75**
13	0.00	0.00	0.00	0.00	0.00%	0.00%	0.00%	0.00%	**0.00**	**0.00**
14	29.00	18.00	0.00	0.00	10.00%	10.00%	0.00%	0.00%	**5.90**	**3.50**
15	31.50	19.00	0.00	0.00	10.00%	10.00%	0.00%	0.00%	**5.90**	**3.50**
16	5.00	3.00	0.00	0.00	5.00%	5.00%	0.00%	0.00%	**2.95**	**1.75**
17	9.00	5.80	0.00	0.00	5.00%	5.00%	0.00%	0.00%	**2.95**	**1.75**
18	16.00	9.00	0.00	0.00	10.00%	10.00%	0.00%	0.00%	**5.90**	**3.50**
19	12.00	8.00	0.00	0.00	5.00%	5.00%	0.00%	0.00%	**2.95**	**1.75**
20	5.50	3.30	0.00	0.00	0.00%	0.00%	0.00%	0.00%	**0.00**	**0.00**
21	7.50	3.20	0.00	0.00	5.00%	5.00%	0.00%	0.00%	**2.95**	**1.75**
22	0.00	0.00	37.00	24.00	0.00%	0.00%	17.22%	16.88%	**0.00**	**0.00**
23	0.00	0.00	23.00	16.00	0.00%	0.00%	11.14%	10.92%	**0.00**	**0.00**
24	4.70	3.70	0.00	0.00	5.00%	5.00%	0.00%	0.00%	**2.95**	**1.75**
25	3.00	2.00	0.00	0.00	5.00%	5.00%	0.00%	0.00%	**2.95**	**1.75**
26	5.50	3.30	0.00	0.00	0.00%	0.00%	0.00%	0.00%	**0.00**	**0.00**
27	0.00	0.00	38.00	28.00	0.00%	0.00%	18.24%	17.87%	**0.00**	**0.00**
28	0.00	0.00	0.00	0.00	0.00%	0.00%	0.00%	0.00%	**0.00**	**0.00**
29	4.00	2.40	0.00	0.00	5.00%	5.00%	0.00%	0.00%	**2.95**	**1.75**
30	7.60	4.00	0.00	0.00	5.00%	5.00%	0.00%	0.00%	**2.95**	**1.75**
Total	201.8	117.7	212.9	141.8	100.00%	100.00%	100.00%	100.00%	**59.00**	**35.00**

Table 4.5.1-3 The prototype and its associated power margins for pattern class III

3. Decision function

As all the coefficients of the VSDFs are selected as pattern features in this simulation, the weighting factors in the Euclidean equation are set to "1" for all the pattern features. This means that all the pattern features have the same influencing power on the pattern recognition. To provide a better distinction and visibility, the values of the load distribution pattern and generation participation pattern are multiplied by 100 in the calculation for the Euclidean Distance. Thus, the decision function used in this simulation has the following format:

$$D^{\Pi i} = [(X_1^{\Pi P} - Z_1^{\Pi iP})^2 + (X_2^{\Pi P} - Z_2^{\Pi iP})^2 + \ldots + (X_k^{\Pi P} - Z_k^{\Pi iP})^2 + \ldots + (X_{30}^{\Pi P} - Z_{30}^{\Pi iP})^2 + (X_1^{\Pi Q} - Z_1^{\Pi iQ})^2 + (X_2^{\Pi Q} - Z_2^{\Pi iQ})^2 + \ldots + (X_k^{\Pi Q} - Z_k^{\Pi iQ})^2 + \ldots + (X_{30}^{\Pi Q} - Z_{30}^{\Pi iQ})^2]^{1/2} \tag{4.5.1–1}$$

where,

$D^{\Pi i}$ is the Euclidean distance for one of the four VSDFs from a target pattern **X** to the prototype of a pattern class i,

$Z^{\Pi i} = \left[Z_1^{\Pi iP} \quad Z_2^{\Pi iP} \quad \ldots \quad Z_k^{\Pi iP} \quad \ldots \quad Z_{30}^{\Pi iP}, Z_1^{\Pi iQ} \quad Z_2^{\Pi iQ} \quad \ldots \quad Z_k^{\Pi iQ} \quad \ldots \quad Z_{30}^{\Pi iQ} \right]$

is a VSDF for the prototype of pattern class i, e.g. Load pattern,

$\mathbf{X}^{\Pi} = \left[X_1^{\Pi P} \quad X_2^{\Pi P} \quad \ldots \quad X_k^{\Pi P} \quad \ldots \quad X_{30}^{\Pi P}, X_1^{\Pi Q} \quad X_2^{\Pi Q} \quad \ldots \quad X_k^{\Pi Q} \quad \ldots \quad X_{30}^{\Pi Q} \right]$

is a VSDF for a target pattern

Π stands for a specific type of VSDFs, $\Pi \in \{L, LD, G, GP\}$

For example, if the prototype of a pattern class is specified as

(i) Load Pattern **L01 = [L01$^{\mathbf{P}}$, L01$^{\mathbf{Q}}$]$^{\mathbf{T}}$**

(ii) Load Distribution Pattern **LD03 =[LD03$^{\mathbf{P}}$, LD03$^{\mathbf{Q}}$]$^{\mathbf{T}}$**

(iii) Generation Pattern **G01 = [G01$^{\mathbf{P}}$, G01$^{\mathbf{Q}}$]$^{\mathbf{T}}$**

(iv) Generation Participation Pattern **GP01 =[GP01$^{\mathbf{P}}$, GP01$^{\mathbf{Q}}$]$^{\mathbf{T}}$**,

the Euclidean distances from a target pattern to the prototype of this pattern class include the following 4 segments:

<u>Load pattern segment:</u>

$$\mathbf{D}^{L01} = [(X_1^{LP} - L01_1^P)^2 + (X_2^{LP} - L01_2^P)^2 \ldots + (X_k^{LP} - L01_k^P)^2 \ldots + (X_{30}^{LP} - L01_{30}^P)^2 + (X_1^{LQ} - L01_1^Q)^2 + (X_2^{LQ} - L01_2^Q)^2 \ldots + (X_k^{LQ} - L01_k^Q)^2 \ldots + (X_{30}^{LQ} - L01_{30}^Q)^2]^{1/2}$$

Load distribution pattern segment:

$$\mathbf{D}^{LD03} = [(X_1^{LDP} - LD03_1^P)^2 + (X_2^{LDP} - LD03_2^P)^2 ... + (X_k^{LDP} - LD03_k^P)^2 ... + (X_{30}^{LDP} - LD03_{30}^P)^2$$
$$+ (X_1^{LDQ} - LD03_1^Q)^2 + (X_2^{LDQ} - LD03_2^Q)^2 ... + (X_k^{LDQ} - LD03_k^Q)^2 ... + (X_{30}^{LDQ} - LD03_{30}^Q)^2]^{1/2}$$

Generation pattern segment:

$$\mathbf{D}^{G02} = [(X_1^{GP} - G02_1^P)^2 + (X_2^{GP} - G02_2^P)^2 ... + (X_k^{GP} - G02_k^P)^2 ... + (X_{30}^{GP} - G02_{30}^P)^2$$
$$+ (X_1^{GQ} - G02_1^Q)^2 + (X_2^{gQ} - G02_2^Q)^2 ... + (X_k^{GQ} - G02_k^Q)^2 ... + (X_{30}^{GQ} - G02_{30}^Q)^2]^{1/2}$$

Generation participation pattern segment:

$$\mathbf{D}^{GP01} = [(X_1^{GPP} - GP01_1^P)^2 + (X_2^{GPP} - GP01_2^P)^2 ... + (X_k^{GPP} - GP01_k^P)^2 ... + (X_{30}^{GPP} - GP01_{30}^P)^2$$
$$+ (X_1^{GPQ} - GP01_1^Q)^2 + (X_2^{GPQ} - GP01_2^Q)^2 ... + (X_k^{GPQ} - GP01_k^Q)^2 ... + (X_{30}^{GPQ} - GP01_{30}^Q)^2]^{1/2}$$

where,

$$\mathbf{X}^{L} = \left[X_1^{LP}\ X_2^{LP}\ ...X_k^{LP}\ ...\ X_{30}^{LP}\ X_1^{LQ}\ X_2^{LQ}\ ...X_k^{LQ} ...\ X_{30}^{LQ}\right]$$

$$\mathbf{X}^{LD} = \left[X_1^{LDP}\ X_2^{LDP}\ ...X_k^{LDP}\ ...\ X_{30}^{LDP}\ X_1^{LDQ}\ X_2^{LDQ}\ ...X_k^{LDQ} ...\ X_{30}^{LDQ}\right]$$

$$\mathbf{X}^{G} = \left[X_1^{GP}\ X_2^{GP}\ ...X_k^{GP}\ ...\ X_{30}^{GP}\ X_1^{GQ}\ X_2^{GQ}\ ...X_k^{GQ} ...\ X_{30}^{GQ}\right]$$

$$\mathbf{X}^{GP} = \left[X_1^{GPP}\ X_2^{GPP}\ ...X_k^{GPP}\ ...\ X_{30}^{GPP}\ X_1^{GPQ}\ X_2^{GPQ}\ ...X_k^{GPQ} ...\ X_{30}^{GPQ}\right]$$

are the VSDFs for the target state.

4. Knowledge rules

The knowledge rules used in this simulation are listed in the following table:

RULES	CONTENTS	NOTES
Rule 1.	**IF** $D^{Lk} = \min\{D^{L01}, D^{L10}, D^{L20}\}$	
	Then $X^{L} \in \mathbf{Lk}$, K=01, 10, 20	
Rule 2.	**IF** $D^{LDk} = \min\{D^{LD05}, D^{LD15}, D^{LD20}\}$	
	Then $X^{LD} \in \mathbf{LDk}$, K=05, 15, 20	
Rule 3.	**IF** $D^{Gk} = \min\{D^{G02}, D^{G06}, D^{G20}\}$	
	Then $X^{G} \in \mathbf{Gk}$, k = 02, 06, 20	
Rule 4.	**IF** $D^{GPk} = \min\{D^{GP01}, D^{GP03}, D^{GP20}\}$	
	Then $X^{GP} \in \mathbf{GPk}$, k = 01, 03, 20	
Rule 5.	**IF** $\mathbf{X^{L} \in L01, X^{G} \in G02, X^{LD} \in LD05, X^{GP} \in GP01}$	
	Then $\mathbf{X^{VSDF}} \in \Phi 1$	The target state belongs to pattern class 1
Rule 6.	**IF** $\mathbf{X^{L} \in L10, X^{G} \in G06, X^{LD} \in LD15, X^{GP} \in GP03}$	
	Then $\mathbf{X^{VSDF}} \in \Phi 2$	The target state belongs to pattern class 2
Rule 7.	**IF** $\mathbf{X^{L} \in L20, X^{G} \in G20 \quad X^{LD} \in LD20, X^{GP} \in GP20}$	
	Then $\mathbf{X^{VSDF}} \in \Phi 3$	the target state belongs to pattern class 3
Rule 8.	**IF** $\mathbf{X^{VSDF}} \in \Phi 1$	
	Then $\mathbf{PM_0}$ = Table 4.5.1 – 5	Initial solution for pattern class 1
Rule 9.	**IF** $\mathbf{X^{VSDF}} \in \Phi 2$	
	Then $\mathbf{PM_0}$ = Table 4.5.1 – 6	Initial solution for pattern class 2
Rule 10.	**IF** $\mathbf{X^{VSDF}} \in \Phi 3$	
	Then $\mathbf{PM_0}$ = Table 4.5.1 – 7	Initial solution for pattern class 3
Rule 11.	**Run** Solution compensation calculation $\mathbf{PM_S = PM_0 + \delta}$ $\Delta P_i = \Delta P_{0i} + \delta^{P}_{i}$; $\Delta Q_i = \Delta Q_{0i} + \delta^{Q}_{i}$	See equations (4.3.1 – 15) (4.3.1 – 16)
Rule 12.	**Run** MMI Routine	Present the final results

Table 4.5.1-4 The knowledge rules used in the simulation

Bus	PM_0 (p.u.)		Compensation δ		PM_S (p.u.)	
	ΔP_L	ΔQ_L	δ^P	δ^Q	$\Delta P_L - \delta^P$	$\Delta Q_L - \delta^Q$
1	0.00	0.00				
2	0.00	0.00				
3	2.48	1.48				
4	9.92	5.92				
5	0.00	0.00				
6	0.00	0.00				
7	9.92	5.92				
8	12.40	7.40				
9	12.40	7.40				
10	7.44	4.44				
11	0.00	0.00				
12	12.40	7.40				
13	0.00	0.00				
14	12.40	7.40				
15	14.88	8.88				
16	9.92	5.92				
17	12.40	7.40				
18	37.20	22.20				
19	29.76	17.76				
20	29.76	17.76				
21	12.40	7.40				
22	0.00	0.00				
23	0.00	0.00				
24	4.96	2.96				
25	2.48	1.48				
26	4.96	2.96				
27	0.00	0.00				
28	0.00	0.00				
29	2.48	1.48				
30	7.44	4.44				
Total	**248.00**	**148.00**				

Table 4.5.1-5 The initial solution (PMo) for the VSDFs belonging to pattern class I

Bus	PM_0 (p.u.)		Compensation δ		PM_S (p.u.)	
	ΔP_L	ΔQ_L	δ^P	δ^Q	$\Delta P_L+\delta^P$	$\Delta Q_L+\delta^Q$
1	0.00	0.00				
2	0.00	0.00				
3	1.56	0.92				
4	3.12	1.84				
5	0.00	0.00				
6	0.00	0.00				
7	2.34	1.38				
8	3.90	2.30				
9	3.90	2.30				
10	2.34	1.38				
11	0.00	0.00				
12	3.12	1.84				
13	0.00	0.00				
14	4.68	2.76				
15	3.90	2.30				
16	3.12	1.84				
17	3.90	2.30				
18	15.60	9.20				
19	7.80	4.60				
20	7.80	4.60				
21	3.90	2.30				
22	0.00	0.00				
23	0.00	0.00				
24	1.56	0.92				
25	0.78	0.46				
26	2.34	1.38				
27	0.00	0.00				
28	0.00	0.00				
29	0.78	0.46				
30	1.56	0.92				
Total	**78.00**	**46.00**				

Table 4.5.1-6 The initial solution (PMo) for the VSDFs belonging to pattern class II

Bus	PM$_0$ (p.u.)		Compensation δ		PM$_S$ (p.u.)	
	ΔP_L	ΔQ_L	δ^P	δ^Q	$\Delta P_L+\delta^P$	$\Delta Q_L+\delta^Q$
1	0.00	0.00				
2	0.00	0.00				
3	2.95	1.75				
4	0.00	0.00				
5	0.00	0.00				
6	0.00	0.00				
7	2.95	1.75				
8	2.95	1.75				
9	2.95	1.75				
10	2.95	1.75				
11	0.00	0.00				
12	2.95	1.75				
13	0.00	0.00				
14	5.90	3.50				
15	5.90	3.50				
16	2.95	1.75				
17	2.95	1.75				
18	5.90	3.50				
19	2.95	1.75				
20	0.00	0.00				
21	2.95	1.75				
22	0.00	0.00				
23	0.00	0.00				
24	2.95	1.75				
25	2.95	1.75				
26	0.00	0.00				
27	0.00	0.00				
28	0.00	0.00				
29	2.95	1.75				
30	2.95	1.75				
Total	**59.00**	**35.00**				

Table 4.5.1-7 The initial solution (PMo) for the VSDFs belonging to pattern class III

4.5.2 Case study

Totally six simulation cases (two test patterns under each configured pattern class) are presented in this section. To illustrate the decision-making process, the interim results produced by this knowledge based system are provided in some of the study cases. Accuracy analysis of the simulation results is made for each study case against the power margins determined by the conventional load flow study.

1. Case Study 1

(1) Test pattern

In this case, the VSDFs for the testing pattern are set as shown in the table below:

Bus	X^L (p.u.)		X^G (p.u.)		X^{LD} (%)		X^{GP} (%)	
	X^{LP}	X^{LQ}	X^{GP}	X^{GQ}	X^{LDP}	X^{LDQ}	X^{GPP}	X^{GPQ}
1	0.00	0.00	4.47	-0.79	0.00%	0.00%	23.89%	11.29%
2	0.00	0.00	4.27	-1.40	0.00%	0.00%	23.95%	17.07%
3	0.24	0.12	0.00	0.00	1.10%	1.10%	0.00%	0.00%
4	0.76	0.36	0.00	0.00	3.60%	3.60%	0.00%	0.00%
5	0.00	0.00	0.00	0.00	0.00%	0.00%	0.00%	0.00%
6	0.00	0.00	0.00	0.00	0.00%	0.00%	0.00%	0.00%
7	1.28	0.59	0.00	0.00	4.40%	4.40%	0.00%	0.00%
8	1.15	0.43	0.00	0.00	4.50%	4.50%	0.00%	0.00%
9	0.90	0.50	0.00	0.00	5.50%	5.50%	0.00%	0.00%
10	0.58	0.20	0.00	0.00	2.70%	2.70%	0.00%	0.00%
11	0.00	0.00	0.00	0.00	0.00%	0.00%	0.00%	0.00%
12	1.12	0.55	0.00	0.00	5.50%	5.50%	0.00%	0.00%
13	0.00	0.00	2.14	-1.17	0.00%	0.00%	11.97%	14.90%
14	0.62	0.36	0.00	0.00	4.50%	4.50%	0.00%	0.00%
15	0.82	0.55	0.00	0.00	6.60%	6.60%	0.00%	0.00%
16	0.35	0.18	0.00	0.00	3.60%	3.60%	0.00%	0.00%
17	0.90	0.58	0.00	0.00	5.50%	5.50%	0.00%	0.00%
18	3.28	1.79	0.00	0.00	13.50%	13.50%	0.00%	0.00%
19	2.30	1.10	0.00	0.00	13.20%	13.20%	0.00%	0.00%
20	1.22	0.67	0.00	0.00	10.80%	10.80%	0.00%	0.00%
21	0.75	0.32	0.00	0.00	5.50%	5.50%	0.00%	0.00%
22	0.00	0.00	2.67	-1.63	0.00%	0.00%	14.92%	22.70%
23	0.00	0.00	1.60	-1.12	0.00%	0.00%	8.83%	14.90%
24	0.47	0.37	0.00	0.00	2.20%	2.20%	0.00%	0.00%
25	0.10	0.07	0.00	0.00	0.90%	0.90%	0.00%	0.00%
26	0.35	0.23	0.00	0.00	2.20%	2.20%	0.00%	0.00%
27	0.00	0.00	2.94	-1.52	0.00%	0.00%	16.44%	19.14%
28	0.00	0.00	0.00	0.00	0.00%	0.00%	0.00%	0.00%
29	0.27	0.19	0.00	0.00	0.90%	0.90%	0.00%	0.00%
30	0.56	0.29	0.00	0.00	3.30%	3.30%	0.00%	0.00%
Total	18.02	9.45	18.09	-7.63	100.00%	100.00%	100.00%	100.00%

Table 4.5.2-1 Test pattern (1) for the case study 1

This is one of the patterns within study group 1 (lightly loaded cluster) for the simulation of power margin similarity in Chapter 3. The further details about this test pattern are given in Table A3-9 of Appendix 3.

(2) Euclidean Distance Calculations

The Euclidean distances to the prototype of each pattern class are calculated by using equation (4.5.1-1) as below:

(i) The Euclidean distance to pattern class I:

The 4 segments of Euclidean distance from the testing pattern (1) to the prototype of pattern class I (**L01, LD05, G02 and GP01** as shown in Table 4.5.1-1) are:

Load pattern segment D^{L01}	0
Load distribution pattern segment D^{LD03}	0
Generation pattern segment D^{G02}	3.94
Generation participation pattern segment D^{GP01}	0.33

Table 4.5.2-2 The Euclidean distance from test pattern (1) to pattern class I

(ii) Euclidean distance to pattern class II:

The Euclidean distance from test pattern (1) to the prototype of pattern class II (**L10, LD15, G06 and GP03** as shown in Table 4.5.1-2) is:

Load pattern segment D^{L12}	23.38
Load distribution pattern segment D^{LD11}	11.55
Generation pattern segment D^{G09}	55.67
Generation participation pattern segment D^{GP06}	53.18

Table 4.5.2-3 The Euclidean distance from test pattern (1) to pattern class 1I

(iii) Euclidean distance to pattern class III:

The Euclidean distance from test pattern (1) to the prototype of pattern class III (**L20, LD20, G20 and GP20** as shown in Table 4.5.1-3) is calculated as:

Load pattern segment D^{L12}	61.25
Load distribution pattern segment D^{LD11}	25.46
Generation pattern segment D^{G09}	114.95
Generation participation pattern segment D^{GP06}	28.37

Table 4.5.2-4 The Euclidean distance from test pattern (1) to pattern class III

(3) Solution searching

By using the calculated Euclidean distances and other data in the database, the solution is searched in the following steps:

Step 1: VSDFs identification

Applying the knowledge rules to the results in Table 4.5.2-2, Table 4.5.2-3, Table 4.5.2-4 the following interim results are obtained:

Rules Applied	Reasoning	Conclusion
RULE (1)	$D^{L01} = \min \{D^{L01}, D^{L10}, D^{L20}\}$,	$X^{L} \in \mathbf{L01}$
RULE (2)	$D^{LD03} = \min \{D^{LD05}, D^{LD15}, D^{LD20}\}$,	$X^{LD} \in \mathbf{LD05}$
RULE (3)	$D^{G02} = \min \{D^{G02}, D^{G06}, D^{G20}\}$,	$X^{G} \in \mathbf{G02}$
RULE (4) :	$D^{GP01} = \min \{D^{GP01}, D^{GP03}, D^{GP20}\}$,	$X^{GP} \in \mathbf{GP01}$

Table 4.5.2-5 The interim results 1 for case study 1

Step 2: Pattern class recognition

Applying the knowledge rules to the interim result 1Table 4.5.2-5, produces:

Rules applied	Reasoning	Conclusion
RULE (5)	$X^{L} \in \mathbf{L01}$, $X^{LD} \in \mathbf{LD05}$, $X^{G} \in \mathbf{G02}$, $X^{GP} \in \mathbf{GP01}$	$X^{VSDF} \in \Phi 1$

Table 4.5.2-6 The interim results 2 for case study 1

Step 3: Initial solution

By applying the knowledge rules to the interim result 2 in Table 4.5.2-6, the initial prediction results are researched as

Rules applied	Reasoning	Conclusion
RULE (7)	$X^{VSDF} \in \Phi 1$	$\mathbf{PM_0}$ = Table 4.5.1 – 5

Table 4.5.2-7 The interim results 3 (initial solution) for case study 1

Step 4: Solution compensation

By running the solution compensation routine (Rule 11) with the interim result 3 in the Table 4.5.2-7, the final prediction results are achieved as:

Bus	PM_0 (p.u.)		Compensation δ		PM_S (p.u.)	
	ΔP_{L0}	ΔQ_{L0}	δ^P	δ^Q	$\Delta P_L = \Delta P_{L0} + \delta^P$	$\Delta Q_L = \Delta Q_{L0} + \delta^Q$
1	0.00	0.00	0.00	0.00	**0.00**	**0.00**
2	0.00	0.00	0.00	0.00	**0.00**	**0.00**
3	2.48	1.48	0.25	0.15	**2.73**	**1.63**
4	9.92	5.92	-0.99	-0.59	**8.93**	**5.33**
5	0.00	0.00	0.00	0.00	**0.00**	**0.00**
6	0.00	0.00	0.00	0.00	**0.00**	**0.00**
7	9.92	5.92	0.99	0.59	**10.91**	**6.51**
8	12.40	7.40	-1.24	-0.74	**11.16**	**6.66**
9	12.40	7.40	1.24	0.74	**13.64**	**8.14**
10	7.44	4.44	-0.75	-0.44	**6.69**	**4.00**
11	0.00	0.00	0.00	0.00	**0.00**	**0.00**
12	12.40	7.40	1.24	0.74	**13.64**	**8.14**
13	0.00	0.00	0.00	0.00	**0.00**	**0.00**
14	12.40	7.40	-1.24	-0.74	**11.16**	**6.66**
15	14.88	8.88	1.49	0.89	**16.37**	**9.77**
16	9.92	5.92	-0.99	-0.59	**8.93**	**5.33**
17	12.40	7.40	1.24	0.74	**13.64**	**8.14**
18	37.20	22.20	-3.72	-2.22	**33.48**	**19.98**
19	29.76	17.76	2.97	1.77	**32.73**	**19.53**
20	29.76	17.76	-2.97	-1.78	**26.79**	**15.98**
21	12.40	7.40	1.24	0.74	**13.64**	**8.14**
22	0.00	0.00	0.00	0.00	**0.00**	**0.00**
23	0.00	0.00	0.00	0.00	**0.00**	**0.00**
24	4.96	2.96	0.49	0.29	**5.45**	**3.25**
25	2.48	1.48	-0.25	-0.15	**2.23**	**1.33**
26	4.96	2.96	0.49	0.29	**5.45**	**3.25**
27	0.00	0.00	0.00	0.00	**0.00**	**0.00**
28	0.00	0.00	0.00	0.00	**0.00**	**0.00**
29	2.48	1.48	-0.25	-0.15	**2.23**	**1.33**
30	7.44	4.44	0.75	0.44	**8.19**	**4.88**
Total	248.00	148.00	0.00	0.00	**248.00**	**148.00**

Table 4.5.2-8 The final (compensated) solution for case study 1

(4) The results produced by the prediction system

By running the user interface routine (Rule 12), the final results together with all the interim results for the case study 1 are presented as:

Bus	X^L (p.u.)		X^G (p.u.)		X^{LD} (%)		X^{GP} (%)		PM_S (p.u.)	
	X^{LP}	X^{LQ}	X^{GP}	X^{GQ}	X^{LDP}	X^{LDQ}	X^{GPP}	X^{GPQ}	ΔP_L	ΔQ_L
1	0.00	0.00	4.47	-0.79	0.00%	0.00%	23.89%	11.29%	**0.00**	**0.00**
2	0.00	0.00	4.27	-1.40	0.00%	0.00%	23.95%	17.07%	**0.00**	**0.00**
3	0.24	0.12	0.00	0.00	1.10%	1.10%	0.00%	0.00%	**2.73**	**1.63**
4	0.76	0.36	0.00	0.00	3.60%	3.60%	0.00%	0.00%	**8.93**	**5.33**
5	0.00	0.00	0.00	0.00	0.00%	0.00%	0.00%	0.00%	**0.00**	**0.00**
6	0.00	0.00	0.00	0.00	0.00%	0.00%	0.00%	0.00%	**0.00**	**0.00**
7	1.28	0.59	0.00	0.00	4.40%	4.40%	0.00%	0.00%	**10.91**	**6.51**
8	1.15	0.43	0.00	0.00	4.50%	4.50%	0.00%	0.00%	**11.16**	**6.66**
9	0.90	0.50	0.00	0.00	5.50%	5.50%	0.00%	0.00%	**13.64**	**8.14**
10	0.58	0.20	0.00	0.00	2.70%	2.70%	0.00%	0.00%	**6.69**	**4.00**
11	0.00	0.00	0.00	0.00	0.00%	0.00%	0.00%	0.00%	**0.00**	**0.00**
12	1.12	0.55	0.00	0.00	5.50%	5.50%	0.00%	0.00%	**13.64**	**8.14**
13	0.00	0.00	2.14	-1.17	0.00%	0.00%	11.97%	14.90%	**0.00**	**0.00**
14	0.62	0.36	0.00	0.00	4.50%	4.50%	0.00%	0.00%	**11.16**	**6.66**
15	0.82	0.55	0.00	0.00	6.60%	6.60%	0.00%	0.00%	**16.37**	**9.77**
16	0.35	0.18	0.00	0.00	3.60%	3.60%	0.00%	0.00%	**8.93**	**5.33**
17	0.90	0.58	0.00	0.00	5.50%	5.50%	0.00%	0.00%	**13.64**	**8.14**
18	3.28	1.79	0.00	0.00	13.50%	13.50%	0.00%	0.00%	**33.48**	**19.98**
19	2.30	1.10	0.00	0.00	13.20%	13.20%	0.00%	0.00%	**32.73**	**19.53**
20	1.22	0.67	0.00	0.00	10.80%	10.80%	0.00%	0.00%	**26.79**	**15.98**
21	0.75	0.32	0.00	0.00	5.50%	5.50%	0.00%	0.00%	**13.64**	**8.14**
22	0.00	0.00	2.67	-1.63	0.00%	0.00%	14.92%	22.70%	**0.00**	**0.00**
23	0.00	0.00	1.60	-1.12	0.00%	0.00%	8.83%	14.90%	**0.00**	**0.00**
24	0.47	0.37	0.00	0.00	2.20%	2.20%	0.00%	0.00%	**5.45**	**3.25**
25	0.10	0.07	0.00	0.00	0.90%	0.90%	0.00%	0.00%	**2.23**	**1.33**
26	0.35	0.23	0.00	0.00	2.20%	2.20%	0.00%	0.00%	**5.45**	**3.25**
27	0.00	0.00	2.94	-1.52	0.00%	0.00%	16.44%	19.14%	**0.00**	**0.00**
28	0.00	0.00	0.00	0.00	0.00%	0.00%	0.00%	0.00%	**0.00**	**0.00**
29	0.27	0.19	0.00	0.00	0.90%	0.90%	0.00%	0.00%	**2.23**	**1.33**
30	0.56	0.29	0.00	0.00	3.30%	3.30%	0.00%	0.00%	**8.19**	**4.88**
Total	18.02	9.45	18.09	-7.63	100.00%	100.00%	100.00%	100.00%	**248.00**	**148.00**

Table 4.5.2-9 The final results by the predication system for case study 1

(5) The results by the conventional load flow study

For the purpose of comparison, the power margins for the test pattern (1) were calculated by using the load flow programme as:

Bus	X^L (p.u.)		X^G (p.u.)		X^{LD} (%)		X^{GP} (%)		**PM** (p.u.)	
	X^{LP}	X^{LQ}	X^{GP}	X^{GQ}	X^{LP}	X^{LQ}	X^{GP}	X^{GQ}	ΔP_L	ΔQ_L
1	0.00	0.00	4.47	-0.79	0.00%	0.00%	23.89%	11.29%	**0.00**	**0.00**
2	0.00	0.00	4.27	-1.40	0.00%	0.00%	23.95%	17.07%	**0.00**	**0.00**
3	0.24	0.12	0.00	0.00	1.10%	1.10%	0.00%	0.00%	**2.77**	**1.66**
4	0.76	0.36	0.00	0.00	3.60%	3.60%	0.00%	0.00%	**9.07**	**5.44**
5	0.00	0.00	0.00	0.00	0.00%	0.00%	0.00%	0.00%	**0.00**	**0.00**
6	0.00	0.00	0.00	0.00	0.00%	0.00%	0.00%	0.00%	**0.00**	**0.00**
7	1.28	0.59	0.00	0.00	4.40%	4.40%	0.00%	0.00%	**11.09**	**6.64**
8	1.15	0.43	0.00	0.00	4.50%	4.50%	0.00%	0.00%	**11.34**	**6.80**
9	0.90	0.50	0.00	0.00	5.50%	5.50%	0.00%	0.00%	**13.86**	**8.31**
10	0.58	0.20	0.00	0.00	2.70%	2.70%	0.00%	0.00%	**6.80**	**4.08**
11	0.00	0.00	0.00	0.00	0.00%	0.00%	0.00%	0.00%	**0.00**	**0.00**
12	1.12	0.55	0.00	0.00	5.50%	5.50%	0.00%	0.00%	**13.86**	**8.31**
13	0.00	0.00	2.14	-1.17	0.00%	0.00%	11.97%	14.90%	**0.00**	**0.00**
14	0.62	0.36	0.00	0.00	4.50%	4.50%	0.00%	0.00%	**11.34**	**6.80**
15	0.82	0.55	0.00	0.00	6.60%	6.60%	0.00%	0.00%	**16.63**	**9.97**
16	0.35	0.18	0.00	0.00	3.60%	3.60%	0.00%	0.00%	**9.07**	**5.44**
17	0.90	0.58	0.00	0.00	5.50%	5.50%	0.00%	0.00%	**13.86**	**8.31**
18	3.28	1.79	0.00	0.00	13.50%	13.50%	0.00%	0.00%	**34.02**	**20.39**
19	2.30	1.10	0.00	0.00	13.20%	13.20%	0.00%	0.00%	**33.26**	**19.93**
20	1.22	0.67	0.00	0.00	10.80%	10.80%	0.00%	0.00%	**27.22**	**16.31**
21	0.75	0.32	0.00	0.00	5.50%	5.50%	0.00%	0.00%	**13.86**	**8.31**
22	0.00	0.00	2.67	-1.63	0.00%	0.00%	14.92%	22.70%	**0.00**	**0.00**
23	0.00	0.00	1.60	-1.12	0.00%	0.00%	8.83%	14.90%	**0.00**	**0.00**
24	0.47	0.37	0.00	0.00	2.20%	2.20%	0.00%	0.00%	**5.54**	**3.32**
25	0.10	0.07	0.00	0.00	0.90%	0.90%	0.00%	0.00%	**2.27**	**1.36**
26	0.35	0.23	0.00	0.00	2.20%	2.20%	0.00%	0.00%	**5.54**	**3.32**
27	0.00	0.00	2.94	-1.52	0.00%	0.00%	16.44%	19.14%	**0.00**	**0.00**
28	0.00	0.00	0.00	0.00	0.00%	0.00%	0.00%	0.00%	**0.00**	**0.00**
29	0.27	0.19	0.00	0.00	0.90%	0.90%	0.00%	0.00%	**2.27**	**1.36**
30	0.56	0.29	0.00	0.00	3.30%	3.30%	0.00%	0.00%	**8.32**	**4.98**
Total	18.02	9.45	18.09	-7.63	100.00%	100.00%	100.00%	100.00%	**251.99**	**151.04**

Table 4.5.2-10 The power margins by the load flow study for case study 1

(6) Accuracy analysis

Accuracy analysis was made for the case study 1 as listed in Table 4.5.2-11. The analysis includes both absolute error and relative error for the initial and final simulation results against the power margins determined by the conventional load flow study. The following formulas are used for calculating the absolute and relative errors:

Absolute Errors:

$$\varepsilon_P = | \Delta P - \Delta Px |$$

$$\varepsilon_Q = | \Delta Q - \Delta Qx |$$

Relative Errors:

$$\eta_P = | (\Delta P - \Delta P_X) / Pmax |$$

$$\eta_Q = | (\Delta P - \Delta P_X) / Qmax |$$

where,

ε_P , ε_Q are the absolute errors for the predicted active and reactive power margins,

ΔP , ΔQ are the active and reactive power margins determined by the conventional load flow study,

ΔPx , ΔQx are the initial or final power margin results produced by the prediction system,

η_P , η_Q are the relative errors for the initial or final results by the prediction system,

Pmax , Qmax are the maximum active and reactive load level for a bus or power system determined by the conventional load flow study.

From Table 4.5.2-11, it can be seen that by using the compensation algorithm, the average relative errors are reduced from 8.94% / 9.00% for the initial solution to 1.48% / 1.89% with the final solution. The maximum relative errors with the individual results are improved from 10.03% / 10.36% for the initial solution to the 1.52% / 1.95% for the final solution.

					For the initial results(PMo)				For the final results (PMs)			
	PM by LF		Max Load		Abs Error (p.u.)		Rel Error (%)		Abs Error (p.u.)		Rel Error (%)	
Bus	ΔP	ΔQ	Pmax	Qmax	ε_P	ε_Q	η_p	η_q	ε_P	ε_Q	η_p	η_q
1	0.00	0.00	0.00	0.00	0.000	0.000	n/a	n/a	0.000	0.000	n/a	n/a
2	0.00	0.00	0.00	0.00	0.000	0.000	n/a	n/a	0.000	0.000	n/a	n/a
3	2.77	1.66	3.01	1.78	0.290	0.180	9.63%	10.11%	0.044	0.033	1.46%	1.88%
4	9.07	5.44	9.83	5.80	0.850	0.480	8.65%	8.28%	0.144	0.109	1.46%	1.89%
5	0.00	0.00	0.00	0.00	0.000	0.000	n/a	n/a	0.000	0.000	n/a	n/a
6	0.00	0.00	0.00	0.00	0.000	0.000	n/a	n/a	0.000	0.000	n/a	n/a
7	11.09	6.64	12.37	7.23	1.170	0.720	9.46%	9.96%	0.176	0.134	1.42%	1.85%
8	11.34	6.80	12.49	7.23	1.060	0.600	8.49%	8.30%	0.180	0.137	1.44%	1.89%
9	13.86	8.31	14.76	8.81	1.460	0.910	9.89%	10.33%	0.219	0.167	1.49%	1.90%
10	6.80	4.08	7.38	4.28	0.640	0.360	8.67%	8.41%	0.108	0.082	1.46%	1.92%
11	0.00	0.00	0.00	0.00	0.000	0.000	n/a	n/a	0.000	0.000	n/a	n/a
12	13.86	8.31	14.98	8.86	1.460	0.910	9.75%	10.27%	0.219	0.167	1.47%	1.89%
13	0.00	0.00	0.00	0.00	0.000	0.000	n/a	n/a	0.000	0.000	n/a	n/a
14	11.34	6.80	11.96	7.16	1.060	0.600	8.86%	8.38%	0.180	0.137	1.50%	1.91%
15	16.63	9.97	17.45	10.52	1.750	1.090	10.03%	10.36%	0.263	0.201	1.51%	1.91%
16	9.07	5.44	9.42	5.62	0.850	0.480	9.02%	8.54%	0.144	0.109	1.52%	1.95%
17	13.86	8.31	14.76	8.89	1.460	0.910	9.89%	10.24%	0.219	0.167	1.49%	1.88%
18	34.02	20.39	37.30	22.18	3.180	1.810	8.53%	8.16%	0.539	0.410	1.44%	1.85%
19	33.26	19.93	35.56	21.03	3.500	2.170	9.84%	10.32%	0.527	0.401	1.48%	1.91%
20	27.22	16.31	28.44	16.98	2.540	1.450	8.93%	8.54%	0.431	0.328	1.52%	1.93%
21	13.86	8.31	14.61	8.63	1.460	0.910	9.99%	10.54%	0.219	0.167	1.50%	1.94%
22	0.00	0.00	0.00	0.00	0.000	0.000	n/a	n/a	0.000	0.000	n/a	n/a

					For the initial results(PMo)				For the final results (PMs)			
	PM by LF		Max Load		Abs Error (p.u.)		Rel Error (%)		Abs Error (p.u.)		Rel Error (%)	
Bus	**ΔP**	**ΔQ**	**Pmax**	**Qmax**	**ε_P**	**ε_Q**	**η_p**	**η_q**	**ε_P**	**ε_Q**	**η_p**	**η_q**
23	0.00	0.00	0.00	0.00	0.000	0.000	n/a	n/a	0.000	0.000	n/a	n/a
24	5.54	3.32	6.01	3.69	0.580	0.360	9.65%	9.76%	0.088	0.067	1.46%	1.81%
25	2.27	1.36	2.37	1.43	0.210	0.120	8.86%	8.39%	0.036	0.027	1.52%	1.91%
26	5.54	3.32	5.89	3.55	0.580	0.360	9.85%	10.14%	0.088	0.067	1.49%	1.88%
27	0.00	0.00	0.00	0.00	0.000	0.000	n/a	n/a	0.000	0.000	n/a	n/a
28	0.00	0.00	0.00	0.00	0.000	0.000	n/a	n/a	0.000	0.000	n/a	n/a
29	2.27	1.36	2.54	1.55	0.210	0.120	8.27%	7.74%	0.036	0.027	1.42%	1.77%
30	8.32	4.98	8.88	5.27	0.880	0.540	9.91%	10.25%	0.132	0.100	1.48%	1.90%
Total	251.99	151.04	270.01	160.49	3.990	3.040	1.48%	1.89%	3.990	3.040	1.48%	1.89%
Average					**0.941**	**0.585**	**8.94%**	**9.00%**	**0.257**	**0.196**	**1.48%**	**1.89%**

Table 4.5.2-11 The accuracy analysis for case study 1

2. Case Study 2

(1) Test pattern

The VSDFs for the testing pattern in this study case are set as:

Bus	X^{L} (p.u.)		X^{G} (p.u.)		X^{LD} (%)		X^{GP} (%)	
	X^{LP}	X^{LQ}	X^{GP}	X^{GQ}	X^{LDP}	X^{LDQ}	X^{GPP}	X^{GPQ}
1	0.00	0.00	3.92	0.91	0.00%	0.00%	24.93%	10.03%
2	0.00	0.00	5.64	1.48	0.00%	0.00%	25.82%	18.64%
3	0.32	0.16	0.00	0.00	1.04%	1.05%	0.00%	0.00%
4	1.00	0.48	0.00	0.00	4.19%	4.19%	0.00%	0.00%
5	0.00	0.00	0.00	0.00	0.00%	0.00%	0.00%	0.00%
6	0.00	0.00	0.00	0.00	0.00%	0.00%	0.00%	0.00%
7	1.69	0.78	0.00	0.00	4.19%	4.19%	0.00%	0.00%
8	1.52	0.57	0.00	0.00	5.24%	5.23%	0.00%	0.00%
9	1.19	0.66	0.00	0.00	5.24%	5.24%	0.00%	0.00%
10	0.77	0.26	0.00	0.00	3.14%	3.14%	0.00%	0.00%
11	0.00	0.00	0.00	0.00	0.00%	0.00%	0.00%	0.00%
12	1.48	0.73	0.00	0.00	5.24%	5.23%	0.00%	0.00%
13	0.00	0.00	1.88	0.82	0.00%	0.00%	10.19%	13.49%
14	0.82	0.48	0.00	0.00	5.24%	5.23%	0.00%	0.00%
15	1.08	0.73	0.00	0.00	6.29%	6.28%	0.00%	0.00%
16	0.31	0.16	0.00	0.00	4.19%	4.20%	0.00%	0.00%
17	0.81	0.53	0.00	0.00	4.29%	4.28%	0.00%	0.00%
18	2.94	1.63	0.00	0.00	12.86%	12.86%	0.00%	0.00%
19	2.06	1.00	0.00	0.00	12.57%	12.57%	0.00%	0.00%
20	1.09	0.61	0.00	0.00	12.57%	12.57%	0.00%	0.00%
21	0.67	0.29	0.00	0.00	4.29%	4.29%	0.00%	0.00%
22	0.00	0.00	3.53	1.72	0.00%	0.00%	12.74%	20.09%
23	0.00	0.00	2.11	1.18	0.00%	0.00%	9.31%	16.30%
24	0.42	0.34	0.00	0.00	2.10%	2.09%	0.00%	0.00%
25	0.09	0.06	0.00	0.00	1.05%	1.05%	0.00%	0.00%
26	0.46	0.30	0.00	0.00	2.10%	2.10%	0.00%	0.00%
27	0.00	0.00	2.81	0.95	0.00%	0.00%	17.02%	21.45%
28	0.00	0.00	0.00	0.00	0.00%	0.00%	0.00%	0.00%
29	0.36	0.25	0.00	0.00	1.04%	1.05%	0.00%	0.00%
30	0.74	0.38	0.00	0.00	3.14%	3.14%	0.00%	0.00%
Total	19.82	10.40	19.89	7.06	100.00%	100.00%	100.00%	100.00%

Table 4.5.2-12 Test pattern (2) for the case study 2

The further details about this test pattern are given in the Table A3-14 of Appendix 3.

(2) Euclidean Distance Calculations

(i) The Euclidean Distance to pattern class I:

The 4 segments of Euclidean distance from testing pattern (2) to the prototype of pattern class I (**L01, LD05, G02 and GP01** as shown in Table 4.5.1-1) are calculated as:

Load pattern segment D^{L01}	1.11
Load distribution pattern segment D^{LD03}	3.67
Generation pattern segment D^{G02}	6.40
Generation participation pattern segment D^{GP01}	5.69

Table 4.5.2-13 The Euclidean distance from test pattern (2) to pattern class I

(ii) The Euclidean distance to pattern class II:

The Euclidean distance from test pattern (1) to the prototype of pattern class II (**L10, LD15, G06 and GP03** as shown in Table 4.5.1-2) is calculated as:

Load pattern segment D^{L12}	23.32
Load distribution pattern segment D^{LD11}	12.14
Generation pattern segment D^{G09}	53.48
Generation participation pattern segment D^{GP06}	50.01

Table 4.5.2-14 The Euclidean distance from test pattern (2) to pattern class 1I

(iii) Euclidean distance to pattern class III:

The Euclidean distance to from test pattern (1) to the prototype of pattern class III **(L20, LD20, G20 and GP20** as shown in Table 4.5.1-3) is calculated as:

Load pattern segment D^{L12}	60.73
Load distribution pattern segment D^{LD11}	26.34
Generation pattern segment D^{G09}	111.12
Generation participation pattern segment D^{GP06}	27.18

Table 4.5.2-15 The Euclidean distance from test pattern (2) to pattern class III

(3) Solution searching

By the same solution searching as illustrated in the case study 1, the initial (**PM_0**) and the final solutions (compensated) are reached as shown in Table 4.5.2-16 The final (compensated) solution for case study

Bus	PM_0 (p.u.)		Compensation δ		PM_S (p.u.)	
	ΔP_{L0}	ΔQ_{L0}	δ^P	δ^Q	$\Delta P_L=\Delta P_{L0}+\delta^P$	$\Delta Q_L=\Delta Q_{L0}+\delta^Q$
1	0.00	0.00	0.00	0.00	0.00	0.00
2	0.00	0.00	0.00	0.00	0.00	0.00
3	2.48	1.48	0.09	0.06	2.57	1.54
4	9.92	5.92	0.40	0.24	10.32	6.16
5	0.00	0.00	0.00	0.00	0.00	0.00
6	0.00	0.00	0.00	0.00	0.00	0.00
7	9.92	5.92	0.39	0.24	10.31	6.16
8	12.40	7.40	0.50	0.30	12.90	7.70
9	12.40	7.40	0.50	0.31	12.90	7.71
10	7.44	4.44	0.29	0.18	7.73	4.62
11	0.00	0.00	0.00	0.00	0.00	0.00
12	12.40	7.40	0.50	0.30	12.90	7.70
13	0.00	0.00	0.00	0.00	0.00	0.00
14	12.40	7.40	0.50	0.30	12.90	7.70
15	14.88	8.88	0.60	0.36	15.48	9.24
16	9.92	5.92	0.40	0.25	10.32	6.17
17	12.40	7.40	-1.85	-1.10	10.55	6.30
18	37.20	22.20	-5.55	-3.29	31.65	18.91
19	29.76	17.76	1.19	0.73	30.95	18.49
20	29.76	17.76	1.19	0.73	30.95	18.49
21	12.40	7.40	-1.85	-1.09	10.55	6.31
22	0.00	0.00	0.00	0.00	0.00	0.00
23	0.00	0.00	0.00	0.00	0.00	0.00
24	4.96	2.96	0.20	0.12	5.16	3.08
25	2.48	1.48	0.10	0.07	2.58	1.55
26	4.96	2.96	0.20	0.12	5.16	3.08
27	0.00	0.00	0.00	0.00	0.00	0.00
28	0.00	0.00	0.00	0.00	0.00	0.00
29	2.48	1.48	0.09	0.06	2.57	1.54
30	7.44	4.44	0.29	0.18	7.73	4.62
Total	248.00	148.00	-1.80	-0.95	246.20	147.05

Table 4.5.2-16 The final (compensated) solution for case study 2

(4) The result produced by the prediction system

The final results for the case study 2 are presented as:

Bus	X^L (p.u.)		X^G (p.u.)		X^{LD} (%)		X^{GP} (%)		PMs (p.u.)	
	X^{LP}	X^{LQ}	X^{GP}	X^{GQ}	X^{LDP}	X^{LDQ}	X^{GPP}	X^{GPQ}	ΔP_L	ΔQ_L
1	0.00	0.00	3.92	0.91	0.00%	0.00%	24.93%	10.03%	**0.00**	**0.00**
2	0.00	0.00	5.64	1.48	0.00%	0.00%	25.82%	18.64%	**0.00**	**0.00**
3	0.32	0.16	0.00	0.00	1.04%	1.05%	0.00%	0.00%	**2.57**	**1.54**
4	1.00	0.48	0.00	0.00	4.19%	4.19%	0.00%	0.00%	**10.32**	**6.16**
5	0.00	0.00	0.00	0.00	0.00%	0.00%	0.00%	0.00%	**0.00**	**0.00**
6	0.00	0.00	0.00	0.00	0.00%	0.00%	0.00%	0.00%	**0.00**	**0.00**
7	1.69	0.78	0.00	0.00	4.19%	4.19%	0.00%	0.00%	**10.31**	**6.16**
8	1.52	0.57	0.00	0.00	5.24%	5.23%	0.00%	0.00%	**12.90**	**7.70**
9	1.19	0.66	0.00	0.00	5.24%	5.24%	0.00%	0.00%	**12.90**	**7.71**
10	0.77	0.26	0.00	0.00	3.14%	3.14%	0.00%	0.00%	**7.73**	**4.62**
11	0.00	0.00	0.00	0.00	0.00%	0.00%	0.00%	0.00%	**0.00**	**0.00**
12	1.48	0.73	0.00	0.00	5.24%	5.23%	0.00%	0.00%	**12.90**	**7.70**
13	0.00	0.00	1.88	0.82	0.00%	0.00%	10.19%	13.49%	**0.00**	**0.00**
14	0.82	0.48	0.00	0.00	5.24%	5.23%	0.00%	0.00%	**12.90**	**7.70**
15	1.08	0.73	0.00	0.00	6.29%	6.28%	0.00%	0.00%	**15.48**	**9.24**
16	0.31	0.16	0.00	0.00	4.19%	4.20%	0.00%	0.00%	**10.32**	**6.17**
17	0.81	0.53	0.00	0.00	4.29%	4.28%	0.00%	0.00%	**10.55**	**6.30**
18	2.94	1.63	0.00	0.00	12.86%	12.86%	0.00%	0.00%	**31.65**	**18.91**
19	2.06	1.00	0.00	0.00	12.57%	12.57%	0.00%	0.00%	**30.95**	**18.49**
20	1.09	0.61	0.00	0.00	12.57%	12.57%	0.00%	0.00%	**30.95**	**18.49**
21	0.67	0.29	0.00	0.00	4.29%	4.29%	0.00%	0.00%	**10.55**	**6.31**
22	0.00	0.00	3.53	1.72	0.00%	0.00%	12.74%	20.09%	**0.00**	**0.00**
23	0.00	0.00	2.11	1.18	0.00%	0.00%	9.31%	16.30%	**0.00**	**0.00**
24	0.42	0.34	0.00	0.00	2.10%	2.09%	0.00%	0.00%	**5.16**	**3.08**
25	0.09	0.06	0.00	0.00	1.05%	1.05%	0.00%	0.00%	**2.58**	**1.55**
26	0.46	0.30	0.00	0.00	2.10%	2.10%	0.00%	0.00%	**5.16**	**3.08**
27	0.00	0.00	2.81	0.95	0.00%	0.00%	17.02%	21.45%	**0.00**	**0.00**
28	0.00	0.00	0.00	0.00	0.00%	0.00%	0.00%	0.00%	**0.00**	**0.00**
29	0.36	0.25	0.00	0.00	1.04%	1.05%	0.00%	0.00%	**2.57**	**1.54**
30	0.74	0.38	0.00	0.00	3.14%	3.14%	0.00%	0.00%	**7.73**	**4.62**
Total	19.82	10.40	19.89	7.06	100.00%	100.00%	100.00%	100.00%	**246.20**	**147.05**

Table 4.5.2-17 The final results by the predication system for case study 2

(5) The results by the conventional load flow study

For the purposed of comparison, the power margins for test pattern (2) are also calculated by the conventional load flow programme as:

Bus	X^{L} (p.u.)		X^{G} (p.u.)		X^{LD} (%)		X^{GP} (%)		PM (p.u.)	
	X^{LP}	X^{LQ}	X^{GP}	X^{GQ}	X^{LP}	X^{LQ}	X^{GP}	X^{GQ}	ΔP_L	ΔQ_L
1	0.00	0.00	3.92	0.91	0.00%	0.00%	24.93%	10.03%	**0.00**	**0.00**
2	0.00	0.00	5.64	1.48	0.00%	0.00%	25.82%	18.64%	**0.00**	**0.00**
3	0.32	0.16	0.00	0.00	1.04%	1.05%	0.00%	0.00%	**2.61**	**1.57**
4	1.00	0.48	0.00	0.00	4.19%	4.19%	0.00%	0.00%	**10.48**	**6.29**
5	0.00	0.00	0.00	0.00	0.00%	0.00%	0.00%	0.00%	**0.00**	**0.00**
6	0.00	0.00	0.00	0.00	0.00%	0.00%	0.00%	0.00%	**0.00**	**0.00**
7	1.69	0.78	0.00	0.00	4.19%	4.19%	0.00%	0.00%	**10.47**	**6.29**
8	1.52	0.57	0.00	0.00	5.24%	5.23%	0.00%	0.00%	**13.09**	**7.86**
9	1.19	0.66	0.00	0.00	5.24%	5.24%	0.00%	0.00%	**13.09**	**7.87**
10	0.77	0.26	0.00	0.00	3.14%	3.14%	0.00%	0.00%	**7.85**	**4.72**
11	0.00	0.00	0.00	0.00	0.00%	0.00%	0.00%	0.00%	**0.00**	**0.00**
12	1.48	0.73	0.00	0.00	5.24%	5.23%	0.00%	0.00%	**13.09**	**7.86**
13	0.00	0.00	1.88	0.82	0.00%	0.00%	10.19%	13.49%	**0.00**	**0.00**
14	0.82	0.48	0.00	0.00	5.24%	5.23%	0.00%	0.00%	**13.09**	**7.86**
15	1.08	0.73	0.00	0.00	6.29%	6.28%	0.00%	0.00%	**15.71**	**9.43**
16	0.31	0.16	0.00	0.00	4.19%	4.20%	0.00%	0.00%	**10.48**	**6.30**
17	0.81	0.53	0.00	0.00	4.29%	4.28%	0.00%	0.00%	**10.71**	**6.43**
18	2.94	1.63	0.00	0.00	12.86%	12.86%	0.00%	0.00%	**32.13**	**19.31**
19	2.06	1.00	0.00	0.00	12.57%	12.57%	0.00%	0.00%	**31.42**	**18.88**
20	1.09	0.61	0.00	0.00	12.57%	12.57%	0.00%	0.00%	**31.42**	**18.88**
21	0.67	0.29	0.00	0.00	4.29%	4.29%	0.00%	0.00%	**10.71**	**6.44**
22	0.00	0.00	3.53	1.72	0.00%	0.00%	12.74%	20.09%	**0.00**	**0.00**
23	0.00	0.00	2.11	1.18	0.00%	0.00%	9.31%	16.30%	**0.00**	**0.00**
24	0.42	0.34	0.00	0.00	2.10%	2.09%	0.00%	0.00%	**5.24**	**3.14**
25	0.09	0.06	0.00	0.00	1.05%	1.05%	0.00%	0.00%	**2.62**	**1.58**
26	0.46	0.30	0.00	0.00	2.10%	2.10%	0.00%	0.00%	**5.24**	**3.15**
27	0.00	0.00	2.81	0.95	0.00%	0.00%	17.02%	21.45%	**0.00**	**0.00**
28	0.00	0.00	0.00	0.00	0.00%	0.00%	0.00%	0.00%	**0.00**	**0.00**
29	0.36	0.25	0.00	0.00	1.04%	1.05%	0.00%	0.00%	**2.61**	**1.57**
30	0.74	0.38	0.00	0.00	3.14%	3.14%	0.00%	0.00%	**7.85**	**4.72**
Total	19.82	10.40	19.89	7.06	100.00%	100.00%	100.00%	100.00%	**249.91**	**150.15**

Table 4.5.2-18 **The power margins by the load flow study for case study 2**

(6) Accuracy analysis

Accuracy analysis for the case study 2 are summarised in the Table 4.5.2-19 below. The average relative errors are reduced from 6.04% / 6.50% with the initial solution to 1.37% / 1.92% with the final solution. The maximum relative errors with the individual prediction results are improved from 14.85% / 14.26% for the initial solution to the 1.44% / 2.01% for the final solution.

					For the initial results(PMo)				For the final results (PMs)			
	PM by LF		Max Load		Abs Error (p.u.)		Rel Error (%)		Abs Error (p.u.)		Rel Error (%)	
Bus	ΔP	ΔQ	Pmax	Qmax	ε_P	ε_Q	η_p	η_q	ε_P	ε_Q	η_p	η_q
1	0.00	0.00	0.00	0.00	0.000	0.000	n/a	n/a	0.000	0.000	n/a	n/a
2	0.00	0.00	0.00	0.00	0.000	0.000	n/a	n/a	0.000	0.000	n/a	n/a
3	2.61	1.57	2.93	1.73	0.130	0.090	4.44%	5.20%	0.039	0.032	1.32%	1.87%
4	10.48	6.29	11.48	6.77	0.560	0.370	4.88%	5.47%	0.156	0.130	1.36%	1.92%
5	0.00	0.00	0.00	0.00	0.000	0.000	n/a	n/a	0.000	0.000	n/a	n/a
6	0.00	0.00	0.00	0.00	0.000	0.000	n/a	n/a	0.000	0.000	n/a	n/a
7	10.47	6.29	12.16	7.07	0.550	0.370	4.52%	5.23%	0.155	0.130	1.28%	1.84%
8	13.09	7.86	14.61	8.43	0.690	0.460	4.72%	5.46%	0.194	0.162	1.33%	1.93%
9	13.09	7.87	14.28	8.53	0.690	0.470	4.83%	5.51%	0.194	0.162	1.36%	1.90%
10	7.85	4.72	8.62	4.98	0.410	0.280	4.76%	5.62%	0.117	0.097	1.35%	1.96%
11	0.00	0.00	0.00	0.00	0.000	0.000	n/a	n/a	0.000	0.000	n/a	n/a
12	13.09	7.86	14.57	8.59	0.690	0.460	4.74%	5.36%	0.194	0.162	1.33%	1.89%
13	0.00	0.00	0.00	0.00	0.000	0.000	n/a	n/a	0.000	0.000	n/a	n/a
14	13.09	7.86	13.91	8.34	0.690	0.460	4.96%	5.52%	0.194	0.162	1.40%	1.95%
15	15.71	9.43	16.79	10.16	0.830	0.550	4.94%	5.41%	0.233	0.195	1.39%	1.92%
16	10.48	6.30	10.79	6.46	0.560	0.380	5.19%	5.88%	0.156	0.130	1.44%	2.01%
17	10.71	6.43	11.52	6.96	1.690	0.970	14.67%	13.94%	0.159	0.133	1.38%	1.91%
18	32.13	19.31	35.07	20.94	5.070	2.890	14.46%	13.80%	0.477	0.399	1.36%	1.90%
19	31.42	18.88	33.48	19.88	1.660	1.120	4.96%	5.63%	0.466	0.390	1.39%	1.96%
20	31.42	18.88	32.51	19.49	1.660	1.120	5.11%	5.75%	0.466	0.390	1.43%	2.00%
21	10.71	6.44	11.38	6.73	1.690	0.960	14.85%	14.26%	0.159	0.133	1.40%	1.98%
22	0.00	0.00	0.00	0.00	0.000	0.000	n/a	n/a	0.000	0.000	n/a	n/a

					For the initial results(PMo)				For the final results (PMs)			
	PM by LF		Max Load		Abs Error (p.u.)		Rel Error (%)		Abs Error (p.u.)		Rel Error (%)	
Bus	**ΔP**	**ΔQ**	**Pmax**	**Qmax**	ε_P	ε_Q	η_p	η_q	ε_P	ε_Q	η_p	η_q
23	0.00	0.00	0.00	0.00	0.000	0.000	n/a	n/a	0.000	0.000	n/a	n/a
24	5.24	3.14	5.66	3.48	0.280	0.180	4.95%	5.17%	0.078	0.065	1.37%	1.86%
25	2.62	1.58	2.71	1.64	0.140	0.100	5.17%	6.10%	0.039	0.033	1.44%	1.99%
26	5.24	3.15	5.70	3.45	0.280	0.190	4.91%	5.51%	0.078	0.065	1.36%	1.89%
27	0.00	0.00	0.00	0.00	0.000	0.000	n/a	n/a	0.000	0.000	n/a	n/a
28	0.00	0.00	0.00	0.00	0.000	0.000	n/a	n/a	0.000	0.000	n/a	n/a
29	2.61	1.57	2.97	1.82	0.130	0.090	4.38%	4.95%	0.039	0.032	1.30%	1.78%
30	7.85	4.72	8.59	5.10	0.410	0.280	4.77%	5.49%	0.117	0.097	1.36%	1.91%
Total	249.91	150.15	269.73	160.55	1.910	2.150	0.71%	1.34%	3.710	3.100	1.38%	1.93%
Average					**0.668**	**0.450**	**6.04%**	**6.50%**	**0.239**	**0.200**	**1.37%**	**1.92%**

Table 4.5.2-19 The accuracy analysis for case study 2

3. Case Study 3

(1) Test pattern

In this case, the VSDFs for the testing pattern are set as shown in the table blow:

Bus	X^L (p.u.)		X^G (p.u.)		X^{LD} (%)		X^{GP} (%)	
	X^{LP}	X^{LQ}	X^{GP}	X^{GQ}	X^{LDP}	X^{LDQ}	X^{GPP}	X^{GPQ}
1	0.00	0.00	35.09	12.31	0.00%	0.00%	38.54%	36.58%
2	0.00	0.00	36.20	14.40	0.00%	0.00%	36.88%	34.15%
3	1.32	0.66	0.00	0.00	2.00%	2.00%	0.00%	0.00%
4	4.18	1.98	0.00	0.00	4.00%	4.00%	0.00%	0.00%
5	0.00	0.00	0.00	0.00	0.00%	0.00%	0.00%	0.00%
6	0.00	0.00	0.00	0.00	0.00%	0.00%	0.00%	0.00%
7	7.04	3.25	0.00	0.00	3.00%	3.00%	0.00%	0.00%
8	6.33	2.37	0.00	0.00	5.00%	5.00%	0.00%	0.00%
9	4.95	2.75	0.00	0.00	5.00%	5.00%	0.00%	0.00%
10	3.19	1.10	0.00	0.00	3.00%	3.00%	0.00%	0.00%
11	0.00	0.00	0.00	0.00	0.00%	0.00%	0.00%	0.00%
12	5.04	2.48	0.00	0.00	4.00%	4.00%	0.00%	0.00%
13	0.00	0.00	0.00	0.00	0.00%	0.00%	0.00%	0.00%
14	2.79	1.62	0.00	0.00	6.00%	6.00%	0.00%	0.00%
15	3.69	2.48	0.00	0.00	5.00%	5.00%	0.00%	0.00%
16	1.58	0.81	0.00	0.00	4.00%	4.00%	0.00%	0.00%
17	4.05	2.61	0.00	0.00	5.00%	5.00%	0.00%	0.00%
18	14.76	8.05	0.00	0.00	20.00%	20.02%	0.00%	0.00%
19	10.35	4.95	0.00	0.00	10.00%	10.00%	0.00%	0.00%
20	5.49	3.02	0.00	0.00	10.00%	10.00%	0.00%	0.00%
21	4.13	1.76	0.00	0.00	5.00%	5.00%	0.00%	0.00%
22	0.00	0.00	0.00	0.00	0.00%	0.00%	0.00%	0.00%
23	0.00	0.00	0.00	0.00	0.00%	0.00%	0.00%	0.00%
24	2.59	2.04	0.00	0.00	2.00%	2.00%	0.00%	0.00%
25	0.55	0.39	0.00	0.00	1.00%	1.00%	0.00%	0.00%
26	1.93	1.26	0.00	0.00	2.99%	3.00%	0.00%	0.00%
27	0.00	0.00	19.80	13.08	0.00%	0.00%	24.58%	29.27%
28	0.00	0.00	0.00	0.00	0.00%	0.00%	0.00%	0.00%
29	1.49	1.04	0.00	0.00	1.00%	1.00%	0.00%	0.00%
30	3.08	1.60	0.00	0.00	2.00%	2.00%	0.00%	0.00%
Total	88.53	46.22	91.09	39.79	100.00%	100.00%	100.00%	100.00%

Table 4.5.2-20 Test pattern (3) for case study 3

This test pattern is one of the patterns within the study group 2 (normally loaded cluster) for the simulation of power margin similarity in Chapter 3. The further details about this test pattern are given in the Table A3-16 in Appendix 3.

(2) Euclidean Distance Calculations

The Euclidean distances to the prototype of each pattern class is calculated by using equation (4.5.1-1) as:

(i) The Euclidean distance to pattern class I:

The 4 segments of the Euclidean distance from the testing pattern (3) to the prototype of pattern class I (**L01, LD05, G02 and GP01** as shown in Table 4.5.1-1) are:

Load pattern segment D^{L01}	21.87
Load distribution pattern segment D^{LD03}	8.95
Generation pattern segment D^{G02}	53.81
Generation participation pattern segment D^{GP01}	53.86

Table 4.5.2-21 The Euclidean distance from test pattern (3) to pattern class I

(ii) The Euclidean distance to pattern class II:

The Euclidean distance from test pattern (3) to the prototype of pattern class II (**L10, LD15, G06 and GP03** as shown in Table 4.5.1-2) is:

Load pattern segment D^{L12}	2.93
Load distribution pattern segment D^{LD11}	0.02
Generation pattern segment D^{G09}	3.23
Generation participation pattern segment D^{GP06}	3.63

Table 4.5.2-22 The Euclidean distance from test pattern (3) to pattern class 1I

(iii) The Euclidean distance to pattern class III:

The Euclidean distance to from test pattern (3) to the prototype of pattern class III (**L20, LD20, G20 and GP20** as shown in Table 4.5.1-3) is:

Load pattern segment D^{L12}	48.40
Load distribution pattern segment D^{LD11}	26.84
Generation pattern segment D^{G09}	73.13
Generation participation pattern segment D^{GP06}	37.13

Table 4.5.2-23 The Euclidean distance from test pattern (3) to pattern class III

(3) Solution searching

The solution searching in this case study includes the following steps:

Step 1: VSDFs identification

By applying the knowledge rules to the results in Table 4.5.2-21, Table 4.5.2-22 and Table 4.5.2-23, the following interim results are obtained:

Rules Applied	**Reasoning**	**Conclusion**
RULE (1)	$D^{L10} = \min \{D^{L01}, D^{L10}, D^{L20}\}$,	$\mathbf{X}^{L} \in$ L10
RULE (2)	$D^{LD15} = \min \{D^{LD05}, D^{LD15}, D^{LD20}\}$,	$\mathbf{X}^{LD} \in$ **LD15**
RULE (3)	$D^{G06} = \min \{D^{G02}, D^{G06}, D^{G20}\}$,	$\mathbf{X}^{G} \in$ **G06**
RULE (4) :	$D^{GP03} = \min \{D^{GP01}, D^{GP03}, D^{GP20}\}$,	$\mathbf{X}^{GP} \in$ **GP03**

Table 4.5.2-24 Interim results 1 for case study 3

Step 2: Pattern class recognition

Applying the knowledge rules to the interim result 1 in Table 4.5.2-24, produces

Rules applied	**Reasoning**	**Conclusion**
RULE (5)	$\mathbf{X}^{L} \in \mathbf{L10}$, $\mathbf{X}^{LD} \in \mathbf{LD15}$, $\mathbf{X}^{G} \in \mathbf{G06}$, $\mathbf{X}^{GP} \in \mathbf{GP03}$	$\mathbf{X}^{VSDF} \in \Phi 2$

Table 4.5.2-25 Interim results 2 for case study 3

Step 3: Initial solution

By applying the knowledge rules to the interim result 2 in Table 4.5.2-25, the initial prediction results are reached as

Rules applied	**Reasoning**	**Conclusion**
RULE (7)	$\mathbf{X}^{VSDF} \in \Phi 2$	$\mathbf{PM_0}$ = Table 4.5.1 – 6

Table 4.5.2-26 Interim results 3 (initial solution) for case study 3

Step 4: Solution compensation

By running the solution compensation routine (Rule 11) with the interim result 3, the final prediction results are achieved as:

Bus	PM_0 (p.u.)		Compensation δ		PM_S (p.u.)	
	ΔP_{L0}	ΔQ_{L0}	δ^P	δ^Q	$\Delta P_L = \Delta P_{L0} + \delta^P$	$\Delta Q_L = \Delta Q_{L0} + \delta^Q$
1	0.00	0.00	0.00	0.00	**0.00**	**0.00**
2	0.00	0.00	0.00	0.00	**0.00**	**0.00**
3	1.56	0.92	0.03	0.02	**1.59**	**0.94**
4	3.12	1.84	0.06	0.04	**3.18**	**1.88**
5	0.00	0.00	0.00	0.00	**0.00**	**0.00**
6	0.00	0.00	0.00	0.00	**0.00**	**0.00**
7	2.34	1.38	0.05	0.03	**2.39**	**1.41**
8	3.90	2.30	0.08	0.05	**3.98**	**2.35**
9	3.90	2.30	0.08	0.05	**3.98**	**2.35**
10	2.34	1.38	0.05	0.03	**2.39**	**1.41**
11	0.00	0.00	0.00	0.00	**0.00**	**0.00**
12	3.12	1.84	0.06	0.04	**3.18**	**1.88**
13	0.00	0.00	0.00	0.00	**0.00**	**0.00**
14	4.68	2.76	0.09	0.06	**4.77**	**2.82**
15	3.90	2.30	0.08	0.05	**3.98**	**2.35**
16	3.12	1.84	0.06	0.04	**3.18**	**1.88**
17	3.90	2.30	0.08	0.05	**3.98**	**2.35**
18	15.60	9.20	0.32	0.21	**15.92**	**9.41**
19	7.80	4.60	0.16	0.10	**7.96**	**4.70**
20	7.80	4.60	0.16	0.10	**7.96**	**4.70**
21	3.90	2.30	0.08	0.05	**3.98**	**2.35**
22	0.00	0.00	0.00	0.00	**0.00**	**0.00**
23	0.00	0.00	0.00	0.00	**0.00**	**0.00**
24	1.56	0.92	0.03	0.02	**1.59**	**0.94**
25	0.78	0.46	0.02	0.01	**0.80**	**0.47**
26	2.34	1.38	0.04	0.03	**2.38**	**1.41**
27	0.00	0.00	0.00	0.00	**0.00**	**0.00**
28	0.00	0.00	0.00	0.00	**0.00**	**0.00**
29	0.78	0.46	0.02	0.01	**0.80**	**0.47**
30	1.56	0.92	0.03	0.02	**1.59**	**0.94**
Total	78.00	46.00	1.57	1.03	**79.57**	**47.03**

Table 4.5.2-27 The final (compensated) solution for case study 3

(4) The results produced by the prediction system

By running the user interface routine (Rule 12), the final results together with all the interim results for case study 3 are presented as:

Bus	X^L (p.u.)		X^G (p.u.)		X^{LD} (%)		X^{GP} (%)		PMs (p.u.)	
	X^{LP}	X^{LQ}	X^{GP}	X^{GQ}	X^{LDP}	X^{LDQ}	X^{GPP}	X^{GPQ}	ΔP_L	ΔQ_L
1	0.00	0.00	35.09	12.31	0.00%	0.00%	38.54%	36.58%	**0.00**	**0.00**
2	0.00	0.00	36.20	14.40	0.00%	0.00%	36.88%	34.15%	**0.00**	**0.00**
3	1.32	0.66	0.00	0.00	2.00%	2.00%	0.00%	0.00%	**1.59**	**0.94**
4	4.18	1.98	0.00	0.00	4.00%	4.00%	0.00%	0.00%	**3.18**	**1.88**
5	0.00	0.00	0.00	0.00	0.00%	0.00%	0.00%	0.00%	**0.00**	**0.00**
6	0.00	0.00	0.00	0.00	0.00%	0.00%	0.00%	0.00%	**0.00**	**0.00**
7	7.04	3.25	0.00	0.00	3.00%	3.00%	0.00%	0.00%	**2.39**	**1.41**
8	6.33	2.37	0.00	0.00	5.00%	5.00%	0.00%	0.00%	**3.98**	**2.35**
9	4.95	2.75	0.00	0.00	5.00%	5.00%	0.00%	0.00%	**3.98**	**2.35**
10	3.19	1.10	0.00	0.00	3.00%	3.00%	0.00%	0.00%	**2.39**	**1.41**
11	0.00	0.00	0.00	0.00	0.00%	0.00%	0.00%	0.00%	**0.00**	**0.00**
12	5.04	2.48	0.00	0.00	4.00%	4.00%	0.00%	0.00%	**3.18**	**1.88**
13	0.00	0.00	0.00	0.00	0.00%	0.00%	0.00%	0.00%	**0.00**	**0.00**
14	2.79	1.62	0.00	0.00	6.00%	6.00%	0.00%	0.00%	**4.77**	**2.82**
15	3.69	2.48	0.00	0.00	5.00%	5.00%	0.00%	0.00%	**3.98**	**2.35**
16	1.58	0.81	0.00	0.00	4.00%	4.00%	0.00%	0.00%	**3.18**	**1.88**
17	4.05	2.61	0.00	0.00	5.00%	5.00%	0.00%	0.00%	**3.98**	**2.35**
18	14.76	8.05	0.00	0.00	20.00%	20.02%	0.00%	0.00%	**15.92**	**9.41**
19	10.35	4.95	0.00	0.00	10.00%	10.00%	0.00%	0.00%	**7.96**	**4.70**
20	5.49	3.02	0.00	0.00	10.00%	10.00%	0.00%	0.00%	**7.96**	**4.70**
21	4.13	1.76	0.00	0.00	5.00%	5.00%	0.00%	0.00%	**3.98**	**2.35**
22	0.00	0.00	0.00	0.00	0.00%	0.00%	0.00%	0.00%	**0.00**	**0.00**
23	0.00	0.00	0.00	0.00	0.00%	0.00%	0.00%	0.00%	**0.00**	**0.00**
24	2.59	2.04	0.00	0.00	2.00%	2.00%	0.00%	0.00%	**1.59**	**0.94**
25	0.55	0.39	0.00	0.00	1.00%	1.00%	0.00%	0.00%	**0.80**	**0.47**
26	1.93	1.26	0.00	0.00	2.99%	3.00%	0.00%	0.00%	**2.38**	**1.41**
27	0.00	0.00	19.80	13.08	0.00%	0.00%	24.58%	29.27%	**0.00**	**0.00**
28	0.00	0.00	0.00	0.00	0.00%	0.00%	0.00%	0.00%	**0.00**	**0.00**
29	1.49	1.04	0.00	0.00	1.00%	1.00%	0.00%	0.00%	**0.80**	**0.47**
30	3.08	1.60	0.00	0.00	2.00%	2.00%	0.00%	0.00%	**1.59**	**0.94**
Total	88.53	46.22	91.09	39.79	100.00%	100.00%	100.00%	100.00%	**79.57**	**47.03**

Table 4.5.2-28 The final results by the predication system for case study 3

(5) The results by the conventional load flow study

For the purposed of comparison, the power margins for test pattern (3) are also calculated by the conventional load flow programme as:

Bus	X^L (p.u.)		X^G (p.u.)		X^{LD} (%)		X^{GP} (%)		PM (p.u.)	
	X^{LP}	X^{LQ}	X^{GP}	X^{GQ}	X^{LP}	X^{LQ}	X^{GP}	X^{GQ}	ΔP_L	ΔQ_L
1	0.00	0.00	35.09	12.31	0.00%	0.00%	38.54%	36.58%	**0.00**	**0.00**
2	0.00	0.00	36.20	14.40	0.00%	0.00%	36.88%	34.15%	**0.00**	**0.00**
3	1.32	0.66	0.00	0.00	2.00%	2.00%	0.00%	0.00%	**1.64**	**0.98**
4	4.18	1.98	0.00	0.00	4.00%	4.00%	0.00%	0.00%	**3.28**	**1.96**
5	0.00	0.00	0.00	0.00	0.00%	0.00%	0.00%	0.00%	**0.00**	**0.00**
6	0.00	0.00	0.00	0.00	0.00%	0.00%	0.00%	0.00%	**0.00**	**0.00**
7	7.04	3.25	0.00	0.00	3.00%	3.00%	0.00%	0.00%	**2.46**	**1.47**
8	6.33	2.37	0.00	0.00	5.00%	5.00%	0.00%	0.00%	**4.10**	**2.45**
9	4.95	2.75	0.00	0.00	5.00%	5.00%	0.00%	0.00%	**4.10**	**2.45**
10	3.19	1.10	0.00	0.00	3.00%	3.00%	0.00%	0.00%	**2.46**	**1.47**
11	0.00	0.00	0.00	0.00	0.00%	0.00%	0.00%	0.00%	**0.00**	**0.00**
12	5.04	2.48	0.00	0.00	4.00%	4.00%	0.00%	0.00%	**3.28**	**1.96**
13	0.00	0.00	0.00	0.00	0.00%	0.00%	0.00%	0.00%	**0.00**	**0.00**
14	2.79	1.62	0.00	0.00	6.00%	6.00%	0.00%	0.00%	**4.92**	**2.94**
15	3.69	2.48	0.00	0.00	5.00%	5.00%	0.00%	0.00%	**4.10**	**2.45**
16	1.58	0.81	0.00	0.00	4.00%	4.00%	0.00%	0.00%	**3.28**	**1.96**
17	4.05	2.61	0.00	0.00	5.00%	5.00%	0.00%	0.00%	**4.10**	**2.45**
18	14.76	8.05	0.00	0.00	20.00%	20.02%	0.00%	0.00%	**16.40**	**9.81**
19	10.35	4.95	0.00	0.00	10.00%	10.00%	0.00%	0.00%	**8.20**	**4.90**
20	5.49	3.02	0.00	0.00	10.00%	10.00%	0.00%	0.00%	**8.20**	**4.90**
21	4.13	1.76	0.00	0.00	5.00%	5.00%	0.00%	0.00%	**4.10**	**2.45**
22	0.00	0.00	0.00	0.00	0.00%	0.00%	0.00%	0.00%	**0.00**	**0.00**
23	0.00	0.00	0.00	0.00	0.00%	0.00%	0.00%	0.00%	**0.00**	**0.00**
24	2.59	2.04	0.00	0.00	2.00%	2.00%	0.00%	0.00%	**1.64**	**0.98**
25	0.55	0.39	0.00	0.00	1.00%	1.00%	0.00%	0.00%	**0.82**	**0.49**
26	1.93	1.26	0.00	0.00	2.99%	3.00%	0.00%	0.00%	**2.45**	**1.47**
27	0.00	0.00	19.80	13.08	0.00%	0.00%	24.58%	29.27%	**0.00**	**0.00**
28	0.00	0.00	0.00	0.00	0.00%	0.00%	0.00%	0.00%	**0.00**	**0.00**
29	1.49	1.04	0.00	0.00	1.00%	1.00%	0.00%	0.00%	**0.82**	**0.49**
30	3.08	1.60	0.00	0.00	2.00%	2.00%	0.00%	0.00%	**1.64**	**0.98**
Total	88.53	46.22	91.09	39.79	100.00%	100.00%	100.00%	100.00%	**81.99**	**49.01**

Table 4.5.2-29 The power margins by the load flow study for case study 3

(6) Accuracy analysis

Accuracy analysis for the case study 3 are summarised in the Table 4.5.2-30. The average relative errors are reduced from 2.33% / 3.10% for the initial solution to 1.41% / 2.04% for the final solution. The maximum relative errors with the individual results are improved from 3.29% / 4.33% for the initial solution to the 1.99% / 2.86% for the final solution.

					For the initial results(PMo)				For the final results (PMs)			
	PM by LF		Max Load		Abs Error (p.u.)		Rel Error (%)		Abs Error (p.u.)		Rel Error (%)	
Bus	ΔP	ΔQ	Pmax	Qmax	ε_P	ε_Q	η_p	η_q	ε_P	ε_Q	η_p	η_q
1	0.00	0.00	0.00	0.00	0.000	0.000	n/a	n/a	0.000	0.000	n/a	n/a
2	0.00	0.00	0.00	0.00	0.000	0.000	n/a	n/a	0.000	0.000	n/a	n/a
3	1.64	0.98	2.96	1.64	0.080	0.060	2.70%	3.66%	0.048	0.040	1.64%	2.41%
4	3.28	1.96	7.46	3.94	0.160	0.120	2.14%	3.05%	0.097	0.079	1.30%	2.01%
5	0.00	0.00	0.00	0.00	0.000	0.000	n/a	n/a	0.000	0.000	n/a	n/a
6	0.00	0.00	0.00	0.00	0.000	0.000	n/a	n/a	0.000	0.000	n/a	n/a
7	2.46	1.47	9.50	4.72	0.120	0.090	1.26%	1.91%	0.073	0.059	0.76%	1.26%
8	4.10	2.45	10.43	4.82	0.200	0.150	1.92%	3.11%	0.121	0.099	1.16%	2.05%
9	4.10	2.45	9.05	5.20	0.200	0.150	2.21%	2.88%	0.121	0.099	1.34%	1.90%
10	2.46	1.47	5.65	2.57	0.120	0.090	2.12%	3.50%	0.073	0.059	1.29%	2.31%
11	0.00	0.00	0.00	0.00	0.000	0.000	n/a	n/a	0.000	0.000	n/a	n/a
12	3.28	1.96	8.32	4.44	0.160	0.120	1.92%	2.70%	0.097	0.079	1.16%	1.78%
13	0.00	0.00	0.00	0.00	0.000	0.000	n/a	n/a	0.000	0.000	n/a	n/a
14	4.92	2.94	7.71	4.56	0.240	0.180	3.11%	3.95%	0.145	0.119	1.88%	2.60%
15	4.10	2.45	7.79	4.93	0.200	0.150	2.57%	3.04%	0.121	0.099	1.55%	2.01%
16	3.28	1.96	4.86	2.77	0.160	0.120	3.29%	4.33%	0.097	0.079	1.99%	2.86%
17	4.10	2.45	8.15	5.06	0.200	0.150	2.45%	2.96%	0.121	0.099	1.48%	1.96%
18	16.40	9.81	31.16	17.86	0.800	0.610	2.57%	3.42%	0.484	0.396	1.55%	2.22%
19	8.20	4.90	18.55	9.85	0.400	0.300	2.16%	3.05%	0.242	0.198	1.30%	2.01%
20	8.20	4.90	13.69	7.92	0.400	0.300	2.92%	3.79%	0.242	0.198	1.77%	2.50%
21	4.10	2.45	8.23	4.21	0.200	0.150	2.43%	3.56%	0.121	0.099	1.47%	2.35%
22	0.00	0.00	0.00	0.00	0.000	0.000	n/a	n/a	0.000	0.000	n/a	n/a
23	0.00	0.00	0.00	0.00	0.000	0.000	n/a	n/a	0.000	0.000	n/a	n/a

					For the initial results(PMo)				For the final results (PMs)			
	PM by LF		Max Load		Abs Error (p.u.)		Rel Error (%)		Abs Error (p.u.)		Rel Error (%)	
Bus	**ΔP**	**ΔQ**	**Pmax**	**Qmax**	ε_P	ε_Q	η_p	η_q	ε_P	ε_Q	η_p	η_q
24	1.64	0.98	4.23	3.02	0.080	0.060	1.89%	1.99%	0.048	0.040	1.14%	1.31%
25	0.82	0.49	1.37	0.88	0.040	0.030	2.92%	3.41%	0.024	0.020	1.77%	2.25%
26	2.45	1.47	4.38	2.73	0.110	0.090	2.51%	3.30%	0.072	0.059	1.65%	2.18%
27	0.00	0.00	0.00	0.00	0.000	0.000	n/a	n/a	0.000	0.000	n/a	n/a
28	0.00	0.00	0.00	0.00	0.000	0.000	n/a	n/a	0.000	0.000	n/a	n/a
29	0.82	0.49	2.31	1.53	0.040	0.030	1.73%	1.96%	0.024	0.020	1.05%	1.29%
30	1.64	0.98	4.72	2.58	0.080	0.060	1.69%	2.33%	0.048	0.040	1.03%	1.53%
Total	81.99	49.01	170.52	95.23	3.990	3.010	2.34%	3.16%	2.420	1.980	1.42%	2.08%
Average					**0.257**	**0.194**	**2.33%**	**3.10%**	**0.156**	**0.128**	**1.41%**	**2.04%**

Table 4.5.2-30 The accuracy analysis for case study 3

4. **Case Study 4**

(1) Test pattern

The testing pattern of VSDFs for this case study is set as:

Bus	X^L (p.u.)		X^G (p.u.)		X^{LD} (%)		X^{GP} (%)	
	X^{LP}	X^{LQ}	X^{GP}	X^{GQ}	X^{LDP}	X^{LDQ}	X^{GPP}	X^{GPQ}
1	0.00	0.00	40.01	17.23	0.00%	0.00%	37.29%	33.93%
2	0.00	0.00	40.54	17.50	0.00%	0.00%	37.63%	35.57%
3	1.32	0.66	0.00	0.00	2.20%	2.20%	0.00%	0.00%
4	4.18	1.98	0.00	0.00	3.60%	3.61%	0.00%	0.00%
5	0.00	0.00	0.00	0.00	0.00%	0.00%	0.00%	0.00%
6	0.00	0.00	0.00	0.00	0.00%	0.00%	0.00%	0.00%
7	7.04	3.25	0.00	0.00	3.31%	3.29%	0.00%	0.00%
8	6.33	2.37	0.00	0.00	4.49%	4.49%	0.00%	0.00%
9	4.95	2.75	0.00	0.00	5.51%	5.51%	0.00%	0.00%
10	3.19	1.10	0.00	0.00	3.31%	3.29%	0.00%	0.00%
11	0.00	0.00	0.00	0.00	0.00%	0.00%	0.00%	0.00%
12	6.16	3.03	0.00	0.00	4.41%	4.39%	0.00%	0.00%
13	0.00	0.00	0.00	0.00	0.00%	0.00%	0.00%	0.00%
14	3.41	1.98	0.00	0.00	5.41%	5.39%	0.00%	0.00%
15	4.51	3.03	0.00	0.00	5.49%	5.49%	0.00%	0.00%
16	1.93	0.99	0.00	0.00	4.39%	4.39%	0.00%	0.00%
17	4.95	3.19	0.00	0.00	4.49%	4.51%	0.00%	0.00%
18	18.04	9.85	0.00	0.00	22.01%	22.01%	0.00%	0.00%
19	12.65	6.05	0.00	0.00	9.00%	9.00%	0.00%	0.00%
20	6.71	3.69	0.00	0.00	9.00%	9.00%	0.00%	0.00%
21	4.13	1.76	0.00	0.00	4.49%	4.51%	0.00%	0.00%
22	0.00	0.00	0.00	0.00	0.00%	0.00%	0.00%	0.00%
23	0.00	0.00	0.00	0.00	0.00%	0.00%	0.00%	0.00%
24	2.59	2.04	0.00	0.00	1.80%	1.78%	0.00%	0.00%
25	0.55	0.39	0.00	0.00	1.10%	1.10%	0.00%	0.00%
26	1.93	1.26	0.00	0.00	2.70%	2.71%	0.00%	0.00%
27	0.00	0.00	22.29	15.70	0.00%	0.00%	25.08%	30.49%
28	0.00	0.00	0.00	0.00	0.00%	0.00%	0.00%	0.00%
29	1.49	1.04	0.00	0.00	1.09%	1.12%	0.00%	0.00%
30	3.08	1.60	0.00	0.00	2.20%	2.20%	0.00%	0.00%
Total	99.14	52.01	102.84	50.43	100.00%	100.00%	100.00%	100.00%

Table 4.5.2-31 Test pattern (4) for case study 4

The further details about this test pattern are given in the Table A3-19 of Appendix 3.

(2) Euclidean Distance Calculations

The Euclidean distances to the prototype of each pattern class are calculated by using equation (4.5.1-1) as below:

(i) The Euclidean distance to pattern class I:

The 4 segments of the Euclidean distance from the testing pattern (4) to the prototype of pattern class I (**L01, LD05, G02 and GP01** as shown in Table 4.5.1-1) are:

Load pattern segment D^{L01}	26.31
Load distribution pattern segment D^{LD03}	12.03
Generation pattern segment D^{G02}	62.86
Generation participation pattern segment D^{GP01}	53.31

Table 4.5.2-32 The Euclidean distance from test pattern (4) to pattern class I

(ii) The Euclidean distance to pattern class II:

The Euclidean distance from test pattern (4) to the prototype of pattern class II (**L10, LD15, G06 and GP03** as shown in Table 4.5.1-2) is :

Load pattern segment D^{L12}	2.93
Load distribution pattern segment D^{LD11}	4.13
Generation pattern segment D^{G09}	7.38
Generation participation pattern segment D^{GP06}	0.06

Table 4.5.2-33 The Euclidean distance from test pattern (4) to pattern class 1I

(iii) The Euclidean distance to pattern class III:

The Euclidean distance to from test pattern (4) to the prototype of pattern class III **(L20, LD20, G20 and GP20** as shown in Table 4.5.1-3) is calculated as:

Load pattern segment D^{L12}	46.90
Load distribution pattern segment D^{LD11}	27.09
Generation pattern segment D^{G09}	66.95
Generation participation pattern segment D^{GP06}	37.17

Table 4.5.2-34 The Euclidean distance from test pattern (4) to pattern class III

(3) Solution searching

By applying the knowledge rules to the results in Table 4.5.2-32, Table 4.5.2-33, and Table 4.5.2-34, the initial and final (compensated) solutions for case study 4 are reached as:

Bus	PM_0 (p.u.)		Compensation δ		PM_S (p.u.)	
	ΔP_{L0}	ΔQ_{L0}	δ^P	δ^Q	$\Delta P_L=\Delta P_{L0}+\delta^P$	$\Delta Q_L=\Delta Q_{L0}+\delta^Q$
1	0.00	0.00	0.00	0.00	**0.00**	**0.00**
2	0.00	0.00	0.00	0.00	**0.00**	**0.00**
3	1.56	0.92	-0.04	-0.01	**1.52**	**0.91**
4	3.12	1.84	-0.64	-0.35	**2.48**	**1.49**
5	0.00	0.00	0.00	0.00	**0.00**	**0.00**
6	0.00	0.00	0.00	0.00	**0.00**	**0.00**
7	2.34	1.38	-0.06	-0.02	**2.28**	**1.36**
8	3.90	2.30	-0.80	-0.45	**3.10**	**1.85**
9	3.90	2.30	-0.10	-0.03	**3.80**	**2.27**
10	2.34	1.38	-0.06	-0.02	**2.28**	**1.36**
11	0.00	0.00	0.00	0.00	**0.00**	**0.00**
12	3.12	1.84	-0.08	-0.03	**3.04**	**1.81**
13	0.00	0.00	0.00	0.00	**0.00**	**0.00**
14	4.68	2.76	-0.95	-0.54	**3.73**	**2.22**
15	3.90	2.30	-0.11	-0.04	**3.79**	**2.26**
16	3.12	1.84	-0.09	-0.03	**3.03**	**1.81**
17	3.90	2.30	-0.80	-0.44	**3.10**	**1.86**
18	15.60	9.20	-0.42	-0.12	**15.18**	**9.08**
19	7.80	4.60	-1.59	-0.89	**6.21**	**3.71**
20	7.80	4.60	-1.59	-0.89	**6.21**	**3.71**
21	3.90	2.30	-0.80	-0.44	**3.10**	**1.86**
22	0.00	0.00	0.00	0.00	**0.00**	**0.00**
23	0.00	0.00	0.00	0.00	**0.00**	**0.00**
24	1.56	0.92	-0.32	-0.19	**1.24**	**0.73**
25	0.78	0.46	-0.02	-0.01	**0.76**	**0.45**
26	2.34	1.38	-0.48	-0.26	**1.86**	**1.12**
27	0.00	0.00	0.00	0.00	**0.00**	**0.00**
28	0.00	0.00	0.00	0.00	**0.00**	**0.00**
29	0.78	0.46	-0.03	0.00	**0.75**	**0.46**
30	1.56	0.92	-0.04	-0.01	**1.52**	**0.91**
Total	78.00	46.00	-9.04	-4.76	**68.96**	**41.24**

Table 4.5.2-35 The final (compensated) solution for case study 4

(4) The results by the prediction system

The final solution together with all the interim results for the case study 4 are presented as:

Bus	X^L (p.u.)		X^G (p.u.)		X^{LD} (%)		X^{GP} (%)		PM_S (p.u.)	
	X^{LP}	X^{LQ}	X^{GP}	X^{GQ}	X^{LDP}	X^{LDQ}	X^{GPP}	X^{GPQ}	ΔP_L	ΔQ_L
1	0.00	0.00	40.01	17.23	0.00%	0.00%	37.29%	33.93%	**0.00**	**0.00**
2	0.00	0.00	40.54	17.50	0.00%	0.00%	37.63%	35.57%	**0.00**	**0.00**
3	1.32	0.66	0.00	0.00	2.20%	2.20%	0.00%	0.00%	**1.52**	**0.91**
4	4.18	1.98	0.00	0.00	3.60%	3.61%	0.00%	0.00%	**2.48**	**1.49**
5	0.00	0.00	0.00	0.00	0.00%	0.00%	0.00%	0.00%	**0.00**	**0.00**
6	0.00	0.00	0.00	0.00	0.00%	0.00%	0.00%	0.00%	**0.00**	**0.00**
7	7.04	3.25	0.00	0.00	3.31%	3.29%	0.00%	0.00%	**2.28**	**1.36**
8	6.33	2.37	0.00	0.00	4.49%	4.49%	0.00%	0.00%	**3.10**	**1.85**
9	4.95	2.75	0.00	0.00	5.51%	5.51%	0.00%	0.00%	**3.80**	**2.27**
10	3.19	1.10	0.00	0.00	3.31%	3.29%	0.00%	0.00%	**2.28**	**1.36**
11	0.00	0.00	0.00	0.00	0.00%	0.00%	0.00%	0.00%	**0.00**	**0.00**
12	6.16	3.03	0.00	0.00	4.41%	4.39%	0.00%	0.00%	**3.04**	**1.81**
13	0.00	0.00	0.00	0.00	0.00%	0.00%	0.00%	0.00%	**0.00**	**0.00**
14	3.41	1.98	0.00	0.00	5.41%	5.39%	0.00%	0.00%	**3.73**	**2.22**
15	4.51	3.03	0.00	0.00	5.49%	5.49%	0.00%	0.00%	**3.79**	**2.26**
16	1.93	0.99	0.00	0.00	4.39%	4.39%	0.00%	0.00%	**3.03**	**1.81**
17	4.95	3.19	0.00	0.00	4.49%	4.51%	0.00%	0.00%	**3.10**	**1.86**
18	18.04	9.85	0.00	0.00	22.01%	22.01%	0.00%	0.00%	**15.18**	**9.08**
19	12.65	6.05	0.00	0.00	9.00%	9.00%	0.00%	0.00%	**6.21**	**3.71**
20	6.71	3.69	0.00	0.00	9.00%	9.00%	0.00%	0.00%	**6.21**	**3.71**
21	4.13	1.76	0.00	0.00	4.49%	4.51%	0.00%	0.00%	**3.10**	**1.86**
22	0.00	0.00	0.00	0.00	0.00%	0.00%	0.00%	0.00%	**0.00**	**0.00**
23	0.00	0.00	0.00	0.00	0.00%	0.00%	0.00%	0.00%	**0.00**	**0.00**
24	2.59	2.04	0.00	0.00	1.80%	1.78%	0.00%	0.00%	**1.24**	**0.73**
25	0.55	0.39	0.00	0.00	1.10%	1.10%	0.00%	0.00%	**0.76**	**0.45**
26	1.93	1.26	0.00	0.00	2.70%	2.71%	0.00%	0.00%	**1.86**	**1.12**
27	0.00	0.00	22.29	15.70	0.00%	0.00%	25.08%	30.49%	**0.00**	**0.00**
28	0.00	0.00	0.00	0.00	0.00%	0.00%	0.00%	0.00%	**0.00**	**0.00**
29	1.49	1.04	0.00	0.00	1.09%	1.12%	0.00%	0.00%	**0.75**	**0.46**
30	3.08	1.60	0.00	0.00	2.20%	2.20%	0.00%	0.00%	**1.52**	**0.91**
Total	99.14	52.01	102.84	50.43	100.00%	100.00%	100.00%	100.00%	**68.96**	**41.24**

Table 4.5.2-36 The final results by the predication system for case study 4

(5) The results by the conventional load flow study

For the purposed of comparison, the power margins for test pattern (4) are also calculated by the conventional load flow programme as:

Bus	X^L (p.u.)		X^G (p.u.)		X^{LD} (%)		X^{GP} (%)		PM (p.u.)	
	X^{LP}	X^{LQ}	X^{GP}	X^{GQ}	X^{LP}	X^{LQ}	X^{GP}	X^{GQ}	ΔP_L	ΔQ_L
1	0.00	0.00	40.01	17.23	0.00%	0.00%	37.29%	33.93%	**0.00**	**0.00**
2	0.00	0.00	40.54	17.50	0.00%	0.00%	37.63%	35.57%	**0.00**	**0.00**
3	1.32	0.66	0.00	0.00	2.20%	2.20%	0.00%	0.00%	**1.52**	**0.90**
4	4.18	1.98	0.00	0.00	3.60%	3.61%	0.00%	0.00%	**2.48**	**1.48**
5	0.00	0.00	0.00	0.00	0.00%	0.00%	0.00%	0.00%	**0.00**	**0.00**
6	0.00	0.00	0.00	0.00	0.00%	0.00%	0.00%	0.00%	**0.00**	**0.00**
7	7.04	3.25	0.00	0.00	3.31%	3.29%	0.00%	0.00%	**2.28**	**1.35**
8	6.33	2.37	0.00	0.00	4.49%	4.49%	0.00%	0.00%	**3.10**	**1.84**
9	4.95	2.75	0.00	0.00	5.51%	5.51%	0.00%	0.00%	**3.80**	**2.26**
10	3.19	1.10	0.00	0.00	3.31%	3.29%	0.00%	0.00%	**2.28**	**1.35**
11	0.00	0.00	0.00	0.00	0.00%	0.00%	0.00%	0.00%	**0.00**	**0.00**
12	6.16	3.03	0.00	0.00	4.41%	4.39%	0.00%	0.00%	**3.04**	**1.80**
13	0.00	0.00	0.00	0.00	0.00%	0.00%	0.00%	0.00%	**0.00**	**0.00**
14	3.41	1.98	0.00	0.00	5.41%	5.39%	0.00%	0.00%	**3.73**	**2.21**
15	4.51	3.03	0.00	0.00	5.49%	5.49%	0.00%	0.00%	**3.79**	**2.25**
16	1.93	0.99	0.00	0.00	4.39%	4.39%	0.00%	0.00%	**3.03**	**1.80**
17	4.95	3.19	0.00	0.00	4.49%	4.51%	0.00%	0.00%	**3.10**	**1.85**
18	18.04	9.85	0.00	0.00	22.01%	22.01%	0.00%	0.00%	**15.18**	**9.02**
19	12.65	6.05	0.00	0.00	9.00%	9.00%	0.00%	0.00%	**6.21**	**3.69**
20	6.71	3.69	0.00	0.00	9.00%	9.00%	0.00%	0.00%	**6.21**	**3.69**
21	4.13	1.76	0.00	0.00	4.49%	4.51%	0.00%	0.00%	**3.10**	**1.85**
22	0.00	0.00	0.00	0.00	0.00%	0.00%	0.00%	0.00%	**0.00**	**0.00**
23	0.00	0.00	0.00	0.00	0.00%	0.00%	0.00%	0.00%	**0.00**	**0.00**
24	2.59	2.04	0.00	0.00	1.80%	1.78%	0.00%	0.00%	**1.24**	**0.73**
25	0.55	0.39	0.00	0.00	1.10%	1.10%	0.00%	0.00%	**0.76**	**0.45**
26	1.93	1.26	0.00	0.00	2.70%	2.71%	0.00%	0.00%	**1.86**	**1.11**
27	0.00	0.00	22.29	15.70	0.00%	0.00%	25.08%	30.49%	**0.00**	**0.00**
28	0.00	0.00	0.00	0.00	0.00%	0.00%	0.00%	0.00%	**0.00**	**0.00**
29	1.49	1.04	0.00	0.00	1.09%	1.12%	0.00%	0.00%	**0.75**	**0.46**
30	3.08	1.60	0.00	0.00	2.20%	2.20%	0.00%	0.00%	**1.52**	**0.90**
Total	99.14	52.01	102.84	50.43	100.00%	100.00%	100.00%	100.00%	**68.98**	**40.99**

Table 4.5.2-37 The power margins by the load flow study for case study 4

(6) Accuracy analysis

Accuracy analysis for the case study 4 are summarised in the Table 4.5.2-38. The average relative errors are reduced from 5.37% / 5.30% with the initial solution to 0.01% / 0.27% with the final solution. The maximum relative errors with the individual results are improved from 13.31% / 13.13% for the initial solution to the 0.02% / 0.39% for the final solution.

					For the initial results(PMo)				For the final results (PMs)			
	PM by LF		Max Load		Abs Error (p.u.)		Rel Error (%)		Abs Error (p.u.)		Rel Error (%)	
Bus	ΔP	ΔQ	Pmax	Qmax	ε_P	ε_Q	η_p	η_q	ε_P	ε_Q	η_p	η_q
1	0.00	0.00	0.00	0.00	0.000	0.000	n/a	n/a	0.000	0.000	n/a	n/a
2	0.00	0.00	0.00	0.00	0.000	0.000	n/a	n/a	0.000	0.000	n/a	n/a
3	1.52	0.90	2.84	1.56	0.040	0.020	1.41%	1.28%	0.000	0.005	0.02%	0.35%
4	2.48	1.48	6.66	3.46	0.640	0.360	9.61%	10.40%	0.001	0.009	0.01%	0.26%
5	0.00	0.00	0.00	0.00	0.000	0.000	n/a	n/a	0.000	0.000	n/a	n/a
6	0.00	0.00	0.00	0.00	0.000	0.000	n/a	n/a	0.000	0.000	n/a	n/a
7	2.28	1.35	9.32	4.60	0.060	0.030	0.64%	0.65%	0.001	0.008	0.01%	0.18%
8	3.10	1.84	9.43	4.21	0.800	0.460	8.48%	10.93%	0.001	0.011	0.01%	0.27%
9	3.80	2.26	8.75	5.01	0.100	0.040	1.14%	0.80%	0.001	0.014	0.01%	0.28%
10	2.28	1.35	5.47	2.45	0.060	0.030	1.10%	1.22%	0.001	0.008	0.01%	0.34%
11	0.00	0.00	0.00	0.00	0.000	0.000	n/a	n/a	0.000	0.000	n/a	n/a
12	3.04	1.80	9.20	4.83	0.080	0.040	0.87%	0.83%	0.001	0.011	0.01%	0.23%
13	0.00	0.00	0.00	0.00	0.000	0.000	n/a	n/a	0.000	0.000	n/a	n/a
14	3.73	2.21	7.14	4.19	0.950	0.550	13.31%	13.13%	0.001	0.013	0.02%	0.32%
15	3.79	2.25	8.30	5.28	0.110	0.050	1.33%	0.95%	0.001	0.014	0.01%	0.26%
16	3.03	1.80	4.96	2.79	0.090	0.040	1.81%	1.43%	0.001	0.011	0.02%	0.39%
17	3.10	1.85	8.05	5.04	0.800	0.450	9.94%	8.93%	0.001	0.011	0.01%	0.22%
18	15.18	9.02	33.22	18.87	0.420	0.180	1.26%	0.95%	0.004	0.055	0.01%	0.29%
19	6.21	3.69	18.86	9.74	1.590	0.910	8.43%	9.34%	0.002	0.023	0.01%	0.23%
20	6.21	3.69	12.92	7.38	1.590	0.910	12.31%	12.33%	0.002	0.023	0.01%	0.30%
21	3.10	1.85	7.23	3.61	0.800	0.450	11.07%	12.47%	0.001	0.011	0.01%	0.31%
22	0.00	0.00	0.00	0.00	0.000	0.000	n/a	n/a	0.000	0.000	n/a	n/a

					For the initial results(PMo)				For the final results (PMs)			
	PM by LF		Max Load		Abs Error (p.u.)		Rel Error (%)		Abs Error (p.u.)		Rel Error (%)	
Bus	ΔP	ΔQ	Pmax	Qmax	ε_P	ε_Q	η_p	η_q	ε_P	ε_Q	η_p	η_q
23	0.00	0.00	0.00	0.00	0.000	0.000	n/a	n/a	0.000	0.000	n/a	n/a
24	1.24	0.73	3.83	2.77	0.320	0.190	8.36%	6.86%	0.000	0.004	0.01%	0.16%
25	0.76	0.45	1.31	0.84	0.020	0.010	1.53%	1.19%	0.000	0.003	0.02%	0.33%
26	1.86	1.11	3.79	2.37	0.480	0.270	12.66%	11.39%	0.001	0.007	0.01%	0.29%
27	0.00	0.00	0.00	0.00	0.000	0.000	n/a	n/a	0.000	0.000	n/a	n/a
28	0.00	0.00	0.00	0.00	0.000	0.000	n/a	n/a	0.000	0.000	n/a	n/a
29	0.75	0.46	2.24	1.50	0.030	0.000	1.34%	0.00%	0.000	0.003	0.01%	0.19%
30	1.52	0.90	4.60	2.50	0.040	0.020	0.87%	0.80%	0.000	0.005	0.01%	0.22%
Total	**68.98**	**40.99**	**168.12**	**93.00**	**9.020**	**5.010**	**5.37%**	**5.39%**	**0.020**	**0.250**	**0.01%**	**0.27%**
Average					**0.582**	**0.323**	**5.37%**	**5.30%**	**0.001**	**0.016**	**0.01%**	**0.27%**

Table 4.5.2-38 The accuracy analysis for case study 4

5. **Case Study 5**

(1) Test pattern

The testing pattern of VSDFs for this case study is set as:

Bus	X^L (p.u.)		X^G (p.u.)		X^{LD} (%)		X^{GP} (%)	
	X^{LP}	X^{LQ}	X^{GP}	X^{GQ}	X^{LDP}	X^{LDQ}	X^{GPP}	X^{GPQ}
1	0.00	0.00	57.90	36.80	0.00%	0.00%	30.03%	29.34%
2	0.00	0.00	57.00	37.00	0.00%	0.00%	29.99%	30.28%
3	3.00	1.80	0.00	0.00	4.49%	4.51%	0.00%	0.00%
4	9.00	5.40	0.00	0.00	0.00%	0.00%	0.00%	0.00%
5	0.00	0.00	0.00	0.00	0.00%	0.00%	0.00%	0.00%
6	0.00	0.00	0.00	0.00	0.00%	0.00%	0.00%	0.00%
7	12.80	5.90	0.00	0.00	4.51%	4.51%	0.00%	0.00%
8	10.50	4.30	0.00	0.00	4.51%	4.51%	0.00%	0.00%
9	9.00	5.00	0.00	0.00	4.51%	4.51%	0.00%	0.00%
10	6.00	3.60	0.00	0.00	4.49%	4.51%	0.00%	0.00%
11	0.00	0.00	0.00	0.00	0.00%	0.00%	0.00%	0.00%
12	11.20	7.00	0.00	0.00	5.51%	5.51%	0.00%	0.00%
13	0.00	0.00	0.00	0.00	0.00%	0.00%	0.00%	0.00%
14	29.00	18.00	0.00	0.00	11.00%	10.98%	0.00%	0.00%
15	31.50	19.00	0.00	0.00	11.00%	10.98%	0.00%	0.00%
16	5.00	3.00	0.00	0.00	5.51%	5.51%	0.00%	0.00%
17	9.00	5.80	0.00	0.00	5.51%	5.48%	0.00%	0.00%
18	16.00	9.00	0.00	0.00	11.00%	10.98%	0.00%	0.00%
19	12.00	8.00	0.00	0.00	5.51%	5.51%	0.00%	0.00%
20	5.50	3.30	0.00	0.00	0.00%	0.00%	0.00%	0.00%
21	7.50	3.20	0.00	0.00	4.49%	4.51%	0.00%	0.00%
22	0.00	0.00	37.00	24.00	0.00%	0.00%	14.99%	15.14%
23	0.00	0.00	23.00	16.00	0.00%	0.00%	10.00%	10.09%
24	4.70	3.70	0.00	0.00	4.51%	4.51%	0.00%	0.00%
25	3.00	2.00	0.00	0.00	4.49%	4.51%	0.00%	0.00%
26	5.50	3.30	0.00	0.00	0.00%	0.00%	0.00%	0.00%
27	0.00	0.00	38.00	28.00	0.00%	0.00%	14.99%	15.14%
28	0.00	0.00	0.00	0.00	0.00%	0.00%	0.00%	0.00%
29	4.00	2.40	0.00	0.00	4.49%	4.48%	0.00%	0.00%
30	7.60	4.00	0.00	0.00	4.49%	4.51%	0.00%	0.00%
Total	201.8	117.7	212.90	141.80	**100.00%**	**100.00%**	100.00%	100.00%

Table 4.5.2-39 Test pattern (5) for case study 5

This test pattern is one of the patterns within the study group 3 (heavily loaded cluster) for the simulation of power margin similarity in Chapter 3. The further details about this test pattern are given in Table A3-23 Appendix 3.

(2) Euclidean Distance Calculations

The Euclidean distances to the prototype of each pattern class are calculated by using equation (4.5.1-1) as below:

(i) The Euclidean distance to pattern class I:

The segments 4 of the Euclidean distance from the testing pattern (5) to the prototype of pattern class I (**L01, LD05, G02 and GP01** as shown in Table 4.5.1-1) are:

Load pattern segment D^{L01}	61.25
Load distribution pattern segment D^{LD03}	25.85
Generation pattern segment D^{G02}	114.96
Generation participation pattern segment D^{GP01}	32.43

Table 4.5.2-40 The Euclidean distance from test pattern (5) to pattern class I

(ii) The Euclidean distance to pattern class II:

The Euclidean distance from test pattern (5) to the prototype of pattern class II (**L10, LD15, G06 and GP03** as shown in Table 4.5.1-2) is:

Load pattern segment D^{L12}	48.00
Load distribution pattern segment D^{LD11}	26.09
Generation pattern segment D^{G09}	71.63
Generation participation pattern segment D^{GP06}	33.97

Table 4.5.2-41 The Euclidean distance from test pattern (5) to pattern class 1I

(iii) The Euclidean distance to pattern class III:

The Euclidean distance from test pattern (5) to the prototype of pattern class III: **L20, LD20, G20 and GP20** (shown in Table 4.5.1-3) is:

Load pattern segment D^{L12}	0.00
Load distribution pattern segment D^{LD11}	3.59
Generation pattern segment D^{G09}	0.00
Generation participation pattern segment D^{GP06}	8.14

Table 4.5.2-42 The Euclidean distance from test pattern (5) to pattern class III

(3) Solution searching

The solution searching in this case study involves the following steps:

Step 1: VSDFs identification

By applying the knowledge rules to the results in Table 4.5.2-40, Table 4.5.2-41 and Table 4.5.2-42, the following interim results are obtained:

Rules Applied	**Reasoning**	**Conclusion**
RULE (1)	$D^{L20} = \min \{D^{L01}, D^{L10}, D^{L20}\}$,	$\mathbf{X}^{L} \in$ L20
RULE (2)	$D^{LD20} = \min \{D^{LD05}, D^{LD15}, D^{LD20}\}$,	$\mathbf{X}^{LD} \in$ **LD**20
RULE (3)	$D^{G20} = \min \{D^{G02}, D^{G06}, D^{G20}\}$,	$\mathbf{X}^{G} \in$ **G**20
RULE (4) :	$D^{GP20} = \min \{D^{GP01}, D^{GP03}, D^{GP20}\}$,	$\mathbf{X}^{GP} \in$ **GP**20

Table 4.5.2-43 Interim results 1 for case study 5

Step 2: Pattern class recognition

By applying the knowledge rules to the interim results 1 in Table 4.5.2-43, produces:

Rules applied	Reasoning	Conclusion
RULE (5)	$\mathbf{X}^{L} \in \mathbf{L20}$, $\mathbf{X}^{LD} \in \mathbf{LD20}$, $\mathbf{X}^{G} \in \mathbf{G20}$, $\mathbf{X}^{GP} \in \mathbf{GP20}$	$\mathbf{X}^{VSDF} \in \Phi 3$

Table 4.5.2-44 Interim results 2 for case study 5

Step 3: Initial solution

By applying the knowledge rules to the interim results 2 in Table 4.5.2-44, the initial prediction results are reached as:

Rules applied	Reasoning	Conclusion
RULE (7)	$\mathbf{X}^{VSDF} \in \Phi 3$	$\mathbf{PM_0}$ = Table 4.5.1 – 7

Table 4.5.2-45 Interim results 3 (initial solution) for case study 5

Step 4: Solution compensation

By running the solution compensation routine (Rule 11) with the interim results 3, the final prediction results are achieved as:

Bus	PM_0 (p.u.)		Compensation δ		PM_S (p.u.)	
	ΔP_{L0}	ΔQ_{L0}	δ^P	δ^Q	$\Delta P_L = \Delta P_{L0} + \delta^P$	$\Delta Q_L = \Delta Q_{L0} + \delta^Q$
1	0.00	0.00	0.00	0.00	**0.00**	**0.00**
2	0.00	0.00	0.00	0.00	**0.00**	**0.00**
3	2.95	1.75	-0.30	-0.17	**2.65**	**1.58**
4	0.00	0.00	0.00	0.00	**0.00**	**0.00**
5	0.00	0.00	0.00	0.00	**0.00**	**0.00**
6	0.00	0.00	0.00	0.00	**0.00**	**0.00**
7	2.95	1.75	-0.29	-0.17	**2.66**	**1.58**
8	2.95	1.75	-0.29	-0.17	**2.66**	**1.58**
9	2.95	1.75	-0.29	-0.17	**2.66**	**1.58**
10	2.95	1.75	-0.30	-0.17	**2.65**	**1.58**
11	0.00	0.00	0.00	0.00	**0.00**	**0.00**
12	2.95	1.75	0.30	0.18	**3.25**	**1.93**
13	0.00	0.00	0.00	0.00	**0.00**	**0.00**
14	5.90	3.50	0.59	0.34	**6.49**	**3.84**
15	5.90	3.50	0.59	0.34	**6.49**	**3.84**
16	2.95	1.75	0.30	0.18	**3.25**	**1.93**
17	2.95	1.75	0.30	0.17	**3.25**	**1.92**
18	5.90	3.50	0.59	0.34	**6.49**	**3.84**
19	2.95	1.75	0.30	0.18	**3.25**	**1.93**
20	0.00	0.00	0.00	0.00	**0.00**	**0.00**
21	2.95	1.75	-0.30	-0.17	**2.65**	**1.58**
22	0.00	0.00	0.00	0.00	**0.00**	**0.00**
23	0.00	0.00	0.00	0.00	**0.00**	**0.00**
24	2.95	1.75	-0.29	-0.17	**2.66**	**1.58**
25	2.95	1.75	-0.30	-0.17	**2.65**	**1.58**
26	0.00	0.00	0.00	0.00	**0.00**	**0.00**
27	0.00	0.00	0.00	0.00	**0.00**	**0.00**
28	0.00	0.00	0.00	0.00	**0.00**	**0.00**
29	2.95	1.75	-0.30	-0.18	**2.65**	**1.57**
30	2.95	1.75	-0.30	-0.17	**2.65**	**1.58**
Total	59.00	35.00	0.00	0.00	**59.00**	**35.00**

Table 4.5.2-46 The final (compensated) solution for case study 5

(4) The results by the prediction system

By running the user interface routine (Rule 12), the final solution together with all the interim results for the case study 5 are presented as:

Bus	X^L (p.u.)		X^G (p.u.)		X^{LD} (%)		X^{GP} (%)		PM_S (p.u.)	
	X^{LP}	X^{LQ}	X^{GP}	X^{GQ}	X^{LDP}	X^{LDQ}	X^{GPP}	X^{GPQ}	ΔP_L	ΔQ_L
1	0.00	0.00	57.90	36.80	0.00%	0.00%	30.03%	29.34%	**0.00**	**0.00**
2	0.00	0.00	57.00	37.00	0.00%	0.00%	29.99%	30.28%	**0.00**	**0.00**
3	3.00	1.80	0.00	0.00	4.49%	4.51%	0.00%	0.00%	**2.65**	**1.58**
4	9.00	5.40	0.00	0.00	0.00%	0.00%	0.00%	0.00%	**0.00**	**0.00**
5	0.00	0.00	0.00	0.00	0.00%	0.00%	0.00%	0.00%	**0.00**	**0.00**
6	0.00	0.00	0.00	0.00	0.00%	0.00%	0.00%	0.00%	**0.00**	**0.00**
7	12.80	5.90	0.00	0.00	4.51%	4.51%	0.00%	0.00%	**2.66**	**1.58**
8	10.50	4.30	0.00	0.00	4.51%	4.51%	0.00%	0.00%	**2.66**	**1.58**
9	9.00	5.00	0.00	0.00	4.51%	4.51%	0.00%	0.00%	**2.66**	**1.58**
10	6.00	3.60	0.00	0.00	4.49%	4.51%	0.00%	0.00%	**2.65**	**1.58**
11	0.00	0.00	0.00	0.00	0.00%	0.00%	0.00%	0.00%	**0.00**	**0.00**
12	11.20	7.00	0.00	0.00	5.51%	5.51%	0.00%	0.00%	**3.25**	**1.93**
13	0.00	0.00	0.00	0.00	0.00%	0.00%	0.00%	0.00%	**0.00**	**0.00**
14	29.00	18.00	0.00	0.00	11.00%	10.98%	0.00%	0.00%	**6.49**	**3.84**
15	31.50	19.00	0.00	0.00	11.00%	10.98%	0.00%	0.00%	**6.49**	**3.84**
16	5.00	3.00	0.00	0.00	5.51%	5.51%	0.00%	0.00%	**3.25**	**1.93**
17	9.00	5.80	0.00	0.00	5.51%	5.48%	0.00%	0.00%	**3.25**	**1.92**
18	16.00	9.00	0.00	0.00	11.00%	10.98%	0.00%	0.00%	**6.49**	**3.84**
19	12.00	8.00	0.00	0.00	5.51%	5.51%	0.00%	0.00%	**3.25**	**1.93**
20	5.50	3.30	0.00	0.00	0.00%	0.00%	0.00%	0.00%	**0.00**	**0.00**
21	7.50	3.20	0.00	0.00	4.49%	4.51%	0.00%	0.00%	**2.65**	**1.58**
22	0.00	0.00	37.00	24.00	0.00%	0.00%	14.99%	15.14%	**0.00**	**0.00**
23	0.00	0.00	23.00	16.00	0.00%	0.00%	10.00%	10.09%	**0.00**	**0.00**
24	4.70	3.70	0.00	0.00	4.51%	4.51%	0.00%	0.00%	**2.66**	**1.58**
25	3.00	2.00	0.00	0.00	4.49%	4.51%	0.00%	0.00%	**2.65**	**1.58**
26	5.50	3.30	0.00	0.00	0.00%	0.00%	0.00%	0.00%	**0.00**	**0.00**
27	0.00	0.00	38.00	28.00	0.00%	0.00%	14.99%	15.14%	**0.00**	**0.00**
28	0.00	0.00	0.00	0.00	0.00%	0.00%	0.00%	0.00%	**0.00**	**0.00**
29	4.00	2.40	0.00	0.00	4.49%	4.48%	0.00%	0.00%	**2.65**	**1.57**
30	7.60	4.00	0.00	0.00	4.49%	4.51%	0.00%	0.00%	**2.65**	**1.58**
Total	201.8	117.7	212.90	141.80	**100.00%**	**100.00%**	100.00%	100.00%	**59.00**	**35.00**

Table 4.5.2-47 The final results by the predication system for case study 5

(5) The results by the conventional load flow study

For the purposed of comparison, the power margins for test pattern (5) are also calculated by the conventional load flow programme as:

Bus	X^L (p.u.)		X^G (p.u.)		X^{LD} (%)		X^{GP} (%)		PM (p.u.)	
	X^{LP}	X^{LQ}	X^{GP}	X^{GQ}	X^{LP}	X^{LQ}	X^{GP}	X^{GQ}	ΔP_L	ΔQ_L
1	0.00	0.00	57.90	36.80	0.00%	0.00%	30.03%	29.34%	**0.00**	**0.00**
2	0.00	0.00	57.00	37.00	0.00%	0.00%	29.99%	30.28%	**0.00**	**0.00**
3	3.00	1.80	0.00	0.00	4.49%	4.51%	0.00%	0.00%	**2.38**	**1.40**
4	9.00	5.40	0.00	0.00	0.00%	0.00%	0.00%	0.00%	**0.00**	**0.00**
5	0.00	0.00	0.00	0.00	0.00%	0.00%	0.00%	0.00%	**0.00**	**0.00**
6	0.00	0.00	0.00	0.00	0.00%	0.00%	0.00%	0.00%	**0.00**	**0.00**
7	12.80	5.90	0.00	0.00	4.51%	4.51%	0.00%	0.00%	**2.39**	**1.40**
8	10.50	4.30	0.00	0.00	4.51%	4.51%	0.00%	0.00%	**2.39**	**1.40**
9	9.00	5.00	0.00	0.00	4.51%	4.51%	0.00%	0.00%	**2.39**	**1.40**
10	6.00	3.60	0.00	0.00	4.49%	4.51%	0.00%	0.00%	**2.38**	**1.40**
11	0.00	0.00	0.00	0.00	0.00%	0.00%	0.00%	0.00%	**0.00**	**0.00**
12	11.20	7.00	0.00	0.00	5.51%	5.51%	0.00%	0.00%	**2.92**	**1.71**
13	0.00	0.00	0.00	0.00	0.00%	0.00%	0.00%	0.00%	**0.00**	**0.00**
14	29.00	18.00	0.00	0.00	11.00%	10.98%	0.00%	0.00%	**5.83**	**3.41**
15	31.50	19.00	0.00	0.00	11.00%	10.98%	0.00%	0.00%	**5.83**	**3.41**
16	5.00	3.00	0.00	0.00	5.51%	5.51%	0.00%	0.00%	**2.92**	**1.71**
17	9.00	5.80	0.00	0.00	5.51%	5.48%	0.00%	0.00%	**2.92**	**1.70**
18	16.00	9.00	0.00	0.00	11.00%	10.98%	0.00%	0.00%	**5.83**	**3.41**
19	12.00	8.00	0.00	0.00	5.51%	5.51%	0.00%	0.00%	**2.92**	**1.71**
20	5.50	3.30	0.00	0.00	0.00%	0.00%	0.00%	0.00%	**0.00**	**0.00**
21	7.50	3.20	0.00	0.00	4.49%	4.51%	0.00%	0.00%	**2.38**	**1.40**
22	0.00	0.00	37.00	24.00	0.00%	0.00%	14.99%	15.14%	**0.00**	**0.00**
23	0.00	0.00	23.00	16.00	0.00%	0.00%	10.00%	10.09%	**0.00**	**0.00**
24	4.70	3.70	0.00	0.00	4.51%	4.51%	0.00%	0.00%	**2.39**	**1.40**
25	3.00	2.00	0.00	0.00	4.49%	4.51%	0.00%	0.00%	**2.38**	**1.40**
26	5.50	3.30	0.00	0.00	0.00%	0.00%	0.00%	0.00%	**0.00**	**0.00**
27	0.00	0.00	38.00	28.00	0.00%	0.00%	14.99%	15.14%	**0.00**	**0.00**
28	0.00	0.00	0.00	0.00	0.00%	0.00%	0.00%	0.00%	**0.00**	**0.00**
29	4.00	2.40	0.00	0.00	4.49%	4.48%	0.00%	0.00%	**2.38**	**1.39**
30	7.60	4.00	0.00	0.00	4.49%	4.51%	0.00%	0.00%	**2.38**	**1.40**
Total	201.8	117.7	212.90	141.80	**100.00%**	**100.00%**	100.00%	100.00%	**53.01**	**31.05**

Table 4.5.2-48 **The power margins by the load flow study for case study 5**

(6) Accuracy analysis

Accuracy analysis for the case study 5 are summarised in the Table 4.5.2-49. The average relative errors are reduced from 3.49% / 3.54% for the initial solution to 2.54% / 2.88% with the final solution. The maximum relative errors with the individual prediction results are improved from 10.59% / 10.94% for the initial solution to the 5.00% / 5.57% for the final solution.

					For the initial results(PMo)				For the final results (PMs)			
	PM by LF		Max Load		Abs Error (p.u.)		Rel Error (%)		Abs Error (p.u.)		Rel Error (%)	
Bus	ΔP	ΔQ	Pmax	Qmax	ε_P	ε_Q	η_p	η_q	ε_P	ε_Q	η_p	η_q
1	0.00	0.00	0.00	0.00	0.000	0.000	n/a	n/a	0.000	0.000	n/a	n/a
2	0.00	0.00	0.00	0.00	0.000	0.000	n/a	n/a	0.000	0.000	n/a	n/a
3	2.38	1.40	5.38	3.20	0.570	0.350	10.59%	10.94%	0.269	0.178	5.00%	5.57%
4	0.00	0.00	9.00	5.40	0.000	0.000	0.00%	0.00%	0.000	0.000	0.00%	0.00%
5	0.00	0.00	0.00	0.00	0.000	0.000	n/a	n/a	0.000	0.000	n/a	n/a
6	0.00	0.00	0.00	0.00	0.000	0.000	n/a	n/a	0.000	0.000	n/a	n/a
7	2.39	1.40	15.19	7.30	0.560	0.350	3.69%	4.79%	0.270	0.178	1.78%	2.44%
8	2.39	1.40	12.89	5.70	0.560	0.350	4.34%	6.14%	0.270	0.178	2.10%	3.12%
9	2.39	1.40	11.39	6.40	0.560	0.350	4.92%	5.47%	0.270	0.178	2.37%	2.78%
10	2.38	1.40	8.38	5.00	0.570	0.350	6.80%	7.00%	0.269	0.178	3.21%	3.56%
11	0.00	0.00	0.00	0.00	0.000	0.000	n/a	n/a	0.000	0.000	n/a	n/a
12	2.92	1.71	14.12	8.71	0.030	0.040	0.21%	0.46%	0.330	0.218	2.34%	2.50%
13	0.00	0.00	0.00	0.00	0.000	0.000	n/a	n/a	0.000	0.000	n/a	n/a
14	5.83	3.41	34.83	21.41	0.070	0.090	0.20%	0.42%	0.659	0.434	1.89%	2.03%
15	5.83	3.41	37.33	22.41	0.070	0.090	0.19%	0.40%	0.659	0.434	1.76%	1.94%
16	2.92	1.71	7.92	4.71	0.030	0.040	0.38%	0.85%	0.330	0.218	4.17%	4.62%
17	2.92	1.70	11.92	7.50	0.030	0.050	0.25%	0.67%	0.330	0.216	2.77%	2.88%
18	5.83	3.41	21.83	12.41	0.070	0.090	0.32%	0.73%	0.659	0.434	3.02%	3.50%
19	2.92	1.71	14.92	9.71	0.030	0.040	0.20%	0.41%	0.330	0.218	2.21%	2.24%
20	0.00	0.00	5.50	3.30	0.000	0.000	0.00%	0.00%	0.000	0.000	0.00%	0.00%
21	2.38	1.40	9.88	4.60	0.570	0.350	5.77%	7.61%	0.269	0.178	2.72%	3.87%
22	0.00	0.00	0.00	0.00	0.000	0.000	n/a	n/a	0.000	0.000	n/a	n/a

					For the initial results(PMo)				For the final results (PMs)			
	PM by LF		Max Load		Abs Error (p.u.)		Rel Error (%)		Abs Error (p.u.)		Rel Error (%)	
Bus	**ΔP**	**ΔQ**	**Pmax**	**Qmax**	ε_P	ε_Q	η_p	η_q	ε_P	ε_Q	η_p	η_q
23	0.00	0.00	0.00	0.00	0.000	0.000	n/a	n/a	0.000	0.000	n/a	n/a
24	2.39	1.40	7.09	5.10	0.560	0.350	7.90%	6.86%	0.270	0.178	3.81%	3.49%
25	2.38	1.40	5.38	3.40	0.570	0.350	10.59%	10.29%	0.269	0.178	5.00%	5.24%
26	0.00	0.00	5.50	3.30	0.000	0.000	0.00%	0.00%	0.000	0.000	0.00%	0.00%
27	0.00	0.00	0.00	0.00	0.000	0.000	n/a	n/a	0.000	0.000	n/a	n/a
28	0.00	0.00	0.00	0.00	0.000	0.000	n/a	n/a	0.000	0.000	n/a	n/a
29	2.38	1.39	6.38	3.79	0.570	0.360	8.93%	9.50%	0.269	0.177	4.22%	4.67%
30	2.38	1.40	9.98	5.40	0.570	0.350	5.71%	6.48%	0.269	0.178	2.69%	3.30%
Total	**53.01**	**31.05**	**254.81**	**148.75**	**5.990**	**3.950**	**2.35%**	**2.66%**	**5.990**	**3.950**	**2.35%**	**2.66%**
Average					**0.386**	**0.255**	**3.49%**	**3.89%**	**0.386**	**0.255**	**2.54%**	**2.88%**

Table 4.5.2-49 The accuracy analysis for case study 5

6. **Case Study 6**

(1) Test pattern

The testing pattern of VSDFs for this case study is set as:

Bus	X^L (p.u.)		X^G (p.u.)		X^{LD} (%)		X^{GP} (%)	
	X^{LP}	X^{LQ}	X^{GP}	X^{GQ}	X^{LDP}	X^{LDQ}	X^{GPP}	X^{GPQ}
1	0.00	0.00	64.80	45.49	0.00%	0.00%	24.42%	23.04%
2	0.00	0.00	62.70	42.55	0.00%	0.00%	33.26%	32.98%
3	3.30	1.98	0.00	0.00	4.50%	4.51%	0.00%	0.00%
4	9.90	5.94	0.00	0.00	0.00%	0.00%	0.00%	0.00%
5	0.00	0.00	0.00	0.00	0.00%	0.00%	0.00%	0.00%
6	0.00	0.00	0.00	0.00	0.00%	0.00%	0.00%	0.00%
7	14.08	6.49	0.00	0.00	4.50%	4.51%	0.00%	0.00%
8	11.55	4.73	0.00	0.00	4.50%	4.51%	0.00%	0.00%
9	9.90	5.50	0.00	0.00	4.50%	4.51%	0.00%	0.00%
10	6.60	3.96	0.00	0.00	4.50%	4.51%	0.00%	0.00%
11	0.00	0.00	0.00	0.00	0.00%	0.00%	0.00%	0.00%
12	12.32	7.70	0.00	0.00	5.50%	5.51%	0.00%	0.00%
13	0.00	0.00	0.00	0.00	0.00%	0.00%	0.00%	0.00%
14	31.90	19.80	0.00	0.00	11.00%	10.97%	0.00%	0.00%
15	34.65	20.90	0.00	0.00	11.00%	10.97%	0.00%	0.00%
16	5.50	3.30	0.00	0.00	5.50%	5.51%	0.00%	0.00%
17	9.90	6.38	0.00	0.00	5.50%	5.46%	0.00%	0.00%
18	17.60	9.90	0.00	0.00	11.00%	10.97%	0.00%	0.00%
19	13.20	8.80	0.00	0.00	5.50%	5.51%	0.00%	0.00%
20	6.05	3.63	0.00	0.00	0.00%	0.00%	0.00%	0.00%
21	8.25	3.52	0.00	0.00	4.50%	4.51%	0.00%	0.00%
22	0.00	0.00	40.70	27.60	0.00%	0.00%	17.07%	16.49%
23	0.00	0.00	25.76	18.40	0.00%	0.00%	10.10%	10.99%
24	5.17	4.07	0.00	0.00	4.50%	4.51%	0.00%	0.00%
25	3.30	2.20	0.00	0.00	4.50%	4.51%	0.00%	0.00%
26	6.05	3.63	0.00	0.00	0.00%	0.00%	0.00%	0.00%
27	0.00	0.00	42.56	32.20	0.00%	0.00%	15.15%	16.49%
28	0.00	0.00	0.00	0.00	0.00%	0.00%	0.00%	0.00%
29	4.40	2.64	0.00	0.00	4.50%	4.51%	0.00%	0.00%
30	8.36	4.40	0.00	0.00	4.50%	4.51%	0.00%	0.00%
Total	221.98	129.47	236.52	166.24	100.00%	100.00%	100.00%	100.00%

Table 4.5.2-50 Test pattern (6) for case study 6

The further details about this test pattern are given in Table A3-24 of Appendix 3.

(2) Euclidean Distance Calculations

The Euclidean distances to the prototype of each pattern class are calculated by using equation (4.5.1-1) as below:

(i) The Euclidean distance to pattern class I:

The 4 segments of the Euclidean distance from the testing pattern (6) to the prototype of pattern class I (**L01, LD05, G02 and GP01** as shown in Table 4.5.1-1) are:

Load pattern segment D^{L01}	67.78
Load distribution pattern segment D^{LD03}	25.86
Generation pattern segment D^{G02}	130.79
Generation participation pattern segment D^{GP01}	30.34

Table 4.5.2-51 The Euclidean distance from test pattern (6) to pattern class I

(ii) The Euclidean distance to pattern class II:

The Euclidean distance from test pattern (6) to the prototype of pattern class II (**L10, LD15, G06 and GP03** as shown in Table 4.5.1-2) is:

Load pattern segment D^{L12}	54.04
Load distribution pattern segment D^{LD11}	26.10
Generation pattern segment D^{G09}	86.56
Generation participation pattern segment D^{GP06}	37.28

Table 4.5.2-52 The Euclidean distance from test pattern (6) to pattern class 1I

(iii) The Euclidean distance to pattern class III:

The Euclidean distance to from test pattern (6) to the prototype of pattern class III (**L20, LD20, G20 and GP20** as shown in Table 4.5.1-3) is:

Load pattern segment D^{L12}	6.55
Load distribution pattern segment D^{LD11}	3.56
Generation pattern segment D^{G09}	16.28
Generation participation pattern segment D^{GP06}	10.40

Table 4.5.2-53 The Euclidean distance from test pattern (6) to pattern class III

(3) Solution searching

By applying the knowledge rules to the results in Table 4.5.2-51, Table 4.5.2-52 and Table 4.5.2-53, the initial and final (compensated) solutions are reached as:

Bus	PM_0 (p.u.)		Compensation δ		PM_S (p.u.)	
	ΔP_{L0}	ΔQ_{L0}	δ^P	δ^Q	$\Delta P_L=\Delta P_{L0}+\delta^P$	$\Delta Q_L=\Delta Q_{L0}+\delta^Q$
1	0.00	0.00	0.00	0.00	0.00	0.00
2	0.00	0.00	0.00	0.00	0.00	0.00
3	2.95	1.75	-1.20	-0.70	1.75	1.05
4	0.00	0.00	0.00	0.00	0.00	0.00
5	0.00	0.00	0.00	0.00	0.00	0.00
6	0.00	0.00	0.00	0.00	0.00	0.00
7	2.95	1.75	-1.20	-0.70	1.75	1.05
8	2.95	1.75	-1.20	-0.70	1.75	1.05
9	2.95	1.75	-1.20	-0.70	1.75	1.05
10	2.95	1.75	-1.20	-0.70	1.75	1.05
11	0.00	0.00	0.00	0.00	0.00	0.00
12	2.95	1.75	-0.81	-0.47	2.14	1.28
13	0.00	0.00	0.00	0.00	0.00	0.00
14	5.90	3.50	-1.63	-0.95	4.27	2.55
15	5.90	3.50	-1.63	-0.95	4.27	2.55
16	2.95	1.75	-0.81	-0.47	2.14	1.28
17	2.95	1.75	-0.81	-0.48	2.14	1.27
18	5.90	3.50	-1.63	-0.95	4.27	2.55
19	2.95	1.75	-0.81	-0.47	2.14	1.28
20	0.00	0.00	0.00	0.00	0.00	0.00
21	2.95	1.75	-1.20	-0.70	1.75	1.05
22	0.00	0.00	0.00	0.00	0.00	0.00
23	0.00	0.00	0.00	0.00	0.00	0.00
24	2.95	1.75	-1.20	-0.70	1.75	1.05
25	2.95	1.75	-1.20	-0.70	1.75	1.05
26	0.00	0.00	0.00	0.00	0.00	0.00
27	0.00	0.00	0.00	0.00	0.00	0.00
28	0.00	0.00	0.00	0.00	0.00	0.00
29	2.95	1.75	-1.20	-0.70	1.75	1.05
30	2.95	1.75	-1.20	-0.70	1.75	1.05
Total	59.00	35.00	-20.18	-11.77	38.82	23.23

Table 4.5.2-54 The initial and final (compensated) solutions for case study 6

(4) The results produced by the prediction system

By running the user interface routine (Rule 12), the final solution together with all the interim results for the case study 1 are presented as:

Bus	X^L (p.u.)		X^G (p.u.)		X^{LD} (%)		X^{GP} (%)		PM_S (p.u.)	
	X^{LP}	X^{LQ}	X^{GP}	X^{GQ}	X^{LDP}	X^{LDQ}	X^{GPP}	X^{GPQ}	ΔP_L	ΔQ_L
1	0.00	0.00	64.80	45.49	0.00%	0.00%	24.42%	23.04%	**0.00**	**0.00**
2	0.00	0.00	62.70	42.55	0.00%	0.00%	33.26%	32.98%	**0.00**	**0.00**
3	3.30	1.98	0.00	0.00	4.50%	4.51%	0.00%	0.00%	**1.75**	**1.05**
4	9.90	5.94	0.00	0.00	0.00%	0.00%	0.00%	0.00%	**0.00**	**0.00**
5	0.00	0.00	0.00	0.00	0.00%	0.00%	0.00%	0.00%	**0.00**	**0.00**
6	0.00	0.00	0.00	0.00	0.00%	0.00%	0.00%	0.00%	**0.00**	**0.00**
7	14.08	6.49	0.00	0.00	4.50%	4.51%	0.00%	0.00%	**1.75**	**1.05**
8	11.55	4.73	0.00	0.00	4.50%	4.51%	0.00%	0.00%	**1.75**	**1.05**
9	9.90	5.50	0.00	0.00	4.50%	4.51%	0.00%	0.00%	**1.75**	**1.05**
10	6.60	3.96	0.00	0.00	4.50%	4.51%	0.00%	0.00%	**1.75**	**1.05**
11	0.00	0.00	0.00	0.00	0.00%	0.00%	0.00%	0.00%	**0.00**	**0.00**
12	12.32	7.70	0.00	0.00	5.50%	5.51%	0.00%	0.00%	**2.14**	**1.28**
13	0.00	0.00	0.00	0.00	0.00%	0.00%	0.00%	0.00%	**0.00**	**0.00**
14	31.90	19.80	0.00	0.00	11.00%	10.97%	0.00%	0.00%	**4.27**	**2.55**
15	34.65	20.90	0.00	0.00	11.00%	10.97%	0.00%	0.00%	**4.27**	**2.55**
16	5.50	3.30	0.00	0.00	5.50%	5.51%	0.00%	0.00%	**2.14**	**1.28**
17	9.90	6.38	0.00	0.00	5.50%	5.46%	0.00%	0.00%	**2.14**	**1.27**
18	17.60	9.90	0.00	0.00	11.00%	10.97%	0.00%	0.00%	**4.27**	**2.55**
19	13.20	8.80	0.00	0.00	5.50%	5.51%	0.00%	0.00%	**2.14**	**1.28**
20	6.05	3.63	0.00	0.00	0.00%	0.00%	0.00%	0.00%	**0.00**	**0.00**
21	8.25	3.52	0.00	0.00	4.50%	4.51%	0.00%	0.00%	**1.75**	**1.05**
22	0.00	0.00	40.70	27.60	0.00%	0.00%	17.07%	16.49%	**0.00**	**0.00**
23	0.00	0.00	25.76	18.40	0.00%	0.00%	10.10%	10.99%	**0.00**	**0.00**
24	5.17	4.07	0.00	0.00	4.50%	4.51%	0.00%	0.00%	**1.75**	**1.05**
25	3.30	2.20	0.00	0.00	4.50%	4.51%	0.00%	0.00%	**1.75**	**1.05**
26	6.05	3.63	0.00	0.00	0.00%	0.00%	0.00%	0.00%	**0.00**	**0.00**
27	0.00	0.00	42.56	32.20	0.00%	0.00%	15.15%	16.49%	**0.00**	**0.00**
28	0.00	0.00	0.00	0.00	0.00%	0.00%	0.00%	0.00%	**0.00**	**0.00**
29	4.40	2.64	0.00	0.00	4.50%	4.51%	0.00%	0.00%	**1.75**	**1.05**
30	8.36	4.40	0.00	0.00	4.50%	4.51%	0.00%	0.00%	**1.75**	**1.05**
Total	221.98	129.47	236.52	166.24	100.00%	100.00%	100.00%	100.00%	**38.82**	**23.23**

Table 4.5.2-55 The final results by the predication system for case study 6

(5) The results by the conventional load flow study

For the purposed of comparison, the power margins for test pattern (6) are also calculated by the conventional load flow programme as:

Bus	X^L (p.u.)		X^G (p.u.)		X^{LD} (%)		X^{GP} (%)		PM (p.u.)	
	X^{LP}	X^{LQ}	X^{GP}	X^{GQ}	X^{LP}	X^{LQ}	X^{GP}	X^{GQ}	ΔP_L	ΔQ_L
1	0.00	0.00	64.80	45.49	0.00%	0.00%	24.42%	23.04%	**0.00**	**0.00**
2	0.00	0.00	62.70	42.55	0.00%	0.00%	33.26%	32.98%	**0.00**	**0.00**
3	3.30	1.98	0.00	0.00	4.50%	4.51%	0.00%	0.00%	**1.44**	**0.86**
4	9.90	5.94	0.00	0.00	0.00%	0.00%	0.00%	0.00%	**0.00**	**0.00**
5	0.00	0.00	0.00	0.00	0.00%	0.00%	0.00%	0.00%	**0.00**	**0.00**
6	0.00	0.00	0.00	0.00	0.00%	0.00%	0.00%	0.00%	**0.00**	**0.00**
7	14.08	6.49	0.00	0.00	4.50%	4.51%	0.00%	0.00%	**1.44**	**0.86**
8	11.55	4.73	0.00	0.00	4.50%	4.51%	0.00%	0.00%	**1.44**	**0.86**
9	9.90	5.50	0.00	0.00	4.50%	4.51%	0.00%	0.00%	**1.44**	**0.86**
10	6.60	3.96	0.00	0.00	4.50%	4.51%	0.00%	0.00%	**1.44**	**0.86**
11	0.00	0.00	0.00	0.00	0.00%	0.00%	0.00%	0.00%	**0.00**	**0.00**
12	12.32	7.70	0.00	0.00	5.50%	5.51%	0.00%	0.00%	**1.76**	**1.05**
13	0.00	0.00	0.00	0.00	0.00%	0.00%	0.00%	0.00%	**0.00**	**0.00**
14	31.90	19.80	0.00	0.00	11.00%	10.97%	0.00%	0.00%	**3.52**	**2.09**
15	34.65	20.90	0.00	0.00	11.00%	10.97%	0.00%	0.00%	**3.52**	**2.09**
16	5.50	3.30	0.00	0.00	5.50%	5.51%	0.00%	0.00%	**1.76**	**1.05**
17	9.90	6.38	0.00	0.00	5.50%	5.46%	0.00%	0.00%	**1.76**	**1.04**
18	17.60	9.90	0.00	0.00	11.00%	10.97%	0.00%	0.00%	**3.52**	**2.09**
19	13.20	8.80	0.00	0.00	5.50%	5.51%	0.00%	0.00%	**1.76**	**1.05**
20	6.05	3.63	0.00	0.00	0.00%	0.00%	0.00%	0.00%	**0.00**	**0.00**
21	8.25	3.52	0.00	0.00	4.50%	4.51%	0.00%	0.00%	**1.44**	**0.86**
22	0.00	0.00	40.70	27.60	0.00%	0.00%	17.07%	16.49%	**0.00**	**0.00**
23	0.00	0.00	25.76	18.40	0.00%	0.00%	10.10%	10.99%	**0.00**	**0.00**
24	5.17	4.07	0.00	0.00	4.50%	4.51%	0.00%	0.00%	**1.44**	**0.86**
25	3.30	2.20	0.00	0.00	4.50%	4.51%	0.00%	0.00%	**1.44**	**0.86**
26	6.05	3.63	0.00	0.00	0.00%	0.00%	0.00%	0.00%	**0.00**	**0.00**
27	0.00	0.00	42.56	32.20	0.00%	0.00%	15.15%	16.49%	**0.00**	**0.00**
28	0.00	0.00	0.00	0.00	0.00%	0.00%	0.00%	0.00%	**0.00**	**0.00**
29	4.40	2.64	0.00	0.00	4.50%	4.51%	0.00%	0.00%	**1.44**	**0.86**
30	8.36	4.40	0.00	0.00	4.50%	4.51%	0.00%	0.00%	**1.44**	**0.86**
Total	221.98	129.47	236.52	166.24	100.00%	100.00%	100.00%	100.00%	**32.00**	**19.06**

Table 4.5.2-56 The power margins by the load flow study for case study 6

(6) Accuracy analysis

Accuracy analysis for the case study 6 are summarised in the Table 4.5.2-57. The average relative errors are reduced from 13.08% / 13.21% for the initial solution to 3.04% / 3.17% for the final solution. The maximum relative errors with the individual prediction results are improved from 31.86% / 31.34% for the initial solution to the 6.47% / 6.63% for the final solutions.

					For the initial results(PMo)				For the final results (PMs)			
	PM by LF		Max Load		Abs Error (p.u.)		Rel Error (%)		Abs Error (p.u.)		Rel Error (%)	
Bus	ΔP	ΔQ	Pmax	Qmax	ε_P	ε_Q	η_p	η_q	ε_P	ε_Q	η_p	η_q
1	0.00	0.00	0.00	0.00	0.000	0.000	n/a	n/a	0.000	0.000	n/a	n/a
2	0.00	0.00	0.00	0.00	0.000	0.000	n/a	n/a	0.000	0.000	n/a	n/a
3	1.44	0.86	4.74	2.84	1.510	0.890	31.86%	31.34%	0.307	0.188	6.47%	6.63%
4	0.00	0.00	9.90	5.94	0.000	0.000	0.00%	0.00%	0.000	0.000	0.00%	0.00%
5	0.00	0.00	0.00	0.00	0.000	0.000	n/a	n/a	0.000	0.000	n/a	n/a
6	0.00	0.00	0.00	0.00	0.000	0.000	n/a	n/a	0.000	0.000	n/a	n/a
7	1.44	0.86	15.52	7.35	1.510	0.890	9.73%	12.11%	0.307	0.188	1.98%	2.56%
8	1.44	0.86	12.99	5.59	1.510	0.890	11.62%	15.92%	0.307	0.188	2.36%	3.37%
9	1.44	0.86	11.34	6.36	1.510	0.890	13.32%	13.99%	0.307	0.188	2.71%	2.96%
10	1.44	0.86	8.04	4.82	1.510	0.890	18.78%	18.46%	0.307	0.188	3.82%	3.90%
11	0.00	0.00	0.00	0.00	0.000	0.000	n/a	n/a	0.000	0.000	n/a	n/a
12	1.76	1.05	14.08	8.75	1.190	0.700	8.45%	8.00%	0.375	0.230	2.66%	2.63%
13	0.00	0.00	0.00	0.00	0.000	0.000	n/a	n/a	0.000	0.000	n/a	n/a
14	3.52	2.09	35.42	21.89	2.380	1.410	6.72%	6.44%	0.750	0.457	2.12%	2.09%
15	3.52	2.09	38.17	22.99	2.380	1.410	6.24%	6.13%	0.750	0.457	1.97%	1.99%
16	1.76	1.05	7.26	4.35	1.190	0.700	16.39%	16.09%	0.375	0.230	5.17%	5.28%
17	1.76	1.04	11.66	7.42	1.190	0.710	10.21%	9.57%	0.375	0.228	3.22%	3.07%
18	3.52	2.09	21.12	11.99	2.380	1.410	11.27%	11.76%	0.750	0.457	3.55%	3.81%
19	1.76	1.05	14.96	9.85	1.190	0.700	7.95%	7.11%	0.375	0.230	2.51%	2.33%
20	0.00	0.00	6.05	3.63	0.000	0.000	0.00%	0.00%	0.000	0.000	0.00%	0.00%
21	1.44	0.86	9.69	4.38	1.510	0.890	15.58%	20.32%	0.307	0.188	3.17%	4.30%
22	0.00	0.00	0.00	0.00	0.000	0.000	n/a	n/a	0.000	0.000	n/a	n/a

					For the initial results(PMo)				For the final results (PMs)			
	PM by LF		Max Load		Abs Error (p.u.)		Rel Error (%)		Abs Error (p.u.)		Rel Error (%)	
Bus	**ΔP**	**ΔQ**	**Pmax**	**Qmax**	**ε_P**	**ε_Q**	**η_p**	**η_q**	**ε_P**	**ε_Q**	**η_p**	**η_q**
23	0.00	0.00	0.00	0.00	0.000	0.000	n/a	n/a	0.000	0.000	n/a	n/a
24	1.44	0.86	6.61	4.93	1.510	0.890	22.84%	18.05%	0.307	0.188	4.64%	3.82%
25	1.44	0.86	4.74	3.06	1.510	0.890	31.86%	29.08%	0.307	0.188	6.47%	6.15%
26	0.00	0.00	6.05	3.63	0.000	0.000	0.00%	0.00%	0.000	0.000	0.00%	0.00%
27	0.00	0.00	0.00	0.00	0.000	0.000	n/a	n/a	0.000	0.000	n/a	n/a
28	0.00	0.00	0.00	0.00	0.000	0.000	n/a	n/a	0.000	0.000	n/a	n/a
29	1.44	0.86	5.84	3.50	1.510	0.890	25.86%	25.43%	0.307	0.188	5.26%	5.38%
30	1.44	0.86	9.80	5.26	1.510	0.890	15.41%	16.92%	0.307	0.188	3.13%	3.58%
Total	**32.00**	**19.06**	**253.98**	**148.53**	**27.000**	**15.940**	**10.63%**	**10.73%**	**6.820**	**4.170**	**2.69%**	**2.81%**
Average					**1.742**	**1.028**	**13.08%**	**13.21%**	**0.440**	**0.269**	**3.04%**	**3.17%**

Table 4.5.2-57 The accuracy analysis for case study 6

4.5.3 Simulation Evaluation

1. Simulation configurations

The IEEE 30 bus power system and its standard data were used for the simulation of the proposed system. Three pattern classes under lightly, normally and heavily loaded conditions were configured for the voltage stability determining factors (VSDFs). These pattern classes represent three typical pattern classes that a power system will normally have. Totally six study cases, two under each configured pattern class were presented in this section. All the test patterns were set up in such way that at least one of its VSDFs have minimum (+/-)10% deviation (randomly applied) from the prototype of the pattern class they belong to. This is to ensure that the test patterns are within the designated pattern class meanwhile have sufficient distance (Euclidean) to the prototype of the pattern class.

2. Decision making speed

All six simulation cases show that the proposed system has extremely fast decision-making speed. This is fundamentally owed to the use of the knowledge-based method and pattern recognition technique, such that the conventional algorithm based numeric computation is avoided.

3. Decision-making accuracy

Accuracy analyses with each case study show that the proposed system is able to produce sufficiently accurate results for prediction of voltage stability. The compensation algorithm significantly improves the accuracy of the predicted results. The average relative errors for all the case studies were well below 5%.

4. Remarks

It must be emphasised here that the decision-making speed and accuracy of this knowledge based system are interactive to each another, and both of them are sensitively affected by the pattern features selection and pattern class determination. In the reality, comprise often has to be made in order to achieve a desired system performance.

4.6 DISCUSSIONS AND CONCLUSIONS

A knowledge based system for prediction of voltage collapse using pattern recognition technique has been proposed in this chapter. It is based on the theory established in chapter 3 that a power system has similar voltage stability when its voltage stability determining factors (VSDFs) stay in the same pattern class.

The principle of this proposed system is to compare a power network to a pre-studied system of which voltage stability (power margins) is known. It has a basic structure of a knowledge based system with a pattern recognition module. To apply such a system to a power system involves a two stage process: off-line training and on-line application. The main task of the off-line training is to develop a knowledge base which contains the power margin results for the prototypes of all the pattern classes of the VSDFs in the power system. At the on-line application, the pattern recognition technique is used to identify the pattern class to which the current state of the power system belongs, its voltage stability can be found in the knowledge base.

The "off-line training" is crucial to the success of this knowledge based system. The pattern feature selection and pattern class determination for the VSDFs are two key elements in this process. They directly affect the decision-making speed and accuracy of the proposed system. Accurate results require a sufficient number of the pattern classes, whereas too many of them will cause heavy computation burden and slow down the decision-making. In practise, comprise often has to be made in choosing a right number of the pattern classes in order to achieve a desired system performance.

To improve the accuracy of the decision-making, a compensation algorithm was developed and introduced in this knowledge based system. The simulation results show that the prediction accuracy has been significantly improved by using the compensation algorithm.

The technical details about designing and developing such a system were intensively discussed in this chapter. The Artificial Intelligence approach used in the proposed system has fundamentally changed the way in which voltage stability is assessed for a power system. It does not require on-line numerical calculations to produce power margins, hence the decision-making time is significantly reduced in comparison with the traditional algorithm based methods. The typical convergence problem of the Newton-Raphson-like load flow algorithm in the vicinity of voltage instability is also avoided in this prediction system.

In addition, as the power margin solutions produced by proposed system are off-line calculated, different algorithms and approaches can be used for the off-line calculations. This is a big advantage, especially for the power systems of which power margins are difficult to determine.

The proposed system has been simulated on the IEEE 30 bus power system. Six study cases were presented in this chapter. The simulation results show that the proposed system is able to reach rather accurate results with a speedy decision-making. Therefore, it has a good potential for on-line application for prediction of voltage collapse.

CHAPTER 5 THE PRINCIPLE OF SECONDARY VOLTAGE CONTROL SYSTEMS

5.1 INTRODUCTION

As a major counter-measure to voltage collapse in power systems, secondary voltage control systems have been intensively investigated in this project.

This is one of three chapters in this thesis to present this part of research. It deals with all the theoretical preparations required for the design and analyse of such a voltage control system. Other chapters include chapter 6: the secondary voltage control system by a classical control design, and chapter 7: the secondary voltage control system by an optimal control design.

In this chapter, the pilot bus based control principle for secondary voltage control is theoretically formularised. A multi-level control structure is defined, and functions at each control level are clarified for this control system. All the system plants involved in secondary voltage control are systematically modelled and mathematically described. This includes the models for generators, power plants and power systems.

Both the centralised and decentralised control schemes for secondary voltage control are discussed in this chapter. It can be seen that the centralised scheme has many advantages over the decentralised one in terms of system efficiency, reliability and implementation. The design criteria for such a control system are also included at the end of this chapter.

5.2 THE PRINCIPLE OF SECONDARY VOLTAGE CONTROL

Voltage control in a power system can be divided into three levels: Primary, Secondary (Regional) and Tertiary. The primary control is to control the voltage at generator terminals. It will be implemented by the Automatic Voltage Regulator (AVR) of a generator.

Secondary Voltage Control also known as the Regional Voltage Regulation (RVR) is to maintain voltage profile in a region of a power system. This can be implemented by keeping the voltage of some buses, called pilot buses, at a desired value (target) by dispatching the reactive generation of some local power plants, called control power plants.

The tertiary control is to automatically or manually co-ordinate the regional voltage controls in a power system. It determines the target voltage for secondary voltage control in each region by using actual state of the power network, forecasted optimal voltage and reactive reserves. In this way a secure and economic operation of a power system will be achieved.

It is clearly seen that secondary voltage control takes a major role in the voltage control of a power system. It receives the targets from the tertiary control and maintains the desired voltage profile in a region through the primary control facilities (AVR).

This section deals with the principle of secondary voltage control. The pilot bus based control principal and centralised/decentralised control schemes are going to be discussed here.

5.2.1 Pilot Buses and Control Power Plants

The principle of secondary voltage control is to maintain a desired voltage profile in a region of a power system by controlling the voltage of pilot buses at a certain values. This is achieved by regulating the reactive generation of the control plants in the region. The pilot buses are buses in a region, of which if their voltage is kept at a desired reference value, the voltage at most buses in the region will be maintained within a certain bandwidth. The control power plants are power plants in a region, of which reactive outputs have a stronger influence on the voltage of pilot buses than other power plants. This pilot bus based control principal is based on "the electrical decoupling" of a power system, can be mathematically formularised as follows:

From linearised load flow equations, there are:

$$[\Delta Q] = [J_{QV}][\Delta V] \qquad (5.2.1\text{–}1)$$

Where,

$[\Delta Q]$ is the reactive power injection variation at all the buses in a power system,

$[\Delta V]$ is the voltage variation at all the buses in a power system,

$[J_{QV}]$ is the Jacob matrix between reactive power injection and voltage at all the buses in a power system.

Assuming $[J_{QV}]$ invertible, and $[S] = [J_{QV}]^{-1}$ then,

$$[\Delta V] = [S][\Delta Q] \qquad (5.2.1\text{–}2)$$

By dividing the voltages into the pilot bus group and non-pilot bus group ($V_P, V_{\bar{P}}$), and the reactive power injections into the control power plant group and load bus group (Q_G, Q_L). the above equation becomes:

$$\begin{bmatrix} \Delta V_P \\ \Delta V_{\bar{P}} \end{bmatrix} = \begin{bmatrix} S_{VG}^{P} & S_{VL}^{P} \\ S_{VG}^{\bar{P}} & S_{VL}^{\bar{P}} \end{bmatrix} \begin{bmatrix} \Delta Q_G \\ \Delta Q_L \end{bmatrix} \qquad (5.2.1\text{–}3)$$

The voltages of this non-pilot bus group $[V_{\bar{P}}]$ represent the voltage profile in a region or a power system. The pilot bus voltage and voltage profile can be described as:

$$[\Delta V_P] = [S_{VG}^{P}][\Delta Q_G] + [S_{VL}^{P}][\Delta Q_L] \qquad (5.2.1\text{–}4)$$

$$\left[\Delta V_{\bar{P}}\right] = \left[S^{\bar{P}}_{VG} \right]\left[\Delta Q_G\right] + \left[S^{\bar{P}}_{VL} \right]\left[\Delta Q_L\right] \tag{5.2.1–5}$$

Assuming that by a certain control design, the following relationship can be established:

$$[\Delta Q_G] = [\Lambda][\Delta V_p] + [\Omega][\Delta Q_L] \tag{5.2.1–6}$$

where,

$[\Lambda] \in \Re^{N_G X N_P}$,

$[\Omega] \in \Re^{N_G X N_Q}$.

By direct substitution with equation (5.2.1- 6), equation (5.2.1 -5) becomes

$$\begin{aligned}[\Delta V_{\bar{P}}] &= \left[S^{\bar{P}}_{VG} \right][\Lambda][\Delta V_p] + \left(\left[S^{\bar{P}}_{VL} \right] + \left[S^{\bar{P}}_{VG} \right][\Omega] \right)[\Delta Q_L] \\ &= [\Re][\Delta V_p] + [\aleph][\Delta Q_L]\end{aligned} \tag{5.2.1–7}$$

where,

$[\Re] = \left[S^{\bar{P}}_{VG} \right][\Lambda]$;

$[\aleph] = \left[S^{\bar{P}}_{VL} \right] + \left[S^{\bar{P}}_{VG} \right][\Omega]$.

From the equation (5.2.1-7), the following statements can be made:

1. It is possible to maintain the voltage profile through controlling the voltages at pilot buses;
2. The success of secondary voltage control relays on a proper methodology for the pilot bus/control power plant selection and control system design. A good selection of pilot buses/control power plants shall make the absolute value of elements in matrix $[\aleph]$ sufficiently small.
3. A good control design shall efficiently and stubbly keep the voltages of the pilot buses at desired value.

5.2.2 Centralised and Decentralised Control Scheme

Generally there are two different schemes for implementing the voltage control in a power system: Centralised and Decentralised Schemes. The centralised scheme is to control the voltage profile for the whole power system through one central controller. The decentralised scheme is to divide a power system into several regions, and the voltage profile for a whole power system can be controlled through the Regional Voltage Regulators (RVRs).

The decentralised control scheme has many advantages over the decentralised one. Firstly the decentralised control scheme uses separate computers for the RVR in each region, it does not have special requirements for the computers; While the centralised control scheme uses a central computer for a whole power system, hence requires massive CPU and memory resources.

Secondly the decentralised control scheme has a better reliability than the centralised one. Problems with a regional voltage regulation will not have significant impact on the voltage control in other regions in a power system. However, single failure with the centralised scheme may cause a total loss of the voltage control for a whole power system.

In addition, for the decentralised scheme, the regional voltage control systems can be installed and commissioned region by region at different times; while the installation of a centralised control system requires an operation outages (out of service) for a whole power system, which is rather difficult to plan.

The decentralisation of a power system is a key task for a secondary voltage control scheme. A common methodology for the decentralisation is based on the sensitivity analysis using the Jacobian matrix of the load flow equations. The fundamental requirements for this decentralisation can be generalised as:

1. The decentralisation should be based on the natural decoupling of a power system.
2. A decentralised region should be a set of buses in a power system, of which the voltage behaviours are strongly coupled with each other internally and loosely tied with the buses external to the region.

3. A successful decentralisation algorithm should take into account the possible voltage oscillation between the regions and ensure that the voltage control action in a region has a negligible effect to other regions.
4. Each decentralised region should have sufficient reactive generation reserve with respect to the specified maximum MVar demand in the region.

5.2.3 Multi-level Control Structure

Secondary voltage control system maintains desired voltages at the pilot buses by regulating the reactive generation of control power plants. To mange the required reactive generation at a control power plant, a control mechanism is needed to automatically allocate the reactive generation among the participated generator units called control generators. The reactive generation demanded from each generator unit will be finally controlled by the generator AVR system. By considering this hierarchical structure and the different dynamic response times, a three level control structure is believed to be necessary for a secondary voltage control system. These three levels are the Regional Voltage Regulation (RVR), the Power Plant Reactive Power Regulation (PQR), and the Generator Automatic Voltage Regulation (AVR).

The RVR will determine the necessary reactive generation or the voltage at the HV busbar (PQR reference) for each control power plant in a region. This is based on the voltage variation at the regional pilot bus with respect to a target value (reference for RVR). To attain this determined reactive generation/voltage, the PQR is used to determine the outputs of the control generators within each control power plant. The demanded reactive generation will eventually be fulfilled by the AVRs with the control generators. The global structure of this three level voltage control system is shown in Figure 5.2.3-1.

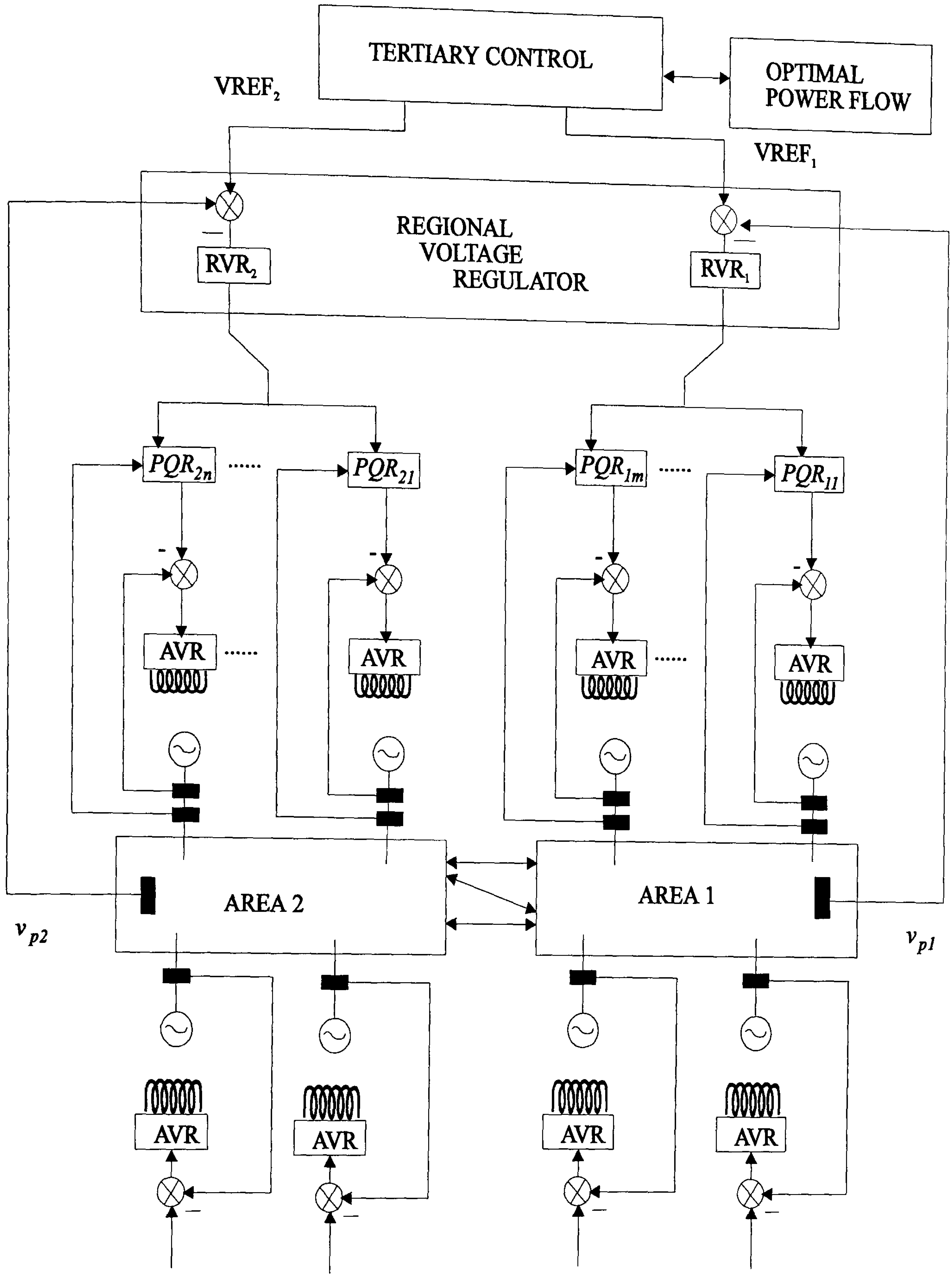

Figure 5.2.3-1 **The three level structure for secondary voltage control**

As the AVR system is regarded as an independent subject in the area of power generators, it is not included in the study of this thesis.

5.3 System Modelling and Descriptions

Properly modelling and described control plant takes a crucial role for the design and analysis of a control system. All the power system components involved in secondary voltage control are systematically modelled and mathematically described in this Section.

5.3.1 System Modelling

1. Control generators

The control generators are the generators in a control power plant, which are used to produce the demanded reactive generation for a secondary voltage control scheme. A control generator has the following model:

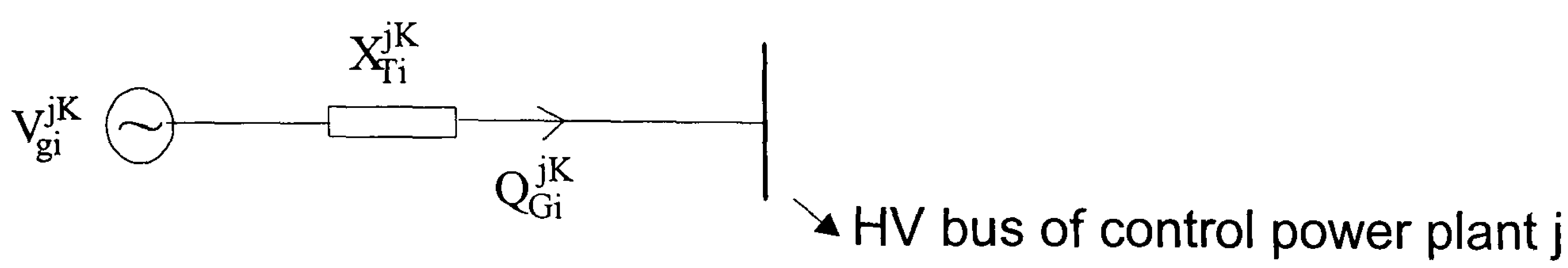

Figure 5.3.1-1 The model for a control generator

Where,

V_{gi}^{jk} is the voltage magnitude of control generator *K* at control power plant *j* within region *i*,

Q_{gi}^{jk} is the reactive generation of control generator *k* at control power plant *j* in region *i*,

X_{Ti}^{jk} is the equivalent reactance between generator k and the HV busbar of control power plant *j* in region *i* .

2. Control power plants

The control power plants are the power plants in a decentralised region, which are selected to participate in a secondary voltage control scheme. In this thesis, a control power plant is simplified to only contain the control generators, its model can be defined as:

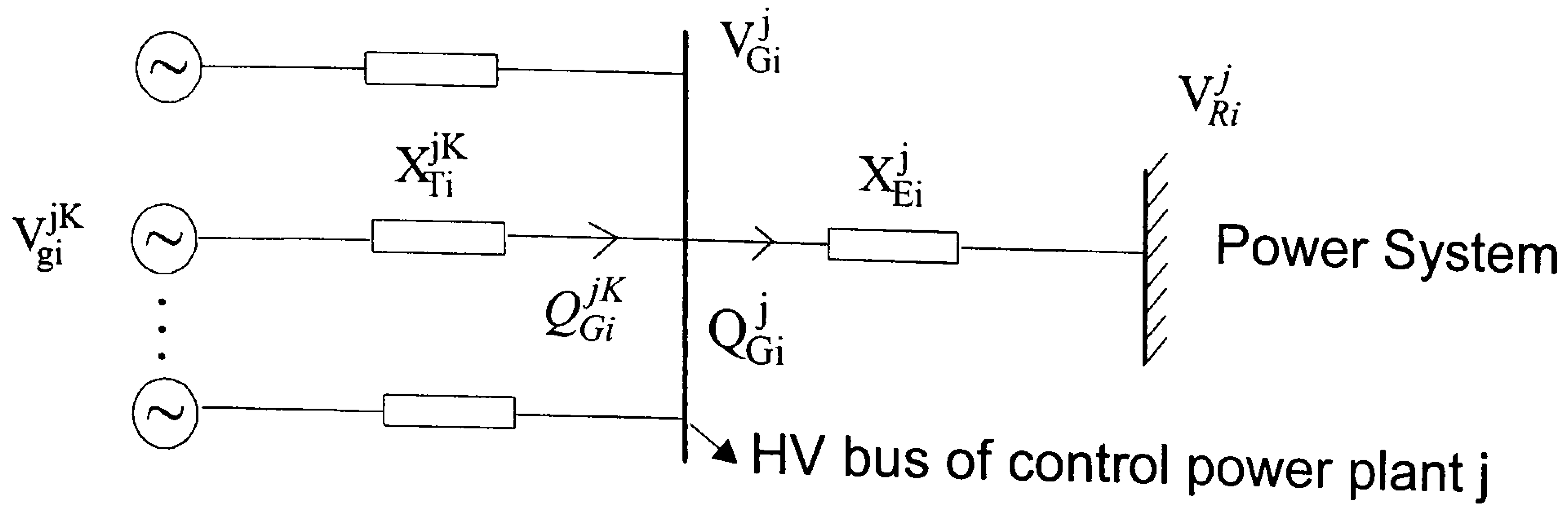

Figure 5.3.1-2 **The model for a control power plant**

The PQR design is based on this model.

Where,

Q_{Gi}^{j} is the reactive power generation of control power plant j in the region i,

V_{Gi}^{j} is the voltage magnitude at HV bus of control power plant j in region i,

V_{Ri}^{j} is the voltage at equivalent system bus for the control power plant j in region i,

X_{Ei}^{j} is the equivalent reactance between the HV bus of control power plant j and the system bus for the power plant.

3. Decentralised regions and power System

It is believed in this thesis that one pilot bus per decentralised region is sufficient for a secondary voltage control scheme. Within a decentralised region, the buses can be divided into one pilot bus, control power plant buses and load buses. The pilot bus is known as the bus of which the voltage has a greater influence on the regional voltage profile than other buses in a region. The control power plant buses and load buses are assumed to only have power generation and load respectively. The power plants which are not involved in secondary voltage control are treated as load buses (with the opposite sign of power injections to the load buses) in this model. Thus, a power system consisting of decentralised regions can be defined to have the model as shown in Figure 5.3.1-3 below. The RVR design is based on this model.

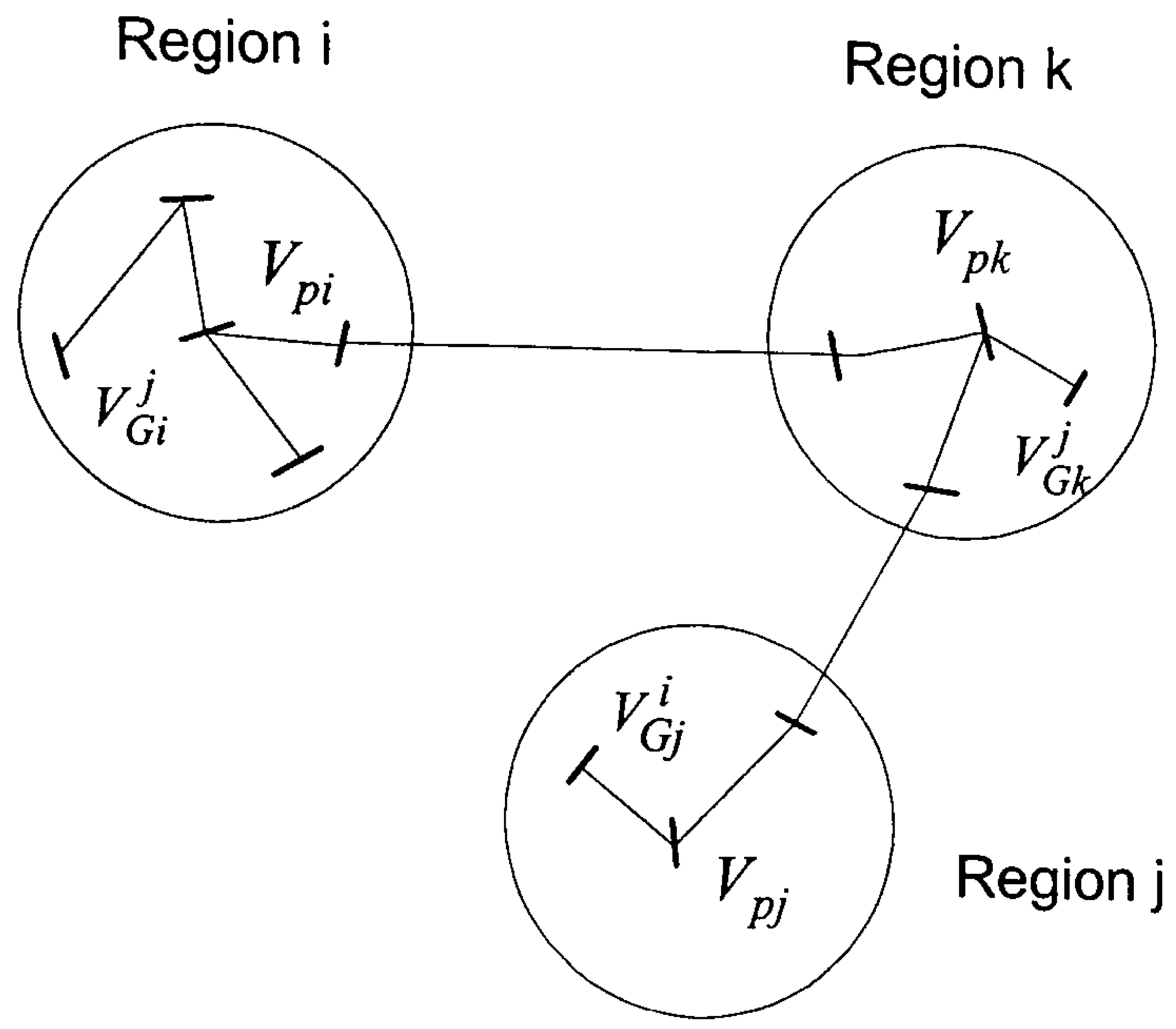

Figure 5.3.1-3 The model for a power system with decentralised regions

where,

V_{Pi}, V_{Pj}, V_{PK} are the voltage magnitudes at pilot bus in region *i* , *j*, *k* respectively;

5.3.2 System Descriptions

The system descriptions for the plant models used for the design of RVR and PQR are presented in this section.

1 System Descriptions for the RVR design

For a power system model shown in Figure 5.3.1-3, the system descriptions for the pilot bus voltage and voltage profile have already be derived in section 5.2.1, and rewritten here:

(1) Pilot buses

$$[\Delta V_P] = [S_{VG}^{P}][\Delta Q_G] + [S_{VL}^{P}][\Delta Q_L] \qquad (5.3.2\text{–}1)$$

(2) Voltage profile

$$\left[\Delta V_{\bar{P}}\right] = \left[S_{VG}^{\bar{P}}\right][\Delta Q_G] + \left[S_{VL}^{\bar{P}}\right][\Delta Q_L] \qquad (5.3.2\text{–}2)$$

It will be seen in Chapter 6 that the classic PI control design for the RVR is based on equation (5.3.2-2).

(3) Control power plants

By using the same linearised load flow equations (5.2.1–2) shown in section 5.2.1, the relationship between reactive generation and voltage at the control power plants can also be derived. By dividing the buses into control power plant group and load bus group (V_G, V_L), (Q_G, Q_L), the equations (5.2.1 -2) becomes

$$\begin{bmatrix} \Delta Q_G \\ \Delta Q_L \end{bmatrix} = \begin{bmatrix} J_{GG} & J_{GL} \\ J_{LG} & J_{LL} \end{bmatrix} \begin{bmatrix} \Delta V_G \\ \Delta V_L \end{bmatrix} \qquad (5.3.2\text{–}3)$$

Thus, the system description for the control power plants is obtained as

$$[\Delta Q_G] = [S^Q_{QV}][\Delta V_G] + [S^Q_{QL}][\Delta Q_L] \qquad (5.3.2\text{–}4)$$

where,

$[S^Q_{QV}] = [J_{GG}] - [J_{GL}][J_{LL}]^{-1}[J_{LG}]$,

$[S^Q_{QL}] = [J_{GL}][J_{LL}]^{-1}$.

$[J_{LL}]$ is assumed to be invertible.

From equation (5.3.2-4) and (5.3.2-2), another form of the system description for the pilot buses can be obtained:

$$[\Delta V_P] = [S^P_{VV}][\Delta V_G] + [S'^P_{VL}][\Delta Q_L] \qquad (5.3.2\text{–}5)$$

where,

$[S^P_{VV}] = [S^P_{VG}][S^Q_{QV}]$

$[S'^P_{VL}] = [S^P_{VG}][S^Q_{QL}] + [S^P_{VL}]$

The optimal control design for the RVR described in Chapter 7 is based on equations (5.3.2-4) and (5.3.2-5).

2 System Descriptions for the PQR design

Two different descriptions for the PQR design are given in this subsection, they are for the classic and optimal control designs for the PQR respectively.

(1) Description for the classic PI control design

Based on the power plant model shown in Figure 5.3.1-2, the system description for the PQR used by the classic control design in chapter 6 can be expressed as:

$$\left[\Delta V_{gi}^{j}\right]-\left[I_{col}\right]\Delta V_{Ri}^{j}=\left[A_{i}^{j}\right]\left[\Delta Q_{gi}^{j}\right] \qquad (5.3.2\text{–}6)$$

where,

$$\left[A_{i}^{j}\right]=\frac{1}{V_{Gi}^{j}(0)}\begin{bmatrix} X_{Ti}^{j}+X_{Ei}^{j} & X_{Ei}^{j} & \cdots & X_{Ei}^{j} \\ X_{Ei}^{j} & X_{Ti}^{j}+X_{Ei}^{j} & \cdots & X_{Ei}^{j} \\ \cdots & \cdots & & \cdots \\ X_{Ei}^{j} & & & X_{Ti}^{j}+X_{Ei}^{j} \end{bmatrix}$$

It is assumed here that,

$X_{Ti}^{j1}=X_{Ti}^{j2}=\ \ldots\ =X_{Ti}^{jN_{gi}^{j}}$.

(2) Description for the optimal control design

By regarding the power plant model shown in Figure 5.3.1-2 as a mini power system, the linearised load flow equations for the power plant can be written as:

$$\begin{bmatrix} \Delta Q_{gi}^{j} \\ \Delta Q_{Gi}^{j} \end{bmatrix}=\begin{bmatrix} L_{gg} & L_{gG} \\ L_{Gg} & L_{GG} \end{bmatrix}\begin{bmatrix} \Delta V_{gi}^{j} \\ \Delta V_{Gi}^{j} \end{bmatrix} \qquad (5.3.2\text{–}7)$$

Based on this equation, another set of system descriptions for the power plant can be derived:

$$\Delta V_{Gi}^{j}=\left[S_{VVi}^{Gj}\right]\left[\Delta V_{gi}^{j}\right]+\left[S_{VLi}^{Gj}\right]\Delta Q_{Gi}^{j} \qquad (5.3.2\text{–}8)$$

$$\Delta Q_{Gi}^{j}=\left[S_{QVi}^{Gj}\right]\left[\Delta V_{gi}^{j}\right] \qquad (5.3.2\text{–}9)$$

where,

$$\Delta Q_{Gi}^{j} = \sum_{k=1}^{N_{gi}^{j}} \Delta Q_{gi}^{jk}$$

$$\left[S_{VVi}^{Gj}\right] = -\left[L_{GG}\right]^{-1}\left[L_{Gg}\right],$$

$$\left[S_{VLi}^{Gj}\right] = -\left[L_{GG}\right]^{-1}.$$

$$\left[S_{QVi}^{Gj}\right] = (1 - \left[I_{row}\right]_{N_{gi}^{j}}\left[L_{gG}\right]\left[L_{GG}\right]^{-1})^{-1}\left[I_{row}\right]_{N_{gi}^{j}}\left[\left[L_{gg}\right] - \left[L_{gG}\right]\left[L_{GG}\right]^{-1}\left[L_{Gg}\right]\right],$$

It is assumed that the scalar $\left|1 - \left[I_{row}\right]_{N_{gi}^{j}}\left[L_{gG}\right]\left[L_{GG}\right]^{-1}\right| \neq 0$.

The equations (5.3.2-8) and (5.3.2-9) are the system descriptions for the PQR used by the optimal control design in the Chapter 7.

5.4 Design Criteria for a Secondary Voltage Control System

Based on the control principle and structure introduced in the section 5.2, different control methods can be used to design a secondary voltage control system. A successful control design should ensure the control system satisfying two main criteria: good stability and integration.

5.4.1 Control System Stability

1 Closed loop stability

As secondary voltage control systems are an on-line closed loop systems, essentially these systems should have good closed loop stability. The closed loop stability generally covers two types of stability: Steady State Stability and Robust Stability.

(1) Steady State Stability

Steady State Stability reflects the ability of a control system to copy with the small perturbation. To examine the steady-state stability, a small change model around an operating point is used to test whether all modes in the closed loop systems are asymptotically stable. In other words, all small perturbation will decay to zero if the system is steady state stable.

(2) Robust Stability

Robust Stability reflects the ability of a control system to copy with the system model perturbation. To study this stability, model perturbations or representations of model uncertainty are used to test whether the closed loop system remains asymptotically stable.

2 Closed loop performance

Another important property linked with this stability is the closed loop performance. It is about the time domain behaviour of a closed loop control system. This includes Reference Tracking, Disturbance Rejection and Robust Performance.

(1) Reference Tracking

Reference Tracking shows how well a control system to reach the designed performance. It can be examined by using the criteria of settle-time, rise-time, maximum overshoot and steady-state error, among others.

(2) Disturbance rejection

Disturbance rejection reflects the ability of a control system to reject the disturbances. It can be examined by using the criteria of maximum overshoot, steady-state error, settle-time, as well as interactions between responses.

(3) Robust Performance

Robust Performance can be examined by observing whether the desired performance is preserved if model is inaccurate or uncertain, and whether the desired performance preserved over a range of operating points.

3 The stability of a secondary voltage control system

As a secondary voltage control system has a multi-level control structure, its stability shall satisfy the following criteria:

(1) Good closed loop stability and performance at each control level including AVR, PQR, and RVR,

(2) Good global stability and performance of the whole control system.

5.4.2 Control System Integration

For the multi-level structure of secondary voltage control systems, the whole system needs to be integrated by certain signals between different control levels. This integration directly affects the success of a secondary voltage control. A good integration of such a multi-level control system should ensure:

1. The offsets with the integration signals between different control levels are sufficient small,
2. All the fast dynamic disturbances will be sufficiently rejected at lower control level, and the slow disturbances will be rejected at highest level to guarantee an efficient voltage control at pilot buses.

5.5 Discussions and Conclusions

The issues concerning the principle of secondary voltage control systems in a power system have been discussed in this chapter. This work is aimed to prepare a systematic and consistent theoretical environment for the design and analyses of secondary voltage systems by different control methods.

In this chapter, the pilot bus based control principle has been theoretically formularised for secondary voltage control. A three-level control has been defined as an essential structure for such a control system, and functions at each control level are clarified. Merits of the centralised, decentralised schemes for implementing a secondary voltage control are also discussed in his chapter. It is shown that the decentralise scheme has many advantages over the centralised one in terms of system reliability, installation and computer requirements.

All the control plants (power system components) involved in secondary voltage control have been systematically modelled and mathematically described. The system descriptions cover the pilot buses, decentralised regions and control power plants, which will be used for both classical and optimal control designs for the RVR and PQR.

The design criteria for a secondary voltage control system have also been discussed. It is concluded that a good closed loop stability and performance, as well as successful system integration are three essential criteria for a secondary voltage control system.

It shall be pointed out that one pilot bus per decentralised region is believed to be sufficient for a secondary voltage control. All the control designs and analyses presented in this thesis are based on this presumption. However, scheme with more than one pilot bus in a region is also feasible, and may be needed when some special system performance is required for secondary voltage control. The design and analysis for a control system with multiple pilot buses per region will have the same principle as for the control system with single pilot bus per region.

CHAPTER 6 THE SECONDARY VOLTAGE CONTROL SYSTEM BY A CLASSICAL CONTROL DESIGN

6.1 INTRODUCTION

Based on the control principle and structure discussed in chapter 5, the secondary voltage control system can be designed using two major control methods: the classical control and the optimal control. In this chapter, a classical PI control design is presented for the secondary voltage control. This includes the design details for the PQR, RVR and the integration of this multi-level control system. The closed loop stability and performance of this PI based control system are analysed by using the traditional frequency domain method. The voltage profile analysis is also performed to examine the efficiency of the secondary voltage control system. For the purpose of comparison, all the design and analysis include both the centralised and decentralised schemes. This system has been simulated the IEEE 39 bus power system, some simulation results are presented at the end of this chapter.

As a large number of common symbols and abbreviations are used in the design and analysis work in this and next chapter, they are centrally noted and defined in Appendix 2 of this thesis.

6.2 CONTROL DESIGN

A classical PI (Proportional and Integral) control design for the secondary voltage control is presented in this section. This design covers both centralised and decentralised control schemes.

6.2.1 Centralised Control Scheme

6.2.1.1 The Design of the Regional Voltage Regulator (RVR)

From the system descriptions given in the section 5.3.2 of chapter 5, it is known that

$$[\Delta V_P] = [S^P_{VG}][\Delta Q_G] + [S^P_{VL}][\Delta Q_L] \qquad (6.2.1\text{–}1)$$

Where,

$[\Delta V_P]$ is the voltage variation at all the pilot buses in a power system,

$[\Delta Q_G]$ is the reactive power generation variation at all the control power plants in a power system,

$[\Delta Q_L]$ is the reactive power demand variation at all the load buses in a power system,

$[S^P_{VG}]$ and $[S^P_{VL}]$ are sensitivity matrices.

By using the control law that all the control power plants having the same participation to a reactive power demand change in each region, there is

$$\Delta q^1_{Gi} = \Delta q^2_{Gi} \ldots = \Delta q^j_{Gi} \ldots = \Delta q_{Ri} \qquad (6.2.1\text{–}2)$$

Where,

Δq^j_{Gi} is the necessary reactive power generation increment in percentage with rated capacity at control power plant j in region i;

Δq_{Ri} is the necessary reactive power generation increment in percentage with respect to the rated capacity in region i;

Considering

$$[\Delta Q_G] = [\Lambda_{G\lim}][\Delta q_G]$$

$$[\Lambda_{G\lim}] = [D_{Gg}][\Lambda_{g\lim}][D_{Gg}]^T$$

$$[\Delta q_G] = [D_{GR}][\Delta q_R]$$

Equation (6.2.1-1) can be re-written as:

$$[\Delta V_P] = [U^P][\Delta q_R] + [S^P_{VL}][\Delta Q_L] \qquad (6.2.1\text{–}3)$$

$$[U^P] = [S^P_{VG}][D_{Gg}][\Lambda_{glim}][D_{Gg}]^T[D_{GR}] \qquad (6.2.1\text{–}4)$$

where,

$$[\Lambda_{glim}] = \text{diag}\left\{Q^{11}_{glimi}, Q^{12}_{glimi}, \ldots, Q^{jk}_{glimi}, \ldots, Q^{N_{GZ}N^{N_{GZ}}_{gZ}}_{glimZ}\right\}.$$

Q^{jk}_{glimi} is rated reactive power generation capacity of generator k at control power plant j in region i;

$[D_{Gg}] = \text{diag}\left\{[I_{row}]_{N^1_{g1}}, [I_{row}]_{N^2_{g1}}, \ldots, [I_{row}]_{N^j_{gi}}, \ldots, [I_{row}]_{N^{N_{GZ}}_{gZ}}\right\}$ is **structure matrix** to represent the structure between all the control power plants and all the control generators in a power system,

$[I_{row}]_n$ is the 1 by n unit row matrix;

As there is only one pilot bus in each region, $[U^P]$ is a square matrix. And assuming $[U^P]^{-1}$ exist,

$$[\Delta q_R] = [U^P]^{-1}[\Delta V_P] - [U^P]^{-1}[S^P_{VL}][\Delta Q_L] \qquad (6.2.1\text{–}5)$$

Based on equations (6.2.1-1)-(6.2.1-5), the RVR can be designed to have following structure:

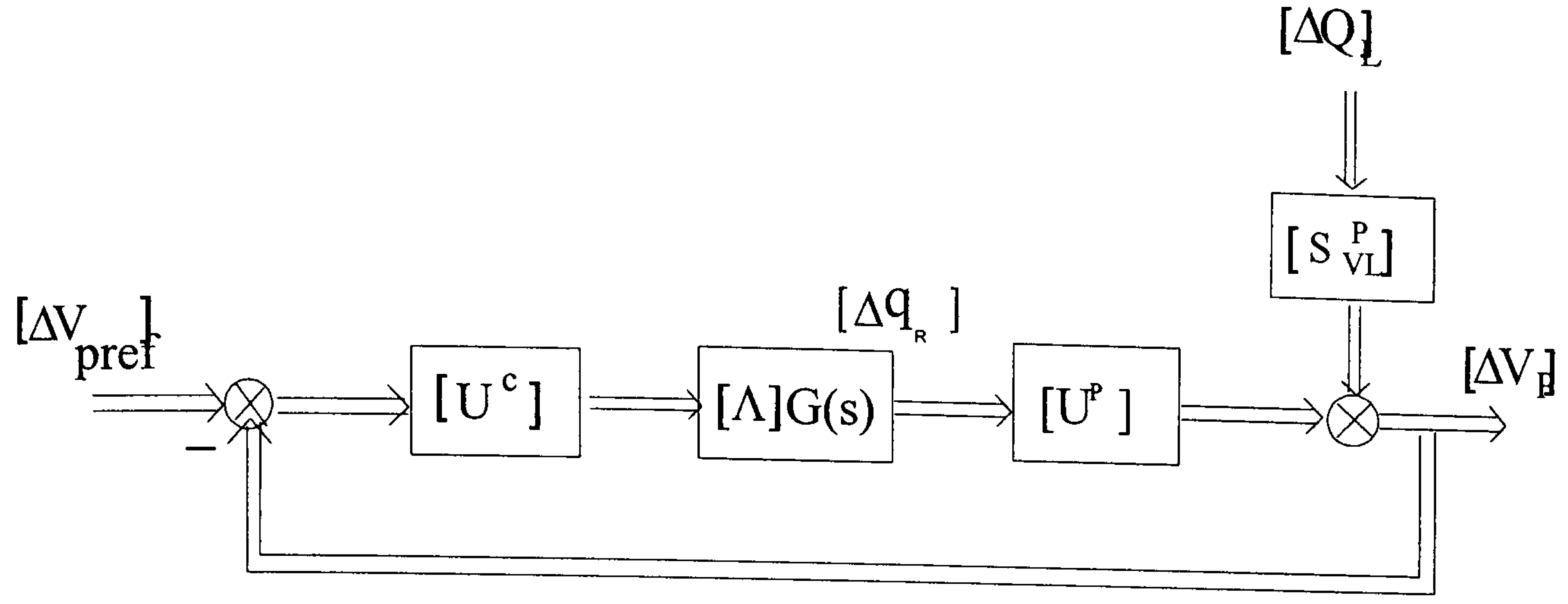

Figure 6.2.1-1 Integral Control for RVR

the RVR control law is

$$[\Delta q_R] = [U^C][\Lambda]G(s)\left([\Delta V_{pref}] - [\Delta V_P]\right) \qquad (6.2.1\text{–}6)$$

Where,

$[\Delta V_{Pref}]$ is the vector of references for all the $[\Delta V_P]$ within a power system,

G(s) is the RVR control method, to which two classical control methods can be applied, PI control: $G(s) = K_P + \frac{K_I}{s}$, or I control: $G(s) = \frac{1}{T_R s}$.

$[U^C] = [U^P]^{-1}$ is the control law matrix. (Assuming $[U^P]$ is invertible.)

6.2.1.2 The Design of Power Plant Reactive Power Regulator (PQR)

From the system description for PQR in the section 5.3.2 of chapter 5, there is:

$$[\Delta V_{gi}^j] - [I_{col}]\Delta V_{Ri}^j = [A_i^j][\Delta Q_{gi}^j] \qquad (6.2.1\text{–}7)$$

Then,

$$[\Delta Q_{gi}^j] = [A_i^j]^{-1}[\Delta V_{gi}^j] - [A_i^j]^{-1}\Delta V_{Ri}^j \qquad (6.2.1\text{–}8)$$

Where,

ΔV_{gi}^j is the vector of voltage variation at all the control generator terminals within control power plant *j* in region *i*,

ΔQ_{gi}^j is the vector of reactive generation of all the control generators within control power plant *j* in region *i*,

$[I_{col}]_n$ is n by 1 unit column matrix,

$[A_i^j]$ is the structure matrix for control power plant j in region i. It is made of the equivalent reactance for all the control generators within the control power plant.

Based on the equations (6.2.1-7) and (6.2.1-8), the PQR can be designed using the integral control as shown in Figure 6.2.1-1.

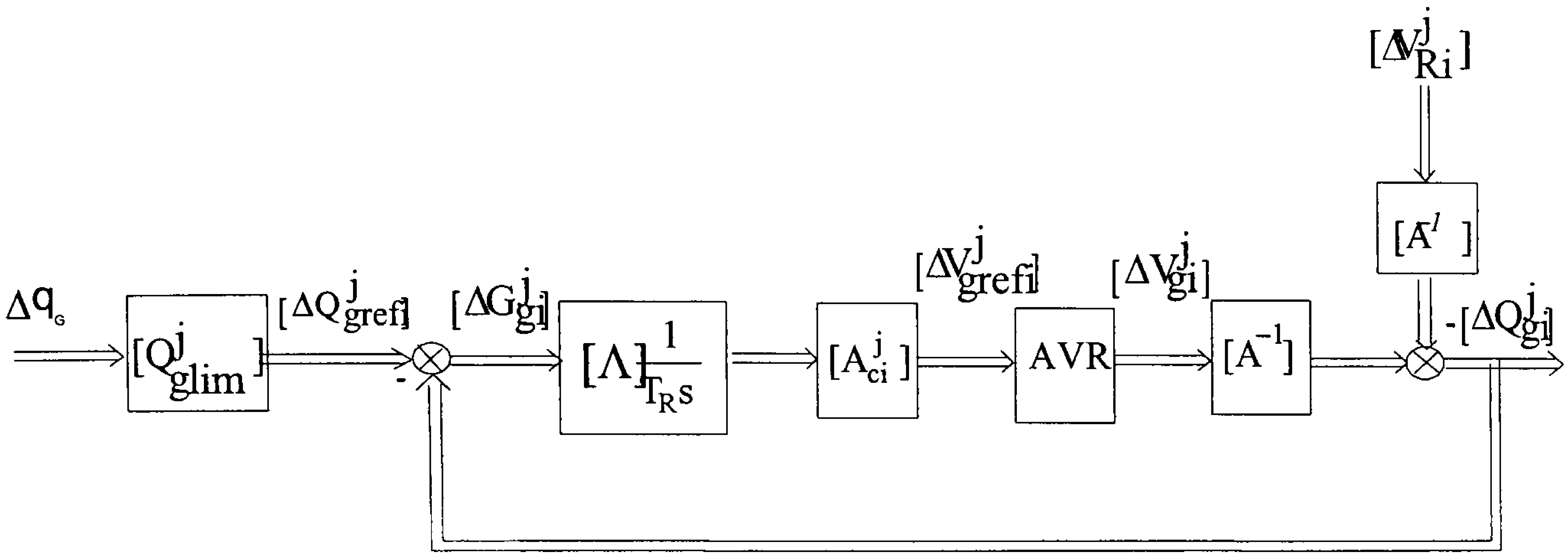

Figure 6.2.1-2 The PQR by the integral control design

The PQR control law is:

$$\left[\Delta V_{grefi}^{j}\right]=\left[A_{ci}^{j}\right]\left[\Lambda\right]\frac{1}{T_Q s}\left(\left[\Delta Q_{grefi}^{j}\right]-\left[\Delta Q_{gi}^{j}\right]\right) \qquad (6.2.1\text{–}9)$$

Where,

$$\left[\Delta Q_{grefi}^{j}\right]=\left[Q_{g\,lim\,i}^{j}\right]\Delta q_{Gi}^{j}$$

$$\left[Q_{g\,lim\,i}^{j}\right]=\left[\Lambda_{g\,lim\,i}^{j}\right]\left[I_{col}\right]_{N_{gi}^{j}},$$

$[V_{gref\,i}^{j}]$ is the vector of references for the terminal voltages of all the control generators $\left[v_{gi}^{j}\right]$ within control power plant j in region i,

$\left[Q_{gref\,i}^{j}\right]$ is the vector of the references for the reactive generations of all the control generators $\left[Q_{gi}^{j}\right]$ within control power plant j in region i,

$[A_{ci}^j]= [A_i^j]^{-1}$ (Assuming $[A_i^j]$ is invertible)

T_Q is the desired time constant for PQR.

6.2.2 Decentralised Control Scheme

The main difference between the centralised and decentralised schemes lies at the RVR level. Technically the decentralised scheme requires a diagonal control law matrix $[U^C]$, so that the secondary voltage control system can be decentralised into several non-interfering regional control systems. These regional control systems can be implemented and used independently in each region. The decentralisation and pilot buses selection are supposed to ensure that the sensitivity matrix $[U^P]$ is a dominantly diagonal matrix. Thus, the $[U^C]$ will be diagonal dominant, and can be simplified into a diagonal matrix.

The decentralised scheme will obviously cause further model mismatch. It can be treated as a special case of model mismatch in the centralised scheme.

The following two methods can be used to produce a diagonal control law matrix $[U^C]$ for the RVRs:

1. Optimisation method

The following optimisation algorithm can be formalised to produce a diagonal $[U^C]$:

$$\text{Min } J(U^c_{ii}) = \sum_{i=1}^{Z} \left\{ (W_{ii} - 1)^2 + \sum_{j \neq i} (W_{ij})^2 \right\} \qquad (6.2.2\text{–}1)$$

where

$[W] = [U^C][U^P]$,

W_{ij} is the (i-j)th entry of $[W]$,

Z is the total number of decentralised regions in a power system.

As this method uses $[U^P]$ which requires the information of the whole power system, the elements of $[U^C]$ need to be determined at the tertiary level and sent to each decentralised region.

2. By the load flow equation

By regarding the load flow on the circuits between decentralised regions as power injections, the load flow equations for a decentralised region (i) can be obtained. From this regional load flow equations (say region i in a power system), there is

$$\begin{bmatrix} \Delta V_{Pi} \\ \Delta V_{\bar{P}i} \end{bmatrix} = \begin{bmatrix} S_{VG}^{Pi} & S_{VL}^{Pi} \\ S_{VG}^{\bar{P}i} & S_{VL}^{\bar{P}i} \end{bmatrix} \begin{bmatrix} \Delta Q_{Gi} \\ \Delta Q_{Li} \end{bmatrix}$$

then,

$$\Delta V_{Pi} = \left[S_{VG}^{Pi}\right]\left[\Delta Q_{Gi}\right] + \left[S_{VL}^{Pi}\right]\left[\Delta Q_{Li}\right]$$

Considering

$$\left[\Delta Q_{Gi}\right] = \left[\Lambda_{G\,lim\,i}\right]\left[\Delta q_{Gi}\right]$$

$$\left[\Delta q_{Gi}\right] = \left[I_{col}\right]_{N_{Gi}} \Delta q_i$$

Then,

$$\Delta V_{Pi} = U_i^P \Delta q + \left[S_{VL}^{Pi}\right]\left[\Delta Q_{Li}\right] \quad (6.2.2\text{–}2)$$

where,

$$U_i^P = \left[S_{VG}^{Pi}\right]\left[\Lambda_{G\,lim\,i}\right]\left[I_{col}\right]_{N_{Gi}}.$$

Thus,

$$U_{ii}^C = 1/U_i^P \qquad (6.2.2\text{–}3)$$

U^c_{ii} is the ii-th element in the diagonal matrix $[U^c]$.

This method requires the measurement of load flow on the circuits between the regions.

6.2.3 Global Structure of a Secondary Voltage Control System

Integrating the above PQR and the RVR together, a secondary voltage control system can be established. The global block diagram of this control system is shown in Figure 6.2.3-1.

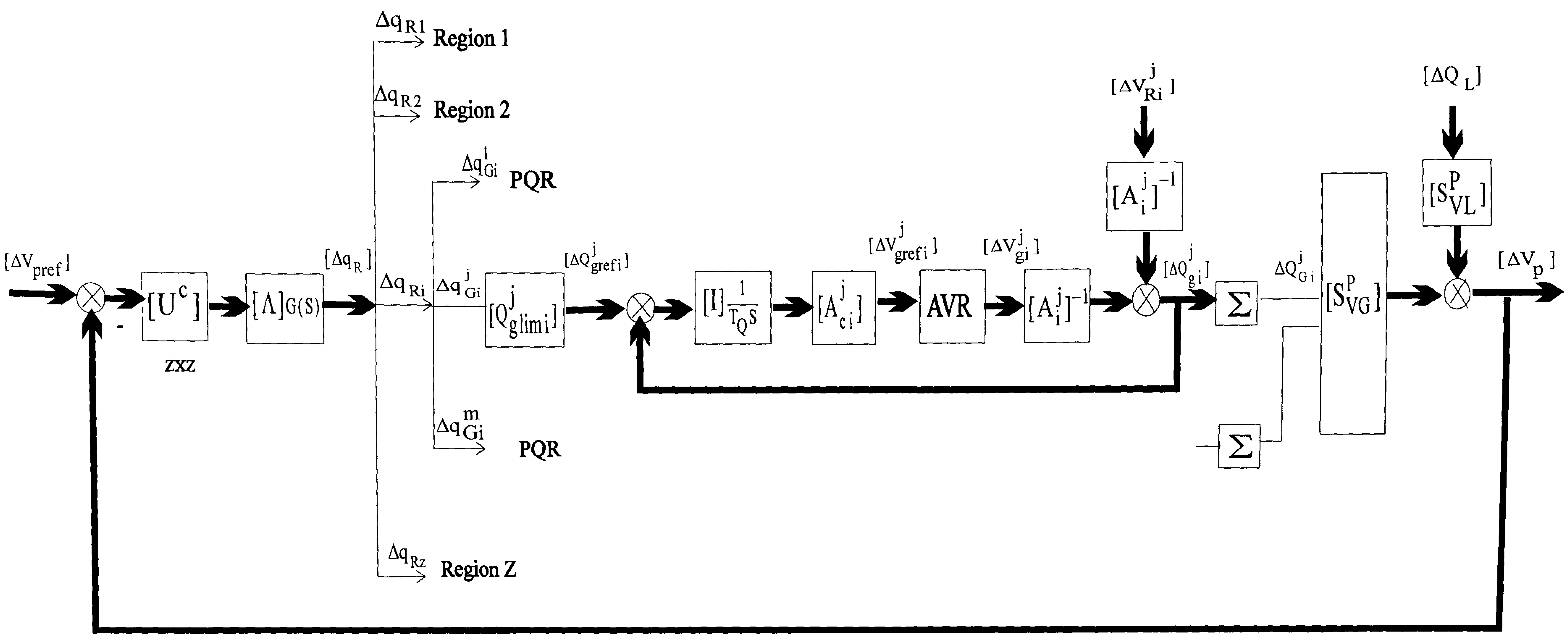

Figure 6.2.3-1 **Global structure of the secondary voltage control system by a classic control design**

6.3 STABILITY ANALYSIS

This section deals with the stability analysis of the secondary voltage control system by the PI control design. The traditional frequency domain(s) method is used to examine the closed loop stability and performance of the control system. The analysis is divided into general case and special cases. The general case is concerning with the system stability with PQR/RVR model mismatches and PQR dynamics; while the special case study is to explore some special properties of the control system under certain simplifications.

6.3.1 The Control System with Centralised Scheme

6.3.1.1 General case (model mismatch + PQR dynamics)

The model mismatches in the PQR and RVR can be mathematically described as

$$\left[A^{j}_{Ci}\right]\left[A^{j}_{i}\right]^{-1} \neq [I]_{N^{j}_{gi}},$$

$$\left[U^{P}\right]\left[U^{c}\right] \neq [I]_{Z}$$

1. The PQR Dynamics

(1) Transfer Function

Assuming all the channels have the same time constant T_Q in the PQRs, the control law equation (6.2.1-9) becomes:

$$\left[\Delta V^{j}_{grefi}\right] = \left[A^{j}_{ci}\right][I]_{N^{j}_{gi}} \frac{1}{T_Q s}\left(\left[\Delta Q^{j}_{grefi}\right] - \left[\Delta Q^{j}_{gi}\right]\right)$$

From the system description for the PQR in chapter 5, it is known

$$\left[\Delta Q^{j}_{gi}\right] = \left[A^{j}_{i}\right]^{-1}\left[\Delta V^{j}_{grefi}\right] - \left[A^{j}_{i}\right]^{-1}\Delta V^{j}_{Ri}$$

Therefore,

$$\begin{aligned}\left[\Delta Q^{j}_{gi}\right] = &\left[sT_Q[I]_{N^{j}_{gi}} + \left[A^{j}_{Ci}\right]\left[A^{j}_{i}\right]^{-1}\right]^{-1}\left[A^{j}_{Ci}\right]\left[A^{j}_{i}\right]^{-1}\left[\Delta Q^{j}_{grefi}\right] \\ &-\left[sT_Q[I]_{N^{j}_{gi}} + \left[A^{j}_{Ci}\right]\left[A^{j}_{i}\right]^{-1}\right]^{-1} sT_Q\left[A^{j}_{i}\right]^{-1}\left[\Delta V^{j}_{Ri}\right]\end{aligned} \qquad (6.3.1\text{-}1)$$

The closed loop transfer function for the PQR in the control power plant j of region i can be obtained from equation (6.3.1-1):

$H_R(s) = \left[sT_Q[I]_{N^j_{gi}} + [A^j_{Ci}][A^j_i]^{-1} \right]^{-1} [A^j_{Ci}][A^j_i]^{-1}$ is the transfer function for reference tracking; and

$H_D(s) = -\left[sT_Q[I]_{N^j_{gi}} + [A^j_{Ci}][A^j_i]^{-1} \right]^{-1} sT_Q[A^j_i]^{-1}$ is the transfer function for disturbance.

Let $[A^j_{Ci}][A^j_i]^{-1} = [T^i_i][\Lambda^j_i][T^i_i]^{-1}$

where,

$[\Lambda^j_i] = \text{diag}\left\{ \lambda^{j1}_i, \lambda^{j2}_i, \ldots, \lambda^{jN^j_{gi}}_i \right\}$ is the eigenvalue matrix of $[A^j_{Ci}][A^j_i]^{-1}$.

Thus, the equation (6.3.1-1) can be rewritten as:

$$[\Delta Q^j_{gi}] = [T^j_i][\Phi^j_i][T^j_i]^{-1}[\Delta Q^j_{gref\,i}] + [d^j_i(s)] \quad (6.3.1\text{–}2)$$

Where,

$$[\Phi^j_i] = \text{diag}\left\{ \frac{\lambda^{j1}_i}{sT_Q + \lambda^{j1}_i}, \frac{\lambda^{j2}_i}{sT_Q + \lambda^{j2}_i}, \ldots, \frac{\lambda^{jN^j_{gi}}_i}{sT_Q + \lambda^{jN^j_{gi}}_i} \right\};$$

$$[d^j_i(s)] = \left[sT_Q[I]_{N^j_{gi}} + [A^j_i]^{-1}[A^j_{Ci}] \right]^{-1} sT_Q[A^j_i]^{-1}[\Delta V^j_{Ri}].$$

(2) Discussion

Some properties about the PQR can be examined at this point:

(i) The PQR poles will occur from

$$\left[sT_Q[I]_{N^j_{gi}} + [A^j_i]^{-1}[A^j_{Ci}] \right] = T\left[sT_Q[I]_{N^j_{gi}} + [\Lambda^j_i] \right] T^{-1} = [0]$$

Thus, the closed loop poles for the PQR will be:

$$s_i = -\frac{\lambda^{j1}_i}{T_Q}, \qquad i = 1, 2, \ldots, N^j_{gi}.$$

Where,

N^j_{gi} is the number of control generators in control power plant j in region i.

As the eigenvalues might be complex (in conjugate pairs), there are possible oscillation and instability with the PQR.

(ii) Assuming the mismatch does not cause closed loop instability, then by Laplace transformation theory (applying a step signal u(t)=1, t>0)

$$\lim_{t\to\infty} F_R^{-1}(t) = \lim_{s\to 0} sF_R(s) = \lim_{s\to 0} sH_R(s)u(s)$$
$$= \lim_{s\to 0} s\left[sT_Q[I]_{N^j_{gi}} + [A^j_i]^{-1}[A^j_{Ci}]\right]^{-1}[A^j_i]^{-1}[A^j_{Ci}]\frac{1}{s} = [I]_{N^j_{gi}}$$

$$\lim_{t\to\infty} F_D^{-1}(t) = \lim_{s\to 0} sF_D(s) = \lim_{s\to 0} sH_D(s)u(s)$$
$$= \lim_{s\to 0} s\left[sT_Q[I]_{N^j_{gi}} + [A^j_i]^{-1}[A^j_{Ci}]\right]^{-1} sT_Q[A^j_i]^{-1}\frac{1}{s} = [0]_{N^j_{gi}}$$

Perfect steady state reference tracking and disturbance rejection occur.

2. The RVR/Global System

(1) Transfer function

Recalling the system description for a power system in chapter 5:

$$[\Delta V_P] = [S^P_{VG}][\Delta Q_G] + [S^P_{VL}][\Delta Q_L]$$

Based on this equation and equation (6.3.1-2), the PQRs' transfer function for the whole power system can be written as:

$$[\Delta Q_g] = [\Lambda_{T\Phi T^{-1}}][\Delta Q_{gref}] + [d(s)]$$

where,

$$[\Lambda_{T\Phi T^{-1}}] = \mathrm{diag}\left\{[T^1_1][\Phi^1_1][T^1_1]^{-1}, [T^2_1][\Phi^2_1][T^2_1]^{-1}, \ldots, [T^{N_{GZ}}_z][\Phi^{N_{GZ}}_z][T^{N_{GZ}}_z]^{-1}\right\}$$

Considering:

$$[\Delta Q_G] = [D_{Gg}][\Delta Q_g]$$

$$[\Delta Q_{gref}] = [\Lambda_{g\lim}][D_{Gg}]^T[\Delta q_G]$$

$$[\Delta q_G] = [D_{GR}][\Delta q_R]$$

Direct substitution yields:

$$[\Delta V_P] = [S^P_{VG}][D_{Gg}][\Lambda_{T\Phi T^{-1}}][\Lambda_{g\lim}][D_{Gg}]^T[D_{GR}][\Delta q_R] + [\tilde{d}(s)] \qquad (6.3.1\text{–}3)$$

where,

$$[\tilde{d}(s)] = [S^P_{VG}][D_{Gg}][d(s)] + [S^P_{VL}][\Delta Q_L].$$

Recalling equation (6.2.1-4),

$$[U^P] = [S^P_{VG}][D_{Gg}][\Lambda_{g\lim}][D_{Gg}]^T[D_{GR}]$$

and,

$$[D_{Gg}]^T[D_{Gg}] = [I]_{N_g}$$

$$[D_{GR}][D_{GR}]^T = [I]_{N_G}$$

$$[\Delta V_P] = [U^P][D_{GR}]^T[D_{Gg}][\Lambda_{g\lim}]^{-1}[\Lambda_{T\Phi T^{-1}}][\Lambda_{g\lim}][D_{Gg}]^T[D_{GR}][\Delta q_R] + [\tilde{d}(s)]$$

Introducing

$$[\alpha^j_i] = [I_{row}]_{N^j_{gi}}[\Lambda^j_{g\lim i}]^{-1}[T^j_i]$$

$$[\beta^j_i] = [T^j_i]^{-1}[\Lambda^j_{g\lim i}][I_{col}]_{N^j_{gi}}$$

then,

$$[\Delta V_P] = [U^P][\Lambda_R][\Delta q_R] + [\tilde{d}(s)] \qquad (6.3.1\text{–}4)$$

where,

$$[\Lambda_R] = \mathrm{diag}\left\{\frac{N_1(s)}{D_1(s)}, \frac{N_2(s)}{D_2(s)}, \ldots, \frac{N_Z(s)}{D_Z(s)}\right\},$$

$$N_i(s) = \sum_{e=1}^{N_{Gi}}\sum_{f=1}^{N^e_{gi}} \alpha^{ef}_i \lambda^{ef}_i \beta^{ef}_i \prod_{j=1}^{N_{Gi}}\prod_{\substack{k=1\\k\neq f}}^{N^j_{gi}} (T_Q s + \lambda^{jk}_i),$$

$$D_i(s) = \prod_{j=1}^{N_{Gi}}\prod_{k=1}^{N^j_{gi}} (T_Q s + \lambda^{jk}_i),$$

$$\mathrm{Deg}(D_i(s)) > \mathrm{Deg}(N_i(s)).$$

Rewriting

$$[\Lambda_R] = [\Lambda_N][\Lambda_D]^{-1}$$

where,

$[\Lambda_N] = \mathrm{diag}\{N_1(s), N_2(s), \ldots, N_Z(s)\}$,

$[\Lambda_D] = \mathrm{diag}\{D_1(s), D_2(s), \ldots, D_Z(s)\}$.

Then, equation (6.3.1-4) can also be re- written as:

$$[\Delta V_P] = [U^P][\Lambda_N][\Lambda_D]^{-1}[\Delta q_R] + [\tilde{d}(s)] \qquad (6.3.1\text{–}5)$$

Assuming all the RVRs have the same time constant T_R, the RVR control Law equation (6.2.1-6) becomes:

$$[\Delta q_R] = [U^C][I]_Z\, G(s)\left([\Delta V_{pref}] - [\Delta V_P]\right) \qquad (6.3.1\text{–}6)$$

From equation (6.3.1-4) and equation (6.3.1-6),

$$\begin{aligned}[\Delta V_P] = {} & \left[[I]_Z + [U^P][\Lambda_R][U^C]G(s)\right]^{-1}[U^P][\Lambda_R][U^C]G(s)[\Delta V_{P\,ref}] \\ & + \left[[I]_Z + [U^P][\Lambda_R][U^C]G(s)\right]^{-1}[\tilde{d}(s)]\end{aligned} \qquad (6.3.1\text{–}7)$$

Thus, the RVR transfer function between $[\Delta V_P]$ and $[\Delta V_{Pref}]$ (for reference tracking):

$$H_{PP}(s) = \left[[I]_Z + [U^P][\Lambda_R][U^C]G(s)\right]^{-1}[U^P][\Lambda_R][U^C]G(s) \qquad (6.3.1\text{–}8)$$

The RVR transfer function between $[\Delta V_P]$ and $[\tilde{d}(s)]$ (for disturbance):

$$H_{PD}(s) = \left[[I]_Z + [U^P][\Lambda_R][U^C]G(s)\right]^{-1} \qquad (6.3.1\text{–}9)$$

For the PI control: $G(s) = K_P + \dfrac{K_I}{s}$,

$$H_{PP}(s) = \left[s[I]_Z + [U^P][\Lambda_R][U^C](K_P s + K_I)\right]^{-1}[U^P][\Lambda_R][U^C](K_P s + K_I) \qquad (6.3.1\text{–}10)$$

$$H_{PD}(s)=\left[s[I]_Z+\left[U^P\right]\left[\Lambda_R\right]\left[U^C\right](K_P s+K_I)\right]^{-1} s \tag{6.3.1–11}$$

For the pure I control: $G(S) = \dfrac{1}{T_R s}$, ($K_P=0$, $K_I=1/T_R$)

$$H_{PP}(s)=\left[T_R s[I]_Z+\left[U^P\right]\left[\Lambda_R\right]\left[U^C\right]\right]^{-1}\left[U^P\right]\left[\Lambda_R\right]\left[U^C\right] \tag{6.3.1–12}$$

$$H_{PD}(s)=\left[T_R s[I]_Z+\left[U^P\right]\left[\Lambda_R\right]\left[U^C\right]\right]^{-1} T_R s \tag{6.3.1–13}$$

(2) Discussion

By using these transfer functions, some general properties about the RVR/global control system can be identified at this stage:

(i) The global stability of this centralised secondary voltage control system is related to the RVR control design G(s) and model mismatch $\left[A_{Ci}^j\right]\left[A_i^j\right]$, $[U^P][U^C]$.

(ii) The stability is also influenced by the PQR dynamics through $[\Lambda_R]$.

(iii) It is difficult to derive the poles/zeros polynomial matrix to generalise the stability of this control system for the general case.

(iv) Provided the closed loop is stable, the DC gain is unity for the reference tracking, and zero for the disturbance for both PI and pure I control designs, this can be examined by

$$\lim_{s\to 0} sH_{PP}(s)\frac{1}{s}=[I]_Z,\ \lim_{S\to 0} sH_{PD}(s)\frac{1}{s}=[0]_Z$$

6.3.1.2 Special Cases

In this subsection, the stability of this centralised secondary voltage control system is examined under two simplified conditions: neglecting PQR dynamics and Perfect Model Match.

1. Neglecting PQR dynamics

(1) Transfer Function

Under this simplification:

$$\left[A_{Ci}^{j}\right]\left[A_{i}^{j}\right]^{-1}=\left[T_{i}^{j}\right]\left[\Phi_{i}^{j}\right]\left[T_{i}^{j}\right]=\left[I\right]_{N_{gi}^{j}},\ i=1,2,\ldots,\quad N_{Gi}$$

Where,

N_{Gi} is the number of control power plant in region i.

Considering

$$\left[D_{Gg}\right]\left[D_{Gg}\right]^{T}=\mathrm{diag}\{N_{g1}^{1},N_{g1}^{2},\ldots,N_{g1}^{N_{G1}},\ldots,N_{gZ}^{N_{GZ}}\}$$

then,

$$\left[\Lambda_{R}\right]=\mathrm{diag}\{N_{g1},N_{g2},\ldots,N_{gi},\ldots,N_{gZ}\}=\left[\Lambda_{N_g}\right]$$

Thus, the RVR transfer functions become:

<u>For the PI control</u>: $G(s)=K_P+\dfrac{K_I}{s}$,

$$\begin{aligned}H_{PP}(s)&=\left[s[I]_Z+\left[U^P\right]\left[\Lambda_{N_g}\right]\left[U^C\right](K_Ps+K_I)\right]^{-1}(K_Ps+K_I)\left[U^P\right]\left[\Lambda_{N_g}\right]\left[U^C\right]\\&=[\Gamma]\left[(([\Lambda_\sigma]K_P+[I]_Z)s+K_I[\Lambda_\sigma]\right]^{-1}(K_Ps+K_I)[\Lambda_\sigma][\Gamma]^{-1}\\&=[\Gamma]\varepsilon[\Gamma]^{-1}\end{aligned}$$

(6.3.1–14)

$$\begin{aligned}H_{PD}(s)&=\left[s[I]_Z+\left[U^P\right]\left[\Lambda_{N_g}\right]\left[U^C\right](K_Ps+K_I)\right]^{-1}s\\&=[\Gamma]\left[(([\Lambda_\sigma]K_P+[I]_Z)s+K_I[\Lambda_\sigma]\right]^{-1}s[\Gamma]^{-1}\\&=[\Gamma]\eta[\Gamma]^{-1}\end{aligned}\qquad(6.3.1\text{–}15)$$

where,

$\left[U^P\right]\left[\Lambda_{N_g}\right]\left[U^C\right]=[\Gamma][\Lambda_\sigma][\Gamma]^{-1}$,

$\left[\Lambda_\sigma\right]=\mathrm{diag}\{\sigma_1,\sigma_2,\ldots,\sigma_Z\}$ is the eigenvalue matrix of $\left[U^P\right]\left[\Lambda_{N_g}\right]\left[U^C\right]$.

$$\varepsilon = \mathrm{diag}\{\frac{(K_P s + K_I)\sigma_1}{(\sigma_1 K_P + 1)s + K_I\sigma_1}, \frac{(K_P s + K_I)\sigma_2}{(\sigma_2 K_P + 1)s + K_I\sigma_2}, \ldots\ldots, \frac{(K_P s + K_I)\sigma_Z}{(\sigma_Z K_P + 1)s + K_I\sigma_Z}\}$$

$$\eta = \mathrm{diag}\{\frac{s}{(\sigma_1 K_P + 1)s + K_I\sigma_1}, \frac{s}{(\sigma_2 K_P + 1)s + K_I\sigma_2}, \ldots\ldots, \frac{s}{(\sigma_Z K_P + 1)s + K_I\sigma_Z}\}.$$

The poles polynomial matrix for both H_{PP} (s) and $H_{PD}(s)$ is

$$\left[((\left[\Lambda_\sigma\right]K_P + [I]_Z)s + \left[\Lambda_\sigma\right]K_I)\right]$$

The zeros polynomial matrix for $H_{PP}(s)$ is

$$[I]_Z(K_P s + K_I)$$

The zeros polynomial matrix for $H_{PD}(s)$ is

$[I]_Z s$.

<u>For the pure I control</u>: $G(s) = \dfrac{1}{T_R s}$, (K_P=0, K_I=1/T_R)

$$\begin{aligned} H_{PP}(s) &= [\Gamma]\left[T_R s[I]_Z + \left[\Lambda_\sigma\right]\right]^{-1}\left[\Lambda_\sigma\right][\Gamma]^{-1} \\ &= [\Gamma]\varepsilon'[\Gamma]^{-1} \end{aligned} \qquad (6.3.1\text{–}16)$$

$$\begin{aligned} H_{PD}(s) &= [\Gamma]\left[T_R s[I]_Z + \left[\Lambda_\sigma\right]\right]^{-1} T_R s[\Gamma]^{-1} \\ &= [\Gamma]\eta'[\Gamma]^{-1} \end{aligned} \qquad (6.3.1\text{–}17)$$

where,

$$\varepsilon' = \mathrm{diag}\{\frac{\sigma_1}{T_R s + \sigma_1}, \frac{\sigma_2}{T_R s + \sigma_2}, \ldots, \frac{\sigma_Z}{T_R s + \sigma_Z}\}$$

$$\eta' = \mathrm{diag}\{\frac{T_R s}{T_R s + \sigma_1}, \frac{T_R s}{T_R s + \sigma_2}, \ldots\ldots \frac{T_R s}{T_R s + \sigma_Z}\}$$

The poles polynomial matrix for both $H_{pp}(s)$ and $H_{pp}(s)$ is

$$\left[(T_R s[I]_Z + \left[\Lambda_\sigma\right])\right]$$

The zeros polynomial matrix for $H_{PP}(s)$ is $[I]_N$

The zeros polynomial matrix for $H_{PD}(s)$ is $[I]_Z T_R$ s.

(2) Discussion

(i) By neglecting PQR dynamics, it can be seen that the global stability of this secondary control system is not only determined by the control parameters K_P and K_I , but also related to the RVR model mismatch and the number of control generators in each decentralised region.

(ii) As the eigenvalues of $\left[U^P\right]\left[\Lambda_{N_g}\right]\left[U^C\right]$ might be complex, potential oscillation is possible with the system outputs.

(iii) Through the matrices $[\Gamma]$ and $[\Gamma]^{-1}$, it is known that the interactions between RVRs are related to the RVR model mismatch and number of control generators in each region. From these matrices, it can also be know that the instability in one RVR could cause the instability in other RVRs as well as the global control system.

(iv) The above analysis clearly shows that PI control provides with the flexible means for improving the control system properties by the selecting the controller parameters, while the pure I control does not possess this advantage when the time constant of control system is fixed.

(v) Other properties remain the same as the general case.

2. Perfect model match

Under this simplification, the model match for both PQR and RVR are assumed to be perfect:

$$\left[U^P\right]\left[U^C\right]=[I]_Z,\ \left[A^j_{Ci}\right]\left[A^j_i\right]^{-1}=[I]_{N^j_{gi}}$$

(1) Incorporating PQR dynamics

(i) Transfer Function

Based on the simplification, there are:

$$\left[\Lambda_N\right]=\mathrm{diag}\left\{(T_Q s+1)^{(N_{g1}-1)}N_{g1},(T_Q s+1)^{(N_{g2}-1)}N_{g2},\ldots,(T_Q s+1)^{(N_{gZ}-1)}N_{gZ}\right\},$$

$$\left[\Lambda_D\right]=\mathrm{diag}\left\{(T_Q s+1)^{N_{g1}},(T_Q s+1)^{N_{g2}},\ldots,(T_Q s+1)^{N_{gZ}}\right\}$$

and,

$$\left[\Lambda_R\right]=\mathrm{diag}\{N_{g1},N_{g2},\ldots,N_{gi},\ldots,N_{gZ}\}(T_Q s+1)^{-1}=\left[\Lambda_{N_g}\right](T_Q s+1)^{-1}$$

Thus, the global transfer functions for the secondary voltage control system can be obtained from equation (6.3.1-10) - (6.3.1-13) above:

<u>For the PI control</u>:

$$H_{PP}(s)=\left[s(T_Q s+1)[I]_Z+\left[U^P\right]\left[\Lambda_{N_g}\right]\left[U^C\right](K_P s+K_I)\right]^{-1}(K_P s+K_I)\left[U^P\right]\left[\Lambda_{N_g}\right]\left[U^C\right]$$

$$H_{PD}(s)=\left[s(T_Q s+1)[I]_Z+\left[U^P\right]\left[\Lambda_{N_g}\right]\left[U^C\right](K_P s+K_I)\right]^{-1}s(T_Q s+1)$$

Recalling,

$$\left[U^P\right]\left[U^C\right]=[I]_Z,\ \left[U^C\right]=\left[U^P\right]^{-1},$$

then,

$$H_{PP}(s)=\left[U^P\right]\left[T_Q s^2[I]_Z+(\left[\Lambda_{N_g}\right]K_P+[I]_Z)s+K_I\left[\Lambda_{N_g}\right]\right]^{-1}(K_P s+K_I)\left[\Lambda_{N_g}\right]\left[U^P\right]^{-1}$$

$$=\left[U^P\right]\varepsilon''\left[U^P\right]^{-1}$$

(6.3.1–18)

$$H_{PD}(s)=\left[U^{P}\right]\left[T_Q s^2[I]_Z+(\left[\Lambda_{N_g}\right]K_P+[I]_Z)s+K_I\left[\Lambda_{N_g}\right]\right]^{-1}s(T_Q s+1)[I]_Z\left[U^{P}\right]^{-1}$$
$$=\left[U^{P}\right]\eta''\left[U^{P}\right]^{-1}$$

(6.3.1–19)

where,

$$\varepsilon''=\mathrm{diag}\{\frac{(K_P S+K_I)N_{g1}}{T_Q S^2+(N_{g1}K_P+1)S+K_I N_{g1}},\frac{(K_P S+K_I)N_{g2}}{T_Q S^2+(N_{g2}K_P+1)S+K_I N_{g2}},$$
$$\ldots,\frac{(K_P s+K_I)N_{gZ}}{T_Q s^2+(N_{gZ}K_P+1)s+K_I N_{gZ}}\}$$
$$=\mathrm{diag}\{\frac{(\frac{K_P}{K_I}s+1)}{\frac{T_Q}{K_I N_{g1}}s^2+(\frac{K_P}{K_I}+\frac{1}{K_I N_{g1}})s+1},\frac{(\frac{K_P}{K_I}s+1)}{\frac{T_Q}{K_I N_{g2}}s^2+(\frac{K_P}{K_I}+\frac{1}{K_I N_{g2}})s+1},$$
$$\ldots,\frac{(\frac{K_P}{K_I}s+1)}{\frac{T_Q}{K_I N_{gZ}}s^2+(\frac{K_P}{K_I}+\frac{1}{K_I N_{gZ}})s+1}$$

$$\eta''=\mathrm{diag}\{\frac{s(T_Q s+1)}{T_Q s^2+(N_{g1}K_P+1)s+K_I N_{g1}},\frac{s(T_Q s+1)}{T_Q s^2+(N_{g2}K_P+1)s+K_I N_{g2}},$$
$$\ldots,\frac{s(T_Q s+1)}{T_Q s^2+(N_{gZ}K_P+1)s+K_I N_{gZ}}$$
$$=\mathrm{diag}\{\frac{s(T_Q s+1)\frac{1}{K_I N_{g1}}}{\frac{T_Q}{K_I N_{g1}}s^2+(\frac{K_P}{K_I}+\frac{1}{K_I N_{g1}})s+1},\frac{s(T_Q s+1)\frac{1}{K_I N_{g2}}}{\frac{T_Q}{K_I N_{g2}}s^2+(\frac{K_P}{K_I}+\frac{1}{K_I N_{g2}})s+1}$$
$$\ldots,\frac{s(T_Q s+1)\frac{1}{K_I N_{gZ}}}{\frac{T_Q}{K_I N_{gZ}}s^2+(\frac{K_P}{K_I}+\frac{1}{K_I N_{gZ}})s+1}\}$$

The poles polynomial matrix for both H_{PP} (s) and H_{PD}(s) is

$$\left[T_Q s^2 [I]_Z + (\left[\Lambda_{N_g}\right] K_P + [I]_Z) s + \left[\Lambda_{N_g}\right] K_I\right]$$

The zeros polynomial matrix for H_{PP}(s) is

$$\left[\Lambda_{N_g}\right](K_P s + K_I)$$

The zeros polynomial matrix for H_{PD}(s) is

$$[I]_Z s(T_Q s+1).$$

<u>For the pure I control</u>: $K_P=0$, $K_I=1/T_R$

$$\begin{aligned} H_{PP}(S) &= \left[U^P\right]\left[T_R T_Q s^2 [I]_Z + T_R [I]_Z s + \left[\Lambda_{N_g}\right]\right]^{-1} \left[\Lambda_{N_g}\right]\left[U^P\right]^{-1} \\ &= \left[U^P\right]\varepsilon'''\left[U^P\right]^{-1} \end{aligned} \qquad (6.3.1\text{–}20)$$

$$\begin{aligned} H_{PD}(S) &= \left[U^P\right]\left[T_R T_Q s^2 [I]_Z + T_R [I]_Z s + \left[\Lambda_{N_g}\right]\right]^{-1} s(T_Q s + 1)\left[U^P\right]^{-1} \\ &= \left[U^P\right]\eta'''\left[U^P\right]^{-1} \end{aligned} \qquad (6.3.1\text{–}21)$$

where,

$$\varepsilon''' = \mathrm{diag}\{\frac{1}{\frac{T_R T_Q}{N_{g1}} s^2 + \frac{T_R}{N_{g1}})s + 1}, \frac{1}{\frac{T_R T_Q}{N_{g1}} s^2 + \frac{T_R}{N_{g1}})s + 1}, \ldots, \frac{1}{\frac{T_R T_Q}{N_{gZ}} s^2 + \frac{T_R}{N_{gZ}} s + 1}\}$$

$$\eta''' = \mathrm{diag}\{\frac{s(T_Q s + 1)\frac{T_R}{N_{g1}}}{\frac{T_R T_Q}{N_{g1}} s^2 + \frac{T_R}{N_{g1}} s + 1}, \frac{s(T_Q s + 1)\frac{T_R}{N_{g2}}}{\frac{T_R T_Q}{N_{g2}} s^2 + \frac{T_R}{N_{g2}} S + 1}, \ldots, \frac{s(T_Q s + 1)\frac{T_R}{N_{gZ}}}{\frac{T_R T_Q}{N_{gZ}} s^2 + \frac{T_R}{N_{gZ}})s + 1}\}$$

The poles polynomial matrix for both H_{PP} (S)and H_{PD}(S) is

$$\left[T_R T_Q S^2 [I]_Z + T_R [I]_Z S + \left[\Lambda_{N_g}\right]\right];$$

The zeros polynomial matrix for $H_{PP}(s)$ is $[I]_Z$;

The zeros polynomial matrix for $H_{PD}(s)$ is $[I]_Z\, s(T_Q s+1)$.

(ii) Discussions

(a) In the case of perfect model mismatch with incorporating PQR dynamics, the transfer functions of this secondary voltage control system become second order.

(b) It can be directly spotted from those transfer functions that the dynamic interactions between the RVRs are determined by the non-diagonal elements of $[U^P]$. Hence, these interactions are heavily influenced by algorithms for the decentralisation/pilot buses selection.

(c) Other properties are same as the general case.

(d) It is known that a standard second order control system has the following characteristic equation:

$$\frac{s^2}{\omega_n^2}+\frac{2\delta}{\omega_n}s+1=0,$$

where the pole positions will be $s=-\omega_n\delta \pm j\omega_n(1-\delta)^{\frac{1}{2}}$. And with $0<\delta<1$, $\delta=1$, and $\delta>1$, the system is underdamped, critically damped and overdamped respectively. By comparing the characteristic equation of each control loop of this secondary voltage control system with this equation, the specification of the closed loop poles can be analysed:

<u>For PI control</u>

Underdamped/overdamped: Specify δ and ω_n, by solving

$$\omega_n^2=\frac{K_I N_{gi}}{T_Q},\quad \frac{2\delta}{\omega_n}=\frac{K_P}{K_I}+\frac{1}{N_{gi}K_I}$$

It can be obtained that,

$$K_I = \frac{T_Q\omega_n^2}{N_{gi}},\ K_P = \frac{1}{N_{gi}}(2T_Q\omega_n\delta - 1) \qquad (6.3.1\text{–}22)$$

Critically damped: $\delta = 1$, ω_n is specified, then

$$K_I = \frac{T_Q\omega_n^2}{N_{gi}},\ K_P = \frac{1}{N_{gi}}(2T_Q\omega_n - 1) \qquad (6.3.1\text{–}23)$$

<u>For Pure I control</u>

For the pure integral control, $K_P = 0$, $K_I = 1/T_R$, then

$$\omega_n = \left(\frac{N_{gi}}{T_R T_Q}\right)^{\frac{1}{2}},\ \delta = \frac{1}{2}\left(\frac{1}{N_{gi}}\frac{T_R}{T_Q}\right)^{\frac{1}{2}}.$$

It can been seen that by pure I control ω_n and δ are determined by the time constant T_R, T_Q for the RVR and PQR, as well as the number of control generators in each region. There is little choice for improving the control system dynamic properties once these time constants are fixed.

(2) Neglecting PQR dynamics

(i) Transfer Functions

Neglecting PQR dynamics in the case of perfect model match, there are:

$$[\Lambda_R] = [\Lambda_{N_g}],\ [U^P][U^C] = [I]_Z.$$

Then, the closed loop transfer functions become:

<u>For the PI control:</u>

$$\begin{aligned} H_{PP}(s) &= [U^P]\left[([\Lambda_{N_g}]K_P + [I]_Z)s + K_I[\Lambda_{N_g}]\right]^{-1}(K_P s + K_I)[\Lambda_{N_g}][U^P]^{-1} \\ &= [U^P][\varepsilon][U^P]^{-1} \end{aligned} \qquad (6.3.1\text{–}24)$$

$$H_{PD}(s)=\left[U^P\right]\left[(\left[\Lambda_{N_g}\right]K_P+[I]_Z)s+K_I\left[\Lambda_{N_g}\right]\right]^{-1}s[I]_Z\left[U^P\right]^{-1}$$
$$=\left[U^P\right]\bar{\eta}\left[U^P\right]^{-1} \tag{6.3.1–25}$$

where,

$$\bar{\varepsilon}=\mathrm{diag}\left\{\frac{(\frac{K_P}{K_I}s+1)}{(\frac{K_P}{K_I}+\frac{1}{K_IN_{g1}})s+1},\frac{(\frac{K_P}{K_I}s+1)}{(\frac{K_P}{K_I}+\frac{1}{K_IN_{g2}})s+1},\ldots,\frac{(\frac{K_P}{K_I}s+1)}{(\frac{K_P}{K_I}+\frac{1}{K_IN_{gZ}})s+1}\right\}$$

$$\bar{\eta}=\mathrm{diag}\left\{\frac{\frac{s}{K_IN_{g1}}}{(\frac{K_P}{K_I}+\frac{1}{K_IN_{g1}})s+1},\frac{\frac{s}{K_IN_{g2}}}{(\frac{K_P}{K_I}+\frac{1}{K_IN_{g2}})s+1},\ldots,\frac{\frac{s}{K_IN_{gZ}}}{(\frac{K_P}{K_I}+\frac{1}{K_IN_{gZ}})s+1}\right\}$$

The poles polynomial matrix for both $H_{PP}(s)$ and $H_{PD}(s)$ is

$$\left[(\left[\Lambda_{N_g}\right]K_P+[I]_Z)s+\left[\Lambda_{N_g}\right]K_I\right]$$

The zeros polynomial matrix for $H_{PP}(s)$ is

$$\left[\Lambda_{N_g}\right](K_Ps+K_I)$$

The zeros polynomial matrix for $H_{PD}(s)$ is

$$[I]_Zs$$

<u>For the pure I control</u>: $K_P=0$, $K_I=1/T_R$

$$H_{PP}(s)=\left[U^P\right]\left[T_R[I]_Zs+\left[\Lambda_{N_g}\right]\right]^{-1}\left[\Lambda_{N_g}\right]\left[U^P\right]^{-1}$$
$$=\left[U^P\right]\bar{\varepsilon}'\left[U^P\right]^{-1} \tag{6.3.1–26}$$

$$H_{PD}(s)=\left[U^P\right]\left[T_R[I]_Zs+\left[\Lambda_{N_g}\right]\right]^{-1}s\left[U^P\right]^{-1}$$
$$=\left[U^P\right]\bar{\eta}'\left[U^P\right]^{-1} \tag{6.3.1–27}$$

where,

$$\bar{\varepsilon}' = \mathrm{diag}\{\frac{1}{\frac{T_R}{N_{g1}}s+1}, \frac{1}{\frac{T_R}{N_{g1}}s+1}, \ldots, \frac{1}{\frac{T_R}{N_{gZ}}s+1}\}$$

$$\bar{\eta}' = \mathrm{diag}\{\frac{s\frac{T_R}{N_{g1}}}{\frac{T_R}{N_{g1}}s+1}, \frac{s\frac{T_R}{N_{g2}}}{\frac{T_R}{N_{g2}}s+1}, \ldots, \frac{s\frac{T_R}{N_{gZ}}}{\frac{T_R}{N_{gZ}}s+1}\}$$

The poles polynomial matrix for both H_{PP} (s)and $H_{PD}(s)$ is

$$\left[T_R[I]_Z s + \left[\Lambda_{N_g}\right]\right].$$

The zeros polynomial matrix for H_{PP} (s) is $[I]_Z$.

The zeros polynomial matrix for $H_{PD}(s)$ is $[I]_Z S$.

(ii) Discussions

(a) The above analysis is subject to a very ideal condition: perfect model match, neglecting PQR dynamics. Under this condition, the global stability of the closed loop voltage control system is guaranteed, because $s = -N_{g\,i}/T_R$, $i = 1,2,\ldots, Z$, $Re(s) < 0$.

(b) From this analysis, it can be seen that global stability of this secondary voltage control system is related to the number of the control generators in each region. The more the control generators, the more stable the control system is.

(c) Other properties are the same as general case.

6.3.2 The Control System with a Decentralised Scheme

As discussed before, the decentralised control scheme can be regarded as a special case of the centralised control scheme: a diagonal control law matrix $[U^C]$ for RVRs. Adding this condition to the analysis for the centralised scheme, the stability analysis for the decentralised scheme can be obtained.

6.3.2.1 General case

1. Transfer functions

The transfer functions for the decentralised scheme can be directly achieved from equations (6.3.1-11) - (6.3.1-12) by considering that $[U^C]$ is a diagonal matrix.

For PI control

$$H_{PP}(s)=\left[s[I]_Z+\left[U^P\right]\left[U^C\right][\Lambda_R](K_P s+K_I)\right]^{-1}\left[U^P\right]\left[U^C\right][\Lambda_R](K_P s+K_I) \quad (6.3.2\text{–}1)$$

$$H_{PD}(s)=\left[s[I]_Z+\left[U^P\right]\left[U^C\right][\Lambda_R](K_P s+K_I)\right]^{-1}s \quad (6.3.2\text{–}2)$$

For the pure I control:

$$H_{PP}(s)=\left[T_R s[I]_Z+\left[U^P\right]\left[U^C\right][\Lambda_R]\right]^{-1}\left[U^P\right]\left[U^C\right][\Lambda_R] \quad (6.3.2\text{–}3)$$

$$H_{PD}(s)=\left[T_R s[I]_Z+\left[U^P\right]\left[U^C\right][\Lambda_R]\right]^{-1}T_R s \quad (6.3.2\text{–}4)$$

2. Discussions

(1) It can be seen that the global stability of this decentralised voltage control system is also related to the RVR model mismatch $\left[U^P\right]\left[U^C\right]$, and PQR model mismatch $\left[A_{Ci}^j\right]\left[A_i^j\right]^{-1}$ through $[\Lambda_R]=[\Lambda_N][\Lambda_D]^{-1}$.

(2) Other discussions are the same as the general case study of the centralised scheme.

6.3.2.2 Special Cases

Similarly, the analyses for the special cases for the decentralised scheme can be achieved by taking into account the diagonal control law matrix $[U^C]$.

1. Neglecting PQR dynamics

The analyses for this special case are same as those for the centralised scheme. For details, see equation (6.3.1-14)-(6.3.1-17) in subsection 6.3.1.2. Note that in this case,

$$\left[U^P\right]\left[\Lambda_{N_g}\right]\left[U^C\right]=\left[U^P\right]\left[U^C\right]\left[\Lambda_{N_g}\right]=[\Gamma][\Lambda_\sigma][\Gamma]^{-1}$$

2. Perfect model match

By considering that

$$\left[U^P\right]\left[U^C\right]=[I]_Z,\ \left[A^j_{Ci}\right]\left[A^j_i\right]^{-1}=[I]_{N^j_{gi}}$$

and $[U^C]$ is a diagonal matrix, the following analyses can be made based on equations (6.3.1-18) - (6.3.1-27).

(1) Incorporating PQR dynamics

The transfer functions for the secondary voltage control system by the PI control:

$$H_{PP}(s)=\left[T_Q s^2[I]_Z+(\left[\Lambda_{N_g}\right]K_P+[I]_Z)s+K_I\left[\Lambda_{N_g}\right]\right]^{-1}(K_P s+K_I)\left[\Lambda_{N_g}\right] \qquad (6.3.2\text{–}5)$$

$$=\varepsilon''$$

$$H_{PD}(s)=\left[T_Q s^2[I]_Z+(\left[\Lambda_{N_g}\right]K_P+[I]_Z)s+K_I\left[\Lambda_{N_g}\right]\right]^{-1}s(T_Q s+1) \qquad (6.3.2\text{–}6)$$

$$=\eta''$$

The transfer functions for the secondary voltage control system by the pure I control:

$$H_{PP}(s)=\left[T_R T_Q s^2[I]_Z+T_R[I]_Z s+\left[\Lambda_{N_g}\right]\right]^{-1}\left[\Lambda_{N_g}\right] \qquad (6.3.2\text{–}7)$$

$$=\varepsilon'''$$

$$H_{PD}(s)=\left[T_R T_Q s^2[I]_Z+T_R[I]_Z s+\left[\Lambda_{N_g}\right]\right]^{-1} s(T_Q s+1) \\ =\eta''' \tag{6.3.2–8}$$

(2) Neglecting PQR dynamics

The transfer functions for the secondary voltage control system by the PI control:

$$H_{PP}(s)=\left[(\left[\Lambda_{N_g}\right]K_P+[I]_Z)s+K_I\left[\Lambda_{N_g}\right]\right]^{-1}(K_P s+K_I)\left[\Lambda_{N_g}\right] \\ =\overline{\varepsilon} \tag{6.3.2–9}$$

$$H_{PD}(s)=\left[(\left[\Lambda_{N_g}\right]K_P+[I]_Z)S+K_I\left[\Lambda_{N_g}\right]\right]^{-1} s(T_Q s+1) \\ =\overline{\eta} \tag{6.3.2–10}$$

For the pure I control ($K_P=0$, $K_I=1/T_R$):

$$H_{PP}(s)=\left[T_R[I]_Z s+\left[\Lambda_{N_g}\right]\right]^{-1}\left[\Lambda_{N_g}\right] \\ =\overline{\varepsilon}' \tag{6.3.2–11}$$

$$H_{PD}(s)=\left[T_R[I]_Z s+\left[\Lambda_{N_g}\right]\right]^{-1} s(T_Q s+1) \\ =\overline{\eta}' \tag{6.3.2–12}$$

(3) Discussions

(i) Under this very ideal situation, the interactions between RVRs disappear.

(ii) The poles/zeros polynomial matrices are same as those in the centralised scheme under the same simplification.

(iii) Other properties are same as those in the case of perfect model match in the centralised scheme.

6.4 VOLTAGE PROFILE ANALYSIS

6.4.1 Analysis

By recalling the voltage profile description (5.3.2-2) given in Chapter 5,

$$\left[\Delta V_{\bar{P}}\right]=\left[S^{\bar{P}}_{VG}\right]\left[\Delta Q_G\right]+\left[S^{\bar{P}}_{VL}\right]\left[\Delta Q_L\right]$$

By considering

$$\left[\Delta Q_G\right]=\left[\Lambda_{G\lim}\right]\left[\Delta q_G\right]$$

$$\left[\Lambda_{G\lim}\right]=\left[D_{Gg}\right]\left[\Lambda_{g\lim}\right]\left[D_{Gg}\right]^T$$

$$\left[\Delta q_G\right]=\left[D_{GR}\right]\left[\Delta q_R\right]$$

It can be obtained that,

$$\left[\Delta V_{\bar{P}}\right]=\left[U^{\bar{P}}\right]\left[\Delta q_R\right]+\left[S^{\bar{P}}_{VL}\right]\left[\Delta Q_L\right].$$

where,

$$\left[U^{\bar{P}}\right]=\left[S^{\bar{P}}_{VG}\right]\left[\Lambda_{G\lim}\right]\left[D_{GR}\right].$$

The RVR control design equation (6.2.1-5) gives

$$\left[\Delta q_R\right]=\left[U^P\right]^{-1}\left[\Delta V_p\right]-\left[U^P\right]^{-1}\left[S^P_{VL}\right]\left[\Delta Q_L\right] \quad \textbf{(6.2.1–5)}$$

Thus,

$$\left[\Delta V_{\bar{P}}\right]=\left[U^{\bar{P}}\right]\left[U^P\right]^{-1}\left[\Delta V_p\right]+\left(\left[S^{\bar{P}}_{VL}\right]-\left[U^{\bar{P}}\right]\left[U^P\right]^{-1}\left[S^P_{VL}\right]\right)\left[\Delta Q_L\right] \qquad (6.4.1–1)$$

$$=\left[\Re\right]\left[\Delta V_p\right]+\left[\aleph\right]\left[\Delta Q_L\right]$$

where,

$$\left[\Re\right]=\left[U^{\bar{P}}\right]\left[U^P\right]^{-1},$$

$$\left[\aleph\right]=\left[S^{\bar{P}}_{VL}\right]-\left[U^{\bar{P}}\right]\left[U^P\right]^{-1}\left[S^P_{VL}\right].$$

6.4.2 Remarks

1. Equation (6.4.1-1) shows that the voltage profile produced from the secondary voltage control system is influenced by both the voltages of pilot buses and load disturbances in a power system

2. A successful methodology for the power system decentralisation and the selection of pilot buses/control power plants should ensure that the matrix $[\aleph]$ is sufficiently close to $[0]$. In this way, the load disturbances influence can be neglected, and the voltage profile can be well controlled by the secondary voltage control system through the pilot buses. This matrix $[\aleph]$ provides a useful measure to assess the algorithms for the decentralisation and pilot buses/control power plants selection.

3. Provided that the load disturbances influence is negligible ($[\aleph] \approx [0]$), the voltage profile will have very similar dynamics to the voltages of the pilot buses in the power system.

6.5 SYSTEM INTEGRATION ANALYSIS

6.5.1 Integration Issues and Signals

6.5.1.1 Integration issues

From the viewpoint of system integration, a secondary voltage control system can be simplified as

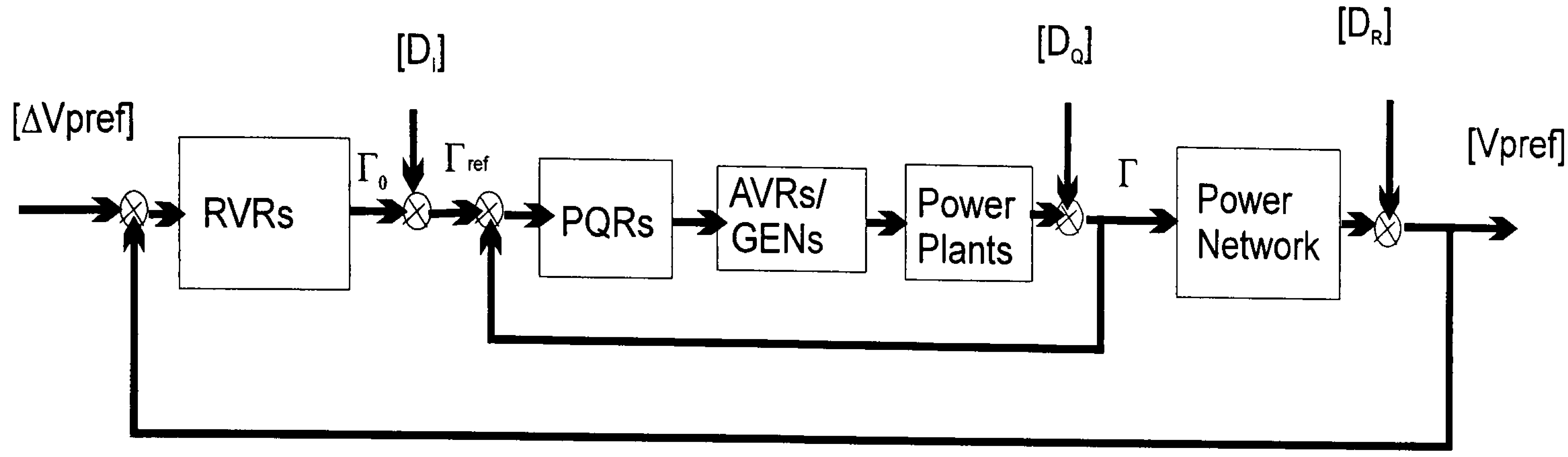

Figure 6.5.1-1 The simplified block diagram of a secondary voltage control system

Where,

Γ : Integration signal,

Γ_0: the integration signal from RVR controllers without disturbance,

D_R : Slow dynamical disturbance in RVR loop,

D_I : Disturbance on Γ_0,

D_Q : Fast dynamical disturbance in PQR loop,

For the integration between the RVR and PQR, the following issues need to be considered:

1. **System output offset elimination**

Two kinds of reference offsets are concerned here: the PQR reference offset and the RVR reference offsets. A successful control design should ensure that the reference offsets with both RVR and PQR close loop outputs are sufficiently small.

2. Disturbance rejections

Three kinds of disturbances need to be considered: the fast dynamical disturbances within PQR loop D_Q, the slow dynamical disturbances with RVR (including the power system disturbance D_R and the one on the integration signal D_I). A good integration should have the following properties:

(1) The fast dynamical disturbance will be sufficiently rejected within PQR loops, so that it has a very limited influence on the RVR loops.

(2) The slow disturbances will be sufficiently rejected within RVR loops so that an efficient voltage regulation can be achieved at pilot buses.

6.5.1.2 Integration Signals

From the control design in Section 6.2, it is known that, by the classic PI control design, the demanded reactive power increment in percentage for each region Δq_{Ri} is the RVR-PQR integration signal:

$$\Gamma = [\Delta q_R],\ \Gamma_{ref} = [\Delta q_{Rref}].$$

The RVR controllers determine the demanded reactive power increment in percentage for each decentralised region. This will be based on the voltage variations at the pilot buses. In each region, as all the control power plants have the same participation to the reactive power demand change (the RVR control law), thus

$$\Delta q^1_{Gi} = \Delta q^2_{Gi} \dots = \Delta q^j_{Gi} \dots = \Delta q_{Ri} \qquad (6.5.1\text{–}1)$$

This demanded reactive power increment in percentage for each region is then used as the reference for each PQR, and RVR and PQR are integrated with the following relationships:

$$[\Delta q_G] = [\Lambda_{G\lim}]^{-1}[\Delta Q_G] \qquad (6.5.1\text{–}2)$$

$$[\Delta q_R] = [D_{GR}]^T[\Delta q_G] \qquad (6.5.1\text{–}3)$$

$$[\Lambda_{G\lim}] = [D_{Gg}][\Lambda_{g\lim}][D_{Gg}]^T \qquad (6.5.1\text{–}4)$$

6.5.2 Integration Analysis

6.5.2.1 The PQR loop

Recalling the stability analysis in Section 6.3, the closed loop transfer function for the PQR at control power plant j of region i can be written as:

$$\left[\Delta Q_{gi}^{j}\right]=H_{ggi}^{j}(s)\left[\Delta Q_{gref\,i}^{j}\right]+H_{gDi}^{j}\left[D_{Qi}^{j}\right] \qquad (6.5.2\text{–}1)$$

where,

$$H_{gg\,i}^{j}(s)=\left[sT_Q[I]_{N_{gi}^{j}}+\left[A_{Ci}^{j}\right]\left[A_{i}^{j}\right]^{-1}\right]^{-1}\left[A_{Ci}^{j}\right]\left[A_{i}^{j}\right]^{-1}$$

$$H_{gD\,i}^{j}(s)=-\left[sT_Q[I]_{N_{gi}^{j}}+\left[A_{Ci}^{j}\right]\left[A_{i}^{j}\right]^{-1}\right]^{-1}sT_Q\left[A_{i}^{j}\right]^{-1}$$

Using equations (6.5.1-1) - (6.5.1-4) and (6.5.2-1), yields:

$$\left[\Delta q_R\right]=H_{qq}(s)\left[\Delta q_{Rref}\right]+H_{qD}(s)\left[D_Q\right]$$

where,

$$H_{qq}(s)=\left[D_{GR}\right]^T\left[D_{Gg}\right]\left[\Lambda_{g\lim}\right]^{-1}\left[\Lambda_{Hgg(s)}\right]\left[\Lambda_{g\lim}\right]\left[D_{Gg}\right]^T\left[D_{GR}\right];$$

$$H_{qD}(s)=\left[D_{GR}\right]^T\left[D_{Gg}\right]\left[\Lambda_{g\lim}\right]^{-1}\left[\Lambda_{HgD(s)}\right]\left[D_{Gg}\right]^T\left[D_{GR}\right];$$

$$\left[\Lambda_{Hgg(s)}\right]=\mathrm{diag}\{H_{gg1}^{1}(s),H_{gg1}^{2}(s),\ldots,H_{gg1}^{N_{G1}}(s),\ldots,H_{ggi}^{1}(s),H_{ggi}^{2}(s),\ldots,H_{ggi}^{N_{Gii}}(s),\ldots,H_{ggZ}^{N_{GZ}}(s)\};$$

$$\left[\Lambda_{HgD(s)}\right]=\mathrm{diag}\{H_{gD1}^{1}(s),H_{gD1}^{2}(s),\ldots,H_{gD1}^{N_{G1}}(s),\ldots,H_{gDi}^{1}(s),H_{gDi}^{2}(s),\ldots,H_{gDi}^{N_{Gii}}(s),\ldots,H_{gDZ}^{N_{GZ}}(s)\}.$$

$$\left[D_Q\right]=\left[\left[D_{Q\ 1}^{1}\right],\ldots,\left[D_{Q\ i}^{j}\right],\ldots,\left[D_{QZ}^{N_{GZ}}\right]\right]$$

It is easy to verify that

$$\lim_{S\to 0} sH_{gg\,i}^{j}(s)\frac{1}{s}=[I]_{N_{gi}^{j}};\quad \lim_{S\to 0} sH_{gD\,i}^{j}(s)\frac{1}{s}=[0]_{N_{Gi}^{j}}$$

and

$$\lim_{S\to 0} sH_{qq}(s)\frac{1}{s}=[I]_Z;\quad \lim_{S\to 0} sH_{qD}(s)\frac{1}{s}=[0]_Z$$

Thus, it is known that the reference offset with the PQR closed loop output is completely eliminated, and the disturbances with the PQR closed loop are completed rejected provided the PQR closed loop is stable.

6.5.2.2 The RVR loop

The stability analysis in Section 6.3 also gives the transfer function for the RVR as:

$$[\Delta V_P] = H_{PP}(s)[\Delta V_{Pref}] + H_{PD}(s)[\Delta D]$$

where,

$$H_{PP}(s) = \left[[I]_Z + [U^P][\Lambda_R][U^C]G(s)\right]^{-1}[U^P][\Lambda_R][U^C]G(s)$$

$$H_{PD}(s) = \left[[I]_Z + [U^P][\Lambda_R][U^C]G(s)\right]^{-1}$$

$$[D] = [S^P_{VG}][D_{Gg}][H_{qD}(s)][D_Q] + [S^P_{VL}][D_R]$$

It can also be verified that

$$\lim_{s\to 0} SH_{PP}(s)\frac{1}{s} = [I]_Z$$

and

$$\lim_{S\to 0} sH_{PD}(s)\frac{1}{s} = [0]_Z$$

Hence, if the RVR closed loop remains stable, perfect reference tracking and disturbance rejection occur. As the disturbance [D] contains both the RVR slow dynamical disturbance [D_R] and the PQR fast disturbances [D_Q], it is known that not only the slow dynamical disturbance can be rejected, but also the remains of fast dynamical disturbances can be rejected if they are not completely eliminated in PQR loop.

6.5.2.3 Integration between the PQRs and the RVRs

For the disturbance $[D_I]$ on the integration signal, as it can be subsumed into the slow dynamical disturbance $[D_R]$ within RVR loops as:

$$[\Delta q_R] = [\Delta q_{R0}] + [D_I]$$

$$\begin{aligned}[\Delta V_P] &= [U^P][\Delta q_R] + [D_R] \\ &= [U^P][\Delta q_{R0}] + [U^P][D_I] + [D_R] \\ &= [U^P][\Delta q_{R0}] + [D]\end{aligned}$$

where,

$$[D] = [U^P][D_I] + [D_R]$$

Therefore, the disturbance $[D_I]$ can also be rejected by the RVR control law.

6.5.3 Remarks

Based on the above integration analysis, following points can be summarised:

1. By the classic PI control design, the reference offsets with both RVR and PQR closed loop outputs can be completely eliminated provided the closed loops are stable;

2. All the disturbances including fast dynamical disturbance [D_Q] within PQR loops and slow disturbances in RVR loops ([D_r] and [D_I]) can be successfully rejected by this PI based control system.

3. In addition, the RVR closed loop disturbance rejection can further eliminate remnants of the fast dynamical disturbances from PQR if they are not completely rejected within PQR loops.

6.6 SIMULATIONS

The simulation of the secondary voltage control system by the classic control design is presented in this section. The IEEE 39 bus power system (the New England System) is used in this simulation.

6.6.1 Simulation Configurations

1. The testing power system

The IEEE 39 bus power system used for this simulation contains 10 power plants and 29 load buses. The bus 10 (power plant) is used as slack bus. The operation diagram and parameters of this testing system are given in Appendix 1.

2. The control system

(1) Control Scheme

The decentralised control scheme was used for this PI control based secondary voltage control system. Each decentralised region has one pilot bus. Apart from the slack bus, all power plants were used as the control power plants.

(2) Pilot buses and control power plants

By using the sensitivity analysis based method [42], the testing power system was decentralised into 6 regions. The pilot bus and control power plants for each decentralised region are shown in the table below.

AREA	PILOT BUS	CONTROL POWER PLANTS
1	bus 13	bus 2, bus 8
2	bus 15	bus 1
3	bus 23	bus 3
4	bus 30	bus 4, bus 5
5	bus 33	bus 6, bus 7
6	bus 38	bus 9

Table 6.6.1-1 The decentralisation and pilot buses/control power plants

6.6.2 Simulation Programme

1. Programme

The secondary voltage control system was programmed by using the Matlab/Simulink. For the sake of simplicity, pure integral control was used in this simulation, the proportional control was replaced by a tuning factor for the RVR gain to avoid overshooting problem of the control output. The discretisation technique was used in the programme to implement the integral control. The number of control steps needs to be specified at the beginning of the simulation as the total control steps for both PQR and RVR.

2. Settings for the secondary voltage control

(1) Voltage reference for the pilot buses

The pilot bus voltages were set with the following reference values:

Pilot buses	13	15	23	30	33	38
VPref	1.009	1.003	1.014	0.982	1.036	1.022

Table 6.6.2-1 The voltage references for the pilot buses

(2) Disturbances

A reactive load increase (20MVA) was given to all the 29 load buses to simulate the voltage disturbances. The voltage variations at the pilot buses were calculated by running a load flow study. The RVR and PQR controls were performed to correct the voltage variations by regulating the reactive outputs of the Control Power Plants.

6.6.3 Simulations Results

Figure 6.6.3-1 to Figure 6.6.3-3 list the simulation results with different control steps (discrete control actions within a given time interval in seconds) and the gain tuning factors.

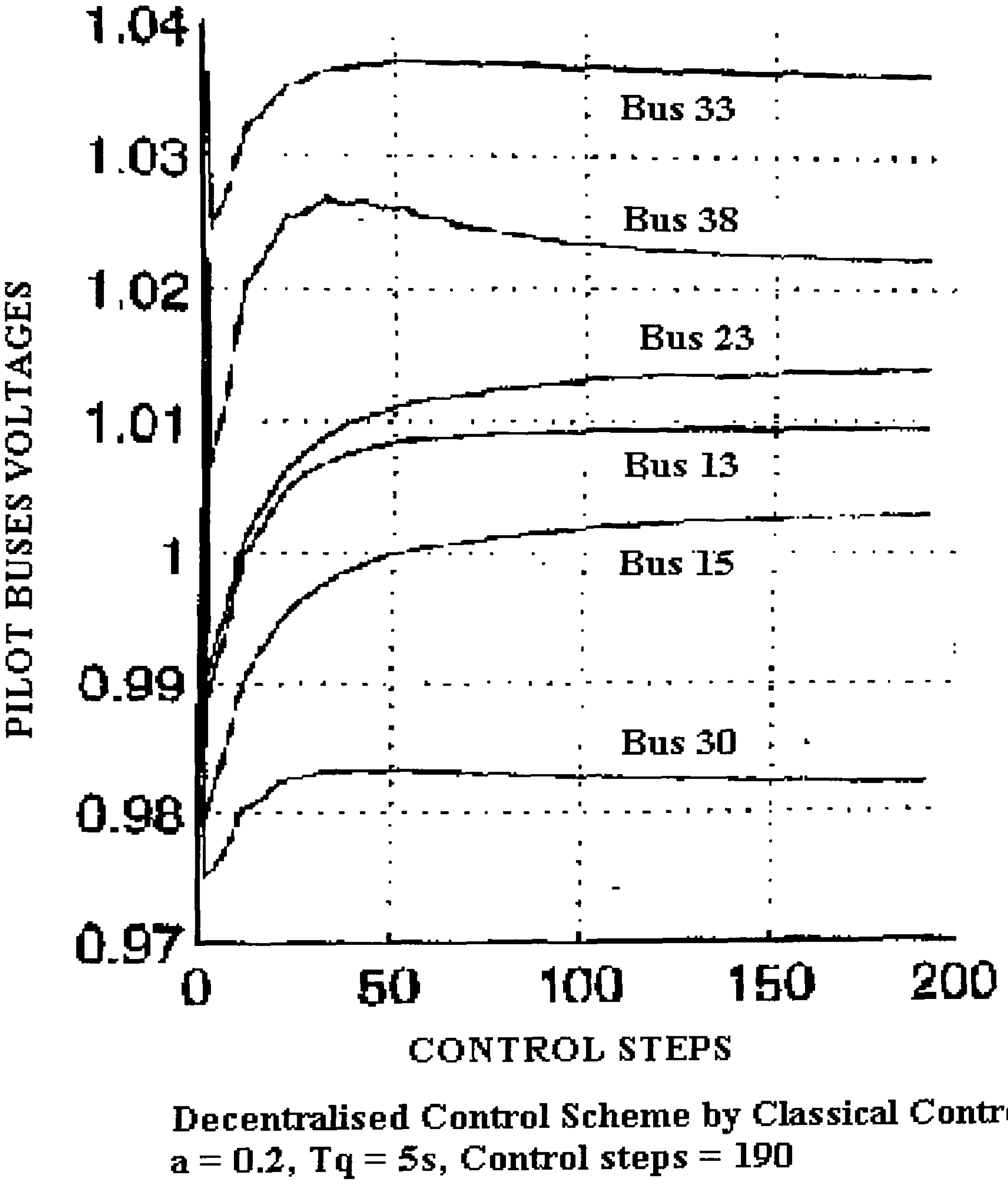

Figure 6.6.3-1 **Simulation results 1 - the secondary voltage control system by classical control design**

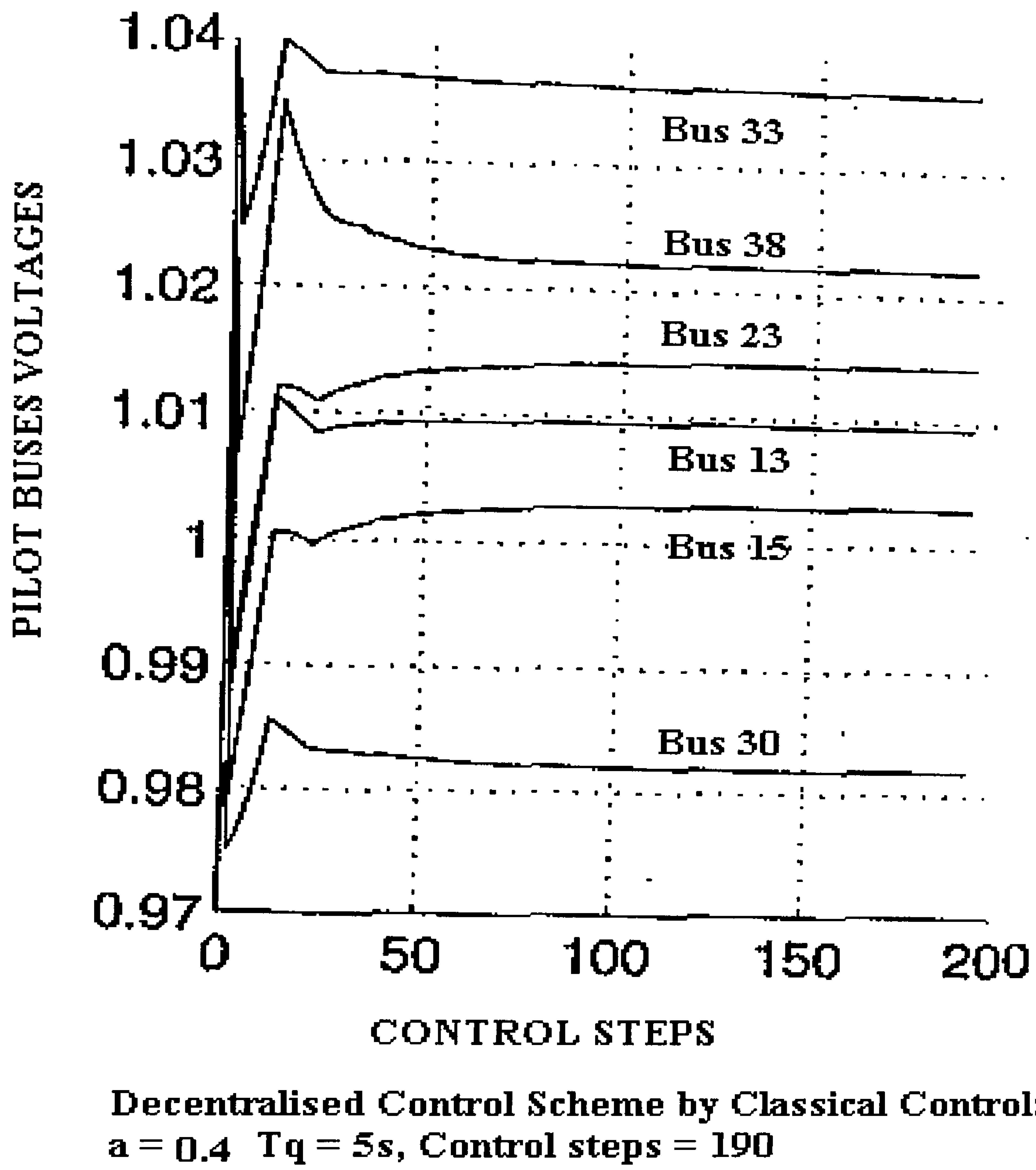

Figure 6.6.3-2 **Simulation results 2 - the secondary voltage control system by classical control design**

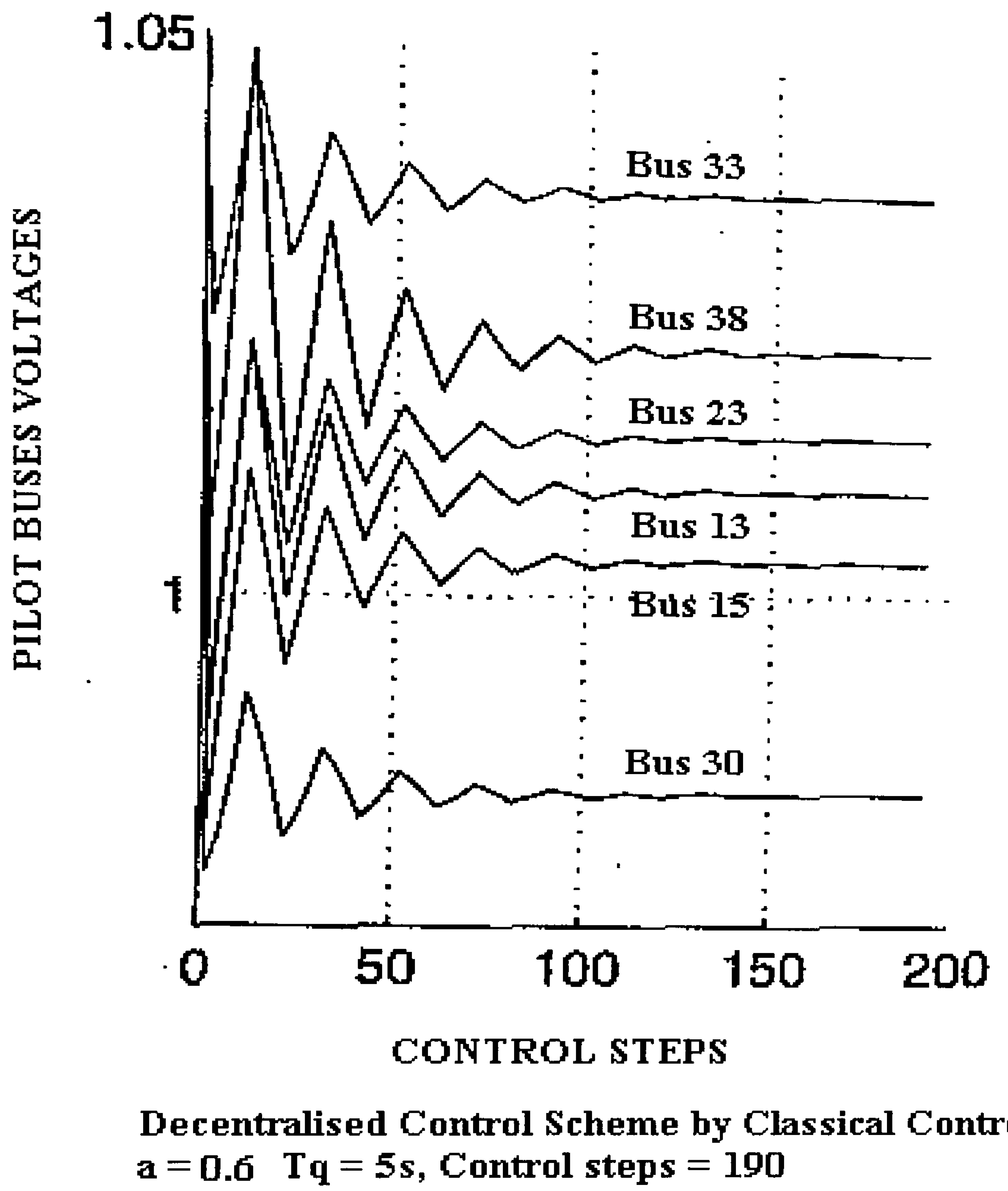

Figure 6.6.3-3 **Simulation results 3 - the secondary voltage control system by classical control design**

6.6.4 Remarks

From the simulation results, it can be seen that a successful secondary voltage control system can be achieved by the classic control design.

The gain tuning factor for RVR has direct impact on the control output (voltages of the pilot buses). This proves that the proportional control is crucial for achieving a good closed loop performance.

The above simulations also show that closed loop stability and performance of the control system are related to the control steps in the discretised control system. A good closed loop stability and performance require a large number of the control steps, while too many of them will slow down the control system. In practice, comprise is needed to determine a proper number of control steps.

6.7 DISCUSSIONS AND CONCLUSIONS

A classical PI control design for the secondary voltage control system has been discussed in this chapter. It includes the design details for the PQR, the RVR as well as their integration of this multi-level control system.

The closed loop stability and performance of this classical control based system have been systematically examined by using the traditional frequency(S) domain method. It is believed that this is the first systematic analysis for such a voltage control system. The transfer functions for reference tracking and disturbances were generically derived for both the PQRs and the RVRs, and some specific properties for those two sub-systems were examined in the special cases under certain simplifications. The following points can be abstracted from the analysis:

1. A satisfactory closed loop stability and performance can be achieved by the classical control designs for such a secondary voltage control system.

2. The global stability of this multi-level secondary voltage control system is related to the RVR/PQR model mismatch, the PQR dynamics as well as the number of control generators in each region.

3. There are dynamic interactions between the RVRs in different decentralised regions. These interactions are mainly caused by the RVR model mismatch. The number of control generators in each of the regions has also an impact on the interactions.

4. Generally, the more control generators in each of the regions, the more stable the closed loop control system is, however the bigger RVRs interactions may occur. This suggests that a compromise might be needed for determining the number of control generators in each region.

5. The PI control design for RVR is superior to the pure I control design. This is because that by PI control, the stability and other dynamic properties of the control system can be improved by properly selecting the parameters K_P and K_I. The Pure I control design does not possess this advantage.

Voltage profile analysis shows that, with a proper decentralisation of a power system and selection of pilot buses/control power plants, the voltage profile (regional and global) can be efficiently regulated by the secondary voltage control system.

It has also been observed from this analysis that voltage profile will have very similar dynamics to the voltages at pilot buses. Through this analysis, a useful measure (matrix $[\aleph]$) was produced for assessing the decentralisation of a power system and the selection of the pilot buses/control power plants.

In the integration analysis, it has been seen that with the classic PI control design, all the reference offsets and disturbances can be sufficiently eliminated within this secondary voltage control system.

The simulation on the IEEE 39 bus system numerically demonstrated that this classical control design is able to produce a satisfactory control results for the secondary voltage control in a power system.

CHAPTER 7 THE SECONDARY VOLTAGE CONTROL SYSTEM BY AN OPTIMAL CONTROL DESIGN

7.1 INTRODUCTION

In this chapter, an optimal control design is presented for the secondary voltage control. In this design, both the RVR and PQR are formularised as constrained optimal control problems. The Receding Horizon principle is used in this optimal control system.

To prepare for the optimal control design and analysis, the discrete system descriptions and error equations are established in the beginning of this chapter. Then, the design for both the PQR and the RVR are discussed. The control design covers both the centralised and decentralised scheme.

As the validation of the closed loop stability for an optimal control system in the presence of all the constraints has always been an unsolved problem, the stability and integration analyses for this optimal control based secondary voltage control system have been intensively examined as a major task in this chapter. A constructive time domain analysis method is proposed and successfully used for the analyses.

The optimal control design for the secondary voltage control has been simulated on the IEEE 39 bus power system, some of the simulation results are included at the end of this chapter.

7.2 DISCRETE SYSTEM DESCRIPTIONS

To use an optimal control for the secondary voltage control, it is essential to have the discrete system descriptions. Based on the system descriptions established in chapter 5, their discrete version can be obtained by discretisation.

7.2.1 Discrete System Descriptions for the RVR

By discretising the equations (5.3.2-4) - (5.3.2-5) in Chapter 5, the discrete system descriptions for the RVR can be achieved with the following time interval:

$$T = t_{k+1} - t_k \quad T > 2\text{-}3 \text{ sec.}$$

7.2.1.1 Pilot Buses

1. The pilot bus voltage descriptions

$$\left[V_p(k+1)\right] = [I\ \ ]_{Np}\left[V_p(k)\right] + [S^P_{VV}]\left[\Delta V_G(k)\right] \qquad (7.2.1\text{-}1)$$

Where,

$\left[\tilde{S}^P_{VV}\right]$ is the **actual** systems sensitivity matrix used in defining any control law,

$\left[S^P_{VV}\right]$ is for the **model** system sensitivity used in system mis-match analyses,

N_P, N_G are the number of pilot buses and control power plants respectively.

The pilot bus voltage system model is shown in Figure 7.2.1-1.

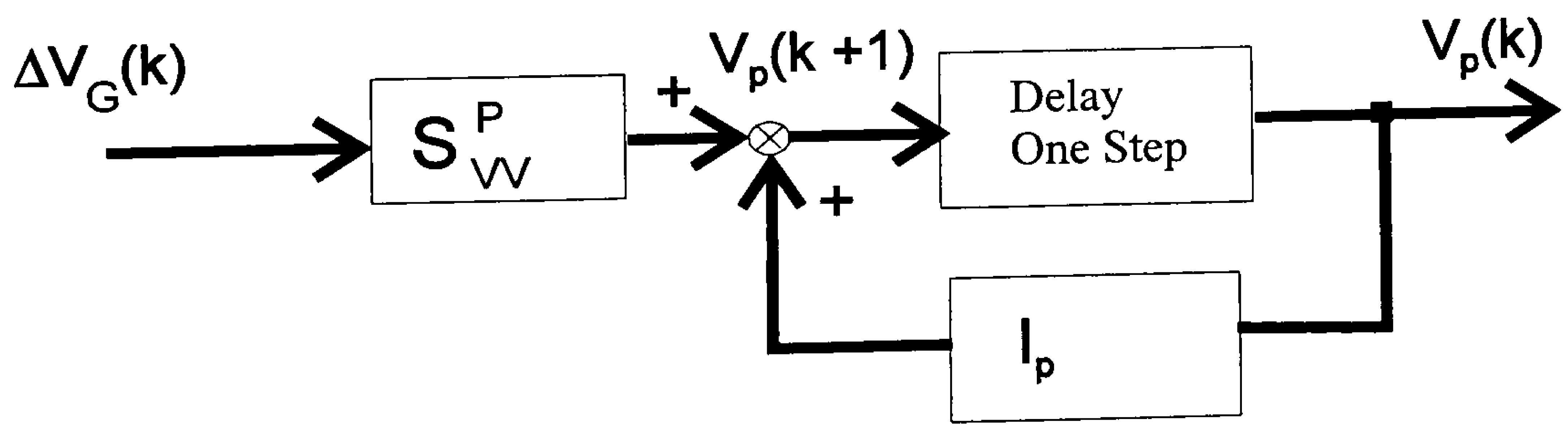

Figure 7.2.1-1 The model pilot bus linear discrete system

2. System Controllability

$$\text{Rank } \aleph = \text{rank}[[S_{VV}^{P}],[S_{VV}^{P}],\ldots,[S_{VV}^{P}]] = \text{rank }[S_{VV}^{P}] \leq \min(N_P,N_G)$$

Thus the number of modes of the pilot bus subsystems which can be assigned (arbitrarily) depends on the rank of the sensitivity matrix $[S_{VV}^{P}]$.

For the system mismatch study, the linear system for the pilot bus voltage is given by

$$[V_p(k+1)] = [I]_{Np}[V_p(k)] + [\tilde{S}_{VV}^{P}][\Delta V_G(k)] + [D_R^P(k)] \quad (7.2.1\text{–}2)$$

for which the system diagram is shown in Figure 7.2.1-2.

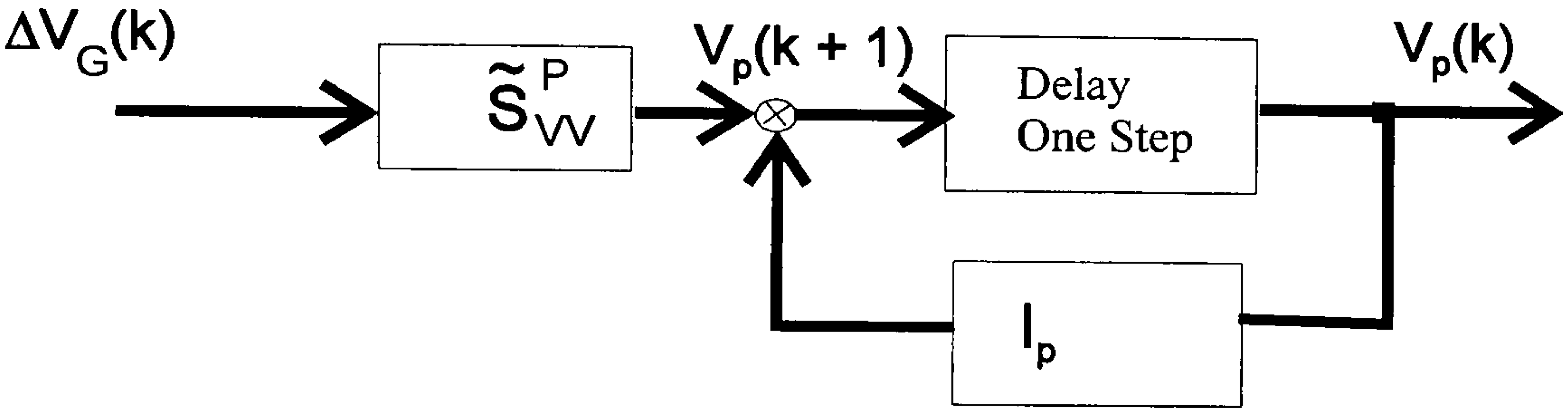

Figure 7.2.1-2 The actual pilot bus linear discrete system

3. The Error Equations for the Pilot Bus Voltages

Using the linear equation (7.2.1-2), two error equations can be established, one for use in control design which uses the model sensitivity matrix $[S_{VV}^{P}]$, and one for use in system mismatch study which uses the actual sensitivity matrix $[\tilde{S}_{VV}^{P}]$.

Error System 1 (For Design)

$$e_p(k+1) = [V_{pref}] - [V_p(k+1)]$$

$$= [V_{pref}] - [I]_{Np} V_p(k) - [S_{VV}^{P}][\Delta V_G(k)]$$

$$e_p(k+1) = [I]_{Np} e_p(k) - [S_{VV}^{P}][\Delta V_G(k)] \quad (7.2.1\text{–}3)$$

Error System 2 (For Analysis)

$$\tilde{e}_p(k+1) = \left[V_{Pref}\right] - \left[V_P(k+1)\right]$$

$$= \left[V_{Pref}\right] - [I]_{Np} V_p(k) - \left[\tilde{S}^P_{VV}\right]\left[\Delta V_G(k)\right] - \left[D^P_R\right]$$

$$\tilde{e}_p(k+1) = [I]_{Np}\, \tilde{e}_p(k) - \left[\tilde{S}^P_{VV}\right]\left[\Delta V_G(k)\right] - \left[D^P_R\right] \qquad (7.2.1\text{–}4)$$

7.2.1.2 Control Power Plants

1. The Discrete Descriptions Of The Reactive Power Generation

The discrete descriptions for the reactive generation of the control power plant are:

$$\left[Q_G(k+1)\right] = [I]_{N_G}\left[Q_G(k)\right] + \left[S^Q_{QV}\right]\left[\Delta V_G(k)\right] \qquad (7.2.1\text{–}5)$$

$$\left[Q_G(k+1)\right] = [I]_{N_G}\left[Q_G(k)\right] + \left[\tilde{S}^Q_{QV}\right]\left[\Delta V_G(k)\right] + \left[D^Q_R\right] \qquad (7.2.1\text{–}6)$$

$\left[S^Q_{QV}\right]$ and $\left[\tilde{S}^Q_{QV}\right]$ are the model and actual sensitivity matrices obtained from the Jacobian matrix. The system diagram is shown in Figure 7.2.1-3.

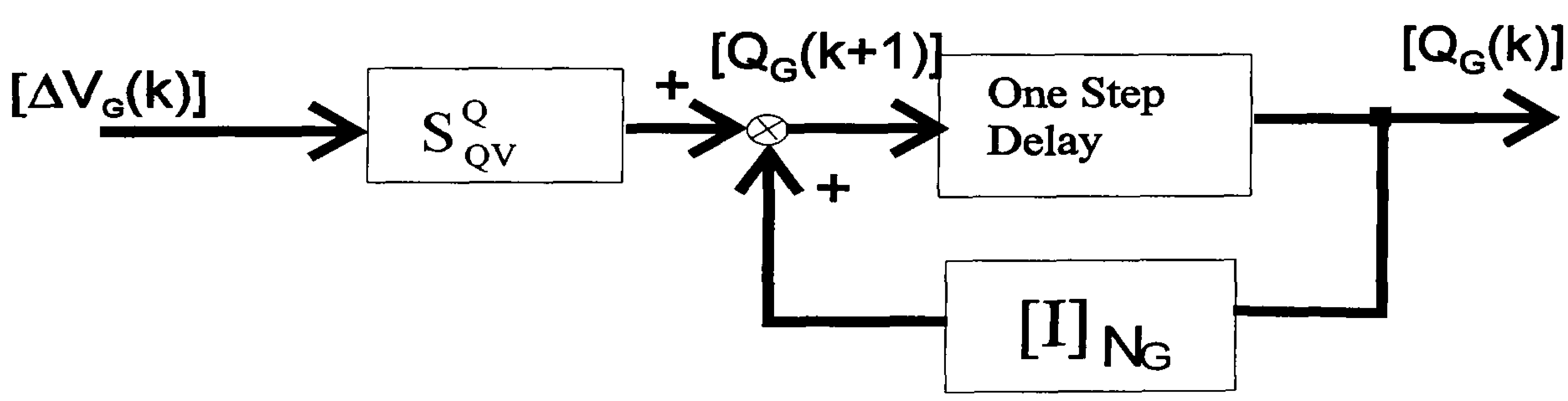

Figure 7.2.1-3 The reactive power generation model

2. System Error Equations

By considering that the reactive generation references will be revised at each control step (see subsection 7.3.1.1), two error equations for the control design and analysis can be written as:

$$e_Q(k+1) = [Q_{Gref}(k+1)] - [Q_G(k+1)]$$
$$= [Q_{Gref}(k)] + M[\Delta d(k)] - [Q_G(k)] - [S_{QV}^{Q}][\Delta V_G(k)] \qquad (7.2.1\text{–}7)$$
$$= [I]_{N_G}\, e_Q(k) + M[\Delta d(k)] - [S_{QV}^{Q}][\Delta V_G(k)]$$

$$\tilde{e}_Q(k+1) = [I]_{N_G}\, \tilde{e}_Q(k) + M[\Delta d(k)] - [\tilde{S}_{QV}^{Q}][\Delta V_G(k)] - [D_R^G] \qquad (7.2.1\text{–}8)$$

7.2.2 Discrete System Descriptions for the PQR

Similarly the discrete system descriptions for the PQR can be produced based on their analogue forms in chapter 5. For control power plant j, in region i of a power system, the three system descriptions for the PQR are:

7.2.2.1 Power plant high voltage bus

1. Discrete System Descriptions

$$V_{Gi}^{j}(k+1) = V_{Gi}^{j}(k) + [S_{VVi}^{Gj}][\Delta V_{gi}^{j}(k)] \qquad (7.2.2\text{–}1)$$

$$V_{Gi}^{j}(k+1) = V_{Gi}^{j}(k) + [\tilde{S}_{VVi}^{Gj}][\Delta V_{gi}^{j}(k)] + [D_{Gi}^{Vj}(k)] \qquad (7.2.2\text{–}2)$$

where,

$[\tilde{S}_{VVi}^{Gj}]$ is the **actual** systems sensitivity matrix;

$[S_{VVi}^{Gj}]$ is the **model** system sensitivity.

2. System Error Equations

$$e_G^V(k+1) = e_G^V(k) - [S_{VVi}^{Gj}][\Delta V_{gi}^{j}(k)] \qquad (7.2.2\text{–}3)$$

$$\tilde{e}_G^V(k+1) = \tilde{e}_G^V(k) - [\tilde{S}_{VVi}^{Gj}][\Delta V_{gi}^{j}(k)] - [D_{Gi}^{Vj}(k)] \qquad (7.2.2\text{–}4)$$

3. **System Controllability**

As V^{j}_{Gi} is a scalar, and $\left[S^{Gj}_{VV}\right] \in \Re^{1XN^{j}_{g}}$, the system is controllable provided $\left[S^{Gj}_{VV}\right] \neq [0]$.

7.2.2.2 Reactive power generation

1. **Discrete System Descriptions**

$$Q^{j}_{Gi}(k+1) = Q^{j}_{Gi}(k) + [S^{Gj}_{QVi}]\left[\Delta V^{j}_{gi}(k)\right] \qquad (7.2.2\text{–}5)$$

$$Q^{j}_{Gi}(k+1) = Q^{j}_{Gi}(k) + [\tilde{S}^{Gj}_{QVi}]\left[\Delta V^{j}_{gi}(k)\right] + \left[D^{Qj}_{Gi}(k)\right] \qquad (7.2.2\text{–}6)$$

where,

$\left[\tilde{S}^{Gj}_{QVi}\right]$ is the **actual** system sensitivity matrix which is for system mis-match analyses,

$\left[S^{Gj}_{QVi}\right]$ is the **model** system sensitivity matrix which is for defining any control law.

2. **System Error Equations**

$$e^{Q}_{G}(k+1) = e^{Q}_{G}(k) - [S^{Gj}_{QVi}]\left[\Delta V^{j}_{gi}(k)\right] \qquad (7.2.2\text{–}7)$$

$$e^{Q}_{G}(k+1) = e^{Q}_{G}(k) - [\tilde{S}^{Gj}_{QVi}]\left[\Delta V^{j}_{gi}(k)\right] - \left[D^{Qj}_{Gi}(k)\right] \qquad (7.2.2\text{–}8)$$

3. **System Controllability**

As Q^{j}_{Gi} is a scalar, and $\left[S^{Gj}_{QVi}\right] \in \Re^{1XN^{j}_{g}}$, the system is controllable provided $\left[S^{Gj}_{QVi}\right] \neq [0]$.

7.2.2.3 Composite system

1. **Discrete System Descriptions**

Joining the above two descriptions for PQR, produces:

$$y_G(k+1) = \begin{pmatrix} V^{j}_{Gi}(k+1) \\ Q^{j}_{Gi}(k+1) \end{pmatrix} = \begin{pmatrix} V^{j}_{Gi}(k) \\ Q^{j}_{Gi}(k) \end{pmatrix} + \begin{pmatrix} \left[S^{Gj}_{VVi}\right] \\ \left[S^{Gj}_{QVi}\right] \end{pmatrix} \left[\Delta V^{j}_{gi}(k)\right] \qquad (7.2.2\text{–}9)$$

$$y_G(k+1) = \begin{pmatrix} V^j_{Gi}(k+1) \\ Q^j_{Gi}(k+1) \end{pmatrix} = \begin{pmatrix} V^j_{Gi}(k) \\ Q^j_{Gi}(k) \end{pmatrix} + \begin{pmatrix} [\tilde{S}^{Gj}_{VVi}] \\ [\tilde{S}^{Gj}_{QVi}] \end{pmatrix} [\Delta V^j_{gi}(k)] + \begin{pmatrix} [D^{Vj}_{Gi}(k)] \\ [D^{Qj}_{Gi}(k)] \end{pmatrix} \qquad (7.2.2\text{–}10)$$

or

$$y_G(k+1) = y_G(k) + [S_G][\Delta V^j_{gi}(k)] \qquad (7.2.2\text{–}11)$$

$$y_G(k+1) = y_G(k) + [\tilde{S}_G][\Delta V^j_{gi}(k)] + D_G(k) \qquad (7.2.2\text{–}12)$$

2. The Composite System Error Equations:

$$e_G(k+1) = \begin{pmatrix} e^V_G(k+1) \\ e^Q_G(k+1) \end{pmatrix} = e_G(k) - [S_G][\Delta V^j_{gi}(k)] \qquad (7.2.2\text{–}13)$$

$$\tilde{e}_G(k+1) = \begin{pmatrix} \tilde{e}^V_G(k+1) \\ \tilde{e}^Q_G(k+1) \end{pmatrix} = \tilde{e}_G(k) - [\tilde{S}_G][\Delta V^j_{gi}(k)] - D_G(k) \qquad (7.2.2\text{–}14)$$

where,

$$S_G = \begin{pmatrix} [S^{Gj}_{VVi}] \\ [S^{Gj}_{QVi}] \end{pmatrix};$$

$$\tilde{S}_G = \begin{pmatrix} [\tilde{S}^{Gj}_{VVi}] \\ [\tilde{S}^{Gj}_{QVi}] \end{pmatrix};$$

$$D_G = \begin{pmatrix} [D^{Vj}_{Gi}] \\ [D^{Qj}_{Gi}] \end{pmatrix}.$$

3. The Composite System Controllability

The dimension of the composite sensitivity matrix S_G is $(2XN^j_{gi})$ where $N^j_{gi} \geq 1$, is the number of the control generators within control plant j in region i.

Thus, the rank condition for the composite system controllability is:

$$\text{rank}(\aleph) = \text{rank}(S_G) \leq \min(2, N^j_{gi}).$$

For the real system sensitivity matrices, this will be rank $(S_G) = 2$ so that the PQR composite system can be completely controllable.

7.3 Control Design

The optimal control design presented in this section covers both centralised and decentralised control schemes.

7.3.1 Centralised Scheme

7.3.1.1 The RVR Design

As discussed before, the RVR aims to maintain a desired voltage value at the pilot bus in each region by regulating the reactive power generations of the regional control power plants. This RVR system is formularised as an optimal control problem. The control targets in this design include both the pilot buses voltages (the first priority) and the reactive generation of the control power plants. This is achieved by minimising the quadratic deviations of the pilot buses voltages and the control plants reactive power generations with respect to their references. The target for the reactive generation is for the best co-ordination of the reactive generations among the control power plants.

1. Reactive Generation Co-ordination

In a decentralised region of a power system, the control power plants may have different reactive generation capacities, and their impacts on the voltage control can be different. Therefore, it is necessary to have a co-ordination among the control power plants in order to

(a) efficiently use reactive generation source to achieve a best voltage control effect,

(b) maximise local reactive generation reserve or best follow the planned reactive generation schedule;

(c) minimise unnecessary reactive power transfer to reduce the voltage control oscillation.

(1) The Reactive Generation Zones

To implement the reactive generation co-ordination, a decentralised region can be further divided into several reactive generation zones. The control power plants in the same zone are electrically close. In each of the zones, a pre-established schedule with reference values are set up for the reactive generation of the control power plants. With respect to the reference value for each control power plant, the best co-ordination can be obtained at each control step by minimising the reactive power generation for the voltage control.

(2) The Displacement Variables

To achieve the reactive generation co-ordination, a displacement free variable d is introduced to each reactive generation zone. With this d variable, the reference values for the reactive power generation of the control power plants can be revised at each control step based on their basic values as

$$[Q_{Gref}] = [Q_{Gref0}] + M[d] \qquad (7.3.1\text{–}1)$$

where,

$[Q_{Gref0}] \in \Re^{N_d \times 1}$ is the vector of the basic reference values for the reactive generation for all the control power plants in a power system,

$M \in \Re^{N_G \times N_d}$ is the schedule matrix containing the slopes for revising the reference values for the reactive generation for all the control power plants. The entry (i,j) is non-zero if the control power plant i belongs to the zone j,

N_d is the number of the reactive generation zones in a whole power system.

Discretizing the equation (7.3.1), yields:

$$[Q_{Gref}(k+1)] = [Q_{Gref}(k)] + M[\Delta d(k)] \qquad (7.3.1\text{–}2)$$

This equation is used for revising the reactive generation references at each control step.

In this optimal control, this variable d will limit the difference between the reactive power generation and its reference. It also has upper and lower bounds, for each zone these bounds can be written as:

$$\mathrm{Max}\left(\frac{Q^j_{G\,min_i} - Q^j_{Gref\,i}}{M^j_i}\right) \le d_i(k) + \Delta d_i(k) \le \mathrm{Min}\left(\frac{Q^j_{G\,max_i} - Q^j_{Gref\,i}}{M^j_i}\right) \quad \forall i \in N_d, \forall j \in N_{Gi}$$

Where,

$[Q_{G\,min}], [Q_{G\,max}]$ are the vector of control power plants reactive generation limits.

2. Formulation

Based on the equations (7.2.1-1) to (7.2.1-8) and (7.3.1-2), the optimisation problem for the RVR can be formularised as:

$$\underset{[\Delta V_{Gref}(k)],[\Delta d(k)]}{\mathrm{Min}} \quad J_R = \left\{ \left\| \alpha[\Delta V_p(k)] - [S^P_{VV}][\Delta V_{Gref}(k)] \right\|^2 \right.$$
$$\left. + q_0 \left\| \alpha([Q_{Gref}] + M[\Delta d(k)] - [Q_G(k)]) - [S^Q_{QV}][\Delta V_{Gref}(k)] \right\|^2 + \delta \left\| [\Delta d(k)] \right\|^2 \right\}$$

(7.3.1–3)

Subject to:

$$[V_{G\,min}] \le [V_G(k)] + [\Delta V_{Gref}(k)] \le [V_{G\,max}]$$

$$[Q_{G\,min}] \le [Q_G(k)] + [S^Q_{QV}][\Delta V_{Ggref}(k)] \le [Q_{G\,max}]$$

$$[\Delta V_{Gref}(k)] \le [|\Delta V_{G\,max}|]$$

$$[V_{c\,min}] \le [V_c(k)] + [S^c_{cv}][\Delta V_{Gref}(k)] \le [V_{c\,max}]$$

$$\mathrm{Max}\left(\frac{Q^j_{G\,min_i} - Q^j_{Gref\,i}}{M^j_i}\right) \le d_i(k) + \Delta d_i(k) \le \mathrm{Min}\left(\frac{Q^j_{G\,max_i} - Q^j_{Gref\,i}}{M^j_i}\right)$$

$$\forall i \in N_d, \forall j \in N_{Gi}$$

where,

N_d is the number of the zones in a power system,

$[d(k)]$ the vector of displacement for each generation zone at time instant k. Its dimension is (N_d x1),

δ a weighting factor,

$[V_{G\min}], [V_{G\max}]$ are the vector of control power plant HV bus voltage limits within the power system,

$[Q_{G\min}], [Q_{G\max}]$ are the vector of control power plants reactive generation limits within the whole power system,

$[V_c]$ is the vector of critical bus voltages,

$[S^c_{cv}]$ is the sensitivity matrix between the critical bus voltages and the control power plant high voltages for the whole power system,

$[V_{c\min}], [V_{c\max}]$ are the vector of the critical bus voltage limits for the whole power system,

α is a weighting factor which determines the closed loop regulator time constant,

q is a weighting factor between pilot bus voltages and reactive power generation.

3. Remarks

It is not difficult to see that in the cost function J, the first two items are the voltage deviation of the pilot buses and the reactive generation deviation of the control power plants at time instant K+1 with a de-tuning factors α and q. The third item is simply a part of the control. These three items together form a basic quadratic programming problem for the RVR.

7.3.1.2 The PQR Design

1. Formulation

Similarly the PQR can also be formularised as an optimal control problem. This optimal control is to minimise the quadratic deviations of the HV bus voltages and the reactive generations at the control power plants with respect to their references.

Based on equations (7.2.2-1) to (7.2.2-8) in Subsection 7.2.2, the PQR optimal control problem can be formularised as below. The reactive power term in the objective function is weighted by a factor P_0 to reflect the importance level to the voltage term.

$$\underset{[\Delta V_{gi}^{j}(k)]}{\text{Min}}\left\{\left\|\Delta V_{Gi}^{j}(k)-\left[S_{VVi}^{Gj}\right]\left[\Delta V_{gi}^{j}(k)\right]\right\|^{2}+p_{0}\left\|\Delta Q_{Gi}^{j}(k)-\left[S_{QVi}^{Gj}\right]\left[\Delta V_{gi}^{j}(k)\right]\right\|^{2}\right\} \quad (7.3.1\text{–}4)$$

Subject to:

$$\left[V_{g\min i}^{j}\right]\leq\left[V_{gi}^{j}(k)\right]+\left[\Delta V_{gi}^{j}(k)\right]\leq\left[V_{g\max i}^{j}\right]$$

$$\left[Q_{g\min i}^{j}\right]\leq\left[Q_{gi}^{j}(k)\right]+\left[S_{QVi}^{Gj}\right]\left[\Delta V_{gi}^{j}(k)\right]\leq\left[Q_{g\max i}^{j}\right]$$

$$\left[\left|\Delta V_{gi}^{j}(k)\right|\right]\leq\Delta V_{g\max i}^{j}$$

$$-\delta\leq\frac{Q_{gi}^{jk}}{Q_{g\lim i}^{jk}}-\frac{Q_{gi}^{jm}}{Q_{g\lim i}^{jm}}\leq\delta,\ \forall k,m\in N_{gi}^{j}$$

where

$\left[V_{g\min i}^{j}\right],\left[V_{g\max i}^{j}\right],\left[Q_{g\min i}^{j}\right],\left[Q_{g\max i}^{j}\right]$ are the variable limits in the vector form,

Q_{gi}^{jk},Q_{gi}^{jm} are the reactive generations of generator k and generator m in the same control power plant j in the region i,

$\left[S_{QVi}^{Gj}\right]$ is the sensitivity matrix between reactive generations and voltages for the control generators in control power plant j,

$Q_{g\lim i}^{jk}$ and $Q_{g\lim i}^{jm}$ are the maximum or minimum limits for Q_{gi}^{jk},Q_{gi}^{jm},

δ is a pre-established tolerance value.

2. Discussions

From the costing function, it can be seen that this PQR control is a typical quadratic programming problem with constraints. And the last constraint ensures that the demanded reactive power generation is evenly shared among the control generators within a control power plant.

7.3.2 Decentralised Control Scheme

For the decentralised control scheme, the PQR control structure will remain the same as the centralised one. Applying the RVR optimal control law to each decentralised region i =1, 2, ..., Z, the decentralised RVR control design can be obtained as:

$$\underset{[\Delta V_{Grefi}(k)],[\Delta d_i(k)]}{\text{Min}} \quad J_R = \left\{ \left\| \alpha \Delta V_{Pi}(k) - [S^P_{VVi}][\Delta V_{Gref\,i}(k)] \right\|^2 \right.$$
$$\left. + q_0 \left\| \alpha([Q_{Grefi}] + M_i[\Delta d_i(k)] - [Q_{Gi}(k)]) - [S^Q_{QVi}][\Delta V_{Grefi}(k)] \right\|^2 + \delta \left\| [\Delta d_i(k)] \right\|^2 \right\}$$

(7.3.2–1)

Subject to:

$$[V_{G\min i}] \le [V_{Gi}(k)] + [\Delta V_{Grefi}(k)] \le [V_{G\max i}]$$

$$[Q_{G\min i}] \le [Q_{Gi}(k)] + [S^Q_{QVi}][\Delta V_{Ggrefi}(k)] \le [Q_{G\max i}]$$

$$[\Delta V_{Grefi}(k)] \le [|\Delta V_{G\max i}|]$$

$$[V_{c\min i}] \le [V_{ci}(k)] + [S^c_{cvi}][\Delta V_{Grefi}(k)] \le [V_{c\max i}]$$

$$\text{Max}\left(\frac{Q^j_{\min i} - Q^j_{Gref\,i}}{M^j_i} \right) \le d_i(k) + \Delta d_i(k) \le \text{Min}\left(\frac{Q^j_{\max i} - Q^j_{Gref\,i}}{M^j_i} \right)$$

$$\forall i \in N_{di}, \forall j \in N_{Gi}$$

where,

N_{di} is the number of the zones in the decentralised region i,

$[d_i(k)]$ the vector of displacement for generation zone in region i,

M_i is a $N_{Gi}xN_{di}$ matrix containing the slope of working line for control power plants in region i,

δ a weighting factor,

$\left[V_{G\min i}\right], \left[V_{G\max i}\right]$ are the vector of control power plant HV bus voltage limits in region i,

$\left[Q_{G\min i}\right], \left[Q_{G\max i}\right]$ are the vectors of control power plants reactive generation limits in region i,

$\left[V_{ci}\right]$ the vector of critical bus voltages in region i,

$\left[S^{P}_{VVi}\right] \left[S^{c}_{cvi}\right] \left[S^{Q}_{QVi}\right]$ are the sensitivity matrices between the pilot bus voltages, critical bus voltages, the control power plant reactive generations and the HV voltage of control power plant in region i,

$\left[V_{c\min i}\right], \left[V_{c\max i}\right]$ are the vectors of the critical bus voltage limits in region i,

α is a weighting factor which determines the closed loop system time constant,

q is a weighting factor between pilot bus voltages and reactive power generation.

It is emphasised that in the cost function here, the $\Delta V_{Pi}(k)$ is a scalar rather than a vector. This is because that that there is only one pilot bus in each decentralised region.

7.4 STABILITY ANALYSIS

7.4.1 Technical Background

To analysis the stability of this optimal control based system, it is useful to review some basic concepts about the modern control theory.

7.4.1.1 Dynamic system equation and controllability

For a linear discrete state space system:

$$\Sigma\!: \quad x(k+1) = Ax(k) + Bu(k) \qquad x(k)\varepsilon\ \Re^{n}, u(k)\varepsilon\ \Re^{m}$$

The system is completely controllable if all the system modes are accessible from the input u(k). This can be tested by the rank condition

$$\text{rank}\ [\aleph] = \text{rank}\ [B, AB, A^2B,\ldots, A^{n-1}B] = n,$$

where, n = order of the system.

Note that if the dynamic system condition is pair (A,B) stabilizable, then all the uncontrolled modes of the system must be asymptotically stable, and hence have modules less than unity.

7.4.1.2 The Receding horizon principle

This is the principle that although an optimal control sequence has been obtained from the current instance to N steps ahead, only the current optimal control u(K) is implemented.

7.4.1.3 Null controllability

The concept of null controllability plays an important role in discussions of constrained problems. System Σ is asymptotically null controllable using controls in set U ε $\Re^m$ if and only if for each x(o) ε $\Re^n$, there is an input sequence $\{u(k)\}_{k=0}^{\infty}$ such that $x(k+1) \to 0\ \varepsilon\ \Re^n$ as $k \to \infty$. Further if for each x(o), there is a finite input sequence $\{u(k)\}_{k=o}^{N}$ for some N such that x(N+1) = 0 then Σ is known as null controllable. (Sontag, 1984).

Basically this concept is needed to see if it is possible to move from any (initial) state x(o) to the origin in a finite number of steps.

7.4.1.4 Null controllability theorem

Consider the discrete linear dynamic system: $x(k+1) = Ax(k) + Bu(k)$ with $x_o = x^*$ where pair (A,B) is completely controllable. Denote by $\lambda_i \varepsilon C$, the eigenvalues of A, then:

(i) If λ_i lie in the closed unit disc ($|\lambda_i| \leq 1$), then for all $x^* \varepsilon \Re^n$ and for all $\varepsilon > o$, there exists integer N finite, and a sequence of controls $\{u(k) \in \Re^m; k = 0, 1, 2, \ldots, N-1\}$ with $|u_j(k)| \leq \varepsilon$, $j=1,\ldots m$ such that if $x_o = x^*$, then $x(N) = 0$.

(ii) If at least one λ_i lies outside the closed unit disc ($|\lambda_i| > 1$ for some, i), then for all $\varepsilon > 0$ and every sequence of control $\{u(k) \in \Re^m;\ k = 0,1,\ldots, N-1\}$ with $|u_j(k)| \leq \varepsilon$, $j = 1,\ldots,m$, if $x_o = x^*$ then $x(N) \neq 0 \ \varepsilon \ \Re^n$. **Proof** (Tsirukis and Morari, 1992)

Part (i) of the theorem guarantees the existence of a control sequence, of bounded magnitude which can move the system from any x^* to the origin. The required conditions are:

(a) $|\lambda_i (A)| \leq 1$; $i = 1,\ldots,n$

(b) Pair (A,B) completely controllable.

Part (ii) of the theorem states that this is not true if just one λ_i (A) lies outside the unit disc.

7.4.1.5 Introducing the constraints

Practical constraints are generally hard constraints for control inputs and are soft constraints when levied on system states or outputs. The usual practical constraints are:

Input magnitude constraints:

$$u_i^{min}(k) \le u_i(k) \le u_i^{max}(k) \qquad i = 1,\ldots,m; \quad k = 0,1,\ldots$$

Input rate constraints:

$$\Delta u_i^{min}(k) \le \Delta u_i(k) \le \Delta u_i^{max}(k) \qquad i = 1,\ldots,m; \quad k = 0,1,\ldots$$

State magnitude constraints:

$$x_i^{min}(k) \le x_i(k) \le x_i^{max}(k) \qquad i = 1,\ldots,n; \quad k = 0,1,\ldots$$

Output magnitude constraints:

$$y_i^{min}(k) \le y_i(k) \le y_i^{max}(k) \qquad i = 1,\ldots,r; \quad k = 0,1,\ldots$$

or equivalently using $y(k) = Cx(k)$

$$y_i^{min}(k) \le \sum_{j=1}^{n} C_{ij} x_j(k) \le y_i^{max}(k)$$

7.4.1.6 Formal constraints and feasibility

All of the above input and state (output) constraints become (in vector notation):

$$Du(k) \le d \qquad k = 0, 1,\ldots$$

$$Hx(k) \le h \qquad k = 1, 2,\ldots$$

For stability purposes, these constraints are assumed to be specified on the infinite time horizon. The control optimisation uses a finite time control sequence $\{u(k+j)\}_{j=0}^{N-1}$, hence the control constraints are reduced to a finite set at each optimisation, namely,

$$Du(k+j) \le d \qquad j = 0, \ldots, N\text{-}1 \;;\; k = 0, 1,\ldots$$

The state constraints on $k = 1, 2,\ldots, \infty$ may be unfeasible particularly for small k, as many examples have been able to demonstrate. Obtaining a set of feasible constraints is essential for a global stability result, otherwise no controller exists for the problem. For difficult systems (those which are unstable) unfeasible state constraints pose a particular problem, since the existence of a feasible solution is a precursor to a closed loop stable system. Two particular solutions have been proposed in the literature.

1. **Constraint Deletion (Rawlings and Muske, 1993)**

In this approach, for small time index $k < k_1$ the state constraints are deleted so that the state constraints become feasible on the infinite time interval

hence

$$Hx(k) \leq h \qquad k = k_1, k_1+1, \ldots, \infty$$

2. **Constraint softening (Zheng and Morari, 1995)**

In this approach, the unfeasible state constraints are managed by the introduction of a slack variable η "softens" these constraints:

$$Hx(k) \leq d + \eta(k)$$

The slack variable which also appears in the cost function:

$$J_s = J_k + \eta^T(k) Q \eta(k)$$

The optimisation is also with respect to the slack variable.

7.4.1.7 The Quadratic Programming Problem

All the control optimisation problems result in a Quadratic Programming (QP) problem, and it is useful to review the fundamentals of such problems. A formal definition of a QP problem is given as (Fletcher, 1987):

$$\underset{\text{w.r.t. } x}{\text{minimise}} \quad J(x) = x^T G x + 2g^T x$$

Subject to $\quad a_i^T x = b_i \qquad i = 1,\ldots,n_i$

and $\quad c_j^T x \leq d_j \qquad j = 1,\ldots,n_j$

where $\quad x,\ a_i, a_j\ \varepsilon \Re^n$.

The matrix G can always be arranged to be symmetric, but it is its definiteness which impacts on the nature of the solution (after allowing for possibilities that the problem may be unfeasible or the solution unbounded). Assuming a solution x^o exists, then if $G \geq 0$, x^o is a global solution and if $G > 0$ then x^o is also a unique solution.

In the situation where on-line QP optimisation occurs, it seems essential to ensure that the QP routine is numerically robust. Extending the minimum error norm cost function to incorporate a positive-definite control cost is one useful way of ensuring this robustness.

7.4.1.8 Closed Loop Stability

Proving closed loop stability in the presence of "hard" actuator/input/control constraints and "soft" output/state constraints has only recently been identified as an urgent research issue. The reason for this interest is the successful industrial application of finite and infinite receding horizon model based predictive control in both unconstrained and constrained varieties. Despite this application success, the search for guaranteed properties is of considerable practical and theoretical value. Four questions are under investigation:

(i) Under what conditions is the control problem feasible on the infinite time axis?

(ii) Under what conditions is the closed loop control problem asymptotically stable?

(iii) What are the stability robustness properties of optimisation controllers? Is stability preserved with model mismatch? How much model mis-match can be tolerated?

(iv) What are the performance robustness and disturbance rejection properties when model mismatch is present?

7.4.2 Stability Analysis for the Centralised Control System

7.4.2.1 The RVR

Re-writing the RVR control design for the centralised control scheme:

$$\underset{[\Delta V_{Gref}(k)],[\Delta d(k)]}{\text{Min}} J_R = \Big\{ \big\| \alpha[\Delta V_p(k)] - [S_{VV}^P][\Delta V_{Gref}(k)] \big\|^2$$

$$+ q_0 \big\| \alpha([Q_{Gref}] + M[\Delta d(k)] - [Q_G(k)]) - [S_{QV}^Q][\Delta V_{Gref}(k)] \big\|^2 + \delta \big\| [\Delta d(k)] \big\|^2 \Big\}$$

Subject to:

$$[V_{G\min}] \le [V_G(k)] + [\Delta V_{Gref}(k)] \le [V_{G\max}]$$

$$[Q_{G\min}] \le [Q_G(k)] + [S_{QV}^Q][\Delta V_{Ggref}(k)] \le [Q_{G\max}]$$

$$[\Delta V_{Gref}(k)] \le [|\Delta V_{G\max}|]$$

$$[V_{c\min}] \le [V_c(k)] + [S_{cV}^c][\Delta V_{Gref}(k)] \le [V_{c\max}]$$

$$\text{Max}\left(\frac{Q^j_{G\min i} - Q^j_{Gref i}}{M_i^j} \right) \le d_i(k) + \Delta d_i(k) \le \text{Min}\left(\frac{Q^j_{G\max i} - Q^j_{Gref i}}{M_i^j} \right)$$

$$\forall i \in N_d, \forall j \in N_{Gi}$$

1. Controllability/Null controllability

Recalling the discrete system descriptions of pilot buses and control power plants:

$$[V_p(k+1)] = [I]_{Np}[V_p(k)] + [S_{VV}^P][\Delta V_G(k)] \tag{7.4.2–1}$$

$$e_p(k+1) = [I]_{Np} e_p(k) - [S_{VV}^P][\Delta V_G(k)] \tag{7.4.2–2}$$

$$[Q_G(k+1)] = [I]_{N_G}[Q_G(k)] + [S_{QV}^Q][\Delta V_G(k)] \tag{7.4.2–3}$$

$$e_Q(k+1) = [I]_{N_G}\, e_Q(k) + M[\Delta d(k)] - [S^Q_{QV}][\Delta V_G(k)] \qquad (7.4.2\text{–}4)$$

Regarding both $\Delta V_G(k)$ and $\Delta d(k)$ as the control variables, two different composite systems can be formed by combining the equations(7.4.2-1), (7.4.2-2), and (7.4.2-3), (7.4.2-4):

Composite system 1 $\quad y(k+1) = [I]_{Np+N_G}\, y(k) + S'_R\,[\Delta U(k)] \qquad (7.4.2\text{–}5)$

Composite system 2 $\quad e_R(k+1) = [I]_{Np+N_G}\, e_R(k) - S_R\,[\Delta U(k)] \qquad (7.4.2\text{–}6)$

where,

$$y(k+1) \triangleq \begin{pmatrix} [V_p(k+1)] \\ [Q_G(k+1)] \end{pmatrix} \in \Re^{Np+N_G}; \qquad e_R(k+1) \triangleq \begin{pmatrix} e_p(k+1) \\ e_Q(k+1) \end{pmatrix} \in \Re^{Np+N_G};$$

$$S'_R = \begin{bmatrix} S^P_{VV} & 0 \\ S^Q_{QV} & 0 \end{bmatrix} \in \Re^{(N_P+N_G)X(N_G+N_d)}; \qquad S_R = \begin{bmatrix} S^P_{VV} & 0 \\ S^Q_{QV} & -M \end{bmatrix} \in \Re^{(N_P+N_G)X(N_G+N_d)};$$

$$U(k) \triangleq \begin{pmatrix} [\Delta V_G(k)] \\ [\Delta d(k)] \end{pmatrix} \in \Re^{N_G+N_d}.$$

(1) The composite system 1

This system is made directly by combining the pilot bus subsystem and the control power plant subsystem. It can be known that:

$$\text{Rank}(S'_R) = \text{Rank}\begin{bmatrix} S^P_{VV} & 0 \\ S^Q_{QV} & 0 \end{bmatrix} = N_G < N_P + N_G \text{ (system order)},$$

therefore, the composite system 1 is not completely controllable.

This tells that it is not feasible to control both the pilot bus voltages and the reactive generation of the control power plant by directly combining the two sub-systems. The reason is that in the viewpoint of a power system, these two sub-systems are linear independent. This can be proven using the system descriptions for the control design:

The system description for pilot buses gives

$$\left[\Delta V_p(k)\right] = \left[V_p(k+1)\right] - [I\ ]_{Np}\left[V_p(k)\right] = [S_{VV}^P][\Delta V_G(k)]$$

And the system description for control power plants gives

$$[\Delta Q_G(k)] = [Q_G(k+1)] - [I]_{N_G}[Q_G(k)] = \left[S_{QV}^Q\right][\Delta V_G(k)]$$

Assuming $\left[S_{QV}^Q\right]$ is invertible, it is known from equation (5.3.2-5)

$$\left[\Delta V_p(k)\right] - \left[S_{VV}^P\right]\left[S_{QV}^Q\right]^{-1}[\Delta Q_G] = [0] \qquad (7.4.2\text{–}7)$$

Hence, the pilot bus subsystem and the control power plant subsystem are linear independent.

(2) The composite system 2

This is actually the error system of the composite system 1 revised with the reactive power co-ordination scheme. The displacement variable d is introduced into this system through the reactive generation co-ordination. The optimal control design for RVR is based on this system.

As $\mathrm{Rank}(S_R) = \mathrm{Rank}\begin{bmatrix} S_{VV}^P & 0 \\ S_{QV}^Q & -M \end{bmatrix} \le N_G + N_d > N_P + N_G$ (normally $N_d > N_P$), the system is completely controllable.

Furthermore, the eigenvalues magnitudes $\left|\lambda_i(I_{N_P+N_G})\right| = 1$, I=1, 2, ..., ($N_P+N_G$), from the Null controllability theorem in Subsection 7.4.1.4, it is known that the system is also null controllable. This shows that it is possible to move the errors with all system modes to zero in a finite number of steps.

Note that the reason why the composite system 2 is controllable is that, by using the displacement variable d, the control references for the reactive generation of the control power plants will be revised at each control step. Effectively the reactive power generation sub-system is revised so that it is no longer linear independent with the pilot bus sub-system.

With consideration of the disturbances D_R, the composite system 2 for model mismatch analysis can be obtained as:

$$\tilde{e}_R(k+1) = [I]_{Np+N_G}\,\tilde{e}_R(k) - \tilde{S}_R[\Delta U(k)] - D_R(k) \qquad (7.4.2\text{–}8)$$

where,

$$D_R = \begin{bmatrix} D_R^P \\ D_R^G \end{bmatrix}, \qquad \tilde{S}_R = \begin{bmatrix} \tilde{S}_{VV}^P & 0 \\ \tilde{S}_{QV}^Q & -M \end{bmatrix} \in \Re^{(N_P+N_G)X(N_G+N_d)}.$$

2. Stability Analysis

Rearrange the costing function for the RVR:

$$\begin{aligned} J_R &= \left\| \alpha[\Delta V_p(k)] - [S_{VV}^P][\Delta V_{Gref}(k)] \right\|^2 \\ &\quad + q_0 \left\| \alpha([Q_{Gref}] + M[\Delta d(k)] - [Q_G(k)]) - [S_{QV}^Q][\Delta V_{Gref}(k)] \right\|^2 + \delta \left\| [\Delta d(k)] \right\|^2 \\ &= \left\| \alpha e_p(k) - [S_{VV}^P][\Delta V_{Gref}(k)] \right\|^2 \\ &\quad + q_0 \left\| \alpha e_Q(k) + \alpha M[\Delta d(k)] - [S_{QV}^Q][\Delta V_{Gref}(k)] \right\|^2 + \delta \left\| [\Delta d(k)] \right\|^2 \end{aligned}$$

$$J_R = (\alpha e_R(k) - SU(k))^T q(\alpha e_R(k) - SU(k)) + U^T(k)RU(k)$$

where,

$$S = \begin{bmatrix} S_{VV}^P & 0 \\ S_{QV}^Q & -\alpha M \end{bmatrix} \in \Re^{(N_P+N_G)X(N_G+N_d)}; \quad q = \begin{bmatrix} I_{N_P} & 0 \\ 0 & q_0 I_{N_G} \end{bmatrix} \in \Re^{(N_P+N_G)X(N_P+N_G)};$$

$$R = \begin{bmatrix} 0 & 0 \\ 0 & \delta I_{N_d} \end{bmatrix} \in \Re^{(N_G+N_d)X(N_G+N_d)}; \qquad e_R(k) \triangleq \begin{pmatrix} e_p(k) \\ e_Q(k) \end{pmatrix} \in \Re^{Np+N_G};$$

$$U(k) \triangleq \begin{pmatrix} \Delta V_{Gref}(k) \\ \Delta d(k) \end{pmatrix} \in \Re^{Np+N_G}; \qquad [\Delta d(k)] \in \Re^{N_d}$$

Hence,

$$J_R = \alpha^2 e_R{}^T(k) q e_R(k) - 2\alpha U(k) S^T q e_R(k) + U^T(k)\left[S^T q S + R\right]U(k)$$

(1) Without considering the constraints:

For optimality

$$\frac{1}{2}\frac{\partial J_R}{\partial U(k)} = -\alpha S^T q e_R(k) + \left[S^T q S + R\right]U(k) = 0$$

$$\begin{aligned} U(k) &= \alpha\left[S^T q S + R\right]^{-1} S^T q e_R(k) \\ &= K e_R(k) \end{aligned}$$

Where, $K = \alpha\left[S^T q S + R\right]^{-1} S^T q$ is the unconstrained control law.

(2) By considering the constraints

Using the unconstrained control law, the feasibility of the control design is assumed to ensure that there exists $\alpha = \alpha_0$ so that

$$\begin{aligned} U(k) &= \alpha_0\left[S_0{}^T q S_0 + R\right]^{-1} S_0{}^T q e_R(k) \\ &= K_0 e_R(k) \end{aligned}$$

will obey all the active constraints. Where, $K_0 = \alpha_0\left[I_{N_G} \quad 0\right]\left[S_0{}^T q S_0 + R\right]^{-1} S_0{}^T q$ is the constrained control law, this is equivalent to a detuned sub-optimal control law.

Recalling the composite error equation for model mismatch analysis:

$$\tilde{e}_R(k+1) = [I]_{Np+N_G}\,\tilde{e}_R(k) - \tilde{S}_R U(k) - D_R(k)$$

By considering

$$U(k) = K_0 \tilde{e}(k)$$

then,

$$\begin{aligned}\tilde{e}_R(k+1) &= [I]_{Np+N_G}\,\tilde{e}_R(k) - \tilde{S}_R K_0 \tilde{e}_R(k) - D_R(k)\\ &= \left[I_{Np+N_G} - \alpha_0 \tilde{S}_R \left[S_0{}^T q S_0 + R\right]^{-1} S_0{}^T q\right]\tilde{e}_R(k) - D_R(k)\\ &= \Phi_R\,\tilde{e}_R(k) - D_R(k)\end{aligned}$$

and

$$\tilde{e}_R(k+n) = (\Phi_R)^n \tilde{e}_R(k) - \sum_{j=1}^{n} (\Phi_R)^{j-1} D_R(k+n-j)$$

Where, $\Phi_R = \left[I_{Np+N_G} - \alpha_0 \tilde{S}_R \left[S_0{}^T q S_0 + R\right]^{-1} S_0{}^T q\right]$

For (a) closed loop stability and

(b) disturbance rejection for a disturbance of finite duration,

it is required that

$$\lim_{n\to\infty} (\Phi_R)^n = 0 \qquad (7.4.2\text{–}9)$$

By eigenvector-eignevalue decomposition:

$$\Phi_R = \Gamma \Lambda \Gamma^{-1}$$

where,

$\Lambda = \mathrm{diag}\{\lambda_1(\Phi_R), \lambda_2(\Phi_R), \ldots, \lambda_{N_{P+}N_G}(\Phi_R)\}$,

$\lambda_i(\Phi_R)$, i=1, 2, ..., N_P+N_G are the eigenvalues of the matrix Φ_R,

$\Gamma \in \Re^{(N_P+N_G)X(N_P+N_G)}$.

Thus, the equation (7.4.2-9) becomes:

$$\lim_{n\to\infty}(\Phi_R)^n = \lim_{n\to\infty}\Gamma(\Lambda)^n\Gamma^{-1} = \lim_{n\to\infty}\Gamma\,\mathrm{diag}\{(\lambda_1(\Phi_R))^n, (\lambda_1(\Phi_R))^n, \ldots, (\lambda_1(\Phi_R))^n\}\Gamma^{-1} = 0$$

Therefore, a necessary and sufficient condition for the closed loop stability and disturbance rejection is

$$|\lambda_i(\Phi_R)| < 1, \quad i=1, 2, \ldots, N_P+N_G$$

where

$$\Phi_R = \left[I_{N_P+N_G} - \alpha_0 \begin{bmatrix} \widetilde{S}_{VV}^{P} & 0 \\ \widetilde{S}_{QV}^{Q} & -M \end{bmatrix} \begin{bmatrix} \left(S_{VV}^{P}\right)^T S_{VV}^{P} + q_0 \left(S_{QV}^{Q}\right)^T S_{QV}^{G} & -\alpha_0 q_0 \left(S_{QV}^{Q}\right)^T M \\ -\alpha_0 q_0 M^T S_{QV}^{Q} & \alpha_0^2 q_0 M^T M + \delta I_{N_d} \end{bmatrix}^{-1} \cdot \begin{bmatrix} \left(S_{VV}^{P}\right)^T & q_0 \left(S_{QV}^{Q}\right)^T \\ 0 & -\alpha_0 q_0 M^T \end{bmatrix} \right]$$

(7.4.2–10)

3. Discussions

(1) The composite system 1 is direct combination of the pilot bus and reactive power generation sub-systems. As these two subsystems are linear independent, the composite system 1 is not completely controllable. This shows that it is unfeasible to design a controller to achieve the desired control targets with this composite system.

(2) With the reactive generation co-ordination scheme, the composite system 2 (in the form of errors) can be re-structured based on the two sub-systems. It has been seen that this composite system 2 is completely controllable and null controllable. This guarantees that it is possible to design a controller to move

all the output of the system modes to the reference values in the finite number of steps. As the optimal control design for the RVR is based on this composite system 2, the feasibility of this control design is theoretically ensured.

(3) The stability analysis shows that, when the condition $|\lambda_i(\Phi_R)| < 1$, i=1, 2, ..., N_P+N_G, is satisfied, the system will be closed loop stable, and the satisfactory reference tracking and disturbance rejection will be well achieved with all the outputs of the system modes. The outputs include the pilot buses voltages and the reactive generation co-ordination scheme.

(4) In the case of perfect model mismatch, $\tilde{S}_R = S_R = \begin{bmatrix} S_{VV}^P & 0 \\ S_{QV}^Q & -M \end{bmatrix}$,

$$\Phi_R = \left[I_{N_P+N_G} - \alpha_0 \begin{bmatrix} S_{VV}^P & 0 \\ S_{QV}^Q & -M \end{bmatrix} \begin{bmatrix} \left(S_{VV}^P\right)^T S_{VV}^P + q_0 \left(S_{QV}^Q\right)^T S_{QV}^G & -\alpha_0 q_0 \left(S_{QV}^Q\right)^T M \\ -\alpha_0 q_0 M^T S_{QV}^Q & \alpha_0^2 q_0 M^T M + \delta I_{N_d} \end{bmatrix}^{-1} \cdot \begin{bmatrix} \left(S_{VV}^P\right)^T & q_0 \left(S_{QV}^Q\right)^T \\ 0 & -\alpha_0 q_0 M^T \end{bmatrix} \right]$$

This shows that the closed loop properties of this control system are related to model mismatch of the control design.

7.4.2.2 The PQR

Re-writing the PQR control design:

$$\underset{[\Delta V_{gi}^j(k)]}{\mathrm{Min}} J_G = \left\{ \left\| \Delta V_{Gi}^j(k) - \left[S_{VVi}^{Gj}\right]\left[\Delta V_{gi}^j(k)\right] \right\|^2 + p_0 \left\| \Delta Q_{Gi}^j(k) - \left[S_{QVi}^{Gj}\right]\left[\Delta V_{gi}^j(k)\right] \right\|^2 \right\}$$

Subject to:

$$\left[V_{g\min i}^j\right] \le \left[V_{gi}^j(k)\right] + \left[\Delta V_{gi}^j(k)\right] \le \left[V_{g\max i}^j\right]$$

$$\left[Q_{g\min i}^j\right] \le \left[Q_{gi}^j(k)\right] + \left[S_{QVi}^{gj}\right]\left[\Delta V_{gi}^j(k)\right] \le \left[Q_{g\max i}^j\right]$$

$$\left[\left\|\Delta V_{gi}^{j}(k)\right\|\right] \le \Delta V_{g\max i}^{j}$$

$$-\delta \le \frac{Q_{gi}^{jk}}{Q_{g\lim i}^{jk}} - \frac{Q_{gi}^{jm}}{Q_{g\lim i}^{jm}} \le \delta, \forall k, m \in N_{gi}^{j}$$

1. Controllability/Null controllability

Recalling the composite discrete system descriptions for PQR:

$$y_G(k+1) = [I]_2 y_G(k) + S_G\left[\Delta V_{gi}^{j}(k)\right] \qquad (7.4.2\text{–}11)$$

$$e_G(k+1) = [I]_2 e_G(k) - S_G\left[\Delta V_{gi}^{j}(k)\right] \qquad (7.4.2\text{–}12)$$

where,

$$y_G(k+1) \triangleq \begin{pmatrix} V_{Gi}^{j}(k+1) \\ Q_{Gi}^{j}(k+1) \end{pmatrix} \in \Re^{2N_{gi}^{j}}; \qquad e_G(k+1) \triangleq \begin{pmatrix} e_G^{V}(k+1) \\ e_G^{Q}(k+1) \end{pmatrix} \in \Re^{2};$$

$$S_G = \begin{bmatrix} S_{VVi}^{Gj} \\ S_{QVi}^{Gj} \end{bmatrix} \in \Re^{2XN_{gi}^{j}}.$$

As $\mathrm{Rank}(S_G) = 2$, the system is completely controllable.

Furthermore, the eigenvalues magnitudes $|\lambda_i(I_2)| = 1$, i=1, 2, therefore the system is also null controllable. Thus, from the error equation (7.4.2-12) it is known that it is possible to remove the system errors in a finite number of control steps.

2. Stability Analysis

Rearrange the costing function

$$\begin{aligned} J_G &= \left\|\Delta V_{Gi}^{j}(k) - \left[S_{VVi}^{Gj}\right]\left[\Delta V_{gi}^{j}(k)\right]\right\|^2 + p_0\left\|\Delta Q_{Gi}^{j}(k) - \left[S_{QVi}^{Gj}\right]\left[\Delta V_{gi}^{j}(k)\right]\right\|^2 \\ &= \left\|e_G^{V}(k) - \left[S_{VVi}^{Gj}\right]\left[\Delta V_{gi}^{j}(k)\right]\right\|^2 + p_0\left\|e_G^{Q}(k) - \left[S_{VVi}^{Gj}\right]\left[\Delta V_{gi}^{j}(k)\right)\right\|^2 \end{aligned}$$

$$J_G = (e_G(k) - S_G \Delta V_{gi}^{j}(k))^T P (e_G(k) - S_G \Delta V_{gi}^{j}(k))$$

Where,

$$P = \begin{bmatrix} I_2 & 0 \\ 0 & p_0 I_2 \end{bmatrix} \in \Re^{4X4}$$

Hence,

$$J_G = e_G{}^T(k) P e_G(k) - 2\left(\Delta V_{gi}^j(k)\right)^T S_G{}^T P e_G(k) + \left(\Delta V_{gi}^j(k)\right)^T \left[S_G{}^T P S_G\right] \Delta V_{gi}^j(k)$$

(1) Without considering the constraints

For optimality

$$\frac{1}{2}\frac{\partial J_G}{\partial \Delta V_{gi}^j(k)} = -S_G{}^T P e_G(k) + S_G{}^T P S_G \Delta V_{gi}^j(k) = 0$$

$$\begin{aligned} \Delta V_{gi}^j(k) &= \left[S_G{}^T P S_G\right]^{-1} S_G{}^T P e_G(k) \\ &= K_G e_G(k) \end{aligned}$$

Where, $K_G = \left[S_G{}^T P S_G\right]^{-1} S_G{}^T P$ is the unconstrained control law.

(2) By considering the constraints

Using the unconstrained control law and tuning factors α,

$$\begin{aligned} \Delta V_{gi}^j(k) &= \alpha K_G e_G(k) \\ &= \alpha\left[S_G{}^T P S_G\right]^{-1} S_G{}^T P e_G(k) \end{aligned}$$

The feasibility of the control design is assumed to ensure that there exists $\alpha=\alpha_0$ so that

$$\begin{aligned} \Delta V_{gi}^j(k) &= \alpha_0 K_G e_G(k) \\ &= \alpha_0\left[S_G{}^T P S_G\right]^{-1} S_G{}^T P e_G(k) \end{aligned}$$

$$\left[\Delta V_{gi}^{j}(k)\right] = K_G^0 e_G(k)$$

will obey all the active constraints. Thus, $K_G^0 = \alpha_0 K_G = \alpha_0 \left[S_G{}^T P S_G\right]^{-1} S_G{}^T P$ is the constrained control law.

Recalling the composite error equation for model mismatch analysis:

$$\tilde{e}_G(k+1) = \tilde{e}_G(k) - \left[\tilde{S}_G\right]\left[\Delta V_{gi}^{j}(k)\right] - D_G(k)$$

By considering

$$\left[\Delta V_{gi}^{j}(k)\right] = K_G^0 \tilde{e}(k)$$

then,

$$\begin{aligned}
\tilde{e}_G(k+1) &= I_2 \tilde{e}_G(k) - \tilde{S}_G K_G^0 \tilde{e}_G(k) - D_G(k) \\
&= \left[I_2 - \alpha_0 \tilde{S}_G \left[S_G{}^T P S_G\right]^{-1} S_G{}^T P\right] \tilde{e}_G(k) - D_G(k) \\
&= \Phi_G \tilde{e}_G(k) - D_G(k)
\end{aligned}$$

and

$$\tilde{e}_G(k+n) = (\Phi_G)^n \tilde{e}_G(k) - \sum_{j=1}^{n} (\Phi_G)^{j-1} D_G(k+n-j)$$

Where, $\Phi_G = \left[I_2 - \alpha_0 \tilde{S}_G \left[S_G{}^T P S_G\right]^{-1} S_G{}^T P\right] \tilde{e}_G(k)$

For (a) closed loop stability and

(b) disturbance rejection for a disturbance of finite duration,

it is required that

$$\lim_{n\to\infty} (\Phi_G)^n = 0.$$

Hence, a necessary and sufficient condition for these requirements is

$$|\lambda_i(\Phi_G)| < 1, \ \text{i=1, 2.}$$

Where,

$$\Phi_G = \left[I_2 - \alpha_0 \begin{bmatrix} \tilde{S}^{Gj}_{VVi} \\ \tilde{S}^{Gj}_{QVi} \end{bmatrix} \left[\left(S^{Gj}_{VVi}\right)^T S^{Gj}_{VVi} + p_0 \left(S^{Gj}_{QVi}\right)^T S^{Gj}_{QVi} \right]^{-1} \left[\left(S^{Gj}_{VVi}\right)^T \quad p_0 \left(S^{Gj}_{QVi}\right)^T \right] \right]$$

3. Discussions

(1) By this PQR control design, the system is completely controllable and null controllable. This theoretically ensures that all the outputs of system can be moved to the demanded reference values by the control law in the finite number of control steps.

(2) When the condition $|\lambda_i(\Phi)| < 1$, i=1, 2, is satisfied, the system closed loop is asymptotically stable, and satisfactory reference tracking and disturbance rejection occur.

(3) In the case of perfect model match, $\tilde{S}_G = S_G = \begin{bmatrix} S^P_{VV} \\ S^Q_{QV} \end{bmatrix}$, then

$$\Phi_G = \left[I_{N_P+N_G} - \alpha_0 \begin{bmatrix} S^{Gj}_{VVi} \\ S^{Gj}_{QVi} \end{bmatrix} \left[\left(S^{Gj}_{VVi}\right)^T S^{Gj}_{VVi} + p_0 \left(S^{Gj}_{QVi}\right)^T S^{Gj}_{QVi} \right]^{-1} \right.$$
$$\left. \left[\left(S^{Gj}_{VVi}\right)^T \quad p_0 \left(S^{Gj}_{QVi}\right)^T \right] \right]$$

Therefore, the system closed loop properties are related to the model mismatch of the control design.

7.4.3 Stability Analysis for the Decentralised Control System

For the optimal control design, as the decentralised scheme has the same PQR design as the centralised one, only the RVR closed loop stability for a decentralised region and a whole power system need to be examined in this stability analysis.

7.4.3.1 Closed Loop Stability of a Regional RVR System

As the RVR control design for a decentralised region is the same as the one for the whole system in the centralised scheme, by directly using the analysis results for the centralised scheme in subsection 7.4.2.1, following discussions can be made:

Re-writing the decentralised RVR design:

$$\underset{[\Delta V_{Grefi}(k)],[d_i(k)]}{\mathrm{Min}} \left\{ \left\| \alpha \Delta V_{Pi}(k) - [S^P_{VVi}][\Delta V_{Gref\,i}(k)] \right\|^2 \right.$$
$$\left. + q_0 \left\| \alpha([Q_{Grefi}] + M_i[d_i(k)] - [Q_{Gi}(k)]) - [S^Q_{QVi}][\Delta V_{Grefi}(k)] \right\|^2 + \delta \left\| [d_i(k)] \right\|^2 \right\}$$

Subject to:

$$[V_{G\min i}] \le [V_{Gi}(k)] + [\Delta V_{Grefi}(k)] \le [V_{G\max i}]$$

$$[Q_{G\min i}] \le [Q_{Gi}(k)] + [S^Q_{QVi}][\Delta V_{Ggrefi}(k)] \le [Q_{G\max i}]$$

$$[\Delta V_{Grefi}(k)] \le [|\Delta V_{G\max i}|]$$

$$[V_{c\min i}] \le [V_{ci}(k)] + [S^c_{cvi}][\Delta V_{Grefi}(k)] \le [V_{c\max i}]$$

$$\mathrm{Max}\left(\frac{Q^j_{\min i} - Q^j_{Gref\,i}}{M^j_i} \right) \le d_i \le \mathrm{Min}\left(\frac{Q^j_{\max i} - Q^j_{Gref\,i}}{M^j_i} \right) \quad \forall i \in N_{di}, \forall j \in N_{Gi}$$

(i) This control design is based a composite system derived from the pilot bus and reactive power generation sub-systems. A reactive generation co-ordination scheme is introduced in this design to avoid the linear independent problem between these two subsystems. As the system is completely controllable and null controllable, it is possible to move all the output of the system modes to the references values by the control law in the finite number of steps.

(ii) When the condition $\left|\lambda_i(\Phi_R)\right| < 1$, i=1, 2, ..., (1+$N_G$), is satisfied, the system will be closed loop stable, and the satisfactory reference tracking and disturbance rejection will be achieved with all the outputs of the system modes. This includes the pilot bus voltage and the reactive generation co-ordination scheme.

Where,

$$\Phi_{Ri} = \left[I_{N_{Pi}+N_{Gi}} - \alpha_0 \begin{bmatrix} \tilde{S}^P_{VVi} & 0 \\ \tilde{S}^Q_{QVi} & -M \end{bmatrix} \begin{bmatrix} \left(S^P_{VVi}\right)^T S^P_{VVi} + q_0 \left(S^Q_{QVi}\right)^T S^G_{QVi} & -\alpha_0 q_0 \left(S^Q_{QVi}\right)^T M \\ -\alpha_0 q_0 M^T S^Q_{QVi} & \alpha_0^2 q_0 M^T M + \delta I_{N_d} \end{bmatrix}^{-1} \cdot \begin{bmatrix} \left(S^P_{VVi}\right)^T & q_0 \left(S^Q_{QVi}\right)^T \\ 0 & -\alpha_0 q_0 M^T \end{bmatrix} \right]$$

(iii) In the case of perfect model mismatch, $\tilde{S}_R = S_R = \begin{bmatrix} S^P_{VV} & 0 \\ S^Q_{QV} & -M \end{bmatrix}$,

$$\Phi_{Ri} = \left[I_{N_{Pi}+N_{Gi}} - \alpha_0 \begin{bmatrix} S^P_{VVi} & 0 \\ S^Q_{QVi} & -M \end{bmatrix} \begin{bmatrix} \left(S^P_{VVi}\right)^T S^P_{VVi} + q_0 \left(S^Q_{QVi}\right)^T S^G_{QVi} & -\alpha_0 q_0 \left(S^Q_{QVi}\right)^T M \\ -\alpha_0 q_0 M^T S^Q_{QVi} & \alpha_0^2 q_0 M^T M + \delta I_{N_d} \end{bmatrix}^{-1} \cdot \begin{bmatrix} \left(S^P_{VVi}\right)^T & q_0 \left(S^Q_{QVi}\right)^T \\ 0 & -\alpha_0 q_0 M^T \end{bmatrix} \right].$$

This shows that the system closed loop properties are related to the model mismatch of the control design.

7.4.3.2 Global Stability of the Decentralised Secondary Control Scheme

The secondary voltage control with the decentralised scheme for a whole power system can be regarded as a special case in the centralised scheme with a block diagonal matrix $\left[S^{P}_{VV}\right]$:

$$\left[S^{P}_{VV}\right] = \mathrm{diag}\left\{\left[S^{P}_{VV1}\right], \left[S^{P}_{VV2}\right], \ldots, \left[S^{P}_{VVZ}\right]\right\}$$

By considering this difference, the following points can be concluded using the stability analysis for the centralised scheme:

(i) The decentralised control scheme causes further model mismatch, however if the condition $\left|\lambda_i(\Phi_R)\right| < 1$, $i=1, 2, \ldots, N_P + N_G$ is satisfied, a closed loop stability for the whole power system can still be achieved by the control design.

(ii) Through the non diagonal elements of the matrix Φ_R, the interactions between the RVRs in different regions can be examined.

(iii) The other properties are the same as those in the centralised case.

7.5 INTEGRATION ANALYSIS

7.5.1 Objectives and Background

1. Objectives

The basic requirements for the integration of a multi-level secondary control system have been clarified for the classical control design in Subsection 6.5.1. The objective of this integration analysis is to see whether the system by this optimal control design satisfies those requirements.

2. Integration Signals

In the optimal control design, the variations of control power plant high voltage ΔV_G and reactive power generation ΔQ_G are used as the signals to integrate the RVR and PQR systems:

$$\Gamma = [\Delta V_G \; \Delta Q_G]^T$$

$$\Gamma_{ref} = [\Delta V_{Gref} \; \Delta Q_{Gref}]^T.$$

The RVR controllers determine the demanded high voltage variations and reactive power generation variations for each of the control power plants. This will be based on the voltage variations at pilot buses. And each control power plant uses these determined variation values as the references for its PQR system. In this way, the RVR and PQR systems are integrated to fulfil secondary voltage control as shown in Figure 6.5.1-1.

7.5.2 Integration Analysis

The stability analysis in section 7.4 gives

$$\tilde{e}(k+n) = (\Phi_R)^n \tilde{e}(k) - \sum_{j=1}^{n} (\Phi_R)^{j-1} D(k+n-j)$$

for the RVR closed loop.

It is known that when

$$\left|\lambda_i(\Phi)\right| < 1, \qquad i = 1,2,\ldots,(N_P + N_G)$$

the RVR closed loop is asymptotically stable, and the satisfactory reference tracking and disturbances rejection with the all outputs of the composite system 2 will be achieved.

For the PQR closed loop, the stability analysis also gives

$$\tilde{e}_G(k+n) = \left(\Phi_G\right)^n \tilde{e}_G(k) - \sum_{j=1}^{n} \left(\Phi_G\right)^{j-1} D(k+n-j)$$

It is also known that if $\left|\lambda_i(\Phi)\right| < 1, i = 1,2$, then $\lim_{n\to\infty}\left(\Phi_G\right)^n = 0$, the PQR closed loop is asymptotically stable, and the reference tracking and disturbance rejection are satisfactory.

These results show that if PQR and RVR closed loops are stable, the reference offset with the outputs of the loops will be sufficiently eliminated, and all the disturbances in the PQR and RVR loops will be sufficiently rejected after certain number of control steps.

For the disturbance on the integration signals D_I,, as it can be subsumed into the disturbances with RVR closed loop D_R:

$$\begin{aligned} \tilde{e}(k+1) &= [I]_{Np+N_G}\, \tilde{e}(k) - \left[\tilde{S}_R\right]\left[U(k) + D_I\right] - D_R \\ &= [I]_{Np+N_G}\, \tilde{e}(k) - \left[\tilde{S}_R\right]\left[U(k)\right] - \left(\left[\tilde{S}_R\right] D_I + D_R\right) \end{aligned}$$

this disturbance will also be rejected when the RVR system is stable.

7.5.3 Remarks

The following points can be summarised from the above integration analysis:

(i) Generally the reference offsets with both PQR and RVR system can be sufficiently eliminated by the optimal control provided that their closed loops are stable.

(ii) The disturbances including the fast dynamic ones within the PQR loops and slow dynamic ones in the RVR systems, as well as those on the RVR-PQR integration signals will be sufficiently rejected subject to the same condition as in item (i).

7.6 SIMULATIONS

The optimal control design for the secondary voltage control has been simulated on the IEEE 39 bus power system. Some of the simulation results are presented in this section.

7.6.1 Simulation Configurations

1. Testing System

The details of the IEEE 39 bus power system are listed in Appendix 1. Its configurations are the same as the simulation for the classical control design in chapter 6.

2. Control Scheme

(1) Control Scheme

The decentralised control scheme was used for this simulation. Each decentralised region was designed to have one pilot bus. Apart from bus 10 (slack bus), all the power plants were chosen as the control power plants.

(2) Pilot buses and control power plants

The IEEE 39 bus power system was decentralised into 4 regions by an optimisation method [7]. The pilot bus and control power plants for each decentralised region were selected as shown in Table 7.6.1-1.

AREA	PILOT BUS	CONTROL POWER PLANTS
1	bus13, 15, 23	bus 1, 2, 3, 8
3	bus 30	bus 4, bus 5
4	bus 33	bus 6, bus 7
5	bus 38	bus 9

Table 7.6.1-1 The Pilot buses and control power plants for the optimal control design

7.6.2 Simulation Programme

1. Programme

this optimal control based secondary voltage control system was programmed by using the Matlab/Simulink. The Matlab optimisation toolbox was used to solve the constrained QP algorithm. The number of control steps needs to be specified in the beginning of the simulation. This number of control steps is the total control steps for the RVR. A tuning factor is also required for the RVR gain to reduce the overshooting problem of the control output.

2. Simulation Settings

(1) Reference values

The voltage references set for the pilot buses V_{Pref} are:

Pilot buses	13	15	23	30	33	38
$\mathbf{V_{Pref}}$	1.0304	1.0050	1.0142	0.9909	1.0450	1.0502

Table 7.6.2-1 The voltage references for the pilot buses

The reference values for the difference between the reactive generations of two power plants are:

Power Plant i – Power plant j	2 - 8	4 - 5	6 - 7
$\mathbf{\Delta Q_{Gref}}$	0.5301	-0.1200	0.10093

Table 7.6.2-2 The references for the reactive generation (differences)

(2) Disturbances

A reactive load disturbance (100MVA) was introduced to load bus 28 and 21 of the test system. The voltage variations caused by those disturbances at pilot buses was calculated by running a load flow programme. The RVR and PQR took control actions to correct the voltage variations.

7.6.3 Simulations Results

Figure 7.6.3-1and Figure 7.6.3-2 list some simulation results with different control steps (discrete control actions within a given time interval in seconds).

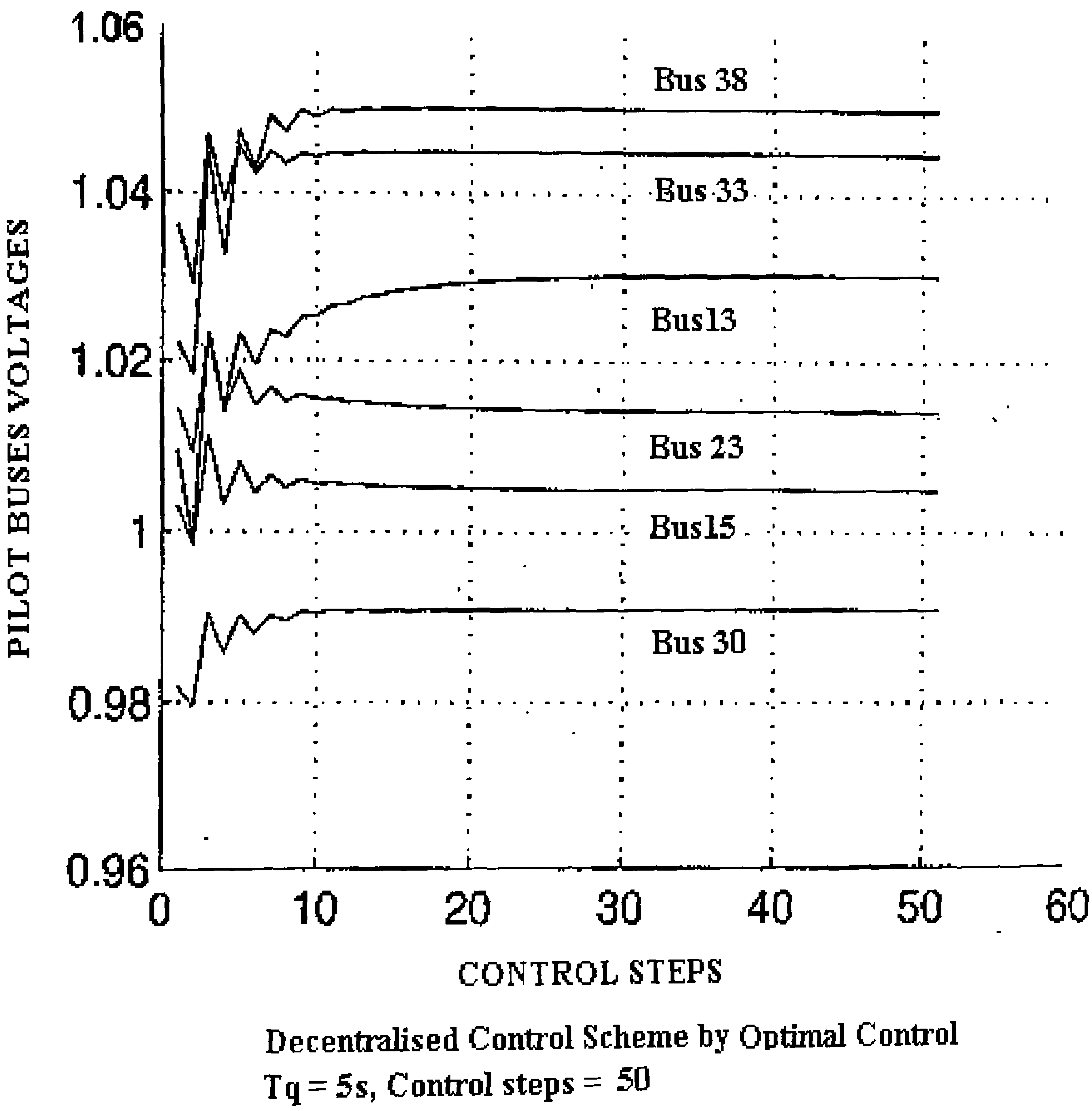

Figure 7.6.3-1 **Simulation results 1 - the secondary voltage control system by the optimal control design**

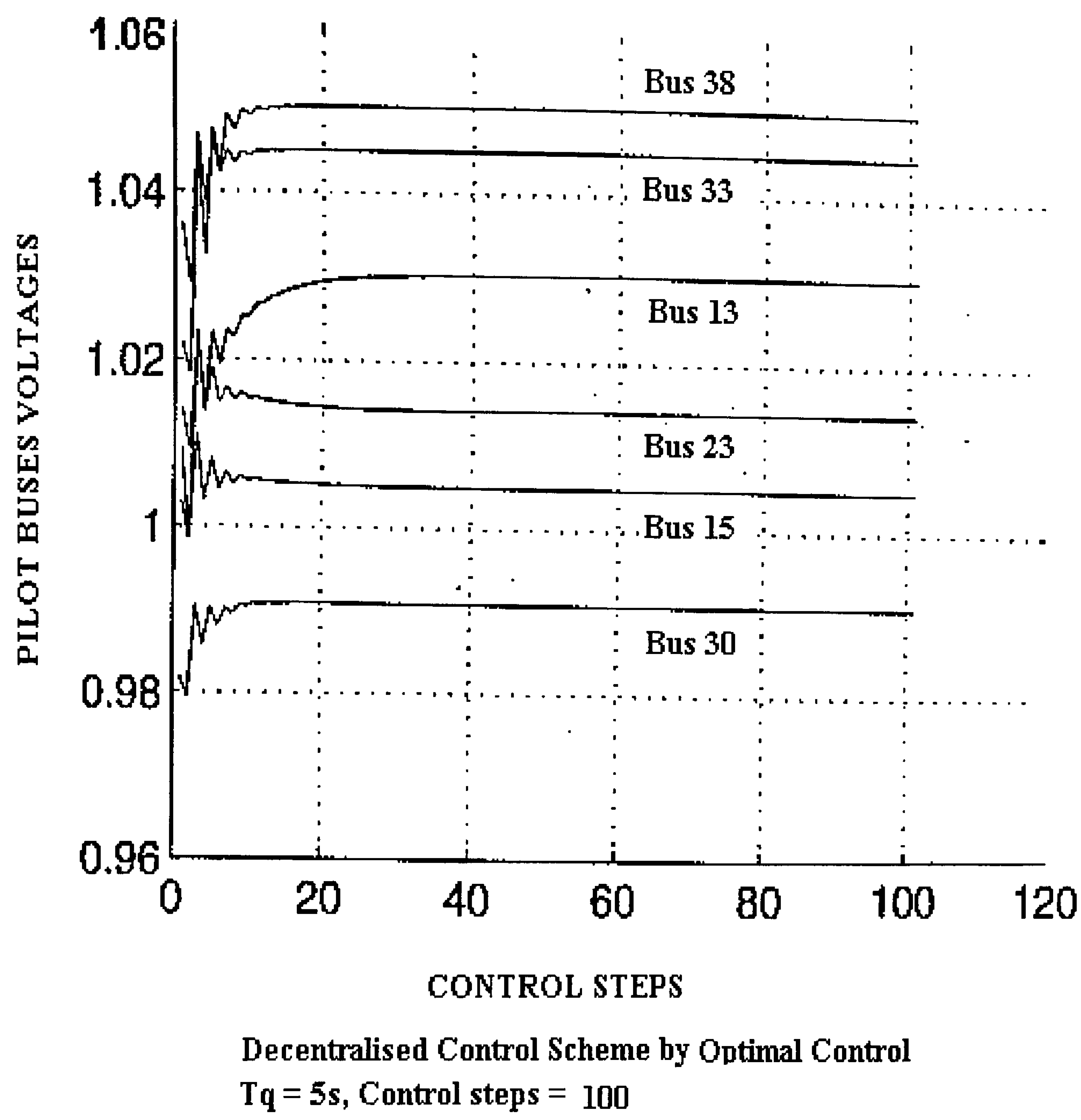

Figure 7.6.3-2 **Simulation results 2 - the secondary voltage control system by optimal control design**

7.6.4 Remarks

The following points can be summarised from the simulation results:

1. From the simulation results, it can be seen that a successful secondary voltage control system can be achieved by the optimal control method.

2. The gain tuning factor is crucial for achieving a good closed loop performance (the voltages of the pilot buses). This point is in consistent with the system by classical control design.

3. The simulation also shown that closed loop stability and performance of the control system are related to the control steps used for the discrete control. A comprise may be needed to determine a proper number of control steps in order to achieve a satisfactory control output with a good control speed.

7.7 Discussions and Conclusions

An optimal control design has been presented for the secondary voltage control system in this chapter. Both the RVR and PQR were formularised as constrained quadratic programming (QP) problems. The Receding Horizon principle is used in this control design. A co-ordination scheme is introduced in the design to optimise the reactive generation. It has been seen in the stability analysis that this co-ordination scheme is crucial for the system controllability.

A time domain method was proposed and successfully used to analyse the closed loop stabilities and performance of this optimal control system. The analysis covers both the centralised and decentralised control schemes. The following points can be generalised from the analyses:

(i) It is unfeasible to design a RVR controller by directly combining the pilot bus and reactive power generation sub-systems. Such a system is not completely controllable because of the linear independent relationship between the two sub-systems.

(ii) With the reactive generation co-ordination scheme, the revised system based on the pilot bus and reactive power generation sub-systems becomes completely controllable and also null controllable. This provides with a theoretical guarantee for the feasibility of the RVR control design.

(iii) By the optimal control design, when the condition ($|\lambda_i(\Phi_R)| \leq 1$, i=1, 2,...., N_P+N_G) is satisfied, the RVR closed loop system will be asymptotically stable with obeying all the constraints, and the satisfactory reference tracking and disturbance rejection will occur the control system.

(iv) By the same control design, the satisfactory closed loop stability, reference tracking and disturbance rejection can be achieved with the PQR when the condition $|\lambda_i(\Phi_G)| < 1$, i=1, 2 is satisfied.

(v) It has been seen that the closed loop properties for either the individual PQR and RVR or the global system are related to the model mismatch of the control design. The decentralised control scheme will cause a further model mismatch. By the non-diagonal elements of the matrix Φ_R, the interactions between the RVRs in different regions can be monitored in the decentralised control scheme.

The integration analysis shows that, by the optimal control design, all the reference offsets and disturbances with this multi-level voltage control system can be sufficiently eliminated. Thus a good integration can be achieved with this control design.

The simulations with the IEEE 39 bus power system numerically demonstrate that satisfactory closed loop stability and performance can be produced from the secondary voltage control system by the optimal control.

It is concluded that the optimal control in the form of constrained quadratic programming can be used for the secondary voltage control in a power system. Satisfactory closed loop stability and performance can be achieved from a secondary voltage control system by this optimal control design.

CHAPTER 8 GENERAL CONCLUSIONS AND FURTHER STUDIES

8.1 OVERVIEW

Under the title of Voltage Stability Analysis and Control, three major objectives were set up in this PhD project: the fundamental study, the on-line prediction method, and the prevention measures for the voltage collapse phenomenon.

The fundamental study is to examine the mechanism of voltage collapse, and identify the determining factors to this phenomenon. This was aimed to lay a theoretical foundation for the rest of research in this project. The on-line prediction method and prevention measures are particularly targeting on the "early prediction and prevention" strategy to tackle the rapid and "uncontrollable" nature of the voltage collapse phenomenon.

Previous literature in the areas of the three objectives was reviewed in chapter 2. Following this literature review, the research directions and methodologies were further identified for each of the study objectives.

The work on the fundamental study was presented in chapter 3 of this thesis. The basic characteristics of voltage collapse were examined, and the theory concerning the voltage stability determining factors (VSDFs) was established. Based on the results in the fundamental study, a knowledge based system for the on-line prediction of voltage collapse was proposed in chapter 4. The design and development of this knowledge based system were intensively discussed in this chapter.

As a prevention measure to voltage collapse, the secondary voltage control system was systematically investigated in Chapter 5, 6, and 7 of this thesis. This part of study covers the details of system modelling, design and analysis of such a multi-level control system in power systems.

All the studies in this project were supported by the simulations on the IEEE 30 or 39 power system. The study results were published in the different international conferences or academic forums [51] [54] [55] [56]. The major achievements with each part of research will be further summarised in section 2 of this chapter.

Improving voltage stability through generation dispatch was also briefly examined in this project. An algorithm aimed at this purpose was proposed to determine the generation participation pattern upon system load increase. This study together with some preliminary simulation results on the IEEE 6 bus (Ward-Hale) system was published in the IEE 2nd International conference on Advances in Power system Control, Operation and Management, 1993 Hong Kong [53]. As this work was not originally planned within the study scope of this PhD project, it is presented in this chapter as a further study.

8.2 GENERAL SUMMARY

All the research work and major achievements of this project are summarised under three headings: the voltage stability determining factors, a knowledge based system for prediction of voltage collapse, and the secondary voltage control systems.

8.2.1 The Voltage Stability Determining Factors

To establish a theoretical foundation for the research in this project, some fundamental aspects of voltage stability problems were examined in chapter 3 of this thesis. The investigation started with a two bus simple power system, and was extended into a multi-bus power system. The V-P and V-Q curves were used to explore the basic characteristics of voltage stability. Based on this fundamental study of voltage stability problems, a typical trajectory of voltage collapse was plotted with consideration of power system major dynamics and non-linearity.

Following the basic characteristics study, the voltage stability determining factors (VSDFs) were identified and defined for a power system. These determining factors are the load pattern, the load distribution pattern as well as the generation pattern and the generation participation pattern. The unique property of the VSDFs was discussed and generalised into a hypothesis, of which the theoretical validation was given in this chapter.

The pattern class feature was also observed with the voltage stability determining factors in this study. It was found that a power system has similar voltage stability when the VSDFs are in the same pattern class.

The simulation was performed on the IEEE 30 bus power system to show the impact of the voltage stability determining factors. Three groups of case studies representing different system loading conditions were presented in this chapter to demonstrate the pattern class feature of the VSDFs.

The theory about the voltage stability determining factors is a significant development in revealing the mechanism of voltage stability in the steady state. Based on this theory, a knowledge based system was proposed in chapter 4 for on-line prediction of voltage collapse using pattern recognition technique.

8.2.2 A Knowledge Based System for Prediction of Voltage Collapse

A knowledge based system for prediction of voltage collapse using pattern recognition technique was presented in chapter 4 of this thesis. It is based on the theory established in chapter 3 that a power system has similar voltage stability when its voltage stability determining factors (VSDFs) stay in the same pattern class.

The principle of this proposed system is to compare a power network to a pre-studied system of which voltage stability (power margins) is known. Its basic structure includes a knowledge based system and a pattern recognition module. To apply such a system to a power system involves a two stage process: the off-line training and the on-line application. During the off-line training, the power margins for the prototypes of all the pattern classes of the VSDFs are determined by using conventional algorithms. Those results will be extracted into the "IF-THEN" rules to form a knowledge base. In the real time, the pattern recognition technique is used to identify the pattern class of the VSDFs for the current state in the power system, the solution to the current prediction of voltage collapse can be found in the knowledge base. The implementation and development of such a system were intensively discussed in this chapter.

To improve the accuracy of the decision-making, a special compensation algorithm was developed and introduced in this knowledge based system. The simulation results show that the compensation algorithm significantly improves the prediction accuracy.

The Artificial Intelligence approach used in the proposed system fundamentally changed the way in which voltage stability is assessed. It does not directly require the algorithm based calculations to determine the power margins, hence the decision-making time is significantly reduced in comparison with the traditional methods. The typical convergence problem of the Newton-Raphson-like load flow algorithm in the vicinity of voltage instability is also avoided with this method.

In addition, as the power margins in the knowledge base of the proposed system are off-line calculated, different algorithms and approaches can be used for the calculation. This is a big advantage, especially for the power systems whose power margins are difficult to determine.

The proposed system has been simulated on the IEEE 30 bus power system. The simulation results show that the proposed system is able to reach rather accurate results with a speedy decision-making. Therefore, it has a good potential for on-line applications for prediction of voltage collapse.

8.2.3 The Secondary Voltage Control Systems

The study on the secondary voltage control systems was presented in chapter 5, 6, and 7 of this thesis. This part of research is summarised here in three sections: the control principal, the classical control design and the optimal control design.

1. The Control Principle

The principle of the secondary voltage control is to decentralise a power system into several regions, and control the regional voltage profile through maintaining the voltages of some pilot buses at certain targets. This is achieved by regulating the reactive generations within each region.

The issues concerning the principle of the secondary voltage control have been discussed in Chapter 5. This is aimed to prepare a systematic and consistent theoretical environment for the design and analyses of such a control system by different control methods. In this chapter, the pilot bus based control principle was theoretically formularised based on power system analysis. All the plants (power system components) involved in the secondary voltage control were systematically modelled and mathematically described. A three level control (Regional –RVR, Power plant-PQR and Generator-AVR) was defined as an essential structure for the secondary voltage control, and the functions at each control level were clarified.

Both the centralised and the decentralised schemes for implementing the secondary voltage control were discussed in this chapter. It was clearly seen that the decentralised control scheme has many advantages over the centralised one. The design criteria for a secondary voltage control system were also given in this chapter.

It shall be pointed out that one pilot bus per decentralised region is believed to be sufficient for a secondary voltage control scheme. All the control design and analyses presented in this thesis are based on this presumption. However, the multiple pilot buses per region scheme is also viable, and indeed may be necessary for the secondary voltage control when some special performance is required. Its design and analysis are principally the same as for the single pilot bus scheme.

2. The Secondary Voltage Control System by a Classical Control Design

A complete design and analysis of a secondary voltage control system by the classical PI control were presented in chapter 6. The control design equations for each control level (RVR and PQR) as well as their relationship were fully established. As a generator normally has a integrated Automatic Voltage Regulator (AVR), the control system at this level was not included in this study. Through the PI control signal, the three control levels were integrated to fulfil the global function of the secondary voltage control.

The traditional frequency domain(s) method was used for the stability analysis of this PI control based system. The analysis shows that satisfactory closed loop stability and performance can be achieved by the control design. The analysis also shows that the RVR/PQR closed loop properties and the interactions between the RVRs are related to the model mismatch of the control design. The decentralised control scheme will cause a further model mismatch.

One interesting finding in the stability analysis was that, the more control power plants in a region, the more stable the closed loop control system is, however the bigger RVR interactions will occur. This indicates that a compromise is needed for determining the number of control power plants in each region.

To assess the global effect of this secondary voltage control system, the voltage profile of a whole power system was analysed. The analysis reveals that the voltage profile has very similar dynamics to the voltages at pilot buses; the efficiency of the secondary voltage control system is related to the decentralisation of a power system and the selection of pilot buses/control power plants.

From the integration analysis, it has been seen that with the classic PI control design, all the reference offsets and disturbances are sufficiently eliminated in the multi-level voltage control system. Hence the whole control system can be well integrated by this PI control design.

This secondary voltage control system was simulated on the IEEE 39 bus power system. The simulation results numerically demonstrated that the classical control design is viable for the secondary voltage control system.

3. The Secondary Voltage Control System by an Optimal Control

The secondary voltage control system by an optimal control was presented in chapter 7 of this thesis. Based on the Receding Horizon principle, both the RVR and PQR were formularised as the constrained quadratic programming problems. To optimise the reactive power generation, a co-ordination plan was also introduced in the RVR formulations. The stability analysis shows that this co-ordination plan is crucial for the system controllability.

For the optimal control, the validation of the closed loop stability in the presence of all the constraints has never been properly solved. In this study, a constructive time domain analysis method was proposed and used for the optimal control design for the secondary voltage control system. The stability analyses show that by this optimal control design, the satisfactory closed loop stability and performance can be achieved for both the RVR and PQR with obeying all the constraints. This is subject to the conditions $|\lambda_i(\Phi_R)| < 1$, i=1, 2,...., N_P+N_G (for RVR), and $|\lambda_i(\Phi_G)| < 1$, i=1, 2 (for PQR).

It has also been seen that the RVR/PQR closed loop properties are affected by the model mismatch of the control design. The decentralised control scheme will cause a further model mismatch. By directly substituting the power system sensitivity matrices into the equation Φ_R and Φ_G, the RVR closed loop stability and performance can be monitored. For the decentralised control scheme, the interactions between the RVRs in different regions can also be examined by the non diagonal elements of the matrix Φ_R.

In the stability analysis, the controllability for the structure of the RVR and PQR has also been fully justified. It can be seen that with this control design, it is unfeasible to achieve a controllable RVR by directly using the pilot bus and reactive power generation sub-systems. By introducing the reactive generation co-ordination plan, the revised system has become completely controllable and also null controllable. This has theoretically guaranteed the feasibility of the RVR system by this optimal control design.

The integration analysis in this study also shows that by this optimal control design, all the reference offsets and disturbances within this multi-level voltage control system can be sufficiently eliminated. Thus a good integration can be achieved with the optimal control design.

The simulation on the IEEE 39 bus power system demonstrates that this optimal control design is also viable for the secondary y voltage control.

8.2.4 General Conclusions

Based on the summary above, it can be concluded that the study objectives set up for this PhD project have been fully achieved. The study activities and major achievements can be highlighted as:

- Through examining the mechanism of voltage collapse phenomenon, a theory about the voltage stability determining factors was established;
- Aimed at on-line application, a knowledge based system was proposed for prediction of voltage collapse using pattern recognition technique;
- As a counter-measure to voltage collapse, the design and analysis of the secondary voltage control systems by both classical and optimal control were systematically investigated.

8.3 FURTHER STUDY – IMPROVE VOLTAGE STABILITY BY GENERATION DISPATCH

Improving voltage stability through generation dispatch was briefly examined in this research project. Some preliminary results from this study are presented in this section.

8.3.1 The Principal of the Method

In chapter 3, the voltage stability determining factors was identified for a power system. These factors are the load pattern, the load distribution pattern, the generation pattern and the generation participation pattern. It has been validated that in the steady state, those factors uniquely determine voltage stability of a power system.

Following this theory, it is easy to see that those determining factors can be potentially used to control voltage stability. However, the load and load distribution patterns are largely determined by the customers of a power system. It will be very difficult to change those two factors apart from load shredding which would be rather expensive if possible at all. The generation and generation participation patterns on the other hand, are relatively easy to be modified through generation dispatch. Based on this consideration, a sensitivity based method is proposed in this study to improve voltage stability through generation dispatch.

8.3.2 An Algorithm for Determining the Generation Participation Pattern

The key issue with the proposed method for the generation dispatch is to determine the generation participation patterns upon a load change in order to maintain good voltage profile.

1. Sensitivity analysis

For a power system, the linearised the load flow equations can be written as:

$$\begin{bmatrix} \Delta P \\ \Delta Q \end{bmatrix} = \begin{bmatrix} J_{P\theta} & J_{PV} \\ J_{Q\theta} & J_{QV} \end{bmatrix} \begin{bmatrix} \Delta\theta \\ \Delta V \end{bmatrix} \qquad (8.3.2\text{–}1)$$

where

$\begin{bmatrix} J_{P\theta} & J_{PV} \\ J_{Q\theta} & J_{QV} \end{bmatrix}$ is the full Jacobian matrix,

ΔP and ΔQ are the vectors of active and reactive power injections at all the buses,

ΔV and $\Delta\theta$ are the vectors of voltage magnitudes and angles at all the buses,

$J_{P\theta}$ is the sensitivity sub-matrix between active power injection and voltage angels,

J_{PV} is the sensitivity sub-matrix between active power injection and voltage magnitudes,

$J_{Q\theta}$ is the sensitivity sub-matrix between reactive power injection and voltage angels,

J_{QV} is the sensitivity sub-matrix between reactive power injections and voltage magnitudes.

Equation (8.3.2-1) can be decomposed into the following two equations:

$$[\Delta P] = [J_{P\theta}][\Delta\theta] + [J_{PV}][\Delta V] \quad (8.3.2\text{–}2)$$

$$[\Delta Q] = [J_{Q\theta}][\Delta\theta] + [J_{QV}][\Delta V] \quad (8.3.2\text{–}3)$$

Without loss of generalities, it can be assumed that $[J_{PV}]$ and $[J_{QV}]$ are invertible. Thus, from equations (8.3.2-2) and (8.3.2-3), there are

$$[\Delta V] = [J_{PV}]^{-1}[\Delta P] - [J_{PV}]^{-1}[J_{P\theta}][\Delta\theta] \qquad (8.3.2\text{–}4)$$

$$[\Delta V] = [J_{QV}]^{-1}[\Delta Q] - [J_{QV}]^{-1}[J_{Q\theta}][\Delta\theta] \qquad (8.3.2\text{–}5)$$

Where,

$[J_{PV}]^{-1}[J_{PV}] = I$,

$[J_{PV}]^{-1}[J_{PV}] = I$.

From equation (8.3.2-4) and (8.3.2-5), the following equation can be produced:

$$\begin{aligned}[\Delta V] = {} & [\ [J_{PV}] - [J_{Q\theta}]^{-1}[J_{P\theta}][J_{QV}]\ ]^{-1}[\Delta P] \\ & + [\ [J_{QV}] - [J_{P\theta}]^{-1}[J_{Q\theta}][J_{PV}]\ ]^{-1}[\Delta Q]\end{aligned} \qquad (8.3.2\text{–}6)$$

Rewrite equation (8.3.2-6) as

$$[\Delta V] = [J_A][\Delta P] + [J_B][\Delta Q] \qquad (8.3.2\text{–}7)$$

Where,

$$[J_A] = [\ [J_{PV}] - [J_{Q\theta}]^{-1}[J_{P\theta}][J_{QV}]\ ]^{-1}$$

$$[J_B] = [\ [J_{QV}] - [J_{P\theta}]^{-1}[J_{Q\theta}][J_{PV}]\ ]^{-1}$$

In matrix $[J_A]$ and $[J_B]$, each row is corresponding to the voltage magnitude at a bus, and each column is corresponding to the power injections at a bus. By removing the columns corresponding to the non power plant buses from the matrices, the two new matrices $[\hat{J}_A]$ and $[\hat{J}_B]$ can be obtained. The elements in these two matrices represent the relationships between system voltage and active, reactive power outputs of power plants respectively.

In matrix $[\hat{J}_B]$, element $(\hat{J}_B)_{ij}$ shows the effect of the change of reactive generation at power plant j on the voltage at bus i. The summation of all the elements in this column j reflects the effect of changing reactive generation at power plant j on the system voltage profile. The elements in matrix $[\hat{J}_A]$ show the similar effects on system voltage by changing the active generations at power plants.

2. The algorithm

From the above analysis, it can be seen that different generation dispatch will result in a different voltage profile, hence different voltage stability in a power system. In order to maintain good voltage profile, the power plants with higher summation of the elements in the corresponding column within the matrix $[\hat{J}_A]$ or $[\hat{J}_B]$ should be given higher priorities for generation dispatch. Based on this consideration, an algorithm for determining the generation participation coefficients is developed to improve voltage stability as:

$$\beta_P^i = \lambda_P^i \Big/ \sum_{i=1}^{M} \lambda_P^i ,$$

$$\beta_Q^i = \lambda_Q^i \Big/ \sum_{i=1}^{M} \lambda_Q^i$$

where,

$\lambda_P^i = \sum_{i=1}^{N}\left(\hat{J}_A\right)_{ji}$,

$\lambda_Q^i = \sum_{i=1}^{N}\left(\hat{J}_B\right)_{ji}$

β_P^i and β_Q^i are the generation participation coefficients for the active and reactive output at power plant *i*,

M is the total number of power plants in a power system,

N is the total number of buses in a power system.

In order to balance the load and generation for both reactive and active power in a power system, it may not be always possible to use both the active and reactive generation participation coefficients determined by the algorithm. As reactive power has a much stronger impact on system voltage than active power (normally 3 times more), in the conflict situation, the reactive participation coefficients will be treated with priority for the generation dispatch, the active ones will be used in a slack manner.

3. Application of the algorithm

For a given load increase (ΔP_L, ΔQ_L), the application procedure of the proposed algorithm includes the following steps:

Step 1: calculate the elements of $\left[\hat{J}_B\right]$ and $\left[\hat{J}_B\right]$ for the current state of a power system.

Step 2: calculate the generation participation coefficients β_P^i and β_Q^i for each power plant (i) by using the proposed algorithm. Determine the generation increase for each power plant as:

$$\Delta P^i = \beta_P^i(\Delta P_L + \delta_P)$$

$$\Delta Q^i = \beta_Q^i(\Delta Q_L + \delta_Q)$$

$$i = 1, 2, \ldots N$$

(δ_P and δ_Q are the adjustable factors to reflect the transmission loss)

Step3: update operational conditions and run load flow simulation to verify the calculated generation change before committing dispatch actions.

As the proposed algorithm is based on the sensitivity analysis of the linearised load flow equations, the load increase has to be sufficiently small in order to achieve satisfactory results. For a big load increase, the total load increase may have to be divided into several small fractions, and run through the application procedure with each fraction successively.

It is known that a power system has different non-linearity at different operational points. With load increasing, this non-linearity will become more and more severe. Under heavily loaded conditions, it is necessary to run the algorithm more often with much finer load increase fractions than the normally loaded situations.

8.3.3 Simulations

The proposed algorithm has been tested on the Ward-Hale 6-bus power system. Some of the simulation results are presented in this section. The detailed information about this 6 bus power system is given in Appendix 3 of this thesis.

1. Simulation configurations

Three study cases were set up to demonstrate the efficiency of this algorithm for improving voltage stability. All the three cases are under exactly the same operation conditions apart from the generation participation pattern. The first two cases are given with the fixed generation participation pattern for generation dispatch, while the proposed algorithm was used for the generation dispatch in the third case. The power margins for the three cases were determined by using the same load flow programme.

2. Simulation results

(1) Study case 1

In this case, a fixed participation pattern is used for generation dispatch. The system conditions and simulation results of power margins are summarised in the Table 8.3.3-1 below:

	Bus	**Initial load**		**Initial Gen**		**Load Dist**		**Gen Par**		**PM (p.u.)**	
		P_L^0	Q_L^0	P_G^0	Q_G^0	LD^P	LD^Q	β_P	β_Q	ΔP_L	ΔQ_L
Load	1	0.30	0.18	0.00	0.00	20.00%	20.00%	0.00%	0.00%	**0.090**	**0.054**
	2	0.50	0.05	0.00	0.00	30.00%	30.00%	0.00%	0.00%	**0.135**	**0.081**
	3	0.00	0.00	0.00	0.00	20.00%	20.00%	0.00%	0.00%	**0.090**	**0.054**
	4	0.50	0.13	0.00	0.00	30.00%	30.00%	0.00%	0.00%	**0.135**	**0.081**
Gen	5	0.00	0.00	1.37	0.38	0.00%	0.00%	100.00%	100.00%	**0.000**	**0.000**
	6	0.00	0.00	0.00	0.00	0.00%	0.00%	0.00%	0.00%	**0.000**	**0.000**
	Total	1.30	0.36	1.37	0.38	100.00%	100.00%	100.00%	100.00%	**0.450**	**0.270**

Table 8.3.3-1 The simulation results for study case 1

(2) Study case 2

This is another case, in which a fixed participation pattern is used for generation dispatch. The system conditions and simulation results of power margins are summarised in the Table 8.3.3-2 .

	Bus	Initial load		Initial Gen		Load Dist		Gen Par		PM (p.u.)	
		P_L^0	Q_L^0	P_G^0	Q_G^0	LD^P	LD^Q	β_P	β_Q	ΔP_L	ΔQ_L
Load	1	0.30	0.18	0.00	0.00	20.00%	20.00%	0.00%	0.00%	**0.168**	**0.102**
	2	0.50	0.05	0.00	0.00	30.00%	30.00%	0.00%	0.00%	**0.252**	**0.153**
	3	0.00	0.00	0.00	0.00	20.00%	20.00%	0.00%	0.00%	**0.168**	**0.102**
	4	0.50	0.13	0.00	0.00	30.00%	30.00%	0.00%	0.00%	**0.252**	**0.153**
Gen	5	0.00	0.00	0.69	0.19	0.00%	0.00%	50.00%	50.00%	**0.000**	**0.000**
	6	0.00	0.00	0.69	0.19	0.00%	0.00%	50.00%	50.00%	**0.000**	**0.000**
	Total	1.30	0.36	1.38	0.38	100.00%	100.00%	100.00%	100.00%	**0.840**	**0.510**

Table 8.3.3-2 The simulation results for study case 2

(3) Study case 3

In this case, the proposed algorithm was used for the generation dispatch. Four steps of load increase were made before the system reaches its maximum load level. The proposed algorithm was used for generation dispatch at each of the load increase steps successively. The simulation results of this study case are summarised in the Table 8.3.3-3 and Table 8.3.3-4.

	Bus	Initial load		Initial Gen		Load Dist		PM (p.u.)	
		P_L^0	Q_L^0	P_G^0	Q_G^0	LD^P	LD^Q	ΔP_L	ΔQ_L
Load	1	0.30	0.18	0.00	0.00	20.00%	20.00%	**0.180**	**0.110**
	2	0.50	0.05	0.00	0.00	30.00%	30.00%	**0.270**	**0.165**
	3	0.00	0.00	0.00	0.00	20.00%	20.00%	**0.180**	**0.110**
	4	0.50	0.13	0.00	0.00	30.00%	30.00%	**0.270**	**0.165**
Gen	5	0.00	0.00	0.69	0.19	0.00%	0.00%	**0.000**	**0.000**
	6	0.00	0.00	0.69	0.19	0.00%	0.00%	**0.000**	**0.000**
	Total	1.30	0.36	1.38	0.38	100.00%	100.00%	**0.900**	**0.550**

Table 8.3.3-3 The simulation results for study case 3

Gen Bus	Step 1 ΔP=0.25 ΔQ=0.15		Step 2 ΔP=0.25 ΔQ=0.15		Step 3 ΔP=0.25 ΔQ=0.15		Step 4 ΔP=0.15 ΔQ=0.10	
	β_P	β_Q	β_P	β_Q	β_P	β_Q	β_P	β_Q
5	32.00%	51.11%	30.88%	51.14%	30.38%	51.13%	32.72%	50.45%
6	68.00%	48.89%	69.12%	48.86%	69.62%	48.87%	67.28%	49.55%

Table 8.3.3-4 The generation participation coefficients for study case 3

3. Remarks

From the simulation results, it is clearly seen that, the power margins of the testing system has been much improved by using the proposed algorithm for generation dispatch.

8.3.4 Discussions and Conclusions

A brief study on improving voltage stability through generation dispatch has been presented in this section. This is also based on the theory about voltage stability determining factors of which two are generation related.

Based on the sensitivity analysis of the Jacobian matrix of load flow equations, an algorithm was developed for determining the generation participation pattern with respect to maintain good voltage stability. The application of this algorithm for generation dispatch upon a load increase has also been discussed in this section.

The proposed algorithm has been tested on the Ward-Hale 6 bus power system. The simulation results show that the power margins of the testing system have been significantly improved by using this algorithm for generation dispatch, in comparison with other dispatch strategies.

The same algorithm may also be used to improve voltage stability under no load change conditions. This will involve "re-dispatching" generations among power plants for the existing load. Furthermore, by following the same principle, a method can be developed for the under voltage load shredding scheme in a power system. Those are the interesting and useful subjects for further development in the area of voltage stability control.

REFERENCES

[1] Thomas, R J and Tiranuchit, A, " Voltage instabilities in electric power networks", the proceeding of 18th Southeast symposium on power system theory, 1986, pp 359-363.

[2] Tiranuchit, and A Thomas, R J, " A posturing strategy against voltage instabilities in electric power systems", IEEE Transactions on Power Systems, Vol.3, No.1, February 1988, pp 87-93"

[3] Tiranuchit, and A Thomas, R J, " Towards a computationally feasible on-line voltage instability index", IEEE Transactions on Power Systems, Vol.3, No.2, May 1988, pp669-675"

[4] Ekwue, A O, Cheng, D T and Song, Y H, " Integrated Methods for Voltage Stability Analysis of the NGC system", the proceeding of IEE colloquium on voltage collapse, April 1997, pp3/1-3/5.

[5] Kundur, P, " Section 14.4, Power system stability and control", EPRI Power System engineering Series, McGraw-Hill, Inc. 1994.

[6] Taylor, C W, "Power system Voltage stability", EPRI Power System engineering Series, McGraw-Hill, Inc. 1994.

[7] Popovic, D S, Calovic, M S, "Secondary voltage control and power system performance in case of voltage instability", Fonctionnement des reseaux, RGE No. 10/94, November 1994, pp8-18.

[8] Arcidiacono, V, Corsi, S, " a real-time voltage stability index for bulk system with secondary voltage regulation", Bulk Power system Voltage Phenomena seminar III, Davos.

[9] Fishchl, R, Mercede, F, Zaragocin, L, Yan, H, ... et. al., "A review of methods for predicting voltage collapse of power system", 9th PSCC, 30th August - 4th september 1987, Lisbon, Portugal.

[10] Tamura, Y, "Summary of presentation, panel session on voltage instability", IEEE Summer Meeting, 1987.

[11] Lemaitre, C, Paul, J P, ...et, al. "An indicator of the risk of voltage profile instability for real-time control application", IEEE Transactions on Power Systems, Vol. 5, No. 1, February 1990, pp154-161.

[12] Obadina, O O, Berg, G J, "Determination of voltage stability limit in multi-machine power systems", IEEE Transactions on Power systems, Vol. 3, No. 4, November 1988, pp 1545 - 1550.

[13] Obadina, O O, Berg, G J, "Identifying electrically weak and strong segments of a power system from a voltage stability viewpoint", IEE Proceeding s, Vol. 137, Pt. C, No. 3, May 1990.

[14] Van Cutsem, T, "A method to compute reactive power margins with respect to voltage collapse", IEEE Transactions on Power Systems, Vol. 6, No. 1, February 1991.

[15] Tamura, Y, et. al..., "Relationship between voltage instability and multiple load flow solutions in electric power system", IEEE Transactions on PAS, Vol. PAS-102, No. 5, May 1985, pp 1115-1122.

[16] Venikogv, V A, et. al..., "Estimation of electric power systems steady state stability in load flow calculation", IEEE Transactions on PAS, Vol. PAS-94, No. 3, May/June 1975, pp 1034-1038.

[17] Jarjis, J, Galiana, F D, "Quantitative analysis of steady state stability in power networks", IEEE Transactions on PAS, Vol. PAS-100, No. 1, January 1981, pp. 318 -326.

[18] Jarjis, J, Galiana, F D, "Analysis and characterisation of security regions in power systems, Part II: load flow feasibility conditions in power networks", Final report, US Department of Energy, Division of Electric Energy Systems, March 1980.

[19] Galiana, F D, "Load flow feasibility and the voltage collapse problem", the proceedings of 23rd conference on decision and control, Las Vegas, NV, December 1984, PP. 485-487.

[20] Schlueter, R A, Chang, M W, Costi, A, "Loss of voltage controllability as a cause of voltage collapse", the proceedings of the 27th conference on decision and control, Austin, Texas, December 1988, pp. 2120-2126.

[21] Schlueter, R A, et al., "Voltage stability and security assessment", EPRI Final report El-5967 on project RP 1999-8, May 1988.

[22] Schlueter, R A, Hu, I, et. al..., "Methods for determining proximity to voltage collapse", IEEE Transactions on Power Systems, Vol. 6, No. 1, February 1991, pp. 285-292.

[23] Venikov, V A, et. al., "Estimation of electric power systems steady state stability in load flow calculation", IEEE Transactions on PAS, Vol. PAS-94, No. 3 May/June 1975, PP. 1034-1038.

[24] Carpentier, J, et. al., "Voltage collapse proximity indicatirs computed from an optimal power flow", the proceedings of 8th PSCC, Helsininli, 1989.

[25] Borremans, P, et. al., "Voltage stability : fundamental concept and comparison of practical criteria", International conference on large high voltage electric system", CIGRE 38-!!, August, 1984.

[26] Chebbo, A M, et. al., "Voltage collapse proximity indicator: behaviour and implications", the IEE proceedings-C, Vol. 139, No. 3, May 1992, pp. 241-252.

[27] Chebbo, A M, et. al., "Reactive power dispatch incorporating voltage stability", the IEE proceedings-C, Vol. 139, No. 3, May 1992, pp. 253-260.

[28] Vournas, C D, Krassas, N D, "Voltage stability as affected by static load characteristics", the IEE proceedings-c, Vol. 140, No. 3, May 1993, pp.221-228.

[29] De Mello, F P, et. al. "Concepts of synchronous machine stability as affected by excitation control", IEEE Transactions on PAS, PAS-88, April 1969, pp. 317-329.

[30] Hiskens, I A, Mclean, C B, "SVC behaviour under voltage collapse conditions", IEEE Transactions on Power Systems, Vol. 7, No. 3, August 1992, pp. 1078-1087.

[31] Rajagopalan, C, et al., "An integrated approach to dynamic and static voltage stability," the proceedings of 1989 American Control Conference, Pittsburgh, PA, June 1989, Vol.3, pp. 1231-1235.

[32] Skine, Y, Ohrsuki, H, "Cascaded voltage collapse", IEEE transactions on power systems, Vol. 5, No 1, February 1990, pp. 250-256.

[33] Lee, B H, Lee, K Y, "A study on voltage collapse mechanism in electric power systems", IEEE transactions on power systems, Vol. 6, No. 3, August 1991, pp. 966 - 973.

[34] Lee, B H, Lee, K Y, "Dynamic and static voltage stability enhancement of power systems", IEEE transactions on power systems, Vol. 8, No. 1, February 1993, pp. 231 - 238.

[35] Stubbe, M, et al., "STAG - A new unified software program for the study of the dynamic behaviour of electrical power systems", IEEE transactions, Vol. PWRS-4, No. 1, pp.129-138, 1989.

[36] Deuse, J, et al., "Dynamic simulation of voltage collapse", IEEE Transactions on power systems, Vol. 8, No. 3, August 1993, pp. 894-904.

[37] Lachs, W R, et al., "Voltage instability in interconnected power systems: a simulation approach", IEEE Transactions on power systems, Vol. 7, No. 2, May 1992, pp. 753-761.

[38] Liu, C C, "Analysis of a voltage collapse mechanism due to effects of on-load tap changers," IEEE ISCAS 1986, Vol.3, May 1986, pp. 1028-1030.

[39] Liu, C C, Vu, K, "Analysis of tap changer dynamics and construction of voltage stability regions," IEEE Transactions on circuits and systems, Vol. 36, No. 4, April 1989, pp. 575-590.

[40] Ohtsuki, H, et al. "Reverse action of on-load tap changer in association with voltage collapse," IEEE Transactions on power systems, Vol. 6, No. 1, February 1991, pp. 300-306.

[41] Sancha, J L, et al, "Analysis of RVR for power systems," project IMPROVE report 1.5-DV-Rev. 0, ESPRIT III Project EP6165, July 1995.

[42] Arcidiacono, V, et. al, "Studies on area voltage and reactive power control at ENEL,"CIGRE Report 32-77-66, Study Committee 32 Meeting in Dortmund.

[43] Arcidiacono, "Automatic voltage and reactive power control in transmission systems," Survey paper E, CIGRE-IFAC Symposium, Florence, 1983.

[44] J L Sancha, et. al, "Secondary voltage control: Analysis, solutions and Simulation results for the Spanish transmission system," PICA conference, Salt Lake, USA, May 1995.

[45] Paul J P, et. al. "Survey of the secondary voltage control in France, Present realisation and investigations," IEEE Transactions on Power systems, Vol. PWRS-2, No. 2, May pp505-511.

[46] Thorp J S, et al. "optimal secondary voltage-var control using pilot point information structure, IEEE CDC, Las Vegas, December 1984.

[47] Florez J., A. Tapia, R. Criado and J.M., Gvijalba, "Secondary voltage control based on a robust multivariable PI controller," Elect. Power and Energy Syst., 1994, Vol. 16, No.3, pp.167-173.

[48] Goméz, T., Conejo, A., de la Fuente, J. I., Pagola, F. L. and Rehn, C. J., 1992, "Decentralised Secondary Voltage Control and Pilot Bus Selection," IFAC Symposium on Control of Power Plants and Power Systems.

[49] Goméz, T., Conejo, A., de la Fuente, J. I., Sancha, J. L., and Fernandez, J. L., "Secondary Voltage Control and Pilot Bus Selection in Electric Power Transmission Systems," IASIED'91, 1991, Zurich.

[50] Paul, J P, Corroyer, C., Jeannel, P., Tesseron, J. M., Maury, F. and Torra, A., 1990, "Improvements in the organisation of secondary voltage control in France," CIGRE paper 38/39-03.

[51] Zhang, X., M. A. Johnson, 'Stability Analysis of the Integrated Multi-level Voltage Regulation in Power System' IMPROVE Report 2.3.1 ESPRINT, April 1996.

[52] Sancha, J L, 'A Multi-level Automatic Voltage control System for the Spanish Transmission Network: Analysis, Proposed solutions and Simulations,' the International Symposium on electric Power Engineering, June 18-22, 1995, Stockholm, Sweden.

[53] Lo, K L, Zhang, X, "Dispatching Outputs of Generators for Enhancing the Power Margins from the Viewpoint of Voltage Stability", the proceeding of the IEE 2nd International Conference on Advances in Power System Control, Operation and Management, Dec 1993, Hong Kong, pp.60-65.

[54] Lo, K L, Zhang, X, "The Effect of Load Increase Distribution Pattern and Generator Participation Pattern on Voltage Collapse in Power Systems" UPEC 1993, Staffordshire, UK.

[55] Lo, K L, Zhang, X, "The Use Of Pattern Recognition Technique for Identifying Electrically Weak Segments In Power Systems", the proceeding of the IEEE Power Tech Conference 1993, Athens, Greece, pp.916-920.

[56] Lo, K L, Zhang, X, "A Real-Time Method to determine the Power Margins and Identify Electrically Weak Segments of a Power System with Respect to Voltage Collapse", the proceeding of the 27th UPEC 1992, Bath, UK, Vol.2 pp.704-707.

[57] Lo, K L, Abidin, Haji I H Z, "The Fuzzy Decision Tree Application to a Power System Problem", International Journal for Computation and Mathematics in Electrical and Electronic Engineering, Vol 23, Issue 2, pp436-451, 2004.

[58] Lo, K L, Zhu, T X, "Arnold Diffusion in a Particular Multi-Machine Power System", IEE Proceedings Generation, Transmission and Distribution, Vol 145, N0 3, May, pp257-264, 1998.

[59] Lo, K L, Zhu, T X, "Chaotic Motion and Diffusion in a Power System", IEEE International Conference on Energy Management and Power Delivery (EMPD'98), Singapore, March, 1998.

[60] Zhu, T X, Tso, S K, Lo, K L, "An Investigation into the OLTC Effects on Voltage Collapse", IEEE Transaction on Power Systems, Vol 15, No 2, pp515-521 2000.

[61] Tso, S K, Zhu, T X, Zeng, Q Y, Lo, K L, "A Fuzzy -Set Approach to Dynamic Voltage Security Assessment", IEE Proceedings, Generation, Transmission and Distribution, Vol 142, pp190-194, 1995.

[62] Tso, S K, Zhu, T X, Zeng, Q Y, Lo, K L, "Fuzzy Reasoning for Knowledge-Based Assessment of Dynamic Voltage Security", IEE Proceedings, Generation, Transmission and Distribution, Vol 143, pp157-162, March, 1996.

[63] Van Cutsem, T, Costas, Vournas, " Voltage Stability of Electric Power Systems", Kluwer Academic Publishers, 1998.

APPENDIX 1 SIMULATION SYSTEM DATA

A1.1 THE IEEE 39 BUS POWER SYSTEM

1. The Single Line Diagram

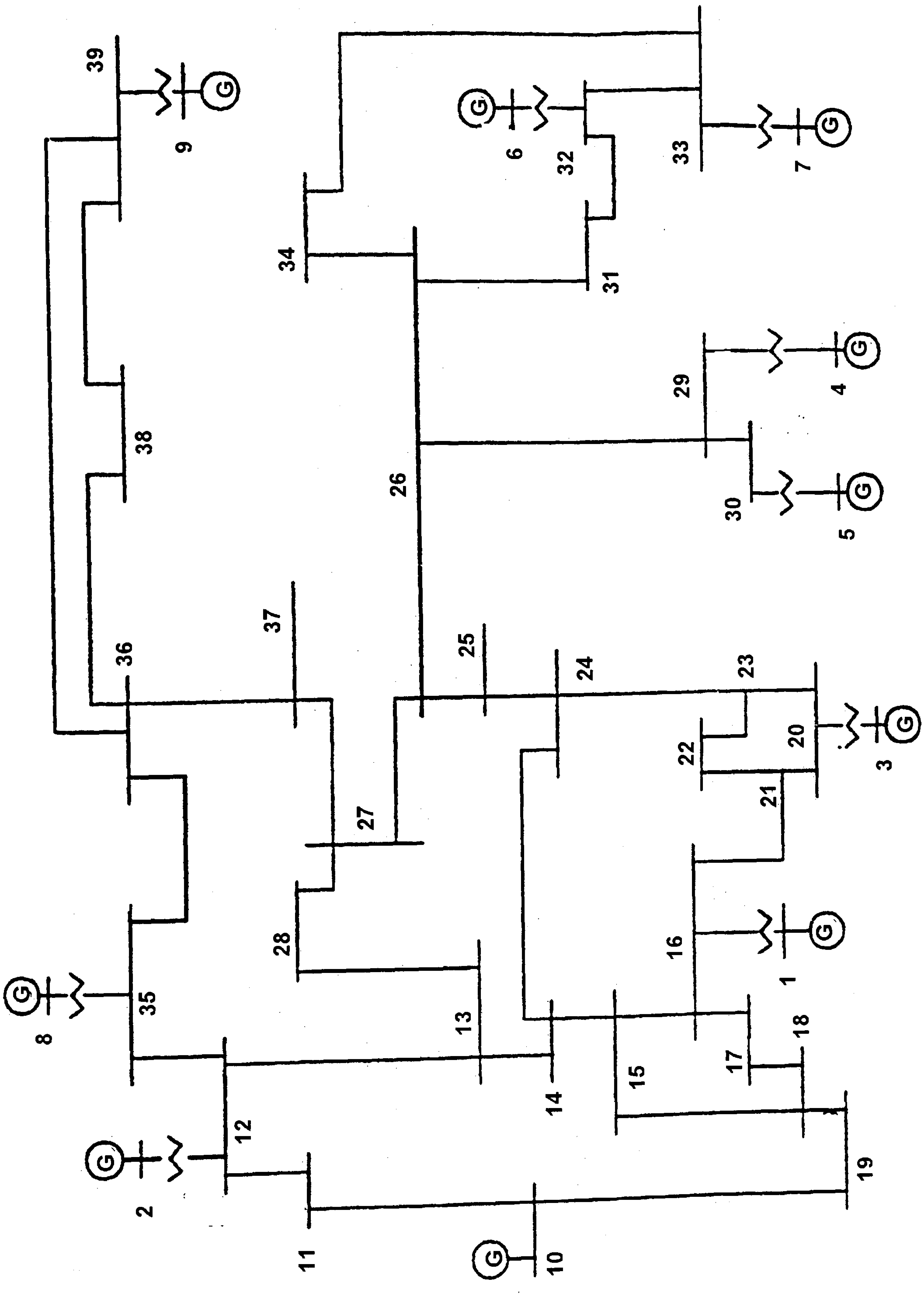

2. The Bus Data

Bus No.	P load	Q load	P gen	V max	Vmin	Vo
1	0.092	0.046	5.732	1.1	0.9	1.0
2	0.000	0.000	2.500	1.1	0.9	1.0
3	0.000	0.000	6.500	1.1	0.9	1.0
4	0.000	0.000	6.320	1.1	0.9	1.0
5	0.000	0.000	5.080	1.1	0.9	1.0
6	0.000	0.000	6.500	1.1	0.9	1.0
7	0.000	0.000	5.600	1.1	0.9	1.1
8	0.000	0.000	5.400	1.1	0.9	1.0
9	0.000	0.000	8.300	1.1	0.9	1.0
10	11.04	2.500	10.00	1.1	0.9	1.0
11	0.000	0.000	0.000	1.1	0.9	1.0
12	0.000	0.000	0.000	1.1	0.9	1.0
13	3.220	0.024	0.000	1.1	0.9	1.0
14	5.000	1.840	0.000	1.1	0.9	1.0
15	0.000	0.000	0.000	1.1	0.9	1.0
16	0.000	0.000	0.000	1.1	0.9	1.0
17	2.338	0.840	0.000	1.1	0.9	1.0
18	5.220	1.760	0.000	1.1	0.9	1.0
19	0.000	0.000	0.000	1.1	0.9	1.0
20	0.000	0.000	0.000	1.1	0.9	1.0
21	0.000	0.000	0.000	1.1	0.9	1.0
22	0.085	0.880	0.000	1.1	0.9	1.0
23	0.000	0.000	0.000	1.1	0.9	1.0
24	0.000	0.000	0.000	1.1	0.9	1.0
25	3.200	1.530	0.000	1.1	0.9	1.0
26	3.294	3.2.30	0.000	1.1	0.9	1.0
27	0.000	0.000	0.000	1.1	0.9	1.0
28	1.580	0.030	0.000	1.1	0.9	1.0
29	0.000	0.000	0.000	1.1	0.9	1.1
30	6.800	1.030	0.000	1.1	0.9	1.0
31	2.740	1.150	0.000	1.1	0.9	1.0
32	0.000	0.000	0.000	1.1	0.9	1.1
33	2.475	8.460	0.000	1.1	0.9	1.0
34	3.086	-0.922	0.000	1.1	0.9	1.0
35	2.240	4.720	0.000	1.1	0.9	1.1
36	1.390	0.170	0.000	1.1	0.9	1.1
37	2.810	0.755	0.000	1.1	0.9	1.0
38	2.060	0.276	0.000	1.1	0.9	1.1
39	2.835	0.269	0.000	1.1	0.9	1.1

3. The Branch Data

Bus from	Bus to	Type	R	X	B	Ratio
12	2	1	0	0.0181	0	1.025
16	1	1	0	0.025	0	1.07
20	3	1	0	0.02	0	1.07
29	4	1	0.0007	0.0142	0	1.07
30	5	1	0.0009	0.018	0	1.009
32	6	1	0	0.0143	0	1.025
33	7	1	0.0005	0.0272	0	1
35	8	1	0.0006	0.0232	0	1.025
39	9	1	0.0008	0.0156	0	1.025
11	12	0	0.0035	0.0411	0.3493	0
11	10	0	0.001	0.025	0.3750	0
12	13	0	0.0013	0.0151	0.1286	0
12	35	0	0.007	0.0086	0.0730	0
13	14	0	0.0013	0.0213	0.1107	0
13	28	0	0.0011	0.0133	0.1069	0
14	15	0	0.0008	0.0128	0.0671	0
14	24	0	0.0008	0.0129	0.0691	0
15	16	0	0.0002	0.0026	0.0217	0
15	18	0	0.0008	0.0112	0.0738	0
16	17	0	0.0006	0.0092	0.0565	0
16	21	0	0.0007	0.0082	0.0694	0
17	18	0	0.0004	0.0046	0.0390	0
18	19	0	0.0023	0.0363	0.1902	0
19	10	0	0.001	0.025	0.6000	0
20	21	0	0.0004	0.0043	0.0365	0
20	23	0	0.0004	0.0043	0.0365	0
22	21	1	0.0016	0.0435	0	1.006
22	23	1	0.0016	0.0435	0	1.006
23	24	0	0.0009	0.0101	0.0862	0
24	25	0	0.0018	0.0217	0.1830	0
25	26	0	0.0009	0.0094	0.0855	0
26	27	0	0.0007	0.0089	0.0671	0
26	29	0	0.0016	0.0195	0.1520	0
26	31	0	0.0008	0.0135	0.1274	0
26	34	0	0.0003	0.0059	0.0340	0
27	28	0	0.0007	0.0082	0.0659	0
27	37	0	0.0013	0.0173	0.1608	0
29	30	1	0.0007	0.0138	0	1.06
31	32	0	0.0008	0.014	0.1283	0
32	33	0	0.0006	0.0096	0.0923	0
33	34	0	0.0022	0.035	0.1805	0
35	36	0	0.0032	0.0323	0.2565	0

Bus from	Bus to	Type	R	X	B	Ratio
36	37	0	0.0014	0.0147	0.1198	0
36	38	0	0.0043	0.0474	0.3901	0
36	39	0	0.0057	0.0625	0.5145	0
38	39	0	0.0014	0.0151	0.1245	0

A1.2 THE IEEE 30 BUS POWER SYSTEM

1. The Single Line Diagram

See next page.

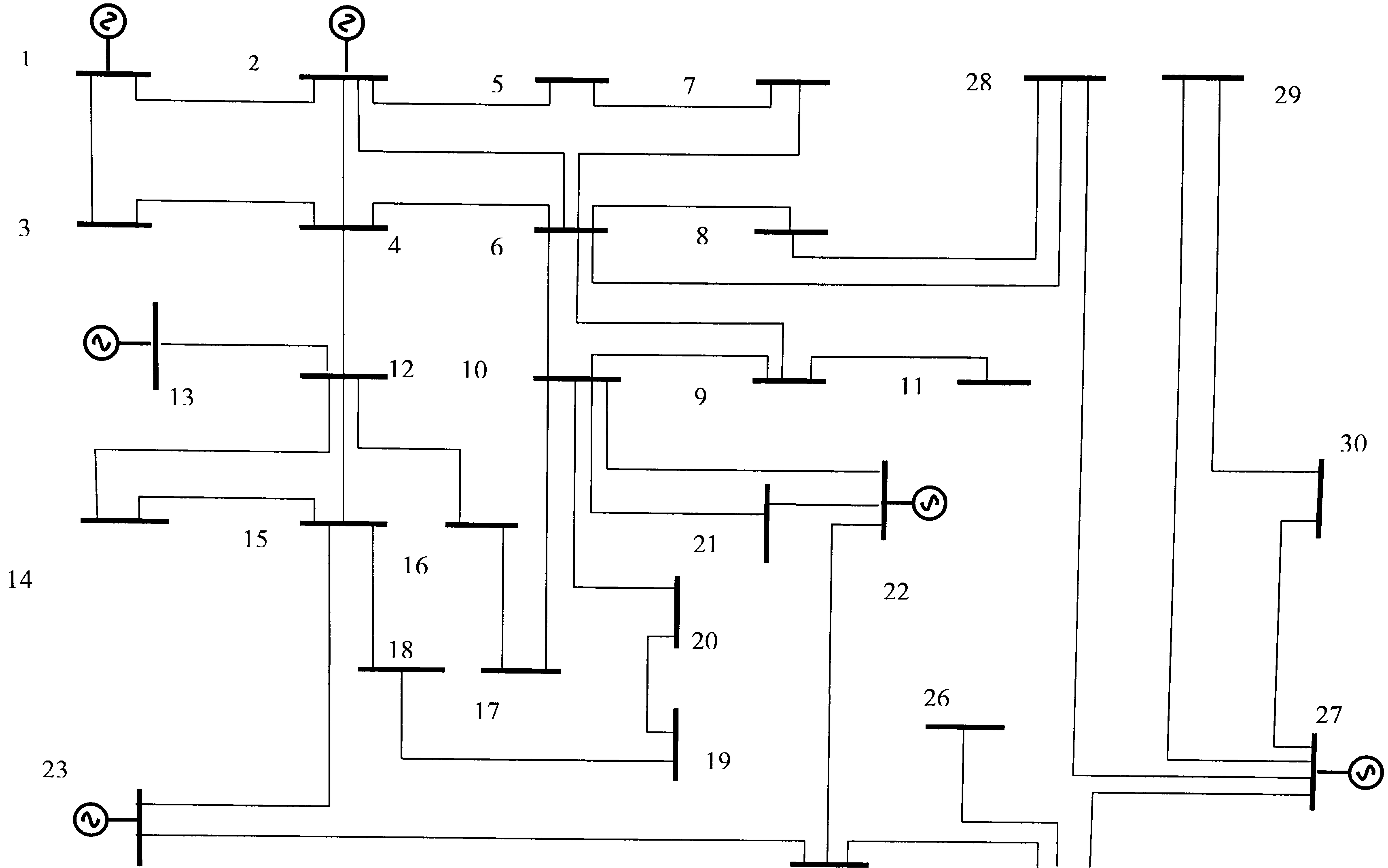
1
2
5
7
28
29
3
4
6
8
13
12
10
9
11
30
15
16
21
22
14
18
20
17
26
27
19
23
24
25

2. The Bus Data

Bus	Type	P load	Q load	Gs	Bs	Base kV	Vmax	Vmin
1	3	0	0	0	0	135	1.05	0.95
2	2	0	0	0	0	135	1.10	0.95
3	1	2.4	1.2	0	0	135	1.05	0.95
4	1	7.6	3.6	0	0	135	1.05	0.95
5	1	0	0	0	0.19	135	1.05	0.95
6	1	0	0	0	0	135	1.05	0.95
7	1	3.8	1.9	0	0	135	1.05	0.95
8	1	0.5	0.3	0	0	135	1.05	0.95
9	1	0	0	0	0	135	1.05	0.95
10	1	5.8	2	0	0	135	1.05	0.95
11	1	0	0	0	0	135	1.05	0.95
12	1	11.2	7.5	0	0	135	1.05	0.95
13	2	0	0	0	0	135	1.1	0.95
14	1	6.2	3.6	0	0	135	1.05	0.95
15	1	8.2	5.5	0	0	135	1.05	0.95
16	1	3.5	1.8	0	0	135	1.05	0.95
17	1	9	5.8	0	0	135	1.05	0.95
18	1	2.80	1.90	0	0	135	1.05	0.95
19	1	3.00	3.00	0	0	135	1.05	0.95
20	1	2.2	1.7	0	0	135	1.05	0.95
21	1	7.50	3.20	0	0	135	1.05	0.95
22	2	0	0	0	0	135	1.1	0.95
23	2	0	0	0	0	135	1.1	0.95
24	1	4.7	3.7	0	0.04	135	1.05	0.95
25	1	0	0	0	0	135	1.05	0.95
26	1	3.5	2.3	0	0	135	1.05	0.95
27	2	0	0	0	0	135	1.1	0.95
28	1	0	0	0	0	135	1.05	0.95
29	1	2.4	1.9	0	0	135	1.05	0.95
30	1	5.6	2.9	0	0	135	1.05	0.95

3. The Branch Data

Bus from	Bus to	R	X	B	Ratio
1	2	0.02	0.06	0.03	0
1	3	0.05	0.19	0.02	0
2	4	0.06	0.17	0.02	0
3	4	0.01	0.04	0	0
2	5	0.05	0.2	0.02	0
2	6	0.06	0.18	0.02	0
4	6	0.01	0.04	0	0
5	7	0.05	0.12	0.01	0
6	7	0.03	0.08	0.01	0
6	8	0.01	0.04	0	0
6	9	0	0.21	0	0
6	10	0	0.56	0	0
9	11	0	0.21	0	0
9	10	0	0.11	0	0
4	12	0	0.26	0	0
12	13	0	0.14	0	0
12	14	0.12	0.26	0	0
12	15	0.07	0.13	0	0
12	16	0.09	0.2	0	0
14	15	0.22	0.2	0	0
16	17	0.08	0.19	0	0
15	18	0.11	0.22	0	0
18	19	0.06	0.13	0	0
19	20	0.03	0.07	0	0
10	20	0.09	0.21	0	0
10	17	0.03	0.08	0	0
10	21	0.03	0.07	0	0
10	22	0.07	0.15	0	0
21	22	0.01	0.02	0	0
15	23	0.1	0.2	0	0
22	24	0.12	0.18	0	0
23	24	0.13	0.27	0	0
24	25	0.19	0.33	0	0
25	26	0.25	0.38	0	0
25	27	0.11	0.21	0	0
28	27	0	0.4	0	0
27	29	0.22	0.42	0	0
27	30	0.32	0.6	0	0
29	30	0.24	0.45	0	0
8	28	0.06	0.2	0.02	0
6	28	0.02	0.06	0.01	0

4. The Generator Data

Bus	P	Q	Qmax	Qmin	V	Mbase	Pmax	Pmin
1	23.54	0	150.00	-20	1.01	100	80	0
2	20.00	0	60.00	-20	1.01	100	80	0
13	12.00	0	44.70	-15	1.00	100	40	0
22	15.00	0	62.50	-15	1.00	100	50	0
23	9.00	0	40.00	-10	1.00	100	30	0
27	20.50	0	48.70	-15	1.00	100	55	0

A1.3 THE WARD-HALE 6 BUS POWER SYSTEM

1. The Single Line Diagram

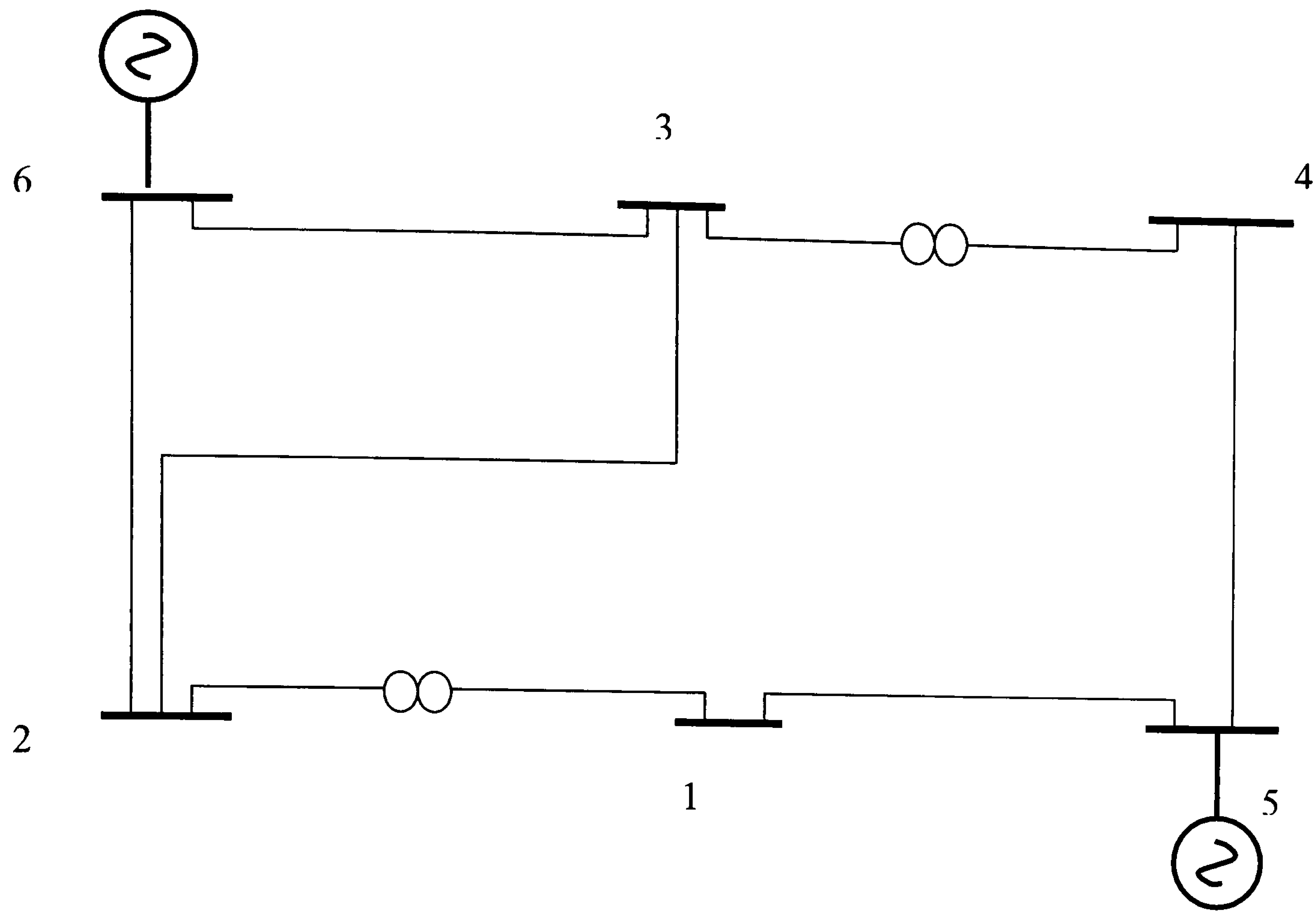

2. The Bus Data

Bus	Type	P Load	Q Load	P Gen	Q Gen	Vmax	Vmin
1	1	0.30	0.18	0.00	0.00	1.05	0.95
2	1	0.50	0.05	0.00	0.00	1.10	0.95
3	1	0.00	0.00	0.00	0.00	1.05	0.95
4	1	0.50	0.13	0.00	0.00	1.05	0.95
5	2	0.00	0.00	0.50	0.00	1.10	0.90
6	3	0.00	0.00	0.00	0.00	1.10	0.90

3. The Branch Data

Bus from	Bus to	R	X	B	Ratio
1	5	0.282	0.640	0.00	0.00
2	1	0.000	0.300	0.00	1.25
2	3	0.097	0.407	0.06	0.00
2	6	0.123	0.518	0.06	0.00
3	4	0.000	0.133	0.00	1.10
3	6	0.080	0.370	0.06	0.00
4	5	0.723	1.050	0.00	0.00

APPENDIX 2 DEFINITIONS AND NOTATIONS IN THE STUDY OF SECONDARY VOLTAGE CONTROL SYSTEMS

This appendix includes the definitions and notations commonly used in the study of secondary voltage control in this thesis. By following the structure of a secondary voltage control system, these notations are categorised into Control Generators, Control Power Plants and Decentralised Regions as well as a whole power system.

A2.1 CONTROL GENERATORS

V_{gi}^{jk} is the voltage magnitude of control generator K at control power plant j in region i ;

V_{grefi}^{jk} is the reference value of V_{gi}^{jk} ;

Q_{gi}^{jk} is the reactive power generation of control generator k at control power plant j in the region i ;

$Q_{gref\,i}^{jk}$ is the reference value for Q_{gi}^{jk} ;

Δq_{gi}^{jk} is the necessary reactive power generation increment in percentage with respect to the rated capacity of control generator k at control power plant j in region i ;

$\Delta q_{gref\,i}^{jk}$ is reference value for Δq_{gi}^{jk} ;

Q_{glimi}^{jk} is rated reactive power generation capacity of generator k at control power plant j in region i;

X_{Ti}^{jk} is the transformer reactance between control generator k and the high voltage bus of control power plant j in region i ;

N_{gi}^{j} the number of control generators at control power plant j in region i ;

N_{gi} the number of control generators at control power plant j in region i ;

N_g the total number of control generators in a power system;

$\left[V_{gi}^{j}\right], \left[V_{gi}\right], \left[V_{g}\right]$ are the vectors of V_{gi}^{jk} for control power plant j, region i and the whole power system respectively;

$\left[V^{j}_{grefi}\right]$, $\left[V_{grefi}\right]$, $\left[V_{gref}\right]$ are the vectors of V^{jk}_{grefi} for control power plant j, region i and the whole power system respectively;

$\left[Q^{j}_{gi}\right]$, $\left[Q_{gi}\right]$, $\left[Q_{g}\right]$ are the vectors of Q^{jk}_{gi} for control power plant j, region i and the whole power system respectively;

$\left[Q^{j}_{grefi}\right]$, $\left[Q_{grefi}\right]$, $\left[Q_{gref}\right]$ are the vectors of Q^{jk}_{grefi} for control power plant j, region i and the whole power system respectively;

$\left[\Delta q^{j}_{gi}\right]$, $\left[\Delta q_{gi}\right]$, $\left[\Delta q_{g}\right]$ are the vectors of Δq^{jk}_{gi} for control power plant j, region i and the whole power system respectively;

$\left[\Delta q^{j}_{grefi}\right]$, $\left[\Delta q_{grefi}\right]$, $\left[\Delta q_{gref}\right]$ are the vectors of Δq^{jk}_{grefi} for control power plant j, region i and the whole power system respectively;

$\left[\Lambda^{j}_{g\lim i}\right] = \mathrm{diag}\left\{Q^{j1}_{g\lim i}, Q^{j2}_{g\lim i}, \ldots, Q^{jN^{j}_{gi}}_{g\lim i}\right\}$;

$\left[\Lambda_{g\lim i}\right] = \mathrm{diag}\left\{Q^{11}_{g\lim i}, Q^{12}_{g\lim i}, \ldots, Q^{jk}_{g\lim i}, \ldots, Q^{N_{Gi}N^{N_{Gi}}_{gi}}_{g\lim i}\right\}$;

$\left[\Lambda_{g\lim}\right] = \mathrm{diag}\left\{Q^{11}_{g\lim i}, Q^{12}_{g\lim i}, \ldots, Q^{jk}_{g\lim i}, \ldots, Q^{N_{GZ}N^{N_{GZ}}_{gZ}}_{g\lim Z}\right\}$.

A2.2 Control Power Plants

V_{Gi}^{j} is the voltage magnitude at HV bus of control power plant *j* in region *i* ;

$V_{Gref\,i}^{j}$ is the reference value of V_{Gi}^{j};

Q_{Gi}^{j} is the reactive power generation of control power plant *j* in the region *i* ;

$Q_{Gref\,i}^{j}$ is the reference value of Q_{Gi}^{j};

Δq_{Gi}^{j} is the necessary reactive power generation increment in percentage with rated capacity at control power plant *j* in region *i* ;

$\Delta q_{Gref\,i}^{j}$ is the reference value of $\Delta q_{Gref\,i}^{j}$;

X_{Ei}^{j} is the equivalent reactance between high voltage bus of control power plant *j* in region *i* and the power system ;

V_{Ri}^{j} is the voltage at equivalent system bus for the control power plant *j* in region *i;*

N_{Gi} is the number of control power plants in region *i* ;

N_G is the total number of control plant in the power system;

$[V_{Gi}]$, $[V_G]$ are the vectors of V_{Gi}^{j} for region i and a whole power system respectively;

$[V_{Gref\,i}]$, $[V_{Gref}]$ are the vectors of $V_{Gref\,i}^{j}$ for region i and the whole power system respectively;

$[Q_{Gi}]$, $[Q_G]$ are the vectors of Q_{Gi}^{j} for the region i and the whole power system respectively;

$[Q_{Gref\,i}]$, $[Q_{Gref}]$ are the vectors of $Q_{Gref\,i}^{j}$ for the region i and the whole power system respectively;

$[\Delta q_{G\,i}]$, $[\Delta q_G]$ are the vectors of Δq_{Gi}^{j} for the region i and the whole power system respectively;

$[\Delta q_{Gref\,i}]$, $[\Delta q_{Gref}]$ are the vectors of $\Delta q_{Gref\,i}^{j}$ for the region i and the whole power system respectively.

A2.3 DECENTRALISED REGIONS

V_{Pi} is the voltage magnitude at pilot bus in region i;

$V_{Pref\,i}$ is the reference value for V_{pi};

$V_{\bar{P}i}^{j}$ is the voltage magnitude for a non-pilot bus j in region i;

Q_{Ri} is the necessary reactive power generation in region i;

Q_{Rrefi} is the reference value of Q_{Ri};

Δq_{Ri} is the necessary reactive power generation increment in percentage with respect to the rated capacity in region i;

Δq_{Rrefi} is the reference value of Δq_{Ri};

Q_{Li}^{j} is the reactive power load at the load bus j in region i;

$[V_P]$, $[V_{Pref}]$, $[\Delta Q_R]$, $[\Delta Q_{Rref}]$, $[\Delta q_R]$, $[\Delta q_{Rref}]$ are the vectors of V_{pi}, $V_{pref\,i}$, ΔQ_{Ri}, ΔQ_{Rrefi}, Δq_{Ri}, Δq_{Rrefi} for the whole power system respectively;

$\left[V_{\bar{P}i}\right]$, $\left[V_{\bar{P}}\right]$ are the vectors of $V_{\bar{P}i}^{j}$ for region i and the whole power system respectively;

$[Q_{Li}]$, $[Q_L]$ are the vectors of Q_{Li}^{j} for region i and the whole power system respectively.

A2.4 A POWER SYSTEM

Z is the number of decentralised regions in the power system;

[V] is the vector of voltage magnitude at all buses in a power system ;

$[\Lambda_X]_n$ is n by n diagonal matrix, $[\Lambda_X]_n = \text{diag}\{x_1, x_2, ..., x_i, ... x_n\}$;

$[I]_n$ is the n by n unit matrix;

$[I_{col}]_n$ is the n by 1 unit column matrix;

$[I_{row}]_n$ is the 1 by n unit row matrix;

$[D_{Gg}] = \text{diag}\left\{[I_{row}]_{N_{g1}^1}, [I_{row}]_{N_{g1}^2}, ..., [I_{row}]_{N_{gi}^j}, ..., [I_{row}]_{N_{gZ}^{NGZ}}\right\}$ is **structure matrix** to represent the structure between all the control power plants and all the control generators in a power system;

$[D_{GR}] = \text{diag}\left\{[I_{col}]_{N_{G1}}, [I_{col}]_{N_{G2}}, ..., [I_{col}]_{N_{Gi}}, ..., [I_{col}]_{N_{GZ}}\right\}$ is **structure matrix** to represent the structure between all the control power plants and all the regions in a power system;

$$[\Delta Q_G] = [D_{Gg}][\Delta Q_g] = [D_{GR}][\Delta Q_R]$$

APPENDIX 3 SIMULATION RESULTS

A3.1 ABBREVIATIONS

L: Load pattern

LD: Load distribution pattern

G: Generation pattern

GP: Generation Participation Pattern

LDP: Load distribution coefficient for active power

LDQ: Load distribution coefficient for reactive power

GPP: Generation participation coefficient for active power

GPQ: Generation participation coefficient for reactive power

P_L0: Initial active load (Load pattern active coefficients)

Q_L0: Initial reactive load (Load pattern reactive coefficients)

Pg0: Initial active generation (Generation pattern active coefficients)

Qg0: Initial active generation (Generation pattern reactive coefficients)

P_LF: Critical (Maximum) active load

Q_LF: Critical (Maximum) reactive load

PgF: Critical (Maximum) active generation

QgF: Critical (Maximum) reactive generation

PM: Power margins

$\Delta Q_L = Q_LF - Q_L0$: Reactive power margins

$\Delta Qg = QgF - Qg0$: Generation increase (Active power)

$\Delta P_L = P_LF - P_L0$: Active power margins

$\Delta Pg = PgF - Pg0$: Generation increase (Active power)

A3.2 Impact of the VSDFs on Voltage Stability

1. Impact of the Load Pattern (L)

Table A3-1 and Table A3-2 list the power margin simulation results on the IEEE 30 bus system **with different Load Patterns** but the same other VSDFs under the same operation conditions.

2. Impact of the Load Distribution Pattern (LD)

Table A3-3, Table A3-4 and Table A3-5 list the power margin simulation results on the IEEE 30 bus system **with different Load distribution Patterns** but the same other VSDFs under the same operation conditions.

3. Impact of the Generation Pattern (G)

Table A3-6 and Table A3-7 list the power margin simulation results on the IEEE 30 system **with different Generation Patterns** but the same other VSDFs under the same operation conditions.

4. Impact of the Generation Participation Pattern (GP)

Table A3-3 and Table A3-8 list the power margin simulation results on the IEEE 30 system **with different Generation Participation Patterns** but the same other VSDFs under the same operation conditions.

Table A3 - 1 **Ref. Case30f01L02LD01G05GP01b**

Bus	L		G						PM				LD		GP	
	P_L0	Q_L0	Pg0	Qg0	P_LF	Q_LF	PgF	QgF	ΔP_L	ΔQ_L	ΔPg	ΔQg	LDP	LDQ	GPP	GPQ
1	0	0	46.35	10.8	0	0	79.52	22.61	0	0	33.17	11.81	0.00%	0.00%	24.80%	9.93%
2	0	0	44.44	18.63	0	0	76	39.05	0	0	31.56	20.42	0.00%	0.00%	23.59%	17.17%
3	2.4	1.2	0		3.89	1.94	0	0	1.49	0.74	0.00	0.00	1.33%	1.27%	0.00%	0.00%
4	7.6	3.6	0		12.31	5.83	0	0	4.71	2.23	0.00	0.00	4.22%	3.81%	0.00%	0.00%
5	0	0	0		0	0	0	0	0	0	0.00	0.00	0.00%	0.00%	0.00%	0.00%
6	0	0	0		0	0	0	0	0	0	0.00	0.00	0.00%	0.00%	0.00%	0.00%
7	12.8	5.9	0		20.74	9.56	0	0	7.94	3.66	0.00	0.00	7.10%	6.24%	0.00%	0.00%
8	11.5	4.3	0		18.63	6.97	0	0	7.13	2.67	0.00	0.00	6.38%	4.55%	0.00%	0.00%
9	9	5	0		14.58	8.1	0	0	5.58	3.1	0.00	0.00	4.99%	5.29%	0.00%	0.00%
10	5.8	2	0		9.4	3.24	0	0	3.6	1.24	0.00	0.00	3.22%	2.12%	0.00%	0.00%
11	0	0	0		0	0	0	0	0	0	0.00	0.00	0.00%	0.00%	0.00%	0.00%
12	11.2	5.5	0		18.14	8.91	0	0	6.94	3.41	0.00	0.00	6.22%	5.82%	0.00%	0.00%
13	0	0	22.21	16.05	0	0	38	34.09	0	0	15.79	18.04	0.00%	0.00%	11.80%	15.17%
14	6.2	3.6	0		10.04	5.83	0	0	3.84	2.23	0.00	0.00	3.44%	3.81%	0.00%	0.00%
15	8.2	5.5	0		13.28	8.91	0	0	5.08	3.41	0.00	0.00	4.55%	5.82%	0.00%	0.00%
16	3.5	1.8	0		5.67	2.92	0	0	2.17	1.12	0.00	0.00	1.94%	1.90%	0.00%	0.00%
17	9	5.8	0		14.58	9.4	0	0	5.58	3.6	0.00	0.00	4.99%	6.14%	0.00%	0.00%
18	32.8	17.9	0		53.14	29	0	0	20.34	11.1	0.00	0.00	18.20%	18.94%	0.00%	0.00%
19	23	11	0		37.26	17.82	0	0	14.26	6.82	0.00	0.00	12.76%	11.64%	0.00%	0.00%
20	12.2	6.7	0		19.76	10.85	0	0	7.56	4.15	0.00	0.00	6.77%	7.09%	0.00%	0.00%
21	7.5	3.2	0		12.15	5.18	0	0	4.65	1.98	0.00	0.00	4.16%	3.39%	0.00%	0.00%
22	0	0	27.78	24.3	0	0	47.5	51.92	0	0	19.72	27.62	0.00%	0.00%	14.74%	23.22%
23	0	0	16.66	16.1	0	0	28.5	34.05	0	0	11.84	17.95	0.00%	0.00%	8.85%	15.09%

Bus	*L*		G						PM				LD		GP	
	P_L0	Q_L0	Pg0	Qg0	P_LF	Q_LF	PgF	QgF	ΔP_L	ΔQ_L	ΔPg	ΔQg	LDP	LDQ	GPP	GPQ
24	*4.7*	*3.7*	0		7.61	5.99	0	0	**2.91**	**2.29**	0.00	0.00	2.61%	3.92%	0.00%	0.00%
25	*1*	*0.7*	0		1.62	1.13	0	0	**0.62**	**0.43**	0.00	0.00	0.55%	0.74%	0.00%	0.00%
26	*3.5*	*2.3*	0		5.67	3.73	0	0	**2.17**	**1.43**	0.00	0.00	1.94%	2.43%	0.00%	0.00%
27	*0*	*0*	30.56	20.51	0	0	52.25	43.61	**0**	**0**	21.69	23.10	0.00%	0.00%	16.21%	19.42%
28	*0*	*0*	0		0	0	0	0	**0**	**0**	0.00	0.00	0.00%	0.00%	0.00%	0.00%
29	*2.7*	*1.9*	0		4.37	3.08	0	0	**1.67**	**1.18**	0.00	0.00	1.50%	2.01%	0.00%	0.00%
30	*5.6*	*2.9*	0		9.07	4.7	0	0	**3.47**	**1.8**	0.00	0.00	3.11%	3.07%	0.00%	0.00%
Total	*180.2*	*94.5*	188	106.39	291.91	153.09	321.77	225.33	**111.71**	**58.59**	133.77	118.94	100%	100%	100.00%	100.00%

Table A3 - 2 Ref. Case30f02L03LD01G05GP01

Bus	*L*		G						PM				LD		GP	
	P_L0	Q_L0	Pg0	Qg0	P_LF	Q_LF	PgF	QgF	ΔP_L	ΔQ_L	ΔPg	ΔQg	LDP	LDQ	GPP	GPQ
1	*0*	*0*	46.35	10.8	0	0	80.62	22.12	**0**	**0**	34.27	11.32	0.00%	0.00%	23.16%	10.36%
2	*0*	*0*	44.44	18.63	0	0	80.08	37.56	**0**	**0**	35.64	18.93	0.00%	0.00%	24.08%	17.32%
3	*2.4*	*1.2*	0		4.19	2.24	0	0	**1.79**	**1.04**	0	0	1.33%	1.27%	0.00%	0.00%
4	*7.6*	*3.6*	0		13.4	6.64	0	0	**5.8**	**3.04**	0	0	4.22%	3.81%	0.00%	0.00%
5	*0*	*0*	0		0	0	0	0	**0**	**0**	0	0	0.00%	0.00%	0.00%	0.00%
6	*0*	*0*	0		0	0	0	0	**0**	**0**	0	0	0.00%	0.00%	0.00%	0.00%
7	*12.8*	*5.9*	0		22.6	10.86	0	0	**9.8**	**4.96**	0	0	7.10%	6.24%	0.00%	0.00%
8	*32.8*	*17.9*	0		41.63	21.58	0	0	**30.13**	**17.28**	0	0	6.38%	4.55%	0.00%	0.00%
9	*23*	*11*	0		29.9	15.24	0	0	**20.9**	**10.24**	0	0	4.99%	5.29%	0.00%	0.00%
10	*12.2*	*6.7*	0		16.62	8.38	0	0	**10.82**	**6.38**	0	0	3.22%	2.12%	0.00%	0.00%
11	*0*	*0*	0		0	0	0	0	**0**	**0**	0	0	0.00%	0.00%	0.00%	0.00%
12	*11.2*	*5.5*	0		19.76	10.14	0	0	**8.56**	**4.64**	0	0	6.22%	5.82%	0.00%	0.00%
13	*0*	*0*	22.21	16.05	0	0	40.03	32.32	**0**	**0**	17.82	16.27	0.00%	0.00%	12.04%	14.89%
14	*6.2*	*3.6*	0		10.89	6.64	0	0	**4.69**	**3.04**	0	0	3.44%	3.81%	0.00%	0.00%
15	*8.2*	*5.5*	0		14.55	10.14	0	0	**6.35**	**4.64**	0	0	4.55%	5.82%	0.00%	0.00%
16	*3.5*	*1.8*	0		6.12	3.32	0	0	**2.62**	**1.52**	0	0	1.94%	1.90%	0.00%	0.00%
17	*9*	*5.8*	0		15.9	10.68	0	0	**6.9**	**4.88**	0	0	4.99%	6.14%	0.00%	0.00%
18	*11.5*	*4.3*	0		36.62	19.42	0	0	**3.82**	**1.52**	0	0	18.20%	18.94%	0.00%	0.00%
19	*9*	*5*	0		26.66	14.28	0	0	**3.66**	**3.28**	0	0	12.76%	11.64%	0.00%	0.00%
20	*5.8*	*2*	0		15.18	7.68	0	0	**2.98**	**0.98**	0	0	6.77%	7.09%	0.00%	0.00%
21	*7.5*	*3.2*	0		13.3	5.92	0	0	**5.8**	**2.72**	0	0	4.16%	3.39%	0.00%	0.00%
22	*0*	*0*	27.78	24.3	0	0	50.13	48.97	**0**	**0**	22.35	24.67	0.00%	0.00%	15.10%	22.58%
23	*0*	*0*	16.66	16.1	0	0	30.1	32.73	**0**	**0**	13.44	16.63	0.00%	0.00%	9.08%	15.22%

Bus	L		G						PM				LD		GP	
	P_L0	***Q_L0***	**Pg0**	**Qg0**	**P_LF**	**Q_LF**	**PgF**	**QgF**	**ΔP_L**	**ΔQ_L**	**ΔPg**	**ΔQg**	**LDP**	**LDQ**	**GPP**	**GPQ**
24	*4.7*	*3.7*	0		8.29	6.82	0	0	**3.59**	**3.12**	0	0	2.61%	3.92%	0.00%	0.00%
25	*1*	*0.7*	0		1.83	1.26	0	0	**0.83**	**0.56**	0	0	0.55%	0.74%	0.00%	0.00%
26	*3.5*	*2.3*	0		6.12	4.22	0	0	**2.62**	**1.92**	0	0	1.94%	2.43%	0.00%	0.00%
27	*0*	*0*	30.56	20.51	0	0	55.02	41.96	**0**	**0**	24.46	21.45	0.00%	0.00%	16.53%	19.63%
28	*0*	*0*	0		0	0	0	0	**0**	**0**	0	0	0.00%	0.00%	0.00%	0.00%
29	*2.7*	*1.9*	0		4.77	3.5	0	0	**2.07**	**1.6**	0	0	1.50%	2.01%	0.00%	0.00%
30	*5.6*	*2.9*	0		9.88	5.38	0	0	**4.28**	**2.48**	0	0	3.11%	3.07%	0.00%	0.00%
Total	*180.2*	*94.5*	188	106.39	318.21	174.34	335.98	215.66	**138.01**	**79.84**	147.98	109.27	100%	100%	100.00%	100.00%

NB: Reached maximum generation capacity 335 MWs

Table A3 - 3 **Ref.:Case30F01pL01LD01G02GP01b**

Bus	L		G						PM				*LD*		GP	
	P_L0	Q_L0	Pg0	Qg0	P_LF	Q_LF	PgF	QgF	ΔP_L	ΔQ_L	ΔPg	ΔQg	*LDP*	*LDQ*	GPP	GPQ
1	0	0	4.47	-0.79	0	0	79.52	22.61	**0**	**0**	75.05	23.40	***0.00%***	***0.00%***	24.71%	10.03%
2	0	0	4.27	-1.4	0	0	76	39.05	**0**	**0**	71.73	40.45	***0.00%***	***0.00%***	23.62%	17.33%
3	0.24	0.12	0	0	3.89	1.94	0	0	**3.65**	**1.82**	0.00	0.00	***1.33%***	***1.27%***	0.00%	0.00%
4	0.76	0.36	0	0	12.31	5.83	0	0	**11.55**	**5.47**	0.00	0.00	***4.22%***	***3.81%***	0.00%	0.00%
5	0	0	0	0	0	0	0	0	**0**	**0**	0.00	0.00	***0.00%***	***0.00%***	0.00%	0.00%
6	0	0	0	0	0	0	0	0	**0**	**0**	0.00	0.00	***0.00%***	***0.00%***	0.00%	0.00%
7	1.28	0.59	0	0	20.74	9.56	0	0	**19.46**	**8.97**	0.00	0.00	***7.10%***	***6.24%***	0.00%	0.00%
8	1.15	0.43	0	0	18.63	6.97	0	0	**17.48**	**6.54**	0.00	0.00	***6.38%***	***4.55%***	0.00%	0.00%
9	0.9	0.5	0	0	14.58	8.1	0	0	**13.68**	**7.6**	0.00	0.00	***4.99%***	***5.29%***	0.00%	0.00%
10	0.58	0.2	0	0	9.4	3.24	0	0	**8.82**	**3.04**	0.00	0.00	***3.22%***	***2.12%***	0.00%	0.00%
11	0	0	0	0	0	0	0	0	**0**	**0**	0.00	0.00	***0.00%***	***0.00%***	0.00%	0.00%
12	1.12	0.55	0	0	18.14	8.91	0	0	**17.02**	**8.36**	0.00	0.00	***6.22%***	***5.82%***	0.00%	0.00%
13	0	0	2.14	-1.17	0	0	38	34.09	**0**	**0**	35.86	35.26	***0.00%***	***0.00%***	11.81%	15.13%
14	0.62	0.36	0	0	10.04	5.83	0	0	**9.42**	**5.47**	0.00	0.00	***3.44%***	***3.81%***	0.00%	0.00%
15	0.82	0.55	0	0	13.28	8.91	0	0	**12.46**	**8.36**	0.00	0.00	***4.55%***	***5.82%***	0.00%	0.00%
16	0.35	0.18	0	0	5.67	2.92	0	0	**5.32**	**2.74**	0.00	0.00	***1.94%***	***1.90%***	0.00%	0.00%
17	0.9	0.58	0	0	14.58	9.4	0	0	**13.68**	**8.82**	0.00	0.00	***4.99%***	***6.14%***	0.00%	0.00%
18	3.28	1.79	0	0	53.14	29	0	0	**49.86**	**27.21**	0.00	0.00	***18.20%***	***18.94%***	0.00%	0.00%
19	2.3	1.1	0	0	37.26	17.82	0	0	**34.96**	**16.72**	0.00	0.00	***12.76%***	***11.64%***	0.00%	0.00%
20	1.22	0.67	0	0	19.76	10.85	0	0	**18.54**	**10.18**	0.00	0.00	***6.77%***	***7.09%***	0.00%	0.00%
21	0.75	0.32	0	0	12.15	5.18	0	0	**11.4**	**4.86**	0.00	0.00	***4.16%***	***3.39%***	0.00%	0.00%
22	0	0	2.67	-1.63	0	0	47.5	51.92	**0**	**0**	44.83	53.55	***0.00%***	***0.00%***	14.76%	23.04%
23	0	0	1.60	-1.12	0	0	28.5	34.05	**0**	**0**	26.90	35.17	***0.00%***	***0.00%***	8.86%	15.11%

Bus	L		G						PM				*LD*		GP	
	P_L0	**Q_L0**	**Pg0**	**Qg0**	**P_LF**	**Q_LF**	**PgF**	**QgF**	**ΔP_L**	**ΔQ_L**	**ΔPg**	**ΔQg**	***LDP***	***LDQ***	**GPP**	**GPQ**
24	0.47	0.37	0	0	7.61	5.99	0	0	**7.14**	**5.62**	0.00	0.00	***2.61%***	***3.92%***	0.00%	0.00%
25	0.1	0.07	0	0	1.62	1.13	0	0	**1.52**	**1.06**	0.00	0.00	***0.55%***	***0.74%***	0.00%	0.00%
26	0.35	0.23	0	0	5.67	3.73	0	0	**5.32**	**3.5**	0.00	0.00	***1.94%***	***2.43%***	0.00%	0.00%
27	0	0	2.94	-1.52	0	0	52.25	43.61	**0**	**0**	49.31	45.13	***0.00%***	***0.00%***	16.24%	19.35%
28	0	0	0	0	0	0	0	0	**0**	**0**	0.00	0.00	***0.00%***	***0.00%***	0.00%	0.00%
29	0.27	0.19	0	0	4.37	3.08	0	0	**4.1**	**2.89**	0.00	0.00	***1.50%***	***2.01%***	0.00%	0.00%
30	0.56	0.29	0	0	9.07	4.7	0	0	**8.51**	**4.41**	0.00	0.00	***3.11%***	***3.07%***	0.00%	0.00%
Total	18.02	9.45	18.09	-7.63	291.91	153.09	321.77	225.33	**273.89**	**143.64**	303.68	232.96	***100%***	***100%***	100%	100%

Table A3 - 4 **Ref.CASE30F06L01LD02G02GP01**

Bus	L		G						PM				*LD*		GP	
	P_L0	Q_L0	Pg0	Qg0	PlF	QlF	PgF	QgF	ΔP_L	ΔQ_L	ΔPg	ΔQg	*LDP*	*LDQ*	GPP	GPQ
1	0	0	4.47	-0.79	0	0	79.62	24.59	**0.00**	**0.00**	75.15	25.38	***0.00%***	***0.00%***	24.71%	10.03%
2	0	0	4.27	-1.4	0	0	79.79	37.7	**0.00**	**0.00**	75.52	39.10	***0.00%***	***0.00%***	23.62%	17.33%
3	0.24	0.12	0	0	15.24	9.12	0	0	**15.00**	**9.00**	0.00	0.00	***5.00%***	***5.00%***	0.00%	0.00%
4	0.76	0.36	0	0	15.76	9.36	0	0	**15.00**	**9.00**	0.00	0.00	***5.00%***	***5.00%***	0.00%	0.00%
5	0	0	0	0	0	0	0	0	**0.00**	**0.00**	0.00	0.00	***0.00%***	***0.00%***	0.00%	0.00%
6	0	0	0	0	0	0	0	0	**0.00**	**0.00**	0.00	0.00	***0.00%***	***0.00%***	0.00%	0.00%
7	1.28	0.59	0	0	16.28	9.59	0	0	**15.00**	**9.00**	0.00	0.00	***5.00%***	***5.00%***	0.00%	0.00%
8	1.15	0.43	0	0	16.15	9.43	0	0	**15.00**	**9.00**	0.00	0.00	***5.00%***	***5.00%***	0.00%	0.00%
9	0.9	0.5	0	0	15.9	9.5	0	0	**15.00**	**9.00**	0.00	0.00	***5.00%***	***5.00%***	0.00%	0.00%
10	0.58	0.2	0	0	15.58	9.2	0	0	**15.00**	**9.00**	0.00	0.00	***5.00%***	***5.00%***	0.00%	0.00%
11	0	0	0	0	0	0	0	0	**0.00**	**0.00**	0.00	0.00	***0.00%***	***0.00%***	0.00%	0.00%
12	1.12	0.55	0	0	16.12	9.55	0	0	**15.00**	**9.00**	0.00	0.00	***5.00%***	***5.00%***	0.00%	0.00%
13	0	0	2.14	-1.17	0	0	39.9	32.96	**0.00**	**0.00**	37.76	34.13	***0.00%***	***0.00%***	11.81%	15.13%
14	0.62	0.36	0	0	15.62	9.36	0	0	**15.00**	**9.00**	0.00	0.00	***5.00%***	***5.00%***	0.00%	0.00%
15	0.82	0.55	0	0	15.82	9.55	0	0	**15.00**	**9.00**	0.00	0.00	***5.00%***	***5.00%***	0.00%	0.00%
16	0.35	0.18	0	0	15.35	9.18	0	0	**15.00**	**9.00**	0.00	0.00	***5.00%***	***5.00%***	0.00%	0.00%
17	0.9	0.58	0	0	15.9	9.58	0	0	**15.00**	**9.00**	0.00	0.00	***5.00%***	***5.00%***	0.00%	0.00%
18	3.28	1.79	0	0	18.28	10.79	0	0	**15.00**	**9.00**	0.00	0.00	***5.00%***	***5.00%***	0.00%	0.00%
19	2.3	1.1	0	0	17.3	10.1	0	0	**15.00**	**9.00**	0.00	0.00	***5.00%***	***5.00%***	0.00%	0.00%
20	1.22	0.67	0	0	16.22	9.67	0	0	**15.00**	**9.00**	0.00	0.00	***5.00%***	***5.00%***	0.00%	0.00%
21	0.75	0.32	0	0	15.75	9.32	0	0	**15.00**	**9.00**	0.00	0.00	***5.00%***	***5.00%***	0.00%	0.00%
22	0	0	2.67	-1.63	0	0	49.71	50.35	**0.00**	**0.00**	47.04	51.98	***0.00%***	***0.00%***	14.76%	23.04%
23	0	0	1.60	-1.12	0	0	29.44	33.01	**0.00**	**0.00**	27.84	34.13	***0.00%***	***0.00%***	8.86%	15.11%

Bus	L		G						PM				*LD*		GP	
	P_L0	**Q_L0**	**Pg0**	**Qg0**	**PlF**	**QlF**	**PgF**	**QgF**	**ΔP_L**	**ΔQ_L**	**ΔPg**	**ΔQg**	***LDP***	***LDQ***	**GPP**	**GPQ**
24	0.47	0.37	0	0	15.47	9.37	0	0	**15.00**	**9.00**	0.00	0.00	***5.00%***	***5.00%***	0.00%	0.00%
25	0.1	0.07	0	0	15.1	9.07	0	0	**15.00**	**9.00**	0.00	0.00	***5.00%***	***5.00%***	0.00%	0.00%
26	0.35	0.23	0	0	15.35	9.23	0	0	**15.00**	**9.00**	0.00	0.00	***5.00%***	***5.00%***	0.00%	0.00%
27	0	0	2.94	-1.52	0	0	54.78	42.32	**0.00**	**0.00**	51.84	43.84	***0.00%***	***0.00%***	16.24%	19.35%
28	0	0	0	0	0	0	0	0	**0.00**	**0.00**	0.00	0.00	***0.00%***	***0.00%***	0.00%	0.00%
29	0.27	0.19	0	0	15.27	9.19	0	0	**15.00**	**9.00**	0.00	0.00	***5.00%***	***5.00%***	0.00%	0.00%
30	0.56	0.29	0	0	15.56	9.29	0	0	**15.00**	**9.00**	0.00	0.00	***5.00%***	***5.00%***	0.00%	0.00%
Total	18.02	9.45	18.09	-7.63	318.02	189.45	333.24	220.93	**300**	**180**	315.15	228.56	***100.00%***	***100.00%***	100.00%	100.00%

NB: Reached the maximum generation capacity 335MWs

Table A3 - 5 **Ref.: CASE30F07pL01LD03G02GP01**

Bus	L		G						PM				*LD*		GP	
	P_L0	Q_L0	Pg0	Qg0	PlF	QlF	PgF	QgF	ΔP_L	ΔQ_L	ΔPg	ΔQg	*LDP*	*LDQ*	GPP	GPQ
1	0	0	4.47	-0.79	0	0	69.91	23.79	**0.00**	**0.00**	65.44	24.58	***0.00%***	***0.00%***	24.71%	10.03%
2	0	0	4.27	-1.4	0	0	69.41	37.53	**0.00**	**0.00**	65.14	38.93	***0.00%***	***0.00%***	23.62%	17.33%
3	0.24	0.12	0	0	2.69	1.55	0	0	**2.45**	**1.43**	0.00	0.00	***1.00%***	***1.00%***	0.00%	0.00%
4	0.76	0.36	0	0	10.56	6.08	0	0	**9.80**	**5.72**	0.00	0.00	***4.00%***	***4.00%***	0.00%	0.00%
5	0	0	0	0	0	0	0	0	**0.00**	**0.00**	0.00	0.00	***0.00%***	***0.00%***	0.00%	0.00%
6	0	0	0	0	0	0	0	0	**0.00**	**0.00**	0.00	0.00	***0.00%***	***0.00%***	0.00%	0.00%
7	1.28	0.59	0	0	11.08	6.31	0	0	**9.80**	**5.72**	0.00	0.00	***4.00%***	***4.00%***	0.00%	0.00%
8	1.15	0.43	0	0	13.4	7.58	0	0	**12.25**	**7.15**	0.00	0.00	***5.00%***	***5.00%***	0.00%	0.00%
9	0.9	0.5	0	0	13.15	7.65	0	0	**12.25**	**7.15**	0.00	0.00	***5.00%***	***5.00%***	0.00%	0.00%
10	0.58	0.2	0	0	7.93	4.49	0	0	**7.35**	**4.29**	0.00	0.00	***3.00%***	***3.00%***	0.00%	0.00%
11	0	0	0	0	0	0	0	0	**0.00**	**0.00**	0.00	0.00	***0.00%***	***0.00%***	0.00%	0.00%
12	1.12	0.55	0	0	13.37	7.7	0	0	**12.25**	**7.15**	0.00	0.00	***5.00%***	***5.00%***	0.00%	0.00%
13	0	0	2.14	-1.17	0	0	34.7	32.8	**0.00**	**0.00**	32.56	33.97	***0.00%***	***0.00%***	11.81%	15.13%
14	0.62	0.36	0	0	12.87	7.51	0	0	**12.25**	**7.15**	0.00	0.00	***5.00%***	***5.00%***	0.00%	0.00%
15	0.82	0.55	0	0	13.07	7.7	0	0	**12.25**	**7.15**	0.00	0.00	***5.00%***	***5.00%***	0.00%	0.00%
16	0.35	0.18	0	0	10.15	5.9	0	0	**9.80**	**5.72**	0.00	0.00	***4.00%***	***4.00%***	0.00%	0.00%
17	0.9	0.58	0	0	13.15	7.73	0	0	**12.25**	**7.15**	0.00	0.00	***5.00%***	***5.00%***	0.00%	0.00%
18	3.28	1.79	0	0	52.28	30.39	0	0	**49.00**	**28.60**	0.00	0.00	***20.00%***	***20.00%***	0.00%	0.00%
19	2.3	1.1	0	0	26.8	15.4	0	0	**24.50**	**14.30**	0.00	0.00	***10.00%***	***10.00%***	0.00%	0.00%
20	1.22	0.67	0	0	25.72	14.97	0	0	**24.50**	**14.30**	0.00	0.00	***10.00%***	***10.00%***	0.00%	0.00%
21	0.75	0.32	0	0	13	7.47	0	0	**12.25**	**7.15**	0.00	0.00	***5.00%***	***5.00%***	0.00%	0.00%
22	0	0	2.67	-1.63	0	0	43.24	50.12	**0.00**	**0.00**	40.57	51.75	***0.00%***	***0.00%***	14.76%	23.04%
23	0	0	1.60	-1.12	0	0	25.61	32.85	**0.00**	**0.00**	24.01	33.97	***0.00%***	***0.00%***	8.86%	15.11%

Bus	L		G						PM				*LD*		GP	
	P_L0	Q_L0	Pg0	Qg0	PlF	QlF	PgF	QgF	ΔP_L	ΔQ_L	ΔPg	ΔQg	*LDP*	*LDQ*	GPP	GPQ
24	0.47	0.37	0	0	5.37	3.23	0	0	**4.90**	**2.86**	0.00	0.00	***2.00%***	***2.00%***	0.00%	0.00%
25	0.1	0.07	0	0	2.55	1.5	0	0	**2.45**	**1.43**	0.00	0.00	***1.00%***	***1.00%***	0.00%	0.00%
26	0.35	0.23	0	0	5.25	3.09	0	0	**4.90**	**2.86**	0.00	0.00	***2.00%***	***2.00%***	0.00%	0.00%
27	0	0	2.94	-1.52	0	0	47.65	42.13	**0.00**	**0.00**	44.71	43.65	***0.00%***	***0.00%***	16.24%	19.35%
28	0	0	0	0	0	0	0	0	**0.00**	**0.00**	0.00	0.00	***0.00%***	***0.00%***	0.00%	0.00%
29	0.27	0.19	0	0	2.72	1.62	0	0	**2.45**	**1.43**	0.00	0.00	***1.00%***	***1.00%***	0.00%	0.00%
30	0.56	0.29	0	0	7.91	4.58	0	0	**7.35**	**4.29**	0.00	0.00	***3.00%***	***3.00%***	0.00%	0.00%
Total	18.02	9.45	18.09	-7.63	263.02	152.45	290.52	219.22	**245**	**143**	272.43	226.85	***100.00%***	***100.00%***	100.00%	100.00%

Table A3 - 6 **Ref.Case30f08L01LD04G01GP03**

Bus	L		G						PM				LD		GP	
	P_L0	Q_L0	*Pg0*	*Qg0*	P_LF	Q_LF	PgF	QgF	ΔP_L	ΔQ_L	ΔPg	ΔQg	LDP	LDQ	GPP	GPQ
1	0	0	***6.98***	***-2.56***	0	0	66.8	52.32	**0**	**0**	59.82	54.88	0.00%	0.00%	37.50%	35.00%
2	0	0	*7.24*	***-2.43***	0	0	67.24	52.17	**0**	**0**	60	54.6	0.00%	0.00%	37.50%	35.00%
3	0.24	0.12			1.67	0.98	0	0	**1.43**	**0.86**	0	0	1.00%	1.00%	0.00%	0.00%
4	0.76	0.36			6.48	3.8	0	0	**5.72**	**3.44**	0	0	4.00%	4.00%	0.00%	0.00%
5	0	0			0	0	0	0	**0**	**0**	0	0	0.00%	0.00%	0.00%	0.00%
6	0	0			0	0	0	0	**0**	**0**	0	0	0.00%	0.00%	0.00%	0.00%
7	1.28	0.59			7	4.03	0	0	**5.72**	**3.44**	0	0	4.00%	4.00%	0.00%	0.00%
8	1.15	0.43			8.3	4.73	0	0	**7.15**	**4.3**	0	0	5.00%	5.00%	0.00%	0.00%
9	0.9	0.5			8.05	4.8	0	0	**7.15**	**4.3**	0	0	5.00%	5.00%	0.00%	0.00%
10	0.58	0.2			4.87	2.78	0	0	**4.29**	**2.58**	0	0	3.00%	3.00%	0.00%	0.00%
11	0	0			0	0	0	0	**0**	**0**	0	0	0.00%	0.00%	0.00%	0.00%
12	1.12	0.55			8.27	4.85	0	0	**7.15**	**4.3**	0	0	5.00%	5.00%	0.00%	0.00%
13	0	0	***0***	***0***	0	0	0	0	**0**	**0**	0	0	0.00%	0.00%	0.00%	0.00%
14	0.62	0.36			7.77	4.66	0	0	**7.15**	**4.3**	0	0	5.00%	5.00%	0.00%	0.00%
15	0.82	0.55			9.4	4.85	0	0	**8.58**	**4.3**	0	0	6.00%	5.00%	0.00%	0.00%
16	0.35	0.18			6.07	3.62	0	0	**5.72**	**3.44**	0	0	4.00%	4.00%	0.00%	0.00%
17	0.9	0.58			8.05	4.88	0	0	**7.15**	**4.3**	0	0	5.00%	5.00%	0.00%	0.00%
18	3.28	1.79			24.73	18.99	0	0	**21.45**	**17.2**	0	0	15.00%	20.00%	0.00%	0.00%
19	2.3	1.1			19.46	9.7	0	0	**17.16**	**8.6**	0	0	12.00%	10.00%	0.00%	0.00%
20	1.22	0.67			18.38	9.27	0	0	**17.16**	**8.6**	0	0	12.00%	10.00%	0.00%	0.00%
21	0.75	0.32			7.9	4.62	0	0	**7.15**	**4.3**	0	0	5.00%	5.00%	0.00%	0.00%
22	0	0	***0***	***0***	0	0	0	0	**0**	**0**	0	0	0.00%	0.00%	0.00%	0.00%
23	0	0	***0***	***0***	0	0	0	0	**0**	**0**	0	0	0.00%	0.00%	0.00%	0.00%

Bus	L		G						PM				LD		GP	
	P_L0	Q_L0	*Pg0*	*Qg0*	P_LF	Q_LF	PgF	QgF	ΔP_L	ΔQ_L	ΔPg	ΔQg	LDP	LDQ	GPP	GPQ
24	0.47	0.37			3.33	2.09	0	0	**2.86**	**1.72**	0	0	2.00%	2.00%	0.00%	0.00%
25	0.1	0.07			1.53	0.93	0	0	**1.43**	**0.86**	0	0	1.00%	1.00%	0.00%	0.00%
26	0.35	0.23			3.21	1.95	0	0	**2.86**	**1.72**	0	0	2.00%	2.00%	0.00%	0.00%
27	0	0	***3.89***	***-2.18***	0	0	43.89	44.62	**0**	**0**	40	46.8	0.00%	0.00%	25.00%	30.00%
28	0	0			0	0	0	0	**0**	**0**	0	0	0.00%	0.00%	0.00%	0.00%
29	0.27	0.19			1.7	1.05	0	0	**1.43**	**0.86**	0	0	1.00%	1.00%	0.00%	0.00%
30	0.56	0.29			4.85	2.87	0	0	**4.29**	**2.58**	0	0	3.00%	3.00%	0.00%	0.00%
Total	18.02	9.45	***18.11***	*-7.17*	161.02	95.45	177.93	149.11	**143**	**86**	159.82	156.28	100.00%	100.00%	100.00%	100.00%

Table A3 - 7 **Ref.:CASE30F09L01LD04G04GP03**

Bus	L		G						PM				LD		GP	
	P_L0	Q_L0	*Pg0*	*Qg0*	P_LF	Q_LF	PgF	QgF	ΔP_L	ΔQ_L	ΔPg	ΔQg	LDP	LDQ	GPP	GPQ
1	0	0	***6.98***	***-2.56***	0	0	75.13	56.28	**0**	**0**	68.15	58.84	0.00%	0.00%	37.50%	35.00%
2	0	0	*7.24*	***-2.43***	0	0	75.86	56.37	**0**	**0**	68.62	58.8	0.00%	0.00%	37.50%	35.00%
3	0.24	0.12			1.89	1.12	0	0	**1.65**	**1**	0	0	1.00%	1.00%	0.00%	0.00%
4	0.76	0.36			7.36	4.36	0	0	**6.6**	**4**	0	0	4.00%	4.00%	0.00%	0.00%
5	0	0			0	0	0	0	**0**	**0**	0	0	0.00%	0.00%	0.00%	0.00%
6	0	0			0	0	0	0	**0**	**0**	0	0	0.00%	0.00%	0.00%	0.00%
7	1.28	0.59			7.88	4.59	0	0	**6.6**	**4**	0	0	4.00%	4.00%	0.00%	0.00%
8	1.15	0.43			9.4	5.43	0	0	**8.25**	**5**	0	0	5.00%	5.00%	0.00%	0.00%
9	0.9	0.5			9.15	5.5	0	0	**8.25**	**5**	0	0	5.00%	5.00%	0.00%	0.00%
10	0.58	0.2			5.53	3.2	0	0	**4.95**	**3**	0	0	3.00%	3.00%	0.00%	0.00%
11	0	0			0	0	0	0	**0**	**0**	0	0	0.00%	0.00%	0.00%	0.00%
12	1.12	0.55			9.37	5.55	0	0	**8.25**	**5**	0	0	5.00%	5.00%	0.00%	0.00%
13	0	0	***0***	***0***	0	0	0	0	**0**	**0**	0	0	0.00%	0.00%	0.00%	0.00%
14	0.62	0.36			8.87	5.36	0	0	**8.25**	**5**	0	0	5.00%	5.00%	0.00%	0.00%
15	0.82	0.55			10.72	5.55	0	0	**9.9**	**5**	0	0	6.00%	5.00%	0.00%	0.00%
16	0.35	0.18			6.95	4.18	0	0	**6.6**	**4**	0	0	4.00%	4.00%	0.00%	0.00%
17	0.9	0.58			9.15	5.58	0	0	**8.25**	**5**	0	0	5.00%	5.00%	0.00%	0.00%
18	3.28	1.79			28.03	21.79	0	0	**24.75**	**20**	0	0	15.00%	20.00%	0.00%	0.00%
19	2.3	1.1			22.1	11.1	0	0	**19.8**	**10**	0	0	12.00%	10.00%	0.00%	0.00%
20	1.22	0.67			21.02	10.67	0	0	**19.8**	**10**	0	0	12.00%	10.00%	0.00%	0.00%
21	0.75	0.32			9	5.32	0	0	**8.25**	**5**	0	0	5.00%	5.00%	0.00%	0.00%
22	0	0	***3.89***	***-2.18***	0	0	49.73	48.22	**0**	**0**	45.84	50.4	0.00%	0.00%	25.00%	30.00%
23	0	0	***0***	***0***	0	0	0	0	**0**	**0**	0	0	0.00%	0.00%	0.00%	0.00%

Bus	L		G						PM				LD		GP	
	P_L0	Q_L0	*Pg0*	*Qg0*	P_LF	Q_LF	PgF	QgF	ΔP_L	ΔQ_L	ΔPg	ΔQg	LDP	LDQ	GPP	GPQ
24	0.47	0.37			3.77	2.37	0	0	**3.3**	**2**	0	0	2.00%	2.00%	0.00%	0.00%
25	0.1	0.07			1.75	1.07	0	0	**1.65**	**1**	0	0	1.00%	1.00%	0.00%	0.00%
26	0.35	0.23			3.65	2.23	0	0	**3.3**	**2**	0	0	2.00%	2.00%	0.00%	0.00%
27	0	0			0	0	0	0	**0**	**0**	0	0	0.00%	0.00%	0.00%	0.00%
28	0	0			0	0	0	0	**0**	**0**	0	0	0.00%	0.00%	0.00%	0.00%
29	0.27	0.19			1.92	1.19	0	0	**1.65**	**1**	0	0	1.00%	1.00%	0.00%	0.00%
30	0.56	0.29			5.51	3.29	0	0	**4.95**	**3**	0	0	3.00%	3.00%	0.00%	0.00%
Total	18.02	9.45	***18.11***	*-7.17*	183.02	109.45	200.72	160.87	**165**	**100**	182.61	168.04	100.00%	100.00%	100.00%	100.00%

Table A3 - 8 **Ref.:CASE30F04L01LD01G02GP02**

Bus	L		G						PM				LD		GP	
	P_L0	Q_L0	Pg0	Qg0	P_LF	Q_LF	PgF	QgF	ΔP_L	ΔQ_L	ΔPg	ΔQg	LDP	LDQ	*GPP*	*GPQ*
1	0	0	4.47	-0.79	0	0	68.05	49.79	**0**	**0**	63.58	50.58	0.00%	0.00%	***31.78%***	***31.15%***
2	0	0	4.27	-1.40	0	0	67.27	50.20	**0**	**0**	63.00	51.60	0.00%	0.00%	***31.49%***	***31.78%***
3	0.24	0.12	0.00	0.00	2.66	1.33	0	0.00	**2.42**	**1.21**	0.00	0.00	1.33%	1.27%	***0.00%***	***0.00%***
4	0.76	0.36	0.00	0.00	8.44	4	0	0.00	**7.68**	**3.64**	0.00	0.00	4.22%	3.81%	***0.00%***	***0.00%***
5	0	0	0.00	0.00	0	0	0	0.00	**0**	**0**	0.00	0.00	0.00%	0.00%	***0.00%***	***0.00%***
6	0	0	0.00	0.00	0	0	0	0.00	**0**	**0**	0.00	0.00	0.00%	0.00%	***0.00%***	***0.00%***
7	1.28	0.59	0.00	0.00	14.21	6.55	0	0.00	**12.93**	**5.96**	0.00	0.00	7.10%	6.24%	***0.00%***	***0.00%***
8	1.15	0.43	0.00	0.00	12.77	4.77	0	0.00	**11.62**	**4.34**	0.00	0.00	6.38%	4.55%	***0.00%***	***0.00%***
9	0.9	0.5	0.00	0.00	9.99	5.55	0	0.00	**9.09**	**5.05**	0.00	0.00	4.99%	5.29%	***0.00%***	***0.00%***
10	0.58	0.2	0.00	0.00	6.44	2.22	0	0.00	**5.86**	**2.02**	0.00	0.00	3.22%	2.12%	***0.00%***	***0.00%***
11	0	0	0.00	0.00	0	0	0	0.00	**0**	**0**	0.00	0.00	0.00%	0.00%	***0.00%***	***0.00%***
12	1.12	0.55	0.00	0.00	12.43	6.11	0	0.00	**11.31**	**5.56**	0.00	0.00	6.22%	5.82%	***0.00%***	***0.00%***
13	0	0	2.14	-1.17	0	0	12.64	7.43	**0**	**0**	10.50	8.60	0.00%	0.00%	***5.25%***	***5.30%***
14	0.62	0.36	0.00	0.00	6.88	4	0	0.00	**6.26**	**3.64**	0.00	0.00	3.44%	3.81%	***0.00%***	***0.00%***
15	0.82	0.55	0.00	0.00	9.1	6.11	0	0.00	**8.28**	**5.56**	0.00	0.00	4.55%	5.82%	***0.00%***	***0.00%***
16	0.35	0.18	0.00	0.00	3.89	2	0	0.00	**3.54**	**1.82**	0.00	0.00	1.94%	1.90%	***0.00%***	***0.00%***
17	0.9	0.58	0.00	0.00	9.99	6.44	0	0.00	**9.09**	**5.86**	0.00	0.00	4.99%	6.14%	***0.00%***	***0.00%***
18	3.28	1.79	0.00	0.00	36.41	19.87	0	0.00	**33.13**	**18.08**	0.00	0.00	18.20%	18.94%	***0.00%***	***0.00%***
19	2.3	1.1	0.00	0.00	25.53	12.21	0	0.00	**23.23**	**11.11**	0.00	0.00	12.76%	11.64%	***0.00%***	***0.00%***
20	1.22	0.67	0.00	0.00	13.54	7.44	0	0.00	**12.32**	**6.77**	0.00	0.00	6.77%	7.09%	***0.00%***	***0.00%***
21	0.75	0.32	0.00	0.00	8.33	3.55	0	0.00	**7.58**	**3.23**	0.00	0.00	4.16%	3.39%	***0.00%***	***0.00%***
22	0	0	2.67	-1.63	0	0	13.17	6.97	**0**	**0**	10.50	8.60	0.00%	0.00%	***5.25%***	***5.30%***
23	0	0	1.60	-1.12	0	0	12.1	7.48	**0**	**0**	10.50	8.60	0.00%	0.00%	***5.25%***	***5.30%***

Bus	L		G						PM				LD		*GP*	
	P_L0	**Q_L0**	**Pg0**	**Qg0**	**P_LF**	**Q_LF**	**PgF**	**QgF**	**ΔP_L**	**ΔQ_L**	**ΔPg**	**ΔQg**	**LDP**	**LDQ**	***GPP***	***GPQ***
24	0.47	0.37	0.00	0.00	5.22	4.11	0	0.00	**4.75**	**3.74**	0.00	0.00	2.61%	3.92%	***0.00%***	***0.00%***
25	0.1	0.07	0.00	0.00	1.11	0.78	0	0.00	**1.01**	**0.71**	0.00	0.00	0.55%	0.74%	***0.00%***	***0.00%***
26	0.35	0.23	0.00	0.00	3.89	2.55	0	0.00	**3.54**	**2.32**	0.00	0.00	1.94%	2.43%	***0.00%***	***0.00%***
27	0	0	2.94	-1.52	0	0	44.94	32.88	**0**	**0**	42.00	34.40	0.00%	0.00%	***20.99%***	***21.18%***
28	0	0	0.00	0.00	0	0	0	0.00	**0**	**0**	0.00	0.00	0.00%	0.00%	***0.00%***	***0.00%***
29	0.27	0.19	0.00	0.00	3	2.11	0	0.00	**2.73**	**1.92**	0.00	0.00	1.50%	2.01%	***0.00%***	***0.00%***
30	0.56	0.29	0.00	0.00	6.22	3.22	0	0.00	**5.66**	**2.93**	0.00	0.00	3.11%	3.07%	***0.00%***	***0.00%***
Total	18.02	9.45	18.09	-7.63	200.05	104.92	218.17	154.75	**182.03**	**95.47**	200.08	162.38	100%	100%	***100%***	***100%***

A3.3 Voltage Stability Similarity in the Pattern Classes of the VSDFs

Some simulation results on the IEEE 30 bus system are given in this section to show the similarities of power margins when the VSDFs are in the same clusters (pattern classes). Three typical pattern classes of the VSDFs were set up in this simulation to represent lightly loaded, normally loaded and heavily loaded system conditions. Each pattern class contains five or six study cases which have similar (but not the same) VSDFs. Those study cases were configured in such way that between any two of them, +/- 10% to +/- 20% variations were "randomly" made to at least one of the four VSDFs as

$$20\% \geq \frac{|\beta_a^P i - \beta_b^P i|}{|\beta_a^P i|} \geq 10\%,$$

$$20\% \geq \frac{|\beta_a^Q i - \beta_b^Q i|}{|\beta_a^Q i|} \geq 10\%,$$

where,

$\beta_a = [\beta_a^P 1, \beta_a^P 2, \ldots \beta_a^P i \quad \beta_a^Q 1, \beta_a^Q 2, \ldots \beta_a^Q i \ldots]$ is a VSDF for the study case a,

$\beta_b = [\beta_b^P 1, \beta_b^P 2, \ldots \beta_b^P i \quad \beta_b^Q 1, \beta_b^Q 2, \ldots \beta_b^Q i \ldots]$ is the same type VSDF for the study case b.

The simulated power margin results together with the configuration information for each study case are listed in the tables below.

In addition, the details of test patterns for the knowledge based system for prediction of voltage collapse (Chapter 4) are also included in this section.

1. **Pattern Class 1 - Lightly Loaded Conditions**

Table A3 - 9 **Ref. CASE30F07L01LD07eG02GP01 (Test pattern 01 Case0701)**

Bus	L		G						PM				LD		GP	
	P_L0	Q_L0	Pg0	Qg0	P_LF	Q_LF	PgF	QgF	ΔP_L	ΔQ_L	ΔPg	ΔQg	LDP	LDQ	GPP	GPQ
1	0.00	0.00	4.47	-0.79	0.00	0.00	71.10	25.75	**0.00**	**0.00**	66.63	26.54	0.00%	0.00%	23.89%	11.29%
2	0.00	0.00	4.27	-1.40	0.00	0.00	71.06	38.74	**0.00**	**0.00**	66.79	40.14	0.00%	0.00%	23.95%	17.07%
3	0.24	0.12	0.00	0.00	3.01	1.78	0.00	0.00	**2.77**	**1.66**	0.00	0.00	1.10%	1.10%	0.00%	0.00%
4	0.76	0.36	0.00	0.00	9.83	5.80	0.00	0.00	**9.07**	**5.44**	0.00	0.00	3.60%	3.60%	0.00%	0.00%
5	0.00	0.00	0.00	0.00	0.00	0.00	0.00	0.00	**0.00**	**0.00**	0.00	0.00	0.00%	0.00%	0.00%	0.00%
6	0.00	0.00	0.00	0.00	0.00	0.00	0.00	0.00	**0.00**	**0.00**	0.00	0.00	0.00%	0.00%	0.00%	0.00%
7	1.28	0.59	0.00	0.00	12.37	7.23	0.00	0.00	**11.09**	**6.64**	0.00	0.00	4.40%	4.40%	0.00%	0.00%
8	1.15	0.43	0.00	0.00	12.49	7.23	0.00	0.00	**11.34**	**6.80**	0.00	0.00	4.50%	4.50%	0.00%	0.00%
9	0.90	0.50	0.00	0.00	14.76	8.81	0.00	0.00	**13.86**	**8.31**	0.00	0.00	5.50%	5.50%	0.00%	0.00%
10	0.58	0.20	0.00	0.00	7.38	4.28	0.00	0.00	**6.80**	**4.08**	0.00	0.00	2.70%	2.70%	0.00%	0.00%
11	0.00	0.00	0.00	0.00	0.00	0.00	0.00	0.00	**0.00**	**0.00**	0.00	0.00	0.00%	0.00%	0.00%	0.00%
12	1.12	0.55	0.00	0.00	14.98	8.86	0.00	0.00	**13.86**	**8.31**	0.00	0.00	5.50%	5.50%	0.00%	0.00%
13	0.00	0.00	2.14	-1.17	0.00	0.00	35.53	33.86	**0.00**	**0.00**	33.39	35.03	0.00%	0.00%	11.97%	14.90%
14	0.62	0.36	0.00	0.00	11.96	7.16	0.00	0.00	**11.34**	**6.80**	0.00	0.00	4.50%	4.50%	0.00%	0.00%
15	0.82	0.55	0.00	0.00	17.45	10.52	0.00	0.00	**16.63**	**9.97**	0.00	0.00	6.60%	6.60%	0.00%	0.00%
16	0.35	0.18	0.00	0.00	9.42	5.62	0.00	0.00	**9.07**	**5.44**	0.00	0.00	3.60%	3.60%	0.00%	0.00%
17	0.90	0.58	0.00	0.00	14.76	8.89	0.00	0.00	**13.86**	**8.31**	0.00	0.00	5.50%	5.50%	0.00%	0.00%
18	3.28	1.79	0.00	0.00	37.30	22.18	0.00	0.00	**34.02**	**20.39**	0.00	0.00	13.50%	13.50%	0.00%	0.00%
19	2.30	1.10	0.00	0.00	35.56	21.03	0.00	0.00	**33.26**	**19.93**	0.00	0.00	13.20%	13.20%	0.00%	0.00%
20	1.22	0.67	0.00	0.00	28.44	16.98	0.00	0.00	**27.22**	**16.31**	0.00	0.00	10.80%	10.80%	0.00%	0.00%
21	0.75	0.32	0.00	0.00	14.61	8.63	0.00	0.00	**13.86**	**8.31**	0.00	0.00	5.50%	5.50%	0.00%	0.00%
22	0.00	0.00	2.67	-1.63	0.00	0.00	44.27	51.73	**0.00**	**0.00**	41.60	53.36	0.00%	0.00%	14.92%	22.70%

Bus	L		G						PM				LD		GP	
	P_L0	Q_L0	Pg0	Qg0	P_LF	Q_LF	PgF	QgF	ΔP_L	ΔQ_L	ΔPg	ΔQg	LDP	LDQ	GPP	GPQ
23	0.00	0.00	1.60	-1.12	0.00	0.00	26.22	33.91	**0.00**	**0.00**	24.62	35.03	0.00%	0.00%	8.83%	14.90%
24	0.47	0.37	0.00	0.00	6.01	3.69	0.00	0.00	**5.54**	**3.32**	0.00	0.00	2.20%	2.20%	0.00%	0.00%
25	0.10	0.07	0.00	0.00	2.37	1.43	0.00	0.00	**2.27**	**1.36**	0.00	0.00	0.90%	0.90%	0.00%	0.00%
26	0.35	0.23	0.00	0.00	5.89	3.55	0.00	0.00	**5.54**	**3.32**	0.00	0.00	2.20%	2.20%	0.00%	0.00%
27	0.00	0.00	2.94	-1.52	0.00	0.00	48.78	43.49	**0.00**	**0.00**	45.84	45.01	0.00%	0.00%	16.44%	19.14%
28	0.00	0.00	0.00	0.00	0.00	0.00	0.00	0.00	**0.00**	**0.00**	0.00	0.00	0.00%	0.00%	0.00%	0.00%
29	0.27	0.19	0.00	0.00	2.54	1.55	0.00	0.00	**2.27**	**1.36**	0.00	0.00	0.90%	0.90%	0.00%	0.00%
30	0.56	0.29	0.00	0.00	8.88	5.27	0.00	0.00	**8.32**	**4.98**	0.00	0.00	3.30%	3.30%	0.00%	0.00%
Total	18.02	9.45	18.09	-7.63	270.01	160.49	296.96	227.48	**251.99**	**151.04**	278.87	235.11	100.00%	100.00%	100.00%	100.00%

Differences between Case30F07 and Case30F07a

Bus	L		G		LD		GP	
1,3,5,7,9,11,12,13,15,17,19,21,23,24,26,28,30					1.1X	1.1X		
Others					0.9X	0.9X		

Table A3 - 10 **Ref. CASE30F07aL01LD05G02GP01 (Prototype of Pattern Class I)**

Bus	L		G						PM				LD		GP	
	P_L0	Q_L0	Pg0	Qg0	P_LF	Q_LF	PgF	QgF	ΔP_L	ΔQ_L	ΔPg	ΔQg	LDP	LDQ	GPP	GPQ
1	0.00	0.00	4.47	-0.79	0.00	0.00	70.45	24.75	**0.00**	**0.00**	65.98	25.54	0.00%	0.00%	23.97%	10.99%
2	0.00	0.00	4.27	-1.40	0.00	0.00	70.12	38.39	**0.00**	**0.00**	65.85	39.79	0.00%	0.00%	23.92%	17.13%
3	0.24	0.12	0.00	0.00	2.72	1.60	0.00	0.00	**2.48**	**1.48**	0.00	0.00	1.00%	1.00%	0.00%	0.00%
4	0.76	0.36	0.00	0.00	10.68	6.28	0.00	0.00	**9.92**	**5.92**	0.00	0.00	4.00%	4.00%	0.00%	0.00%
5	0.00	0.00	0.00	0.00	0.00	0.00	0.00	0.00	**0.00**	**0.00**	0.00	0.00	0.00%	0.00%	0.00%	0.00%
6	0.00	0.00	0.00	0.00	0.00	0.00	0.00	0.00	**0.00**	**0.00**	0.00	0.00	0.00%	0.00%	0.00%	0.00%
7	1.28	0.59	0.00	0.00	11.20	6.51	0.00	0.00	**9.92**	**5.92**	0.00	0.00	4.00%	4.00%	0.00%	0.00%
8	1.15	0.43	0.00	0.00	13.55	7.83	0.00	0.00	**12.40**	**7.40**	0.00	0.00	5.00%	5.00%	0.00%	0.00%
9	0.90	0.50	0.00	0.00	13.30	7.90	0.00	0.00	**12.40**	**7.40**	0.00	0.00	5.00%	5.00%	0.00%	0.00%
10	0.58	0.20	0.00	0.00	8.02	4.64	0.00	0.00	**7.44**	**4.44**	0.00	0.00	3.00%	3.00%	0.00%	0.00%
11	0.00	0.00	0.00	0.00	0.00	0.00	0.00	0.00	**0.00**	**0.00**	0.00	0.00	0.00%	0.00%	0.00%	0.00%
12	1.12	0.55	0.00	0.00	13.52	7.95	0.00	0.00	**12.40**	**7.40**	0.00	0.00	5.00%	5.00%	0.00%	0.00%
13	0.00	0.00	2.14	-1.17	0.00	0.00	35.06	33.56	**0.00**	**0.00**	32.92	34.73	0.00%	0.00%	11.96%	14.95%
14	0.62	0.36	0.00	0.00	13.02	7.76	0.00	0.00	**12.40**	**7.40**	0.00	0.00	5.00%	5.00%	0.00%	0.00%
15	0.82	0.55	0.00	0.00	15.70	9.43	0.00	0.00	**14.88**	**8.88**	0.00	0.00	6.00%	6.00%	0.00%	0.00%
16	0.35	0.18	0.00	0.00	10.27	6.10	0.00	0.00	**9.92**	**5.92**	0.00	0.00	4.00%	4.00%	0.00%	0.00%
17	0.90	0.58	0.00	0.00	13.30	7.98	0.00	0.00	**12.40**	**7.40**	0.00	0.00	5.00%	5.00%	0.00%	0.00%
18	3.28	1.79	0.00	0.00	40.48	23.99	0.00	0.00	**37.20**	**22.20**	0.00	0.00	15.00%	15.00%	0.00%	0.00%
19	2.30	1.10	0.00	0.00	32.06	18.86	0.00	0.00	**29.76**	**17.76**	0.00	0.00	12.00%	12.00%	0.00%	0.00%
20	1.22	0.67	0.00	0.00	30.98	18.43	0.00	0.00	**29.76**	**17.76**	0.00	0.00	12.00%	12.00%	0.00%	0.00%
21	0.75	0.32	0.00	0.00	13.15	7.72	0.00	0.00	**12.40**	**7.40**	0.00	0.00	5.00%	5.00%	0.00%	0.00%
22	0.00	0.00	2.67	-1.63	0.00	0.00	43.68	51.27	**0.00**	**0.00**	41.01	52.90	0.00%	0.00%	14.90%	22.77%
23	0.00	0.00	1.60	-1.12	0.00	0.00	25.88	33.61	**0.00**	**0.00**	24.28	34.73	0.00%	0.00%	8.82%	14.95%
24	0.47	0.37	0.00	0.00	5.43	3.33	0.00	0.00	**4.96**	**2.96**	0.00	0.00	2.00%	2.00%	0.00%	0.00%

Bus	L		G						PM				LD		GP	
	P_L0	Q_L0	Pg0	Qg0	P_LF	Q_LF	PgF	QgF	ΔP_L	ΔQ_L	ΔPg	ΔQg	LDP	LDQ	GPP	GPQ
25	0.10	0.07	0.00	0.00	2.58	1.55	0.00	0.00	**2.48**	**1.48**	0.00	0.00	1.00%	1.00%	0.00%	0.00%
26	0.35	0.23	0.00	0.00	5.31	3.19	0.00	0.00	**4.96**	**2.96**	0.00	0.00	2.00%	2.00%	0.00%	0.00%
27	0.00	0.00	2.94	-1.52	0.00	0.00	48.14	43.10	**0.00**	**0.00**	45.20	44.62	0.00%	0.00%	16.42%	19.21%
28	0.00	0.00	0.00	0.00	0.00	0.00	0.00	0.00	**0.00**	**0.00**	0.00	0.00	0.00%	0.00%	0.00%	0.00%
29	0.27	0.19	0.00	0.00	2.75	1.67	0.00	0.00	**2.48**	**1.48**	0.00	0.00	1.00%	1.00%	0.00%	0.00%
30	0.56	0.29	0.00	0.00	8.00	4.73	0.00	0.00	**7.44**	**4.44**	0.00	0.00	3.00%	3.00%	0.00%	0.00%
Total	18.02	9.45	18.09	-7.63	266.02	157.45	293.33	224.68	**248.00**	**148.00**	275.24	232.31	100.00%	100.00%	100.00%	100.00%

Table A3 - 11 **Ref. Case30f07bL04LD05G02GP01e**

Bus	L		G						PM				LD		GP	
	P_L0	Q_L0	Pg0	Qg0	PLF	QLF	PgF	QgF	ΔP_L	ΔQ_L	ΔPg	ΔQg	LDP	LDQ	GPP	GPQ
1	0.00	0.00	4.46	-1.20	0.00	0.00	70.25	25.13	**0.00**	**0.00**	65.79	26.33	0.00%	0.00%	23.73%	11.21%
2	0.00	0.00	4.27	-1.40	0.00	0.00	70.82	38.74	**0.00**	**0.00**	66.55	40.14	0.00%	0.00%	24.00%	17.09%
3	0.29	0.14	0.00	0.00	2.79	1.64	0.00	0.00	**2.50**	**1.50**	0.00	0.00	1.00%	1.00%	0.00%	0.00%
4	0.91	0.43	0.00	0.00	10.91	6.43	0.00	0.00	**10.00**	**6.00**	0.00	0.00	4.00%	4.00%	0.00%	0.00%
5	0.00	0.00	0.00	0.00	0.00	0.00	0.00	0.00	**0.00**	**0.00**	0.00	0.00	0.00%	0.00%	0.00%	0.00%
6	0.00	0.00	0.00	0.00	0.00	0.00	0.00	0.00	**0.00**	**0.00**	0.00	0.00	0.00%	0.00%	0.00%	0.00%
7	1.54	0.71	0.00	0.00	11.54	6.71	0.00	0.00	**10.00**	**6.00**	0.00	0.00	4.00%	4.00%	0.00%	0.00%
8	1.38	0.52	0.00	0.00	13.88	8.02	0.00	0.00	**12.50**	**7.50**	0.00	0.00	5.00%	5.00%	0.00%	0.00%
9	1.08	0.60	0.00	0.00	13.58	8.10	0.00	0.00	**12.50**	**7.50**	0.00	0.00	5.00%	5.00%	0.00%	0.00%
10	0.70	0.24	0.00	0.00	8.20	4.74	0.00	0.00	**7.50**	**4.50**	0.00	0.00	3.00%	3.00%	0.00%	0.00%
11	0.00	0.00	0.00	0.00	0.00	0.00	0.00	0.00	**0.00**	**0.00**	0.00	0.00	0.00%	0.00%	0.00%	0.00%
12	1.34	0.66	0.00	0.00	13.84	8.16	0.00	0.00	**12.50**	**7.50**	0.00	0.00	5.00%	5.00%	0.00%	0.00%
13	0.00	0.00	2.14	-1.17	0.00	0.00	35.41	33.86	**0.00**	**0.00**	33.27	35.03	0.00%	0.00%	12.00%	14.91%
14	0.74	0.43	0.00	0.00	13.24	7.93	0.00	0.00	**12.50**	**7.50**	0.00	0.00	5.00%	5.00%	0.00%	0.00%
15	0.98	0.66	0.00	0.00	15.98	9.66	0.00	0.00	**15.00**	**9.00**	0.00	0.00	6.00%	6.00%	0.00%	0.00%
16	0.29	0.15	0.00	0.00	10.29	6.15	0.00	0.00	**10.00**	**6.00**	0.00	0.00	4.00%	4.00%	0.00%	0.00%
17	0.73	0.48	0.00	0.00	13.23	7.98	0.00	0.00	**12.50**	**7.50**	0.00	0.00	5.00%	5.00%	0.00%	0.00%
18	2.67	1.48	0.00	0.00	40.17	23.98	0.00	0.00	**37.50**	**22.50**	0.00	0.00	15.00%	15.00%	0.00%	0.00%
19	1.88	0.91	0.00	0.00	31.88	18.91	0.00	0.00	**30.00**	**18.00**	0.00	0.00	12.00%	12.00%	0.00%	0.00%
20	0.99	0.55	0.00	0.00	30.99	18.55	0.00	0.00	**30.00**	**18.00**	0.00	0.00	12.00%	12.00%	0.00%	0.00%
21	0.61	0.26	0.00	0.00	13.11	7.76	0.00	0.00	**12.50**	**7.50**	0.00	0.00	5.00%	5.00%	0.00%	0.00%
22	0.00	0.00	2.67	-1.63	0.00	0.00	44.13	51.73	**0.00**	**0.00**	41.46	53.36	0.00%	0.00%	14.95%	22.72%
23	0.00	0.00	1.60	-1.12	0.00	0.00	26.14	33.91	**0.00**	**0.00**	24.54	35.03	0.00%	0.00%	8.85%	14.91%
24	0.38	0.31	0.00	0.00	5.38	3.31	0.00	0.00	**5.00**	**3.00**	0.00	0.00	2.00%	2.00%	0.00%	0.00%

Bus	L		G						PM				LD		GP	
	P_L0	Q_L0	Pg0	Qg0	PLF	QLF	PgF	QgF	ΔP_L	ΔQ_L	ΔPg	ΔQg	LDP	LDQ	GPP	GPQ
25	0.08	0.06	0.00	0.00	2.58	1.56	0.00	0.00	**2.50**	**1.50**	0.00	0.00	1.00%	1.00%	0.00%	0.00%
26	0.42	0.28	0.00	0.00	5.42	3.28	0.00	0.00	**5.00**	**3.00**	0.00	0.00	2.00%	2.00%	0.00%	0.00%
27	0.00	0.00	2.94	-1.52	0.00	0.00	48.62	43.49	**0.00**	**0.00**	45.68	45.01	0.00%	0.00%	16.47%	19.16%
28	0.00	0.00	0.00	0.00	0.00	0.00	0.00	0.00	**0.00**	**0.00**	0.00	0.00	0.00%	0.00%	0.00%	0.00%
29	0.32	0.23	0.00	0.00	2.82	1.73	0.00	0.00	**2.50**	**1.50**	0.00	0.00	1.00%	1.00%	0.00%	0.00%
30	0.67	0.35	0.00	0.00	8.17	4.85	0.00	0.00	**7.50**	**4.50**	0.00	0.00	3.00%	3.00%	0.00%	0.00%
Total	18.02	9.45	18.08	-8.04	268.00	159.45	295.37	226.86	**249.98**	**150.00**	277.29	234.90	100.00%	100.00%	100.00%	100.00%

Differences between Case30F07b and Case30F07a

Bus	L		G		LD		GP	
1 to 15	1.20x	1.20x						
16 to 25	0.83x	0.83x						
26 to 30	1.20x	1.20x						

Table A3 - 12 **Ref. CASE30F07cL04LD05G03GP01**

Bus	L		G						PM				LD		GP	
	P_L0	Q_L0	Pg0	Qg0	PLF	QLF	PgF	QgF	ΔP_L	ΔQ_L	ΔPg	ΔQg	LDP	LDQ	GPP	GPQ
1	0.00	0.00	3.58	-1.05	0.00	0.00	70.52	24.93	**0.00**	**0.00**	66.94	25.98	0.00%	0.00%	24.04%	11.03%
2	0.00	0.00	5.13	-1.68	0.00	0.00	71.68	38.63	**0.00**	**0.00**	66.55	40.31	0.00%	0.00%	23.90%	17.12%
3	0.29	0.14	0.00	0.00	2.80	1.64	0.00	0.00	**2.51**	**1.50**	0.00	0.00	1.00%	1.00%	0.00%	0.00%
4	0.91	0.43	0.00	0.00	10.95	6.43	0.00	0.00	**10.04**	**6.00**	0.00	0.00	4.00%	4.00%	0.00%	0.00%
5	0.00	0.00	0.00	0.00	0.00	0.00	0.00	0.00	**0.00**	**0.00**	0.00	0.00	0.00%	0.00%	0.00%	0.00%
6	0.00	0.00	0.00	0.00	0.00	0.00	0.00	0.00	**0.00**	**0.00**	0.00	0.00	0.00%	0.00%	0.00%	0.00%
7	1.54	0.71	0.00	0.00	11.58	6.71	0.00	0.00	**10.04**	**6.00**	0.00	0.00	4.00%	4.00%	0.00%	0.00%
8	1.38	0.52	0.00	0.00	13.93	8.02	0.00	0.00	**12.55**	**7.50**	0.00	0.00	5.00%	5.00%	0.00%	0.00%
9	1.08	0.60	0.00	0.00	13.63	8.10	0.00	0.00	**12.55**	**7.50**	0.00	0.00	5.00%	5.00%	0.00%	0.00%
10	0.70	0.24	0.00	0.00	8.23	4.74	0.00	0.00	**7.53**	**4.50**	0.00	0.00	3.00%	3.00%	0.00%	0.00%
11	0.00	0.00	0.00	0.00	0.00	0.00	0.00	0.00	**0.00**	**0.00**	0.00	0.00	0.00%	0.00%	0.00%	0.00%
12	1.34	0.66	0.00	0.00	13.89	8.16	0.00	0.00	**12.55**	**7.50**	0.00	0.00	5.00%	5.00%	0.00%	0.00%
13	0.00	0.00	1.71	-0.94	0.00	0.00	34.98	34.25	**0.00**	**0.00**	33.27	35.19	0.00%	0.00%	11.95%	14.94%
14	0.74	0.43	0.00	0.00	13.29	7.93	0.00	0.00	**12.55**	**7.50**	0.00	0.00	5.00%	5.00%	0.00%	0.00%
15	0.98	0.66	0.00	0.00	16.04	9.66	0.00	0.00	**15.06**	**9.00**	0.00	0.00	6.00%	6.00%	0.00%	0.00%
16	0.29	0.15	0.00	0.00	10.33	6.15	0.00	0.00	**10.04**	**6.00**	0.00	0.00	4.00%	4.00%	0.00%	0.00%
17	0.73	0.48	0.00	0.00	13.28	7.98	0.00	0.00	**12.55**	**7.50**	0.00	0.00	5.00%	5.00%	0.00%	0.00%
18	2.67	1.48	0.00	0.00	40.32	23.98	0.00	0.00	**37.65**	**22.50**	0.00	0.00	15.00%	15.00%	0.00%	0.00%
19	1.88	0.91	0.00	0.00	32.00	18.91	0.00	0.00	**30.12**	**18.00**	0.00	0.00	12.00%	12.00%	0.00%	0.00%
20	0.99	0.55	0.00	0.00	31.11	18.55	0.00	0.00	**30.12**	**18.00**	0.00	0.00	12.00%	12.00%	0.00%	0.00%
21	0.61	0.26	0.00	0.00	13.16	7.76	0.00	0.00	**12.55**	**7.50**	0.00	0.00	5.00%	5.00%	0.00%	0.00%
22	0.00	0.00	3.20	-1.96	0.00	0.00	44.66	51.63	**0.00**	**0.00**	41.46	53.59	0.00%	0.00%	14.89%	22.76%
23	0.00	0.00	1.92	-1.34	0.00	0.00	26.46	33.84	**0.00**	**0.00**	24.54	35.18	0.00%	0.00%	8.81%	14.94%
24	0.38	0.31	0.00	0.00	5.40	3.31	0.00	0.00	**5.02**	**3.00**	0.00	0.00	2.00%	2.00%	0.00%	0.00%

Bus	L		G						PM				LD		GP	
	P_L0	Q_L0	Pg0	Qg0	PLF	QLF	PgF	QgF	ΔP_L	ΔQ_L	ΔPg	ΔQg	LDP	LDQ	GPP	GPQ
25	0.08	0.06	0.00	0.00	2.59	1.56	0.00	0.00	**2.51**	**1.50**	0.00	0.00	1.00%	1.00%	0.00%	0.00%
26	0.42	0.28	0.00	0.00	5.44	3.28	0.00	0.00	**5.02**	**3.00**	0.00	0.00	2.00%	2.00%	0.00%	0.00%
27	0.00	0.00	2.55	-1.08	0.00	0.00	48.24	44.12	**0.00**	**0.00**	45.69	45.20	0.00%	0.00%	16.41%	19.20%
28	0.00	0.00	0.00	0.00	0.00	0.00	0.00	0.00	**0.00**	**0.00**	0.00	0.00	0.00%	0.00%	0.00%	0.00%
29	0.32	0.23	0.00	0.00	2.83	1.73	0.00	0.00	**2.51**	**1.50**	0.00	0.00	1.00%	1.00%	0.00%	0.00%
30	0.67	0.35	0.00	0.00	8.20	4.85	0.00	0.00	**7.53**	**4.50**	0.00	0.00	3.00%	3.00%	0.00%	0.00%
Total	18.02	9.45	18.09	-8.05	269.00	159.45	296.54	227.40	**250.98**	**150.00**	278.45	235.45	100.00%	100.00%	100.00%	100.00%

Differences between Case30F07c and Case30F07b

Bus	L		G		LD		GP	
1			0.80x	0.80x				
2			1.20x	1.20x				
13			0.80x	0.80x				
22			1.20x	1.20x				
23			1.20x	1.20x				
27			0.87x	0.71x				

Table A3 - 13 **Ref. CASE30F07dL04LD05G03GP04**

Bus	L		G						PM				LD		GP	
	P_L0	Q_L0	Pg0	Qg0	PLF	QLF	PgF	QgF	ΔP_L	ΔQ_L	ΔPg	ΔQg	LDP	LDQ	GPP	GPQ
1	0.00	0.00	3.58	-1.05	0.00	0.00	68.27	22.26	**0.00**	**0.00**	64.69	23.31	0.00%	0.00%	23.39%	9.91%
2	0.00	0.00	5.13	-1.68	0.00	0.00	78.03	42.63	**0.00**	**0.00**	72.90	44.31	0.00%	0.00%	26.35%	18.84%
3	0.29	0.14	0.00	0.00	2.78	1.62	0.00	0.00	**2.49**	**1.48**	0.00	0.00	1.00%	1.00%	0.00%	0.00%
4	0.91	0.43	0.00	0.00	10.87	6.35	0.00	0.00	**9.96**	**5.92**	0.00	0.00	4.00%	4.00%	0.00%	0.00%
5	0.00	0.00	0.00	0.00	0.00	0.00	0.00	0.00	**0.00**	**0.00**	0.00	0.00	0.00%	0.00%	0.00%	0.00%
6	0.00	0.00	0.00	0.00	0.00	0.00	0.00	0.00	**0.00**	**0.00**	0.00	0.00	0.00%	0.00%	0.00%	0.00%
7	1.54	0.71	0.00	0.00	11.50	6.63	0.00	0.00	**9.96**	**5.92**	0.00	0.00	4.00%	4.00%	0.00%	0.00%
8	1.38	0.52	0.00	0.00	13.83	7.92	0.00	0.00	**12.45**	**7.40**	0.00	0.00	5.00%	5.00%	0.00%	0.00%
9	1.08	0.60	0.00	0.00	13.53	8.00	0.00	0.00	**12.45**	**7.40**	0.00	0.00	5.00%	5.00%	0.00%	0.00%
10	0.70	0.24	0.00	0.00	8.17	4.68	0.00	0.00	**7.47**	**4.44**	0.00	0.00	3.00%	3.00%	0.00%	0.00%
11	0.00	0.00	0.00	0.00	0.00	0.00	0.00	0.00	**0.00**	**0.00**	0.00	0.00	0.00%	0.00%	0.00%	0.00%
12	1.34	0.66	0.00	0.00	13.79	8.06	0.00	0.00	**12.45**	**7.40**	0.00	0.00	5.00%	5.00%	0.00%	0.00%
13	0.00	0.00	1.71	-0.94	0.00	0.00	30.43	30.62	**0.00**	**0.00**	28.72	31.56	0.00%	0.00%	10.38%	13.42%
14	0.74	0.43	0.00	0.00	13.19	7.83	0.00	0.00	**12.45**	**7.40**	0.00	0.00	5.00%	5.00%	0.00%	0.00%
15	0.98	0.66	0.00	0.00	15.92	9.54	0.00	0.00	**14.94**	**8.88**	0.00	0.00	6.00%	6.00%	0.00%	0.00%
16	0.29	0.15	0.00	0.00	10.25	6.07	0.00	0.00	**9.96**	**5.92**	0.00	0.00	4.00%	4.00%	0.00%	0.00%
17	0.73	0.48	0.00	0.00	13.18	7.88	0.00	0.00	**12.45**	**7.40**	0.00	0.00	5.00%	5.00%	0.00%	0.00%
18	2.67	1.48	0.00	0.00	40.02	23.68	0.00	0.00	**37.35**	**22.20**	0.00	0.00	15.00%	15.00%	0.00%	0.00%
19	1.88	0.91	0.00	0.00	31.76	18.67	0.00	0.00	**29.88**	**17.76**	0.00	0.00	12.00%	12.00%	0.00%	0.00%
20	0.99	0.55	0.00	0.00	30.87	18.31	0.00	0.00	**29.88**	**17.76**	0.00	0.00	12.00%	12.00%	0.00%	0.00%
21	0.61	0.26	0.00	0.00	13.06	7.66	0.00	0.00	**12.45**	**7.40**	0.00	0.00	5.00%	5.00%	0.00%	0.00%
22	0.00	0.00	3.20	-1.96	0.00	0.00	39.25	46.07	**0.00**	**0.00**	36.05	48.03	0.00%	0.00%	13.03%	20.42%
23	0.00	0.00	1.92	-1.34	0.00	0.00	28.21	37.17	**0.00**	**0.00**	26.29	38.51	0.00%	0.00%	9.50%	16.38%
24	0.38	0.31	0.00	0.00	5.36	3.27	0.00	0.00	**4.98**	**2.96**	0.00	0.00	2.00%	2.00%	0.00%	0.00%

Bus	L		G						PM				LD		GP	
	P_L0	Q_L0	Pg0	Qg0	PLF	QLF	PgF	QgF	ΔP_L	ΔQ_L	ΔPg	ΔQg	LDP	LDQ	GPP	GPQ
25	0.08	0.06	0.00	0.00	2.57	1.54	0.00	0.00	**2.49**	**1.48**	0.00	0.00	1.00%	1.00%	0.00%	0.00%
26	0.42	0.28	0.00	0.00	5.40	3.24	0.00	0.00	**4.98**	**2.96**	0.00	0.00	2.00%	2.00%	0.00%	0.00%
27	0.00	0.00	2.55	-1.08	0.00	0.00	50.52	48.34	**0.00**	**0.00**	47.97	49.42	0.00%	0.00%	17.34%	21.02%
28	0.00	0.00	0.00	0.00	0.00	0.00	0.00	0.00	**0.00**	**0.00**	0.00	0.00	0.00%	0.00%	0.00%	0.00%
29	0.32	0.23	0.00	0.00	2.81	1.71	0.00	0.00	**2.49**	**1.48**	0.00	0.00	1.00%	1.00%	0.00%	0.00%
30	0.67	0.35	0.00	0.00	8.14	4.79	0.00	0.00	**7.47**	**4.44**	0.00	0.00	3.00%	3.00%	0.00%	0.00%
Total	18.02	9.45	18.09	-8.048	267	157.45	294.71	227.09	**248.98**	**148.00**	276.62	235.14	100.00%	100.00%	100.00%	100.00%

Differences between Case30F07d and Case30F07c

Bus	L		G		LD		GP	
1							0.91x	0.86x
2							1.10x	1.10x
13							0.90x	0.90x
22							0.90x	0.90x
23							1.10x	1.10x
27							1.10x	1.10x

Table A3 - 14 **Ref. CASE30F07t2L0t2LD0t2G0t2GP0t2 (Test pattern 02 Case0702)**

Bus	L		G						PM				LD		GP	
	P_L0	Q_L0	Pg0	Qg0	PLF	QLF	PgF	QgF	ΔP_L	ΔQ_L	ΔPg	ΔQg	LDP	LDQ	GPP	GPQ
1	0.00	0.00	3.92	0.91	0.00	0.00	73.02	23.26	**0.00**	**0.00**	69.10	22.35	0.00%	0.00%	24.93%	10.03%
2	0.00	0.00	5.64	1.48	0.00	0.00	77.22	43.01	**0.00**	**0.00**	71.58	41.53	0.00%	0.00%	25.82%	18.64%
3	0.32	0.16	0.00	0.00	2.93	1.73	0.00	0.00	**2.61**	**1.57**	0.00	0.00	1.04%	1.05%	0.00%	0.00%
4	1.00	0.48	0.00	0.00	11.48	6.77	0.00	0.00	**10.48**	**6.29**	0.00	0.00	4.19%	4.19%	0.00%	0.00%
5	0.00	0.00	0.00	0.00	0.00	0.00	0.00	0.00	**0.00**	**0.00**	0.00	0.00	0.00%	0.00%	0.00%	0.00%
6	0.00	0.00	0.00	0.00	0.00	0.00	0.00	0.00	**0.00**	**0.00**	0.00	0.00	0.00%	0.00%	0.00%	0.00%
7	1.69	0.78	0.00	0.00	12.16	7.07	0.00	0.00	**10.47**	**6.29**	0.00	0.00	4.19%	4.19%	0.00%	0.00%
8	1.52	0.57	0.00	0.00	14.61	8.43	0.00	0.00	**13.09**	**7.86**	0.00	0.00	5.24%	5.23%	0.00%	0.00%
9	1.19	0.66	0.00	0.00	14.28	8.53	0.00	0.00	**13.09**	**7.87**	0.00	0.00	5.24%	5.24%	0.00%	0.00%
10	0.77	0.26	0.00	0.00	8.62	4.98	0.00	0.00	**7.85**	**4.72**	0.00	0.00	3.14%	3.14%	0.00%	0.00%
11	0.00	0.00	0.00	0.00	0.00	0.00	0.00	0.00	**0.00**	**0.00**	0.00	0.00	0.00%	0.00%	0.00%	0.00%
12	1.48	0.73	0.00	0.00	14.57	8.59	0.00	0.00	**13.09**	**7.86**	0.00	0.00	5.24%	5.23%	0.00%	0.00%
13	0.00	0.00	1.88	0.82	0.00	0.00	30.12	30.89	**0.00**	**0.00**	28.24	30.07	0.00%	0.00%	10.19%	13.49%
14	0.82	0.48	0.00	0.00	13.91	8.34	0.00	0.00	**13.09**	**7.86**	0.00	0.00	5.24%	5.23%	0.00%	0.00%
15	1.08	0.73	0.00	0.00	16.79	10.16	0.00	0.00	**15.71**	**9.43**	0.00	0.00	6.29%	6.28%	0.00%	0.00%
16	0.31	0.16	0.00	0.00	10.79	6.46	0.00	0.00	**10.48**	**6.30**	0.00	0.00	4.19%	4.20%	0.00%	0.00%
17	0.81	0.53	0.00	0.00	11.52	6.96	0.00	0.00	**10.71**	**6.43**	0.00	0.00	4.29%	4.28%	0.00%	0.00%
18	2.94	1.63	0.00	0.00	35.07	20.94	0.00	0.00	**32.13**	**19.31**	0.00	0.00	12.86%	12.86%	0.00%	0.00%
19	2.06	1.00	0.00	0.00	33.48	19.88	0.00	0.00	**31.42**	**18.88**	0.00	0.00	12.57%	12.57%	0.00%	0.00%
20	1.09	0.61	0.00	0.00	32.51	19.49	0.00	0.00	**31.42**	**18.88**	0.00	0.00	12.57%	12.57%	0.00%	0.00%
21	0.67	0.29	0.00	0.00	11.38	6.73	0.00	0.00	**10.71**	**6.44**	0.00	0.00	4.29%	4.29%	0.00%	0.00%
22	0.00	0.00	3.53	1.72	0.00	0.00	38.85	46.48	**0.00**	**0.00**	35.32	44.76	0.00%	0.00%	12.74%	20.09%
23	0.00	0.00	2.11	1.18	0.00	0.00	27.92	37.50	**0.00**	**0.00**	25.81	36.32	0.00%	0.00%	9.31%	16.30%
24	0.42	0.34	0.00	0.00	5.66	3.48	0.00	0.00	**5.24**	**3.14**	0.00	0.00	2.10%	2.09%	0.00%	0.00%

Bus	L		G						PM				LD		GP	
	P_L0	Q_L0	Pg0	Qg0	PLF	QLF	PgF	QgF	ΔP_L	ΔQ_L	ΔPg	ΔQg	LDP	LDQ	GPP	GPQ
25	0.09	0.06	0.00	0.00	2.71	1.64	0.00	0.00	**2.62**	**1.58**	0.00	0.00	1.05%	1.05%	0.00%	0.00%
26	0.46	0.30	0.00	0.00	5.70	3.45	0.00	0.00	**5.24**	**3.15**	0.00	0.00	2.10%	2.10%	0.00%	0.00%
27	0.00	0.00	2.81	0.95	0.00	0.00	49.99	48.76	**0.00**	**0.00**	47.18	47.81	0.00%	0.00%	17.02%	21.45%
28	0.00	0.00	0.00	0.00	0.00	0.00	0.00	0.00	**0.00**	**0.00**	0.00	0.00	0.00%	0.00%	0.00%	0.00%
29	0.36	0.25	0.00	0.00	2.97	1.82	0.00	0.00	**2.61**	**1.57**	0.00	0.00	1.04%	1.05%	0.00%	0.00%
30	0.74	0.38	0.00	0.00	8.59	5.10	0.00	0.00	**7.85**	**4.72**	0.00	0.00	3.14%	3.14%	0.00%	0.00%
Total	19.82	10.4	19.89	7.06	269.73	160.55	297.12	229.9	**249.91**	**150.15**	277.23	222.84	100.00%	100.00%	100.00%	100.00%

Differences between Case30F07t2 and Case30F07d

Bus	L		G		LD		GP	
17 to 21					0.9X	0.9X		
19, 20					1.0X	1.0X		
others					1.1X	1.1X		
1 to 30	1.1X	1.1X						

2. Pattern Class II - Normally Loaded Conditions

Table A3 - 15 Ref. Case30F015L010LD15G06GP03 (Prototype of Pattern Class II)

Bus	L		G						PM				LD		GP	
	P_L0	Q_L0	Pg0	Qg0	PLF	QLF	PgF	QgF	ΔP_L	ΔQ_L	ΔPg	ΔQg	LDP	LDQ	GPP	GPQ
1	0.00	0.00	36.99	14.92	0.00	0.00	71.48	50.96	**0.00**	**0.00**	34.49	36.04	0.00%	0.00%	37.24%	33.92%
2	0.00	0.00	36.20	14.58	0.00	0.00	71.08	52.38	**0.00**	**0.00**	34.88	37.80	0.00%	0.00%	37.66%	35.58%
3	1.20	0.60	0.00	0.00	2.76	1.52	0.00	0.00	**1.56**	**0.92**	0.00	0.00	2.00%	2.00%	0.00%	0.00%
4	3.80	1.80	0.00	0.00	6.92	3.64	0.00	0.00	**3.12**	**1.84**	0.00	0.00	4.00%	4.00%	0.00%	0.00%
5	0.00	0.00	0.00	0.00	0.00	0.00	0.00	0.00	**0.00**	**0.00**	0.00	0.00	0.00%	0.00%	0.00%	0.00%
6	0.00	0.00	0.00	0.00	0.00	0.00	0.00	0.00	**0.00**	**0.00**	0.00	0.00	0.00%	0.00%	0.00%	0.00%
7	6.40	2.95	0.00	0.00	8.74	4.33	0.00	0.00	**2.34**	**1.38**	0.00	0.00	3.00%	3.00%	0.00%	0.00%
8	5.75	2.15	0.00	0.00	9.65	4.45	0.00	0.00	**3.90**	**2.30**	0.00	0.00	5.00%	5.00%	0.00%	0.00%
9	4.50	2.50	0.00	0.00	8.40	4.80	0.00	0.00	**3.90**	**2.30**	0.00	0.00	5.00%	5.00%	0.00%	0.00%
10	2.90	1.00	0.00	0.00	5.24	2.38	0.00	0.00	**2.34**	**1.38**	0.00	0.00	3.00%	3.00%	0.00%	0.00%
11	0.00	0.00	0.00	0.00	0.00	0.00	0.00	0.00	**0.00**	**0.00**	0.00	0.00	0.00%	0.00%	0.00%	0.00%
12	5.60	2.75	0.00	0.00	8.72	4.59	0.00	0.00	**3.12**	**1.84**	0.00	0.00	4.00%	4.00%	0.00%	0.00%
13	0.00	0.00	0.00	0.00	0.00	0.00	0.00	0.00	**0.00**	**0.00**	0.00	0.00	0.00%	0.00%	0.00%	0.00%
14	3.10	1.80	0.00	0.00	7.78	4.56	0.00	0.00	**4.68**	**2.76**	0.00	0.00	6.00%	6.00%	0.00%	0.00%
15	4.10	2.75	0.00	0.00	8.00	5.05	0.00	0.00	**3.90**	**2.30**	0.00	0.00	5.00%	5.00%	0.00%	0.00%
16	1.75	0.90	0.00	0.00	4.87	2.74	0.00	0.00	**3.12**	**1.84**	0.00	0.00	4.00%	4.00%	0.00%	0.00%
17	4.50	2.90	0.00	0.00	8.40	5.20	0.00	0.00	**3.90**	**2.30**	0.00	0.00	5.00%	5.00%	0.00%	0.00%
18	16.40	8.95	0.00	0.00	32.00	18.15	0.00	0.00	**15.60**	**9.20**	0.00	0.00	20.00%	20.00%	0.00%	0.00%
19	11.50	5.50	0.00	0.00	19.30	10.10	0.00	0.00	**7.80**	**4.60**	0.00	0.00	10.00%	10.00%	0.00%	0.00%
20	6.10	3.35	0.00	0.00	13.90	7.95	0.00	0.00	**7.80**	**4.60**	0.00	0.00	10.00%	10.00%	0.00%	0.00%
21	3.75	1.60	0.00	0.00	7.65	3.90	0.00	0.00	**3.90**	**2.30**	0.00	0.00	5.00%	5.00%	0.00%	0.00%
22	0.00	0.00	0.00	0.00	0.00	0.00	0.00	0.00	**0.00**	**0.00**	0.00	0.00	0.00%	0.00%	0.00%	0.00%

Bus	L		G						PM				LD		GP	
	P_L0	Q_L0	Pg0	Qg0	PLF	QLF	PgF	QgF	ΔP_L	ΔQ_L	ΔPg	ΔQg	LDP	LDQ	GPP	GPQ
23	0.00	0.00	0.00	0.00	0.00	0.00	0.00	0.00	**0.00**	**0.00**	0.00	0.00	0.00%	0.00%	0.00%	0.00%
24	2.35	1.85	0.00	0.00	3.91	2.77	0.00	0.00	**1.56**	**0.92**	0.00	0.00	2.00%	2.00%	0.00%	0.00%
25	0.50	0.35	0.00	0.00	1.28	0.81	0.00	0.00	**0.78**	**0.46**	0.00	0.00	1.00%	1.00%	0.00%	0.00%
26	1.75	1.15	0.00	0.00	4.09	2.53	0.00	0.00	**2.34**	**1.38**	0.00	0.00	3.00%	3.00%	0.00%	0.00%
27	0.00	0.00	19.90	13.08	0.00	0.00	43.15	45.48	**0.00**	**0.00**	23.25	32.40	0.00%	0.00%	25.10%	30.50%
28	0.00	0.00	0.00	0.00	0.00	0.00	0.00	0.00	**0.00**	**0.00**	0.00	0.00	0.00%	0.00%	0.00%	0.00%
29	1.35	0.95	0.00	0.00	2.13	1.41	0.00	0.00	**0.78**	**0.46**	0.00	0.00	1.00%	1.00%	0.00%	0.00%
30	2.80	1.45	0.00	0.00	4.36	2.37	0.00	0.00	**1.56**	**0.92**	0.00	0.00	2.00%	2.00%	0.00%	0.00%
Total	90.10	47.25	93.09	42.58	168.10	93.25	185.71	148.82	**78.00**	**46.00**	92.62	106.24	100.00%	100.00%	100.00%	100.00%

Table A3 - 16 Ref. Case30F015aL015LD15G06GP03 (Test pattern 03 Case1501)

Bus	L		G						PM				LD		GP	
	P_L0	Q_L0	Pg0	Qg0	PLF	QLF	PgF	QgF	ΔP_L	ΔQ_L	ΔPg	ΔQg	LDP	LDQ	GPP	GPQ
1	0.00	0.00	35.09	12.31	0.00	0.00	72.33	52.42	**0.00**	**0.00**	37.24	40.11	0.00%	0.00%	38.54%	36.58%
2	0.00	0.00	36.20	14.40	0.00	0.00	71.83	51.85	**0.00**	**0.00**	35.63	37.45	0.00%	0.00%	36.88%	34.15%
3	1.32	0.66	0.00	0.00	2.96	1.64	0.00	0.00	**1.64**	**0.98**	0.00	0.00	2.00%	2.00%	0.00%	0.00%
4	4.18	1.98	0.00	0.00	7.46	3.94	0.00	0.00	**3.28**	**1.96**	0.00	0.00	4.00%	4.00%	0.00%	0.00%
5	0.00	0.00	0.00	0.00	0.00	0.00	0.00	0.00	**0.00**	**0.00**	0.00	0.00	0.00%	0.00%	0.00%	0.00%
6	0.00	0.00	0.00	0.00	0.00	0.00	0.00	0.00	**0.00**	**0.00**	0.00	0.00	0.00%	0.00%	0.00%	0.00%
7	7.04	3.25	0.00	0.00	9.50	4.72	0.00	0.00	**2.46**	**1.47**	0.00	0.00	3.00%	3.00%	0.00%	0.00%
8	6.33	2.37	0.00	0.00	10.43	4.82	0.00	0.00	**4.10**	**2.45**	0.00	0.00	5.00%	5.00%	0.00%	0.00%
9	4.95	2.75	0.00	0.00	9.05	5.20	0.00	0.00	**4.10**	**2.45**	0.00	0.00	5.00%	5.00%	0.00%	0.00%
10	3.19	1.10	0.00	0.00	5.65	2.57	0.00	0.00	**2.46**	**1.47**	0.00	0.00	3.00%	3.00%	0.00%	0.00%
11	0.00	0.00	0.00	0.00	0.00	0.00	0.00	0.00	**0.00**	**0.00**	0.00	0.00	0.00%	0.00%	0.00%	0.00%
12	5.04	2.48	0.00	0.00	8.32	4.44	0.00	0.00	**3.28**	**1.96**	0.00	0.00	4.00%	4.00%	0.00%	0.00%
13	0.00	0.00	0.00	0.00	0.00	0.00	0.00	0.00	**0.00**	**0.00**	0.00	0.00	0.00%	0.00%	0.00%	0.00%
14	2.79	1.62	0.00	0.00	7.71	4.56	0.00	0.00	**4.92**	**2.94**	0.00	0.00	6.00%	6.00%	0.00%	0.00%
15	3.69	2.48	0.00	0.00	7.79	4.93	0.00	0.00	**4.10**	**2.45**	0.00	0.00	5.00%	5.00%	0.00%	0.00%
16	1.58	0.81	0.00	0.00	4.86	2.77	0.00	0.00	**3.28**	**1.96**	0.00	0.00	4.00%	4.00%	0.00%	0.00%
17	4.05	2.61	0.00	0.00	8.15	5.06	0.00	0.00	**4.10**	**2.45**	0.00	0.00	5.00%	5.00%	0.00%	0.00%
18	14.76	8.05	0.00	0.00	31.16	17.86	0.00	0.00	**16.40**	**9.81**	0.00	0.00	20.00%	20.02%	0.00%	0.00%
19	10.35	4.95	0.00	0.00	18.55	9.85	0.00	0.00	**8.20**	**4.90**	0.00	0.00	10.00%	10.00%	0.00%	0.00%
20	5.49	3.02	0.00	0.00	13.69	7.92	0.00	0.00	**8.20**	**4.90**	0.00	0.00	10.00%	10.00%	0.00%	0.00%
21	4.13	1.76	0.00	0.00	8.23	4.21	0.00	0.00	**4.10**	**2.45**	0.00	0.00	5.00%	5.00%	0.00%	0.00%
22	0.00	0.00	0.00	0.00	0.00	0.00	0.00	0.00	**0.00**	**0.00**	0.00	0.00	0.00%	0.00%	0.00%	0.00%
23	0.00	0.00	0.00	0.00	0.00	0.00	0.00	0.00	**0.00**	**0.00**	0.00	0.00	0.00%	0.00%	0.00%	0.00%
24	2.59	2.04	0.00	0.00	4.23	3.02	0.00	0.00	**1.64**	**0.98**	0.00	0.00	2.00%	2.00%	0.00%	0.00%

Bus	L		G						PM				LD		GP	
	P_L0	Q_L0	Pg0	Qg0	PLF	QLF	PgF	QgF	ΔP_L	ΔQ_L	ΔPg	ΔQg	LDP	LDQ	GPP	GPQ
25	0.55	0.39	0.00	0.00	1.37	0.88	0.00	0.00	**0.82**	**0.49**	0.00	0.00	1.00%	1.00%	0.00%	0.00%
26	1.93	1.26	0.00	0.00	4.38	2.73	0.00	0.00	**2.45**	**1.47**	0.00	0.00	2.99%	3.00%	0.00%	0.00%
27	0.00	0.00	19.80	13.08	0.00	0.00	43.55	45.18	**0.00**	**0.00**	23.75	32.10	0.00%	0.00%	24.58%	29.27%
28	0.00	0.00	0.00	0.00	0.00	0.00	0.00	0.00	**0.00**	**0.00**	0.00	0.00	0.00%	0.00%	0.00%	0.00%
29	1.49	1.04	0.00	0.00	2.31	1.53	0.00	0.00	**0.82**	**0.49**	0.00	0.00	1.00%	1.00%	0.00%	0.00%
30	3.08	1.60	0.00	0.00	4.72	2.58	0.00	0.00	**1.64**	**0.98**	0.00	0.00	2.00%	2.00%	0.00%	0.00%
Total	88.53	46.22	91.09	39.79	170.52	95.23	187.71	149.45	**81.99**	**49.01**	96.62	109.66	100.00%	100.00%	100.00%	100.00%

Differences between Case30F015a and Case30F015

Bus	L		G		LD		GP	
1 to 10	1.1x	1.1x						
11 to 20	0.9x	0.9x						
21 to 30	1.1x	1.1x						
1			0.95x	0.83x				
2			1.00x	1.00x				
27			1.00x	1.00x				

Table A3 - 17 **Ref. Case30F015bL010LD15bG06GP03**

Bus	L		G						PM				LD		GP	
	P_L0	Q_L0	Pg0	Qg0	PLF	QLF	PgF	QgF	ΔP_L	ΔQ_L	ΔPg	ΔQg	LDP	LDQ	GPP	GPQ
1	0	0	36.99	14.92	0.00	0.00	72.42	52.65	**0.00**	**0.00**	35.43	37.73	0.00%	0.00%	37.62%	35.17%
2	0	0	36.2	14.58	0.00	0.00	71.45	52.03	**0.00**	**0.00**	35.25	37.45	0.00%	0.00%	37.43%	34.91%
3	1.2	0.6	0	0	2.96	1.66	0.00	0.00	**1.76**	**1.06**	0.00	0.00	2.20%	2.21%	0.00%	0.00%
4	3.8	1.8	0	0	7.32	3.91	0.00	0.00	**3.52**	**2.11**	0.00	0.00	4.40%	4.40%	0.00%	0.00%
5	0	0	0	0	0.00	0.00	0.00	0.00	**0.00**	**0.00**	0.00	0.00	0.00%	0.00%	0.00%	0.00%
6	0	0	0	0	0.00	0.00	0.00	0.00	**0.00**	**0.00**	0.00	0.00	0.00%	0.00%	0.00%	0.00%
7	6.4	2.95	0	0	9.04	4.53	0.00	0.00	**2.64**	**1.58**	0.00	0.00	3.30%	3.29%	0.00%	0.00%
8	5.75	2.15	0	0	10.15	4.79	0.00	0.00	**4.40**	**2.64**	0.00	0.00	5.50%	5.50%	0.00%	0.00%
9	4.5	2.5	0	0	8.90	5.14	0.00	0.00	**4.40**	**2.64**	0.00	0.00	5.50%	5.50%	0.00%	0.00%
10	2.9	1	0	0	5.54	2.58	0.00	0.00	**2.64**	**1.58**	0.00	0.00	3.30%	3.29%	0.00%	0.00%
11	0	0	0	0	0.00	0.00	0.00	0.00	**0.00**	**0.00**	0.00	0.00	0.00%	0.00%	0.00%	0.00%
12	5.6	2.75	0	0	9.12	4.86	0.00	0.00	**3.52**	**2.11**	0.00	0.00	4.40%	4.40%	0.00%	0.00%
13	0	0	0	0	0.00	0.00	0.00	0.00	**0.00**	**0.00**	0.00	0.00	0.00%	0.00%	0.00%	0.00%
14	3.1	1.8	0	0	8.38	4.97	0.00	0.00	**5.28**	**3.17**	0.00	0.00	6.60%	6.60%	0.00%	0.00%
15	4.1	2.75	0	0	8.50	5.39	0.00	0.00	**4.40**	**2.64**	0.00	0.00	5.50%	5.50%	0.00%	0.00%
16	1.75	0.9	0	0	5.27	3.01	0.00	0.00	**3.52**	**2.11**	0.00	0.00	4.40%	4.40%	0.00%	0.00%
17	4.5	2.9	0	0	8.10	5.06	0.00	0.00	**3.60**	**2.16**	0.00	0.00	4.50%	4.50%	0.00%	0.00%
18	16.4	8.95	0	0	30.80	17.59	0.00	0.00	**14.40**	**8.64**	0.00	0.00	18.00%	18.00%	0.00%	0.00%
19	11.5	5.5	0	0	18.70	9.82	0.00	0.00	**7.20**	**4.32**	0.00	0.00	9.00%	9.00%	0.00%	0.00%
20	6.1	3.35	0	0	13.30	7.67	0.00	0.00	**7.20**	**4.32**	0.00	0.00	9.00%	9.00%	0.00%	0.00%
21	3.75	1.6	0	0	7.35	3.76	0.00	0.00	**3.60**	**2.16**	0.00	0.00	4.50%	4.50%	0.00%	0.00%
22	0	0	0	0	0.00	0.00	0.00	0.00	**0.00**	**0.00**	0.00	0.00	0.00%	0.00%	0.00%	0.00%
23	0	0	0	0	0.00	0.00	0.00	0.00	**0.00**	**0.00**	0.00	0.00	0.00%	0.00%	0.00%	0.00%
24	2.35	1.85	0	0	4.11	2.91	0.00	0.00	**1.76**	**1.06**	0.00	0.00	2.20%	2.21%	0.00%	0.00%

Bus	L		G						PM				LD		GP	
	P_L0	Q_L0	Pg0	Qg0	PLF	QLF	PgF	QgF	ΔP_L	ΔQ_L	ΔPg	ΔQg	LDP	LDQ	GPP	GPQ
25	0.5	0.35	0	0	1.38	0.88	0.00	0.00	**0.88**	**0.53**	0.00	0.00	1.10%	1.10%	0.00%	0.00%
26	1.75	1.15	0	0	4.39	2.73	0.00	0.00	**2.64**	**1.58**	0.00	0.00	3.30%	3.29%	0.00%	0.00%
27	0	0	19.9	13.08	0.00	0.00	43.40	45.18	**0.00**	**0.00**	23.50	32.10	0.00%	0.00%	24.95%	29.92%
28	0	0	0	0	0.00	0.00	0.00	0.00	**0.00**	**0.00**	0.00	0.00	0.00%	0.00%	0.00%	0.00%
29	1.35	0.95	0	0	2.23	1.48	0.00	0.00	**0.88**	**0.53**	0.00	0.00	1.10%	1.10%	0.00%	0.00%
30	2.8	1.45	0	0	4.56	2.51	0.00	0.00	**1.76**	**1.06**	0.00	0.00	2.20%	2.21%	0.00%	0.00%
Total	90.1	47.25	93.09	42.58	170.10	95.25	187.27	149.86	**80.00**	**48.00**	94.18	107.28	100.00%	100.00%	100.00%	100.00%

Differences between Case30F015b and Case30F015

Bus	L		G		LD		GP	
17 to 21					0.9x	0.9x		
others					1.1x	1.1x		

Table A3 - 18 Ref. Case30F015cL015LD15bG06GP015

Bus	L		G						PM				LD		GP	
	P_L0	Q_L0	Pg0	Qg0	PLF	QLF	PgF	QgF	ΔP_L	ΔQ_L	ΔPg	ΔQg	LDP	LDQ	GPP	GPQ
1	0	0	36.99	14.92	0.00	0.00	74.81	57.24	**0.00**	**0.00**	37.82	42.32	0.00%	0.00%	40.14%	39.95%
2	0	0	36.2	14.58	0.00	0.00	64.40	46.38	**0.00**	**0.00**	28.20	31.80	0.00%	0.00%	29.93%	30.02%
3	1.2	0.6	0.00	0.00	2.96	1.63	0.00	0.00	**1.76**	**1.03**	0.00	0.00	2.20%	2.19%	0.00%	0.00%
4	3.8	1.8	0.00	0.00	7.32	3.87	0.00	0.00	**3.52**	**2.07**	0.00	0.00	4.40%	4.40%	0.00%	0.00%
5	0	0	0.00	0.00	0.00	0.00	0.00	0.00	**0.00**	**0.00**	0.00	0.00	0.00%	0.00%	0.00%	0.00%
6	0	0	0.00	0.00	0.00	0.00	0.00	0.00	**0.00**	**0.00**	0.00	0.00	0.00%	0.00%	0.00%	0.00%
7	6.4	2.95	0.00	0.00	9.04	4.50	0.00	0.00	**2.64**	**1.55**	0.00	0.00	3.30%	3.30%	0.00%	0.00%
8	5.75	2.15	0.00	0.00	10.15	4.74	0.00	0.00	**4.40**	**2.59**	0.00	0.00	5.50%	5.51%	0.00%	0.00%
9	4.5	2.5	0.00	0.00	8.90	5.09	0.00	0.00	**4.40**	**2.59**	0.00	0.00	5.50%	5.51%	0.00%	0.00%
10	2.9	1	0.00	0.00	5.54	2.55	0.00	0.00	**2.64**	**1.55**	0.00	0.00	3.30%	3.30%	0.00%	0.00%
11	0	0	0.00	0.00	0.00	0.00	0.00	0.00	**0.00**	**0.00**	0.00	0.00	0.00%	0.00%	0.00%	0.00%
12	5.6	2.75	0.00	0.00	9.12	4.82	0.00	0.00	**3.52**	**2.07**	0.00	0.00	4.40%	4.40%	0.00%	0.00%
13	0	0	0.00	0.00	0.00	0.00	0.00	0.00	**0.00**	**0.00**	0.00	0.00	0.00%	0.00%	0.00%	0.00%
14	3.1	1.8	0.00	0.00	8.38	4.90	0.00	0.00	**5.28**	**3.10**	0.00	0.00	6.60%	6.59%	0.00%	0.00%
15	4.1	2.75	0.00	0.00	8.50	5.34	0.00	0.00	**4.40**	**2.59**	0.00	0.00	5.50%	5.51%	0.00%	0.00%
16	1.75	0.9	0.00	0.00	5.27	2.97	0.00	0.00	**3.52**	**2.07**	0.00	0.00	4.40%	4.40%	0.00%	0.00%
17	4.5	2.9	0.00	0.00	8.10	5.02	0.00	0.00	**3.60**	**2.12**	0.00	0.00	4.50%	4.51%	0.00%	0.00%
18	16.4	8.95	0.00	0.00	30.80	17.41	0.00	0.00	**14.40**	**8.46**	0.00	0.00	18.00%	17.99%	0.00%	0.00%
19	11.5	5.5	0.00	0.00	18.70	9.73	0.00	0.00	**7.20**	**4.23**	0.00	0.00	9.00%	9.00%	0.00%	0.00%
20	6.1	3.35	0.00	0.00	13.30	7.58	0.00	0.00	**7.20**	**4.23**	0.00	0.00	9.00%	9.00%	0.00%	0.00%
21	3.75	1.6	0.00	0.00	7.35	3.72	0.00	0.00	**3.60**	**2.12**	0.00	0.00	4.50%	4.51%	0.00%	0.00%
22	0	0	0.00	0.00	0.00	0.00	0.00	0.00	**0.00**	**0.00**	0.00	0.00	0.00%	0.00%	0.00%	0.00%
23	0	0	0.00	0.00	0.00	0.00	0.00	0.00	**0.00**	**0.00**	0.00	0.00	0.00%	0.00%	0.00%	0.00%
24	2.35	1.85	0.00	0.00	4.11	2.88	0.00	0.00	**1.76**	**1.03**	0.00	0.00	2.20%	2.19%	0.00%	0.00%

Bus	L		G						PM				LD		GP	
	P_L0	Q_L0	Pg0	Qg0	PLF	QLF	PgF	QgF	ΔP_L	ΔQ_L	ΔPg	ΔQg	LDP	LDQ	GPP	GPQ
25	0.5	0.35	0.00	0.00	1.38	0.87	0.00	0.00	**0.88**	**0.52**	0.00	0.00	1.10%	1.11%	0.00%	0.00%
26	1.75	1.15	0.00	0.00	4.39	2.70	0.00	0.00	**2.64**	**1.55**	0.00	0.00	3.30%	3.30%	0.00%	0.00%
27	0	0	19.9	13.08	0.00	0.00	48.10	44.88	**0.00**	**0.00**	28.20	31.80	0.00%	0.00%	29.93%	30.02%
28	0	0	0.00	0.00	0.00	0.00	0.00	0.00	**0.00**	**0.00**	0.00	0.00	0.00%	0.00%	0.00%	0.00%
29	1.35	0.95	0.00	0.00	2.23	1.47	0.00	0.00	**0.88**	**0.52**	0.00	0.00	1.10%	1.11%	0.00%	0.00%
30	2.8	1.45	0.00	0.00	4.56	2.48	0.00	0.00	**1.76**	**1.03**	0.00	0.00	2.20%	2.19%	0.00%	0.00%
Total	90.1	47.25	93.09	42.58	170.10	94.27	187.31	148.50	**80.00**	**47.02**	94.22	105.92	100.00%	100.00%	100.00%	100.00%

Differences between Case30F015c and Case30F015b

Bus	L		G		LD		GP	
1							1.06xb	1.14xb
2							0.80xb	0.86xb
27							1.20xb	1.00xb

Table A3 - 19 **Ref. Case30F015t2L015t1LD15t2G06GP03 (Test pattern 04 Case1502)**

Bus	L		G						PM				LD		GP	
	P_L0	Q_L0	Pg0	Qg0	PLF	QLF	PgF	QgF	ΔP_L	ΔQ_L	ΔPg	ΔQg	LDP	LDQ	GPP	GPQ
1	0.00	0.00	40.01	17.23	0.00	0.00	70.86	50.28	**0.00**	**0.00**	30.85	33.05	0.00%	0.00%	37.29%	33.93%
2	0.00	0.00	40.54	17.50	0.00	0.00	71.67	52.15	**0.00**	**0.00**	31.13	34.65	0.00%	0.00%	37.63%	35.57%
3	1.32	0.66	0.00	0.00	2.84	1.56	0.00	0.00	**1.52**	**0.90**	0.00	0.00	2.20%	2.20%	0.00%	0.00%
4	4.18	1.98	0.00	0.00	6.66	3.46	0.00	0.00	**2.48**	**1.48**	0.00	0.00	3.60%	3.61%	0.00%	0.00%
5	0.00	0.00	0.00	0.00	0.00	0.00	0.00	0.00	**0.00**	**0.00**	0.00	0.00	0.00%	0.00%	0.00%	0.00%
6	0.00	0.00	0.00	0.00	0.00	0.00	0.00	0.00	**0.00**	**0.00**	0.00	0.00	0.00%	0.00%	0.00%	0.00%
7	7.04	3.25	0.00	0.00	9.32	4.60	0.00	0.00	**2.28**	**1.35**	0.00	0.00	3.31%	3.29%	0.00%	0.00%
8	6.33	2.37	0.00	0.00	9.43	4.21	0.00	0.00	**3.10**	**1.84**	0.00	0.00	4.49%	4.49%	0.00%	0.00%
9	4.95	2.75	0.00	0.00	8.75	5.01	0.00	0.00	**3.80**	**2.26**	0.00	0.00	5.51%	5.51%	0.00%	0.00%
10	3.19	1.10	0.00	0.00	5.47	2.45	0.00	0.00	**2.28**	**1.35**	0.00	0.00	3.31%	3.29%	0.00%	0.00%
11	0.00	0.00	0.00	0.00	0.00	0.00	0.00	0.00	**0.00**	**0.00**	0.00	0.00	0.00%	0.00%	0.00%	0.00%
12	6.16	3.03	0.00	0.00	9.20	4.83	0.00	0.00	**3.04**	**1.80**	0.00	0.00	4.41%	4.39%	0.00%	0.00%
13	0.00	0.00	0.00	0.00	0.00	0.00	0.00	0.00	**0.00**	**0.00**	0.00	0.00	0.00%	0.00%	0.00%	0.00%
14	3.41	1.98	0.00	0.00	7.14	4.19	0.00	0.00	**3.73**	**2.21**	0.00	0.00	5.41%	5.39%	0.00%	0.00%
15	4.51	3.03	0.00	0.00	8.30	5.28	0.00	0.00	**3.79**	**2.25**	0.00	0.00	5.49%	5.49%	0.00%	0.00%
16	1.93	0.99	0.00	0.00	4.96	2.79	0.00	0.00	**3.03**	**1.80**	0.00	0.00	4.39%	4.39%	0.00%	0.00%
17	4.95	3.19	0.00	0.00	8.05	5.04	0.00	0.00	**3.10**	**1.85**	0.00	0.00	4.49%	4.51%	0.00%	0.00%
18	18.04	9.85	0.00	0.00	33.22	18.87	0.00	0.00	**15.18**	**9.02**	0.00	0.00	22.01%	22.01%	0.00%	0.00%
19	12.65	6.05	0.00	0.00	18.86	9.74	0.00	0.00	**6.21**	**3.69**	0.00	0.00	9.00%	9.00%	0.00%	0.00%
20	6.71	3.69	0.00	0.00	12.92	7.38	0.00	0.00	**6.21**	**3.69**	0.00	0.00	9.00%	9.00%	0.00%	0.00%
21	4.13	1.76	0.00	0.00	7.23	3.61	0.00	0.00	**3.10**	**1.85**	0.00	0.00	4.49%	4.51%	0.00%	0.00%
22	0.00	0.00	0.00	0.00	0.00	0.00	0.00	0.00	**0.00**	**0.00**	0.00	0.00	0.00%	0.00%	0.00%	0.00%
23	0.00	0.00	0.00	0.00	0.00	0.00	0.00	0.00	**0.00**	**0.00**	0.00	0.00	0.00%	0.00%	0.00%	0.00%
24	2.59	2.04	0.00	0.00	3.83	2.77	0.00	0.00	**1.24**	**0.73**	0.00	0.00	1.80%	1.78%	0.00%	0.00%

Bus	L		G						PM				LD		GP	
	P_L0	Q_L0	Pg0	Qg0	PLF	QLF	PgF	QgF	ΔP_L	ΔQ_L	ΔPg	ΔQg	LDP	LDQ	GPP	GPQ
25	0.55	0.39	0.00	0.00	1.31	0.84	0.00	0.00	**0.76**	**0.45**	0.00	0.00	1.10%	1.10%	0.00%	0.00%
26	1.93	1.26	0.00	0.00	3.79	2.37	0.00	0.00	**1.86**	**1.11**	0.00	0.00	2.70%	2.71%	0.00%	0.00%
27	0.00	0.00	22.29	15.70	0.00	0.00	43.04	45.40	**0.00**	**0.00**	20.75	29.70	0.00%	0.00%	25.08%	30.49%
28	0.00	0.00	0.00	0.00	0.00	0.00	0.00	0.00	**0.00**	**0.00**	0.00	0.00	0.00%	0.00%	0.00%	0.00%
29	1.49	1.04	0.00	0.00	2.24	1.50	0.00	0.00	**0.75**	**0.46**	0.00	0.00	1.09%	1.12%	0.00%	0.00%
30	3.08	1.60	0.00	0.00	4.60	2.50	0.00	0.00	**1.52**	**0.90**	0.00	0.00	2.20%	2.20%	0.00%	0.00%
Total	99.14	52.01	102.84	50.43	168.12	93.00	185.57	147.83	**68.98**	**40.99**	82.73	97.4	100.00%	100.00%	100.00%	100.00%

Differences between Case30F015t2 and Case30F015

Bus	L		G		LD		GP	
1 to 30	1.1x	1.1x						
1			1.12x	1.2x				
2			1.12x	1.2x				
27			1.12x	1.2x				
4,8,14,17,19,20,21,24,26					0.9x	0.9x		
others					1.1x	1.1x		

3. Pattern Class III - Heavily Loaded Conditions

Table A3 - 20 Ref. Case30F020L020LD020G020GP020 (Prototype of Pattern Class III)

Bus	L		G						PM				LD		GP	
	P_L0	Q_L0	Pg0	Qg0	PLF	QLF	PgF	QgF	ΔP_L	ΔQ_L	ΔPg	ΔQg	LDP	LDQ	GPP	GPQ
1	0.00	0.00	57.90	36.80	0.00	0.00	75.89	56.75	**0.00**	**0.00**	17.99	19.95	0.00%	0.00%	26.04%	27.51%
2	0.00	0.00	57.00	37.00	0.00	0.00	75.90	56.44	**0.00**	**0.00**	18.90	19.44	0.00%	0.00%	27.36%	26.81%
3	3.00	1.80	0.00	0.00	5.95	3.55	0.00	0.00	**2.95**	**1.75**	0.00	0.00	5.00%	5.00%	0.00%	0.00%
4	9.00	5.40	0.00	0.00	9.00	5.40	0.00	0.00	**0.00**	**0.00**	0.00	0.00	0.00%	0.00%	0.00%	0.00%
5	0.00	0.00	0.00	0.00	0.00	0.00	0.00	0.00	**0.00**	**0.00**	0.00	0.00	0.00%	0.00%	0.00%	0.00%
6	0.00	0.00	0.00	0.00	0.00	0.00	0.00	0.00	**0.00**	**0.00**	0.00	0.00	0.00%	0.00%	0.00%	0.00%
7	12.80	5.90	0.00	0.00	15.75	7.65	0.00	0.00	**2.95**	**1.75**	0.00	0.00	5.00%	5.00%	0.00%	0.00%
8	10.50	4.30	0.00	0.00	13.45	6.05	0.00	0.00	**2.95**	**1.75**	0.00	0.00	5.00%	5.00%	0.00%	0.00%
9	9.00	5.00	0.00	0.00	11.95	6.75	0.00	0.00	**2.95**	**1.75**	0.00	0.00	5.00%	5.00%	0.00%	0.00%
10	6.00	3.60	0.00	0.00	8.95	5.35	0.00	0.00	**2.95**	**1.75**	0.00	0.00	5.00%	5.00%	0.00%	0.00%
11	0.00	0.00	0.00	0.00	0.00	0.00	0.00	0.00	**0.00**	**0.00**	0.00	0.00	0.00%	0.00%	0.00%	0.00%
12	11.20	7.00	0.00	0.00	14.15	8.75	0.00	0.00	**2.95**	**1.75**	0.00	0.00	5.00%	5.00%	0.00%	0.00%
13	0.00	0.00	0.00	0.00	0.00	0.00	0.00	0.00	**0.00**	**0.00**	0.00	0.00	0.00%	0.00%	0.00%	0.00%
14	29.00	18.00	0.00	0.00	34.90	21.50	0.00	0.00	**5.90**	**3.50**	0.00	0.00	10.00%	10.00%	0.00%	0.00%
15	31.50	19.00	0.00	0.00	37.40	22.50	0.00	0.00	**5.90**	**3.50**	0.00	0.00	10.00%	10.00%	0.00%	0.00%
16	5.00	3.00	0.00	0.00	7.95	4.75	0.00	0.00	**2.95**	**1.75**	0.00	0.00	5.00%	5.00%	0.00%	0.00%
17	9.00	5.80	0.00	0.00	11.95	7.55	0.00	0.00	**2.95**	**1.75**	0.00	0.00	5.00%	5.00%	0.00%	0.00%
18	16.00	9.00	0.00	0.00	21.90	12.50	0.00	0.00	**5.90**	**3.50**	0.00	0.00	10.00%	10.00%	0.00%	0.00%
19	12.00	8.00	0.00	0.00	14.95	9.75	0.00	0.00	**2.95**	**1.75**	0.00	0.00	5.00%	5.00%	0.00%	0.00%
20	5.50	3.30	0.00	0.00	5.50	3.30	0.00	0.00	**0.00**	**0.00**	0.00	0.00	0.00%	0.00%	0.00%	0.00%
21	7.50	3.20	0.00	0.00	10.45	4.95	0.00	0.00	**2.95**	**1.75**	0.00	0.00	5.00%	5.00%	0.00%	0.00%
22	0.00	0.00	37.00	24.00	0.00	0.00	48.90	36.24	**0.00**	**0.00**	11.90	12.24	0.00%	0.00%	17.22%	16.88%

Bus	L		G						PM				LD		GP	
	P_L0	Q_L0	Pg0	Qg0	PLF	QLF	PgF	QgF	ΔP_L	ΔQ_L	ΔPg	ΔQg	LDP	LDQ	GPP	GPQ
23	0.00	0.00	23.00	16.00	0.00	0.00	30.70	23.92	**0.00**	**0.00**	7.70	7.92	0.00%	0.00%	11.14%	10.92%
24	4.70	3.70	0.00	0.00	7.65	5.45	0.00	0.00	**2.95**	**1.75**	0.00	0.00	5.00%	5.00%	0.00%	0.00%
25	3.00	2.00	0.00	0.00	5.95	3.75	0.00	0.00	**2.95**	**1.75**	0.00	0.00	5.00%	5.00%	0.00%	0.00%
26	5.50	3.30	0.00	0.00	5.50	3.30	0.00	0.00	**0.00**	**0.00**	0.00	0.00	0.00%	0.00%	0.00%	0.00%
27	0.00	0.00	38.00	28.00	0.00	0.00	50.60	40.96	**0.00**	**0.00**	12.60	12.96	0.00%	0.00%	18.24%	17.87%
28	0.00	0.00	0.00	0.00	0.00	0.00	0.00	0.00	**0.00**	**0.00**	0.00	0.00	0.00%	0.00%	0.00%	0.00%
29	4.00	2.40	0.00	0.00	6.95	4.15	0.00	0.00	**2.95**	**1.75**	0.00	0.00	5.00%	5.00%	0.00%	0.00%
30	7.60	4.00	0.00	0.00	10.55	5.75	0.00	0.00	**2.95**	**1.75**	0.00	0.00	5.00%	5.00%	0.00%	0.00%
Total	201.8	117.7	212.9	141.8	260.80	152.70	281.99	214.31	**59.00**	**35.00**	69.09	72.51	100.00%	100.00%	100.00%	100.00%

Table A3 - 21 **Ref. Case30F020aL020aLD020G020aGP020**

Bus	L		G						PM				LD		GP	
	P_L0	Q_L0	Pg0	Qg0	PLF	QLF	PgF	QgF	ΔP_L	ΔQ_L	ΔPg	ΔQg	LDP	LDQ	GPP	GPQ
1	0.00	0.00	55.39	33.74	0.00	0.00	79.92	58.90	**0.00**	**0.00**	24.53	25.16	0.00%	0.00%	27.86%	27.69%
2	0.00	0.00	55.86	34.41	0.00	0.00	79.35	58.71	**0.00**	**0.00**	23.49	24.30	0.00%	0.00%	26.68%	26.74%
3	3.30	1.98	0.00	0.00	7.10	4.28	0.00	0.00	**3.80**	**2.30**	0.00	0.00	5.00%	5.00%	0.00%	0.00%
4	9.90	5.94	0.00	0.00	9.90	5.94	0.00	0.00	**0.00**	**0.00**	0.00	0.00	0.00%	0.00%	0.00%	0.00%
5	0.00	0.00	0.00	0.00	0.00	0.00	0.00	0.00	**0.00**	**0.00**	0.00	0.00	0.00%	0.00%	0.00%	0.00%
6	0.00	0.00	0.00	0.00	0.00	0.00	0.00	0.00	**0.00**	**0.00**	0.00	0.00	0.00%	0.00%	0.00%	0.00%
7	14.08	6.49	0.00	0.00	17.88	8.79	0.00	0.00	**3.80**	**2.30**	0.00	0.00	5.00%	5.00%	0.00%	0.00%
8	11.55	4.73	0.00	0.00	15.35	7.03	0.00	0.00	**3.80**	**2.30**	0.00	0.00	5.00%	5.00%	0.00%	0.00%
9	9.90	5.50	0.00	0.00	13.70	7.80	0.00	0.00	**3.80**	**2.30**	0.00	0.00	5.00%	5.00%	0.00%	0.00%
10	6.60	3.96	0.00	0.00	10.40	6.26	0.00	0.00	**3.80**	**2.30**	0.00	0.00	5.00%	5.00%	0.00%	0.00%
11	0.00	0.00	0.00	0.00	0.00	0.00	0.00	0.00	**0.00**	**0.00**	0.00	0.00	0.00%	0.00%	0.00%	0.00%
12	10.08	6.30	0.00	0.00	13.88	8.60	0.00	0.00	**3.80**	**2.30**	0.00	0.00	5.00%	5.00%	0.00%	0.00%
13	0.00	0.00	0.00	0.00	0.00	0.00	0.00	0.00	**0.00**	**0.00**	0.00	0.00	0.00%	0.00%	0.00%	0.00%
14	26.10	16.20	0.00	0.00	33.70	20.80	0.00	0.00	**7.60**	**4.60**	0.00	0.00	10.00%	10.00%	0.00%	0.00%
15	28.35	17.10	0.00	0.00	35.95	21.70	0.00	0.00	**7.60**	**4.60**	0.00	0.00	10.00%	10.00%	0.00%	0.00%
16	4.50	2.70	0.00	0.00	8.30	5.00	0.00	0.00	**3.80**	**2.30**	0.00	0.00	5.00%	5.00%	0.00%	0.00%
17	8.10	5.22	0.00	0.00	11.90	7.52	0.00	0.00	**3.80**	**2.30**	0.00	0.00	5.00%	5.00%	0.00%	0.00%
18	14.40	8.10	0.00	0.00	22.00	12.70	0.00	0.00	**7.60**	**4.60**	0.00	0.00	10.00%	10.00%	0.00%	0.00%
19	10.80	7.20	0.00	0.00	14.60	9.50	0.00	0.00	**3.80**	**2.30**	0.00	0.00	5.00%	5.00%	0.00%	0.00%
20	4.95	2.97	0.00	0.00	4.95	2.97	0.00	0.00	**0.00**	**0.00**	0.00	0.00	0.00%	0.00%	0.00%	0.00%
21	8.25	3.52	0.00	0.00	12.05	5.82	0.00	0.00	**3.80**	**2.30**	0.00	0.00	5.00%	5.00%	0.00%	0.00%
22	0.00	0.00	36.26	22.32	0.00	0.00	51.05	37.62	**0.00**	**0.00**	14.79	15.30	0.00%	0.00%	16.80%	16.84%
23	0.00	0.00	22.54	14.88	0.00	0.00	32.11	24.78	**0.00**	**0.00**	9.57	9.90	0.00%	0.00%	10.87%	10.90%
24	5.17	4.07	0.00	0.00	8.97	6.37	0.00	0.00	**3.80**	**2.30**	0.00	0.00	5.00%	5.00%	0.00%	0.00%

Bus	L		G						PM				LD		GP	
	P_L0	Q_L0	Pg0	Qg0	PLF	QLF	PgF	QgF	ΔP_L	ΔQ_L	ΔPg	ΔQg	LDP	LDQ	GPP	GPQ
25	3.30	2.20	0.00	0.00	7.10	4.50	0.00	0.00	**3.80**	**2.30**	0.00	0.00	5.00%	5.00%	0.00%	0.00%
26	6.05	3.63	0.00	0.00	6.05	3.63	0.00	0.00	**0.00**	**0.00**	0.00	0.00	0.00%	0.00%	0.00%	0.00%
27	0.00	0.00	37.24	26.04	0.00	0.00	52.90	42.24	**0.00**	**0.00**	15.66	16.20	0.00%	0.00%	17.79%	17.83%
28	0.00	0.00	0.00	0.00	0.00	0.00	0.00	0.00	**0.00**	**0.00**	0.00	0.00	0.00%	0.00%	0.00%	0.00%
29	4.40	2.64	0.00	0.00	8.20	4.94	0.00	0.00	**3.80**	**2.30**	0.00	0.00	5.00%	5.00%	0.00%	0.00%
30	8.36	4.40	0.00	0.00	12.16	6.70	0.00	0.00	**3.80**	**2.30**	0.00	0.00	5.00%	5.00%	0.00%	0.00%
Total	198.14	114.85	207.29	131.39	274.14	160.85	295.33	222.25	**76.00**	**46.00**	88.04	90.86	100.00%	100.00%	100.00%	100.00%

NB: Generation reached max capacity, low voltage 0.704 p.u. at bus 14

Differences between Case30F020a and Case30F020

Bus	L		G		LD		GP	
1 to 10	1.1x	1.1x						
11 to 20	0.9x	0.9x						
21 to 30	1.1x	1.1x						
1			0.98x	0.93x				
2			0.98x	0.93x				
22			0.98x	0.93x				
23			0.98x	0.93x				
27			0.98x	0.93x				

Table A3 - 22 Ref. Case30F020bL020LD020bG020GP020

Bus	L		G						PM				LD		GP	
	P_L0	Q_L0	Pg0	Qg0	PLF	QLF	PgF	QgF	ΔP_L	ΔQ_L	ΔPg	ΔQg	LDP	LDQ	GPP	GPQ
1	0.00	0.00	57.90	36.80	0.00	0.00	75.30	55.78	**0.00**	**0.00**	17.40	18.98	0.00%	0.00%	26.24%	26.26%
2	0.00	0.00	57.00	37.00	0.00	0.00	75.09	56.71	**0.00**	**0.00**	18.09	19.71	0.00%	0.00%	27.28%	27.27%
3	3.00	1.80	0.00	0.00	5.52	3.33	0.00	0.00	**2.52**	**1.53**	0.00	0.00	4.50%	4.50%	0.00%	0.00%
4	9.00	5.40	0.00	0.00	9.00	5.40	0.00	0.00	**0.00**	**0.00**	0.00	0.00	0.00%	0.00%	0.00%	0.00%
5	0.00	0.00	0.00	0.00	0.00	0.00	0.00	0.00	**0.00**	**0.00**	0.00	0.00	0.00%	0.00%	0.00%	0.00%
6	0.00	0.00	0.00	0.00	0.00	0.00	0.00	0.00	**0.00**	**0.00**	0.00	0.00	0.00%	0.00%	0.00%	0.00%
7	12.80	5.90	0.00	0.00	15.32	7.43	0.00	0.00	**2.52**	**1.53**	0.00	0.00	4.50%	4.50%	0.00%	0.00%
8	10.50	4.30	0.00	0.00	13.02	5.83	0.00	0.00	**2.52**	**1.53**	0.00	0.00	4.50%	4.50%	0.00%	0.00%
9	9.00	5.00	0.00	0.00	11.52	6.53	0.00	0.00	**2.52**	**1.53**	0.00	0.00	4.50%	4.50%	0.00%	0.00%
10	6.00	3.60	0.00	0.00	8.52	5.13	0.00	0.00	**2.52**	**1.53**	0.00	0.00	4.50%	4.50%	0.00%	0.00%
11	0.00	0.00	0.00	0.00	0.00	0.00	0.00	0.00	**0.00**	**0.00**	0.00	0.00	0.00%	0.00%	0.00%	0.00%
12	11.20	7.00	0.00	0.00	14.28	8.87	0.00	0.00	**3.08**	**1.87**	0.00	0.00	5.50%	5.50%	0.00%	0.00%
13	0.00	0.00	0.00	0.00	0.00	0.00	0.00	0.00	**0.00**	**0.00**	0.00	0.00	0.00%	0.00%	0.00%	0.00%
14	29.00	18.00	0.00	0.00	35.16	21.74	0.00	0.00	**6.16**	**3.74**	0.00	0.00	11.00%	11.00%	0.00%	0.00%
15	31.50	19.00	0.00	0.00	37.66	22.74	0.00	0.00	**6.16**	**3.74**	0.00	0.00	11.00%	11.00%	0.00%	0.00%
16	5.00	3.00	0.00	0.00	8.08	4.87	0.00	0.00	**3.08**	**1.87**	0.00	0.00	5.50%	5.50%	0.00%	0.00%
17	9.00	5.80	0.00	0.00	12.08	7.67	0.00	0.00	**3.08**	**1.87**	0.00	0.00	5.50%	5.50%	0.00%	0.00%
18	16.00	9.00	0.00	0.00	22.16	12.74	0.00	0.00	**6.16**	**3.74**	0.00	0.00	11.00%	11.00%	0.00%	0.00%
19	12.00	8.00	0.00	0.00	15.08	9.87	0.00	0.00	**3.08**	**1.87**	0.00	0.00	5.50%	5.50%	0.00%	0.00%
20	5.50	3.30	0.00	0.00	5.50	3.30	0.00	0.00	**0.00**	**0.00**	0.00	0.00	0.00%	0.00%	0.00%	0.00%
21	7.50	3.20	0.00	0.00	10.02	4.73	0.00	0.00	**2.52**	**1.53**	0.00	0.00	4.50%	4.50%	0.00%	0.00%
22	0.00	0.00	37.00	24.00	0.00	0.00	48.39	36.41	**0.00**	**0.00**	11.39	12.41	0.00%	0.00%	17.18%	17.17%
23	0.00	0.00	23.00	16.00	0.00	0.00	30.37	24.03	**0.00**	**0.00**	7.37	8.03	0.00%	0.00%	11.11%	11.11%
24	4.70	3.70	0.00	0.00	7.22	5.23	0.00	0.00	**2.52**	**1.53**	0.00	0.00	4.50%	4.50%	0.00%	0.00%

Bus	L		G						PM				LD		GP	
	P_L0	Q_L0	Pg0	Qg0	PLF	QLF	PgF	QgF	ΔP_L	ΔQ_L	ΔPg	ΔQg	LDP	LDQ	GPP	GPQ
25	3.00	2.00	0.00	0.00	5.52	3.53	0.00	0.00	**2.52**	**1.53**	0.00	0.00	4.50%	4.50%	0.00%	0.00%
26	5.50	3.30	0.00	0.00	5.50	3.30	0.00	0.00	**0.00**	**0.00**	0.00	0.00	0.00%	0.00%	0.00%	0.00%
27	0.00	0.00	38.00	28.00	0.00	0.00	50.06	41.14	**0.00**	**0.00**	12.06	13.14	0.00%	0.00%	18.19%	18.18%
28	0.00	0.00	0.00	0.00	0.00	0.00	0.00	0.00	**0.00**	**0.00**	0.00	0.00	0.00%	0.00%	0.00%	0.00%
29	4.00	2.40	0.00	0.00	6.52	3.93	0.00	0.00	**2.52**	**1.53**	0.00	0.00	4.50%	4.50%	0.00%	0.00%
30	7.60	4.00	0.00	0.00	10.12	5.53	0.00	0.00	**2.52**	**1.53**	0.00	0.00	4.50%	4.50%	0.00%	0.00%
Total	201.8	117.7	212.9	141.8	257.80	151.70	279.21	214.07	**56.00**	**34.00**	66.31	72.27	100.00%	100.00%	100.00%	100.00%

Differences between Case30F020b and Case30F020

Bus	L		G		LD		GP	
1 to 10					0.9x	0.9x		
11 to 20					1.1x	1.1x		
21 to 30					0.9x	0.9x		

Table A3 - 23 **Ref. Case30F020cL020LD020bG020GP020c (Test pattern 05 Case2001)**

Bus	L		G						PM				LD		GP	
	P_L0	Q_L0	Pg0	Qg0	PLF	QLF	PgF	QgF	ΔP_L	ΔQ_L	ΔPg	ΔQg	LDP	LDQ	GPP	GPQ
1	0.00	0.00	57.90	36.80	0.00	0.00	76.83	57.15	**0.00**	**0.00**	18.93	20.35	0.00%	0.00%	30.03%	29.34%
2	0.00	0.00	57.00	37.00	0.00	0.00	75.90	58.00	**0.00**	**0.00**	18.90	21.00	0.00%	0.00%	29.99%	30.28%
3	3.00	1.80	0.00	0.00	5.38	3.20	0.00	0.00	**2.38**	**1.40**	0.00	0.00	4.49%	4.51%	0.00%	0.00%
4	9.00	5.40	0.00	0.00	9.00	5.40	0.00	0.00	**0.00**	**0.00**	0.00	0.00	0.00%	0.00%	0.00%	0.00%
5	0.00	0.00	0.00	0.00	0.00	0.00	0.00	0.00	**0.00**	**0.00**	0.00	0.00	0.00%	0.00%	0.00%	0.00%
6	0.00	0.00	0.00	0.00	0.00	0.00	0.00	0.00	**0.00**	**0.00**	0.00	0.00	0.00%	0.00%	0.00%	0.00%
7	12.80	5.90	0.00	0.00	15.19	7.30	0.00	0.00	**2.39**	**1.40**	0.00	0.00	4.51%	4.51%	0.00%	0.00%
8	10.50	4.30	0.00	0.00	12.89	5.70	0.00	0.00	**2.39**	**1.40**	0.00	0.00	4.51%	4.51%	0.00%	0.00%
9	9.00	5.00	0.00	0.00	11.39	6.40	0.00	0.00	**2.39**	**1.40**	0.00	0.00	4.51%	4.51%	0.00%	0.00%
10	6.00	3.60	0.00	0.00	8.38	5.00	0.00	0.00	**2.38**	**1.40**	0.00	0.00	4.49%	4.51%	0.00%	0.00%
11	0.00	0.00	0.00	0.00	0.00	0.00	0.00	0.00	**0.00**	**0.00**	0.00	0.00	0.00%	0.00%	0.00%	0.00%
12	11.20	7.00	0.00	0.00	14.12	8.71	0.00	0.00	**2.92**	**1.71**	0.00	0.00	5.51%	5.51%	0.00%	0.00%
13	0.00	0.00	0.00	0.00	0.00	0.00	0.00	0.00	**0.00**	**0.00**	0.00	0.00	0.00%	0.00%	0.00%	0.00%
14	29.00	18.00	0.00	0.00	34.83	21.41	0.00	0.00	**5.83**	**3.41**	0.00	0.00	11.00%	10.98%	0.00%	0.00%
15	31.50	19.00	0.00	0.00	37.33	22.41	0.00	0.00	**5.83**	**3.41**	0.00	0.00	11.00%	10.98%	0.00%	0.00%
16	5.00	3.00	0.00	0.00	7.92	4.71	0.00	0.00	**2.92**	**1.71**	0.00	0.00	5.51%	5.51%	0.00%	0.00%
17	9.00	5.80	0.00	0.00	11.92	7.50	0.00	0.00	**2.92**	**1.70**	0.00	0.00	5.51%	5.48%	0.00%	0.00%
18	16.00	9.00	0.00	0.00	21.83	12.41	0.00	0.00	**5.83**	**3.41**	0.00	0.00	11.00%	10.98%	0.00%	0.00%
19	12.00	8.00	0.00	0.00	14.92	9.71	0.00	0.00	**2.92**	**1.71**	0.00	0.00	5.51%	5.51%	0.00%	0.00%
20	5.50	3.30	0.00	0.00	5.50	3.30	0.00	0.00	**0.00**	**0.00**	0.00	0.00	0.00%	0.00%	0.00%	0.00%
21	7.50	3.20	0.00	0.00	9.88	4.60	0.00	0.00	**2.38**	**1.40**	0.00	0.00	4.49%	4.51%	0.00%	0.00%
22	0.00	0.00	37.00	24.00	0.00	0.00	46.45	34.50	**0.00**	**0.00**	9.45	10.50	0.00%	0.00%	14.99%	15.14%
23	0.00	0.00	23.00	16.00	0.00	0.00	29.30	23.00	**0.00**	**0.00**	6.30	7.00	0.00%	0.00%	10.00%	10.09%
24	4.70	3.70	0.00	0.00	7.09	5.10	0.00	0.00	**2.39**	**1.40**	0.00	0.00	4.51%	4.51%	0.00%	0.00%

Bus	L		G						PM				LD		GP	
	P_L0	Q_L0	Pg0	Qg0	PLF	QLF	PgF	QgF	ΔP_L	ΔQ_L	ΔPg	ΔQg	LDP	LDQ	GPP	GPQ
25	3.00	2.00	0.00	0.00	5.38	3.40	0.00	0.00	**2.38**	**1.40**	0.00	0.00	4.49%	4.51%	0.00%	0.00%
26	5.50	3.30	0.00	0.00	5.50	3.30	0.00	0.00	**0.00**	**0.00**	0.00	0.00	0.00%	0.00%	0.00%	0.00%
27	0.00	0.00	38.00	28.00	0.00	0.00	47.45	38.50	**0.00**	**0.00**	9.45	10.50	0.00%	0.00%	14.99%	15.14%
28	0.00	0.00	0.00	0.00	0.00	0.00	0.00	0.00	**0.00**	**0.00**	0.00	0.00	0.00%	0.00%	0.00%	0.00%
29	4.00	2.40	0.00	0.00	6.38	3.79	0.00	0.00	**2.38**	**1.39**	0.00	0.00	4.49%	4.48%	0.00%	0.00%
30	7.60	4.00	0.00	0.00	9.98	5.40	0.00	0.00	**2.38**	**1.40**	0.00	0.00	4.49%	4.51%	0.00%	0.00%
Total	201.8	117.7	212.9	141.8	254.81	148.75	275.93	211.15	**53.01**	**31.05**	63.03	69.35	100.00%	100.00%	100.00%	100.00%

Differences between Case30F020c and Case30F020b

Bus	L		G		LD		GP	
1							1.11xb	1.11xb
2							1.11xb	1.11xb
22							0.88xb	0.88xb
23							0.91xb	0.91xb
27							0.83xb	0.83xb

Table A3 - 24 **Ref. Case30F020tL020tLD020bG020tGP020t (Test pattern 06 Case2002)**

Bus	L		G						PM				LD		GP	
	P_L0	Q_L0	Pg0	Qg0	PLF	QLF	PgF	QgF	ΔP_L	ΔQ_L	ΔPg	ΔQg	LDP	LDQ	GPP	GPQ
1	0.00	0.00	64.80	45.49	0.00	0.00	74.23	55.55	**0.00**	**0.00**	9.43	10.06	0.00%	0.00%	24.42%	23.04%
2	0.00	0.00	62.70	42.55	0.00	0.00	75.54	56.95	**0.00**	**0.00**	12.84	14.40	0.00%	0.00%	33.26%	32.98%
3	3.30	1.98	0.00	0.00	4.74	2.84	0.00	0.00	**1.44**	**0.86**	0.00	0.00	4.50%	4.51%	0.00%	0.00%
4	9.90	5.94	0.00	0.00	9.90	5.94	0.00	0.00	**0.00**	**0.00**	0.00	0.00	0.00%	0.00%	0.00%	0.00%
5	0.00	0.00	0.00	0.00	0.00	0.00	0.00	0.00	**0.00**	**0.00**	0.00	0.00	0.00%	0.00%	0.00%	0.00%
6	0.00	0.00	0.00	0.00	0.00	0.00	0.00	0.00	**0.00**	**0.00**	0.00	0.00	0.00%	0.00%	0.00%	0.00%
7	14.08	6.49	0.00	0.00	15.52	7.35	0.00	0.00	**1.44**	**0.86**	0.00	0.00	4.50%	4.51%	0.00%	0.00%
8	11.55	4.73	0.00	0.00	12.99	5.59	0.00	0.00	**1.44**	**0.86**	0.00	0.00	4.50%	4.51%	0.00%	0.00%
9	9.90	5.50	0.00	0.00	11.34	6.36	0.00	0.00	**1.44**	**0.86**	0.00	0.00	4.50%	4.51%	0.00%	0.00%
10	6.60	3.96	0.00	0.00	8.04	4.82	0.00	0.00	**1.44**	**0.86**	0.00	0.00	4.50%	4.51%	0.00%	0.00%
11	0.00	0.00	0.00	0.00	0.00	0.00	0.00	0.00	**0.00**	**0.00**	0.00	0.00	0.00%	0.00%	0.00%	0.00%
12	12.32	7.70	0.00	0.00	14.08	8.75	0.00	0.00	**1.76**	**1.05**	0.00	0.00	5.50%	5.51%	0.00%	0.00%
13	0.00	0.00	0.00	0.00	0.00	0.00	0.00	0.00	**0.00**	**0.00**	0.00	0.00	0.00%	0.00%	0.00%	0.00%
14	31.90	19.80	0.00	0.00	35.42	21.89	0.00	0.00	**3.52**	**2.09**	0.00	0.00	11.00%	10.97%	0.00%	0.00%
15	34.65	20.90	0.00	0.00	38.17	22.99	0.00	0.00	**3.52**	**2.09**	0.00	0.00	11.00%	10.97%	0.00%	0.00%
16	5.50	3.30	0.00	0.00	7.26	4.35	0.00	0.00	**1.76**	**1.05**	0.00	0.00	5.50%	5.51%	0.00%	0.00%
17	9.90	6.38	0.00	0.00	11.66	7.42	0.00	0.00	**1.76**	**1.04**	0.00	0.00	5.50%	5.46%	0.00%	0.00%
18	17.60	9.90	0.00	0.00	21.12	11.99	0.00	0.00	**3.52**	**2.09**	0.00	0.00	11.00%	10.97%	0.00%	0.00%
19	13.20	8.80	0.00	0.00	14.96	9.85	0.00	0.00	**1.76**	**1.05**	0.00	0.00	5.50%	5.51%	0.00%	0.00%
20	6.05	3.63	0.00	0.00	6.05	3.63	0.00	0.00	**0.00**	**0.00**	0.00	0.00	0.00%	0.00%	0.00%	0.00%
21	8.25	3.52	0.00	0.00	9.69	4.38	0.00	0.00	**1.44**	**0.86**	0.00	0.00	4.50%	4.51%	0.00%	0.00%
22	0.00	0.00	40.70	27.60	0.00	0.00	47.29	34.80	**0.00**	**0.00**	6.59	7.20	0.00%	0.00%	17.07%	16.49%
23	0.00	0.00	25.76	18.40	0.00	0.00	29.66	23.20	**0.00**	**0.00**	3.90	4.80	0.00%	0.00%	10.10%	10.99%
24	5.17	4.07	0.00	0.00	6.61	4.93	0.00	0.00	**1.44**	**0.86**	0.00	0.00	4.50%	4.51%	0.00%	0.00%

Bus	L		G						PM				LD		GP	
	P_L0	Q_L0	Pg0	Qg0	PLF	QLF	PgF	QgF	ΔP_L	ΔQ_L	ΔPg	ΔQg	LDP	LDQ	GPP	GPQ
25	3.30	2.20	0.00	0.00	4.74	3.06	0.00	0.00	**1.44**	**0.86**	0.00	0.00	4.50%	4.51%	0.00%	0.00%
26	6.05	3.63	0.00	0.00	6.05	3.63	0.00	0.00	**0.00**	**0.00**	0.00	0.00	0.00%	0.00%	0.00%	0.00%
27	0.00	0.00	42.56	32.20	0.00	0.00	48.41	39.40	**0.00**	**0.00**	5.85	7.20	0.00%	0.00%	15.15%	16.49%
28	0.00	0.00	0.00	0.00	0.00	0.00	0.00	0.00	**0.00**	**0.00**	0.00	0.00	0.00%	0.00%	0.00%	0.00%
29	4.40	2.64	0.00	0.00	5.84	3.50	0.00	0.00	**1.44**	**0.86**	0.00	0.00	4.50%	4.51%	0.00%	0.00%
30	8.36	4.40	0.00	0.00	9.80	5.26	0.00	0.00	**1.44**	**0.86**	0.00	0.00	4.50%	4.51%	0.00%	0.00%
Total	221.98	129.47	236.52	166.24	253.98	148.53	275.13	209.90	**32.00**	**19.06**	38.61	43.66	100.00%	100.00%	100.00%	100.00%

Differences between Case30F020t and Case30F020

Bus	L		G		LD		GP	
1 to 30	1.1x	1.1x						
1			1.12x	1.15x			0.9x	0.85x
2			1.12x	1.15x			1.23x	1.22x
22			1.12x	1.15x			1.00x	0.97x
23			1.12x	1.15x			0.92x	1.00x
27			1.12x	1.15x			0.84x	0.92x
1 to 10					0.9x	0.9x		
11 to 20					1.1x	1.1x		
21 to 30					0.9x	0.9x		